BOSTON

CHARGING INTO THE FUTURE

FIELD TRIP GUIDEBOOK FOR THE NORTHEASTERN UNITED STATES: 1993 BOSTON GSA

Volume 2

For
1993 Geological Society of America Annual Meeting &
85th Annual New England Intercollegiate Geological Conference
October 25-28
Boston, Massachussetts

BOSTON

CHARGING INTO THE FUTURE

FIELD TRIP GUIDEBOOK FOR THE NORTHEASTERN UNITED STATES: 1993 BOSTON GSA

Volume 2

For
1993 Geological Society of America Annual Meeting &
85th Annual New England Intercollegiate Geological Conference
October 25-28
Boston, Massachussetts

EDITED BY:

JOHN T. CHENEY
DEPARTMENT OF GEOLOGY
AMHERST COLLEGE

J. CHRISTOPHER HEPBURN
DEPARTMENT OF GEOLOGY
BOSTON COLLEGE

CONTRIBUTION NO. 67
DEPARTMENT OF GEOLOGY AND GEOGRAPHY, UNIVERSITY OF MASSACHUSETTS
AMHERST, MASSACHUSETTS 01003

EDITORS' REMARKS

Our goal in assembling this field trip program and accompanying guidebook was to showcase the geology of the northeastern United States and the significant contributions of those who have worked here. The trips and authors were selected in an attempt to offer an interesting excursion for nearly every geologist while insuring access to the rich and diverse geological heritage of New England and environs. However, the papers appearing in these volumes have not been formally edited. In fact, time did not permit even a quick reading of most manuscripts. Our editorial role was limited to that of compiling these two volumes by setting the format, establishing reasonable page limits, attempting to enforce both the page limits and necessary deadlines, and insuring that the original was delivered to the printer in time to produce the books for the running of the field trips. Thus the articles appearing here are the original, uncut and unabridged offerings of their authors.

ACKNOWLEDGEMENTS

Organizing and bringing to fruition a project of this scope is only possible with the complete and amicable cooperation of all of those trip leaders and co-leaders who planned the trips, set up the logistics, and wrote the articles. We are most grateful to <u>all</u> of these geologists for their friendly understanding, prompt responses to our many requests and professional conduct of this enterprise. The efforts of the GSA staff on our collective behalf are most gratefully acknowledged. We have benefitted immensely from Sue Beggs' experienced best efforts to keep us out of trouble and Kathy Lynch's knowledge. Most of all however, we are deeply appreciative of the organization, dedication and hard work of Becky Martin, the GSA Field Trip Coordinator. Jackie Newberry provided professional, prompt and cheerful assistance at Amherst. Thanks to the efforts of all of these people, the task was immeasurably simplified and indeed the much dreaded job of Field Trip Organizers was in fact most entertaining.

Howard Dimmick was instrumental in securing the flexible transportation contract with Crystal Bus lines of Boston. The University of Massachusetts Duplicating Service, directed by Leo St. Denis, printed the text . The cover, binding and the fold out map in chapter B were done by the Hamilton I. Newell Company of Amherst, Massachusetts.

Finally we would like to thank Professor Peter Robinson of the University of Massachusetts, Amherst for showing us so many times how to do this job right and for giving us the opportunity. Peter was clearly the choice to Chair the field trip committee. However, when asked by Fr. Skehan in 1988, Peter modestly declined due to <u>age</u> and gracefully suggested us!

For sale by:

The Department of Geology and Geography
University of Massachusetts
Amherst, Massachusetts 01003

VOLUME 2
CONTENTS

Volume 2 Contents continued

Chapter O

High-Pressure, Taconian, and Subsequent Polymetamorphism of Southern Quebec and Northern Vermont

By Jo Laird, Walter E. Trzcienski, Jr., and Wallace A. Bothner

Field Trip Guidebook for the Northeastern United States:
1993 Boston GSA

Volume 2
Contribution No. 67, Department of Geology and Geography, University of Massachusetts, Amherst, Massachusetts

HIGH-PRESSURE, TACONIAN, AND SUBSEQUENT POLYMETAMORPHISM OF SOUTHERN QUEBEC AND NORTHERN VERMONT

by

Jo Laird, Department of Earth Sciences, University of New Hampshire, Durham, NH 03824
Walter E. Trzcienski, Jr., Départment de géologie, Université de Montréal, Montréal, Canada H3C 3J7
Wallace A. Bothner, Department of Earth Sciences, University of New Hampshire, Durham, NH 03824

INTRODUCTION

The first stratigraphic syntheses of the areas we are to visit in southern Quebec and north-central Vermont were provided by Clark (1936) and Doll et al. (1961). Unconformably overlying the Grenville basement are rocks of the Oak Hill (QUE) and Camels Hump (VT) Groups of the Sutton/Green Mountains anticlinoria. To the east in Quebec lies the Caldwell Group which may be correlative to the Oak Hill Group and, in Vermont, to the Hazens Notch Formation in the Camels Hump Group. In Quebec the Caldwell is commonly in contact to the east with large bodies of ultramafic and associated rocks; small slivers of ultramafic rocks are also found locally within the Caldwell. In Vermont the largest ultramafic body is at Belvidere Mountain (western Hazens Notch Fm.). More commonly ultramafic rocks crop out as slivers both within the Hazens Notch Fm. and within the Ottauquechee, Stowe, and Missisquoi Formations to the east.

The Oak Hill, Caldwell, and Camels Hump Groups contain mafic volcanics and volcanoclastics, quartzo-feldspathic sandstones, and pelites. Additionally, micaceous carbonates occur in the Oak Hill Group. In Vermont pelites, volcanics, and volcanoclastics compose the Ottauquechee and Stowe Formations (nomenclature of Doll et al., 1961). Farther west is pinstriped granofels and metadiabase of the Missisquoi Fm. East of these pre-Silurian rocks and across the RMC (Taconian Line of Hatch, 1982) are metamorphosed Silurian and Devonian felsic, calcareous, pelitic, and mafic rocks of the Connecticut Valley - Gaspé Trough.

The first detailed structural analysis of the complex Oak Hill slice of Clark (1936) was that done in the Knowlton-Richmond area by Osberg (1965). He showed the nature of the termination of the Sutton/Green Mountains anticlinoria and the correlation between the Québec and Vermont stratigraphies.

As shown by Doll et al. (1961) pelitic rocks within the pre-Silurian section of northern Vermont are primarily biotite grade with garnet and kyanite grade metamorphism occurring along the Green Mountain anticlinorium and the Elmore/ Worcester/ Northfield Mountains (see Figures 1 & 2 for the locations of these structures). In general, isograds are oriented NNE - SSW along the structural trend. Farther east and within the Connecticut Valley - Gaspé Trough, biotite to sillimanite grade pelitic rocks crop out, and metamorphic isograds are spatially related to Devonian peraluminous granites.

Albee (1965, 1968) published the first detailed petrologic studies of pelitic schists from northern Vermont. He championed the idea that polymetamorphism is preserved in these rocks (Albee, 1957, 1968), and Lanphere and Albee (1974) confirmed the presence of Taconian and Acadian metamorphism via $^{40}Ar/^{39}Ar$ age dating.

With the advent of plate tectonics, the structure of the area was reinterpreted and subdivided into lithotectonic zones by St-Julien and Hubert (1975) and Williams (1976). Concurrently, Laird and Albee (1975, 1981a) discovered glaucophane and omphacite at Tillotson Peak indicating high pressure facies series metamorphism, and Trzcienski (1976) identified crossite in the Richmond area (see Figures 1 and 2 for both localities). Furthermore, barroisite rimmed by actinolite was identified at several locations in pre-Silurian mafic rocks from northern Vermont (Laird and Albee, 1981b) implying medium-high-pressure facies series metamorphism. Compilation of all of these data from southern Quebec and northern Vermont define an envelope of Taconian, high pressure metamorphism about the Sutton/Green Mountains anticlinoria (Figure 2).

Subsequent field and laboratory data have elaborated on the tectonic, petrologic, geochemical, and isotopic relationships found within and adjacent to this envelope. Many of these data are summarized in recent

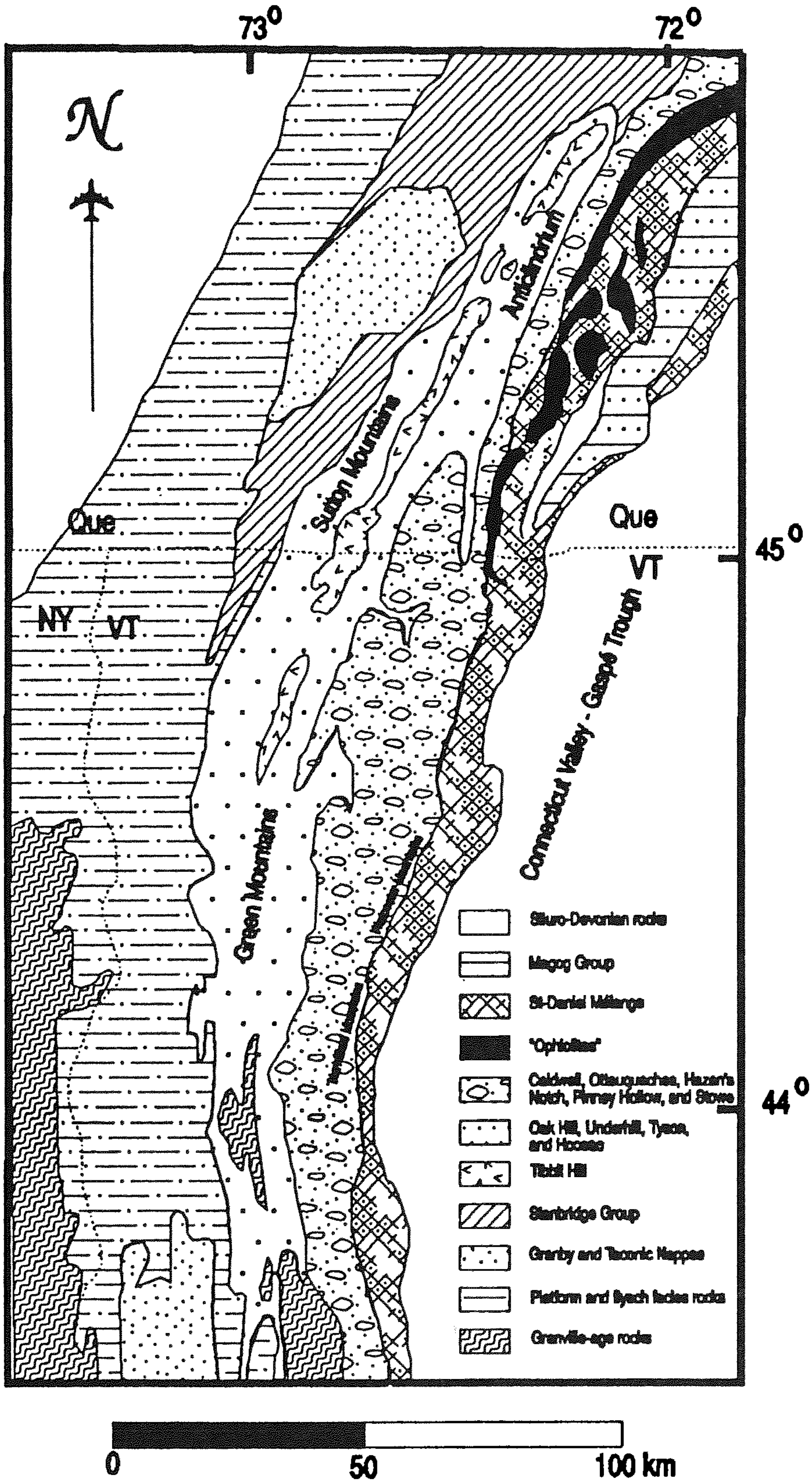

Figure 1: Generalized lithotectonic map of southeastern Québec and north-central Vermont (After Williams, 1978).

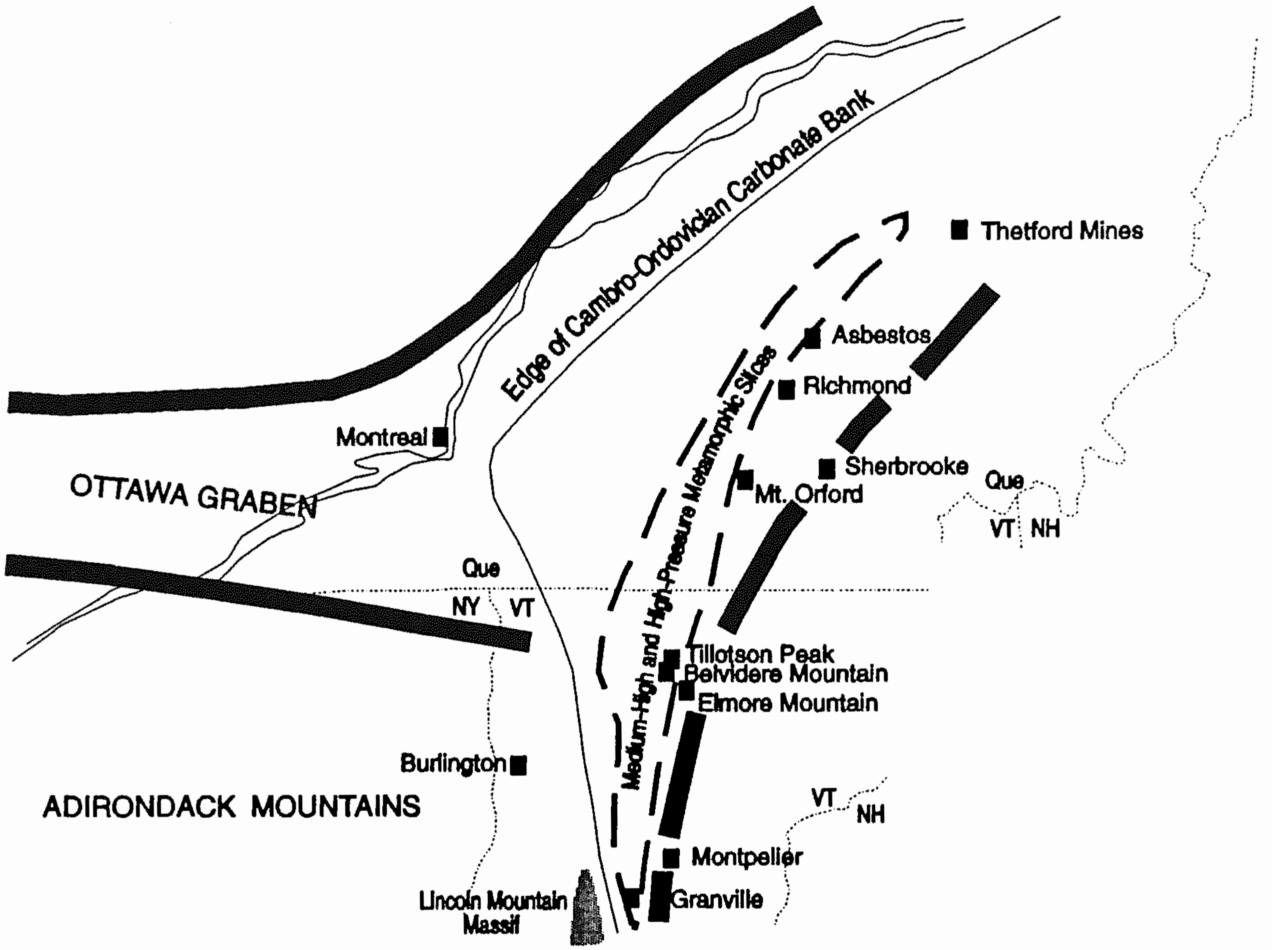

Figure 2: Sketch map showing the "western" shore of Iapetos, the approximate edge of the carbonate bank, and the position of the Ottawa graben.

The present position of the Taconian medium-high to high-pressure metamorphic facies series "envelope" is superimposed (From Bothner and Laird, 1991).

DNAG publications of the Geological Society of America (Roy, 1987; Hatcher et al., 1989, and Thompson et al., 1993).

The purpose of this field trip is to examine several localities within, and astride, the high pressure metamorphic envelope (Figure 2). The metamorphic history will be examined in the context of the geologic setting, and emphasis will be placed on areas where detailed petrologic and geochemical studies are published and ongoing. Day one will be spent in the Richmond area, Quebec looking at the Caldwell and Oak Hill Groups and ultramafic and associated rocks. Day two will be a traverse among the glaucophane and omphacite assemblages of Tillotson Peak. Day three will include the classic polymetamorphic pelitic rocks at Elmore Mountain and mafic rocks at the south end of the high pressure envelope.

To and from the fieldtrip area we will drive across several tectono-metamorphic terranes discussed in other field guides in this volume. We start in the Coastal Lithotectonic Belt and drive through the Central Maine Terrane, over the Bronson Hill anticlinorium into the Connecticut Valley - Gaspé Trough and then into the Sutton Mountain/Green Mountain anticlinorium (Figure 1).

In addition to this guide, field trip guides specific to the outcrops we shall visit are: Marquis et al. (1987), Laird and Bothner (1986), Bothner and Laird (1987), Albee (1972), Lyons and Bothner (1989), and Stanley et al. (1987 and herein). If your enthusiasm wanes during the trip, please remember that in the northern Appalachians very special rocks often hide among the trees, beneath moss and lichen, and up hill!

METAMORPHISM SOUTHERN QUÉBEC

Petrology

Metamorphism of the Cambro-Ordovician rocks along the western margin of the Québec Appalachians is the result of the Taconian Orogeny where little to no evidence is found for Acadian effects. Our visit will be to two different suites of rocks; those derived from the continental margin/slope (Oak Hill and Caldwell Groups) and those thought to be associated with ocean-floor processes. The former are now metamorphosed sediments and volcanics overlying a Grenville basement (St-Julien and Hubert, 1975), and the latter are interpreted (Williams and St-Julien, 1982) to be the trace of a suture zone separating the Laurentian margin to the northwest from a younger Iapetos Ocean to the southeast.

Oak Hill Group. At the base of the Oak Hill sequence (Clark, 1936) are the Tibbit Hill volcanics that in their present state are epidote-albite-chlorite-quartz-amphibole±white mica±stilpnomelane±magnetite±sphene ±calcite greenstones. Epidote nodules and vesicular textures are common. The only vestiges of an igneous precursor are kaersutite cores in some of the larger amphibole grains. These cores, trace element geochemistry, and tectonic variation diagrams (Pintson et al., 1985) indicate an alkaline, within plate, continental setting during crystallization. This fits well with the idea that the volcanics represent the early stages of rifting that led to the formation of an Iapetan ocean in Cambrian time. U-Pb zircon analyses of a felsic unit within the Tibbit Hill near Waterloo, Québec have yielded a crystallization age of 554 Ma (Kumarapeli et al., 1989). Overlying the Tibbit Hill volcanics is the pelitic Call Mill Formation. Distinctive in the field because of its black, phyllitic nature, the Call Mill commonly contains splays of chloritoid within a matrix of white mica, quartz, chlorite, plagioclase and ilmenite. The Pinnacle Formation that overlies the Call Mill in the Richmond area is predominantly a quartzo-feldspathic unit with some intercalated phyllite. In many places it is seen to be highly sheared. Elsewhere the Pinnacle is a massive quartzite, and in the Sutton area to the south of Richmond, linear, massive magnetite beds are common. Above the Pinnacle lies the White Brook Formation composed primarily of calcite and dolomite with minor quartz, chlorite, and feldspar. Marquis (1991) states that this formation is the first that clearly represents a sedimentary marine environment. The Gilman Formation that overlies the White Brook is a composite of phyllite and quartzite, and is the thickest of the Oak Hill formations (Clark, 1936). It has undergone a series of subdivisions and redefinitions over the past two decades but has been restored by Marquis (1991), based on historical priorities, to that originally described by Clark (1936) (see Marquis, 1991, pg. 15 for discussion). Limited fossil evidence (Clark, 1934, 1936) suggests a Lower Cambrian age for the Gilman. The Dunham Formation, overlying in a transitional contact the Gilman (Marquis, 1991), is a buff-weathering dolomite that is also Lower Cambrian in age based on trilobites described by Clark (1936). The classic Oak Hill sequence of Clark (1936) is topped by the Sweetsburg Formation. This latter unit is a series of interstratified phyllites and carbonate-bearing quartzitic sandstones. Marquis (1991) has found fossil fragments that indicate that the Sweetsburg may be as young as Late Cambrian or Early Ordovician. In recent remapping of the Richmond area Marquis (1991) has shown that the Sweetsburg Formation is overlain concordantly and grades into the overlying Melbourne Formation. He argues that the Melbourne is actually the top of the Oak Hill sequence as originally proposed by Cooke (1952). The argument against including the Melbourne within the Oak Hill is that it, the Melbourne, is not seen in the type locality of the Oak Hill sequence near Sutton, Québec. The Melbourne is a distinctive, graphitic, mica-bearing carbonate. Conodonts described by Nowlan (1987) are Middle to Late Ordovician in age and have a North Atlantic affinity.

Caldwell Group. In fault contact that truncates in places the Oak Hill sequence are rocks of the Caldwell Group. These rocks are interstratified volcanics and sandstones. The mafic volcanics have been shown by Gariepy (1978) to be rift related. The sandstones are quartz-rich with a finer-grained chlorite, white mica matrix that imparts a characteristic green patina to the rocks. Chips of phyllite are observed locally along with minor quartz clasts. Caught up along fault planes within the Caldwell are slivers of ultramafic rock derived from the massive ultramafics lying just to the east. No age data are available but based upon tectonic and paleogeographic considerations St-Julien and Hubert (1975) assign a Cambrian age to the group.

Ultramafic Suite. Originally thought to be remnants of Iapetan oceanic crust, ultramafic and associated rocks are found more or less continuously, in fault contact, east of the Caldwell Group. Many of these ultramafites are now completely serpentinized and highly deformed by a late-stage brittle deformation, thus any semblance to original igneous characteristics is commonly lacking. Associated mafic rocks on the other hand retain igneous textures and are overprinted by prehnite-pumpellyite metamorphism. Included amongst these latter group of rocks are metagabbros, diorites/granites, and calcsilicate lenses that may originally have been anorthosite layers. Tectonic discrimination diagrams indicate that the diorites/granites are volcanic arc-type granites similar to continental margin granites.

Thermobarometry. Most of the Québec sequence of rocks are either greenschist facies or lower. The only high-grade rocks are garnet-clinopyroxene amphibolites associated with serpentinites at Thetford Mines and Asbestos. Feininger (1981) has estimated P and T at Thetford Mines to be between 5 and 7 kbars and at least ≥500 °C to ~780 °C. These amphibolites are highly localized and are not typical of the regional metamorphism. The typical assemblages contain prehnite and/or pumpellyite and grossular in metamorphosed gabbros and "anorthosites" and stilpnomelane and amphibole in diorites/tonalites associated with the ultramafites. The metavolcanics throughout the area contain the common assemblage chlorite, amphibole, quartz, albite, epidote and commonly magnetite, white mica, stilpnomelane and/or calcite.

Thermobarometry of subassemblages from these two different suites of rocks were investigated using TWEEQU (Berman, 1991). Common to the serpentinites are layers and lenses of calcsilicate that contain various combinations of prehnite, pumpellyite, epidote/zoisite, Ca-Mn garnet, chlorite, idocrase, and remnant grains of twinned plagioclase, biotite, and diopside. In places these layers are bounded by beds of chromitite. Geochemical analyses from two of these layers occurring between chromitites produced REE patterns (Fig 3) that fall within the maximum and minimum REE values of Stillwater anorthosite layers (Salpas et al. 1983). Based on the mineralogy and geochemistry of these layers, it is suggested that they are remnants of original anorthosite layers within the ultramafic complex. Incorporating microprobe analyses of garnet, zoisite, chlorite, prehnite, and pumpellyite from one of these layers the following reaction stabilities were calculated using TWEEQU:

15 Qtz + 10 Pump + 6Gr + 2H_2O = 2Chl +29Prh (1)
2Zo + 3Qtz + 2Gr + 4H_2O = 5Prh (2)
27Qtz + 20Pump + 10Gr = 4Chl + 53Prh + 2Zo (3)
5Pump = 5Zo + 2Prh + 2Gr + Chl + 9H_2O (4)
25Pump = 29Zo + 6Qtz + 14Gr + 5Chl + 53H_2O (5)
5Pump + 3Qtz = 3Zo + 7Prh + Chl +5H_2O (6).

For garnet the solution model within TWEEQU (Berman, 1991) was used. For chlorite and zoisite solutions, ideal mixing on sites (Powell, 1978) was used. Because analyzed prehnite was nearly pure $Ca_2Al_2Si_3O_{10}(OH)_2$, $a_{Prehnite} = 1$, and $a_{Pumpellyite}$ was calculated after the model of Frey et al. (1991). Since both the zoisite and garnet show chemical zoning, four different equilibrium points were calculated for rim-core compositions (Fig. 4). For garnet cores, higher in Ca and lower in Mn than the rims, P-T estimates are slightly higher for either zoisite composition used than for garnet rims. Also, quartz is a rare quantity in these assemblages, thus calculated equilibria will be maxima for any given point where quartz is not present. Given that this assemblage is common throughout the ultramafic belt the calculated P-T of 3-5 kbars and 300°C to 400°C is probably a decent approximation of the maximum recrystallization conditions of these rocks as presently found.

A similar approach, with TWEEQU, was used for the common metavolcanic assemblage chlorite, amphibole, albite, quartz and epidote in the endmember equilibria:

3Chl + 7Qtz + 6Cz = 5Tsch + 2An + 10H_2O (7)
14 Qtz + 5Tsch + 12Cz = 3Tr + 28An +8H_2O (8)
12Cz + 15Tsch + 14 Qtz = 44An + 4Chl + 5Tr (9)
5Tsch + 4H_2O = Tr + 2Chl + 8An (10)
14Chl + 28Qtz + Tr + 24 Cz = 25 Tsch + 44H_2O (11)
Chl + 7Qtz + 6Cz = Tr + 10An + 6H_2O (12).

Tr = tremolite, Tsch = tschermakite, An = anorthite

Solution models of plagioclase and amphibole are those incorporated within TWEEQU (Berman, 1991) and those for clinozoisite and chlorite are ideal mixing on sites (Powell, 1978). Amphibole microprobe analyses were recalculated using the scheme of Spear and Kimball (1984) to estimate Fe^{3+} by using the average Fe^{3+} value.

A number of Tibbit Hill samples from across the metamorphic envelope (Fig. 2) were used in the calculations to estimate P-T conditions. With the pronounced zoning common to the amphiboles and less so in the epidotes, maximum and minimum P-T estimates within one sample vary considerably (Fig. 5). In Québec, this amphibole zoning is irregular, but with the general trend indicating a higher pressure environment during early stages of amphibole crystallization followed by decreasing pressure. The degree of pressure variability is not the same from sample to sample. Over the center of the gravity high near Richmond (Innes and Argun-Weston, 1967) pressure estimates vary between 4 and 7 kbars (samples RI3A and RI17B - Fig. 5), whereas to the north (samples TB6 and RI10A) and south (sample Q3C) of the high there is greater variation. For the Québec samples, where only one metamorphism is seen, the calculation scheme produces realistic results given all the pitfalls inherent in these types of calculations. Taking analyses from Granville and Elmore, Vt. (see below), and the Tibbit Hill volcanics 20 km south of the Québec-Vermont border, where polymetamorphism is prevalent, similar calculations produce inconsistent intersections and very high pressures (see discussion below).

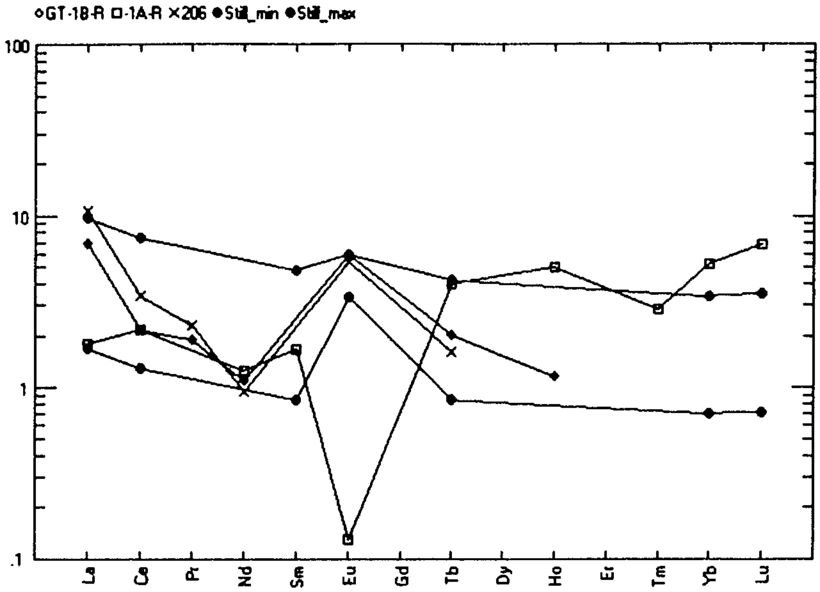

Figure 3. Rare earth element patterns for two samples (GT-1B-R and 1A-R) of calcsilicate-bearing assemblages associated with chromitites from the ultramafic complex north of Richmond, Québec. Also shown is a typical REE pattern for an ultramafic (serpentinite) sample (206) from the same locality. For comparison, the maximum (Still_max) and the minimum (Still_min) values for anorthosites from the Stillwater Complex (Salpas et al., 1983) are included.

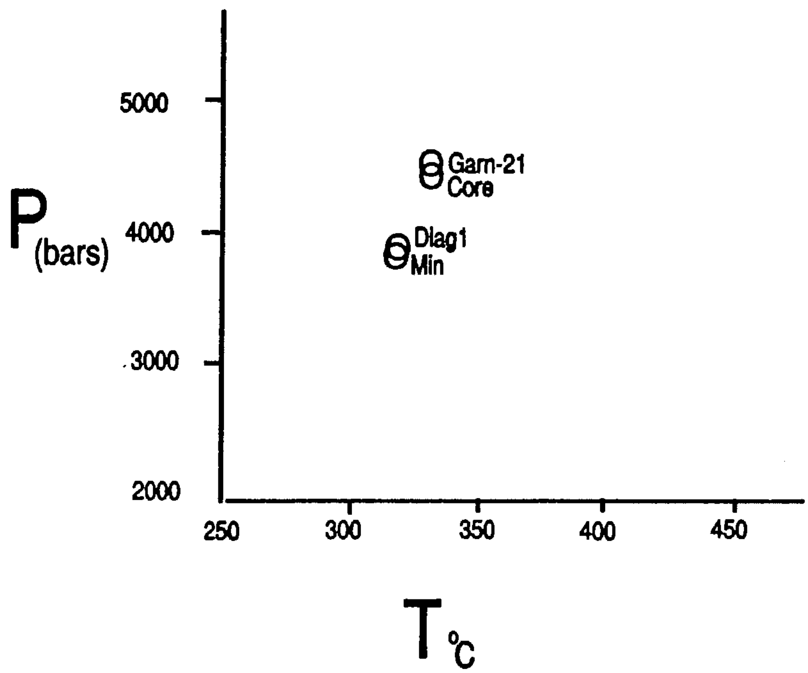

Figure 4. Estimated P-T conditions for the formation of the metamorphic calcsilicate assemblages within the ultramafic complex north of Richmond, Québec. The points were generated by the intersection of reactions (1)-(6) as calculated by TWEEQU (Berman, 1991).

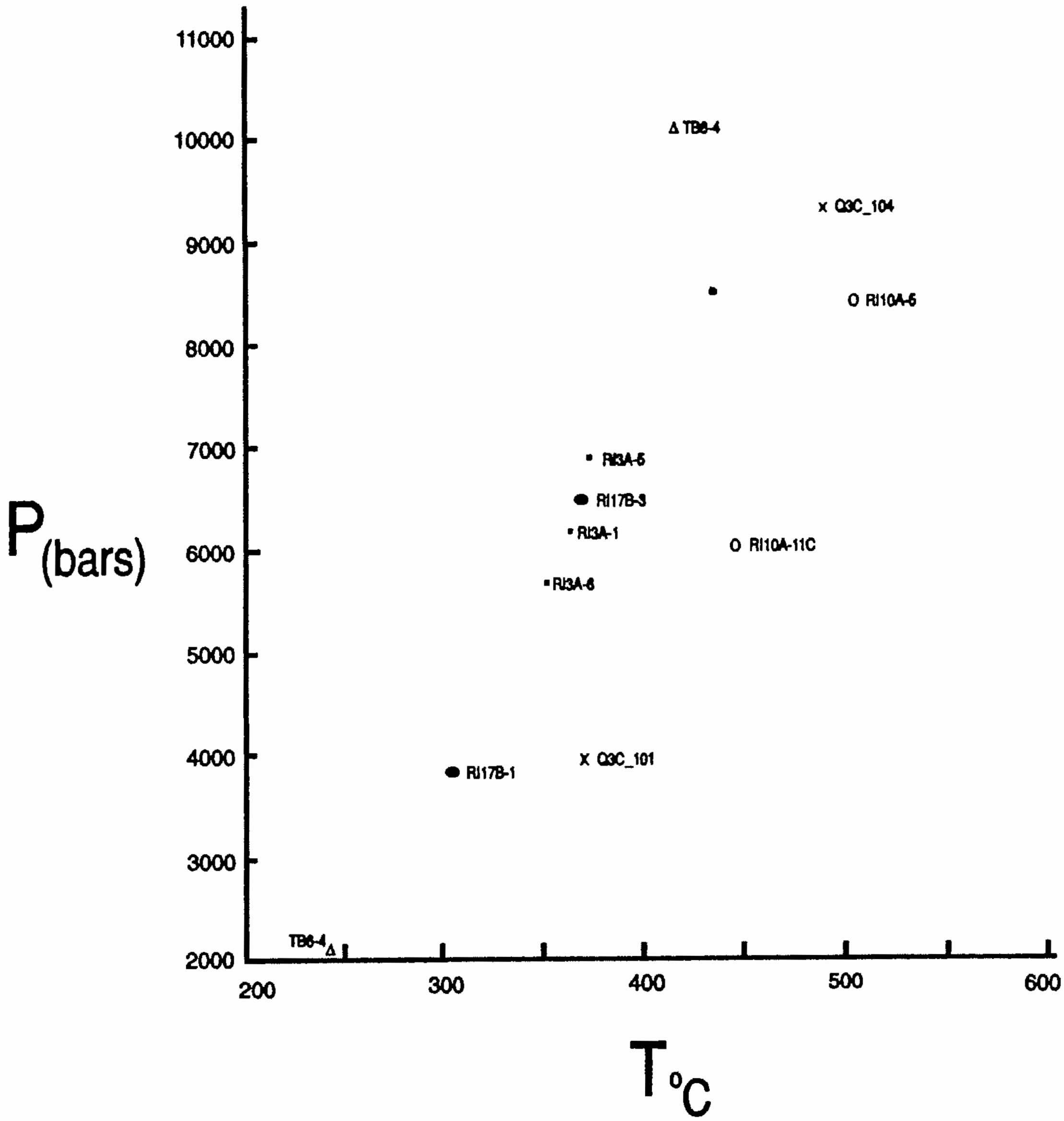

Figure 5. Estimated P-T conditions of formation of the common assemblage amphibole, chlorite, epidote, albite, and quartz in several samples of the Tibbit Hill metavolcanics in Québec. The points were generated from the intersection of the ideal reactions (7)-(12), using microprobe analyses of coexisting minerals, as calculated by the geothermobarometry program TWEEQU (Berman, 1991).

Chloritoid-bearing metapelites within the Oak Hill Group are high variance assemblages, and therefore are, not good petrologic indicators. However, Fe-Mg partitioning between chloritoid-chlorite pairs in these rocks gives a $K_D \approx 5.7$. A similar K_D is typical of epidote zone metasediments associated with New Caledonian blueschists (Ghent et al., 1987) that recrystallized at temperatures above 400 °C and below 535 °C and at pressures less than 10 kbars. These values are in good agreement with the postulated P-T conditions based on equilibria calculated from the common assemblage in the adjacent metavolcanics in the Richmond area.

Geochronologic data are sparse for the Québec sector. Mentioned above is the zircon date of 554 Ma for the Tibbit Hill. In addition zircon dates for a plagiogranite (478 Ma, Dunning et al., 1986) from Thetford Mines, and one (504 ±3 Ma, J. David, pers. com., 1993) from Mt. Orford are available. $^{40}Ar/^{39}Ar$ for the Thetford Mines garnet-clinopyroxene amphibolite has been variously dated at 491 Ma (Claque et al., 1981) and 482 Ma (Lux, 1984). Preliminary Kober analyses of zircons, by W. Trzcienski (unpub. data), from several calc-silicate lenses within the ultramafic units give a span of ages that vary from about 1100 Ma to 500 Ma. Physically these zircons are seen to have an igneous zoned core with one or two growth horizons encircling the core.

METAMORPHISM IN NORTHERN VERMONT

Petrology

Pelitic Rocks. Albee (1968, Figures 25-2, 25-3, and 25-5) documented the sequence of pelitic assemblages and compositional variation of chlorite, biotite, garnet, chloritoid, and staurolite in northern Vermont. Garlick and Epstein (1967) presented oxygen isotope temperatures for many of the samples studied by Albee. Thompson and Norton (1968, Figure 24-1)) compiled a metamorphic map for New England and identified the probable reactions for the first occurrence of pelitic index minerals. Subsequently, Carmichael (1978, Figures 2 and 4) delineated pelitic bathozones in New England.

Thompson and Norton (1968) interpreted the boundary in northeastern Vermont between staurolite + andalusite (to the north) and staurolite + kyanite (to the south) zones as a triple point isobar and speculated that it continued westward and down the west limb of the Green Mountain anticlinorium. After the discovery of glaucophane in mafic rocks (see below), glaucophane was also identified in the pelitic rocks from Tillotson Peak, ending the speculation that the triple point isobar continues westward into pre-Silurian rocks.

In the pre-Silurian section and along the Elmore/Worcester Mountains, the garnet- and kyanite- grade assemblages are retrograded (Albee, 1957, 1968). Kyanite is pseudomorphed by chloritoid and fine-grained muscovite; garnet is altered to chlorite + magnetite; and biotite is replaced by chlorite. As discussed in the section on **Geochronology**, Lanphere and Albee (1974) proposed that the higher grade metamorphism was Ordovician and the lower grade metamorphism Devonian.

Mafic Rocks. Bulk rock geochemistry obtained by Coish et al. (1985, 1986; see also Stanley et al., this volume) show that from west to east, mafic rocks within the pre-Silurian section were emplaced into the following tectonic environments: within plate (continental), within plate and ocean ridge, and at an ocean ridge.

Laird and Albee (1981b) summarized the variation in mineral chemistry and mode seen in metamorphosed mafic rocks from Vermont. The major changes occur among the phases amphibole, chlorite, epidote, plagioclase, and quartz (Laird, 1980) and can be illustrated in a three- dimensional reaction space (Thompson et al., 1982). Two of the reactions dominate the metamorphism and control the $NaSiCa_{-1}Al_{-1}$ (PL) substitution in amphibole and plagioclase and the $Al_2Mg_{-1}Si_{-1}$ (TK) substitution in amphibole and chlorite. TK increases with metamorphic grade, and PL increases with pressure of metamorphism (Laird et al., 1984, Figures 2 and 3; Fig. 6 herein). The whole rock experiments of Liou et al. (1974) and Apted and Liou (1983) show that these relationships hold for a range of mafic compositions and oxygen fugacities (Laird, 1988, Figure 20).

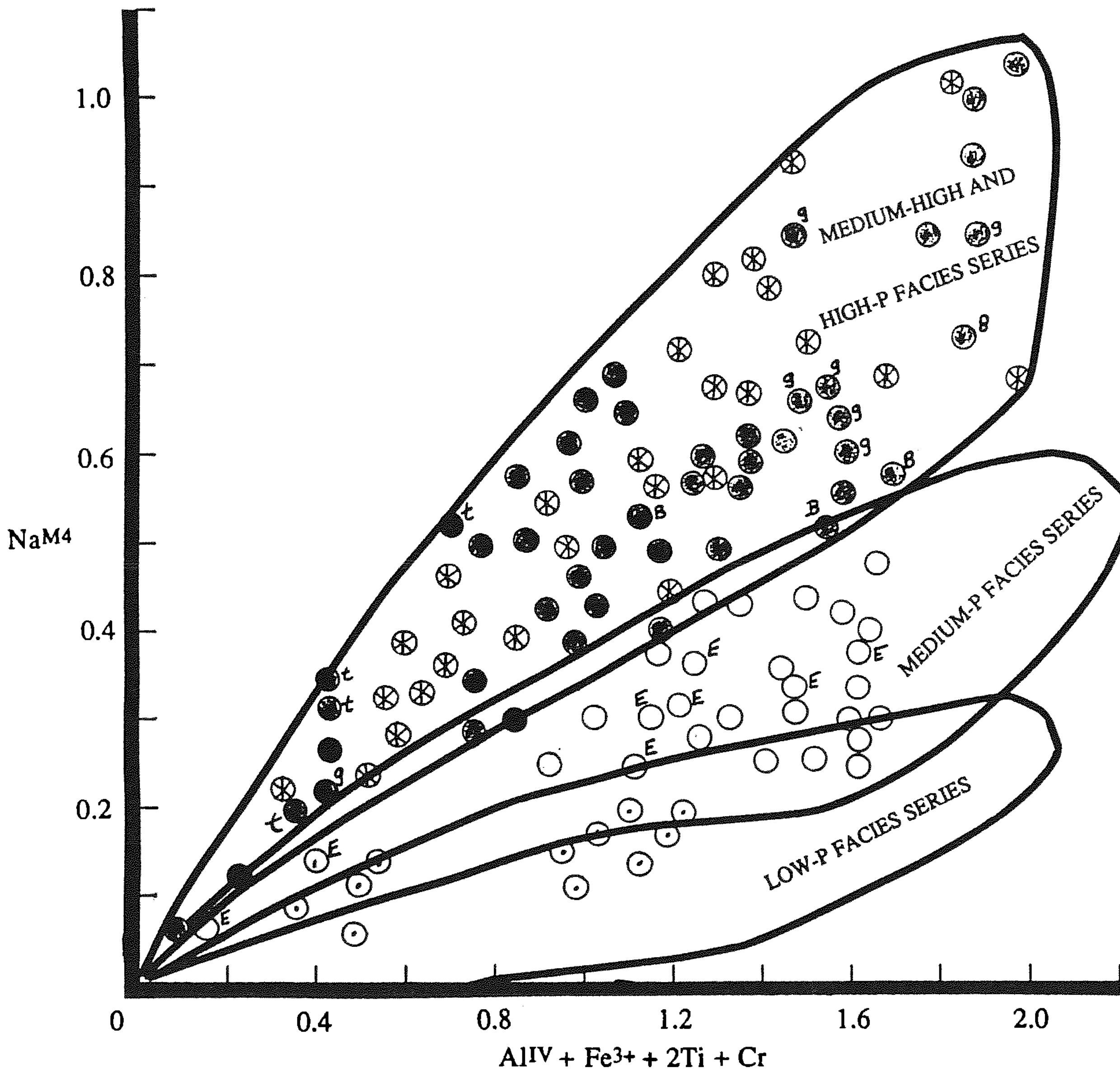

Figure 6. Sodic-calcic and calcic amphibole analyses (normalized to total cations - (Ca+Na+K)=13) from mafic schist west of the RMC, northern Vermont. Envelopes delimiting facies series are after Laird et al. (1984, Figure 2) and are defined by amphibole analyses from northern, central, and southeastern Vermont (both west and east of the RMC). Increasing temperature of metamorphism results in increasing advancement along the TK vector and thus the horizontal axis; the PL vector increases along the vertical axis. Circles with internal X are from the Tillotson Peak area; filled circles are from within the high pressure envelope; and open circles are outside the envelope with those with a dot in the center from Moretown Fm. metadiabase. t = Tibbit Hill, B = Belvidere Mountain, E = Elmore Mountain, and g = Granville Notch.

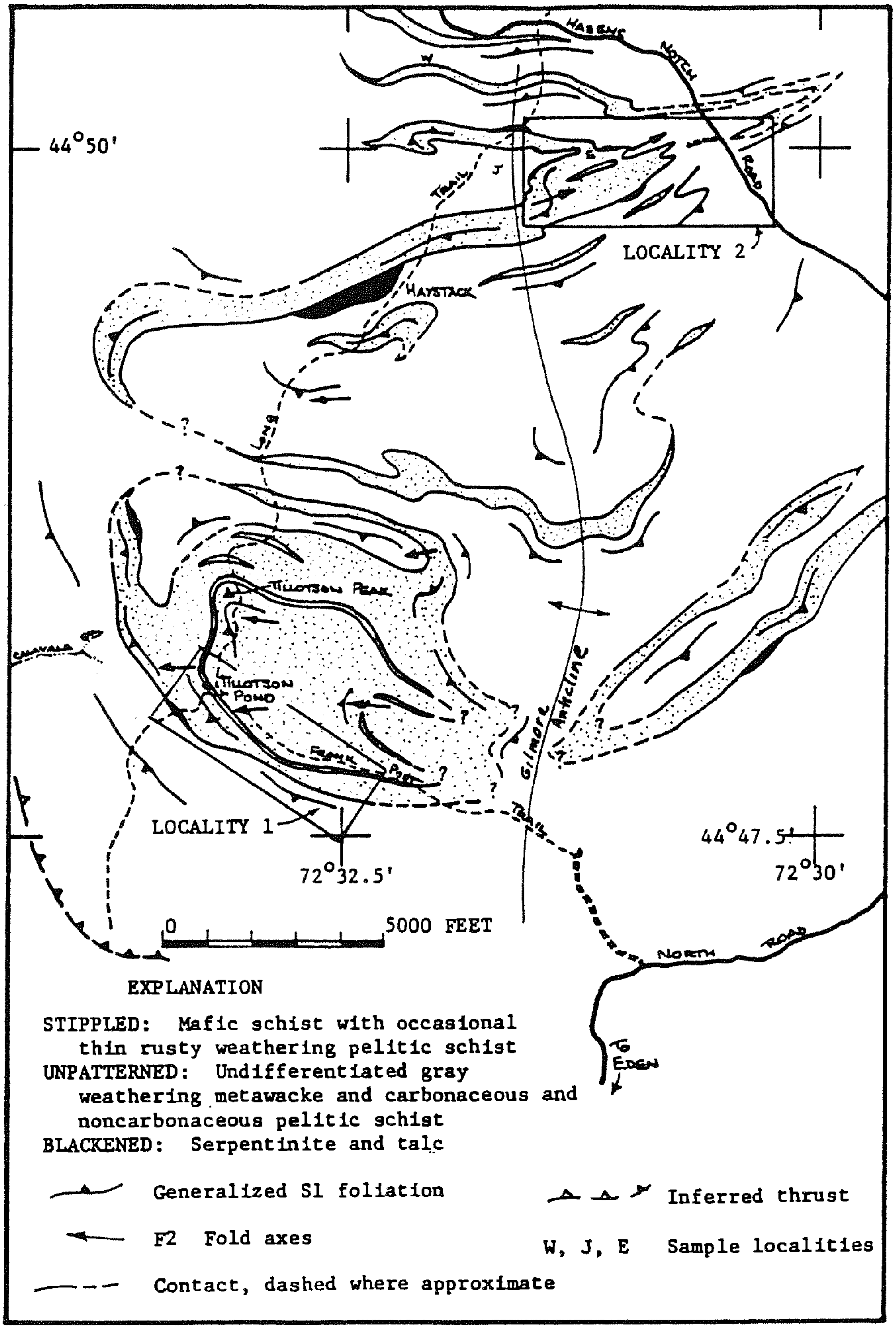

Figure 7. Geologic map of the Tillotson Peak area from Bothner and Laird (1987, Figure 1). Lockwood Brook is south of the Frank Post Trail. Sample localities are referred to in the text; sample VLB40 is from E. Belvidere Mountains is south of the inferred thrust in the southwest corner of the map.

Using these data, Laird and Albee (1981b, Figure 1) delineated an area in north central Vermont where medium-high- and high-pressure facies series metamorphism occurs (see high pressure envelope, Figure 2). The highest pressure is preserved in the Tillotson Peak area where Laird and Albee (1981a) discovered glaucophane + epidote and omphacite + garnet + plagioclase + quartz in mafic rocks. Detailed mapping of this area by Bothner and Laird (1987 and ongoing) has clarified the structural and petrologic relationships (Fig. 7).

Outside of this structural envelope and within pre-Silurian rocks amphibole from mafic rocks indicates medium-P facies series metamorphism (Fig. 6). In the area of this field trip, medium-P facies series metamorphism occurs at Elmore Mountain (Figure 2). Within the Connecticut Valley Trough, amphibole in mafic rocks intercalated with pelitic schist below (north of) the triple point isobar of Thompson and Norton (1968) show less PL than that from above (south of) the isobar and are used to delimit the low-P facies series envelope of Figure 6.

Amphiboles from pre-Silurian rocks in Vermont are commonly discontinuously zoned (see Plates 1 and 2 in Laird and Albee, 1981a,b, respectively). For example, magnesio-hornblende is overgrown by actinolite at Elmore Mountain, barroisite is overgrown by actinolite at Granville Notch and Tillotson Peak, and the Tibbit Hill Formation contains actinolite with optically distinct cores richer in PL than the rims. Laird and Albee interpret these amphiboles as polymetamorphic.

Laird and Albee (1981a) suggest that glaucophane and actinolite coexist at Tillotson Peak. Subsequent TEM/AEM data by Smelik and Veblen (1992) shows the occurrence of glaucophane cores with actinolite exsolution lamellae and of later glaucophane and actinolite, both without exsolution lamellae. Perhaps these glaucophane cores were at one time in equilibrium with barroisite which occurs only as cores of amphibole grains rimmed by actinolite and as inclusions in garnet. (While you should be able to collect samples with the overgrowth textures described by Laird and Albee, 1981a,b and the exsolution textures identified by Smelik and Veblen, 1992, the cummingtonite lamellae discovered by Smelik and Veblen, 1989, is now under water due to active beavers.)

In the Tillotson Peak area glaucophane and omphacite are commonly partially to completely replaced by fine-grained symplectite (Plate 1C, Laird and Albee, 1981a); locally garnet is altered to chlorite $\pm$ green-brown biotite. This alteration of garnet also occurs at Belvidere Mountain (Figure 2) and is pervasive east of the Gilmore antiform and near Hazens Notch Road (see Fig. 7 for locations of these geographic and structural features).

Thermobarometry. Given the disequilibrium described above, thermobarometry in the pre-Silurian rocks from northern Vermont is particularly hazardous, notwithstanding the problems of deciding which experimental data and thermodynamic model to use. With this in mind and an understanding of potential petrologic pitfalls, we present the following P-T estimates.

A sample unearthed by Bothner (Locality 2, Fig. 7) reveals omphacite included within and outside garnet with quartz and albite, providing an opportunity to estimate the pressure-temperature-relative time path taken by high pressure metamorphism at Tillotson Peak. Using the garnet-clinopyroxene geothermometer of Powell (1985) and isopleths on the reaction albite=jadeite+quartz (Holland, 1980) gives the P-T relationships shown in Figure 8. (Garnet and pyroxene are normalized to 8 and 4 cations, respectively, and Fe2+ and 3+ are estimated from charge balance.) Metamorphism recorded within the cores of garnets is lower temperature and pressure than that recorded by garnet rims in contact with omphacite outside the garnet. Pressures and temperatures estimated from omphacite inclusions and adjacent garnet compositions range from 9.4 Kbar, 360°C to 11.2 Kbar, 470°C while garnet rim - omphacite pairs are 12.2 Kbar, 520°C to 14.1 Kbar, 620°C.

Garnet - clinopyroxene pairs from other samples at Tillotson Peak give pressures and temperatures within this total range but do not get as high as those at Eclogite Brook (Fig. 8). The temperature for

Lockwood Brook from garnet-clinopyroxene geothermometry is similar to that obtained from the garnet-hornblende geothermometer of Graham and Powell (1984) - 479 to 443 °C depending on what garnet one thinks is in equilibrium with what calcic or sodic-calcic amphibole. This geothermometer gives about 415°C at the top of Tillotson Peak.

Other calibrations were explored with the aid of the THERMOBAROMETRY computer program of Kohn and Spear (1990). The garnet-clinopyroxene geothermometer of Pattison and Newton (1989) gives temperatures about 150°C lower for garnet rim - omphacite pairs and unreasonably low temperatures (100°C or less) for omphacite inclusions in garnet. Pressures using the garnet-plagioclase-clinopyroxene-quartz geobarometer of Powell and Holland (1988) with the Hodges and Spear (1982) garnet activity model are reasonable for the omphacite inclusions (e.g. 12 Kbar at 400 °C) but unlikely for garnet rim-omphacite pairs (22 Kbar at 600 °C) as kyanite + omphacite has not been identified at Tillotson Peak.

The mafic assemblages at Tillotson Peak indicate metamorphism at pressures below the reaction albite + chlorite = glaucophane + paragonite (Fig. 9). However, higher pressure metamorphism is suggested locally in pelitic rocks. Chloritoid + glaucophane occurs along the Long Trail north of Tillotson Pond (Fig. 7), and the assemblage phengite + quartz + garnet (with chloritoid inclusions) + paragonite + glaucophane (altered to fine-grained symplectite) + chlorite + epidote has also been identified west of Eclogite Brook (Fig. 7). These data imply metamorphism above the reaction paragonite + chlorite = chloritoid + glaucophane (Fig. 9). Metamorphism at Tillotson Peak, therefore, may have reached that seen in the Sesia Zone, Italy, and the island of Sifnos, Greece and subsequently been more similar to that seen in the omphacite-zone metasedimentary rocks from New Caledonia described by Ghent et al. (1987 and references therein).

The pelitic rocks also bracket metamorphic temperature at Tillotson Peak. The reaction chloritoid + albite = paragonite + garnet + H_2O gives a minimum temperature of about 440°C at 10 Kbar (Ghent et al., 1987). Kyanite is not observed, indicating that the maximum temperature of metamorphism is less than that for the reaction chloritoid + quartz = kyanite + garnet + H_2O (567°C at 10 Kbar). The range of temperatures estimated from the garnet-omphacite geothermometer is somewhat larger (Fig. 8).

Garnet amphibolite crops out at the top of Belvidere Mountain across a fault and to the south of the Tillotson Peak area. The absence of glaucophane indicates lower pressures than are identified in the Tillotson Peak area. Belvidere Mountain is put in the high-pressure envelope based on amphibole composition (Fig. 6) and on the fact that a large ultramafic body is exposed here (see Chidester et al., 1978, for detailed maps and petrologic data). Nd and Sr isotopic data show that this amphibolite has a depleted mantle signature and is interpreted as a fragment of oceanic crust (Shaw and Wasserburg, 1984). Garnet-hornblende temperatures (Graham and Powell, 1984, calibration) are 550 to 650°C, somewhat higher than is seen at Tillotson Peak.

Figures 10 and 11 illustrate in reaction space the variation in temperature and pressure implied by pre-Silurian mafic rocks. Samples from the Stowe Formation at Elmore Mountain and from the Missisquoi Fm. to the west indicate peak metamorphism at pressures between 7 and 5 Kbar, while samples farther west show peak metamorphism at pressures above 7 Kbar (but well below the high pressure metamorphism at Tillotson Peak) and are thus shown in the medium-high-P envelope delimited in Figure 6. Pressures estimated for the retrograde metamorphism are 3 to 6 Kbar as estimated from the actinolite - chlorite geobarometer of Cho (pers. comm. and listed in Laird, 1988, p.442).

At Elmore Mountain outward zoning in amphibole cores is up grade, to above 550°C (Fig. 11), consistent with the highest grade pelitic assemblage of biotite + garnet + kyanite. Maximum temperatures from samples within the Hazens Notch and Pinney Hollow Formations are estimated to be between 500 and 550°C (Fig. 10). Amphibole rims on all of these samples are actinolite, and temperatures are low, perhaps 400°C based on the whole rock experiments of Liou et al. (1974) and Apted and Liou (1983).

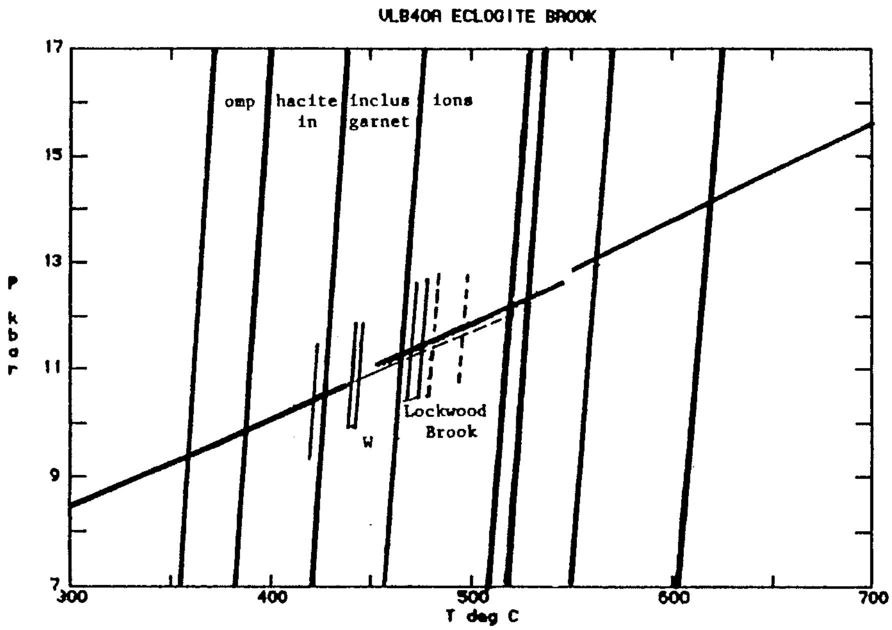

Figure 8. Garnet - clinopyroxene geothermometer of Powell (1985) and isopleths on the albite = jadeite + quartz geobarometer of Holland (1980) calculated using the computer program of Kohn and Spear (1990). The sample from Eclogite Brook (E, Fig. 7) contains omphacite inclusions in garnet and omphacite in the matrix in contact with garnet. Also shown are the P-T intersections estimated from samples at Lockwood Brook (dashed lines) and at W on Fig. 7 (straight lines).

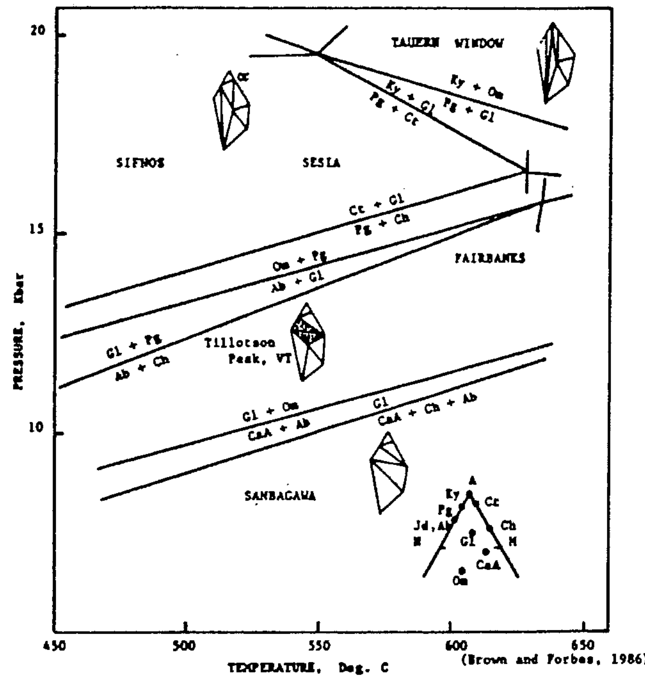

Figure 9. P-T grid for high-P facies series metamorphism from Brown and Forbes (1986, Figure 14). Mineral assemblages at Tillotson Peak are stippled. Chloritoid + glaucophane may also have coexisted; see text. Brown and Forbes (1986) used the parageneses from several classic high-P terranes (as shown on the figure) to construct the grid. The composition diagram is an epidote + garnet + quartz + H2O projection onto Al + Fe3 (A), Na (N), and Mg (M). Ab (albite), Ct (chloritoid), Ch (chlorite), CaA (calcic amphibole), Gl (glaucophane), Jd (jadeite), Ky (kyanite), Om (omphacite).

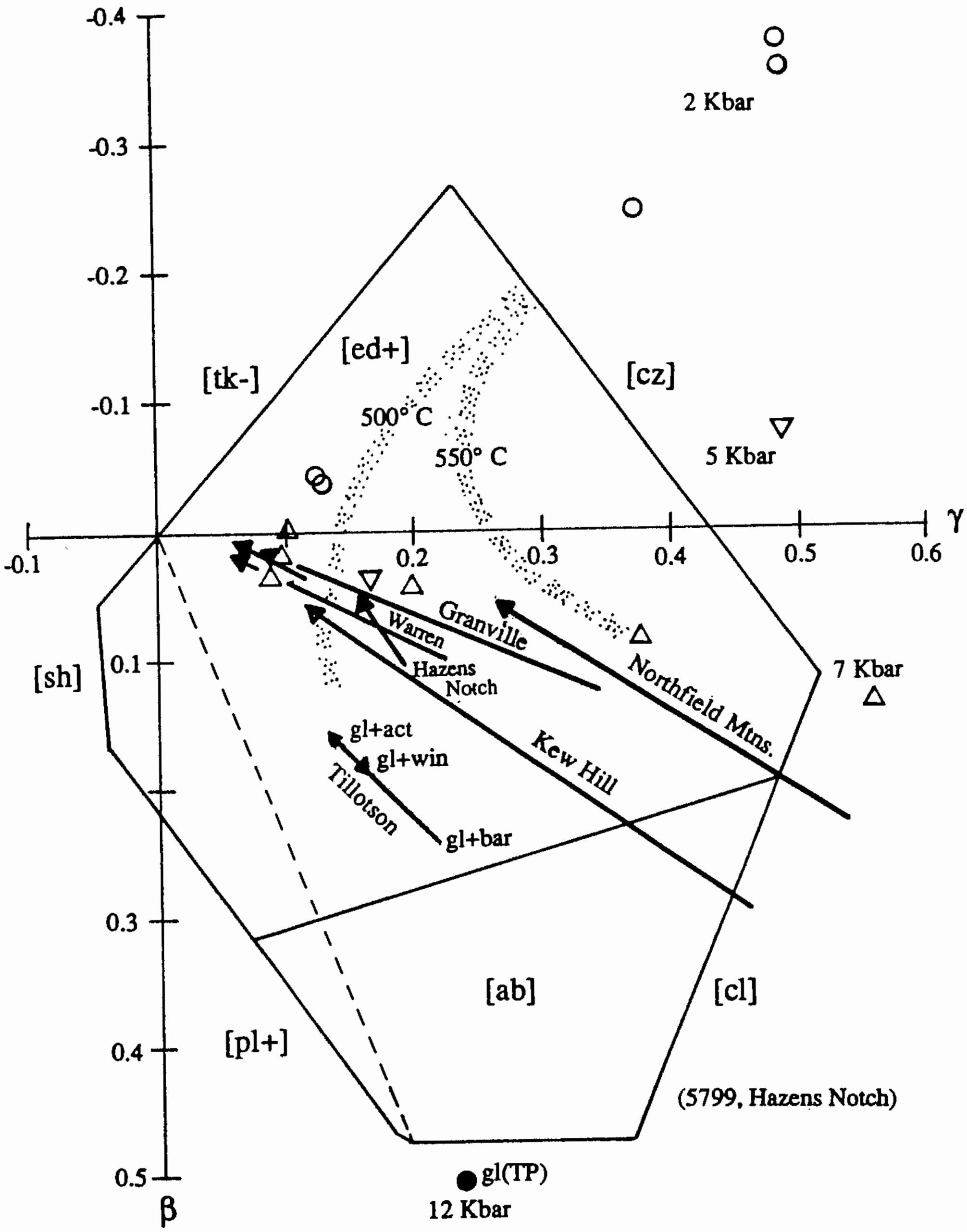

Figure 10. Reaction space for samples within the Hazens Notch and Pinney Hollow Fms. calculated by the method of Thompson et al. and fit to a Hazens Notch Fm. mafic sample from Kew Hill (bulk composition from Ray Coish, written communication, 1987). All samples are from within the high pressure envelope on Figure 2. Arrows connect the calculated positions using amphibole core and rim compositions. Circles represent data from the whole rock experiments of Liou et al. (1974) at 2 Kbar. Upside down and right-side-up triangles represent data from the whole rock experiments of Apted and Liou (1983) at 5 and 7 Kbar, respectively (NNO buffer). Temperature increases away from the origin, and dotted isotherms are estimated from these whole rock data and from geothermometry on mafic rocks from Vermont. Reaction gamma represents increasing advancement on TK, while reaction beta represents increasing advancement on PL and TK.

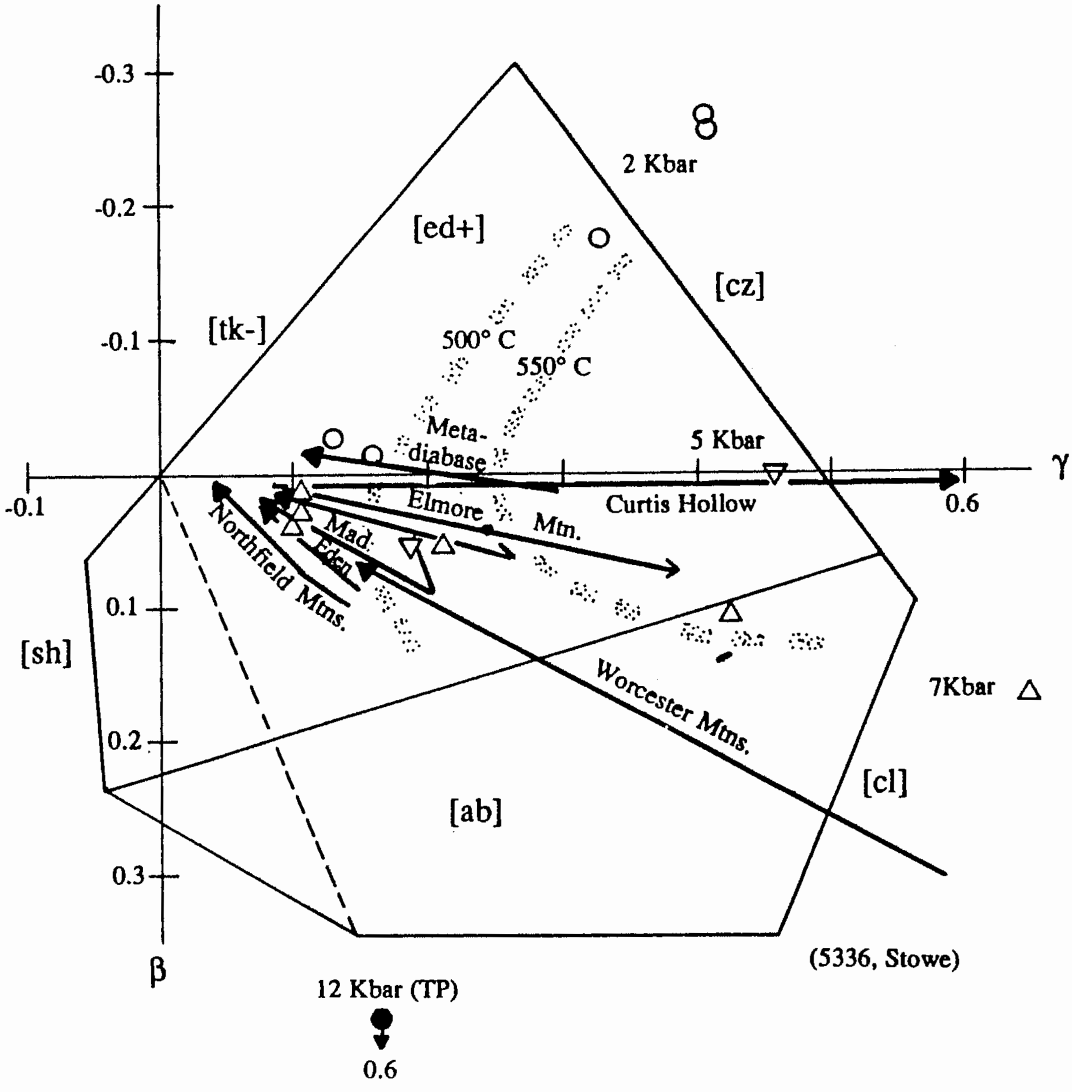

Figure 11. Reaction space for samples from the Stowe and Missisquoi Fms. calculated by the method of Thompson et al. and fit to greenschist from the Mad River (Coish et al., 1985). Samples from Elmore Mountain and the Missisquoi Fm (labelled metadiabase and Curtis Hollow) indicate medium-pressure facies series metamorphism, while the other samples are within the high-pressure envelope on Figure 2. Arrows, symbols, and estimated isotherms as for Figure 10. At Elmore Mountain metamorphism of amphibole cores increases up temperature and, the cores are overgrown by rims giving a reaction space position near the origin.

Geochronology

A summary of the isotopic ages in pre-Silurian metamorphic rocks from the U.S. Appalachians is presented by Drake et al., 1989). Much of the data pertinent to the outcrops we will visit in northern Vermont are presented by Laird et al. (1984) or were just obtained by Laird and Mick Kunk and are thus given here. All the data cited below are $^{40}Ar/^{39}Ar$ ages.

Total fusion ages on amphibole indicate that Taconian metamorphism in the northern Appalachians is 465 $\pm$ 10 Ma. In northern Vermont Taconian, total fusion and plateau amphibole ages (from many of the outcrops we shall visit) are 460 to 471 Ma. Muscovite and biotite total fusion ages between 355 and 386 $\pm$ 5 Ma are also reported in pre-Silurian rocks from northern Vermont and assigned to the Devonian, Acadian orogeny (Laird et al., 1984).

Lanphere and Albee (1974) proposed that the kyanite grade metamorphism in the Worcester Mountains is Taconian while the retrograde metamorphism is Acadian. They reported a 445 $\pm$ 9 Ma plateau age on coarse-grained muscovite and a 363 $\pm$ 4 Ma plateau age on muscovite pseudomorphous after kyanite. Subsequent laser dating of the coarse-grained muscovite reported by Hames (1992) gives 451 to 457 Ma for the core and 400 to 430 Ma along the rim. Laird et al. (1984) come to the same conclusion as Lanphere and Albee (1974) for zoned amphibole at Elmore Mountain. While total fusion amphibole ages are 415 to 449 Ma, the age spectrum is discordant with a plateau age of 470 $\pm$ 12.6 Ma and isochron age of 460 $\pm$ 6.1 for high temperature steps and 376 to 400 Ma apparent ages for low temperature steps.

Laird and Albee (1984) suggested that other samples with discontinuously zoned amphibole (higher temperature core than rim, e.g., Fig. 10 and 11) recorded Taconian metamorphism overprinted by lower grade Acadian metamorphism. They were not successful at demonstrating this by separating cores from rims for total fusion analysis, although it might be argued that at Granville Notch the 471Ma total fusion ages represent Taconian metamorphism while the 448 Ma total fusion age is a composite of Taconian and Acadian metamorphism.

Laird et al (1984) obtained a total fusion age of 439 $\pm$ 10 Ma for zoned amphibole with more PL in the core than rim from the Tibbit Hill (Figure 1). Recent age spectra from another separate of the same split give a preferred age of 463 Ma and a 467 $\pm$ 2 Ma age on an inverse correlation diagram (Fig. 12). Trace biotite in the mineral separate probably explains lower apparent ages in the low temperature steps that may well have grown during the Acadian.

Laird et al. (1984) reported a 490 $\pm$ 8 Ma total fusion age on barroisite from Belvidere Mountain. As this is older than conventional wisdom has it for Taconian metamorphism, this age has been called into question (rumor has it). Recent age spectra on a barroisite separate from the same locality gives a plateau age of 505 $\pm$ 2 Ma (Fig. 13). Belvidere Mountain is in fault contact with the high-pressure rocks at Tillotson Peak (Fig. 7). If the 468 $\pm$ 6 Ma total fusion age on glaucophane from Tillotson Peak "holds up", there must be two ages of fairly high pressure metamorphism preserved in this area so that (to jump ahead to **ARM WAVING**) the ultramafic and associated rocks at Belvidere Mountain could have been present to act as a buttress for facilitating the ascent of the high pressure rocks at Tillotson Peak. Shaw and Wasserburg (1984) presented Sr and Nd isotopic compositions from the sample studied by Laird et al. (1984) that indicate that the mafic and ultramafic rocks at Belvidere Mountain constitute a fragment of oceanic crust.

ARM WAVING

Why is the highest pressure metamorphism of the high pressure envelope at Tillotson Peak and why is there a westward broadening of this envelope? The answer, my friends, is in the rocks.

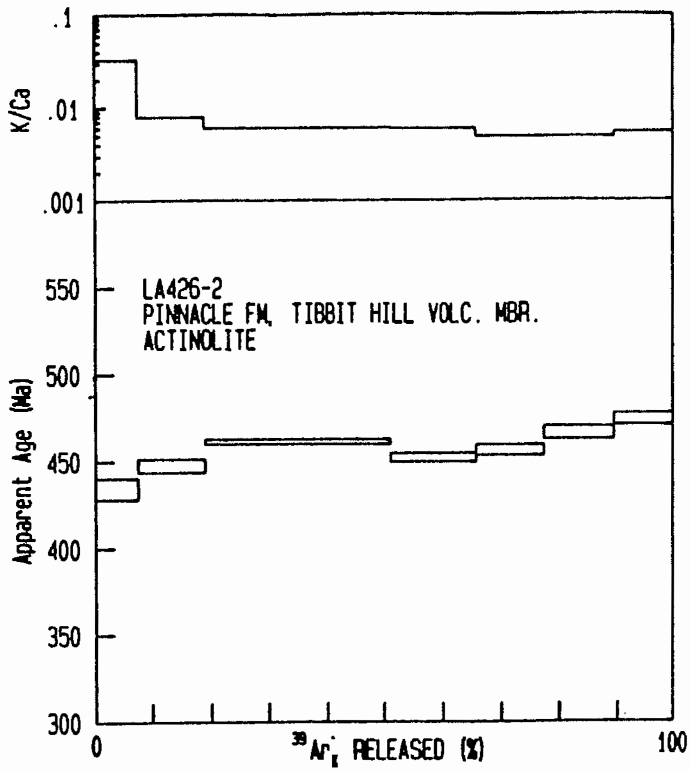

Figure 12. Age spectrum and apparent K/Ca diagrams for a sample from the Tibbit Hill Volcanics, Vermont. While the data do not plateau, the majority of potassium-derived 39Ar released for this and another split run over larger temperature steps "to give more gas" gives a preferred age of 463 Ma. Low apparent ages are probably due to inseparable, intergrown biotite based on the K/Ca and on petrographic observations.

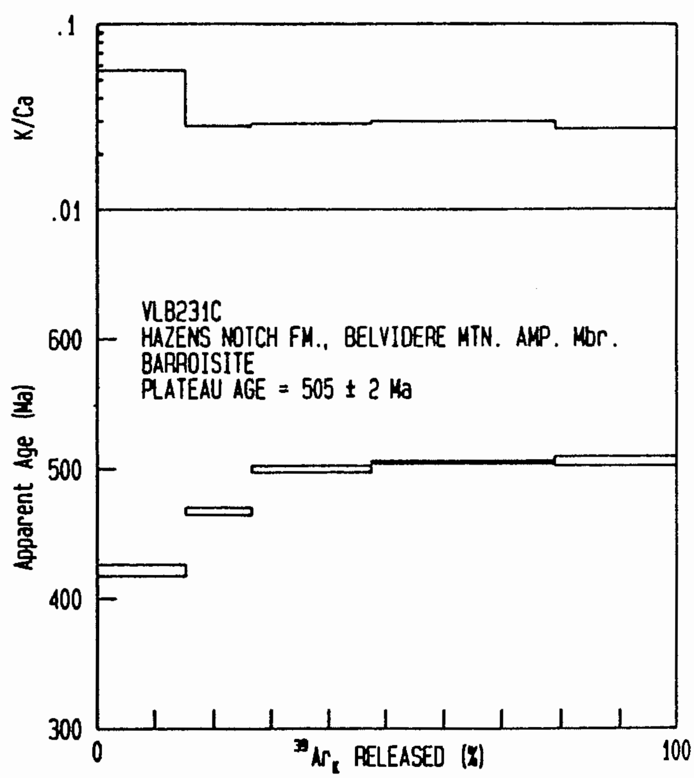

Figure 13. Age spectrum and apparent K/Ca diagrams for mafic schist from Belvidere Mountain, Vermont. The high temperature steps plateau; low apparent ages are probably due to inseparable, intergrown biotite based on the K/Ca and on petropraphic observations.

The high pressure metamorphic envelope coincides with a gravity high along the Green/Sutton Mountains as delineated by Diment(1968) and Innes and Argun-Weston (1967). The high pressure envelope broadens westward along the failed Ottawa graben, and Tillotson Peak is at the "intersection" of the Ottawa graben and the Green Mountain anticlinorium (see Figure 2). Tillotson Peak coincides with an inferred deep-seated structure based on filtered regional gravity data (Bothner and Kucks, in press). This suggests a model by which thè mantle rose nearer to the surface at the intersection of a triple junction (rather than within or along any of the arms of the rift system). This would provide the means by which lower crustal, high pressure/temperature rocks could be transported relatively rapidly toward the surface as suggested by Bothner and Laird, (1991). Ultramafic rocks along the thrust contacts would act as "grease" to facilitate transport.

ACKNOWLEDGEMENTS

Support of this research from the National Science Foundation is gratefully acknowledged (Grants No. DES 69-0064 and EAR 75-03416 to Arden Albee and EAR 83-19383 to Laird and Bothner). John Sutter afforded J.L. the opportunity to obtain isotopic data at the U.S. Geological Survey, Reston; and Mick Kunk's expertise at separating minerals and obtaining quality isotopic data is to be credited for the age spectra presented herein. The field mapping and structural/tectonic interpretations of Tillotson Peak are primarily those of Bothner; J.L. argues that without his diligent pace and compass traverses, we would surely be lost.

W.E.T., Jr. gratefully acknowledges financial support from the Natural Sciences and Engineering Research Council and Energy, Mines, and Resources, Canada. For their patient tutoring in structural and regional complexities he is indebted to Jacques Béland, Pierre St-Julien, and Robert Marquis.

ROAD LOG

DAY 1. RICHMOND AREA AND LAC ORFORD, QUÉBEC

Most of the stops will be along Autoroute 55 east and west of Richmond, Québec (Fig. 14), a town that is accessed off Autoroute 55 by Rte 116. The best access to Richmond from the south is US Interstate 91 to Derby Line, Vt. There, one crosses the international border and continues north on 55 to Richmond, bypassing Sherbrooke. Several of the stops are those described in Marquis et al. (1987) from which some of the following descriptions have been pilfered.

Depending upon time, weather , and mood, we will select the following stops as they are approached. All need not and probably will not be made.

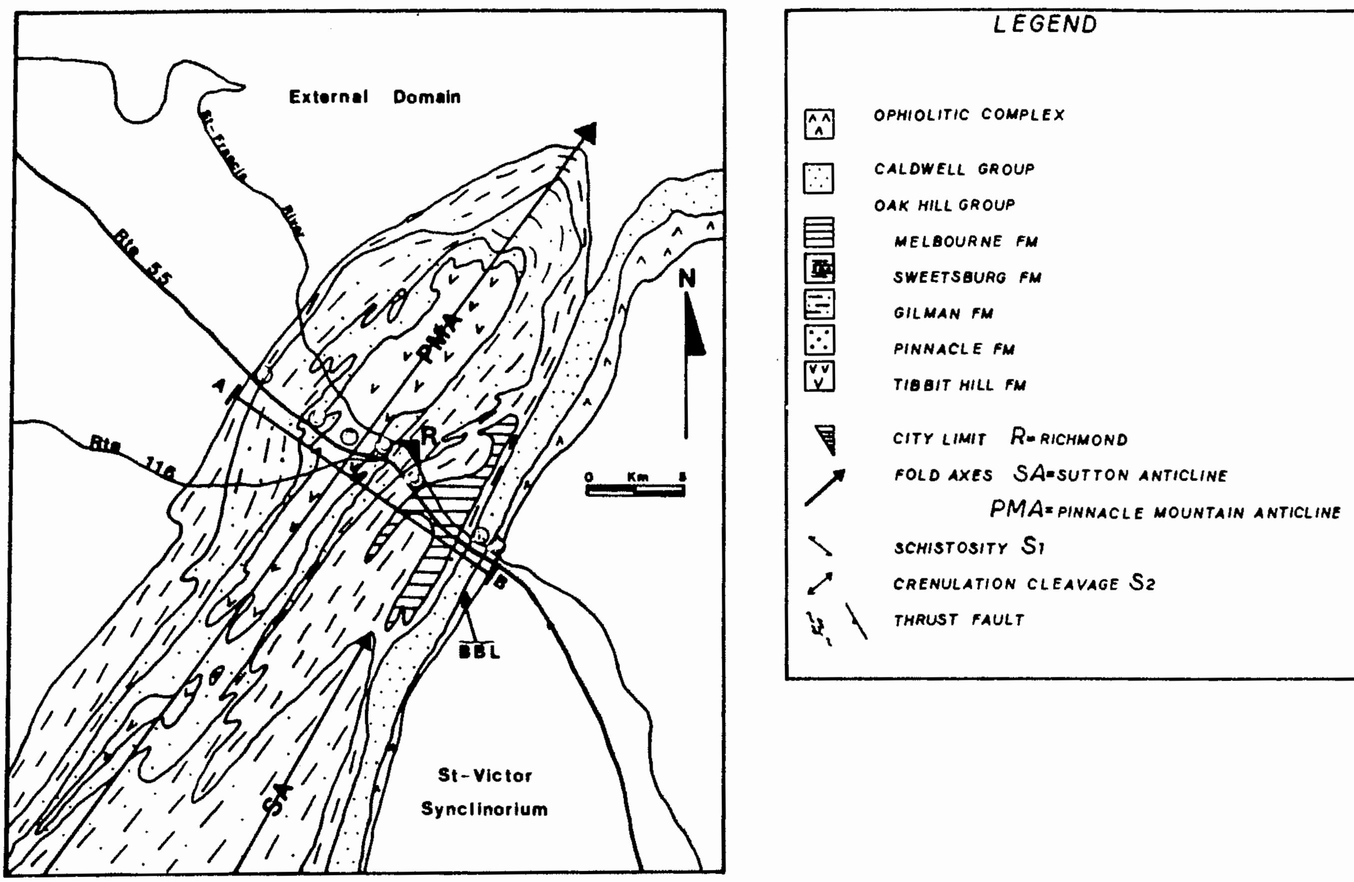

Figure 14. Geologic map of the Richmond area, Québec (Taken from Marquis et al., 1987)

STOP 1. CALDWELL GROUP (4.3 MILES EAST OF THE RTE 116-55 INTERCHANGE). This stop in the Caldwell demonstrates the character of interpreted continental margin rocks. They are an interbedded, but not everywhere present, sequence of sandstones, shales, and volcanic rocks. At this locality the predominant lithology is a green, quartz-rich sandstone, uncommonly graded with tops toward the east (from where we just came). The volcanics are albite + chlorite + quartz-bearing greenstones. In places green spots are observed and are found to be, in thin section, rosettes of green stilpnomelane. Minor carbonate-rich beds weather to a buff color. Red and green slates, although not common here, form a major component of the Caldwell elsewhere. A northeasterly directed regional cleavage is cut by a late slip cleavage. The Caldwell is taken to represent sedimentary conditions ranging from relative quiescence to high turbulence on a continental margin. It is correlated to the Stowe Formation of northern Vermont.

RETURN TO VEHICLE(S)

STOP 2. SWEETSBURG FORMATION (1.2 MILES EAST OF THE RTE 116-55 INTERCHANGE). This formation represents the top of Clark's (1936) classic Oak Hill sequence. This rather nice outcrop affords a pleasant backdrop for lunch, where one sees black phyllite interbedded with thin, buff-colored, dolomitic sandstone beds in an overturned fold. The axial plane of the fold strikes northeasterly and dips 60° northwest which is contrary to the vergence direction expected for the northwest transport of the "Québec Allocthon" (St-Julien and Hubert, 1975). On a mesoscopic scale, one observes the refraction of the penetrative schistosity where it crosscuts centimeter-wide sandstone beds. This early schistosity also exhibits small corrugations. These minute crinkles are produced by the intersection of the schistosity with a late crenulation cleavage that strikes northeasterly and dips 80° to the southwest.

RETURN TO VEHICLE(S)

DIRECTIONS: Continue west on Autoroute 55 and exit onto Rte 116. Turn right at 116 and head north across the St-Francois River into Richmond. Turn right at the lights in Richmond and then, almost immediately, left (closed Texaco gas station on southeast corner of intersection) onto Chemin Valley (Road). Continue east on Valley Road, past the Brown Shoe Company, approximately 2.3 miles to Chemin Pease (Road). Turn right onto Pease Road and cross over "railroad" bed, and follow Pease Road to Ruisseau Steele (Stream). The outcrops seen along the road are of the Caldwell. Immediately after crossing Steele Stream turn right into the Coddington farmyard. The outcrops of interest are directly south, of the farm buildings, in the woods.

STOP 3. ULTRAMAFIC ROCKS AND ASSOCIATED DIORITES/GRANITES. This is one of the more accessible localities to see granites and/or diorites that are intimately associated with the serpentinites. Throughout much of the Québec ultramafic belt one sees these "felsic" rocks in an uncertain relationship with the serpentinites. In outcrop the contact between various "felsic" facies is sharp in places and gradational in others. Blue, riebekitic amphiboles are the primary Fe-Mg phase in these rocks along with feldspar and quartz. Fibers of actinolitic amphibole are commonly seen sprouting out from the bluish amphibole as well as in the matrix. Brown stilpnomelane is also commonly seen as a metamorphic mineral. Several whole rock geochemical analyses from this locality indicate that these "felsic" rocks are volcanic arc granites that are characteristically found along continental margins. Zircons have been identified in thin section and as this field guide is being written their separation is underway. The ultramafic rocks are totally serpentinized and highly deformed by a late-stage deformation. Slickensided surfaces with fiber growth on the surfaces is a common phenomenon. In many places several directions of fiber orientation are superimposed one on the other. A structural analysis of fiber and slickenside orientations pretty well covers a stereonet, a most frustrating result.

RETURN TO VEHICLE(S)

DIRECTIONS: Return to Rte 116 in Richmond and then back across the St-Francois River to rejoin Autoroute 55 westward toward Drummondville. About 3.8 miles west of the Rte 116-55 interchange and beyond an overpass, stop at outcrop on right side of road.

STOP 4. TIBBIT HILL AND CALL MILL FORMATIONS. The western part of the outcrop is atypical Tibbit Hill metavolcanic. An outstanding feature here is a zone within the Tibbit Hill that is composed of rounded structures. The mineralogy of these structures is primarily quartz + feldspar that pass gradually into an encircling rind of chlorite, amphibole, albite, quartz and epidote that is characteristic of the metavolcanic in general. These structures are of various sizes and show variable degrees of deformation. To be debated on the outcrop is whether or not these may have been either pillows or bombs (lapilli) in their initial state.

Walking eastward along the outcrop the Tibbit Hill passes into a dark, fine-grained phyllite (pelite) of the Call Mill Formation. Near the east end of the outcrop, small, dark, round spots become evident in the rock. These are splays of chloritoid in a muscovite-chlorite-quartz-ilmenite-rutile matrix. This is one of the chloritoid assemblages discussed above in the petrology section.

RETURN TO VEHICLE(S)

DIRECTIONS: Continue west along the highway to a rest area on the south side of the road. The outcrops on the road here are in the Dunham Formation. Turn around in the rest area and head back toward the east to the exit for Rte 166. Turn right onto Rte 116 and head southwestward about 0.75 miles. Turn left onto Converse Road and continue southward about 3 miles to a sharp right-bearing curve in the road near the top of the knoll.

STOP 5. TIBBIT HILL VOLCANICS. For some 300 feet on both sides of the road here, in the ditch line, there are exposures of the Tibbit Hill volcanics. It is from this locality that Trzcienski (1976) first described Na-Ca amphiboles. The rocks contain the common assemblage amphibole+chlorite+albite+epidote+quartz±magnetite±stilpnomelane±calcite. Some of the larger amphibole grains may have a core of kaersutite that, in thin section, is easily discernible by its brown pleochroism. Samples RI3A and RI17B in Fig. 5 are from this locality. They indicate P-T conditions that vary between 4 to 7 kbars and 300 to 375°C. This area is also part of the regional gravity high culmination (Innes and Argun-Weston, 1967).

RETURN TO THE VEHICLE(S)

DIRECTIONS: Continue west along the road to rejoin Rte 116. Turn right onto Rte 116 to return eastward and rejoin Autoroute 55. Upon rejoining Autoroute 55 head east and south back towards Sherbrooke then west to join the Eastern Townships Autoroute (#10 - Autoroute des Cantons de l'Est). Continue west on the Townships Autoroute beyond where Autoroute 55 leaves it to head south towards Vermont. Leave Autoroute 10 at Exit 115 and get onto Rte 112 heading west toward Eastman (BE ATTENTIVE HERE, THE INTERSECTION IS CONVOLUTED). Head west on Rte 112 about 3 miles to where Lac Orford and a picnic area are on the right side of the road. Pull off into the picnic area.

STOP 6. MOUNT ORFORD ULTRAMAFIC COMPLEX. Just to the northeast of the lake is Mount Orford. Across the road from the picnic area is serpentinite (**WHOOPEE!**). Within this serpentinite occur several lenses of calc-silicate rock - elsewhere interpreted as "anorthosite". Along fractures in the easternmost lense one can see good crystals of grossular. The rock itself is composed of grossular, epidote, albite and commonly prehnite. Some idocrase may be present locally. Elsewhere, in similar bulk chemistries, amphibole, diopside and pumpellyite, not all together, may also be found. North of Richmond, chromite is also an accessory mineral in these calc-silicate assemblages. A better and larger exposure of this calc-silicate and its relationship to the surrounding serpentinite can be seen at 60 MPH up on the autoroute. Potential road kill prevents us from stopping there.

As is typical of the serpentinites nearly everywhere from Thetford Mines south, deformation is intense.

Here one sees the nice development of large "fish-scale" structures and well polished slickenside surfaces. In fact, on the west end of the outcrop, mirror-like surfaces have developed on which one can see oneself in the now-present moonlight.

RETURN TO VEHICLE(S)

DIRECTIONS: Continue west on Rte 112 to the center of Eastman, turn left onto Rte 245 to go south to Rte 243, the international border, North Troy, and eventually Morrisville, Vermont.

DAY 2. Starting point is from the Sunset Motel, intersection of Rtes. 100/15, Morrisville, Vermont.

Mileage
0.0 Sunset Motel, turn west (left) on Rtes. 100/15.
1.8 Outcrops of carbonaceous and sulfitic schists of the Ottauquechee Formation. Turn north on Rte. 100.
7.0 Junction Rtes 100 and 100C. Continue north on Rte. 100 through North Hyde Park.
11.4 Intersection of Rtes. 100 and 118. Continue north on Rte. 100 to Eden Mills.
12.7 Intersection of Rte. 100 and North Road, Eden Mills. Turn left (N) onto North Road.
16.4 Entrance to the Belvidere Mountain asbestos mine (Vermont Asbestos Group). Chidester et al. (1978) present detailed maps and discussion of the ultramafic body. Gale (1986) gives alternative arguments for the emplacement of this body and associated mafic and pelitic rocks. Mafic schist exposed beneath the fire tower at the top of the mountain is locality VLB231/VJL360 discussed herein.
17.9 Turn left (west) onto gravel road that leads to the base of the Frank Post Trail.
18.4 Continue beyond the house on the dirt road heading north and park. **DO NOT PARK IN THE DRIVEWAY OR ON THE LAWN OF THE HOUSE!**

STOP 1. TILLOTSON PEAK TRAVERSE. HIGH PRESSURE MAFIC, PELITIC, AND FELSIC ROCKS OF THE HAZENS NOTCH FORMATION. ULTRAMAFIC SLIVERS ALONG FAULT ZONES. (Hazens Notch 7.5' quadrangle). We will concentrate on the high-pressure facies series mineral assemblages, on the structural relationships among the rock types, and on the tectonic setting. Cady et al. (1963) were the first to map these rocks and emphasize their "unusual" structural orientation. Specifically, east-west folds are preserved, but the dominant folds in Vermont are generally north-south.

This is an all day hike. Bring your lunch, rain gear, and determination to fight downed trees and peel moss. (If you come in the Summer, be sure to bring bug dope!) Bring the geologic map (Fig. 7). We spend the morning and part of the afternoon at LOCALITY 1 following the guidebook from Bothner and Laird (1987) and liberally plagiarized (with permission) below. Later we will follow the Long Trail to Tillotson Peak so that you can collect more aluminous assemblages in the mafic rocks. If time permits and you are ready for another hike, we may be able to visit LOCALITY 2 after returning to the vehicle(s) and driving up Hazens Notch Road.

The Frank Post Trail starts at the large boulders beyond the driveway to the house and is marked by a blue blaze. Initially the trail is over muddy glacial till, and it takes about an hour to hike up to the first outcrops. At about 2100' elevation proceed into the woods about 100 yards S20W to Lockwood Brook where outcrop is continuous for about 300 feet.

This outcrop is composed primarily of well layered (less than 1 cm to about 10 cm), massive to foliated amphibolite composed of amphibole + calcite + chlorite + epidote + garnet + albite + titanite + phengite + magnetite + apatite ± omphacite ± pyrite ± chalcopyrite (see Laird and Albee, 1981, ABM100, for mineral analyses). Glaucophane is common but pseudomorphed by a fine-grained symplectite of chlorite + plagioclase + white mica + calcic amphibole. Omphacite occurs locally (e.g., 25' from the base of the exposure and at the top of the falls); it is pseudomorphed by a fine-grained symplectite.

Also present are minor pelitic layers composed of garnet + quartz + phengite + chlorite + calcite + albite + titanite + magnetite ± calcite ± glaucophane with accessory apatite, epidote, chalcopyrite, and pyrite. Locally garnet grains show a Becke line between Mn-rich cores and Mn-poor rims; ilmenite and rutile are confined to the cores. Near the bottom of this outcrop and above a 35 cm thick layer containing garnet porphyroblasts up to a cm across is a 40 cm thick layer of pelite with black, pod-like masses (clasts?) that are flattened in the plane of foliation and may represent iron-rich concretions. Epidote here and along strike is locally Mn3+ rich.

Multiple periods of mineral growth and of deformation are wonderfully shown in this outcrop. Barroisite cores are overgrown by rims zoned outward from actinolite to actinolitic hornblende. Early F1 isoclinal folds occur normal to layering, and warps in the main foliation are related to mesoscopic F2 reclined folds. At the top of this exposure, layering in the mafic rocks is locally discordant and may be interpreted as a premetamorphic fault or an originally cross-cutting relationship.

Continue upstream about 200' from the top of the falls to 2230' elevation. Here, and about 100' SW of the stream, is layered, schistose feldspathic metawacke composed of albite + quartz + chlorite + epidote + white mica + magnetite + biotite with pseudomorphs of probable glaucophane. The trace of the contact with the intercalated mafic and pelitic rocks (not exposed here) is marked farther upslope and on the Long Trail by an ultramafic sliver (Fig. 7) and will be seen after lunch.

Continue upstream to about 2400' in elevation and about 800' from the top of the falls to a series of outcrops of infolded amphibolite (glaucophane + carbonate + chlorite + epidote + garnet + quartz and actinolite + glaucophane + epidote + garnet + quartz + titanite ± chlorite, carbonate, and gold-colored sulfides) and pelitic schist (white mica + garnet + quartz + glaucophane + titanite ± chlorite, carbonate, tourmaline, and epidote).

The contact between mafic and pelitic rocks from here upstream is everywhere parallel and assumed conformable. The pelitic schist is traceable (within the constraints of outcrop exposure) around Tillotson Peak (Fig. 7). Both rock types are folded about F2 whose nearly reclined character is apparent here.

Return to Frank Post Trail via a side drainage (about 170' N20E). Sheared amphibolite from this drainage gives an unpublishable $^{40}Ar/^{39}Ar$ age spectrum (Laird and Mick Kunk). Each temperature step gives a drastically different apparent age - the problems with trying to date sheared amphiboles with low K contents.

Follow the trail to about 2480' and several outcrops of amphibolite composed of calcic amphibole + garnet + epidote + titanite + quartz + chlorite ± glaucophane. Calcic amphibole is coarser grained than that seen in the brook; it is generally zoned with magnesio-hornblende cores and actinolite rims. Chlorite and calcic amphibole analyses indicate that these rocks are marginally more Mg rich than garnet amphibolite from Lockwood Brook.

Mesoscopic F2 folds are exposed in the ledges 100-200' NE of the trail and support the presence of a macroscopic WNW-plunging, approximately reclined fold identified from structural data (Bothner and Laird, 1987, Figure 4). Farther up the trail F1 isoclinal folds refolded about broad open warps on the upper limb of an F2 fold are preserved. **PLEASE** DO NOT HAMMER ON THESE ROCKS!

Continue up the trail to Tillotson Camp, where we enjoy lunch and a fine view of the Missisquoi valley and Lowell Mountains. The mafic schist here preserves the same assemblages as we sampled along the Lockwood Brook. The rock is well foliated and contains well developed S2 crenulation cleavage. Early F1 isoclinal folds are exposed on the east-facing joint surface below the camp.

The Long Trail is behind the camp and marked with a white blaze. Toward Tillotson Pond minor pelitic schist is intercalated within the dominant mafic schist. About 1000' south of the pond and miserably buried under brush is sheared serpentinite marking the contact between garnet amphibolite (to the N) and feldspathic metawacke (to the S). The amphibolite contains glaucophane ± omphacite and garnet poikiloblasts up to 1 cm across with inclusions of glaucophane. The metawacke contains the assemblage quartz + plagioclase + white mica + chlorite + epidote + piemontite + biotite + magnetite + apatite. The north-facing surface of this outcrop can be followed about 50 feet along strike to the west where actinolite knots up to 25 cm across and crinkled, actinolite + chlorite rich layers occur. Bothner and Laird interpret this surface as a fault.

North of the camp and along the Long Trail the primary lithology is mafic; mineral assemblages are similar to those seen along Lockwood Brook. Under downed trees west of the trail at Tillotson Pond, you may be rewarded with the assemblage epidote + glaucophane + omphacite + quartz + dolomite + calcite + titanite + magnetite + apatite + chalcopyrite (VJL383, Laird and Albee, 1981a). Chloritoid + glaucophane + garnet pelite occurs; we can argue if it is in place.

Ascending the trail to a peak at about 3040', you come to the "type locality" of blueschist at Tillotson Peak. (If you come to pelitic schist on the trail and are going down hill, you are north of the peak and have gone too far.) West of the trail and under the brush awaits fine-grained mafic rock with the assemblages epidote + glaucophane + chlorite + albite + paragonite + phengite + titanite + quartz + apatite along with epidote + calcite + chlorite + calcic amphibole + glaucophane + quartz + titanite + magnetite + chalcopyrite + pyrite + pyrrhotite + millerite (samples VJL337, Laird and Albee, 1981a). Probable F2 folds fold foliation. Along the ridge to the northwest foliation changes from striking NW to NE (Figure Fig. 7), and quartz + white mica + chlorite + garnet (up to 50 mm across) + magnetite schist occurs infolded with garnet amphibolite.

Return to the Frank Post Trail. If you go cross country rather than take the Long Trail, be sure to pace and use a compass. Depending on time and enthusiasm we may stop at an outcrop off the Frank Post Trail of sheared amphibolite with dismembered layers (clasts?).

Return to vehicle(s). If time and weather permit we will go to Locality 2 (Fig. 7) where the eclogite discussed in Figure 8 was collected (see Bothner and Laird, 1987, for field guide). Otherwise, we will return to Morrisville with a possible stop at Belvidere Mountain.

DAY 3. Starting point is from the Sunset Motel, intersection of Rtes. 100/15, Morrisville, Vermont (see Fig. 14).

Mileage

0.0 Sunset Motel, turn east (left) on Rtes. 100/15 and then south (right) on Rte. 100.

1.0 At T intersection turn left, cross the bridge and at another T intersection turn right. You are still on Rte. 100S.

1.3 At the stoplight turn left onto Rte. 12. Bear right at the Y and follow Rte. 12 eastward out of Morrisville. Pass round barn, outcrops of Stowe Formation amphibolite and of pelitic schist with garnet retrograded to chlorite, and

5.8 Turn right into Elmore State Park. From the entrance drive west past side roads to the left and right and past small outcrops of amphibolite cut by calcite-filled fractures. This is not a good place to collect; it is better to stop on Rte. 12, 1.1 mile south of Elmore Village where amphibole (tschermakitic hornblende rimmed by actinolite, VFig. 114, Laird et al., 1984) up to an inch long occurs in epidote pods and layers.

Drive up hill to the nature center and park (about 1450' in elevation).

STOP 1. ELMORE MOUNTAIN TRAVERSE. POLYMETAMORPHIC PELITIC AND MAFIC SCHISTS OF THE STOWE FORMATION (Hyde Park 15' quadrangle; geologic map by Albee, 1957; see Fig. 14 herein). The purpose of this stop is to demonstrate that in pelitic schist garnet is pseudomorphed by chlorite and kyanite is pseudomorphed by fine-grained white mica and chloritoid. (In thin section you will also find that probable biotite is pseudomorphed by chlorite.) Along the way we will stop at intercalated mafic schist too small to map at the 15' scale. As discussed in the text, $^{40}Ar/^{39}Ar$ age dating from similar polymetamorphic pelitic rocks in the Worcester Mountains to the south and zoned amphibole in mafic rocks from Elmore Mountain (VJL44 and 50, see Laird and Albee, 1981b for mineral chemistry data and Laird et al., 1984 for isotopic data from these samples) indicate Taconian overprinted by Acadian metamorphism. You will also see ample evidence for glaciation.

We hike up the haulage road, which eventually becomes a trail as the grade steepens, starting in the garnet grade and ascending into the kyanite grade (highest grade of metamorphism). There are good outcrops along the road and trail, requiring minimal pulling of moss and scraping of lichen compared to the afternoon of Day 2. Initially, the pelitic schist (quartz + white mica + chlorite) is strongly sheared with quartz knots that are tightly folded. The road bends to follow strike (10 to 20 degrees east and west of north) and a drainage. From about 1550 to 1600' in elevation, garnet, some up to 4mm, is chloritized. Fine grained white mica may be paragonite and coarse-grained white mica muscovite.

At about 1660' in elevation you will find a picnic table, an overgrown cart road to the south, and a trail to the west. Proceed up the trail (yellow blaze) and up hill. At about 1840' a 3-5 mm thick magnetite + chloritoid(?) layer "carries" epidote S surfaces. The outcrop on the west cliff face is very magnetic mafic schist that is "layered" with respect to amphibole grain size and contains epidote lenses and chlorite pockets. Following the crop uphill and angling over to the trail reveals a very disturbed zone with epidote-rich and amphibole-rich blocks and may be a fault.

Pulling moss from outcrops east and west of the trail at about 1900' reveals quartz + white mica + garnet + chlorite schist with porphyroblasts of kyanite. While garnet is still pink, kyanite is altered to fine-grained white mica (the differential hardness test will fail). Press on up the trail past epidote amphibolite and pelitic schist with garnet altered to chlorite and with kyanite altered to white mica and chloritoid. Time and interest will dictate at which of the two following outcrops we will admire during lunch. Both have magnificent views of Lake Elmore and her valley to the east.

Possible lunch stop 1, 2440'. Kyanite + garnet (both altered) + chloritoid + chlorite pelitic/epidote amphibolite contact at old firetower cabin (now reduced to foundation and stone chimney). The contact "passes through" the NW of the foundation; we can argue if it is gradational. Look behind the chimney and outside the foundation for coarse-grained kyanite. A better place to collect kyanite and chloritoid, but of course up hill, is at:

Possible lunch stop 2. Scramble up and over the ledges another 100' in elevation to the intersection with the Firetower/Balancing Rock trail. Forego the firetower and turn north toward Balancing Rock, stopping at the first lookout and ledges dominated by coarse-grained quartz in lenticles and pods, kyanite blades $\pm$ chloritoid, and enclaves of pelitic schist with kyanite.

Were you to continuing north along the trail you would come to ledges from which you can see the Green Mountains and then to a glacial erratic (Balancing Rock). Today we shall retrace our steps to the vehicle(s).

Leaving Elmore State Park turn left (northwest) onto Rte 12 and return to :

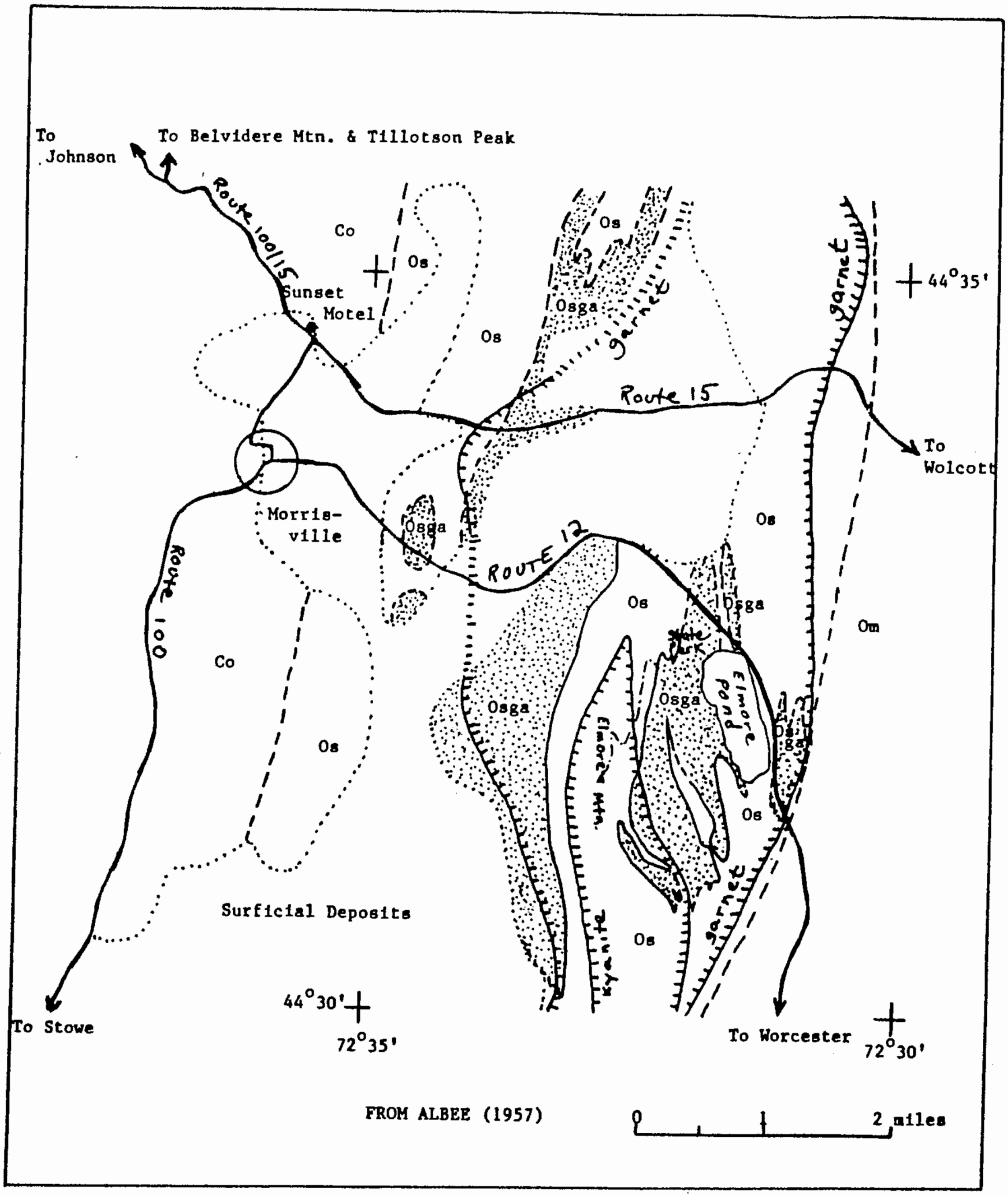

Figure 15. Geologic map of the Elmore Mountain area taken from Albee (1957). From oldest to youngest (following Doll et al., 1961), are black phyllite of the Ottauquechee Fm. (Co), pelitic and mafic schists of the Stowe Fm. (Os and Osga, respectively), and pinstripped granofels of the Moretown Member of the Missisquoi Fm. (Om). Isograds are shown for the highest grade seen in the pelitic rocks; hachers are on the high-grade side. See text for discussion of the alteration of the garnet, kyanite, and, in the mafic rocks, amphibole.

Mileage

0 Morrisville. At stoplight turn left (south) on Rte. 100S Figure Fig. 15) to

9 Stowe. Mount Mansfield and Smuggler's Notch are found up Rte. 108 to the NW. We continue south on Rte. 100 to 16 Waterbury Center. Stowe Formation greenschist. The Worcester Mountains are to the east and reach kyanite grade. If time permits we can drive to a quarry within the Stowe amphibolite with magnesio-hornblende (VJL5, Laird and Albee, 1981b) dated by Lanphere and Albee (1974, LA385) at 463 Ma ($^{40}Ar/^{39}Ar$ total fusion). This outcrop is within the high-pressure envelope. It seems that the mafic rocks from the Stowe Formation show medium-P metamorphism at Elmore Mountain but medium-high-P metamorphism in the western Worcester Mountains (Fig. 11). The highest grade metamorphism in both areas is Taconian.

From Waterbury Center it is 3 miles on Rte. 100S to 19 Waterbury, I-89, Ben and Jerry's, and tightly folded, black phyllite of the Ottauquechee Fm. Continue south on Rte.100 passing up a marvelous outcrop of folded Ottauquechee Formation exposed in a miniature golf "establishment" and follow the Mad River to 37 Warren. Were we to turn west up the Lincoln Gap road we would come to the Hazens Notch Formation with garnet isolated in plagioclase porphyroblasts and amphibole with magnesio-hornblende cores and actinolite rims (VJL246, Laird et al., 1984; Warren on Fig. 10). For now we will be content to smile at the covered bridge in Warren and continue south on Rte. 100. One finds evidence for the high pressure envelope in the Northfield Mountains to the east as well as in the Green Mountains (Fig. 10 and 11).

44 Granville Notch/Granville Gulf. Park in picnic area on west side of Rte.100. Walk south to roadcut. **BE VERY CAREFUL THIS ROADCUT IS ON A CURVE, AND THE ENGINEERS PUT THE ROAD TOO CLOSE TO THE ROCKS.**

STOP 2. PINNEY HOLLOW FORMATION GREENSCHIST CONTAINING AMPHIBOLE WITH BARROISITE CORES AND ACTINOLITE RIMS (Warren 7.5' quadrangle) We are very close to the south end of the high pressure envelope (as far as we know). This is one of the easiest places to collect amphibole with barroisite cores and actinolite rims (VJL14J, Laird and Albee, 1981b). Barroisite occurs as cores within actinolite; actinolite is also associated with quartz veins. $^{40}Ar/^{39}Ar$ total fusion ages on two separates of zoned amphibole are 471 and 448 Ma; the actinolite found associated with veins gives a 471 Ma total fusion age. As speculated in the text above, both Taconian and Acadian metamorphism may be preserved here.

This outcrop is critical to the structural studies of Rolfe Stanley and the geochemical work of Ray Coish. Please see Stanley et al. (this guidebook) for a detailed discussion of their work and description of the outcrop. The outcrop is the best place for us to argue the nature of these contacts between chlorite schist and greenschist.

Mileage

0 Our return trip to Boston takes us south on Rte. 100 past 10, the road to the Rochester ultramafic body.

12 We pass a marvelous outcrop of folded chlorite schist just north of Rochester. Turn east at the Rochester Green and take a road over Rochester Mountain with super, newly blasted outcrops within the Ottauquechee, Stowe, and Missisquoi Formations (as per Doll et al., 1961).

22 Taking Rte 12 south (right) into Bethel and then Rte 107 east we cross into the Connecticut Valley Trough.

25 At Royalton pick up I-89 south passing up, alas, the outcrops discussed by Hatch (1987).

47 Stay on I-89 and cross the Connecticut River into New Hampshire. I-89 takes us across the Bronson Hill anticlinorium and Central Maine Terrane and by classic localities studied by James B. Thompson, Jr., John B. Lyons, and their students and colleagues.

110 I-89 ends at I-93 which we will take south to Boston. It is about 70 miles to Boston from here.

REFERENCES CITED

Albee, A.L., 1957, Geology of the Hyde Park Quadrangle, Vermont, U.S. Geological Survey Geologic Quadrangle Map GQ-102, scale 1:62,500.

Albee, A.L., 1965, Phase equilibria in three assemblages of kyanite-zone pelitic schists, Lincoln Mountain Quadrangle, central Vermont: Journal of Petrology, v. 6, p. 246-301.

Albee, A.L., 1968, Metamorphic zones in Northern Vermont, *in* Zen, E-an, White, W.S., Hadley, J.B., and Thompson, J.B., Jr., eds, Studies of Appalachian Geology: Northern and Maritime, New York, Wiley Interscience, p. 329-341.

Albee, A.L., 1972, Stratigraphic and structural relationships across the Green Mountain anticlinorium in north central Vermont, *in* Doolan, B.L. and Stanley R.S., eds, Guidebook for fieldtrips in Vermont, New England Intercollegiate Geological Conference, 64th annual Meeting, Burlington, Vt., p. 179-194.

Apted, M.J., and Liou, J.G., 1983, Phase relations among greenschist, epidote-amphibolite, and amphibolite in a basaltic system, in Greenwood, H.J., ed., Studies in Metamorphism and Metasomatism (Orville vol.): American Journal of Science, v. 283-A, p. 328-354.

Berman, R.G., 1991, Thermobarometry using multi-equilibrium calculations: A new technique, with petrological applications, Canadian Mineralogist, v. 29, p. 833-855.

Bothner, W.A., and Kucks, R.P., in press, Bouguer gravity anomaly maps and filtered maps of New Hampshire and Vermont: U.S. Geological Survey Miscellaneous Investigations Maps GP-1005, scales 1:250,000 and 1:500,000.

Bothner, W.A., and Laird, Jo, 1987, Structure and metamorphism at Tillotson Peak, north-central Vermont, in Westerman, D.S., ed. Guidebook for Field Trips in Vermont, Volume 2: New England Intercollegiate Geological Conference, 79th Annual Meeting, Northfield, Vermont, p. 380-405.

Bothner, W.A., and Laird, Jo, 1991, Iapetan crustal edges and the preservation of high-pressure metamorphism in Vermont: Geological Society of America, Abstracts with Programs, v. 23, p. 10.

Brown, W.H., and Forbes, R.B., 1986,Phase petrology of eclogitic rocks in the Fairbanks district, Alaska: in
Evans, B.W., and Brown, E.H., eds., Blueschists and Eclogites: Geological Society of America Memoir 164, p. 155-168.

Cady, W.M., Albee, A.L., and Chidester, A.H., 1963,Bedrock geology and asbestos deposits of the upper Missisquoi Valley and vicinity, Vermont: U.S. Geological Survey Bulletin 1122-B, 78 p.

Carmichael, D.M., 1978, Metamorphic bathozones and bathograds: A measure of the depth of post-metamorphic uplift and erosion on the regional scale: American Journal of Science, v. 278, p. 769-797.

Chidester, A.H., Albee, A.L., and Cady, W.M., 1978, Petrology, structure, and genesis of the asbestos-bearing ultramafic rocks of the Belvidere Mountain area in Vermont: U.S. Geological Survey Professional Paper 1016, 95 p.

Clark, T.H., 1934, Structure and stratigraphy of Southern Québec, Geological. Society. America Bull., v. 45, p. 1-20.

Clark, T.H., 1936, A Lower Cambrian series from Southern Quebec, Royal Canadian Institute Transactions, v. 21, pt. 1, p. 135-151.

Clague, D.A., Rubin, J., and Brackett, R., 1981, The age and origin of the dynamothermal aureole underlying the Thetford Mines ophiolite, Canadian Journal of Earth Sciences, v. 18, p. 469-486.

Coish, R.A., Perry, D.A., Anderson, C.D., and Bailey, D, 1986, Metavolcanic rocks from the Stowe Formation, Vermont: remnants of ridge and intraplate volcanism in the Iapetus ocean: American Journal of Science, v. 286, p. 1-28.

Cooke, H.C., 1952, Geology of parts of Richmond and Drummondville map-areas, Eastern Townships, Québec, Ministère des Richesses Naturelles, Québec, DP 467, 45 p.

Diment, W.H., 1968, Gravity anomalies in Northern New England, *in* Zen, E-an, White, W.S., Hadley, J.B., and Thompson, J.B., Jr., eds, Studies of Appalachian Geology: Northern and Maritime, New York, Wiley Interscience, p. 399-413.

Doll, C.G., Cady, W.M., Thompson, J.B.T., Jr., and Billings, M.P., 1961, Centennial geological map of Vermont, Montpelier, Vermont Geol. Survey, scale 1:250,000.

Drake, A.A., Jr., Sinha, A.K., Laird, Jo, and Guy, R.E., 1989, The Taconic orogen, in Hatcher, R.D., Jr., Thomas, W.A., and Viele, G.W., eds., The Appalachian-Ouachita Orogen in the United States: Geological Society of America, The Decade of North American Geology, v. F-2, p. 101-177.

Dunning, G.R., Krogh, T.E., and Pedersen, R.B., 1986, U/Pb zircon ages of Appalachian-Caledonian ophiolites, Terra Cognita, v. 6, Abstract L51.

Feininger, T., 1981, Amphibolite associated with the Thetford Mines ophiolite complex at Belmina Ridge, Québec, Canadian Journal of Earth Sciences, v. 18, p. 1878-1892.

Frey, M., DeCapitani, C., and Liou, J.G., 1991, A new petrogenetic grid for low-grade metabasites, Journal of Metamorphic Geology, v. 9, p. 497-509.

Gale, M.H., 1986, Geologic map of the Belvidere Mountain area, Eden and Lowell, Vermont: U.S. Geological Survey Miscellaneous Investigations Series Map I-1560, scale 1:24,000.

Garlick, G.D., and Epstein, Samuel, 1967, Oxygen isotope ratios in coexisting minerals of regionally metamorphosed rocks: Geochimica et Cosmochimica Acta, v. 31, p. 181-214.

Gariepy, C., 1978, Stratigraphie et géochimie des laves cambriennes (?) du groupe de Caldwell dans la région du Lac Etchemin, appalaches du Québec, MSc thesis, Université de Montréal, 161 p.

Ghent, E.D., Stout, M.Z., Black, P.M., and Brothers, R.N., 1987, Chloritoid-bearing rocks associated with blueschists and eclogites, northern New Caledonia, Journal of Metamorphic Geology, v. 5, p. 239-254.

Graham, C.M., and Powell, Roger, 1984, A garnet-hornblende geothermometer: calibration, testing, and application to the Pelona Schist, Southern California: Journal of Metamorphic Geology, v. 2, p. 13-31.

Hames, W.E., 1992, Laser 40Ar/39Ar dating of polymetamorphic 2M1 muscovite, an example from northern Vermont: Geological Society of America, Abstracts with Programs, v. 24, p. A219.

Hatch, N.L., Jr., 1982, Taconian Line in western New England and its implications to Paleozoic tectonic history, in St-Julien, Pierre and Béland, J., eds. Major structural zones and faults of the northern Appalachians: Geological Association Canada Special Paper 24, p. 67-85.

Hatch, N.L., Jr., 1987, Lithofacies, stratigraphy, and structure in the rocks of the Connecticut Valley Trough, eastern Vermont, in Westerman, D.S., ed. Guidebook for field trips in Vermont Volume 2: New England Intercollegiate Geological Conference, 79th Annual Meeting, Montpelier, Vermont, p. 192-212.

Hatcher, R.D., Jr., Thomas, W.A., and Viele, G.W., 1989, The Appalachian-Ouachita Orogen in the United States: Geological Society of America, The Decade of North American Geology, v. F-2, 767 p.

Holland, T.J.B., 1980, The reaction albite = jadeite + quartz determined experimentally in the range 600-1200 °C American Mineralogist, v. 65, p. 129-134.

Kohn, M.J., and Spear, F.S., 1990, Computer program THERMOBAROMETRY: Copyright to Frank S. Spear.

Innes, M.J.S. and Argun-Weston, A., 1967, Gravity measurements in appalachia and their structural implications, *in* Appalachian Tectonics, T.H. Clark, editor, University of Toronto Press, Toronto, p. 69-83.

Kumarapeli, P.S., Dunning, G.R., Pintson, H., and Shaver, J., 1989, Geochemistry and U-Pb zircon age of commenditic metafelsites of the Tibbit Hill Formation, Québec Appalachians, Canadian Journal of Earth Sciences, v. 26, p. 1374-1383.

Laird, Jo, 1980, Phase equilibria in mafic schist from Vermont: Journal of Petrology, v. 21, p. 1-37.

Laird, Jo, 1988, Chlorites: Metamorphic petrology, in Bailey, S.W., ed., Hydrous Phyllosilicates: Mineralogical Society of America Reviews in Mineralogy, v. 19, p.405-453.

Laird, Jo, and Albee, A.L., 1975, Polymetamorphism and the first occurrence of glaucophane and omphacite in northern Vermont: Geological Society of America, Abstracts with Programs, v. 7, p. 1159.

Laird, Jo, and Albee, A.L., 1981a, High-pressure metamorphism in mafic schist from northern Vermont: American Journal of Science, v. 281, p. 97-126.

Laird, Jo, and Albee, A.L., 1981b, Pressure, temperature, and time indicators in mafic schist: Their application to reconstructing the polymetamorphic history of Vermont: American Journal of Science, v. 281, p. 127-175.

Laird, Jo, and Bothner, W.A., 1986, Metamorphism in the northern Green Mountains of Vermont, in Robinson, Peter, ed., Regional metamorphism and metamorphic phase relations in northwestern and central New England, Field trip B-5, 14th General Meeting, International Mineralogical Association: Amherst, Massachusetts, University of Massachusetts, Department of Geology and Geography Contribution no. 59, p. 11-36.

Laird, Jo, Lanphere, M.A., and Albee, A.L., 1984, Distribution of Ordovician and Devonian metamorphism in mafic and pelitic schists from northern Vermont: American Journal of Science, v. 284, p. 376-413.

Laird, Jo, and Bothner, W.A., 1986, Metamorphism in the northern Green Mountains of Vermont, in Robinson, Peter, ed., Regional metamorphism and metamorphic phase relations in northwestern and central New England, Field trip B-5, 14th General Meeting, International Mineralogical Association: Amherst, Massachusetts, University of Massachusetts, Department of Geology and Geography Contribution no. 59, p. 11-36.

Lanphere, M.A, and Albee, A.L., 1974, $^{40}Ar/^{39}Ar$ age measurements in the Worcester Mountains: Evidence of Ordovician and Devonian metamorphic events in Northern Vermont, American Journal of Science, v. 274, p. 545-555.

Lux, D.R., 1984, A maximum age estimate for emplacement of the Thetford Mines ophiolite (abs), Geological Society of America Northeastern Section, Abstracts with Programs, v. 16, p. 48.

Liou, J.G., Kuniyoshi, S., and Ito, K., 1974, Experimental studies of the phase relations between greenschist and amphibolite in a basaltic system: American Journal of Science, v. 274, p. 613-632.

Lyons, J.B. and Bothner, W.A., 1989, A transect through the New England Appalachians, 28th International Geological Congress Field Trip Guidebook T162: American Geophysical Union, Washington, D.C., 64 p.

Marquis, R., 1991, Géologie de l'anticlinorium des monts Sutton (région de Richmond,) Québec, Ministère de l'Énergie et des Ressources, ET 89-02, 86p.

Marquis, R., Béland, J., and Trzcienski, W.E., Jr., 1987, The Oak Hill Group, Richmond, Québec: Termination of the Green Mountains-Sutton Mountains Anticlinorium, *in* Geological Society of America Field Guide Northeastern Section, D. Roy (ed), p. 363-368.

Nowlan, G.S., 1987, Report on five samples from Ordovician strata in southern Québec, Canada Geological Survey, Report 013-GSN-1987, 2 p.

Osberg, P.H., 1965, Structural geology of the Knowlton-Richmond area, Quebec, Geological Society of America Bulletin, v. 76, p. 223-250.

Pintson, H., Kumarapeli, P.S., and Morency, M., 1985, Tectonic significance of the Tibbit Hill volcanics: geochemical evidence from Richmond area, Québec, *in* Current Research, Part A, Geological Survey of Canada, Paper 85-1a, p. 123-130.

Powell, R., 1978, Equilibrium Thermodynamics in Petrology, Harper & Row Ltd., London, 284 p.

Powell, Roger, 1985, Regression diagnostics and robust regression in geothermometer/geobarometer calibration: The garnet-clinopyroxene geothermometer revisited: Journal of Metamorphic Geology v. 3, p. 231-243.

Powell, Roger, and Holland, T.J.B., 1988, An internally consistent thermodynamic dataset with uncertainties and correlations: 3. Applications to geobarometry, worked examples and a computer program: Journal of Metamorphic Geology, v. 6, p. 173-204.

Roy, D.C., 1987 , Northeastern Section of the Geological Society of America: Geological Society of America, The Decade of North American Geology, Centennial Field Guide Volume 5, 481 p.

Salpas, P.A., Haskin, L.A., and McCallum, I.S., 1983, Stillwater anorthosites: A lunar analog?, Proceedings of the Fourteenth Lunar and Planetary Science Conference, Part 1, Journal of Geophysical Research, v. 88, Supplement, p. B27-B39.

Shaw, H.F., and Wasserburg, G.J., 1984, Isotopic constraints on the origin of Appalachian mafic complexes: American Journal of Science, v. 284, p. 319-349.

Smelik, E.G., and Veblen, D.R., 1989, A five-amphibole assemblage from blueschists in northern Vermont: American Mineralogist, v. 74, p. 960-964.

Smelik, E.A., and Veblen, D.R., 1992, Exsolution of Ca-amphibole from glaucophane and the miscibility gap between sodic and calcic amphiboles: Contributions to Mineralogy and Petrology, v. 112, p. 178-195.

Stanley, R.S., Armstrong, Thomas, Kraus, Jerome, Walsh, Gregory, Prewitt, Jeffery, Kimball, Christine, and Cua, Athena, 1987, The pre-Silurian hinterland along the valleys of the White and Mad Rivers, central Vermont, in Westerman, D.S., ed., Guidebook for field trips in Vermont Volume 2: New England Intercollegiate Geological Conference 79th Annual Meeting, Montpelier, Vermont, p. 314-338.

Stanley, R.S., Martin,Delbert, Coish, and Laird, Jo, 1993, A transect through the Taconide zone of central Vermont, ... this volume

Spear, F.S. and Kimball, K.L., 1984, RECAMP - a FORTRAN program for estimating Fe^{3+} contents in amphiboles, Computers and Geosciences, v. 10, p. 317-325.

St-Julien, p. and Hubert, C., 1975, Evolution of the Taconian Orogen in the Québec Appalachians, American Journal of Science, v. 275A, p. 337-352.

Thompson, J.B., Jr., Bothner, W.A., Robinson, Peter, and Klitgord, K.D. 1993, E-1 Adirondacks to Georges Bank: Geological Society of America, Centennial Continent/Ocean Transect #17.

Thompson, J.B., Jr., Laird, Jo, and Thompson, A.B., 1982, Reactions in amphibolite, greenschist, and blueschist: Journal of Petrology;, v. 23, p. 1-27.

Thompson, J.B., Jr., and Norton, S.A., 1968, Paleozoic regional metamorphism in New England and adjacent areas, in, Zen, E-an, White, W.S., Hadley, J.B., and Thompson, J.B., Jr., eds., Studies of Appalachian geology: Northern and maritime: New York, Wiley Interscience, p. 319-327.

Trzcienski, W.E., Jr., 1976, Crossitic amphibole and its possible tectonic significance in the Richmond area, southeastern Québec, Canadian Journal of Earth Sciences, v. 5, p. 711-714.

Williams, H., 1978, Tectonic lithofacies map of the Appalachian Orogen, Memorial University of Newfoundland, St. John's, Map No. 1.

Williams, H. and St-Julien, P., 1982, The Baie Verte-Brompton Line - Early Paleozoic continent-ocean interface in the Canadian Appalachians, Geological Association of Canada, Special Paper 24, p. 177-208.

Chapter P

Paleoenvironmental Traverse Across the Early Mesozoic Hartford Rift Basin, Connecticut

By Gregory S. Horne, Nicholas G. McDonald, Peter M. LeTourneau, and Jelle Z. de Boer

Field Trip Guidebook for the Northeastern United States:
1993 Boston GSA

Volume 2
Contribution No. 67, Department of Geology and Geography, University of Massachusetts, Amherst, Massachusetts

PALEOENVIRONMENTAL TRAVERSE ACROSS THE EARLY MESOZOIC HARTFORD RIFT BASIN, CONNECTICUT

by
Gregory S. Horne, Nicholas G. McDonald, Peter M. LeTourneau, and Jelle Z. de Boer
Department of Earth & Environmental Sciences
Wesleyan University, Middletown, CT 06459

INTRODUCTION

This two-day field excursion focuses on reconstructing the sedimentary and tectonic paleoenvironments of the early Mesozoic volcanic and nonmarine sedimentary rocks exposed in the Hartford Basin, one of the earliest studied rift basins in North America. Following a general east-west traverse across central Connecticut, the ten field stops highlight both the vertical succession and the lateral diversity of facies and their interpreted paleoenvironments including: proximal alluvial fan and mid-fan facies, distal fan and lakeshore facies, alternating shallow-to-deep lacustrine facies, basalt flows, playa and shoreline facies, alluvial plain facies, and the unconformable and faulted western margin of the basin.

The Lower Mesozoic Newark Supergroup fills a series of block-faulted rift basins along the eastern side of the Appalachian orogen from the Maritimes to the Carolinas (Froelich and Olsen, 1984), formed during the incipient rifting of North America and Africa in the Late Triassic and Early Jurassic. One of these, the Hartford Basin, is an elongate north-trending asymmetric graben, approximately 140 km long and 30 km wide in central Connecticut (Fig. 1). It contains more than four km thickness of Upper Triassic and Lower Jurassic terrestrial sedimentary strata (Table 1), and several intercalated tholeiitic basalts (Cornet, 1977; Olsen and others, 1989). A transverse basement horst partially separates the Hartford Basin from the Deerfield Basin to the north (Wise, 1992); the basin terminates at some unknown distance to the south beneath Long Island Sound. West-dipping listric and en echelon faults define the eastern margin of the basin, toward which the strata generally dip and young (Wise and Robinson, 1982). Therefore, our paleoenvironmental traverse will descend from the youngest through to the oldest strata as we move west.

Structural Setting

The Hartford Basin displays the asymmetric half-graben morphology characteristic of most modern and ancient continental rifts (Leeder and Gawthorpe, 1987; Lambiase, 1990), though at depth, the structural geometry may be considerably more complex. Exposed strata typically dip 10-20° toward the eastern boundary of the basin, which is delineated by alternating segments of N-S trending and NE-SW trending normal faults (Fig. 2). The eastern border faults are characterized by relatively steep westerly dips near the surface (45-65°), which shallow to about 20° at depths of more than 2 km (Wise, 1981; Zen, 1983). Gravity and seismic studies (Eaton and Rosenfeld, 1960; Chang, 1968; Wenk, 1984) reveal that the deepest part of the basin (~ 5 km) is near its axis, considerably west of the eastern basin margin.

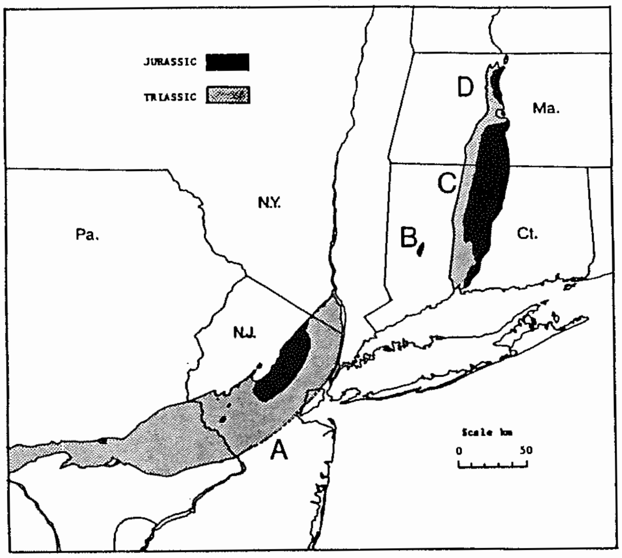

Figure 1. Index map of the (A) Newark, (B) Pomperaug, (C) Hartford, and (D) Deerfield basins (Olsen, 1980).

This presumably indicates the presence of step faults or rider blocks along the eastern margin of the basin. Eastward-thickening rock units, repeated coarsening-up vertical sequences, alluvial fan geometries and paleocurrent directions (Eaton and Rosenfeld, 1960; LeTourneau, 1985) confirm that the eastern border fault system controlled depositional processes in the eastern part of the basin throughout the Early Jurassic. However, its role during initial basin development and early sedimentation in the Triassic is unclear.

For much of its length the western margin of the Hartford Basin is marked by N-striking, E-dipping normal faults, but in some locations early Mesozoic strata unconformably overstep Paleozoic crystalline basement. Westward thickening of the New Haven Arkose (Wenk, 1989) indicates the presence of depocenters along the western margin, and suggests that the western fault system may have played an important role in the early phases of basin subsidence (de Boer and Clifton, 1988). In the earliest Jurassic, rising magma apparently utilized some western faults, emplacing large intrusive bodies adjacent to the western margin of the basin.

In the central part of the basin the structure may be very complicated. The presence of a major axial fault zone at depth is suggested by a swarm of normal faults that intersect and offset the ridges formed by the lava flows. Most of these faults trend northeasterly and dip steeply west. Cumulative displacement is estimated to be about 1.5 km down to the west. An accumulating body of evidence indicates that many of these oblique, intrabasinal, axial faults were syndepositionally active (Philpotts and Martello, 1986; Wenk, 1990a, 1990b). The presence of half-meter diameter crystalline clasts in the New Haven Arkose near the center of the basin (Davis, 1898; Rice and Gregory, 1906) argues for early activity of intrabasinal horsts. Lambiase (1990) has observed that in many continental rift basins, block faulting occurs prior to significant synrift sedimentation, and initially the basin floors are composed of a mosaic of tilted fault blocks at slightly lower elevations than the rift margins.

TABLE 1: NEWARK SUPERGROUP - HARTFORD BASIN

Formation	Thickness	Age
Portland Fm	900-2000 m	Hettangian-Pleinsbachian
Hampden Basalt	60-100 m	
East Berlin Fm	170 m	Hettangian
Holyoke Basalt	100-150 m	
Shuttle Meadow Fm	100 m	Hettangian
Talcott Basalt	65 m	
New Haven Arkose	>2000 m	Carnian-Hettangian

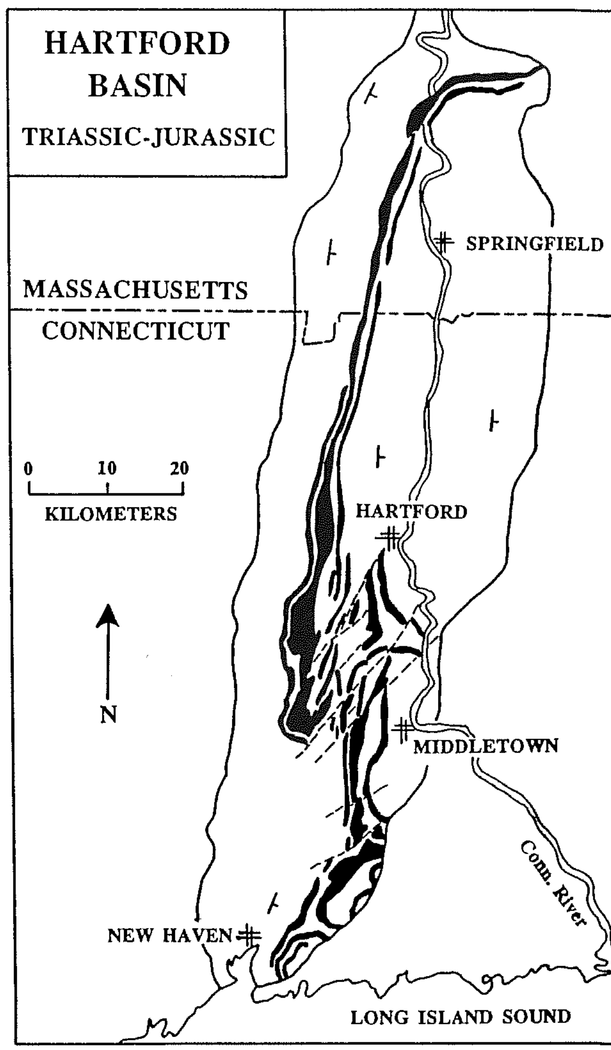

Figure 2. Outline map of the Hartford Basin, showing basalt flows in solid black.

Seismic reflection, magnetic, and gravity data from the New York Bight Basin (Hutchinson and others, 1986), which may be an offshore extension of the Hartford Basin, indicate that its southern portion is underlain by chaotic block-faulted basement. Intrabasinal reflectors are tilted and discontinuous, suggesting that sediment was deposited between blocks contemporaneously with faulting. Early rifting in the Hartford Basin may have been analogous, resulting in a physiography similar to the Basin and Range region of the western U.S., where horsts and grabens, decollements, and complex listric faults are distributed over broad areas (Hutchinson and others, 1986).

Evolution of Paleogeographic Concepts

The Hartford Basin has been the subject of geologic investigation for more than two centuries. Noteworthy American geologists who conducted research in the basin include: B. Silliman, E. Hitchcock, J.G. Percival, J.D. Dana, J.S. Newberry, O.C. Marsh, I.C. Russell, W.M. Davis, B.K. Emerson, J. Barrell, C.R. Longwell, and P.D. Krynine. Only a few of these formulated depositional models or attempted paleogeographic interpretations for the basin, and a review of these concepts over the past century is informative.

William Morris Davis conducted structural and physiographic investigations in central Connecticut for nearly 20 years. In his 1898 monograph, The Triassic Formation of Connecticut, Davis hypothesized sedimentation taking place in an elongate, downwarped trough, bowl-shaped in cross section, with detritus being supplied from both margins and accumulating in near-horizontal layers. Recognizing the shallow-water nature of much of the strata, he realized that depression of the trough and deposition must have taken place simultaneously. Davis believed that basin margin conglomerates were laid down by streams, and suggested (1898, p. 35): "Shallow lakes may have now and then overflowed a *middle* [italics ours] strip or a greater part of the trough, and there finer sediments would gather. The lake floors were sometimes slowly shoaling, ... sometimes sinking to greater depth." Later in his report, he postulated a master axial river draining the basin to the south (p. 155-156). Unfortunately, Davis did not recognize the subtle evidence for synsedimentary activity on the faults which he so carefully and accurately mapped, and he believed instead that most faults within and bordering the basin were postdepositional (Lorenz, 1988).

Joseph Barrell was the first to theorize that the faults which bound the eastern edge of the Hartford Basin were intermittently active during sedimentation, and exerted a primary influence on basin geometry (Barrell, 1915; Eaton and Rosenfeld, 1960). He hypothesized that deposition occurred in a flat-bottomed, wedge-shaped trough, subsiding on the eastern edge, with most of the sediments originating from highlands adjacent to the eastern boundary faults. During sedimentation, according to Barrell, the surface of the basin remained almost horizontal, or perhaps slightly inclined to the west, but the bottom of the trough assumed an increasing eastward inclination due to the weight of the detritus entering the basin from the east. Barrell makes little mention of a western hinged margin of the basin (or west-derived sediment), except to suggest that the basin probably extended well beyond its present western limit, perhaps as far as New Jersey (1915, p. 29). In this regard it is clear that he was profoundly influenced by the now discredited "broad-terrane" hypothesis of Russell (1879), which advocated that the Hartford Basin and the similar Newark Basin of New Jersey (Fig. 1) are erosional remnants of a much larger full-graben, the basins being later uplifted, block-faulted and separated by a broad postdepositional longitudinal arch (Olsen and others, 1989). Nevertheless, Barrell originated the half-graben model to explain the structural development of the Hartford Basin, a model which still has many adherents.

Chester R. Longwell (1922) examined the apron of coarse alluvial fan deposits along the eastern margin, confirming Barrell's ideas of synsedimentary faulting along that boundary. In a later report with E.S. Dana (1932, p. 56-57), Longwell comments: "... the red sandstones and shales, with included sheets of trap, probably covered much of the area between central Connecticut and northern New Jersey". Further studies on the relationship between faulting and sedimentation in the basin led Longwell to proclaim that the entire body of sediments in southern Connecticut was furnished by the highlands to the east of the basin:
"Thus, there is indicated a wide piedmont deposit, tapering in thickness westward ... all derived from a block that

was lifted progressively by faulting as sedimentation proceeded." (Longwell, 1937, p. 437-438).

Paul D. Krynine carried out detailed mineralogic and petrographic investigations of sedimentary rocks from the Hartford Basin in the 1930s, but his comprehensive report remained unpublished until 1950. Although Krynine's petrographic work was of value in the areas of stratigraphy and structural geology, his quantitative and statistical data added little to the existing understanding of the origin or conditions of deposition of the rocks of the Hartford Basin (Lorenz, 1988). In the area of paleogeography, his findings were almost entirely in accord with those of Barrell and Longwell: 1) the eastern border faults were syndepositionally active, 2) the sediments show an exclusive eastern provenance, 3) the basin floor was gently inclined to the west during deposition, and 4) tilting and block-faulting of the basin occurred postdepositionally from the rise of a geanticline between the Hartford and Newark basins. Krynine (1950) agreed with most of the tenets of the broad-terrane hypothesis, but thought that the deposits in the Hartford Basin had originally wedged out in western Connecticut, some 3.5 km west of the Pomperaug Valley (Fig. 1), a small basin of early Mesozoic strata often correlated with the Hartford Basin.

In the most thorough study of the western margin of the basin to date, Girard Wheeler (1937) found evidence for faulting along the western boundary, and concluded that the basin was in part a graben. However, he found no evidence for western sources of detritus in the basin, and did not believe the western faults were syndepositionally active. A staunch advocate of broad-terrane paleogeography, Wheeler argued for the interconnection of the Hartford and Newark basins.

Recent Paleogeographic Studies

Interest in the Hartford Basin resumed in the 1960s with the studies of John E. Sanders and George deVries Klein. Sanders (1968), a supporter of Barrellian ideas, interpreted some of the fine-grained, well-bedded strata of the Jurassic formations as lacustrine deposits with dominant east- and southeast-trending paleocurrent directions, but attributed the paleocurrent trend to irregularities of lake bottom topography, rather than to the influence of regional paleoslope. He also recognized the interbedding of "deep lake" strata and conglomeratic units along the eastern margin, but maintained that in general, lacustrine deposits occupied positions near the center of the basin, passing laterally into coarser-grained strata at the basin margin (Sanders, 1968). Klein (1968) identified locally-derived clasts in the New Haven Arkose near New Haven, thus confirming a western provenance for at least some of the earliest basin deposits. He also recorded easterly directed cross-stratification in sandstones of the East Berlin Formation, and noted the varied lithologies and extreme cyclicity of that formation. In 1969, Klein took an anti-broad-terrane stance, and interpreted the provenance and paleocurrents in the Newark Basin to indicate that it had been filled from all directions of the compass, and thus there could be no persistent connection with the Hartford Basin during deposition. His data also indicated that the Hartford Basin was filled from both sides, and he concluded: "... the dominant flow direction of depositional streams in Connecticut during [early Mesozoic] sedimentation was to the west; data from the basal New Haven Arkose and the East Berlin Formation, however, also indicate deposition by some east-flowing streams" (Klein, 1969, p. 1827).

A series of sedimentological studies by John F. Hubert and his students published over the last two decades are valuable contributions to understanding the geology of the Hartford Basin (Hubert and others, 1976, 1978, 1982). They described the diverse paleoenvironments found in the basin, assembled detailed paleocurrent data for the various sedimentary formations, produced the first paleogeographic maps of the region, and outlined the sedimentary history and distribution of alluvial, fluvial, lacustrine and playa deposits. In their earlier paleogeographic reconstructions of the basin, however, they did not consider the evidence for western provenance and easterly paleoslopes presented by Sanders (1968) and Klein (1969), and adopted a modified broad-terrane viewpoint essentially like that of Krynine (1950). Recently, Hubert and others (1992) integrated their earlier studies with provenance and diagenetic data to analyze the structural and hydrocarbon history of the basin.

Recent studies (McDonald and LeTourneau, 1988, 1989, 1990; Smoot, 1991) have verified the presence of easterly paleoslopes in the basin hypothesized by Klein (1969). In detailed investigations of alluvial fan deposits in the Middletown area, LeTourneau (1985) documented the interfingering of coarse conglomerates with perennial lacustrine strata along the eastern fault margin, and demonstrated that in most cases the lake deposits are thickest adjacent to that margin (Fig. 3). Earlier investigators had envisioned lakes as occupying middle regions of the basin and shallowing toward both margins. The restriction of productive fossil fish localities (McDonald, 1975) to areas close to the eastern margin, and patterns of fossil preservation (McDonald and LeTourneau, 1989) further confirm that perennial lakes were deepest and persisted longest adjacent to the eastern boundary of the basin. Syndepositional eastward tilting of the basin floor in the Jurassic also limited the western progradation of coarse detritus, producing a series of localized, discrete alluvial fans alongside the eastern margin (LeTourneau and McDonald, 1985). Recognition of western shoreline and deltaic deposits in the central portion of the basin (McDonald and LeTourneau, 1988) indicates that the lakes gradually shoaled to the west, where fine-grained detrital and allochemical sedimentation was predominant. In mid-basin areas the persistent trend of paleocurrents in the Shuttle Meadow, East Berlin and Portland formations is to the NE, E and SE (Hubert and others, 1978; McDonald and LeTourneau, 1988). The latest interpretations of Hubert and others (1992), based on paleocurrent, provenance and petrographic studies, also support the hypothesis that the Hartford Basin received detritus from both eastern and western margins during the Late Triassic and Early Jurassic.

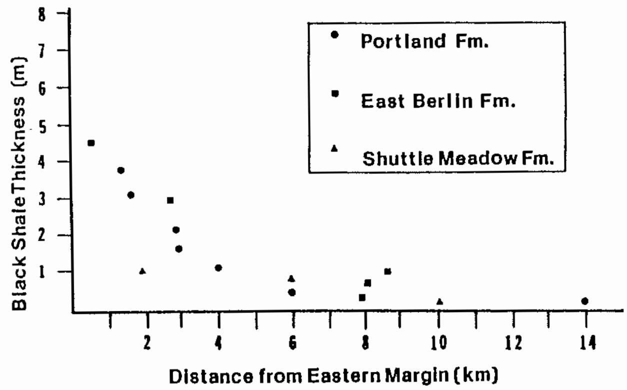

Figure 3. Relation between thickness of black shale beds and distance from the eastern faulted margin of the Hartford Basin.

Stratigraphy and the Basin Model

Interpretations of the paleogeography and paleoclimate of the Hartford Basin have been presented by Krynine (1950), Hubert and others (1978, 1992), and McDonald and LeTourneau (1988, 1989, 1990). The basal New Haven Arkose is mainly composed of coarse redbeds deposited on alluvial fans and braid plains by streams which flowed from Paleozoic crystalline highlands bordering both basin margins. Caliche paleosols suggest that the Late Triassic climate was tropical and semi-arid, with perhaps 100-500 mm of seasonal rain and a long dry season (Hubert, 1978).

An increase in lithospheric extension in the earliest Jurassic (Schlische and Olsen, 1990) led to greater subsidence along the eastern margin of the basin, periodically tapping underlying magma sources, and producing an internally-drained half graben with regional paleoslopes to the east. Following extrusion of the Talcott Basalt, mudstones and sandstones of the Shuttle Meadow Formation were deposited on floodplains and in ephemeral and perennial lakes. The western uplands were the primary sediment source area for the gently inclined hanging wall dip slope of the basin. Sheetfloods and small streams distributed sediment eastward across broad alluvial fans onto a wide braid plain punctuated by playas (Fig. 4). During wet intervals stratified perennial lakes occupied much of the basin floor, perhaps attaining depths of 100 m adjacent to the eastern side of the basin. West-flowing streams only supplied detritus locally along the eastern margin. The Shuttle Meadow is highly fossiliferous; vertebrate footprints are common in fine-grained redbeds, articulated fossil fishes and plants are present in laminated black shales, and plant fragments are locally found in gray mudstones (McDonald, 1992).

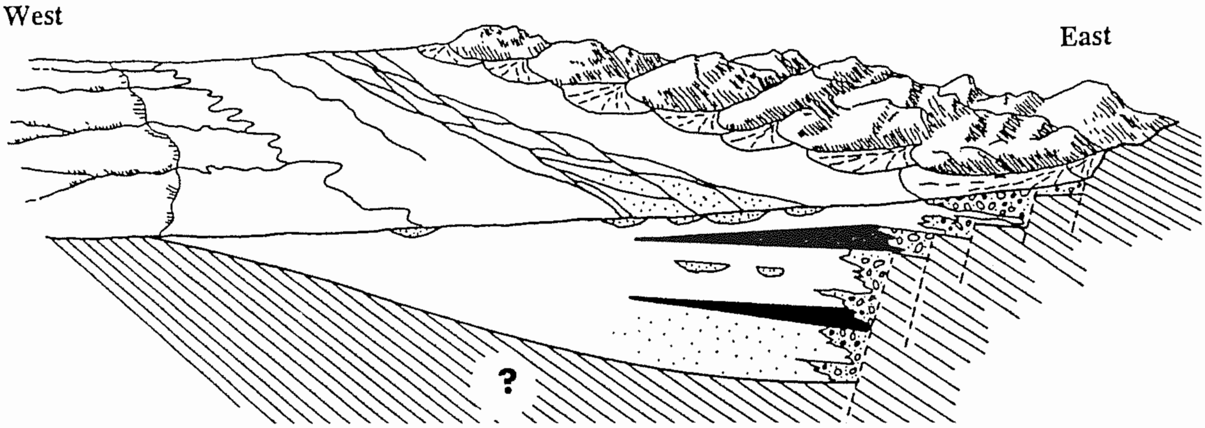

Figure 4. Paleogeographic model of the Hartford Basin during an arid interval in the Early Jurassic (modified from Steel, 1977). Solid black indicates perennial lake deposits; igneous rocks omitted.

After extrusion of the Holyoke Basalt, renewed alluvial fan, floodplain, playa and lacustrine environments are represented by the strata of the East Berlin Formation. Symmetrical cycles of gray mudstone-black shale-gray mudstone, which record the periodic expansion and contraction of large perennial lakes, are most conspicuous in East Berlin outcrops (Hubert and others, 1978; Olsen and others, 1989). Detailed stratigraphic analysis demonstrates that these cycles were climate controlled, perhaps in response to Milankovitch-type fluctuations in the earth's orbit (Olsen, 1986). The region was under the influence of a subtropical, probably monsoonal climate characterized by alternating seasons of high precipitation and aridity. The East Berlin is also rich in fossils.

A third episode of extension and renewed subsidence produced the flows of the Hampden Basalt and aided the development of extensive lacustrine conditions during the deposition of the lower portion of the Portland Formation (Fig. 5). Some of the most productive fossil fish localities occur in perennial lake-bed strata of the basal Portland. The Portland Formation has locally produced numerous dinosaur tracks. The upper part of the Portland is an alluvial fan and alluvial plain facies consisting of red mudstone, sandstone, and conglomerate (LeTourneau and McDonald, 1985).

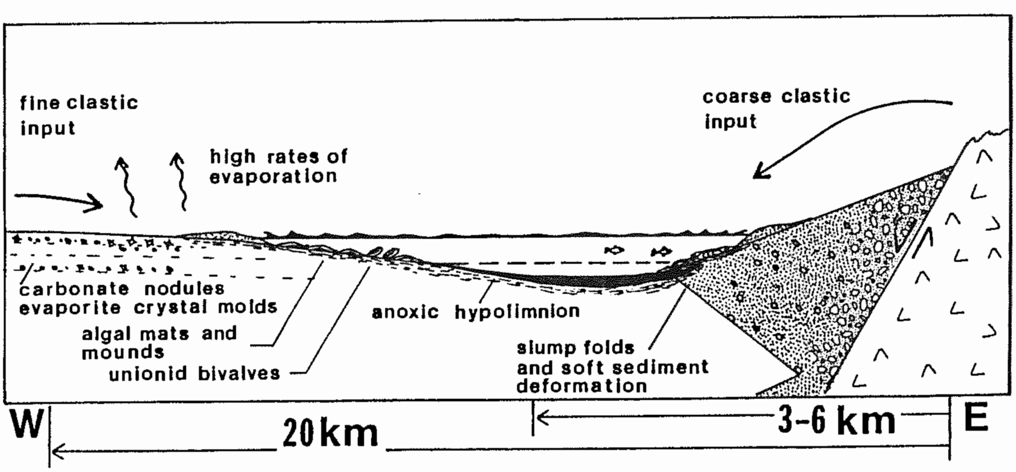

Figure 5. Paleogeographic model of stratified lacustrine conditions in the Hartford Basin in central Connecticut during a wet interval in the Early Jurassic.

HARTFORD BASIN FACIES

The deposits in the Hartford Basin are characterized by lateral and vertical variability, intertonguing and interfingering relationships, and a general lack of strata or fossils that can be confidently correlated across broad areas of the basin. Further complicating the stratigraphic relationships is the block faulting and pervasive eastward tilting of the strata. Strata become progressively younger from west to east across the basin, and also tend to become coarser grained toward the east. The stratigraphy of the basin is largely based on the position of strata relative to the basalt flows, although in some areas of structural complexity even that relationship is not entirely clear.

Early workers in the basin advanced only gross generalizations about the areal distribution of rock types. The lateral and vertical variability of the rocks prevented the development of a comprehensive paleoenvironmental model for the basin. Later workers (Hubert and others, 1978, 1982; LeTourneau and McDonald, 1985) recognized the repetitive association of certain rock types as facies assemblages, and this led to paleoenvironmental reconstructions and the development of a paleogeographic model for the basin. The definition of facies assemblages provided a sense of order to the distribution of rock types that early workers sought in individual units or beds.

The facies analysis presented herein is largely based on detailed studies in the Portland Formation (LeTourneau, 1985). However, work of others in the New Haven, Shuttle Meadow, and East Berlin Formations corroborates the Portland facies models (Hubert and others, 1976, 1978, 1982; Demicco and Gierlowski-Kordesch, 1986; Olsen and others, 1989). Three distinct facies in the basin may be subdivided into nine subfacies (Table 2), each indicative of a discrete depositional environment based on grain size, color, diagnostic fossils, sedimentary structures, and associations with other subfacies.

Subfacies and Depositional Environments

Conglomerate-Sandstone Facies. The texture, fabric, sedimentary structures, clast-size distribution, bedding geometry, and sediment dispersal patterns of Subfacies 1 to 4 are characteristic of alluvial fan deposits. These are the coarsest deposits in the basin, and they occur in discrete lobes adjacent to the eastern border faults. These lithosomes are wedge and prism shaped bodies that thin and fine radially away from the coarsest and central parts of the lobes.

<u>Subfacies 1</u>: consisits of poorly sorted boulder and cobble beds that compare favorably with descriptions of modern and ancient debris flow deposits. Diagnostic features include: random or chaotic orientation of major clasts in mud-rich matrix, concentration of larger clasts near the upper and outer contacts of the deposits, hummocky and irregular upper contacts, planar and distinct lower contacts, and indistinct or poor internal organization. Subfacies 1 lithosomes are interbedded within the deposits of Subfacies 2.

<u>Subfacies 2</u>: consists of thinly bedded and poorly stratified conglomerate and pebbly sandstone in normal-graded and laterally discontinuous beds. The depositional units fine upwards and are commonly capped with a silt drape, often with desiccation features. Cross-bedding is not common, although poorly developed inclined stratification or small scale trough cross-stratification is locally present. These beds are interpreted as ephemeral braided stream deposits on alluvial fans.

<u>Subfacies 3</u>: consists of trough and planar cross-stratified fine conglomerate and pebbly sandstone. Cross-bed set thickness is about 30 cm, but may be as much as 1.5 m. Cobbles and pebbles are dispersed in a sandy matrix or exist as small lenses within the beds; imbricate pebbles lie along the lower contacts and foresets. Upper and lower contacts are discontinuous and the beds are lenticular. These conglomerates and sandstones are interpreted

TABLE 2: ENVIRONMENTAL INTERPRETATION OF NEWARK SUPERGROUP LITHOFACIES, HARTFORD BASIN

Facies	Subfacies	Description	Interpretation	Depositional Setting	
Conglomerate-sandstone	1	Matrix-supported, poorly sorted cobble and boulder conglomerate	Debris flow	Alluvial Fan	Proximal fan
	2	Clast-supported, poorly stratified pebble and cobble conglomerate	Ephemeral braided stream		Mid-fan
	3	Cross-stratified pebble conglomerate and sandstone	Perennial braided stream		Mid-to distal fan
	4	Planar-stratified and ripple-cross-stratified silty fine sandstone	Sheetflood and very shallow stream		Distal fan
Sandstone-siltstone	5	Trough cross-stratified medium-to-coarse sandstone with interbedded siltstone	Ephemeral braided streams and desiccated floodplains	Floodplain	Basin floor
	6	Thin-bedded siltstone and medium-coarse sandstone lenses	Perennial meandering river		Basin floor
Siltstone-shale	7	Dark siltstone with interbedded well sorted ripple-cross-laminated sandstone	Lacustrine shoreline and sublittoral zone	Lake margin	
	8	Dark siltstone and laminated black shale with fish remains	Lacustrine profundal zone	Perennial lake floor	
	9	Massive mudstone with desiccation cracks and evaporite minerals	Playa	Ephemeral lake bed	

as deposits of braided streams on alluvial fans. This interpretation is based on sedimentary features indicative of persistent stream flow: well developed large and small scale cross-stratification, moderate sorting, and absenceof silt drapes and desiccation features. These features are common in modern deposits of seasonal streams with a substantial volume of flow.

Subfacies 4: consists of thin beds of planar and ripple cross-stratified, poorly sorted, silty fine sandstone with very thin granule interbeds. The sandstone typically contains carbonate cement and pore fillings. Subfacies 4 is interpreted as very shallow stream or sheetflow deposits at the distal portions of alluvial fans. It includes the finest-grained alluvial fan deposits, transitional between the lower fan and basin floor. These beds often form a distinctive horizon at the base of coarsening-upwards alluvial fan cycles.

Sandstone-Siltstone Facies. The sandstone and siltstone (and minor shale) of Subfacies 5 and 6 are typical of alluvial plain deposits and dominate the central portion of the Hartford Basin. Subfacies 5 and 6 are closely related, representing end members of varied sandstone/siltstone ratios. A large degree of variability exists within the fluvial deposits of Subfacies 5 and 6, depending on river sinuosity, channel deposits, depth and duration of flow, and floodplain character.

Subfacies 5: consists of fining-up beds of poorly sorted pebbly sandstone with subordinate pebble conglomerate, enclosed within surrounding siltstone. The sandstone beds typically are trough cross-stratified, often with irregular bases scoured into underlying siltstone. The siltstone commonly contains desiccation cracks and burrows; caliche horizons and carbonate intraclasts are locally present. In some areas angular clasts of siltstone from channel bank collapse and mud peloid ripples are abundant in the sandstone. Green-grey mottling from localized reduction of iron oxides is common. This subfacies is interpreted as deposits of ephemeral braided streams and desiccated floodplains.

Subfacies 6: consists of rhythmically stacked, fining-up sequences of sandstone, siltstone, and mudstone. Sandstone beds are often cross-bedded at their base, grading upwards to ripple cross-lamination, and with a bioturbated siltstone-mudstone cap. Internally, the sandstones often have large foresets with coarse grained toes, probably formed as lateral accretion surfaces on point bars. Soft sediment deformation features are common. Subfacies 6 is interpreted as deposits of perennial rivers meandering across broad floodplains on the basin floor.

Siltstone-Shale Facies. The sedimentary structures and fossils in the gray siltstone, minor gray sandstone, black shale, and massive mudstone of Subfacies 7, 8, and 9 are comparable to both modern and ancient lacustrine or playa deposits. These facies are most prevalent in the eastern half of the Hartford Basin, and also generally thicken towards the east.

Subfacies 7: consists of gray, ripple-laminated and wavy-bedded siltstone with intercalations of claystone and very fine sandstone, and gray sandstone beds with a wide variety of wave-generated primary structures, including oscillatory ripples and tabular, low-angle accretionary lenses. Both siltstone and sandstone are very well sorted and characteristically contain abundant plant remains. The sandstones become coarser grained and conglomeratic near the eastern margin of the basin where they interfinger with alluvial fan facies. Vertebrate tracks are locally abundant, and mollusk shell casts, carbonate peloids, and tufa crusts are occasionally present.

Subfacies 7 is interpreted as deposits of offshore-onshore lake margin environments. The gray, wavy bedded siltstone was deposited at or below wave base in a lake. The intercalations of laminated clay and fine sand is indicative of the variable energy conditions that existed between the nearshore and deeper water environments. The gray sandstone was deposited in the sublittoral and littoral zones. Large-scale tabular cross stratification in the coarse sandstone and minor conglomerate along the eastern margin may have been formed in beach ridges built by wave reworking of alluvial fan sediment.

Subfacies 8: consists of thinly bedded, laminated-microlaminated black shale with abundant and well preserved fossil fishes. The black shales were deposited under reducing conditions in periodically or permanently stratified lakes. The preservation of fine laminations indicates that burrowing organisms were not present. Anoxic bottom conditions which excluded a benthic fauna may have resulted from either thermal or chemical stratification of the lake.

In the eastern portions of the basin within the Shuttle Meadow, East Berlin and Portland Formations the Siltstone-Shale Facies is interbedded with alluvial fan conglomerates and sandstones. The stratigraphic succession in these areas indicates that the lake margins expanded and contracted across the slopes of the alluvial fans. In central areas of the basin these subfacies are interbedded with fluvial sandstone and siltstone. At several locations within the Portland Formation deltaic sandstones are interbedded with lacustrine black shale.

Subfacies 9: consists of massive mudstone with extensive desiccation cracks, often from multiple generations of cracking, infilled with sand and silt. Euhedral-subhedral gypsum and halite molds or vugs are locally abundant. Carbonate deposits include thin limestone beds and locally abundant carbonate nodules and concretions. Thin, ripple cross-laminated sandstone lenses are widespread, and often contain sand-sized mud peloids defining ripple slip faces. This subfacies is interpreted as deposits of a dry lake bed or playa, with alternating inundation and desiccation, episodic aeolian influx of fine detritus, and evaporative reflux of interstitial brines.

Climate Hypothesis

Past workers have variously characterized the depositional environments of Hartford Basin deposits as estuarine, marine, fluvial, lacustrine, savannah, or playa, formed under climatic conditions ranging from arid to humid. Usually, one type of climatic regime was used to characterize all of the strata within the basin. The work of Hubert and others (1978, 1982, 1992), LeTourneau and McDonald (1985), Demicco and Gierlowski-Kordesch (1986), and Olsen and others (1989) has indicated that one type of climatic regime can not characterize all deposits in the basin. Mutually exclusive facies assemblages record the influence of contrasting climate regimes within specific stratigraphic intervals. For example, in the lower Portland Formation (LeTourneau, 1985) vertical alternations between distinct assemblages of subfacies probably represent repetitive wet and dry depositional cycles (Fig. 6). Similar climatically controlled depositional cycles have been described from the Triassic Lockatong Formation in the Newark Basin (Olsen, 1986) and from the East Berlin Formation in the Hartford Basin (Hubert and others, 1978; Demicco and Gierlowski-Kordesch, 1986).

Dry cycle assemblages in the Hartford Basin are composed of Subfacies 1-2-4-5-9 (Table 2), which were deposited on alluvial fans and floodplains in the basin by ephemeral fluvial activity. Debris flows (Subfacies 1) are most common on fans in semiarid climates (Blissenbach, 1954; Hooke, 1967). The preservation potential of debris flow deposits is better in dry climates where they are not subjected to large scale reworking by streams. The presence of unreworked debris-flow deposits and desiccation features including abundant mudcracks, caliche horizons, and evaporite minerals suggests that this subfacies assemblage was deposited under arid to semi-arid conditions.

Wet cycle assemblages in the Hartford Basin are composed of Subfacies 3-6-7-8 (Table 2), which were deposited in fluvial and perennial lacustrine environments. These subfacies are indicative of meandering, sinuous rivers, lacustrine deltas, fan deltas, alluvial braid plains, and biologically productive floodplains and basin floors. The record of perennial, stratified deep lakes with well developed food webs (Olsen, 1980; McDonald, 1992) indicates humid climatic regimes. Coarse-grained subfacies of wet cycle assemblages are interstratified with more common dry cycle subfacies in several stratigraphic levels within the lower Portland Formation along the eastern margin of the basin (as close as one kilometer from the border faults). Interbedded alluvial fan and lacustrine deposits also are recognized near the basin margin in the Shuttle Meadow and East Berlin formations.

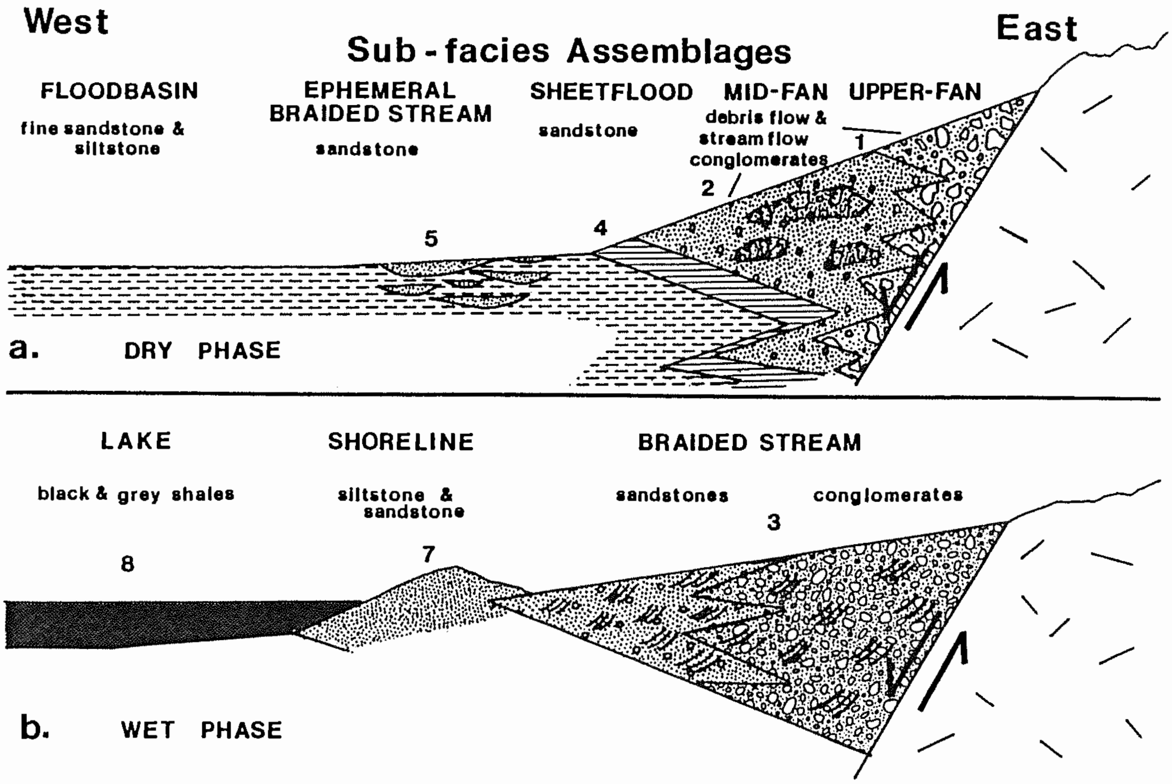

Figure 6. Relation between subfacies in (a.) dry and (b.) wet phases, resulting in distinct facies assemblages in the Portland Formation; subfacies 6 and 9 not shown (LeTourneau, 1985).

Tectonic Hypothesis

Various lines of evidence support the conclusion that syndepositional tectonic rejuvenation of the eastern border faults in the Early Jurassic also controlled the style of sedimentation and the distribution of lithofacies in the Hartford Basin. The grain-size distribution and the paleocurrent patterns in Subfacies 1 through 4 indicate that discrete, small radius alluvial fans were banked against the eastern border faults. This sort of fan distribution is typically associated with rapidly subsiding basin margins, as along the eastern side of Death Valley (Denny, 1965; Bull and McFadden, 1977). In contrast, the less active hinged margins of modern rift basins typically contain broad, low angle, coalescing fan complexes (Hooke, 1972; Steel, 1976; Leeder and Gawthorpe, 1987).

Syndepositional asymmetric basin subsidence is also suggested by the thickness of lacustrine strata. In the Shuttle Meadow, East Berlin, and Portland formations lacustrine strata consistently thicken eastward towards the border faults (Fig. 3), where they become interbedded with alluvial fan conglomerate and sandstone (LeTourneau, 1985). The eastward thickening of individual black shales is also an indirect indication of increasing lake depth; quiet euxinic conditions persisted longer adjacent to the eastern margin (Fig. 5).

Boulders and cobbles of tholeiitic basalt are common within several conglomeratic intervals in the Shuttle Meadow, East Berlin, and Portland formations near the eastern margin of the basin. The trace element geochemical signature of basalt clasts in the Portland Formation is very similar to that of the underlying Hampden Basalt (LeTourneau, 1985). If the Hampden were the source for the basalt clasts in the lower

Portland, then tectonic activity is demanded. It is postulated that the relatively thick Hampden flow may have encroached into the drainage outlets of the eastern crystalline highlands during a pre-Portland interval of relatively low relief between the highlands and the basin. Renewed uplift of the highlands in early Portland time would result in erosion of portions of the flow located east of the basin margin and transport of basalt clasts onto the adjacent fans.

Implications of Cyclicity

Repeated alternations of depositional sequences indicate that cyclicity, both autocyclic and allocyclic in nature, exists on several scales. Small-scale (few meters or less) fining-up or coarsening-up sequences indicate individual depositional events or autocyclic channel entrenchment and avulsion. Syndepositional tectonic rejuvenation of relief at the basin margin produced progradational fan lobes consisting of coarsening-up sequences tens of meters thick. The alternations between wet and dry facies assemblages exist on a scale of hundreds of meters, and probably represent nonseasonal climatic fluctuations that may correlate with global cyclical events (Olsen, 1986).

The sedimentary succession within the Hartford Basin records the influence of both episodic (tectonic) and periodic (climatic) forces on depositional processes and environments. The interplay of tectonic and climatic controls has resulted in complex interfingering and intercalation of subfacies. In the central portion of the basin the climatic signature is more pronounced than the tectonic signature due to the widespread, fine-grained depositional regime. Small changes in climatically controlled lake depth produced wide lateral migrations of lake margins. Increased rainfall produced broad meandering rivers and extensive floodplains in areas adjacent to the lakes. In contrast, near the basin margin evidence of climatic influences on sedimentation are less obvious than the effect of tectonic subsidence, which controlled the geometry of both the alluvial fans and lake basins. Climatic cycles are still indicated by the intercalation of lake and fan deposits, but the marked asymmetry of the lake deposits is a result of the tectonic architecture of the basin.

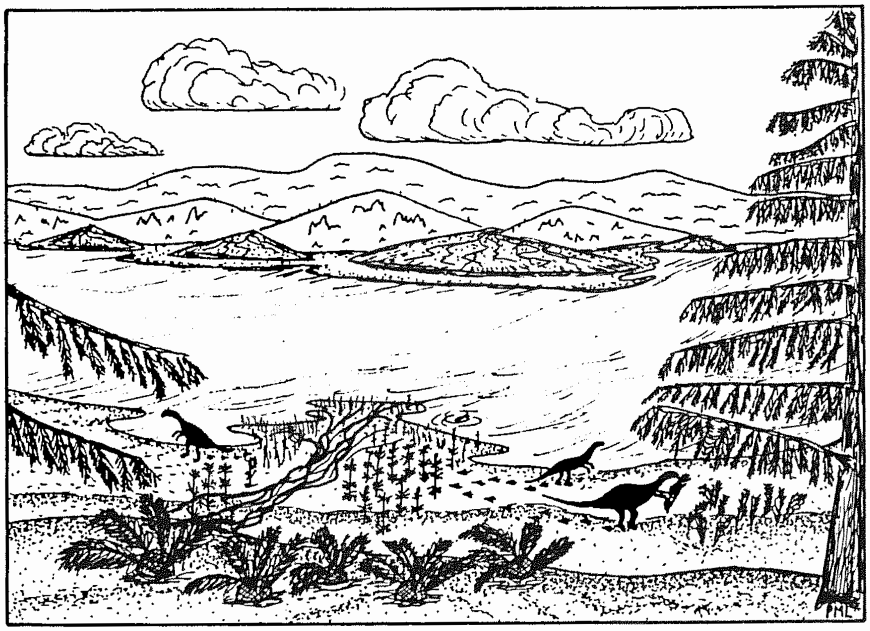

Figure 7. Hypothetical eastward view across the central part of the Hartford Basin in the Early Jurassic.

STOP DESCRIPTIONS

Stops 1 and 2 are about 3 km west of the eastern margin of the Hartford Basin on Round Hill, a glacially scoured and heavily vegetated bedrock hill that typifies the quality of natural exposures in low relief areas of Southern New England such as the Connecticut Valley. Scattered outcrops of conglomerate and sandstone are found along numerous linear ridges, small ledges, and bedding plane exposures. No single outcrop in the Round Hill study area is adequate to characterize the range of local alluvial fan deposits. The alluvial fan depositional model was developed from observations of virtually all of the accessible exposures in the area.

STOP 1: UPPER FAN FACIES OF PORTLAND FM.

Stop 1 provides an excellent example of the range of depositional styles in the coarsest units to be observed in the Hartford Basin. The central areas of Round Hill are notable for extremely large boulders, up to 2 m in length. The vertical section at this stop consists of coarsening-up sandstone and conglomerate units interpreted from base to top as: sheetflow sandstone; shallow, ephemeral, braided stream deposits of cross-stratified coarse and pebbly sandstone; and debris flow deposits of cobble and boulder conglomerate.

A boulder bed is the most prominent feature in the 10 m high outcrop. At the north end of the boulder bed a number of features indicative of debris flows can be observed, including: inverse grading, unsorted matrix-supported major clasts with a random or chaotic fabric, depositional units with planar lower contacts and hummocky or irregular upper contacts, and abrupt textural contrasts with adjacent units. Gray-green weathered basalt clasts in the debris flow conglomerates are geochemically similar to the Hampden Basalt, which underlies the Portland Formation. Approximately 50 m north of the boulder bed several large boulders shelter underlying remnants of debris flow fabrics. Other large boulders occur as isolated clasts in a poorly sorted pebbly sand matrix. These isolated boulders are thought to have been freighted out on the alluvial fan surface by debris flows, which were subsequently eroded removing most or all of the finer-grained constituents, leaving a lag deposit of large, isolated clasts.

The debris flows are surrounded by discontinuous beds of poorly sorted and normal-graded conglomerate and pebbly sandstone that constitute the bulk of the alluvial fan deposits. These deposits were formed by deposition and reworking of alluvial sediment in ephemeral, shifting, braided or bifurcating streams on the fan surface. The beds internally contain variable planar to trough low-angle cross-stratification and scattered scour-and-fill structures. Draped lenses of silt are common along the upper surfaces of beds. The base of the exposure consists of planar to wavy, laminated, silty fine sandstone, interpreted as distal fan deposits. The vertical succession exposed here is thought to represent a progradational fan episode.

STOP 2: MID-FAN FACIES OF PORTLAND FM.

Stop 2 is laterally equivalent to the ridges seen at Stop 1, and is located only 1 km along strike to the north. Two parallel ridges of alluvial fan conglomerate and sandstone illustrate the lateral changes in facies from the previous stop. These exposures also comprise coarsening-up progradational sequences, but containing fining-up units of finer texture and thinner succession. Debris flow deposits have not been recognized here. Maximum clast size is smaller than at Stop 1, but cobbles and boulders do occur in clast-supported, imbricated layers and lenses.

The exposure along the western lower ridge consists of thin, fining-up depositional units representing decelerating flow events. Individual units are well stratified and most of the cross-stratification is small scale. At the south end of the ridge a shallow stream channel (~1 m thick and ~5 m wide) with a scoured lower contact, defined by a cobble-pebble lag deposit, and planar upper contact is present. The channel fill is noticeably finer grained and better sorted than the surrounding units, and internal cross-stratification is very well developed. Comparision of the depositional style within the channel with the surrounding units is indicative of the contrast between more frequent and persistent stream flow in an alluvial fan channel and less frequent short-duration, high velocity flow over broad surfaces of a fan during high discharge events.

The exposure along the eastern upper ridge shows features similar to those described in the lower ridge. However, the eastern ridge provides a better example of the overall coarsening-up nature of the sequences, interpreted as successive alluvial fan progradational cycles. At the base of the exposure a small, cross-stratified channel deposit in fine-grained strata is present. Near the north end of the ridge a thick unit of well-stratified and well-sorted sandstone probably represents a distal fan deposit, but may be partly of aeolian origin.

STOP 3: EASTERN LAKE MARGIN FACIES OF PORTLAND FM.

Stop 3 is located less than one km from the eastern margin of the Hartford Basin, and illustrates several fundamental aspects of the paleogeographic model for the rift basin proposed herein. This stop is significant because of its proximity to the faulted eastern border, the extremely wide range of grain sizes in vertical association, the three dimensional aspect of the exposure, and the presence of paleoenvironmentally diagnostic fossils. In a very limited succession, this small exposure displays a wide range of rift basin depositional facies, including deep water lacustrine laminites, shallow lacustrine littoral sands, fan-delta conglomerates, and alluvial fan sandstones and conglomerates. Sediment grain size from base to top ranges from mud to very large boulders (~2 m long). The exposure illustrates the intimate association of alluvial fan and lacustrine environments along the eastern faulted margin of the rift basin.

The base of the outcrop consists of dark-gray to black laminated shale containing well preserved, articulated fish remains. The overlying fine-grained sandstone is ripple cross-laminated and contains abundant plant debris and evidence of soft sediment deformation; a large slump fold is present in the central portion of the outcrop, and asymmetric interstratal folds are present near the top of the unit. The top of the fine sandstone is marked by an abrupt contact with overlying pebbly and cobbly sandstone. The conglomeratic sandstone rapidly coarsens upward into cobble and boulder conglomerate.

The south side of the outcrop has an extrordinary bedding plane exposure of coarse conglomerate; clasts consist of both low-grade and high-grade metamorphic rocks. The western end of the outcrop displays several small sections of the internal fabric of the deposit along joint surfaces. The range of depositional fabrics through the outcrop indicate that the lower portion of the conglomerate was deposited subaqueously, presumably near the shore of a perennial stratified lake. The the upper portion exhibits the crude stratification and internal laminations typical of alluvial fan or fan delta deposits.

The cyclic nature of the alluvial fan and lake deposits is indicated by the presence of a coarse, fining-up conglomerate located immediately north of the exposure viewed here. The conglomerate underlies the dark shale in this exposure, and is not as coarse grained as the upper conglomerate. However, it does contain a similar assemblage of clast types.

STOP 4: LACUSTRINE-FLUVIAL CYCLES IN EAST BERLIN FM.

The three extensive roadcuts at this stop expose the upper two thirds of the East Berlin Formation in a nearly continuous section 120 m thick. Overlying the East Berlin at the eastern end of the cuts, almost all of the Hampden Basalt is exposed. Although the variety of colors, fabrics, and textures in the East Berlin strata had been previously recognized (Davis, 1898; Krynine, 1950), the existence of lacustrine cycles in the formation was first clearlydocumented by Klein (1968) and confirmed by most recent workers (Hubert and others, 1976, 1978; Demicco and Gierlowski-Kordesch, 1986; Olsen and others, 1989).

The East Berlin Formation here consists of cyclical red, gray, and black lacustrine strata with subordinate interbedded fluvial units. Three cycles in the middle part of the East Berlin Formation are exposed at the west end of the southernmost roadcut as sequences of gray mudstone - black shale - gray mudstone, thought to record the expansion - high stand - contraction of large perennial lakes. The expansion and contraction of lakes was partly climate-controlled, perhaps in response to Milankovitch-type orbital forcing (Olsen, 1986). Similar cyclical deposits in the Triassic Lockatong Formation in New Jersey (Van Houten, 1964) have been called "Van Houten cycles" (Olsen, 1986).

The upper cycle in this triplet contains a distinctive black, laminated carbonate-rich shale bed correlative with the Westfield Fish Bed (McDonald, 1982; Olsen, 1988), a unit which is widely traceable in the East Berlin Formation and contains a characteristic fossil assemblage. Here this bed has produced whole, but dephosphatized specimens of the fishes <u>Semionotus</u> and <u>Redfieldius</u> (McDonald and LeTourneau, 1989), as well as coprolites, conchostracans, and fern and conifer fragments. The associated gray mudstones in this cycle are palynologically productive and have also yielded carbonized leaf and twig fragments of the conifers <u>Brachyphyllum</u> and <u>Pagiophyllum</u> and the cycadophyte <u>Otozamites</u>. During the excavation of these roadcuts in 1988, numerous dinosaur tracks and invertebrate trails were collected from the red and gray units.

A 35 m-thick interval of red, gray, and purple strata separate the lower three Van Houten cycles here from three more lacustrine cycles in the upper East Berlin. The upper cycles are best exposed in the central (CT9) and northernmost (CT372) cuts, and are correlative with three dark shale cycles expose at the I91/CT9 interchange, about 4 km to the east. The upper cycles have produced abundant dinosaur tracks (as at Dinosaur State Park), conchostracans, and fragmentary plants, but no articulated fish. Paleocurrents in the upper cycles trend strongly northeast (Hubert and others, 1978), indicating that the source for much of the East Berlin detritus lay to the west.

STOP 5: FAULTED AND MINERALIZED HAMPDEN BASALT

This stop provides an exposure of the Hampden Basalt (Fe-rich, high TiO_2, quartz normative tholeiite), the youngest of the three major Early Jurassic volcanic flows in the Hartford Basin. The <100 m-thick basaltic unit presumably flowed east to northeast (Ellefsen and Rydel, 1985) away from a feeder dike and fissures in the metamorphic basement complex to the west (Philpotts and Martello, 1986). The Hampden consists of at least eight individual units separated by thin vesicular horizons which can be correlated over distances of more than 30 km (Chapman, 1965). The Hampden Basalt here is cut by numerous sub-vertical, NE-trending extensional fractures and normal faults. Hot brines apparently rose along these faults from underlying arkosic aquifers, leaching the basalt and emplacing quartz, sulfides, carbonates, barite, and small vitreous blobs of bitumen (Gray, 1988). Fluid inclusions in quartz crystals indicate that the brines were moderately saline, near CO_2 saturation, and precipitated most minerals at temperatures between 90° and 220°C.

Thermal maturity levels of the lacustrine black mudstones in the Shuttle Meadow and East Berlin formations indicate pyrolytic fields with temperatures between 435° and 460°C in the central portion of the Hartford Basin (Pratt and others, 1988). High heat flow along the axial zone of the rift valley may have been responsible for heating the brines, and seismic pumping may have aided in forcing the hot brines upward into a NE-trending set of fractures and faults. This thermal event postdated the three major volcanic events (Talcott, Holyoke and Hampden). Elsewhere in the basin it seems to have reset K-Ar ages (Seidemann and others, 1984; Sutter, 1988) and introduced a chemical remanent magnetization (de Boer and Snider, 1979; Witte and Kent, 1989). The relatively high radioactive content of the mineralized fractures allows them to be traced northeast into the lower section of the Portland Formation (Simpson, 1966). This indicates that the thermal events responsible for the mineralization occurred late in the evolutionary history of the Hartford Basin.

STOP 6: MID-BASIN FACIES OF SHUTTLE MEADOW FM.

DANGER: This is an unstable quarry face; do not approach the exposure!

Approximately 60 m of mudstone, siltstone and sandstone from the upper half of the Shuttle Meadow Formation (in contact with the overlying Holyoke Basalt) are exposed in this former rock quarry. In general, the lower part of the exposure consists of red-brown, fine-grained floodplain deposits and the upper part consists of buff-brown to gray sandstone lenses and layers interbedded with similar fine-grained deposits. Two thin micritic limestone beds (rarely found elsewhere) are located near the base of the far west end of the exposure.

The fine-grained units dominate the section and contain a wide variety of sedimentary structures including: climbing ripple cross-lamination, mud peloid ripples, desiccation cracks, vertebrate tracks, soft sediment deformation features, burrowed horizons, planar lamination, parting lineations, low-angle planar cross-stratification, and minor trough cross-stratification. The sandstones contain both planar and trough cross-stratification.

A prominent channel located halfway up the exposure is a lateral accretion feature that grades into floodplain mudstones to the west and abruptly terminates against flooplain deposits to the east. The geometry of the sandstone channel fill and the type of sedimentary structures within the sandstone are typical of a high sinuosity meandering river. The thin gray mudstone associated with the channel sandstone may represent a shallow, organic-rich floodplain lake or an abandoned meander bend.

Hubert and others (1978) interpreted the limestones here as deposits of shallow, alkaline lakes or playas with substantial dissolved magnesium, calcium, carbonate, and sulfate. The limestones are primarily a sandy and muddy dolomitic micrite. The lower limestone contains round fragments of micrite containing gypsum crystals and sparry calcite and pieces of algal tufa; sparse ostracod shells and fish bones have also been observed (Hubert and others, 1978). The sedimentary characteristics of the limestone units and surrounding strata are consistent with a playa depositional environment (Hubert and others, 1982). Massive mudstone surrounding the limestone contains abundant evidence of both desiccation and flashy, ephemeral flow.

The contrast between the lower and upper portion of the outcrop may represent a transition from dry to humid climatic conditions. The fine-grained deposits in the lower portion of the section contain more features indicative of dryer conditions, including desiccation cracks, paleosol features, and playa fabrics. The sandstones and mudstones in the upper part of the section have fewer desiccation features, and appear to be meander plain deposits. The progression from thick, desiccation-cracked mudstones to fluvial mudstones and sandstones may indicate a long term change in climatic regime during the deposition of the section.

STOP 7: BRAID PLAIN FACIES OF NEW HAVEN ARKOSE

The middle part of the 2000 m-thick New Haven Arkose exposed in this large roadcut has been extensively studied by John Hubert and his students (Hubert, 1978; Hubert and others, 1978), from which the following description has been abstracted. This 72 m-thick section is interpreted as an alluvial plain sequence of sandstones and fine conglomerates deposited in channels and longitudinal bars within braided streams, interbedded with sandy mudstones deposited on interfluvial floodplains.

The sandstones and pebble conglomerates are in lenticular and plane beds, with planar, tangential, and trough cross-beds in sets up to 1 m thick. Of special interest are the numerous sets of avalanche foresets, cut-and-fill structures, and well preserved channels and bars with up to 2 m of relief. Paleocurrent directions are generally toward the southwest, but have a very wide ranging distribution. These deposits have been interpreted (Hubert and others, 1978) as representing relatively wide and shallow ephemeral rivers of high gradient and low sinuosity, floored by braided channels with intervening bars, and carrying a coarse bedload of pebbly sand.

Red, planar-laminated, sandy mudstone in lenticular and planar beds is interbedded with the sandstones and conglomerates, and comprises about 15% of the section exposed here. It also is present as large clasts and blocks within some of the channel deposits. The mudstones are considered to be overbank floodplain deposits. Many of the mudstone beds have grayish calcareous horizons in their upper portions, with small green patches and lenses. The calcareous material is nodular, and increases in abundance upwards through an individual bed commonly to a laminated or brecciated calcareous crust at the top. Tubular structures that thin and radiate downwards through these beds are thought to be rhizomorphs or root casts. These calcareous horizons have been interpreted (Hubert, 1978) as paleosol horizons with well developed caliche profiles.

STOP 8: WEST PEAK OF HANGING HILLS

West Peak is supported by the upper, glaciated surface of the Holyoke Basalt, a low TiO_2, quartz normative, tholeiite that is the second and most voluminous of the three Early Jurassic extrusive units in the Hartford Basin. It spread over a distance of at least 3500 km^2, and it has a thickness of >100 m, for a cumulative volume of at least 350 km^3. Its feeder system is unknown, but geophysical evidence suggests that the central segment of the axial fault zone may have been the feeder (de Boer, 1992). The exposure here shows cross sections of differentially weathered polygonal cooling columns. Differential weathering indicates more rapid cooling along the joints. Sets of NNE-trending joints and minor faults intersect the cooling joints and become more abundant towards a major (steeply west dipping) fault zone east of the peak. Downdip motion of the hanging (western) block along this fault zone and at least eight similar and parallel fault zones further east between Meriden and Berlin, is responsible for the apparent sinistral offset of the Holyoke ridge in the central part of the Hartford Basin. Similar motions account for the relatively abrupt deepening of this basin to the northwest (Wenk, 1984, 1989; de Boer and Clifton, 1988).

The topography of the glaciated Hartford Basin can usually be seen clearly from this site. To the west lies a minor valley underlain by the New Haven Arkose, and to the northeast one can see the depression occupied by the Connecticut River valley, underlain by the Portland Formation. Directly south are the outlines of the Sleeping Giant, a massive diabase sill with Talcott affinity, and East Rock and West Rock, large dike-sill complexes which encircle the city of New Haven.

STOP 9: MEANDER PLAIN FACIES OF NEW HAVEN ARKOSE

This description is based on recent work by McInerney (1993). About 130 m of the Upper Triassic New Haven Arkose are exposed in this roadcut, in a succession with up to 22 couplets of fluvial channel sandstone-conglomerate and floodplain mudstone, with numerous caliche horizons in the floodplain mudstones.

The most prominent feature at this stop is the alternation of sequences of light-colored sandstone and conglomerate and darker, fine-grained units. These sequences represent a variety of channel deposits formed by high sinuosity shallow rivers on a broad, intermittently flooded, vegetated floodplain. The channel deposits contain structures formed as bedforms or bars within the rivers. Lateral accretion surfaces, trough cross-bedding, low angle cross-bedding, ripple cross-lamination, and burrows are abundant. The channel units generally fine upward and often contain basal concentrations of pebbles or irregular mudstone clasts derived from cut bank collapse. The floodplain mudstones are characteristically bioturbated by plants and invertebrates. A complete range of partially to wholly bioturbated deposits can be observed.

McInerney (1993) defined 8 types of architectural-depositional units here: isolated channel sheet, amalgamated channel sheet, isolated channel ribbon, minor channel sheet, muddy sandstone (crevasse splay and levee),"U"-shaped fill units, massive mudstone, and caliche units. Each of these represents distinct depositional sub-environments in the meandering river environment. Paleocurrent directions are variable, as expected on a meander plain, but indicate a dominant flow direction to the south and southeast. Petrology of the channel sandstones and conglomerates indicate that some of the detritus was derived from the west side of the basin.

STOP 10: ALLUVIAL PLAIN FACIES OF BASAL NEW HAVEN ARKOSE, THE "GREAT UNCONFORMITY"

Since its discovery in 1890, the angular uncomformity between Late Triassic conglomeratic arkose and steeply tilted Paleozoic mica schist exposed in Roaring Brook has been one of Connecticut's most famous outcrops, often called the "Great Unconformity". Extrapolation of the structure of this single exposure along the entire western margin of the basin led Barrell (1915) and many later investigators to conclude that basin subsidence was controlled primarily by fault displacements along its eastern boundary. Therefore, the western boundary was inferred to be a hinge zone and the basin as a whole was considered a half graben. Subsequent studies, however, have revealed that much of the western margin of the basin also is bounded by faults, some of which apparently were syndepositionally active. The Roaring Brook exposures are bounded both to the east and west by E-dipping, NNE-trending normal faults (Fritts, 1963).

Davis (1898) used this exposure to advance his hypothesis that initial sedimentation in the basin took place on a peneplained basement surface, with detritus entering the basin from both sides. He emphasized that some clasts in the Triassic arkose immediately above the unconformity were locally derived: "...the pebbly sandstones contain fragments of quartz and schist, some of which may be identified as corresponding to the crystalline rocks in place in their neighborhood; and this gives assurance that the sandstones were made from the ruins of the foundation rocks on which they lie." (Davis, 1898, p. 20). Noting angular clasts of quartz and feldspar in the arkose at this locality, Rice and Foye argued for their local provenance from the abundant quartz veins and pegmatite dikes in the underlying schist: "The arkose is composed of very local material. Fresh fragments of feldspar, two or three inches in diameter, still retain bits of tourmaline adhering to them. Their probable source may be found in pegmatite dikes only a few yards away." (1927, p. 135).

However, advocates of the broad-terrane hypothesis have repeatedly denied the existence of a western provenance or locally derived sediment at the Roaring Brook locality. Longwell (1933, p. 112) states: "No fragments of the schist are recognizable in the sediments above it." Agreeing with Longwell's assertions, Wheeler (1937) also concluded that the faults at this locality were postdepositional. Krynine (1950) petrographically compared quartzose clasts with pegmatite vein quartz at this locality, and concluded that none of the sediment was of local origin; he also suggested that the arkose was derived from the eastern crystalline highlands, 27 km to the east.

Recent examination of the Roaring Brook exposures confirms the presence in the arkose of small, but abundant fragments of mica schist which closely resemble the underlying mica schist. Furthermore, it seems unlikely that angular and unweathered clasts of quartz and feldspar in the arkose could have been transported across the basin without appreciable abrasion or disintegration. Easterly-directed paleocurrents obtained from the Roaring Brook exposures (Hubert and others, 1978) support a western provenance for some of this sediment.

ROAD LOG

Mileage (see Fig. 8 for route)

FIRST DAY

0.0 Mileage starts at parking lot entrance of Holiday Inn, Cromwell, CT; turn left onto Sebethe Dr.
0.1 Turn left onto CT372E.
0.4 Turn left onto I91N.
1.4 Turn off at Exit 22 onto CT9S; keep right towards Middletown.

Figure 8. Route map of field trip through central Connecticut, taken from Connecticut State Highway Map.

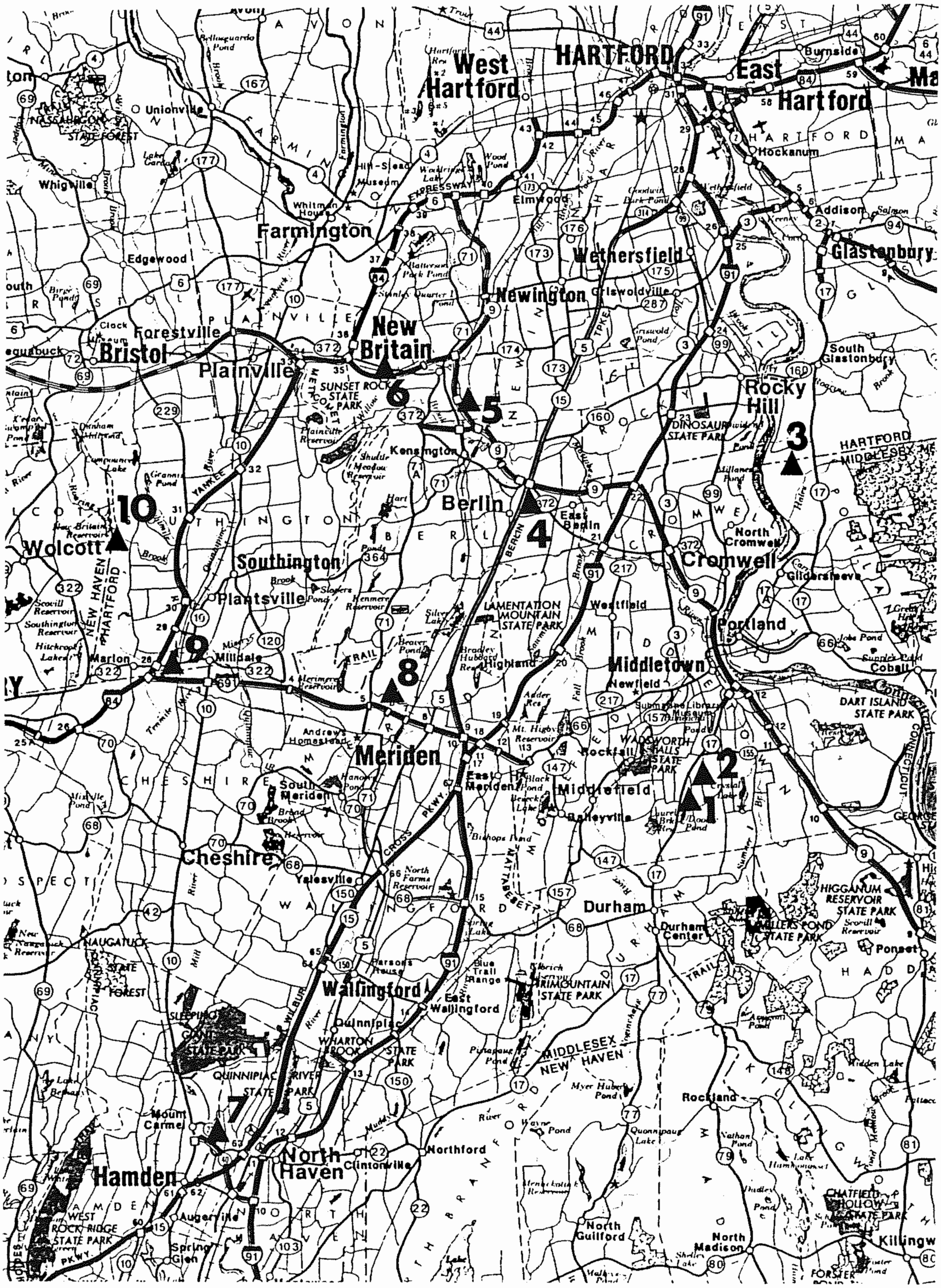
HARTFORD
West Hartford
East Hartford
Unionville
Farmington
Wethersfield
Newington
Glastonbury
Bristol
Forestville
Plainville
New Britain
SUNSET ROCK STATE PARK
Rocky Hill
South Glastonbury
Kensington
Berlin
East Berlin
DINOSAUR STATE PARK
HARTFORD MIDDLESEX
Wolcott
Southington
Plantsville
Cromwell
North Cromwell
Portland
LAMENTATION MOUNTAIN STATE PARK
Middletown
Westfield
Newfield
Marion
Milldale
Meriden
South Meriden
East Meriden
Highland
Rockfall
WADSWORTH FALLS STATE PARK
Middlefield
Baileyville
DART ISLAND STATE PARK
Cobalt
Cheshire
Yalesville
Durham
Durham Center
HIGGANUM RESERVOIR STATE PARK
MILLERS POND STATE PARK
Wallingford
East Wallingford
TRIMOUNTAIN STATE PARK
SLEEPING GIANT STATE PARK
QUINNIPIAC RIVER STATE PARK
WHARTON BROOK STATE PARK
Mount Carmel
Hamden
North Haven
Clintonville
Northford
MIDDLESEX
NEW HAVEN
Rockland
WEST ROCK RIDGE STATE PARK
Augerville
Spring Glen
North Guilford
North Madison
CHATFIELD HOLLOW STATE PARK
Killingw
1
2
3
4
5
6
7
8
9
10

6.9 Stoplight on CT9S at Middletown under Connecticut River bridge; continue south on CT9 and note small outcrops of Jurassic Portland Fm. redbeds for next 3 miles.
10.1 Stop on right shoulder at merge sign just past Exit 11 (Randolph Rd.).

OVERVIEW OF EASTERN BASIN (5 minutes)

Continue south on CT9 across border fault.
10.8 Roadcuts in Brimfield Schist (Ordovician) on the Bronson Hill Anticlinorium.
11.6 Turn off at Exit 10 onto Aircraft Rd.
12.2 U-TURN at stoplight at bottom of exit ramp.
12.4 Return to CT9N; overview of basin as you proceed north.
14.1 Turn off at Exit 11 towards Randolph Rd.; note metamorphic rocks in cuts to right (east); you are descending the fault line scarp of the eastern border fault.
14.4 At bottom of exit ramp turn left (W) onto Randolph Rd.; note low outcrop of Portland Fm. sandstone by union hall just before passing under CT9 overpass; you have just crossed the eastern border fault.
16.6 Turn left at stoplight onto CT17S.
17.1 Turn left onto Coleman Rd. just past Stonegate Apts.; note outcrops of conglomerate along road to left.
18.1 Turn left onto Kelsey St.
18.3 Pull off across from small lane to left just over the crest of the hill; follow lane to north across field and through woods to west-facing ledges of conglomerate.

STOP 1: UPPER FAN FACIES OF PORTLAND FM. (30 minutes)

18.4 Turn left at Y onto Maple Shade Rd.
19.1 Pull off just past house #275 on left; enter field to left through gate along stone wall; outcops of sandstone are located both ahead (west) behind the house and to the right (north) below the road.

STOP 2: MID-FAN FACIES OF PORTLAND FM. (30 minutes)

19.3 Turn left and continue south on Maple Shade Rd.
19.6 Turn right onto Randolph Rd.
21.8 Turn right onto CT9N.
25.1 Turn left at second stoplight (just before bridge), entering Middletown and onto CT66E and CT17N.
25.3 Turn right at stoplight just past church in Middletown; follow CT66E and CT17N over bridge.
26.3 Stoplight in Portland; continue straight ahead on CT17A.
29.4 Turn left onto CT17N.
30.0 Ascending eastern fault line scarp of basin.
31.4 Crossing ridge of Ordovician Brimfield Schist; Devonian Glastonbury Gneiss supports hills to the east, with line of famous pegmatite mineral quarries between them.
32.2 Turn left onto Old Maid's Lane; note low roadcut of schist to right (east) at turn; you will cross the border fault and enter the basin within 500 m.
32.6 Turn left onto gravel road just before third tobacco barn on left; proceed past orchard over hill and into gravel pit. Walk north across gravel pit to moundlike outcrop.

STOP 3: EASTERN LAKE MARGIN FACIES OF PORTLAND FM. (30 minutes)

Retrace route back through Portland to Middletown via CT17S, CT17A, and CT66.
LUNCH at Wesleyan University Science Tower.
Return to CT9N under bridge over Connecticut River.

0.0 Reset mileage at stoplight entering CT9 under bridge in Middletown; turn left onto CT9N.
4.8 Bear left on CT9N towards New Britain.
5.4 Roadcuts in East Berlin Formation: equivalent units will be seen at the next stop.
6.0 View to left (south) of Mt. Higby, supported by Holyoke Basalt.
7.3 Turn off at Exit 21 onto CT372W.
7.7 Roadcuts through Hampden Basalt and East Berlin Fm.
8.2 Turn left at stoplight towards US5/CT15S.
8.3 Turn left again at second stoplight.
8.5 Turn right onto US5 and CT15S.
8.9 U-turn at stoplight back onto US5/CT15N.
9.4 Pull off highway to right by school bus route sign, just before entry ramp onto CT9S towards Middletown; proceed on foot up south side of entry ramp towards CT9S to examine roadcut; **do not try to cross entry ramp!**

STOP 4: LACUSTRINE-FLUVIAL CYCLES IN EAST BERLIN FM. (30 minutes)

Proceed north on US5/CT15.
9.7 Exit right towards CT9N and follow signs to CT9N towards New Britain.
10.1 Turn left onto CT9N.
12.9 Pull off to right shoulder just past Exit 25 (Ellis St.) and beneath overpass at 35 mile marker; **beware of entering traffic on ramp!**

STOP 5: FAULTED AND MINERALIZED HAMPDEN BASALT (15 minutes)

Continue on CT9N.
13.5 Exit left at Exit 28 onto CT72W.
16.9 Turn off at Exit 34.
17.2 Turn right onto Crooked St. and proceed to stoplight at intersection with CT372.
17.4 Turn right at stoplight onto CT372E and pull into parking area on right just past Sunoco station.
17.5 Carefully cross street to large exposure to east of Mobil station.

STOP 6: MID-BASIN FACIES OF SHUTTLE MEADOW FM. (30 minutes)

Return to Holiday Inn in Cromwell via CT72E, CT9E, and I91S; end of first day.

SECOND DAY

0.0 Reset mileage at Holiday Inn parking lot; exit lot to left onto Sebethe Drive; turn left at stoplight onto CT372E, and left again at second stoplight onto I91S.
3.0 View of Mt. Higby (Holyoke Basalt) ahead.
5.6 View to right (west) of Hanging Hills of Meriden.
19.9 Turn off at Exit 10 onto CT40 towards Hamden.
21.7 Pull off onto righthand shoulder of highway at overpass by long roadcut of sandstone and conglomerate.

STOP 7: BRAID PLAIN FACIES OF NEW HAVEN ARKOSE (45 minutes)

Continue ahead to end of highway.
22.6 Turn left onto CT10S; keep right for immediate turn.
22.7 Pull off to right into front parking area of New Haven Savings Bank, pull through lot and U-turn back onto CT10N, and immediately turn right back onto CT40 towards I91.
25.2 Exit left onto I91N.

37.8 Turn off at Exit 17 towards I691.
38.8 Turn off at Exit 68W onto I691W.
39.6 Hanging Hills in foreground. Note several long roadcuts in New Haven Arkose for next few miles.
43.4 Turn off at Exit 4 to CT322 towards Southington.
43.7 Turn left onto CT322E and cross over I691.
44.6 Turn left into park just before pond, go around pond to right.
44.9 Continue straight ahead at stop sign.
45.0 Turn left at second stop sign.
45.1 Gate at foot of Hanging Hills under I691 overpass; continue ahead into fault line gorge.
46.4 Turn left at dam and cross over dam.
47.8 Keep right at Y in road (**not** towards Castle Craig).
48.2 Stop in parking lot at top of mountain by towers. Proceed south on foot to cliff edge; **be very careful!**

STOP 8: WEST PEAK OF HANGING HILLS; OVERVIEW AND LUNCH STOP (one hour)

Retrace route back to I691.
52.7 Turn left onto I691W.
55.7 Pull off highway onto righthand shoulder at roadcut just before Exit 2 to I84E.

STOP 9: MEANDER PLAIN FACIES OF NEW HAVEN ARKOSE (30 minutes)

55.8 Continue west and exit just ahead at Exit 2 onto I84E.
57.8 Turn off at Exit 30 towards Marion Ave.
58.0 Turn left onto Marion Ave.
58.8 Turn right onto Frost St.
59.5 Turn right onto Mt. Vernon Rd.
61.4 Turn left onto Roaring Brook Rd., just past sharp right curve.
61.6 Stop in cul-de-sac at end of Roaring Brook Rd. Proceed on foot from power supply box to west of house #112 along path ~100 m north to exposures along Roaring Brook.

STOP 10: ALLUVIAL PLAIN FACIES OF BASAL NEW HAVEN ARKOSE AND THE "GREAT UNCONFORMITY" (45 minutes)

Retrace route back to I84 and enter I84E towards Boston. **END OF TRIP.**

REFERENCES CITED

Barrell, Joseph, 1915, Central Connecticut in the geologic past: Connecticut State Geological and Natural History Survey Bulletin, no. 23, 44 p.

Blissenbach, E., 1954, Geology of alluvial fans in semi-arid regions: Geological Society of America Bulletin, v. 65, p. 175-189.

Bull, W.B. and McFadden, L.D., 1977, Tectonic geomorphology north and south of the Garlock fault, California, in Doehring, D.O., (ed.), Geomorphology in arid regions: Publications in Geomorphology, State University of New York, Binghamton, New York, p. 115-138.

Chang, C.C., 1968, A gravity study of the Triassic valley in southern Connecticut: M.A. Thesis, Wesleyan University, Middletown, Connecticut, 108 p.

Chapman, R.W., 1965, Stratigraphy and petrology of the Hampden Basalt in central Connecticut: Connecticut State Geological and Natural History Survey Report of Investigations, no. 3, 38 p.

Cornet, Bruce, 1977, The palynostratigraphy and age of the Newark Supergroup: Ph.D. Dissertation, Pennsylvania State University, State College, Pennsylvania, 505 p.

Davis, W.M., 1898, The Triassic formation of Connecticut: U.S. Geological Survey Annual Report, no. 18, part 2, p. 1-192.

de Boer, J.Z., 1992, Stress configurations during and following emplacement of ENA basalts in the northern Appalachians, in Puffer, J.H. and Ragland, P.C., (eds.), Eastern North American Mesozoic Magmatism: Geological Society of American Special Paper, no. 268, p. 361-378.

de Boer, J.Z. and Clifton, A.E., 1988, Mesozoic tectogenesis: development and deformation of Newark rift zones in the Appalachians (with special emphasis on the Hartford Basin, Connecticut), in Manspeizer, W., (ed.), Triassic-Jurassic rifting: continental breakup and the origin of the Atlantic Ocean and Passive Margins: Elsevier, Amsterdam, p. 275-306.

de Boer, J.Z. and Snider, F.G., 1979, Magnetic and chemical variations of Mesozoic diabase dikes from eastern North America: evidence for a hotspot in the Carolinas?: Geological Society of America Bulletin, v. 90, part 1, p. 185-198.

Demicco, R.V. and Gierlowski-Kordesch, E.G., 1986, Facies sequences of a semi-arid closed basin: the Lower Jurassic East Berlin Formation of the Hartford Basin, New England, U.S.A.: Sedimentology, v. 33, p. 107-118.

Denny, C.S., 1965, Alluvial fans in the Death Valley region, California and Nevada: U.S. Geological Survey Professional Paper, no. 466, 62 p.

Eaton, G.P. and Rosenfeld, J.L., 1960, Gravimetric and structural investigations in central Connecticut: International Geological Congress Report, 21st Session, Copenhagen, part 2, p. 168-178.

Ellefsen, K.J. and Rydel, P.L., 1985, Flow direction of the Hampden Basalt in the Hartford Basin, Connecticut and southern Massachusetts: Northeastern Geology, v. 7, p. 33-36.

Fritts, C.E., 1963, Bedrock geology of the Southington quadrangle, Connecticut: U.S. Geological Survey Geologic Quadrangle Map, GQ-200, 1:24,000, 1 sheet, text.

Froelich, A.J. and Olsen, P.E., 1984, Newark Supergroup, a revision of the Newark Group in eastern North America: U.S. Geological Survey Bulletin, no. 1537-A, p. A55-A58.

Gray, N.H., 1988, The origin of copper occurrences in the Hartford Basin, in Froelich, A.J. and Robinson, G.R., Jr., (eds.), Studies of the early Mesozoic basins of the eastern United States: U.S. Geological Survey Bulletin, no. 1776, p. 341-349.

Hooke, R.L., 1967, Processes on arid-region alluvial fans: Journal of Geology, v. 75, p. 438-460.

Hooke, R.L., 1972, Geomorphic evidence for late Wisconsin and Holocene tectonic deformation, California: Geological Society of America Bulletin, v. 83, p. 2073-2098.

Hubert, J.F., 1978, Paleosol caliche in the New Haven Arkose, Newark Group, Connecticut: Palaeogeography, Palaeoclimatology, Palaeoecology, v. 24, p. 151-168.

Hubert, J.F., Reed, A.A. and Carey, P.J., 1976, Paleogeography of the East Berlin Formation, Newark Group, Connecticut Valley: American Journal of Science, v. 276, p. 1183-1207.

Hubert, J.F., Reed, A.A., Dowdall, W.L. and Gilchrist, J.M., 1978, Guide to the Mesozoic redbeds of central

Connecticut: Connecticut State Geological and Natural History Survey Guidebook, no. 4, 129 p.

Hubert, J.F., Gilchrist, J.M. and Reed, A.A, 1982, Jurassic redbeds of the Connecticut Valley, in Joesten, R., and Quarrier, S.S., (eds.), Guidebook for Fieldtrips in Connecticut and south-central Massachusetts: Connecticut State Geological and Natural History Survey Guidebook, no. 5, p. 103-141.

Hubert, J.F., Feshbach-Meriney, P.E. and Smith, M.A., 1992, The Triassic-Jurassic Hartford Rift Basin, Connecticut and Massachusetts: evolution, sandstone diagenesis, and hydrocarbon history: American Association of Petroleum Geologists Bulletin, v. 76, p. 1710-1734.

Hutchinson, D.R., Klitgord, K.D. and Detrick, R.S., 1986, Rift basins of the Long Island platform: Geological Society of America Bulletin, v. 97, p. 688-702.

Klein, G. deV., 1968, Sedimentology of Triassic rocks in the lower Connecticut valley, in Orville, P.M., (ed.), Guidebook for fieldtrips in Connecticut; New England Intercollegiate Geological Conference, 60th Ann. Mtg., New Haven, Connecticut: Connecticut State Geological and Natural History Survey Guidebook, no. 2, trip C-1, p. 1-19.

Klein, G. deV., 1969, Deposition of Triassic sedimentary rocks in separate basins, eastern North America: Geological Society of America Bulletin; v. 80, p. 1825-1832.

Krynine, P.D., 1950, Petrology, stratigraphy, and origin of the Triassic sedimentary rocks of Connecticut: Connecticut State Geological and Natural History Survey Bulletin, no. 73, 247 p.

Lambiase, J.J., 1990, A model for tectonic control of lacustrine stratigraphic sequences in continental rift basins, in Katz, B.J., (ed.), Lacustrine basin exploration: case studies and modern analogs: American Association of Petroleum Geologists Memoir, no. 50, p. 265-276.

Leeder, M.R. and Gawthorpe, R.L., 1987, Sedimentary models for extensional tilt-block/half-graben basins, in Coward, M.P., Dewey, J.F. and Hancock, P.L., (eds.), Continental extensional tectonics: Geological Society Special Publication, no. 28, p. 139-152.

LeTourneau, P.M., 1985, The sedimentology and stratigraphy of the Lower Jurassic Portland Formation, central Connecticut: M.A. Thesis, Wesleyan University, Middletown, Connecticut, 247 p.

LeTourneau, P.M. and McDonald, N.G., 1985, The sedimentology, stratigraphy and paleontology of the Lower Jurassic Portland Formation, Hartford Basin, central Connecticut, in Tracy, R.J., (ed.), Guidebook for fieldtrips in Connecticut and adjacent areas of New York and Rhode Island; New England Intercollegiate Geological Conference, 77th Ann. Mtg., New Haven, Connecticut: Connecticut State Geological and Natural History Survey Guidebook, no. 6, trip B-7, p. 353-391.

Longwell, C.R., 1922, Notes on the structure of the Triassic rocks in southern Connecticut: American Journal of Science, series 5, v. 4, p. 223-236.

Longwell, C.R., 1933, Hartford to New Haven, Connecticut, in Longwell, C.R., (ed.), Eastern New York and western New England: International Geological Congress, 16th Session, United States, Guidebook 1, Excursion A-1, p. 111-116.

Longwell, C.R., 1937, Sedimentation in relation to faulting: Geological Society of America Bulletin, v. 48, p. 433-442.

Longwell, C.R. and Dana, E.S., 1932, Walks and rides in central Connecticut and Massachusetts: Published by the authors, New Haven, Connecticut, 229 p.

Lorenz, J.C., 1988, Triassic-Jurassic rift-basin sedimentology - history and methods: Van Nostrand Reinhold Co., New York, N.Y., 315 p.

McDonald, N.G., 1975, Fossil fishes from the Newark Group of the Connecticut Valley: M.A. Thesis, Wesleyan University, Middletown, Connecticut, 230 p.

McDonald, N.G., 1982, Paleontology of the Mesozoic rocks of the Connecticut Valley, in Joesten, R. and Quarrier, S.S., (eds.), Guidebook for fieldtrips in Connecticut and south-central Massachusetts; New England Intercollegiate Geological Conference, 74th Ann. Mtg., Storrs, Connecticut: Connecticut State Geological and Natural History Survey Guidebook, no. 5, trip M-2, p. 143-172.

McDonald, N.G., 1992, Paleontology of the early Mesozoic (Newark Supergroup) rocks of the Connecticut Valley: Northeastern Geology, v. 14, p. 185-199.

McDonald, N.G. and LeTourneau, P.M., 1988, Paleoenvironmental reconstruction of a fluvial-deltaic-lacustrine sequence, Lower Jurassic Portland Formation, Suffield, Connecticut, in Froelich, A.J. and Robinson, G.R., Jr., (eds.), Studies of the early Mesozoic basins of the eastern United States: U.S. Geological Survey Bulletin, no. 1776, p. 24-30.

McDonald, N.G. and LeTourneau, P.M., 1989, Taphonomic phosphate loss in Early Jurassic lacustrine fishes, East Berlin Formation, Hartford Basin, New England, USA: International Geological Congress, 28th Session, Washington, D.C., Abstracts, v. 2, p. 398.

McDonald, N.G. and LeTourneau, P.M., 1990, Revised paleogeographic model for Early Jurassic deposits, Connecticut Valley: regional easterly paleoslopes and internal drainage in an asymmetrical extensional basin: Geological Society of America Abstracts, v. 22, no. 2, p. 54.

McInerney, D.P., 1993, Fluvial architecture and contrasting fluvial styles of the lower New Haven Arkose and mid-upper Portland Formation, of early Mesozoic age, Hartford Basin, central Connecticut: M.S. Thesis, University of Massachusetts, Amherst, Massachusetts (in preparation).

Olsen, P.E., 1980, A comparison of the vertebrate assemblages from the Newark and Hartford Basins (early Mesozoic, Newark Supergroup) of eastern North America, in Jacobs, L.L., (ed.), Aspects of vertebrate history - Essays in honor of Edwin Harris Colbert: Museum of Northern Arizona Press, Flagstaff, Arizona, p. 35-53.

Olsen, P.E., 1986, A 40-million-year lake record of early Mesozoic orbital climatic forcing: Science, v. 234, p. 842-848.

Olsen, P.E., 1988, Continuity of strata in the Newark and Hartford basins, in Froelich, A.J. and Robinson, G.R., Jr., (eds.), Studies of the early Mesozoic basins of the eastern United States: U.S. Geological Survey Bulletin, no. 1776, p. 6-18.

Olsen, P.E., Schlische, R.W. and Gore, P.J.W., (eds.), 1989, Tectonic, depositional, and paleoecological history of early Mesozoic rift basins, eastern North America: 28th International Geological Congress, Washington, D.C., Field Trip Guidebook T351, 174 p.

Philpotts, A.R. and Martello, Angela, 1986, Diabase feeder dikes for the Mesozoic basalts in southern New England: American Journal of Science, v. 286, p. 105-126.

Pratt, L.M., Shaw, C.A. and Burruss, R.C., 1988, Thermal histories of the Hartford and Newark basins inferred from maturation indices of organic matter, in Froelich, A.J. and Robinson, G.R., Jr., (eds.), Studies of the early Mesozoic basins of the eastern United States: U.S. Geological Survey Bulletin, no. 1776, p. 58-63.

Rice, W.N. and Foye, W.G., 1927, Guide to the geology of Middletown, Connecticut, and vicinity: Connecticut State Geological and Natural History Survey Bulletin, no. 41, 137 p.

Rice, W.N. and Gregory, H.E., 1906, Manual of the geology of Connecticut: Connecticut State Geological and Natural History Survey Bulletin, no. 6, 273 p.

Russell, I.C., 1879, On the physical history of the Triassic formation in New Jersey and the Connecticut Valley: New York Academy of Sciences Annals, v. 1, p. 220-254.

Sanders, J.E., 1968, Stratigraphy and primary sedimentary structures of fine-grained, well-bedded strata, inferred lake deposits, Upper Triassic, central and southern Connecticut, in Klein, G. deV., (ed.), Late Paleozoic and Mesozoic continental sedimentation, northeastern North America: Geological Society of America Special Paper, no. 106, p. 265-305.

Schlische, R.W. and Olsen, P.E., 1990, Quantitative filling model for continental extensional basins with applications to early Mesozoic rifts of eastern North America: Journal of Geology, v. 98, p. 135-155.

Seidemann, D.E., Masterson, W.D., Dowling, M.P. and Turekian, K.K., 1984, K-Ar dates and $^{40}Ar/^{39}Ar$ age spectra for Mesozoic basalt flows of the Hartford Basin, Connecticut, and the Newark Basin, New Jersey: Geological Society of America Bulletin, v. 95, p. 594-598.

Simpson, H.E., 1966, Bedrock geologic map of the New Britain quadrangle, Connecticut: U.S. Geological Survey Geologic Quadrangle Map, GQ-494, 1:24,000, 1 sheet.

Smoot, J.P., 1991, Sedimentary facies and depositional environments of early Mesozoic Newark Supergroup basins, eastern North America: Palaeogeography, Palaeoclimatology, Palaeoecology: v. 84, p. 369-423.

Steel, R.J., 1976, Devonian basins of western Norway - sedimentary response to tectonism and varying tectonic context: Tectonophysics, v. 36, p. 207-224.

Steel, R.J., 1977, Triassic rift basins of northwest Scotland - their configuration, infilling and development, in

Finstad, K.G. and Selley, R.C., (coordinators), Proceedings of the Mesozoic Northern North Sea Symposium, 1977: Norwegian Petroleum Society, MNNSS-7, p. 1-18.

Sutter, J.F., 1988, Innovative approaches to the dating of igneous events in the early Mesozoic basins of the eastern United States, in Froelich, A.J. and Robinson, G.R., Jr., (eds.), Studies of the early Mesozoic basins of the eastern United States: U.S. Geological Survey Bulletin, no. 1776, p. 194-200.

Van Houten, F.B., 1964, Cyclic lacustrine sedimentation, Upper Triassic Lockatong Formation, central New Jersey and adjacent Pennsylvania, in Merriam, D.F., (ed.), Symposium on cyclic sedimentation: Kansas Geological Survey Bulletin, no. 169, v. 2, p. 497-531.

Wenk, W.J., 1984, Seismic refraction model of depth of basement in the Hartford Rift Basin, Connecticut and Massachusetts: Northeastern Geology, v. 6, p. 196-202.

Wenk, W.J., 1989, Seismic model of the thickness of the Triassic-Jurassic New Haven Formation in the Hartford Basin, Connecticut and Massachusetts: Northeastern Geology, v. 11, p. 112-115.

Wenk, W.J., 1990a, Syndepositional block faulting in the Mesozoic Hartford Rift Basin of southern New England: Northeastern Geology, v. 12, p. 99-102.

Wenk, W.J., 1990b, Syndepositional timing of transverse warps in Mesozoic rocks of the Hartford Rift Basin, southern New England: Northeastern Geology, v. 12, p. 132-137.

Wheeler, Girard, 1937, The west wall of the New England Triassic lowland: Connecticut State Geological and Natural History Survey Bulletin, no. 58, 73 p.

Wise, D.U., 1981, Fault, fracture and lineament data for western Massachusetts and western Connecticut: U.S. Nuclear Regulatory Commission Report, NUREG/CR-2292, 253 p.

Wise, D.U., 1992, Dip domain method applied to the Mesozoic Connecticut Valley rift basins: Tectonics, v. 11, p. 1357-1368.

Wise, D.U. and Robinson, Peter, 1982, Tectonics of the Mesozoic Connecticut Valley graben: Geological Society of America Abstracts, v. 14, no. 1-2, p. 96.

Witte, W.K. and Kent, D.V., 1989, A middle Carnian to early Norian (~225 Ma) paleopole from sediments of the Newark Basin, Pennsylvania: Geological Society of America Bulletin, v. 101, p. 1118-1126.

Zen, E-an, (ed.), 1983, Bedrock geologic map of Massachusetts: U.S. Geological Survey, 1:250,000, 3 sheets.

Chapter Q

Petrogenesis of Two Diverse Mid-Paleozoic Complexes of Eastern Massachusetts: A-Type Cape Ann Granite and I-Type Sharpners Pond Quartz Diorite

By Rudolph Hon, Matthew L. Paige, and Christer J. Loftenius

Field Trip Guidebook for the Northeastern United States:
1993 Boston GSA

Volume 2
Contribution No. 67, Department of Geology and Geography, University of Massachusetts, Amherst, Massachusetts

PETROGENESIS OF TWO DIVERSE MID - PALEOZOIC COMPLEXES OF EASTERN MASSACHUSETTS: A - TYPE CAPE ANN GRANITE AND I - TYPE SHARPNERS POND QUARTZ DIORITE.

by
Rudolph Hon,[1] Matthew L. Paige,[2] and Christer J. Loftenius[3]

1. Department of Geology and Geophysics, Chestnut Hill, MA 02167
2. Department of Geological Sciences, Indiana University, Bloomington, IN 47405
3. Engineering Science, Pasadena, CA 91101

FOREWORD

Since the pioneering effort by Bowen (1928) and Tuttle and Bowen (1945), the origin of granitic rocks still remains a question, now and then revived in the hope of major breakthroughs and landmark insights. It has not been so. Bowen gave us the elegant tools of phase diagrams of the alkali feldspar, plagioclase, and quartz system showing that granites are either the end product of crystal fractionation or the first melt formed by partial melting of common crustal protoliths. The origin of the granites visited on this field trip will be pondered as anatectic melts formed in response to elevated temperatures due to intrusions of mafic magmas. Rocks of intermediate composition are then either mixtures of these two liquids, fractionates of the mafic magma, or both.

Many geochemical data will be used to assist many of the field observations. On the first day, we will visit the Cape Ann hypersolvus plutonic complex, a work of Matt Paige, who studied the Cape Ann granites and the related rocks as his Master of Science thesis. Christer Loftenius did his Master of Science thesis on the Sharpners Pond suite which will be visited on the second day. Both theses were done at Boston College.

REGIONAL GEOLOGY OF NORTHEASTERN MASSACHUSETTS

Geologic framework of eastern Massachusetts consists of three different tectonic terranes which have a dissimilar geologic history and which are separated from each other by large fault systems. The easternmost terrane is the Boston Avalon terrane composed mainly of volcanic and plutonic rocks of the late Proterozoic age intruded by Ordovician and Devonian A-type alkaline granites (Buma et . al., 1971; Zen ed. 1983). The adjacent Nashoba terrane adjoins the Boston Avalon terrane by a large fault zone, the Bloody Bluff fault. The displacement along this fault zone is estimated to be large since no rocks on either side of the fault can be correlated with each other (Barosh, 1984a and 1984b).

The Nashoba block consists mainly of pelitic metasediments, amphibolites and felsic gneisses (Bell and Alvord, 1976) intruded by large amounts of felsic and intermediate magmas. The third terrane, separated from the Nashoba terrane by Clinton-Newbury fault system, is the Merrimack trough, which lies to the northwest of the Nashoba Block. In Northeastern Massachusetts the Merrimack terrane consists of pelitic and calcareous sediments (Barosh, 1984a) intruded by several plutons ranging in composition from gabbros to granites (Barosh, 1984a). Some of the granites have been dated to be early Silurian (430 ma) in age (Zartman, Naylor, 1984).

CAPE ANN PLUTONIC COMPLEX

The Cape Ann Complex is a Late Ordovician A-type suite with a radiometric age of 450 ± 25 Ma (Zartman and Marvin, 1991). It extends north of Boston for approx. 25 to 30 km across the Cape Ann peninsula between Salem and Rockport, Massachusetts. Its land exposures are about 300 sq. km with additional exposures of an unknown extent beneath the Atlantic ocean. The complex affords excellent outcrops both along the scenic coast as well as well inland.

During the Ordovician to Middle Devonian time interval, magmatic activity was sporadic but widespread throughout the southeastern New England. Its manifestation within the Boston Avalon terrane was almost exclusively as alkali hypersolvus granites with a subsidiary but petrogenetically relevant activity of alkali basalts. During the same time period within the neighboring Nashoba terrane the magmatism was limited to I-type and S-type plutonism. I-type volcanic rocks are today preserved within a tectonic sliver of Newbury Basin wedged between the Boston Avalon and the Nashoba terranes. A tectonic model that integrates the magmatic activities of both of the terranes is a one of a subduction related continental arc (Nashoba and Newbury Basin) and a behind the arc zone (Boston Avalon). Original placements of these terranes is unknown but it was during the ensuing Acadian orogeny that the individual crustal sections were telescoped and possibly transported some distance by a strike slip motion.

OVERVIEW

The Cape Ann complex consists of several lithological types of which the hypersolvus Cape Ann Granite and Beverly Syenite (Dennen, 1981) are the most dominant. Both designations are actually better described as facies separated from each other by modal quartz content of 5%. A smaller but distinct and possibly not genetically related to the hypersolvus granites and syenites is the Squam Granite (Dennen, 1981), a two feldspar ferrohornblende biotite granite.

Petrogenetically important are co-intrusive mafic magmas found as magmatic pillows, enclaves, and pull-apart or segmented mafic dikes. Their presence is limited to several local regions with a more substantial concentration found near the city of Salem, Mass., at Salem Neck. Magnetic and gravity signatures reflect the higher abundance of mafic rocks by pronounced positive anomalies, not shown anywhere else over the complex. Possibly, the complex was extruded along a feeder near this area.

PETROGENESIS OF THE CAPE ANN IGNEOUS COMPLEX

Although the dominant petrological type of the Cape Ann complex is the Cape Ann Granite, many other types totally engulfed by the granite are also recognized. The granite consists primarily of perthitic alkali feldspar (60 to 65 modal %), quartz (30 to 35 modal %) and usually less than 5 modal % of ferrobiotite and ferrohastingsite. It is of a notable interest to point out that the ferrous end member of the biotite solid solution, annite, is named after Cape Ann. Silica content is typically > 75 wt. % with subequal amounts of Na_2O and K_2O at 4 wt. %. CaO only rarely exceeds 0.5 wt. %. Granites are metaluminous, their agpaitic index varies from 0.93 to 1.05.

With the increasing accumulation of alkali feldspar (up to 80 modal %) the granites become more calcic and also more mafic. Color index rises from about 3% up to 15% and at the same time modal quartz decreases down to near 5 %. These rocks tend to cluster into several regions but they are observed to grade back and forth with the granites, even on scale of a single outcrop. In contrast to the granites, this suite of rocks is designated as the mixed suite, suggesting an involvement of a mafic magma component.

In addition, a third group of rocks can be recognized. In this suite modal quartz is virtually absent, although the modal content of alkali feldspars may be as high as 70%. Their finer grain appearance and frequent association with the localized occurrence of basaltic melts suggest their genetic dependence on the mafic rocks. As we will discuss later these uncommon rocks are best geochemically modeled as a fractionation series from the parental alkali basalt melts.

ZR / HF DISCRIMINATION

Zirconium and hafnium are two trace elements which belong to the second and third transition series, respectively. Both share many of the same chemical characteristics: the same charge (+4), same atomic radii, same electronegativities, and nearly identical ionic radii, and ionization energies (Table 1). It can be shown on examples of cogenetic fractionation suites that this ration remains unaffected through the fractionation process. Perhaps the geochemical affinity of Zr and Hf are very similar to each other that fractionation does not result in an appreciable separation. In this respect Zr and Hf have a geochemical behavior similar to isotopes. Noticeable separation between these two trace elements is observed whenever a vapor phase is involved (pegmatites or aplites).

On the basis of Zr to Hf ratios, the same three groups can be identified geochemically. The Cape Ann Granite yields a Zr/Hf ratio of 29.5 which correlates with other crustally derived magmas (Paige, 1991). On the other hand samples of the mafic rocks and fractionates from the alkali basalts have Zr/Hf ratios equal to 44. The mixed series have their Zr/Hf ratios fall between the two limiting values. Modeling of mixing between the Cape Ann Granite magma and various magmas that resulted by fractionation of the alkali basalt is shown on plots of Sc vs. Zr/Hf (Fig. 2) and SiO2 vs. Zr/Hf (Fig. 3).

Samples	CA-24	CA-6	CA-16D	CA-15A-G	CA-15A-M	CA-30A	BS-2	SN-6	SN-4	BS-3
SiO2	73.60	72.49	74.10	69.24	54.34	47.33	61.63	58.27	49.05	45.78
TiO2	0.22	0.20	0.26	0.56	1.74	2.62	0.52	0.67	2.42	3.20
Al2O3	13.57	13.31	12.39	13.75	17.34	16.62	17.10	18.63	16.43	15.02
Fe2O3	2.32	2.65	3.10	4.99	9.14	13.01	6.19	7.11	11.77	13.94
MnO	0.05	0.07	0.08	0.13	0.18	0.20	0.15	0.15	0.17	0.19
MgO	0.13	0.78	0.03	0.28	1.87	4.79	0.27	0.82	3.86	5.93
CaO	0.78	0.54	0.24	1.64	6.96	7.57	1.66	1.91	7.76	9.80
Na2O	3.18	3.98	4.53	4.53	4.96	4.03	6.71	7.45	5.21	4.58
K2O	5.59	5.30	4.94	4.83	2.57	3.02	5.42	4.95	2.08	1.29
P2O5	0.03	0.03	0.01	0.11	0.85	0.82	0.06	0.17	0.44	0.63
Totals	99.45	99.35	99.68	100.05	99.95	99.99	99.71	100.12	99.20	100.34
Norms										
NS			0.25							
Or	33.09	31.38	29.25	28.66	15.31	18.08	32.21	29.43	12.41	7.74
Ab	26.99	33.76	36.33	38.5	42.31	19.16	50.96	42.11	26.44	17.62
An	3.68	2.48		2.94	17.6	18.55	0.54	2.79	15.47	16.81
Q	30.62	25.29	27.53	18.96						
Ne						8.32	3.33	11.57	9.84	11.72
Ol					5.63	15.32	4.16	6.66	10.44	13.41
Fo					1.64	6.6	0.29	1.12	4.22	6.41
Fa					3.99	8.72	3.87	5.53	6.22	7
Hy	3.32	5.47	3.89	4.97	2.55					
En	0.32	1.94	0.07	0.49	0.8					
Fs	2.99	3.52	3.82	4.48	1.76					
Di			1	3.98	9.9	11.73	6.48	4.88	17.2	23.38
Wo			0.47	1.9	4.87	5.88	3.07	2.35	8.59	11.8
En			0.01	0.21	1.57	2.66	0.26	0.46	3.68	5.82
Fs			0.52	1.88	3.47	3.19	3.15	2.07	4.92	5.76
Ac			0.9							
Ap	0.07	0.07	0.02	0.26	2	1.93	0.14	0.4	1.02	1.49
Il	0.42	0.38	0.49	1.06	3.32	5.03	0.99	1.27	4.65	6.15
C	0.94	0.12								
Mt	0.33	0.39		0.72	1.33	1.91	0.9	1.04	1.73	2.04
Totals	99.46	99.34	99.66	100.05	99.95	100.03	99.71	100.15	99.2	100.36
La	73.69	109.69	117.85	112.35	37.72	48.80	32.40	64.52	32.84	30.38
Ce	146.61	226.31	246.75	233.00	84.68	99.04	66.82	135.62	70.26	64.93
Nd	63.70	107.76	117.07	107.40	47.00	48.00	30.98	60.42	37.70	35.49
Sm	11.94	18.34	20.91	17.59	9.33	8.68	6.08	9.94	7.21	7.13
Eu	1.07	1.69	1.24	2.46	3.49	2.62	1.63	1.19	2.48	2.26
Tb	1.72	1.90	2.43	1.88	1.01	0.93	0.83	0.98	1.00	0.88
Yb	4.98	5.73	7.18	5.38	2.66	2.27	3.04	1.83	1.99	2.05
Lu	0.74	0.85	1.01	0.88	0.46	0.35	0.50	0.31	0.31	0.31
Hf	10.09	14.32	19.07	20.52	6.64	5.64	8.41	11.07	7.46	5.20
Zr	327	424	659	772	283	256	348	444	326	235
Th	19	11	10	14	10	10	10	10	10	10
Ga	24	25	36	32	21	23	26	26	22	20
Zr/Hf	32.41	29.61	34.56	37.62	42.62	45.39	41.38	40.11	43.70	45.19

Table 1. Chemical analyses and CIPW norms for representative samples of the Cape Ann Complex. Major elements and Zr, Th, and Ga by XRF, all others by INAA. Major elements in wt. %, trace elements in ppm. Samples CA-24, CA-6, and CA-16D are of the Cape Ann Granite; sample CA-15A-G is of the mixed series; all others are alkali basalts and their fractionates.

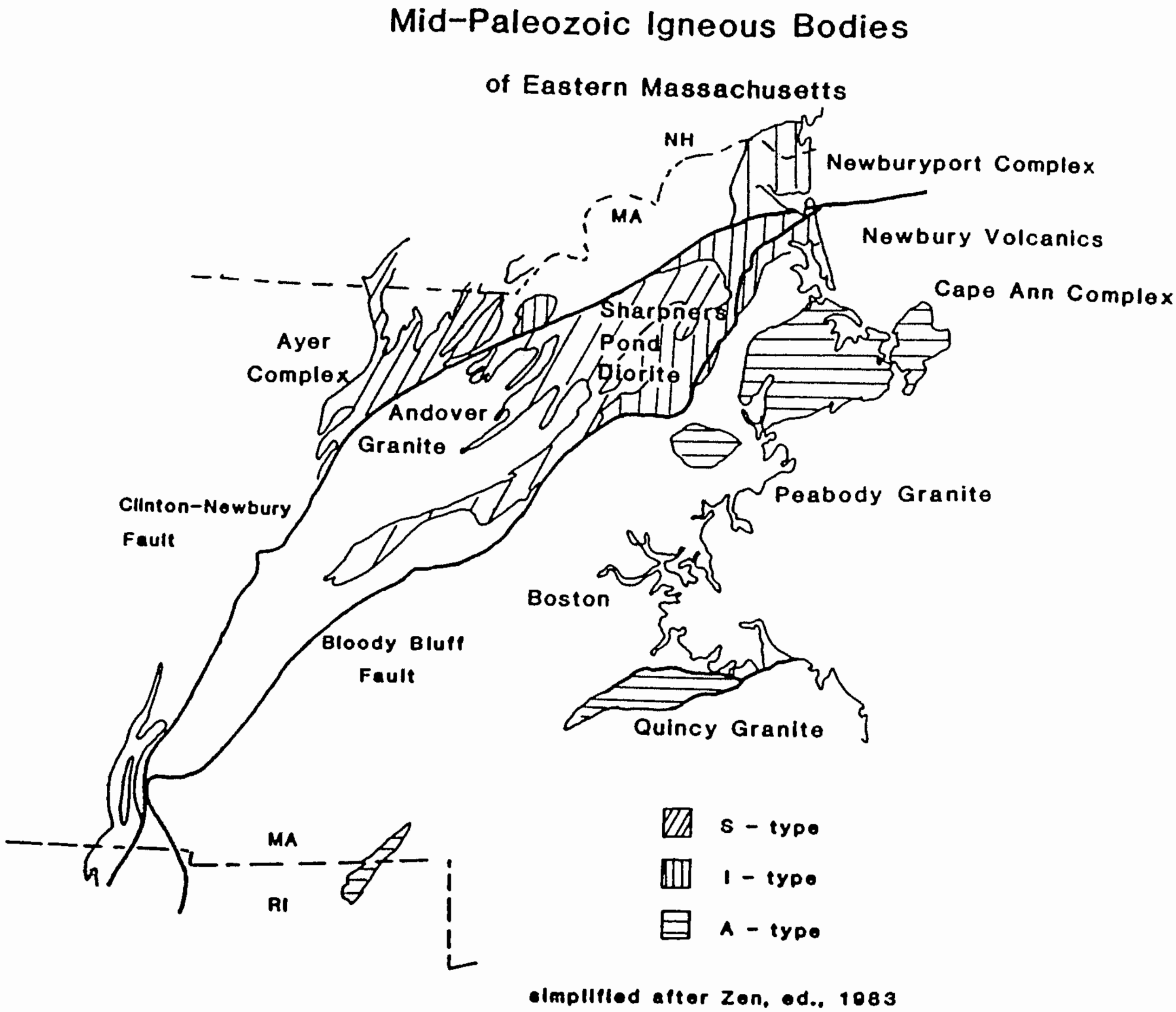

Figure 1. Simplified geologic map of eastern Massachusetts with the location of mid-Paleozoic intrusive complexes. Terrane boundaries are defined by the Bloody Bluff and by the Clinton-Newbury fault systems. From east to west the terranes are Boston Avalon Terrane, Nashoba Terrane, and Merrimack Trough Terrane. Modified after Zen, ed., 1983.

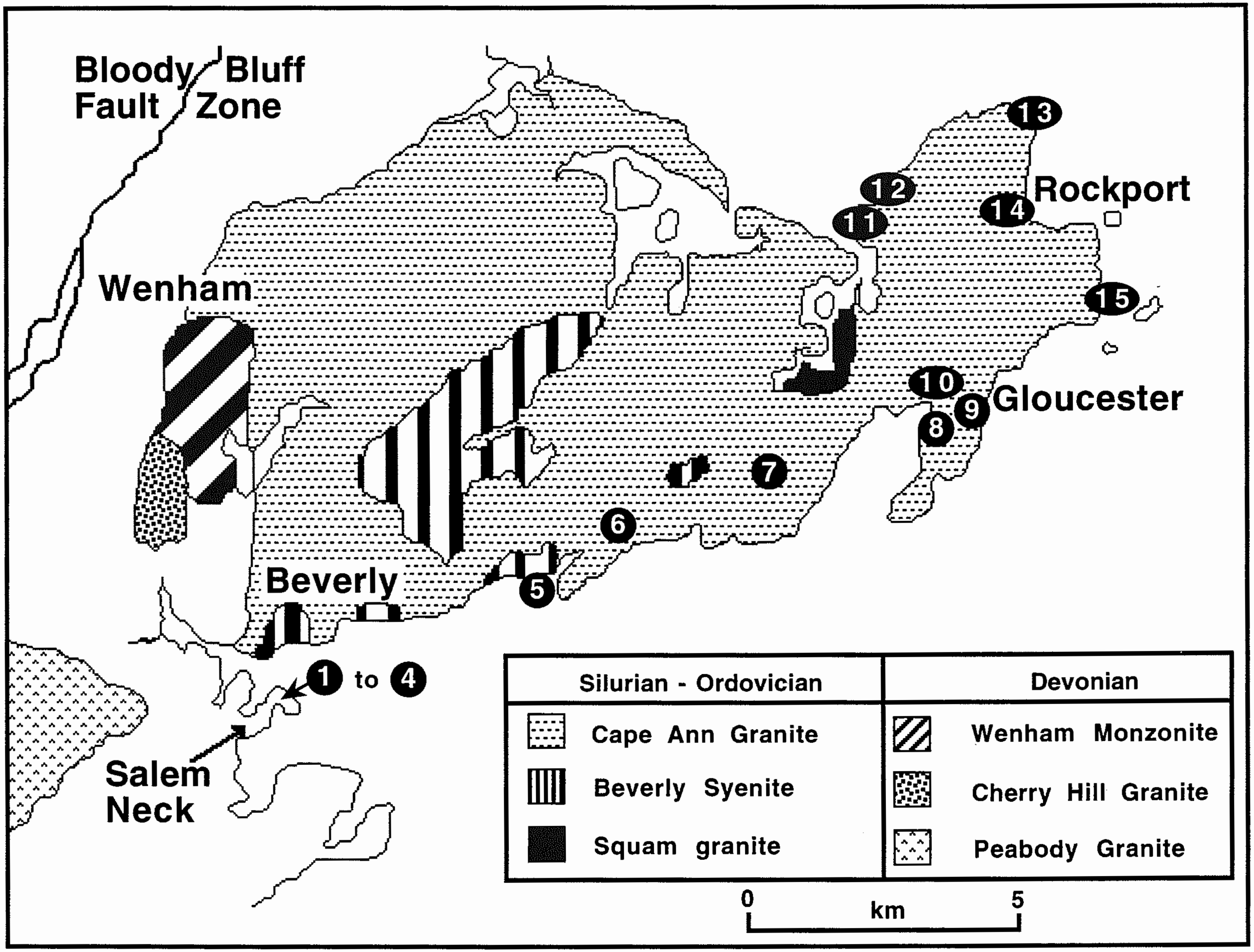

Figure 2. Geologic map of the Cape Ann area and location of the field trip stops for Day 1. Modified after Zen, ed., 1983.

Transition Series Elements

III A	IV A	V A	VI A	VII A	VIIIA	VIIIA	VIIIA	I B	IIB
Sc	Ti	V	Cr	Mn	Fe	Co	Ni	Cu	Zn
Y	**Zr**	Nb	Mo	Tc	Ru	Rd	Pd	Ag	Cd
La*	**Hf**	Ta	W	Re	Os	Ir	Pt	Au	Hg

	Atomic Radius in Å	Ionic Radius in Å	Ionization Energies 4th valency in eV	Electro-negativity
40 Zr^{+4}	2.16	.79	34.34	1.3
72 Hf^{+4}	2.16	.78	33.33	1.3

Mantle Ratio

[Enstatite Chondrites: Ehmann et.al (1977)]

Zr/Hf = 43.8

Solar Ratio

[C1 Chondries: Anders and Ebihara (1982)]

Zr/Hf = 31.2

Figure 3. Portion of the periodic table listing elements of the first, second, and third transition groups. Additional chemical data are given for zirconium and hafnium as well as for the *Zr/Hf* ratios.

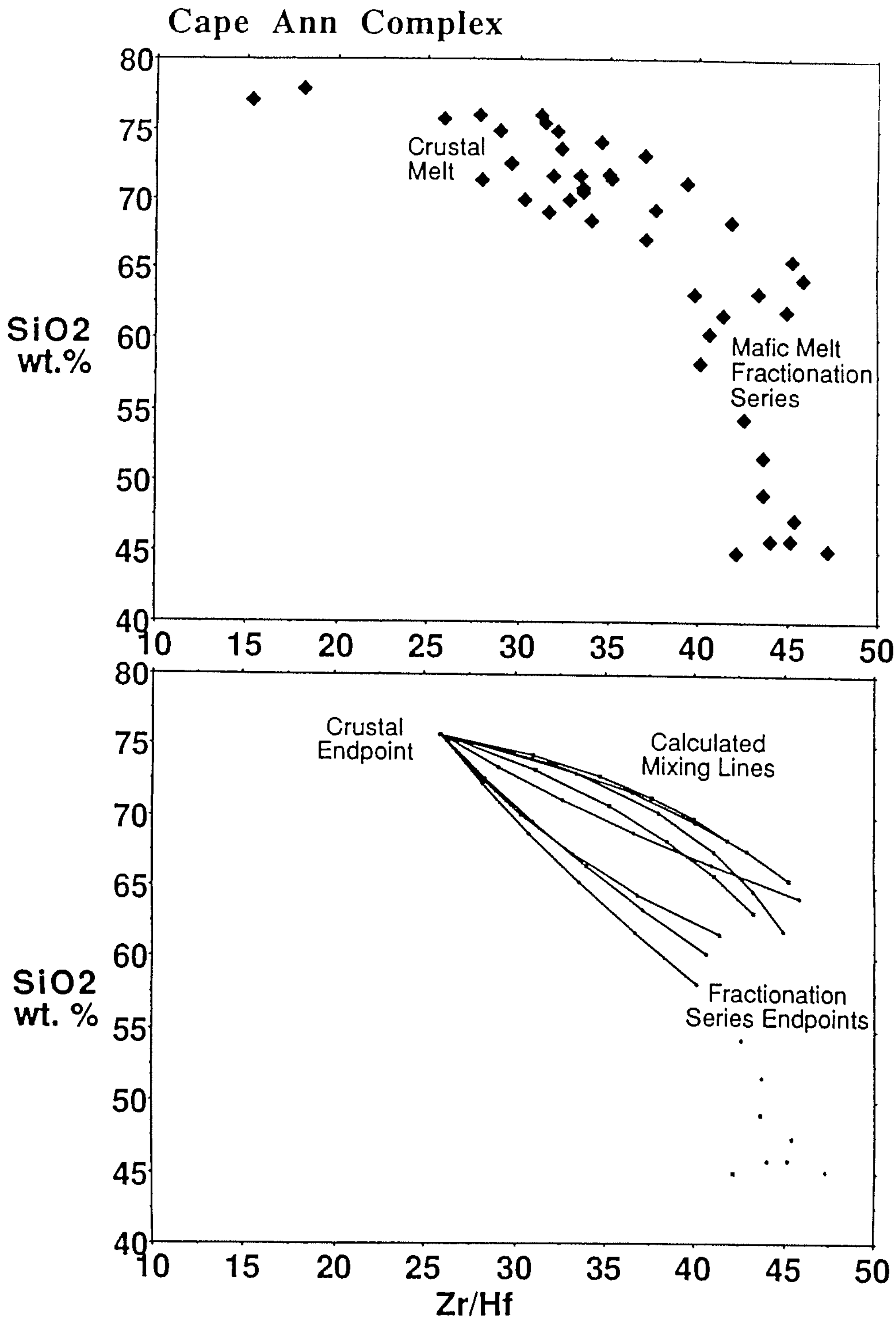

Figure 4. Plot of SiO_2 wt. % vs. Zr/Hf ratio. The diagram at the top shows plotted points for all analyzed samples of the Cape Ann plutonic complex. The bottom diagram is a plot of mixing trajectories between the crustal melt point and points of several melts being the likely candidates of the mafic parental magmas. The latter formed by fractional crystallization of the alkali basalt melts. Samples with Zr/Hf ratio >40 represent alkali basalt melts and their fractionated descendents; melts with ratios<32 are of the anatectic crustal origin. Samples with intermediate ratios represent melts formed by mixing of mafic and silicic parental liquids. Note, that the calculated lines define a region occupied by all samples with the intermediate Zr/Hf ratios.

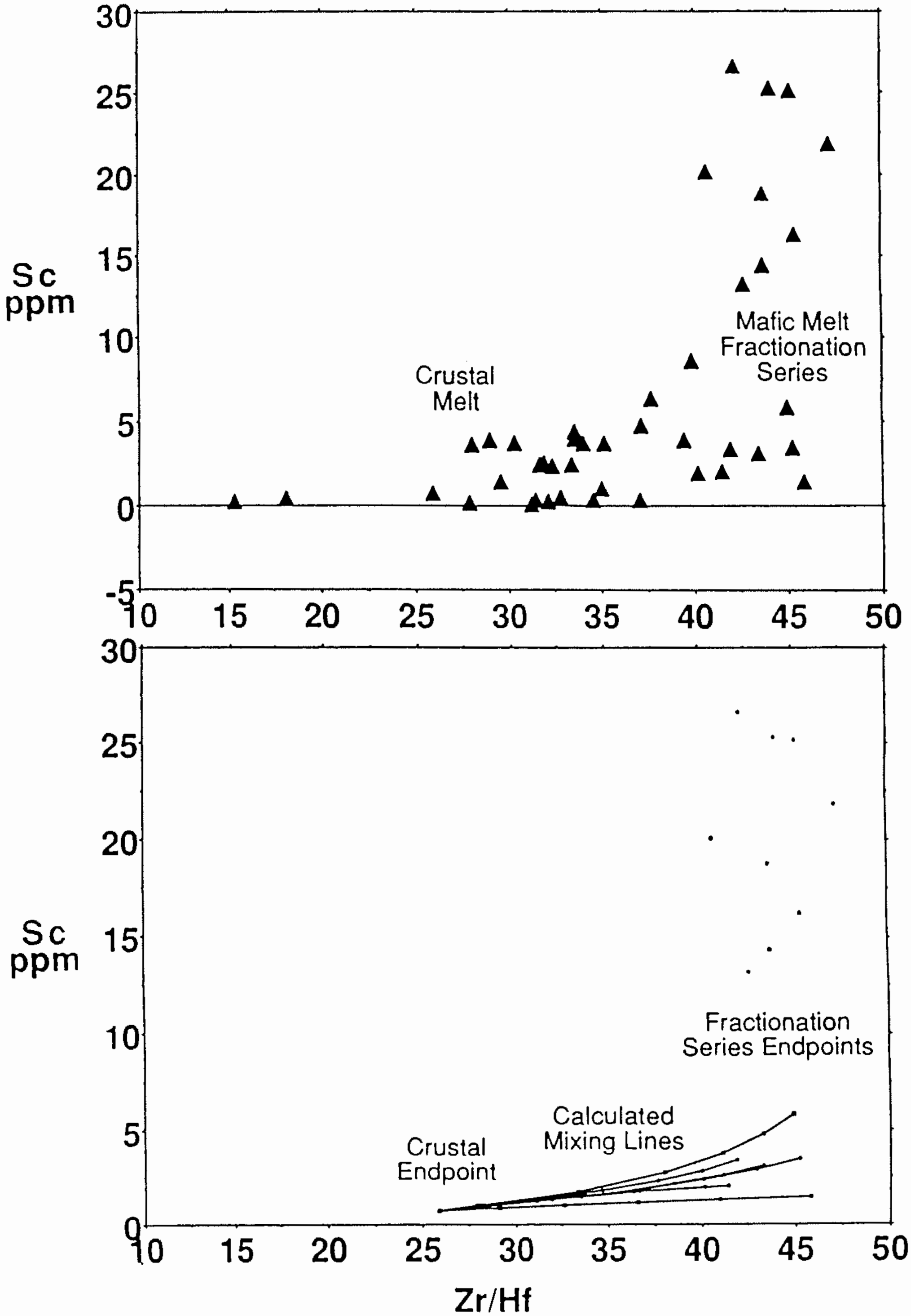

Figure 5. Plot of Sc ppm vs. Zr/Hf ratio. The diagram at the top shows plotted points for all analyzed samples of the Cape Ann plutonic complex. The bottom diagram is a plot of mixing trajectories between the crustal melt point and points of several melts being the likely candidates of the mafic parental magma. The latter formed by fractional crystallization of the alkali basalt melts. Samples with Zr/Hf ratio >40 represent alkali basalt melts and their fractionated descendents; melts with ratios<32 are of the anatectic crustal origin. Samples with intermediate ratios represent melts formed by mixing of mafic and silicic parental liquids. Note, that the calculated lines define a region occupied by all samples with the intermediate Zr/Hf ratios.

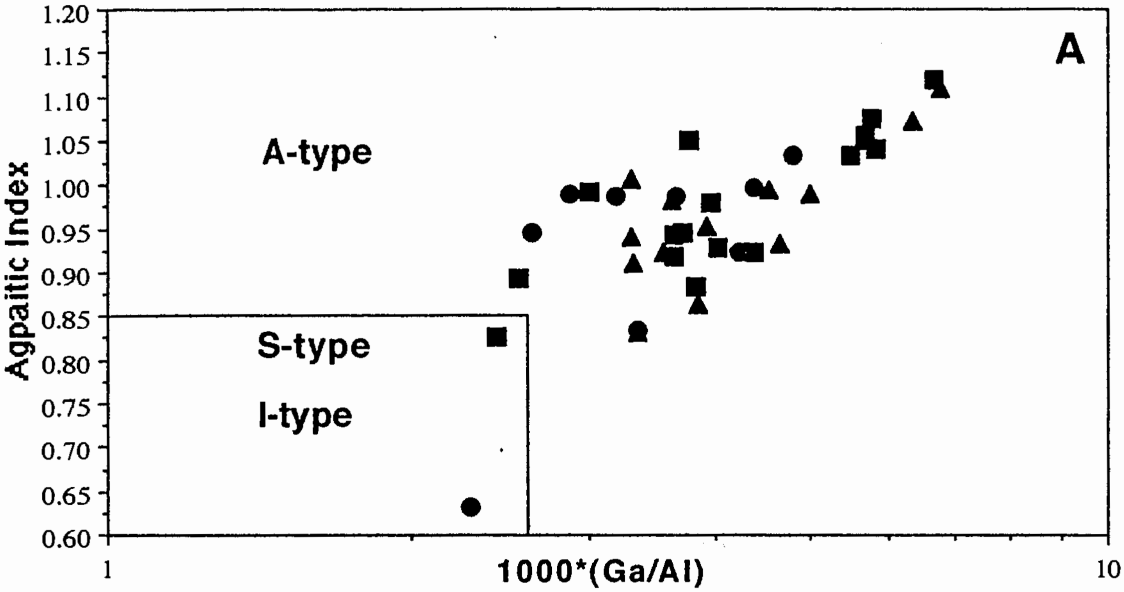

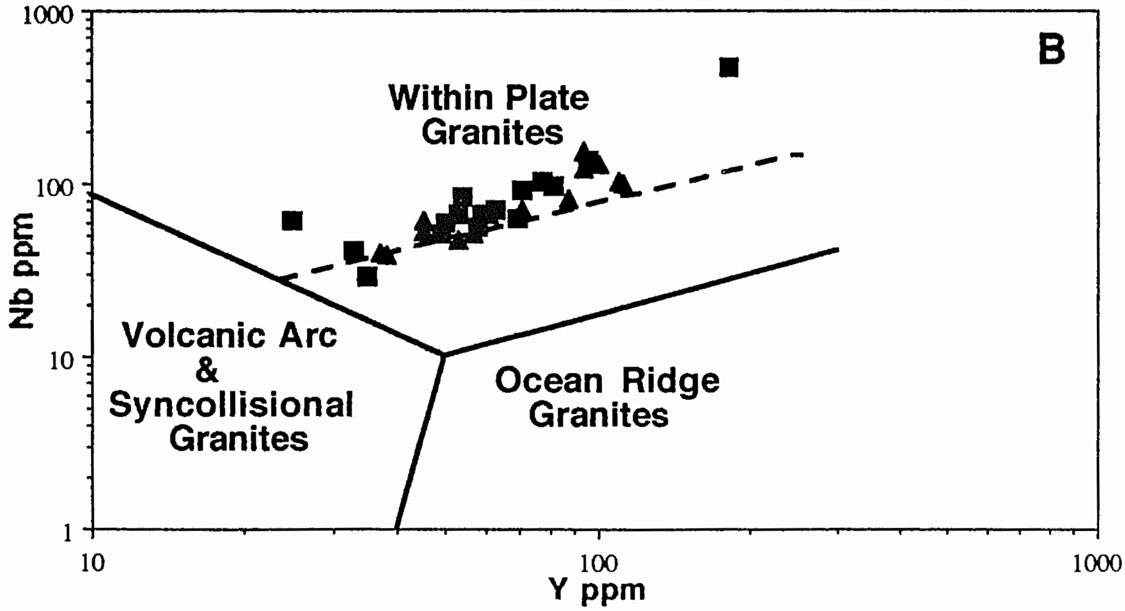

Figure 6. Top: The plot of Cape Ann granites and syenites on a discrimination diagram of agpaitic index ((Na+K)/Al] vs. 1000*Ga/Al (after Whalen et. al., 1987).

Bottom: Nb vs. Y tectonic discrimination diagram showing granites and syenites of the Cape Ann plutonic complex (after Pearce et al., 1984).

DISCUSSION AND CONCLUSION

The Cape Ann complex consists of crustally derived Cape Ann Granite and a suite of rocks that can be modeled as either the fractionation series of alkali basalts or by mixing of the Cape Ann Granite magma with the fractionation series. The Cape Ann Granite is a minimum granite clustering on the projected Q-Ab-Or diagram near a point within the water undersaturated domain. The origin of the granitic melt was likely under water deficient conditions resulting in a magma with crystallization temperatures exceeding the crest of alkali feldspar solvus. The origin of Squam Granite remains enigmatic and does not appear to be genetically related to the rest of the Cape Ann Complex.

SHARPNERS POND PLUTONIC SUITE

The Sharpners Pond Plutonic suite intrudes the metamorphic rocks of the Nashoba terrane near the northeastern terminus of the terrane in northeastern Massachusetts. The pluton extends from Wilmington (north of Boston) to the Atlantic coast and covers an area of approximately 300 km^2. The Sharpners Pond pluton can be divided based on the field observation into three different types of rocks, (1) an intermingled series with fine-grained gabbro mingled with biotite granites, (2) intermediate rocks consisting of diorite to tonalite, and (3) medium- to coarse-grained homogeneous cumulitic rocks, consisting of medium-grained gabbro through diorite. The Sharpners Pond pluton is intruded by an unnamed medium-grained biotite granite, labeled SGr on the Massachusetts geological map (Zen ed., 1983). Prior to 1964, the Sharpners Pond plutonic suite was correlated to rocks within the Boston Avalon terrane (Emerson, 1917). In 1964 the Sharpners Pond pluton was recognized as a separate unit (Castle, 1964). Castle (1965) named these rocks the Sharpners Pond "tonalite" and divided them into three separate, gradational phases: hornblende diorite phase, hornblende-biotite tonalite phase and a biotite tonalite phase. Since Castle (1964) often found all of the three phases within the same outcrop, he mapped the Sharpners Pond pluton according to the most abundant phase found in the outcrops.

Zircon dating performed by Zartman and Naylor (1984) yielded an age of 430 ±5 my for the Sharpners Pond pluton which is also the presumed age or younger for a biotite granite which occurs near the outlines of the Sharpners Pond complex (Wones and Goldsmith, 1991) and most likely it is related or de facto a member of the complex. The Sharpners Pond pluton intrudes felsic gneisses, the Fish Brook Gneiss, amphibolites, and metasediments of the Nashoba Formation (Castle, 1964). The age of the Fish Brook Gneiss yielded an emplecement age at 520 Ma and a metamorphic age at 425 ± 3 Ma (see more discussion in Chapter X, this volume).

PETROGRAPHY OF THE SHARPNERS POND PLUTON

INTERMINGLED GABBRO-BIOTITE GRANITE

This rock unit consists of a fine-grained gabbro intermingled with a medium-grained predominantly granitic rock (Loftenius, 1988). The gabbro is found commonly in magmatic pillows or as partly digested lumps with diffuse boundaries. About 70-80 % of the total rock unit consists of gabbro, but locally on a small scale the felsic rock may be more dominant. The intermingled unit is most often found near the borders of the Sharpners Pond pluton. Small irregular dikes containing intermingled gabbro and granite, often with plastically deformed contacts occur locally within the rocks of other types of the Sharpners Pond suite and within the adjacent country rocks. The major minerals in the mafic rock are zoned plagioclase and hornblende. Opaque minerals, biotite and quartz are minor minerals found in the mafic rocks. Accessory minerals consist of apatite and sphene. Up to three percent of sphene can be found in some partially altered dioritic rocks. Hornblende often contain a lighter core with a yellow-green pleochroism in the thin sections, surrounded by more iron rich hornblende with a green-brown pleochroism.

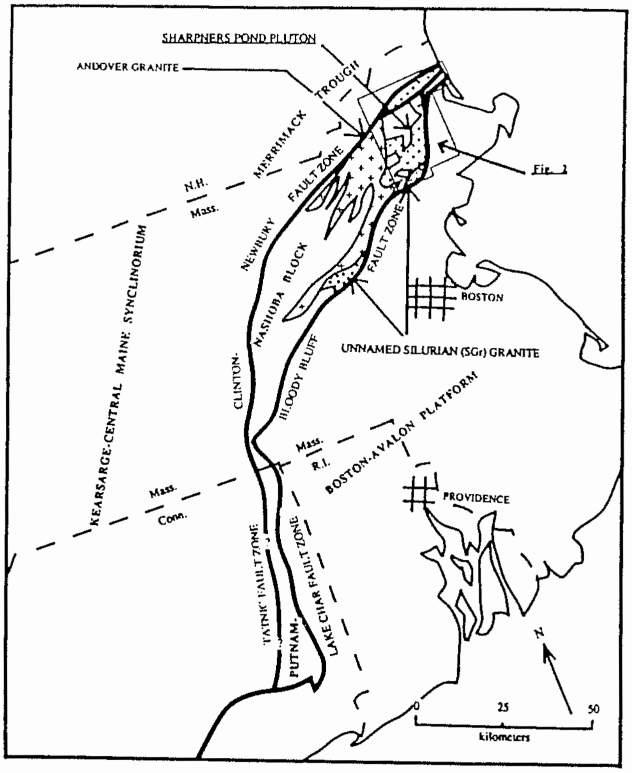

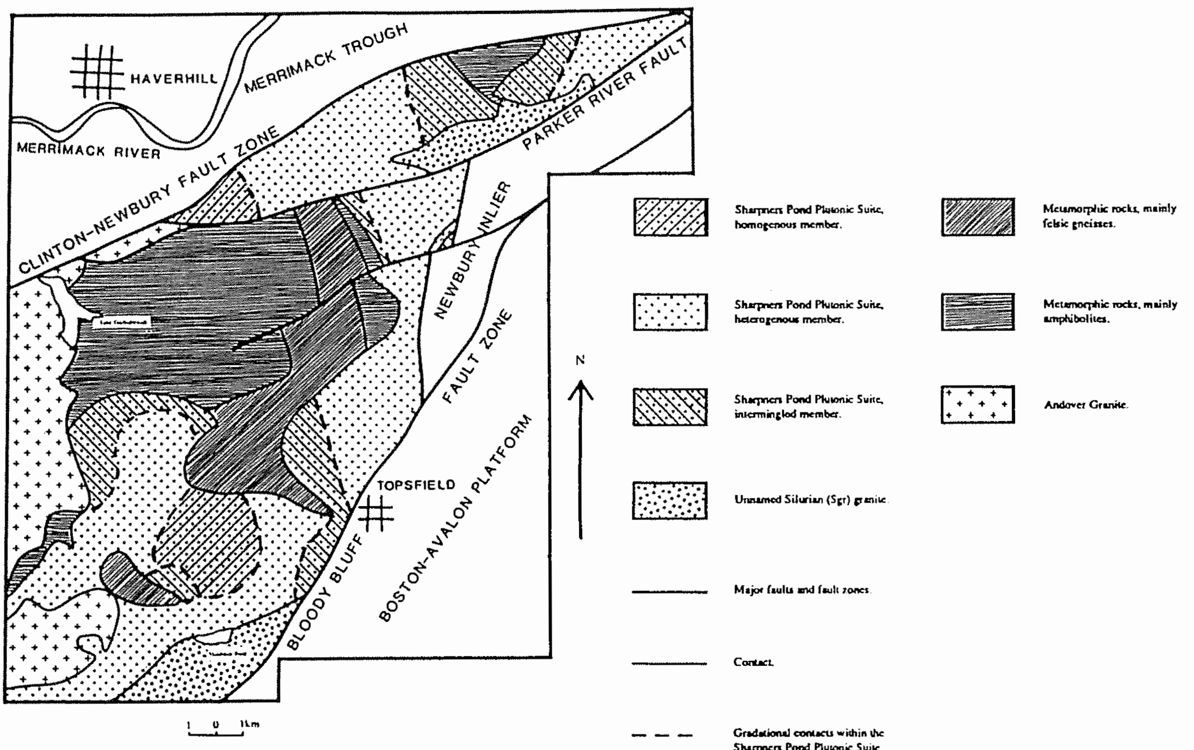

Figure 7. Top: Index map of the Sharpners Pond plutonic suite and its relation to the major terrane boundaries of SE New Engand.

Bottom: Detailed geologic map of the Sharpners Pond plutonic suite showing distribution of the principal petrologic types and the location of the unnamed biotite granite (SGR of the State Geologic Map, Zen, ed., 1983).

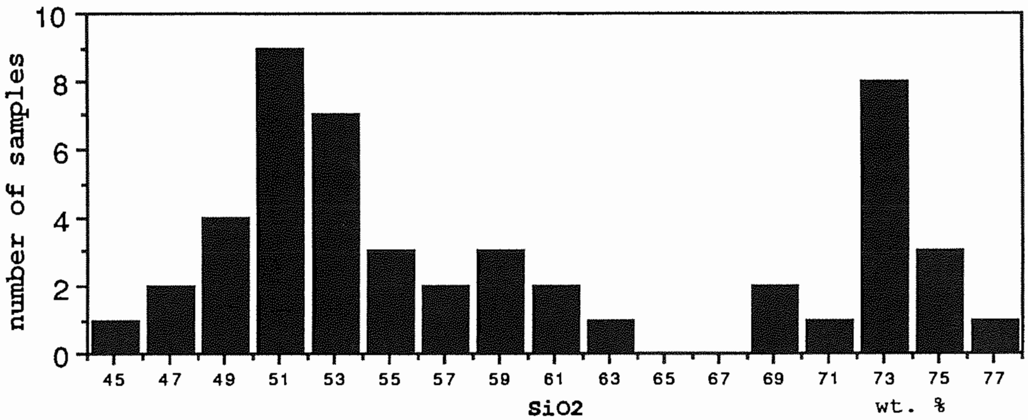

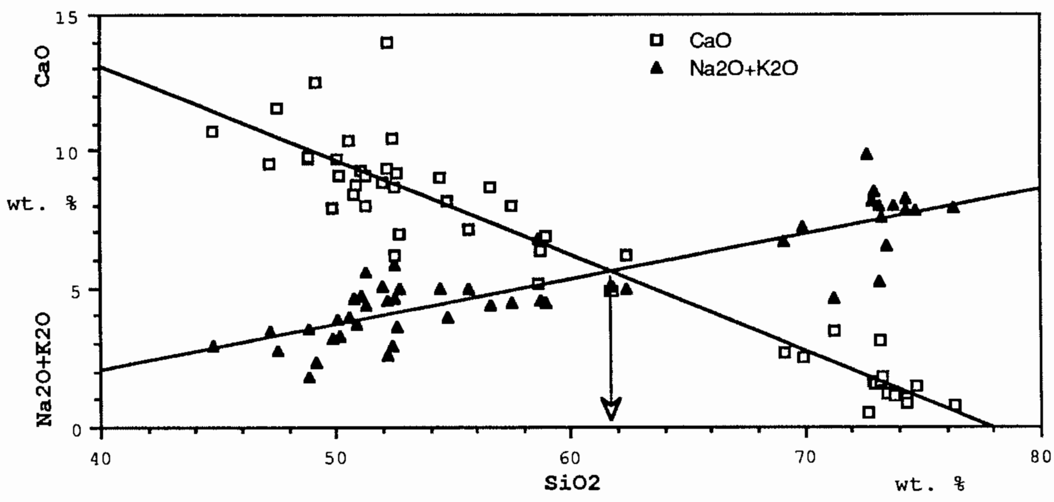

Figure 8. Top: Histogram of number of samples vs. SiO_2 wt. % of all analyzed samples of the Sharpners Pond plutonic suite. The number of samples represents a number of rocks that fall within 2 wt. % intervals in steps of even values of SiO_2 wt. %.

Bottom: Alkali - lime vs. SiO_2 wt. % of all analyzed rocks of the Sharpners Pond plutonic suite. This diagram is also known as the Peacock plot. The intersection of the trend lines defines a SiO_2 wt. % abundance that delimits the character of the suite. An intercept at 61 wt. % SiO_2 falls within the calc-alkali field.

The most characteristic feature of the fine grained dioritic rocks is the 1 to 2 mm wide glomerules of crystalloblastic hornblende crystals. These glomerules may locally contains remnants of plagioclase and quartz crystals in the center of the glomerules. Biotite occurs in all samples of the mafic rock but it is more common in the more silica-rich mafic rock. It forms subhedral interstitial grains but is also seen replacing hornblende.

The felsic rock consists mainly of plagioclase, quartz and biotite with locally larger amounts of sphene. The plagioclase crystals are unzoned and euhedral with interstitial subhedral-anhedral quartz and biotite. Sphene may occur as honey brown euhedral crystals in abundance near the contact to the mafic rock and could constitute up to 3% of the total rock. Apatite may occur as small needles (<0.1mm)in the biotite together with small grains of metamict zircon.

The hornblende porphyroblasts in the mafic rock have often been deformed giving the rock a weak lineation. This lineation is parallel with the longer axis of the magmatic pillows and partially digested mafic fragments. This deformation is not a result of a regional deformation, but was formed by a plastic flow during solidification. Unlike the mafic rock, the felsic rock show no sign of foliation, and its texture is unaffected by any later deformation.

HETEROGENEOUS INTERMEDIATE ROCKS

Heterogeneous diorite to tonalite comprise most of the Sharpners Pond pluton (Loftenius, 1988). There exist complex relationships within these rocks. The characteristic feature is a fine to medium grained quartz diorite to tonalite, containing rounded, elongated mafic inclusions of a gabbroic to dioritic composition (Loftenius, 1988). Compositional contrast between these two components varies from "ghost" outlines to well defined enclaves. Due to their heterogeneous nature, the rocks in thin sections consist of the same minerals but in different proportions depending on their respective place within the outcrop.

The major minerals are plagioclase, hornblende, biotite and quartz. Minor minerals consist of potassium feldspar, sphene, and magnetite. Apatite, zircon and allanite are accessory minerals. Clinozoisite, epidote, sericite and chlorite have formed through alteration of the primary mineral phases. In the mafic inclusions, plagioclase and hornblende are the dominant minerals and occur in approximately equal proportions. Plagioclase grains often show signs of chemical disequilibrium, documented by resorbed crystals with more sodic outer zones. Reverse and oscillatory zoning is observed, especially in rocks where mafic clots are common.

Hornblende has a brown-green pleochroism in the thin sections. The crystals are euhedral to subhedral. Biotite occurs abundantly, especially in the tonalitic parts where it may become the dominant mafic phase. It forms subhedral to anhedral grains that often had been altered to chlorite. This rock type is sometimes foliated which may in some places be strongly developed. Some of this foliation may be due to regional stress but alignment of undeformed plagioclase crystals in the thin sections point toward a flow induced crystal alignment. The alignment is commonly parallel with the borders of the Sharpners Pond pluton. Alteration has commonly transformed biotite to chlorite and plagioclase shows a cloudy sericitization and saussuritization. Hornblende is locally altered to chlorite.

HOMOGENEOUS GABBRO TO DIORITE

Homogeneous diorites are found mainly in the center of the pluton in the area northwest of the town of Middleton (Loftenius, 1988). This unit occurs also in the northeastern portions of the pluton. In the outcrops, this unit is characterized by its uniform grain size and mineralogical homogeneity. The grain size is approximately 2 to 4 mm, locally becoming even coarser.

The most common minerals in this units are plagioclase, hornblende and magnetite. Minor minerals are clinopyroxene, orthopyroxene, and very locally also quartz. The main accessory mineral is apatite, sphene and zircon may occur in small amounts. The plagioclase is usually unzoned but often contains saussuritized cores. This rock type is altered more commonly than the other rock types of the Sharpners Pond pluton, often to the point that the alteration has nearly obliterated the original mineralogy. The most common alteration products are chlorite, actinolitic hornblende, clinozoisite, epidote and sericite. Some samples show orthocumulate textures, but these rocks usually are among the most altered.

The orthocumulate texture grade into a hypidiomorphic-granular texture when approaching the more heterogeneous domains of the Sharpners Pond pluton. Rocks with this texture consist of euhedral plagioclase and subhedral hornblende and usually lack clinopyroxene cores in the hornblende.

UNNAMED BIOTITE GRANITE (SGR GRANITE OF THE STATE GEOL. MAP)

The unnamed medium-grained biotite granite occurs on the southeast side of the pluton along the Bloody Bluff fault zone. Biotite granite, identical to the unnamed granite, is also found in small intrusions within the Sharpners Pond pluton (Loftenius, 1988). These intrusion may locally contain magmatic pillows of a fine-grained basalt.

The granite is composed by equal amounts of plagioclase, quartz and microcline. Minor minerals are biotite and opaque minerals. Apatite, zircon, allanite and sphene are the accessory minerals. A leucotonalite occurring occasionally within the granite may locally show cumulate textures with euhedral plagioclase surrounded by subhedral-anhedral biotite and anhedral quartz.

The Sharpners Pond pluton is sometimes intruded by aplites and less often by biotite granite pegmatite. The aplite and the pegmatite has the same mineralogy as the biotite granite. The grain size is less than 0.1 mm but plagioclase crystals may form 1-3 mm large phenocrysts. These plagioclase phenocrysts contain a calcic, irregular core which is clouded by alteration products.

GEOCHEMISTRY

The scarcity of rocks containing between 63% wt and 69% wt SiO_2 strongly indicates that the felsic portions of Sharpners Pond pluton did not form through a continuos fractional crystallization (Loftenius, 1988). Samples with less than 53% wt SiO_2 show a large variation in MgO, Cr and Ni, which separate them from the rocks containing more than 53% wt SiO_2. These rocks also often contain cumulate textures in the medium-grained gabbros and diorites which also separate them from the more silicic rocks. Four different series of rocks can then be correlated with each other geochemically:

(a) Mafic rocks with less than 53% wt SiO_2. The mafic rocks have a large variation in MgO, Cr and Ni, indicating crystallization of olivine(?) and pyroxenes and removal of Mg and Ni by olivine(?) and Cr by pyroxenes. The occurrence of euhedral plagioclase also indicate crystallization of plagioclase as well. The homogeneous gabbro and the mafic rocks in the intermingled rocks of the Sharpners Pond pluton are part of this group.

(b) Intermediate rocks with more than 53 % wt SiO_2 and less than 65 % wt SiO_2. The intermediate rocks show a linear variation of the major elements (except TiO_2) with SiO_2. The linear relationship between the major elements and SiO_2 indicate a mixing relationship between the mafic and felsic magmas. found in the Sharpners Pond pluton.

(c) Granites with more than 65% wt SiO_2 and more than 2.5% wt of K_2O.

(d) Leucotonalites with more than 65% wt SiO_2 and less than 2.5% wt K_2O. The leucotonalites are found occasionally together with the biotite granite.

MAFIC ROCKS

The mafic rocks are characterized by large variation of MgO and to a lesser degree of CaO. The magnesium numbers vary from 0.7 to 0.5. Of the trace elements Cr and Ni show the largest variations where the magnesium richest rocks have also the highest Cr and Ni abundances. Magma modeling by using the routines described by Conrad (1987) indicate that this series have evolved through Rayleigh fractional crystallization of olivine, clinopyroxene and plagioclase. Crystallization of 40% olivine, 20% clinopyroxene and 40% plagioclase gives approximately the best fit for the trends in the variation diagrams (Conrad and Kay, 1983; Green, 1981; Snoke et. al. 1981). The increase in V seems to rule out any crustal assimilation or magma mixing since the increase of Ti and V correlate with the decreasing MgO. The large variation in Cr and Ni together with the rather uniform content of the immobile incompatible elements (Y, Zr, Nb, heavy lanthanides, Hf and Ta) also rules out open system crystal fractionation with continuous magma replenishment. The elevated concentration of Al_2O_3 and fairly low amount of Ti and high field strength ion elements indicate these rocks are similar to high alumina basalts found at destructive

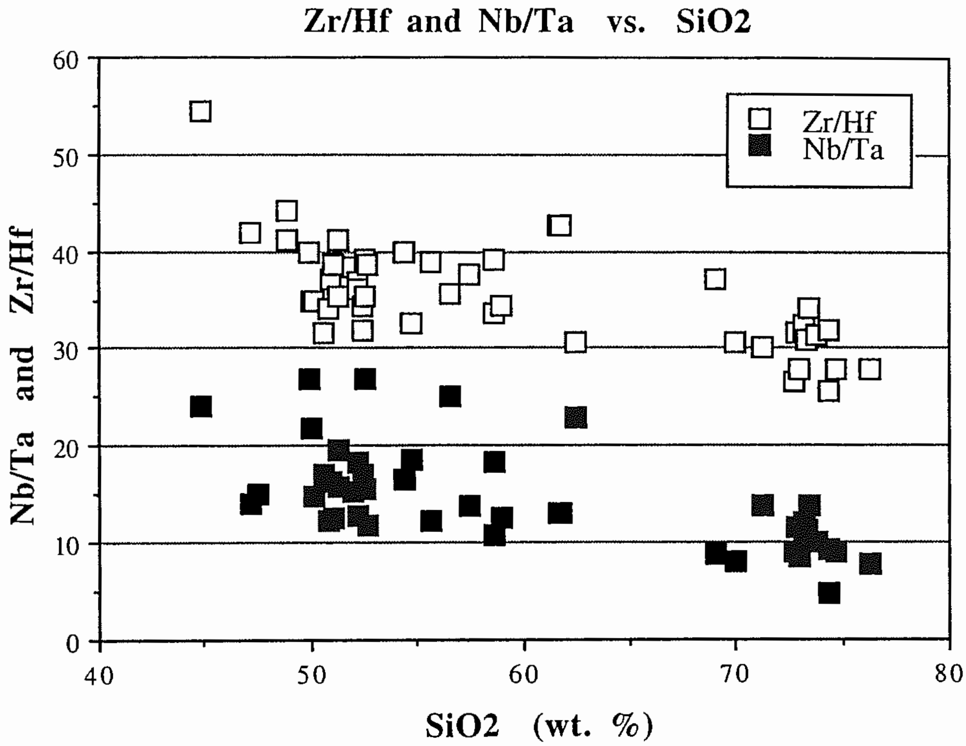

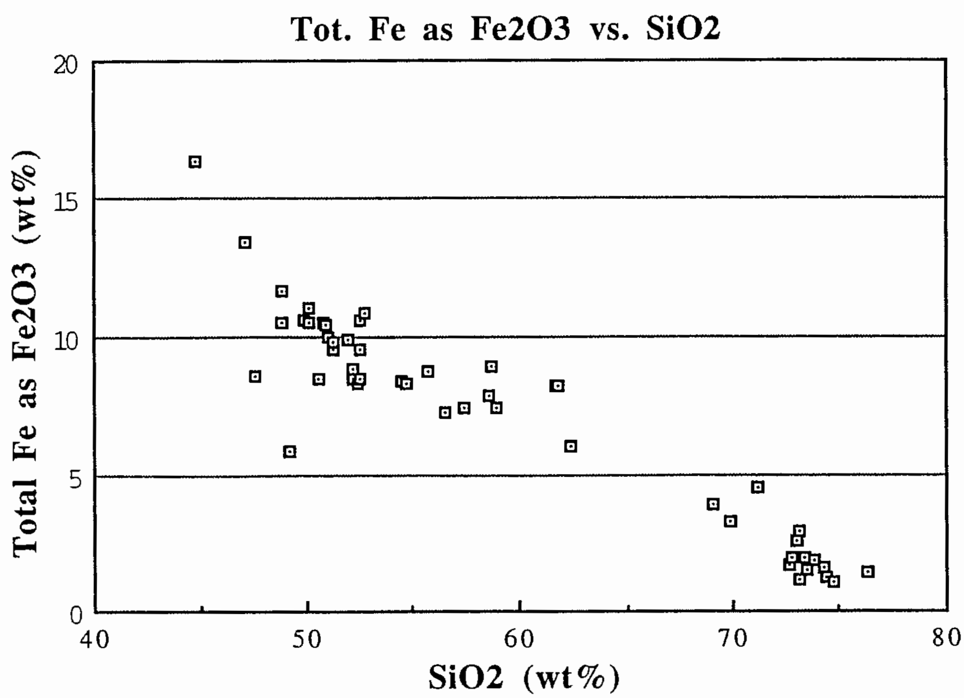

Figure 9. Top: Plot of Zr/Hf and Nb/Ta ratios vs. SiO_2 wt. % for rocks of the Sharpners Pond plutonic suite. The granites have lower values than the mafic and intermediate types. The granites formed as anatectic melts (both ratios have crustal values) whereas the mafic types approximate the typical upper mantle values.

Bottom: Plot of total Fe as Fe_2O_3 vs. SiO_2 wt % for rocks of the Sharpners Pond plutonic suite. The trend shows the granitic and basaltic magmas as end members for the intermediate series.

plate margins (Basaltic Study Project, 1981; Green, 1980). Tectonic discrimination diagrams presented by Loftenius (1988) also indicate that these rocks are related to high alumina basalts. These diagrams indicate that these rocks are of the same type as the calc-alkali basalts found in association with andesites-dacites-rhyolites in modern destructive continental margins.

INTERMEDIATE ROCKS

The intermediate rocks have a silica content between 53% wt SiO_2 and 65% wt SiO_2. These rocks are characterized by disequilibrium textures with reverse and oscillatory zoned plagioclase, two different types of plagioclase where one type is more zoned than the other, resorbed crystals and overgrowths of hornblende on plagioclase and quartz etc. The intermediate rocks are characterized by linear trends in most variation diagrams. These linear trends are interpreted as mixing lines between a mafic magma and a felsic magma. Evidence for this mixing are abundant as mentioned above in the petrographic description. No fractionation of any major minerals seems to have taken place in the intermediate series. In a study by Frost and Mahood (1987), authors came to a conclusion that magmas with a silica content above 63% wt SiO_2 are not likely to form. Instead co-mingling would be more likely process for magma chambers containing abundant felsic magma and small amounts of mafic magma. This is in agreement with the data from the Sharpners Pond pluton where rocks containing between 65-69% wt SiO_2 are virtually absent.

GRANITES

Granites are the most common felsic rocks. Characteristic for the granites is the absence of muscovite and commonly red colored potassium feldspar. Quartz, oligoclase and microcline are the most common minerals. Biotite constitutes the only ferromagnesian phase in these rocks. Homogeneous plagioclase cores indicate some restite material (Noyes et. al., 1983) in the granodioritic-granitic series. The source rock may be weakly corundum normative but minimum melt I-granites may also be weakly corundum normative (White and Chappell, 1977). A likely source rock is a biotite gneiss possibly containing hornblende. The negative europium anomalies indicate a plagioclase-rich restite. The protolith may most likely be a metasedimentary rock consisting mainly of volcanogenic material mixed or interlayered with small amounts of pelitic material. Some of the biotite gneisses in the Nashoba terrane such as the Fish Brook Gneiss may be likely candidates (Bell and Alvord, 1976). The relatively high abundances of heavy lanthanides point also to a restite that does not contain garnets nor hornblende(Loftenius, 1988).

LEUCOTONALITES

The leucotonalites are far less abundant than granites. A possible origin for some of the leucotonalite is through partial melting of an amphibolite (Gromet and Silver, 1987). The amphibolites such as the Boxford Member of the Nashoba Formation or similar amphibolites at depth are possible candidates as the source materials. Locally, very small amounts of leucotonalite has been observed in the amphibolites of the Boxford Member, adjacent to the intrusion of the rocks belonging to the Sharpners Pond pluton.

THE TECTONIC SETTING FOR THE SHARPNERS POND PLUTON AND THE BIOTITE GRANITE.

The mafic rocks appears to be related to the calc-alkali basaltic province formed at a destructive continental margin. The Newbury volcanics is a block of volcanic and sedimentary rocks found in the area east of the Sharpners Pond pluton. The sedimentary rocks were paleontologically dated as Upper Silurian (Shride, 1976) and the volcanics have been determined (Hon and Thirwall, 1985) to have formed at a destructive plate margin. The similarity in chemistry (Hon pers. comm.) and proximity in time of formation of the Newbury Volcanics (Shride, 1976) with some of the plutonic rocks in the Nashoba terrane may indicate a genetic relationship. Paige and Hon (1988) argue for an eastward dip of a subduction zone under the Avalonian microcontinent. Perhaps, the Sharpners Pond plutonic suite is a core of a continental island arc and the Newbury basin is a sliver of the arc that was proximal to the Boston Avalon terrane.

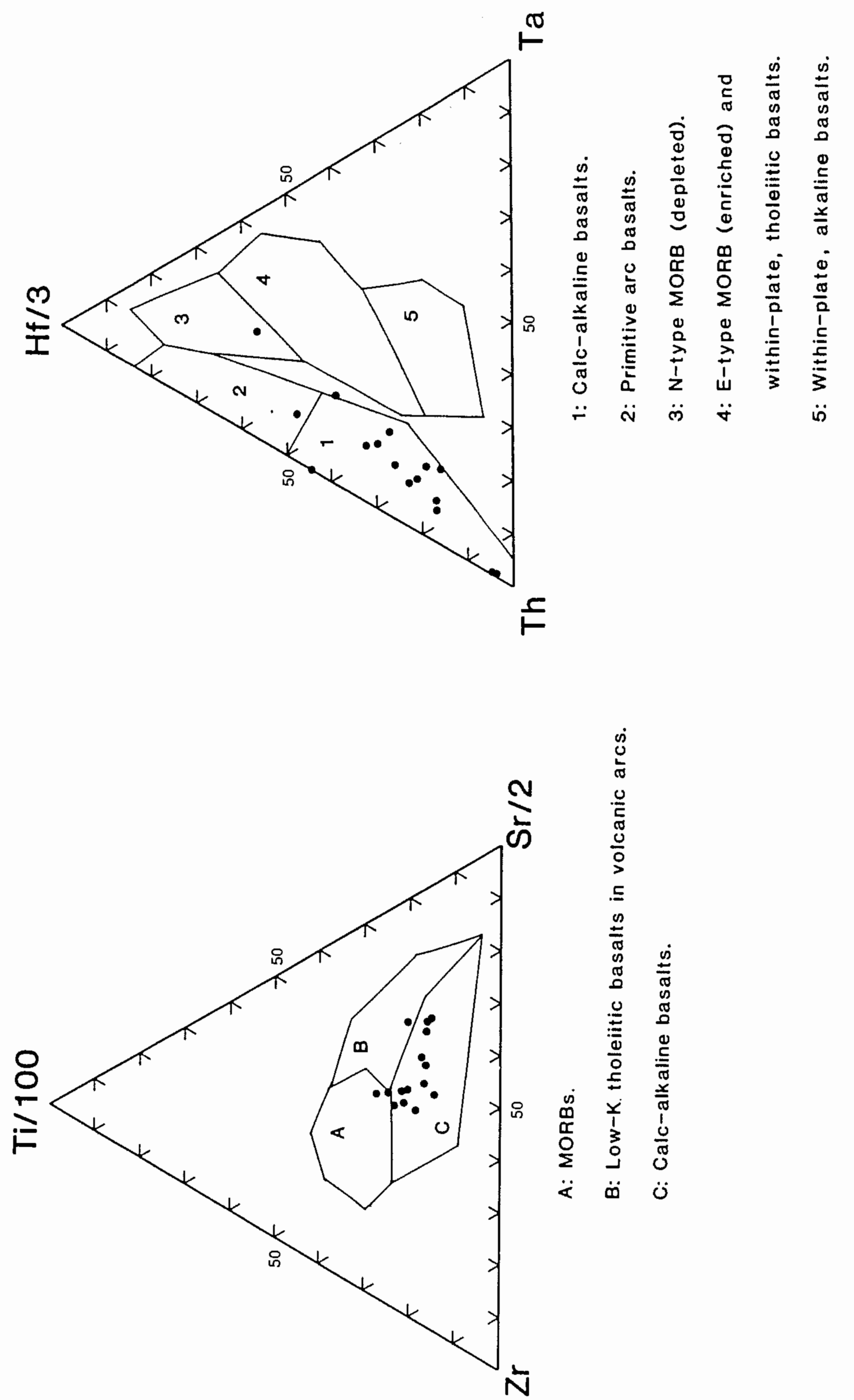

Figure 10. Top: Hf/3 - Th - Ta tectonic discrimination diagram for mafic rocks of the Sharpners Pond plutonic suite (after Wood 1980).

Bottom: Ti/100 - Zr - Sr/2 tectonic discrimination diagram for mafic rocks of the Sharpners Pond plutonic suite (after Pearce and Cann, 1973).

CONCLUSIONS

The evolution of the four different geochemical groups could be characterized as interaction of mafic, mantle derived magma with the rocks of the middle to upper crust. A high alumina basalt that was formed in a destructive margin along the west side of the Avalonian microcontinent intruded in the mid to upper part of the crust, forming the homogeneous gabbro-diorite and the fine-grained gabbros in the intermingled gabbros and granites. The heat given off by this mafic magma caused partial melting of the crust.

The mafic rocks evolved through fractional crystallization, and crystallized primarily olivine and pyroxene. The partially melted crustal rocks in the crust formed mainly granitic magma and lesser amounts of leucotonalitic magma. These felsic magmas intermingled with high alumina basalt magmas and formed the intermingled gabbros and granites near the borders of the Sharpners Pond pluton. The lower temperatures near the borders of the pluton prevented a complete mixing of the mafic and felsic magmas. Cr and Ni poor, evolved mafic magmas of the mafic series, however, mixed with the felsic magma and formed the intermediate rocks of the Sharpners Pond plutonic suite.

The evolution of the Sharpners Pond pluton is similar to a model for calc-alkaline rocks proposed by Grove and Baker (1984) who argue for olivine, plagioclase and clinopyroxene fractionation to take place in mafic calc-alkaline rocks. Rocks evolved through this fractionation may continue to fractionate plagioclase, orthopyroxene, pigeonite, augite and magnetite (Grove and Baker, 1984). This later fractionation process was not important in the Sharpners Pond pluton but observed hypersthene and magnetite accumulations indicate that some of these minerals have crystallized in the late stages of the evolution of the mafic series. Grove and Baker (1984) also point out the importance of input of crustal material either by assimilation or mixing with felsic magmas during the evolution of calc-alkaline rocks, which is well illustrated within the Sharpners Pond pluton, in which magma mixing between mantle-derived magma and crust-derived magmas played an important role in the evolution of the pluton. There was a continued formation of felsic magma after most of the activity of the mafic magma had subsided. This continued formation of felsic magma might have been the cause for the intrusions of the biotite granite near the perimeter of the pluton. The presence of mafic magmas is documented by sparse magmatic pillows near the contacts of the biotite granite and the related small intrusions of biotite granites.

CONCLUDING REMARKS AND EPILOGUE

Data and discussions presented in this paper were kept limited to either the Cape Ann plutonic complex or the Sharpners Pond series. In this regard, the petrogenesis of the two different plutonic suites, each in its own right a prominent magmatic complex, may be seen as separate entities related in time and possibly in space, but otherwise viewed as events accidental to each other. It might perhaps be appropriate to reflect and contrast both of these events as processes that occur within the crust irrespective of the nature of the intruding basaltic magma. In both instances, there is an overwhelming evidence that points toward petrogenetic processes which are virtually identical yet one suite is designated as the I-type and the other as the A-type. In the case of the Cape Ann complex, an alkali basalts interacts with the crust and initiates an anatectic event leading to a formation of felsic magmas. These magmas are undersaturated with respect to water and are characterized by a very low oxygen fugacity, but compositionally they are not so different from the felsic magmas formed by anatexis within the Sharpners Pond suite.

There are, of course, differences in their mineralogical make up, but these can be understood as consequential to crystallization temperatures. Water saturated magmas will crystallize at lower temperatures, under a regime where liquidus intersects the feldspar solvus. Water undersaturated magmas will crystallize at higher temperatures, above the feldspar solvus hence the difference between the hypersolvus and subsolvus mineralogy. Other differences include Fe enriched biotites and amphiboles.

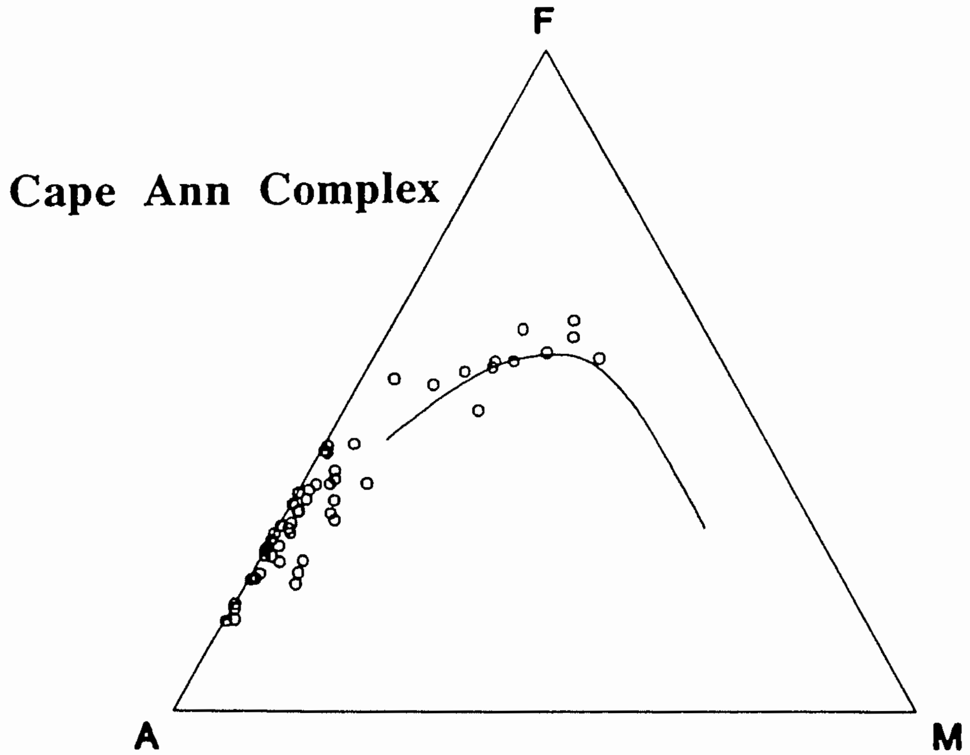

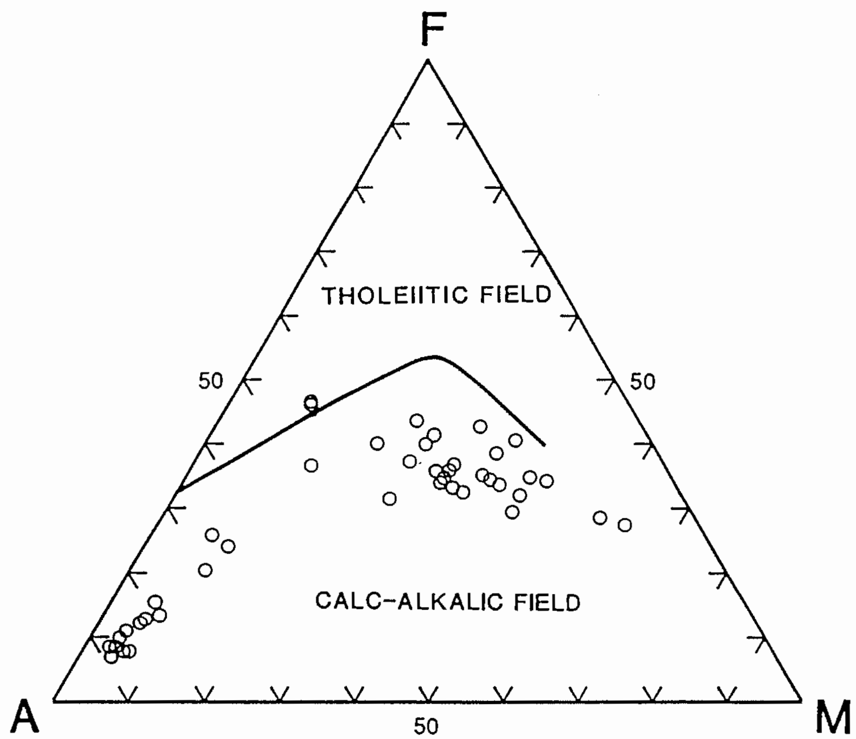

Figure 11. Top: Ternary FMA (alkalis-FeO-MgO) diagram of all analyzed rocks of the Cape Ann plutonic complex
Bottom: Ternary FMA (alkalis-FeO-MgO) diagram of all analyzed rocks of the Sharpners Pond plutonic suite.

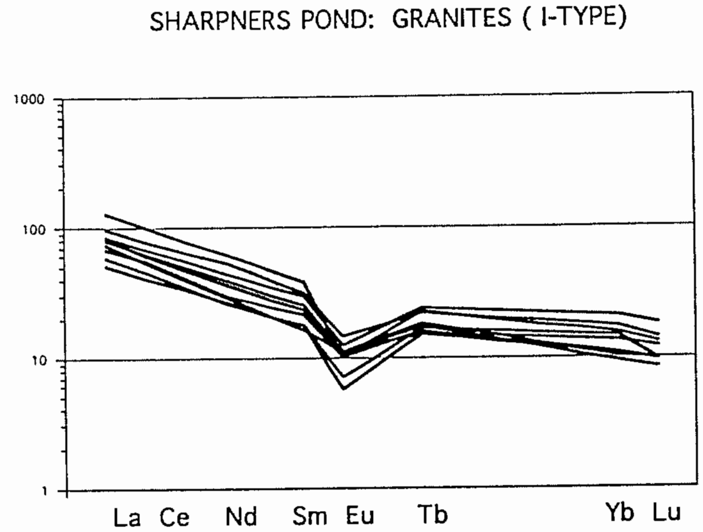

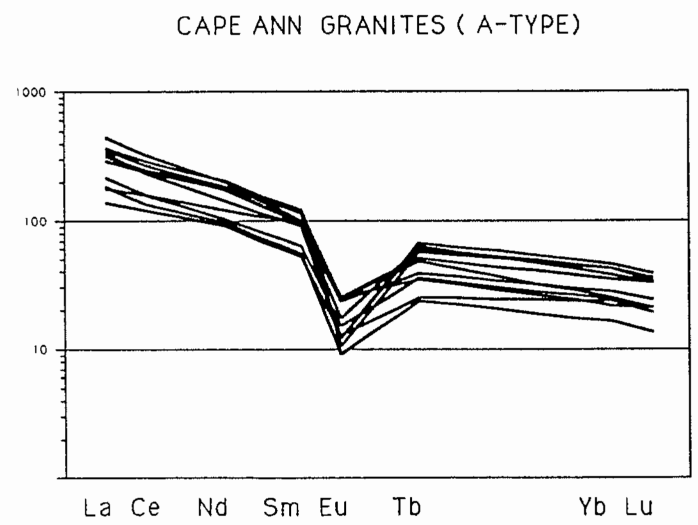

Figure 12. Top: Chondrite normalized plot of rare earth elements in rocks of the Sharpners Pond plutonic suite. Bottom: Chondrite normalized plot of rare earth elements in rocks of the Cape Ann plutonic complex..

But there are also surprising similarities. For instance, both types of the anatectic melts have essentially the same Zr/Hf ratio. Major element geochemical compositions are also very similar. Their REE plots are very similar as well (Fig. 12). The Cape Ann granites REE patterns have just a little bit higher absolute abundances with a little deeper Eu anomalies than the corresponding REE patterns for the Sharpners Pond granites. The Eu anomaly differences probably reflect differences in their oxygen fugacities tilting the balance in favor of Eu +2 and allowing feldspars to accommodate more Eu on their lattices. Overall higher abundances of REE in the Cape Ann granites is due to either lower degree of partial melting or higher temperature. But what strikes most is that their relative REE distributions (except for Eu) are once again nearly identical.

In closing, the formation of the granitic melts is perhaps not so enigmatic. However, it is the magmas that provides the heat source to which our attention should be turned to and to the mechanism by which the initiating and anatectic melts interact.

REFERENCES

Arculus R. J., Wills K. J. A., 1980: The petrology of plutonic blocks and inclusions from the Lesser Antilles island arc, Jour. Petrol., v. 21, p. 743-799.

Barosh P.J., 1984a: Regional geology and tectonic history of southeastern New England, in Hanson S.L. ed.: New England Intercoll. Geol. Conf. 76th ann. meeting, Salem State College, Salem, Massachusetts, p. I-1 to I-35.

Barosh P.J., 1984b: The Bloody Bluff Fault System,_in_ Hanson S.L. ed.: New England Intercoll. Geol. Conf. 76:th ann. meeting, Salem State College, Salem, Massachusetts, p. 310-324.

Basaltic Study Project, 1981: Basaltic volcanism on terrestrial planets., Pergamon Press, Inc., New York, 1286 pp.

Bell K.G., Alvord C.A., 1976: Pre-Silurian Stratigraphy of northeastern Massachusetts, Geol. Soc. Am. , memoir 148, p. 179-216.

Bowen, N.L., 1928: The Evolution of the Igneous Rocks. Princeton University Press, Princeton, N.J.

Tuttle, O.F., Bowen, N.L., 1958: Origin of Granite in the Light of Experimental Studies in the System $NaAlSi_3O_8$-$KAlSi_3O_8$-SiO_2-H_2O. Geological Socirty of America, Memoir 74.

Buma G., Frey F. A. and Wones D. R., 1971: New England granites: Trace element evidence regarding their origin and differentiation, Contrib. Mineral. Petrol., v. 31, p. 300-320.

Carmichael D. M., 1969: On the mechanism of prograde metamorphic reactions in quartz-bearing pelitic rocks, Contrib. Miner. Petrol., v. 20, p. 244-267.

Carmichael I. S. E., Turner F. J., Verhoogen J. ,1974: Igneous Petrology, McGraw-Hill publishing co., New York.

Castle R.O., 1964: Geology of the Andover Granite and surrounding rocks, Massachusetts, U.S. Geological Survey open file report #64-33.

Castle R.O., 1965a: A proposed revision of the subalkalic intrusive rocks of northeastern Massachusetts, U. S. Geological Survey, prof. papers 525-C, p. C:74-80.

Conrad W. K., 1987: A FORTRAN program for simulating major- and trace-element variations during Rayleigh fractionation with melt replenishment or assimilation, Computers and Geosciences, v. 13, no 1, p. 1-12.

Conrad W. K. and Kay R. W., 1983: Ultramafic and mafic inclusions from Adak Island: crystallization history and implications for the nature of primary magmas and crustal evolution in the Aleutian Arc., Jour. Petrol., v. 25, part 1, p. 88-125.

DePaolo D. J., 1981: Trace element and isotopic effects of combined wallrock assimilation and crystal fractionation, Earth Planet. Science Lett., v. 53, p. 189-202.

Dennen W.H., 1981: Bedrock geology of the Cape Ann area, Massachusetts: U.S. Nuclear Regulatory Commission Rept. NUREG/CR-088, 83 p.

Emerson B. K., 1917: Geology of Massachusetts and Rhode Island, U.S. Geological Survey, bull. v. 597

Frost T. P., Mahood G. A., 1987: Field, chemical and physical constraints on mafic-felsic magma interaction in the Lamarck Granodiorite, Sierra Nevada, California., Geol. Soc. Am. Bull., v. 99, p. 272-291.

Green T. H., 1980: Island arc and continent-building magmatism - a review of petrogenic models based on experimental petrology and geochemistry., Tectonoph., v.63, p. 367-385.

Gromet L. P., Silver L. T., 1987: REE variations across the Peninsular Ranges batholith: implications for batholithic petrogenesis and crustal growth in magmatic arcs, Jour. Petrol., v. 28, p. 75-125.

Grove T. L., Baker M. B., 1984: Phase equilibrium controls on the tholeiitic versus calc-alkaline differentiation trends., JGR, v. 89, no B5, p. 3253-3274.

Gust D. A. and Johnson R. W., 1981:Amphibole bearing inclusions from Boisa Island, Papua New Guinea: evaluation of the role of fractional crystallization in an andesitic volcano, Jour. Geol., v. 89, p. 219-232.

Hanson G. N., 1978: The Application of Trace Elements to the Petrogenesis of Igneous Rocks of Granitic Composition., Earth and Planet. Science Lett., v. 38, p. 26-43.

Hon R. and Thirlwall M. F., 1985: Newbury Volcanics-a late Silurian island arc (?), Geol. Soc. Am., Abstracts with Programs, v. 17, p. 25.

Loftenius C.J., 1988: The Geochemistry and the Petrogenesis of the Sharpners Pond Plutonic Suite, NE Massachussetts, MS Thesis, Boston College, 284 pp.

Noyes H. J., Wones D. R. and Frey F. A, 1983: A tale of two plutons: petrographic and mineralogic constraints on the petrogenesis of the Red Lake and Eagle Peak Plutons, central Sierra Nevada, California, Jour. Geol., v. 91, p. 353-379.

O'Hara M. J., 1977: Geochemical evolution during fractional crystallization of a periodically refilled magma chamber, Nature, v. 266, p. 503-507.

Olszewski W.J., 1980: The geochronology of some stratified metamorphic rocks in northeastern Massachusetts, Can. Jour. Earth Sci., v.17 p. 1407-1416.

Paige M.L., and R. Hon, 1988: Geochemical Study and Tectonic Setting of the Cape Ann Complex, Northeastern Massachusetts, Northeastern Geol. Soc. Am., Program with Abstracts, p. 60.

Shride A.F., 1976: Preliminary map of bedrock geology in the Newburyport East and West quadrangles, Massachusetts-New Hampshire, U. S. Geological Survey, open file report #76-488

Snoke A. W., Quick J. E. and Bowman H. R., 1981: Bear Mointain Igneous Complex, Klamath Mountains, California: an ultrabasic to silicic calc-alkaline suite., Jour. Petrol., v. 22, part 4, p. 501-552.

Wones, D.R. and Goldsmith,R., 1991 : Intrusive Rocks of Eastern Massachusetts: in The Bedrock Geology of Masachusetts, US Geol. Survey Professional Paper 1366-I, p. I1-I61.

Watson E. B. and Jurewicz S. R., 1984: Behavior of alkalies during diffusive interaction of granitic xenoliths with basaltic magma, Jour. Geol., v. 92, no 2, p. 121-131.

White A.J.R., Chappell B.W., 1977: Ultrametamorphism and granitoid genesis, Tectonoph., v. 43, p. 7-22.

Zartman R.E.and Marvin, R.F, 1991 : Radiometric Ages of Rocks in Massachusetts: in The Bedrock Geology of Masachusetts, US Geol. Survey Professional Paper 1366-J, p. J1-J19.

Zartman R.E.and Naylor R. S., 1984 : Structural implications of some radio metric ages of igneous rocks in southeastern New England: Geol. Soc. Am. Bull. v. 95, p. 522-539.

Zen E-an, ed., 1983: Bedrock geologic map of Massachusetts, U. S. Geological Survey, scale 1:250 000.

ROAD LOG - DAY 1

CAPE ANN PLUTONIC COMPLEX

From Boston take Rte I-93 north to Rte 128 north. Take Exit 25A (Rte 114 east) towards Salem.

0.0 Begin road log at the stop sign at the end of the ramp.
0.4 Rt. 114 sharp left turn
0.5 Rt. 114 sharp right turn
1.0 Intersection Rt. 135, Bear to right. Continue on Rt. 114
1.4 Enter the Town of Salem
2.3 Exit Rt. 114 onto Rt. 107 north towards Beverly and Rt. 1A
2.9 Intersect Rt. 1A. Continue straight.
3.1 Turn right onto Webb street
3.4 Turn left onto Essex St.
3.6 Turn left into Collins Cove Condominiums, park to the left. Walk through the development to exposures along the shoreline facing Collins Cove.

STOP 1-1. SALEM NECK - MAGMATIC PILLOWS (Salem, MA; 30 minutes). Magmatic pillows of alkali basalt and its fractionates in hypersolvus syenitic host. The outcrop contains multiple exposures of magmatic pillows. The composition of the pillows is variable, but is predominantly alkaline basalt. Access to the outcrop is to the left around the condominiums. The outcrop extends along the cove coast to the north. The exposures near and around Salem Neck show an abundant evidence of coexistence of two melts. (Samples: SN-2, SN-3, Table 1)

3.6 Return to street and turn left onto Essex St. Turn left onto Memorial Drive
3.9 Park to the right near powerlines.

STOP 1-2. (Optional). SALEM NECK - MAGMATIC PILLOWS (Salem, MA; 15 minutes). Walk up the clear-cut area under the powerlines and examine the bedrock exposures. This is another example of predominantly alkaline basaltic magmatic pillows and associated syenite. (SN-4).

3.9 Continue up the road.
4.2 Turn right by athletic fields.
4.3 Intersection: Turn to the right and then immediately left onto road opposite to the one has left.
4.35 Turn left at the stone wall.
4.6 Entrance to Winter Island Park. Enter park and park to the left.

STOP 1-3. SALEM NECK - MAGMATIC PILLOWS IN A SYENITIC HOST (Salem, MA; 25 minutes).
Excellent exposure along the coast line. Traverse counter clockwise around lighthouse point (sample SN-6, Table 1).

4.6 Entrance of Winter Island Park.
4.9 Turn left and then immediately left into the parking area of Cat Cove Marine Lab.

STOP 1-4. (optional) SALEM NECK - MAGMATIC PILLOWS IN A SYENITIC HOST (Salem, MA; 25 minutes).
Several pillow compositions, excellent exposure along the coast line. (Get permission from Cat Cove Labs before proceeding to the shore line. No Sampling).

4.9 Turn left at entrance into the Marine Lab.
5.4 Road bears to the right onto Fort street.
5.8 Turn right onto East Collins Street.
6.1 Turn left onto Lathrop Street
6.2 Turn right onto Rt. 1A north (Bridge Street).
6.6 Cross waterway.
6.9 Bear to the right onto Rt. 22 (Cabot Street).

7.3 Turn right onto Rt. 127 north (Lathrop Street).
8.1 Turn left onto Hale Street, continue following the signs for Rt. 127 north.
12.8 Turn right after red fire hydrant through stone wall onto Boardman Ave (Private way).
13.1 Park to the right and walk up the drive way to Chubb point. Permission is required to access the coast from the owners.

STOP 1-5. BEVERLY SYENITE (Manchester-by-the-Sea, MA; 20 minutes). Syenite and multiple 'pull-apart' dikes.

13.1 Return to Rt. 127 and turn right.
14.2 Enter the center of Manchester-by-the-Sea.
14.4 Turn right onto Pine street.
14.45 Park at outcrop to the right. Street address is 21 Pine street. Do not enter condominiums.

STOP 1-6. CAPE ANN GRANITE (Manchester-by-the-Sea, MA; 20 minutes). Two phases of the Cape Ann granite.

14.45 Return to Rt. 127 and turn left.
18.0 Turn left onto Magnolia Street in Gloucester.
19.0 Turn left into Cape Ann Industrial Park (Kondelin Road).
19.4 Turn left into Lot 15 (Farm Creek Construction), park at the top of the hill after the road turns to the right.

STOP 1-7. CAPE ANN GRANITE AND QUARTZ SYENITE (Gloucester, MA; 20 minutes). Magmatic pillows at the top of the drive and at the southern end of the lot fresh outcrop for sampling (samples CA-60A & CA-60B). Additional exposure is found on Kondelin Road under the radio towers next to Lot 15.

19.4 Return to Rt. 127
20.9 Turn left onto Rt. 127 north.
23.9 Intersect Rt. 133 and cross draw bridge continue on Rt. 127 north through Gloucester.
25.2 Bear right, following signs for Rt. 128 Truck Rt.. (Rt. 127 north bears to the left.)
25.3 Turn right onto Parker Street.
25.4 Park opposite Gloucester Truck and Auto Lot. Enter lot on foot.

STOP 1-8. CAPE ANN GRANITE - MAFICS RICH PHASE (Gloucester, MA; 20 minutes). Mafic rich granite shows evidence of mixing at the northern end of exposure.

25.4 Continue south on Parker street. The road bears to the left and becomes very narrow.
25.6 Turn right
25.6 Turn left onto East Main Street.
25.8 Stop sign, go straight onto Rt. 127A north (Sayward Road).
26.0 Turn right into parking lot of Charlies' Liquor Chest. The outcrop is on the east side on the buildings.

STOP 1-9. CAPE ANN GRANITE - MAFICS RICH PHASE (Gloucester, MA; 20 minutes). Mafic rich granite with small inclusions similar to that of Stop 10.

26.0 Turn left out of lot onto Rt. 127A south and continue on Rt. 127A south
26.5 Turn right at lights onto Rt. 128 south (This is the northern terminus of the Rt.).
26.7 Turn right at the lights onto Rt. 127 north.
26.8 Turn left onto Harrison Ave and park. Walk back to Rt. 128 follow the road to the right.

STOP 1-10. CAPE ANN GRANITE - MAFICS RICH PHASE (Gloucester, MA; 35 minutes). Mafic Granitic host and labradorite phenocrystic basaltic magmatic pillows and hornblende phenocrysts rimmed with plagioclase basaltic magmatic pillows (sample CA-15).

26.8 Turn right onto Rt. 127 south.
26.9 Turn right onto Rt. 128 south.
28.4 At Grant Circle, bear right onto Rt. 127 north.

31.4 Turn left towards Anisquam Village and then an immediate right hand turn onto Nashua Ave. This is a dead end road.
31.5 Bear right onto Private Way.
At fork, stay left.
At fork, stay right.
31.8 Straight through clearing
31.9 Park on lawn by Cedar shingle garage with white doors. Walk down road to Davis Neck (Private Property, permission must obtained from nearest occupied residence).

STOP 1-11. DAVIS NECK. ANORTHOSITE RAFTS IN BASALTIC DIKE (Gloucester, MA; 35 minutes). Davis Neck - Cape Ann Granite and Syenite, aplite dike, labradorite phenocrystic basaltic dike and anorthosite.

31.9 Return to Rt. 127 north.
32.4 Turn left onto Rt. 127 north.
33.4 Park at right.

STOP 1-12. PLUM COVE. ENCLAVES OF PHENOCRYSTIC BASALT (Gloucester, MA; 15 minutes). Cape Ann Granite with xenoliths of labradorite phenocrystic basalt. The xenoliths are located on the north side on the cove out past the point.

35.0 Folly Cove (lunch or just a stop to look at the granite on the pier.
35.7 Turn left between two field stone pillars onto Haven Road.
36.1 Second right onto Linwood Ave (dirt road).
36.2 Turn left onto Pt. DeChene Road.
36.3 Intersection of Pt. DeChene Road and Long Branch Ave. Park and walk along Long Branch Road to the coast.

STOP 1-13. ANDREWS POINT. FENITIZED DIKE (Rockport, MA; 25 minutes). Pegmatite with Blue Quartz, hypersolvus granite, hypabyssal granite with 'pull-apart' dikes and fenitized dike of Martin (1977) (Sample CA-30).

36.3 Return down Pt. DeChene Road.
36.5 Turn left onto Phillips Road
36.8 Bear left at the intersection with LaCrosse Road.
36.9 Turn right onto Cathedral Ave.
36.95 Turn left onto Rt. 127 heading south (Granite Street).
37.8 Turn left onto Wharf Road.
37.9 At Base on the hill, a hard right onto a dirt road.
38.0 Park and continue up the road on foot into the Quarry.

STOP 1-14. (Optional). ROCKPORT QUARRY. CAPE ANN GRANITE (Rockport, MA; 25 minutes). Hypersolvus granite. Sample taken from here has very low Zr/Hf ratio.

38.0 Return to Rt. 127. Turn left onto Rt. 127 and follow to Rt. 127A.
39.0 Turn left onto Rt. 127A south.
39.4 Rockport Harbor, turn right onto Mt. Pleasant Street (Rt. 127 south).
41.1 Turn left by Turk's Head Motor Inn. Bear to the left onto Penzance Road. At each intersection continued to go to the left.
41.6 Turn left onto Old Penzanze Road. Park if going to 41 Old Penzance Road or continue to dead end.
41.7 Park. Take path to the right towards the ocean. The outcrop of interest is 500 yards down the shore line from this point.

STOP 1-15. VOLCANIC PIPE (Rockport, MA; 25 minutes). Phenocrysts of perthite and quartz in a devitrified ground mass.

41.7 Return to Rt. 127A south. Turn left. The road will take you to Rt. 128 south in direction to Boston.

ROAD LOG - DAY 2

SHARPNERS POND PLUTONIC SUITE

This road log starts at the intersection of Rt. 1 and Rt. 133 north of Boston (approx. 37 mi north of Boston on Rt.1).

STOP 2-1A. NEWBURY VOLCANIC COMPLEX, LATE SILURIAN- PORPHYRITIC ANDESITE (Rowley, MA; 20 minutes). From the intersection of Rt. 1 and Rt. 133 continue north approx. 3.7 mi. At the intersection with Central St. turn left (east) onto Central St. and park along the road. Outcrops are on both sides of Central St. near the intersection with Rt. 1.

The Newbury Volcanic Complex consists of a series of andesitic and rhyolitic volcanic rocks and associated sediments within faulted slivers along the Bloody Bluff Fault Zone, 'squeezed' in between the Boston Avalon and Nashoba Terranes. The exposures here are tuffs and flows of aphyric and porphyritic andesites. The top of each flow is recognizable by the presence of a vesicular band.

Geochemically the Newbury Volcanic Complex consists of a bimodal volcanic suite of andesites and rhyolites (McKenna et al, 1993). The andesites are high-alumina calc-alkaline rocks with trace element signatures indicative of formation on a continental margin above a subduction zone. Hon et al. (1986) suggested that the similarity in chemistry between the Newbury and the plutonic rocks of the Sharpners Pond plutonic suite may indicate the Newbury are preserved volcanic remnants of a now eroded continental arc. Geochemical composition of these volcanics are very similar to mafic rocks of the Sharpners Pond suite.

STOP 2-1B. NEWBURY VOLCANIC COMPLEX, LATE SILURIAN-EARLY DEVONIAN, RHYOLITIC MEMBER (Newbury, MA; 20 minutes). Proceed north on Rt. 1 for approx. 0.9 mi. Turn left on Elm St. and park along the exposures on your right side.

These exposures are of a rhyolitic member within the Newbury Inlier. The rhyolites are geochemically correlated with the anatectic melts of the Sharpners Pond suite.

STOP 2-2. INTRUSION OF SGR GRANITE INTO THE SHARPNERS POND PLUTON (Newbury, MA; 20 minutes). Return to Rt.1 north and continue north on for 2.7 mi. Turn right onto Boston Road and approx. 0.5 mi turn right onto Hay St. The outcrop is located approximately 200 meters SE of the intersection of Boston Road and Hay Street.

A biotite granite intrudes a medium-grained hornblende gabbro. Xenoliths of the gabbro are common within the granite as well as the fine-grained magmatic pillows of a dioritic composition. Note, how the magmatic pillows are wrapped around some of the gabbro xenoliths, suggesting that their emplacement was in a semi-liquid state.

STOP 2-3 BORDER ZONE OF THE SHARPNERS POND PLUTON (Newbury, MA; 20 minutes). Return to Rt. 1. Continue on Rt. 1 north. After approx 1.6 mi take a left (west) turn onto Middle St. Park immediately along the road.

Exposures are on both sides of the road plus several outcrops along the west side of US Route 1 at the Middle Street intersection. This is a rather complex outcrop; fine-grained gabbro is found here intermingled with medium-grained diorite to tonalite, forming magmatic pillows. A granite has intruded the earlier gabbros and diorites. Aplites and pegmatites are common in this outcrop. A medium-grained diorite is found as xenoliths within the granite. The granite contains a few inclusions of a fine-grained gabbro to diorite that locally contain glomerophyric hornblende porphyroblasts. A weak foliation can be observed in some of the porphyroblast bearing pillows. Continue south on Middle Street

STOP 2-4. INTERMINGLING OF MAFIC AND FELSIC MAGMAS OF THE SHARPNERS POND SUITE (Newbury, MA; 30 minutes). Continue on Middle St. for 3/4 mi. Turn right (north) on Highfield Road. Proceed north 1.1 mi to Scotland Road. Turn left (west) on Scotland Road and continue 3.6 mi west. Park your cars immediately before the northbound onramp to Interstate 95. Walk toward exposures following the northbound entrance ramp to I-95.

This large outcrop is located along the east side of the northbound onramp at the I-95 and Scotland Road intersection. This stop is another complex outcrop which is characteristic for the border zone of the Sharpners Pond Pluton. Several types of igneous rocks have been intruded into each other at different times. The oldest intrusions consist of a fine-grained gabbro to diorite intermingled with a light medium-grained biotite granite. Approximately 10 % of this intrusion consists of granite. Locally, this intrusion has been homogenized, forming a quartz diorite to tonalite. The second intrusion consists of a homogeneous, medium-grained quartz diorite. The third intrusion and last one associated with the Sharpners Pond Pluton consists of a few aplitic dikes. Northeast-striking, steeply dipping diabase dikes of a younger date can be observed crosscutting the rocks associated with the Sharpners Pond Pluton. Geochemically, these dikes differ from the Sharpners Pond Pluton. The diabase dike has an alkaline affinity, compared to the calc-alkaline Sharpners Pond Pluton.

STOP 2-5. INTERMINGLING AND MIXING OF MAFIC AND FELSIC MAGMAS OF THE SHARPNERS POND SUITE (Georgetown, MA; 20 minutes). Take I-95 south by turning left at the next onramp. Continue south to Rt. 133 (exit 54) in the direction of Georgetown. At the end of the exit ramp turn right and after 1.2 MI turn right again (north) onto Tenet St. Proceed 3.1 MI passing over I-95 to a 'T' intersection with Jewel Street. Park along the road just prior to the intersection.

This outcrop is located at Tenet St., Georgetown 200 meter southwest of the intersection of Tenney St. and Jewett St. At this locality samples have been taken for zircon dating (Zartman and Naylor, 1984) yielding age of the intrusion at 430 ± 25 Ma. The outcrop shows a banded appearance. Quartz diorite and tonalite alternate within these bands. The quartz diorite and tonalite were intruded simultaneously, forming flow bands parallel to the direction of flow. Elongated magmatic pillows of a fine-grained gabbro to diorite can be observed in the thicker tonalic flow bands.

STOP 2-6. MIXED MAFIC AND FELSIC MAGMAS WITH INCLUSIONS OF MAFIC MAGMATIC PILLOWS (Boxford, MA; 20 minutes). Retrace your way back to I-95. Take I-95 south and continue south to Rt. 97 (exit 53) in the direction of Georgetown. At the end of the exit ramp turn right (west) and after 0.2 mi turn left (south) on Pond St. Proceed 0.8 mi, cross Ipswich Road, and after another 0.5 mi turn right (south) on Depot Road. After 0.1 mi (right after the bridge over Pye Brook) turn left (east) onto Bare Hill Road. Proceed 0.2 mi and park along the road.

The outcrop is located along the Bare Hill Road, approximately 350 meter south of the intersection of Bare Hill Road and Depot Road. A medium-grained quartz diorite dominate the outcrop. Approximately 10 % of the outcrop consist of a fine-grained gabbro to diorite as rounded inclusions (partially digested and resorbed magmatic pillows). This outcrop is a typical example of the most common intrusive type of the Sharpners Pond suite.

STOP 2-7. INTERMINGLED MAFIC AND FELSIC MAGMAS NEAR A CONTACT WITH THE FISH BROOK GNEISS (Boxford, MA; 30 minutes). Turn around and retrace your way back to Depot Road. Turn right (south) on Depot Rd, proceed 0.6 mi and turn right (west) onto Boren Road, a site of recent construction and development. Continue approx. 0.2 mi and park along the road. The exposures are on your right side.

This outcrop is located on Boren Rd approximately 250 meter west of the intersection of Boren Rd and Depot Rd in Boxford. The outcrop consist of a commingled fine-grained gabbro and a medium-grained granite. The outcrop shows a beautiful example of magmatic commingling with well developed magmatic pillows of gabbro, surrounded by the granite. A few inclusions of Fish Brook Gneiss are also found. An outcrop located approximately 150 meter further down the road (west) consists of the Fish Brook Gneiss. The gneiss contains quartz, plagioclase and biotite with minor potassium feldspar. The biotite forms swirling bands which are characteristic of the Fish Brook Gneiss.

STOP 2-8. LEUCOCRATIC FISH BROOK GNEISS (Boxford, MA; 20 minutes). Turn around and retrace your way back to Depot Road. Turn right (south) on Depot Rd, proceed 1.2 mi and cross Georgetown Road. At this point you are on Middleton Road. Proceed on Middleton Road 0.6 mi and cross Main St. (this is dangerous intersection, proceed with caution). Continue 0.7 mi and turn right at the second road leading into a new development area. Drive slowly 0.1 mi and the outcrop is along the road just at the cross road connector.

The outcrop consists of a very plagioclase-rich gneiss of the Fish Brook Gneiss. This outcrop illustrate the abundance of leucocratic minerals in the Fish Brook Gneiss, giving it a low water content. The Fish Brook gneiss is most likely an original rhyolitic complex emplaced at 520 Ma ago and metamorphosed at 425 Ma ago (zircon and monazite ages; see description of stop 2-8 Chapter X, this volume)

STOP 2-9. MIXED MAFIC AND FELSIC ROCKS WITH XENOLITHS OF THE BOXFORD FORMATION (Boxford, MA; 25 minutes). Turn around and retrace your way back to Middleton Road. Turn right (east) on Middleton Rd, proceed 1.8 mi to Moonpenny Road on your right (south) side. Turn right and proceed to the end of the road.

This outcrop is located at the end of Moonpenny Rd adjacent to the cul-de-sac, Boxford. This outcrop consists of a fine- to medium-grained tonalite with rounded inclusions of a fine-grained gabbro to diorite. Xenoliths of calc-silicates from the Boxford Formation are found in this tonalite. This tonalite has later been intruded by a more felsic tonalite.

STOP 2-10. MIXED MAFIC AND FELSIC MAGMAS NEAR THE CUMILITIC PHASE OF THE SHARPNERS POND PLUTON (North Andover, MA; 35 minutes). Turn around and retrace your way back to Middleton Road. Turn right (east) on Middleton Rd, and follow signs to I-95 south. Take I-95 south and proceed to the next exit to Rt. 1 south. take Rt. south to the next exit onto Rt. 62 west in the direction of Middleton. Take Rt. 62 west and proceed approx. 2.3 mi to the center of the town of Middleton. Take Rt. 114 (also known as Main St. and Salem Turnpike) west/north and proceed 3.3 mi to Sharpners Pond Road on your right (north). Turn right and proceed approx. 0.3 mi. The outcrops are along the road.

This stop is located at Sharpners Pond Rd, in North Andover, approximately 450 meters northeast of the intersection between Sharpners Pond Road and Rte 114. The outcrop consist of a medium grained diorite with minor amounts of biotite. The diorite is weakly foliated due to flow alignment of hornblende during the emplacement of the rock. Some inclusions of a fine-grained gabbro occur, these inclusions are aligned along the foliation of the rock. The diorite also contain stringers of a leucocratic biotite tonalite.

STOP 2-11. CUMULATE HORNBLENDE GABBRO TO DIORITE (North Andover, MA; 35 minutes). These exposures are along a powerline clear cut. Proceed in the same direction to the powerlines. Park along the right side of the road.

This stop is located at an intersection between a powerline and Sharpners Pond Rd, in N. Andover, approximately 500 meters northeast of the intersection between Sharpners Pond Road and Rte 114. The outcrop is dominated by a medium-grained diorite with cumulate texture where most of the hornblende forms the cumulitic phase and plagioclase the intercumulus. We are here Narrow dikes of pegmatite and aplite cut across the outcrop. A leucocratic biotite tonalite can be observed intruding the cumulitic hornblende.

STOP 2-12. (Optional) CUMULITIC HORNBLENDE GABBRO TO DIORITE (North Andover, MA; 30 minutes). This outcrop is located 100 meter to the south of Stop 2-11, under the power line.

A medium-grained cumulitic hornblende gabbro is intruded by up to 10 cm wide aplitic dikes. Some of the dikes have been offset by faulting. This faulting has taken place during the emplacement of the dikes, since the dikes have partially penetrated the fault plane. Return to the cars. Drive back the same way as you came from in Sharpners Pond Road, turn left on Route 114. Follow Route 114 to Interstate 95. Go south on Interstate 95 back to Boston..

End of Field Trip

Chapter R

Methods of Characterizing Fluid Movement and Chemical Transport in Fractured Rock

By Paul A. Hsieh, Allen M. Shapiro, Christopher C. Barton, F. Peter Haeni, Carole D. Johnson, C. Wayne Martin, Frederick L. Paillet, Thomas C. Winter, and David L. Wright

Field Trip Guidebook for the Northeastern United States: 1993 Boston GSA

Volume 2
Contribution No. 67, Department of Geology and Geography, University of Massachusetts, Amherst, Massachusetts

METHODS OF CHARACTERIZING FLUID MOVEMENT AND CHEMICAL TRANSPORT IN FRACTURED ROCK

by
Paul A. Hsieh, U. S. Geological Survey, Menlo Park CA 94025
Allen M. Shapiro, U. S. Geological Survey, Reston VA 22092
Christopher C. Barton, U. S. Geological Survey, Lakewood CO 80225
F. Peter Haeni, U. S. Geological Survey, Hartford CT 06103
Carole D. Johnson, U. S. Geological Survey, Bow NH 03304
C. Wayne Martin, U. S. Forest Service, West Thornton NH 03223
Frederick L. Paillet, U. S. Geological Survey, Lakewood CO 80225
Thomas C. Winter, U. S. Geological Survey, Lakewood CO 80225
David L. Wright, U. S. Geological Survey, Lakewood CO 80225

INTRODUCTION

A major problem encountered in characterizing fluid movement and chemical transport in fractured rock is how to deal with the high degree of heterogeneity in the rock. In crystalline rocks, for example, hydraulic conductivity can vary by several orders of magnitude over a distance of several meters. If the rock contains zones of highly permeable fractures, these zones can exert a strong control on ground-water flow and chemical transport. Depending on the objective, a site investigation effort may require the explicit identification and characterization of these highly permeable zones, or may be focused on determining the overall properties of the fractured rock mass on a large scale. In either case, the characterization effort requires a variety of field methods to map fractures and to determine their hydraulic and transport properties. During this field trip, we demonstrate a selection of these methods for characterizing fluid flow and chemical transport in fractured crystalline rocks.

This field trip visits a research site in the Mirror Lake area, located partially within the Hubbard Brook Experimental Forest in central New Hampshire. At this site, an ongoing study, supported by the U. S. Geological Survey's Toxic Substances Hydrology Program and the National Research Program in the Water Resources Division, seeks to integrate hydrologic, geologic, geophysical, and geochemical methods to characterize fluid flow and chemical transport in fractured rocks. As discussed by Shapiro and Hsieh (1991), the objectives of this study are to develop monitoring, testing, and interpretive methods, and to establish a site for long-term study. Although the Mirror Lake area is not contaminated, the techniques and understanding developed in this study are directly transferable to other fractured rock sites that have been contaminated with chemical wastes.

AN OVERVIEW OF FIELD METHODS FOR FRACTURE CHARACTERIZATION

The field methods demonstrated in this field trip can be divided into three categories: mapping fractures on exposed surfaces, mapping fractures in the subsurface, and hydrologic testing and monitoring. From these three categories, selected examples are demonstrated. Each method has its strengths and weaknesses. When applied individually, the methods generally yield limited information on fracture characteristics. However, when applied together, these methods enhance each other by reducing uncertainty and nonuniqueness associated with individual methods.

Mapping Fractures on Exposed Surfaces

Because fractures are conduits in the subsurface, the geometric pattern of a fracture network exerts a strong control on flow and transport. For example, in a sparse and poorly connected network of fractures, flow is likely to be highly concentrated (or "channelized") along tortuous pathways. In contrast, in a dense and well connected network, flow is likely to be diffuse, similar to flow in a granular medium. Thus, understanding the geometric pattern of the fracture network provides a basis for making inferences and predictions about the flow and transport properties in the subsurface.

Fracture patterns are most easily studied by mapping fractures on exposed surfaces such as outcrops or mine tunnels. In contrast to traditional methods, which center on measuring fracture orientation (strike and dip), modern methods call for mapping the entire fracture pattern. Properties of individual fractures, such as orientation, length, aperture, and surface morphology are measured. The network pattern is characterized in terms of fracture intersections, nature of termination, density, and scaling properties. The measured properties are analyzed statistically, yielding results that can be used as input data for synthetically generating fracture networks. With this approach, the synthetic networks retain the same statistical characteristics as the natural fracture networks. Computer simulation of flow and transport through synthetic networks is currently a topic of much research interest.

Another purpose of mapping fracture patterns is to infer the processes through which the fractures were created. Recent advances in fracture mechanics have made it possible to quantitatively analyze how fractures initiate, propagate, and interact with each other (see, for example, Pollard and Aydin, 1988). For geologically simple areas, these analyses demonstrate how a fracture pattern depends on stress history and material properties of the rock. For areas that have undergone complex deformations, analysis is substantially more difficult, and understanding of fracture development is far from complete. However, as research progresses, the hope is that fracture patterns can be predicted from knowledge of the geological structure of an area. Such an ability will substantially enhance the prediction of flow and transport properties in fractured rocks.

Mapping Fractures in the Subsurface

Because direct observations can sample only those fractures exposed on rock surfaces, fractures in the subsurface must be mapped remotely, often by geophysical methods applied from land surface or in boreholes. Lewis and Haeni (1987) discuss the use of surface geophysical methods to detect fractures in bedrock. Paillet (1991a) provides an overview of geophysical well logs for evaluating crystalline rocks.

Conventional geophysical methods exploit the fact that fractures have different physical properties than the intact rock. A geophysical survey generally yields an inferred distribution of a rock-mass property, from which one must then infer the presence of fractures. This second inference is often subject to substantial uncertainty because anomalies attributed to fractures can also be caused by inhomogeneities in the rock. The integration of multiple geophysical methods (see, for example, Lieblich and others, 1991, 1992a, 1992b) can reduce the ambiguity by correlating interpretations from different data sets to obtain an overall interpretation.

A general class of surface geophysical methods, based on azimuthal survey, is suitable for detecting one or more sets of closely spaced, steeply dipping fractures in a rock mass. If the intact rock is homogeneous and isotropic with respect to a certain physical property, such as compressional wave velocity, the presence of steeply dipping, closely spaced fractures can cause anisotropy (in the horizontal plane) with respect to that property. This horizontal anisotropy can be detected by an azimuthal survey in which the survey line or array is rotated on land surface. The strike of the fracture set can then be determined from the directions along which the property attains its maximum or minimum values.

Other surface geophysical methods are suited for detecting a single fracture or a fracture zone. For example, the inductive terrain conductivity method detects induced currents that are caused by conductors (fluid-filled fractures) in the subsurface. Ground-penetrating radar (Ulriksen, 1982) emits short pulses of electromagnetic energy and detects the presence of reflectors, which occur at interfaces of strong contrast in electrical properties between fractures and the intact rock. In general, these methods work well in terrane with little or no overburden covering the bedrock.

Borehole geophysical surveys allow probing of the subsurface through boreholes. Conventional logging methods such as gamma, electrical resistivity, and neutron logs are highly developed for identifying lithology encountered by boreholes in sedimentary formations. However, their application for fracture detection is problematic. In many cases, inhomogeneities in rock properties can yield the same anomaly as fractures, so that log interpretation is often nonunique. Furthermore, most conventional logs average rock properties over a sample volume ranging from 20 to 60 cm in diameter. It is difficult to resolve the properties of individual fractures within these volumes. Consequently, conventional logs are generally used to define the large scale structure of the rock mass along the borehole.

In recent years, a number of borehole geophysical methods have been developed specifically for fracture detection. Among these developments are borehole televiewer (Zemanek and others, 1970), downhole video camera, borehole flow meter (Paillet and others, 1987), borehole radar (Olsson and others, 1992a, 1992b), and well-to-well tomography (Dines and Lytle, 1979; Kak and Slaney, 1988) using electromagnetic or seismic waves. Selected examples of these methods are demonstrated in this field trip.

Hydrologic Testing and Monitoring

Hydrologic testing, consisting of hydraulic and tracer tests, is a direct way to determine flow and transport properties in the subsurface. Hydrologic tests generally involve artificially inducing a perturbation in the subsurface and measuring the resulting response. In a hydraulic test, a pressure perturbation is created by injecting or withdrawing fluid in a borehole. The response is the change in fluid pressure in the same borehole or in nearby observation boreholes. In a tracer test, a concentration perturbation is created by introducing a solute (tracer) in the subsurface. The movement of this solute is monitored by sampling for solute concentration at locations downstream from the tracer introduction point. Generally speaking, hydraulic and tracer tests can sample on a scale ranging from several meters to several hundred meters.

The analysis of hydraulic or tracer test data is a two-step procedure consisting of (1) identifying an appropriate model to represent flow or transport in the rock mass, and (2) determining the model parameters (hydraulic or transport properties) such that the model response matches the field response. Because of the complexities of fractured rocks, it is generally not possible to identify, based solely on the test response, a unique model for test analysis. Instead, additional information obtained via geological and geophysical investigations is needed to infer the flow geometry, boundaries, and the nature of heterogeneity. Here again, the need for a multidisciplinary approach to investigate flow and transport in fractured rocks is evident.

On the scale of several kilometers or more, hydrologic tests in fractured rocks become ineffective. Over these distances, the response to fluid injection or pumping is generally too small to be measurable, and solute transport times are too long to run a tracer test. To investigate flow and transport on these scales, one approach is to monitor the response of the ground-water system to natural perturbations and long-term human disturbances. For example, recharge events such as rainfall and snowmelt can cause fluctuations in hydraulic head. By monitoring the recharge and discharge of ground water, and the hydraulic head distribution in the rock mass, one may be able to infer hydraulic properties on the scale of several kilometers or more.

Collecting ground-water samples for chemical analyses is another approach to investigating flow and transport on a scale of several kilometers or more. As ground water flows from a recharge area to a discharge area, its chemical composition evolves as the water reacts with the rock. Understanding the chemical "signature" of ground water can help to identify ground-water flow paths. Recent advances in the detection of man-made chemicals such as chlorofluorocarbons (used as refrigerants, aerosols propellants, etc.) and the parent-daughter isotopes tritium and helium-3 (produced from atmospheric testing of thermonuclear devices) have made it possible to use these chemicals for determining the age of shallow ground waters (Busenberg and Plummer, 1992; Solomon and others, 1992). Knowledge of the spatial distribution of ground-water ages can also help to identify flow paths. If lengths of flow paths are known, ground-water velocities can be determined.

GEOLOGIC AND HYDROLOGIC SETTINGS OF THE MIRROR LAKE AREA

Mirror Lake is near the lower end of the Hubbard Brook valley in the southern portion of the White Mountains of New Hampshire (Figure 1). Hubbard Brook, which drains the valley, flows into the Pemigewasset River, a major drainage in central New Hampshire. For the purpose of this field guide, the "Mirror Lake area" refers to an area of approximately 1000 ha bounded to the east by the Pemigewasset River, to the north by Leemans Brook, to the west by Paradise Brook, and to the south by Hubbard Brook. Topography in this area is steep along the mountain sides, and flat along the Pemigewasset River. Altitude ranges from 180 m at the Pemigewasset River to 720 m at the northwestern corner of the area.

Within the Mirror Lake area, our field investigation has concentrated mainly on a subregion that drains into Mirror Lake (Figure 2). This drainage basin occupies 85 ha, and varies in altitude from 213 m at the lake surface to 481 m at the highest point of the drainage divide. Three perennial streams flow into Mirror Lake. These streams and their respective drainage basins are designated as W, NW, and E. Mirror Lake drains via an outlet stream into Hubbard Brook.

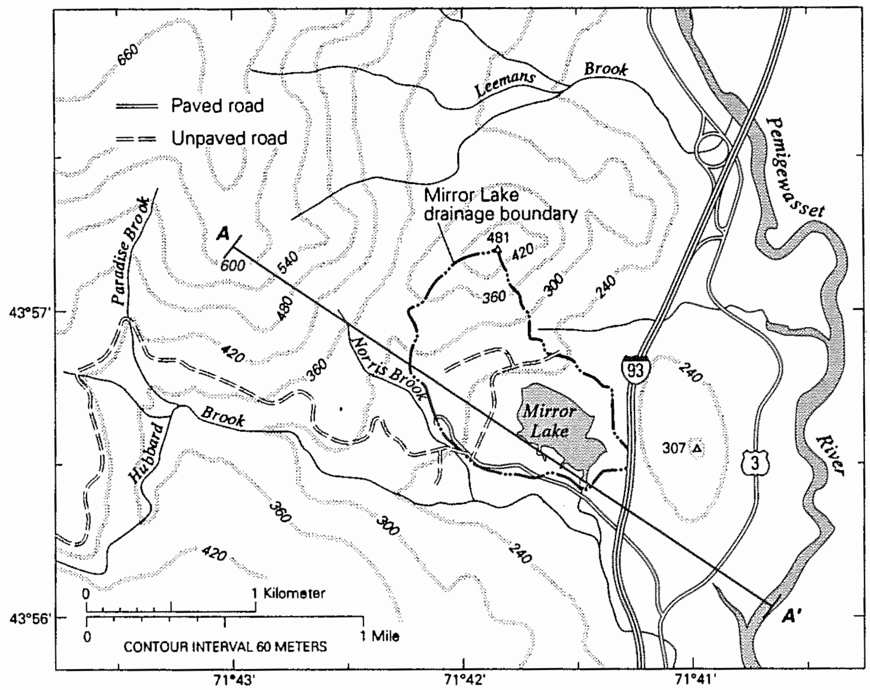

Figure 1. Map of Mirror Lake area in central New Hampshire.

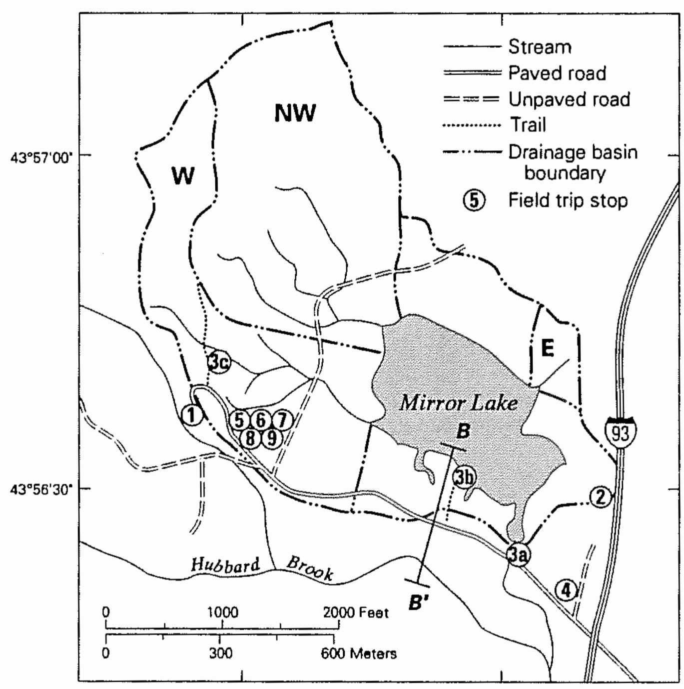

Figure 2. Map of Mirror Lake drainage basin.

Surficial Geology

Glacial drift overlies the bedrock in much of the Mirror Lake area. Stratified drift occupies the Pemigewasset River valley, while till covers much of the mountain sides. Within the Mirror Lake drainage basin, the drift varies in thickness from 0 to 55 m, and consists mainly of silty and sandy till, with numerous cobbles and boulders. Test drilling and surface geophysical surveys indicate that Mirror Lake overlies a bedrock saddle. Bedrock valleys descend to the north and to the south away from the lake. The ridge north of the lake is a moraine. Where the moraine overlies the northern bedrock valley, the drift thickness is as much as 55 m. South of Mirror Lake, in the area between Mirror Lake and Hubbard Brook, the silty sand and gravel are believed to be a delta-type deposit that formed when Hubbard Brook adjusted its grade to the Pemigewasset River during deglaciation. Kame terraces, consisting of fine- to coarse-grained sandy ice-contact deposits, are found at several levels on the mountain sides. Examples of these terraces are those on which the Forest Service station (Stop 1) and the FSE well field (Stops 5-9) are located.

Bedrock Geology

As shown on the preliminary geologic map of New Hampshire (Lyons and others, 1989), the bedrock underlying the Mirror Lake area lies in the Merrimack synclinorium (Central Maine Terrane). The bedrock includes pelitic schists of the early Silurian Rangeley Formation. The pelites were multiply folded and metamorphosed during the Acadian orogeny (mid-Devonian) to a low sillimanite grade (approximately 600^{0} C and 4 kb, equivalent to burial to approximately 15 km). In the Mirror Lake area, the Rangeley schist is extensively intruded by dikes, anastomosing fingers, and pods of late Devonian Concord granite. The Rangeley schist and Concord granite are cut by dikes and interfolial intrusions of pegmatite of unknown age, possibly a residual differentiate of the Concord granite. All three rocks are cut by lamprophyre dikes whose age is not specifically known but is likely between middle Jurassic and early Cretaceous, based on the ages of similar dikes elsewhere in the region (McHone, 1984).

Based on the work of Lyons and others (1989), we classify the bedrock in the Mirror Lake area into four types. The following descriptions are modified from those given by Lyons and others (1989).

Rangeley Formation. (438-428 MY) Early Silurian. Lyons and others (1989) divide the Rangeley Formation into the lower and upper members. The lower Rangeley is a medium to coarse grained, thinly laminated (5-25 mm), non-rusty weathering, black and white pelitic schist. It contains feldspar, quartz, biotite, muscovite, sillimanite; but calc-silicate pods are rare. It bears quartz boudins, clots of fine-grained garnet, and thin laminae of quartz and garnets, and is locally sulfidic. The foliation is strong, corrugated, planar, and locally folded. The upper Rangeley is a medium to coarse grained, rusty weathering pelitic schist. It contains feldspar, quartz, biotite, muscovite, and sillimanite; calc-silicate beds and pods are common. It bears quartz boudins, clots of fine-grained garnet, and is locally sulfidic. Foliation is strong, corrugated, planar, and locally folded.

Concord granite. (370-365 MY) Late Devonian. A part of the regional Concord Intrusive Suite, the Concord granite is an anatectic, two-mica granite, locally grading to tonalite. It is medium grained, gray to light gray, hypidiomorphic, and equigranular. It contains muscovite, biotite, chlorite, and sparse dark purple-red garnet. X-ray modal analysis of a sample collected on the I-93 road cut shows that it contains plagioclase but little or no orthoclase feldspar (i.e., the sample is tonalitic).

Pegmatite. (not dated) The pegmatite is white, coarse-grained, plagioclase-rich, and contains biotite, muscovite, and quartz. Individual grains are generally shattered and deformed, but the rock is coherent. Pegmatite is commonly associated with fine-grained, white aplite. Intruded as dikes and pods, the pegmatite cross cuts and interlayers with the schist and granites. It is possibly a late-stage Concord granite differentiate.

Lamprophyre. (190-95 MY) Middle Jurassic through Early Cretaceous. The lamprophyre ranges from light greenish-gray to dark bluish-gray, and commonly shows rusty weathering. It is aphanitic or porphyritic with an aphanitic groundmass. While commonly massive and featureless, some lamprophyres carry visible pyrite and magnetite, and greenish-white, euhedral plagioclase phenocrysts as much as several millimeters in length. It is vesicular or amygdaloidal with vesicles lined with chlorite, drusy carbonate, or clay. Lamprophyre occurs as dikes and composite dikes, which crosscut all other rocks at the site.

Ground-Water Hydrology

Ground-water flow in the Mirror Lake area is typical of mountain-and-valley terrain of the New England uplands. Water from precipitation and snow melt infiltrates into the subsurface, flows through the glacial drift and the fractured bedrock, and discharges into streams, lakes, and rivers, and by evapotranspiration. Estimates of recharge to ground water in the Mirror Lake drainage basin vary from 20 to 45 cm/year. In the northern and western part of the drainage basin, ground water moves generally down the mountain slopes, discharging into the W and NW Streams or directly into Mirror Lake. On the south side of Mirror Lake, lake water seeps into the subsurface and flows towards Hubbard Brook (Winter, 1984).

Figure 3 illustrates a conceptualization of the ground-water flow pattern along a vertical section (AA' in Figure 1) running from the high point at the northwest corner of the Mirror Lake area to the low point at the Pemigewasset River. The flow pattern contains flow cells of different sizes. Local flow systems begin at water-table highs and end at adjacent lows. Intermediate flow systems pass at depth beneath local flow systems. The regional flow system begins at the regional topographic high and discharges at the regional topographic low. From Figure 3, one can see that the drainage divide northwest of Mirror Lake lies on a relatively small knoll that is situated on a mountain side with much greater relief. Thus, it is not difficult to imagine that an intermediate flow system can begin high on the mountain side outside the Mirror Lake drainage basin, pass beneath the local drainage divide, and discharge either into streams that flow into Mirror Lake, or directly into Mirror Lake. Furthermore, a regional flow system can flow under Mirror Lake and discharge into the Pemigewasset River.

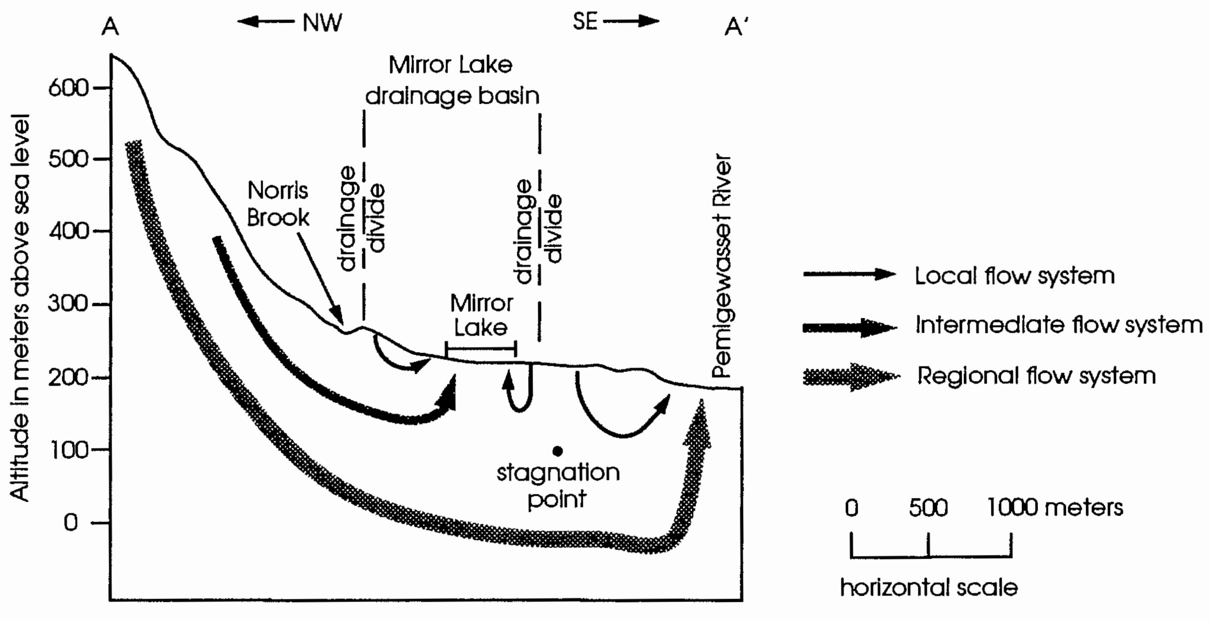

Figure 3. Vertical section AA' (see Figure 1) illustrating local, intermediate, and regional flow systems in the Mirror Lake area (modified from Harte, 1992).

The major features controlling ground-water flow in the Mirror Lake area are (1) the steep slope of the mountain sides, (2) the low hydraulic conductivity of the glacial till and the bedrock, (3) the presence of surface water bodies such as streams, Mirror Lake, and the Pemigewasset River.

Within the Mirror Lake drainage basin, the slope of the mountain side exceeds 0.2 m per m. As pointed out by Forster and Smith (1988), a mountain having high relief results in deep, regional ground-water flow. The depth of circulation will be enhanced if the bedrock contains subvertical fractures that are highly transmissive. In the Mirror

Lake area, the presence of deep circulation of ground water is supported by cross-sectional flow model analysis by Harte (1992), and also by preliminary results of ground-water age dating with the chlorofluorocarbon technique developed by Busenberg and Plummer (1992). In one bedrock well, water 25 years old was sampled at a depth of 146 m.

Hydraulic conductivities of glacial drift and bedrock in the Mirror Lake area have been estimated from hydraulic tests. Based on slug tests in piezometers, hydraulic conductivity of the till is estimated to range between 10^{-6} to 10^{-5} m/s. Hydraulic conductivity of sands in kame terraces is approximately 10 times higher than that of till. Results of single-hole, straddle-packer tests using 5-m test intervals indicate that the bedrock hydraulic conductivity is highly heterogeneous, varying over many orders of magnitude. The average value of hydraulic conductivity determined through testing the upper 100 m of the bedrock is 3×10^{-7} m/s. However, single-borehole tests sample the rock in a small region around the borehole. Therefore, the average value of 3×10^{-7} m/s does not necessarily represent the hydraulic conductivity controlling regional flow through bedrock in the Mirror Lake area.

The relatively low hydraulic conductivity of glacial till and bedrock on the mountain sides results in the water table being close to land surface. Within the Mirror Lake drainage basin, depth to the water table is typically less than 10 m. An exception to this is the moraine north of Mirror Lake, where the water table is more than 20 m below land surface. Local topography, such as terraces, can also affect local patterns of ground-water flow. At Stop 3c, we discuss the effect of a mountain side terrace on vertical components of ground-water flow.

Streams in the Mirror Lake drainage basin serve generally as ground-water drains. (An exception, occurring along a section of the W stream, is discussed at Stop 3c.) Analysis of the baseflow component of streamflow indicates the ground-water discharge to stream W is 95,000 m^3/year, and to stream NW is 150,000 m^3/year.

Mirror Lake, occupying 15 ha at the base of the drainage basin, plays an important role in the ground-water flow system. Subsurface seepage to and from the lake occurs primarily in the littoral zone along the lake perimeter. Much of the lake bottom is covered by organic sediments (gyttja) of low vertical hydraulic conductivity (estimated to be 10^{-9} to 10^{-10} m/s). Ground water enters the lake along three-quarters of the perimeter, while lake water seeps into the subsurface along a portion of the south shore. Based on ten years of data, Rosenberry and Winter (1993) estimate that the ground-water seepage into Mirror Lake is 60,000 m^3/year, which represents about 10% of the total inflow into Mirror Lake (sum of precipitation, surface-water and ground-water inflows). Seepage from Mirror Lake into the subsurface is estimated at 260,000 m^3/year, which represents about 46% of the total outflow from Mirror Lake (sum of evaporation, surface and subsurface outflows).

An interesting feature that results from the interaction between ground water and Mirror Lake is a stagnation point in the ground-water flow system. Hydraulic head data indicate that a stagnation point occurs at the CO well field east of the lake. The stagnation point separates a local flow system, which flows towards the lake, from the underlying regional flow system, which flows under the lake and toward the Pemigewasset River (Figure 3). At the CO well field, the stagnation point is probably in the upper part of the bedrock.

Computer modeling studies are currently underway to analyze the ground-water flow system in the Mirror Lake area. By calibrating the model to simulate the observed recharges, discharges, and hydraulic heads, we hope to determine the large-scale distribution of hydraulic properties within the glacial drift and bedrock. Of particular interest is the comparison between the large-scale properties determined from model calibration versus the small-scale properties determined from hydraulic tests. Another objective is to use observed ground-water ages to aid model calibration and to identify the heterogeneities that control ground-water flow paths and travel times in a drift-bedrock environment.

FIELD TRIP STOPS

The field trip begins at the U. S. Department of Agriculture (USDA) Forest Service station at the Hubbard Brook Experimental Forest, near the town of West Thornton in central New Hampshire. All stops on this field trip are within 2 km of the Forest Service station and can be reached by walking or by a combination of driving and walking. The following road log gives directions to the Forest Service station. To reach the start of the road log, take Highway I-93, get off at Exit 29, and turn left (north) onto Route 3. The road log begins where the end of the exit ramp meets Route 3.

Road Log

0.0 km (0.0 miles)	Road log begins where Exit 29 from Highway I-93 enters Route 3. Proceed north on Route 3.
7.6 km (4.7 miles)	Road crosses over Hubbard Brook.
7.7 km (4.8 miles)	Turn left (west) onto Mirror Lake Road.
8.4 km (5.2 miles)	Highway I-93 passes overhead.
8.7 km (5.4 miles)	On the right is outlet of Mirror Lake.
8.8 km (5.5 miles)	The driveway on right leads to the public beach on Mirror Lake.
9.3 km (5.8 miles)	Bear right at fork.
9.7 km (6.0 miles)	Arrive USDA Forest Service station.

STOP 1. OVERVIEW OF ECOSYSTEM STUDIES AT THE HUBBARD BROOK EXPERIMENTAL FOREST (HBEF). USDA Forest Service station. Operated by the Northeastern Forest Experiment Station of the USDA Forest Service, the HBEF was established in 1955 as a center for watershed management research in the northeastern United States. The original mandate from the Congress of the United States charged that the Experimental Forest be used for basic and applied research of the hydrologic cycle. The goal was to understand the physical and chemical nature of the hydrologic cycle in a northern hardwood forest ecosystem, and to investigate the ramifications of human activity within the forest.

Beginning in 1963, the Forest Service, Dartmouth College, and later Yale and Cornell Universities and the Institute of Ecosystem Studies developed the Hubbard Brook Ecosystem Study (HBES), a long-term multidisciplinary investigation of the structure, function, and interactions between atmospheric, terrestrial, and aquatic ecosystems. As such, the HBES has attracted investigators from a large variety of disciplines. The HBES provides investigators with background data from the long-term records of climate, hydrology, precipitation and stream-water chemistry, and ecological data from many completed and ongoing studies. Cooperative studies, in turn, are linked to other studies to contribute to an integrated understanding of the structure and function of the northern hardwood forest ecosystem. In 1992, more than 100 scientists, professors, graduate students, and technicians from 3 government agencies and 10 universities participated in research at the HBEF.

An important research method pioneered at the HBEF is the "small-watershed approach" to studying nutrient cycling in an ecosystem. This approach selects small watersheds (having areas of tens of hectares) as the basic unit for determining inputs, outputs, and internal cycling of water, nutrients, and energy. In the HBEF, eight watersheds have been equipped to measure the amount and chemistry of precipitation and stream flow. Using these data, scientists at the HBEF determine the sources, sinks, and fluxes of nutrients in the watershed ecosystem.

The long-term record of precipitation and stream flow also provide a basis for evaluating experimental treatments of watersheds. Since 1965, four watersheds have been treated by cutting the forest using different methods and assessing the effects on the nutrient cycles. A publication prepared by the USDA Forest Service (1986) summarizes the major findings of these long-term studies. Among these findings are the significant changes in the chemistry of soil and stream waters, the lack of appreciable increase in erosion and sedimentation, and the rapid regeneration of vegetation.

Because of its long term and multidisciplinary nature, research at the HBEF has gained national and international recognition. Acid precipitation in North America was first documented and reported at the HBEF. In 1976, UNESCO designated the HBEF as a Biosphere Reserve in the Man and Biosphere Program, designed to preserve representative ecosystems and to provide opportunities for long-term interdisciplinary research on the effects of humans on the biosphere. In 1978, the HBEF became a part of the National Atmospheric Deposition Program's network of more than 150 sites in the United States for standardized collection and chemical analysis of precipitation. In 1987, the HBEF was awarded a Long-Term Ecological Research grant through the National Science Foundation.

Research findings at the HBEF are reported in numerous papers, reports, and books. A publication prepared by the USDA Forest Service (1991) gives a selected listing. A complete list of titles up to 1991 has been compiled by Likens (1991). Some of the research results have been synthesized in three books, the latest of which is edited by Likens (1985).

STOP 2. BEDROCK GEOLOGY AND FRACTURE MAPPING. I-93 Roadcut, 0.3 km north of Mirror Lake Road.

Caution: This stop spans a high speed limited access highway where pedestrians are not expected and are normally forbidden. For your own safety, please cross quickly as a group and stand far off the roadway.

The purpose of this stop is to introduce the local bedrock geology and to demonstrate the quantitative methods used to measure the hydrologically important fracture characteristics in the field. The roadcut exposes the bedrock that underlies the Mirror Lake area. All of the rock types described above and their cross-cutting relations can be observed.

The characteristics of individual fractures and the architecture of the fracture network are analyzed by the "pavement method" of fracture mapping developed by Barton and Larsen (1985) and described in detail by Barton and Hsieh (1989). This method consists of 1) making a detailed map of the fractures on an exposed rock surface (pavement), 2) measuring the orientation, surface roughness, aperture, mineralization and trace length of each fracture, and 3) measuring the connectivity, density, and scaling characteristics of the fracture network. The resulting fracture map is a two-dimensional section through a three-dimensional fracture network. If several surfaces are available for mapping, then it is also possible to examine whether fractures from one surface project to connect with fractures on another surface.

Fracture mapping at the roadcut is made possible by the presence of five exposed surfaces—four subvertical faces exposed by blasting and one subhorizontal face that was glacially cleaned and polished. Figure 4 shows the fracture map of a portion of the road cut. In making a fracture map, it is always necessary to choose a cutoff size below which fractures are ignored. In producing Figure 4, we ignore a fracture if its trace length is less than 1 m. Fractures induced by blasting, excavation of the roadcut, and weathering are also excluded from this map.

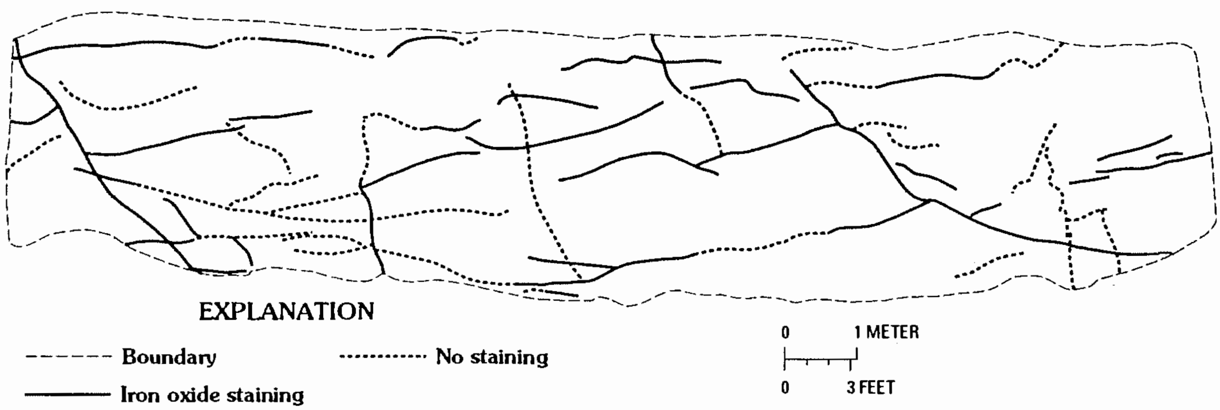

Figure 4. Fracture map of a portion of the road cut on Highway I-93.

Orientation has historically been considered the single most important characteristic of fractures. If a number of fractures share a small isolated range in orientation, they are said to form a set. Orientation is measured in the traditional manner by use of a Brunton compass. As shown in Figure 5a, the strikes of fractures at the I-93 road cut have a preferred direction of approximately N30°E and preferred dips ranging from 10° northeast to 85° southeast.

Surface Roughness is an important fracture characteristic because it controls the aperture variation and, therefore, the spatial distribution of fluid flow between the fracture walls. Surface roughness is measured by using a 15-cm-long contour gauge to copy the profile of an exposed, unweathered fracture surface. The measured profile is converted into a roughness coefficient (RC) by visually comparing it to a standard set of profiles of known RC, which range in integer values from 0 to 20 (Barton and Choubey, 1977). At the I-93 roadcut, the RC values range from 0 to 18, with the mode lying between 5 to 6 (Figure 5b).

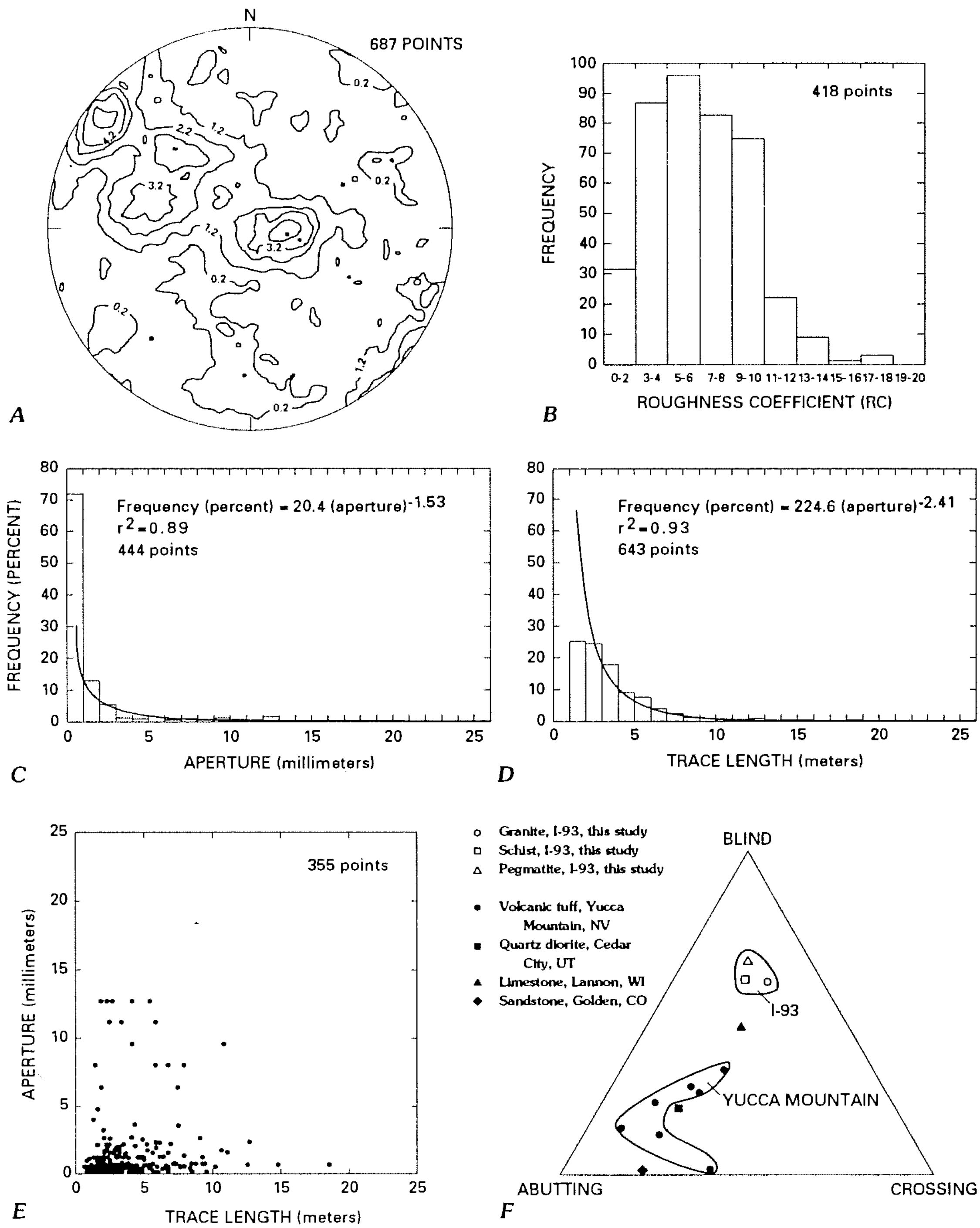

Figure 5. Characteristics of fractures exposed on five faces of the I-93 roadcut. (a) Contoured lower-hemisphere projection of poles to fractures. (b) Histogram of roughness coefficient. (c) Histogram of mechanical aperture. (d) Histogram of trace length. (e) Plot of trace length versus mechanical aperture. (f) Ternary diagram of percentages of fracture intersection and terminations. Data from sites mapped at Yucca Mountain, Nevada are shown for comparison.

Aperture is a major parameter that controls the flow characteristics of a fracture. The parlance of fracture hydrology distinguishes between the hydraulic aperture, which is determined by hydraulic testing, and the mechanical aperture, which is determined by using a ruler or a similar device to measure the gap between opposing fracture walls. At the I-93 outcrop, we measure the mechanical aperture with an automotive feeler gage or a finely grided ruler. A representative aperture is determined by visual inspection at places where weathering is minimal and mineralization is absent. The histogram of mechanical apertures is shown in Figure 5c. The scaling of mechanical apertures is shown by a power law fit with a scaling exponent of -1.53.

Relating the mechanical apertures to the apertures *in situ* is problematic. At land surface, fracture apertures are affected by the removal of overlying rocks and exposure to surface weathering. Although these surface disturbances can be minimized by measuring apertures in boreholes using borehole image logs, such an approach is not without drawbacks. The portion of a fracture intersecting a borehole can be affected by the abrasion of the drilling bit and by stress redistribution around the borehole. It does not appear possible, therefore, to measure mechanical apertures that are unaffected, either at the surface or in boreholes. Nevertheless, an imperfect measure of aperture is preferable to no measure. Scaling analysis of fractures whose apertures were fixed at depth by mineralization (Barton and Hsieh, 1989) suggests that unloading affects the scaling exponent but not the power-law form of the aperture distribution.

Mineralization (i.e., minerals deposited on fracture faces) is direct evidence that water has flowed through the fracture network in the past. At the I-93 roadcut, all of the natural fractures (as opposed to those that were induced by blasting) exhibit coatings of ferric hydroxide, which also precipitated in the rock matrix, in a zone extending as much as 1 m from the fracture into the rock. The iron staining sometimes forms a continuous band, and sometimes forms a rhythmic series of Liesegang bands. The deposition on fracture surface and in the rock matrix provides clues to understanding the history of ground-water circulation through the fracture network.

Trace Length is measured from the fracture maps or directly on the outcrop. The histogram of trace length at the I-93 roadcut is shown in Figure 5d. The scaling of trace length is shown by a power law fit with a scaling exponent of -2.41. The distribution is cut off at both the upper and lower ends. The upper limit is imposed by the size of the outcrop; fractures extending beyond the outcrop have their lengths truncated. The lower limit is imposed by our choice to ignore fractures having trace lengths of less than 1 m. As shown by Figure 5e, there is no apparent correlation between trace length and aperture. Such a correlation might be found for isolated non-intersecting fractures, but is not expected for networks of interconnected fractures.

Fracture Connectivity has a strong effect on the fluid-flow properties of a fracture network. Fractures that are not highly interconnected contribute little to the overall hydraulic conductivity of the rock mass. Connectivity can be represented by the ratios of the three types of fracture termination or interactions; those that (1) terminate in the rock matrix (blind endings), (2) cross, or (3) abut other fractures. The percentage of fracture terminations and crossings mapped at this site are shown on Figure 5f. The high proportion of blind endings suggests that the fracture network is poorly interconnected compared to fracture networks mapped elsewhere, such as Yucca Mountain, Nevada. Therefore, ground-water flow through the fracture network is expected to occur along highly tortuous pathways.

Density and scaling characteristics of the fracture network at the I-93 road cut are still being analyzed, and the results are not yet available. In general, an areal fracture density can be expressed as the sum of fracture trace lengths per unit area of the pavement surface. Scaling characteristics refer to the relationships between fracture network at different length scales. If the network exhibits self-similarity over a range of length scales, then fractal geometry is a useful tool for analysis. A fractal dimension of the fracture network can be determined by overlying square grids of various spacings on the fracture map and counting the number of cells intersected by the fracture traces. Knowledge of the scaling characteristics may eventually aid in predicting the effective properties (such as hydraulic conductivity) of the fracture network at one scale based on measurements made at a different scale

STOP 3. TOUR OF AREA HYDROLOGY. This tour visits three locations in the Mirror Lake area. Stops 3a and 3b are at the south side of Mirror Lake. Stop 3c is about a third of the way up the W Watershed.

Stop 3a. At the outlet of Mirror Lake, the outlet structure, lake stage gage, and Parshall flume can be observed. (Similar Parshall flumes have been installed to measure flow on the three inlet streams to Mirror Lake.) For many years the surface discharge from the lake at the outlet was measured by considering the dam itself as a broad-crested weir. However, this method was considered inadequate because of leakage through the boards and the changing condition of the top board. Therefore, in 1989 a Parshall flume was installed downstream from the dam. This flume was further modified in 1992 to be converted to a weir at times of low flow, when the flume loses sensitivity. To permit year-round operation, the flume is insulated and heated in winter, as are the Parshall flumes on the three inlet streams.

Stop 3b. K1 piezometer-well nest. Looking from the shore towards the center of Mirror Lake, one can see a raft on which are mounted instruments for determining lake evaporation. The instruments measure wind speed at three levels (1,2, and 3 m) above the lake surface, air temperature and vapor pressure at the 2-m level, and water surface temperature. When supplemented with short-wave solar and long-wave atmospheric radiation measured at the Forest Service station, the data allow for computation of lake evaporation by the energy-budget method and the mass-transfer method. The energy-budget method was used for six years (1982-1987) for two reasons: (1) To provide a standard against which simpler and less expensive empirical methods can be evaluated, and (2) to calibrate an empirical mass-transfer coefficient, so evaporation could be monitored over the long term by the mass-transfer method, which requires less data.

The piezometer-well nest at this stop is part of a network to monitor the three-dimensional distribution of hydraulic head in the ground-water flow system in the Mirror Lake area. At each piezometer-well nest, piezometers were installed at different depths in the drift, and a well was installed in the bedrock. Each piezometer was constructed by placing a 0.6-m long screen on 5-cm diameter PVC casing in a drill hole. The annular space between the casing and the hole was sealed with grout. A pedal cement basket positioned above the screen prevented the grout from reaching the screen. Bedrock wells were constructed by drilling 3 m into the bedrock, emplacing and grouting in a casing, then drilling into the bedrock to the desired depth. Also installed in the Mirror Lake area are several tens of water-table wells, which are piezometers whose screens just penetrate the water table. At the K1 piezometer-well nest, an automated recording system continually monitors the hydraulic heads in the piezometers, the bedrock well, and in a string of five water-table wells leading away from the lake. This arrangement permits monitoring the shape of the water table and the vertical distribution of hydraulic head in an area immediately adjacent to the lake.

A complex flow pattern, involving both downward and upward components of flow, can be inferred from the hydraulic heads at the K1 nest. In the upper part of the drift, a downward component of flow from the lake into the drift indicates that the K1 nest is situated in an area of seepage from Mirror Lake. This area, extending from about the K1 nest to the outlet dam, has a estimated seepage discharge of 260,000 m^3/year (Rosenberry and Winter, 1993). This discharge is approximately 46% of the total outflow from Mirror Lake. In the deeper part of the drift and in the shallow bedrock, hydraulic heads at the K1 nest show a strong upward gradient from the bedrock to the drift. As evidenced by the data from two additional piezometer-well nests, K2 and K3, this upward gradient continues along the entire vertical section BB' from Mirror Lake to Hubbard Brook (Figure 6).

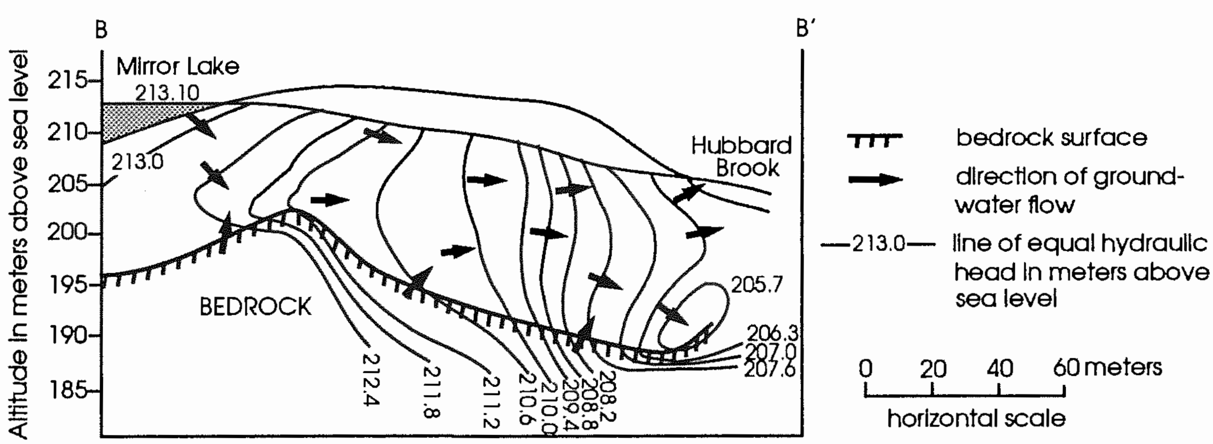

Figure 6. Vertical section BB' illustrating ground-water flow between Mirror Lake and Hubbard Brook.

Stop 3c. FS1 piezometer-well nest. The piezometer-well nest at FS1 is similar to the nest at K1 with one exception: the bedrock well at FS1 is instrumented with packers. In the absence of packers, a well can act as an open conduit connecting fractures that are otherwise unconnected. If the hydraulic heads in these fractures are different, water from the fractures with higher heads will enter the well, flow along the well bore, and exit into fractures with lower heads. This well-bore flow causes a mixing that is undesirable from the standpoint of geochemical sampling. Furthermore, the water level in the open well does not represent the heads in the individual fractures. To eliminate the well-bore connection, packers are installed at unfractured portions of the well to isolate the highly transmissive fractures or fracture zones from each other. The hydraulic head in each packer-isolated interval is measured in a 5-cm diameter PVC pipe that is connected to the interval via nylon tubing (Fig. 7).

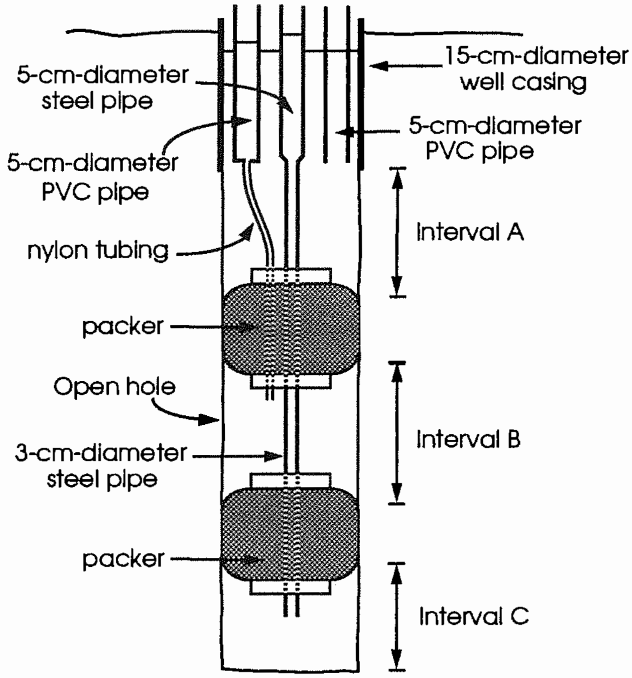

Figure 7. Instrument for multilevel monitoring of hydraulic head in bedrock well.

Hydraulic heads at the FS1 nest, which is situated on a kame terrace, exhibit the influence of the terrace on the local ground-water flow. In the upper part of the drift, the hydraulic gradient indicates an upward component of flow toward the water table. In the lower part of the drift, the hydraulic gradient indicates a downward component of flow into the bedrock. This divergence of flow may be due to the presence of the terrace, which causes breaks in the slope of the water table. On the uphill side of the terrace, an upward break in the water-table slope enhances upward flow. On the downhill side, a downward break in slope enhances downward flow. Preliminary cross-sectional modeling of hypothetical settings and of the Mirror Lake area (Harte, 1992) indicates that such a local flow perturbation may be common along mountain slopes. The presence of a terrace results in a rather complex interchange of ground water between the upper part of the bedrock and the lower part of the drift.

A study conducted near the FS1 nest illustrates another complexity in the ground-water flow pattern on a mountain side. In general, it might be expected that streams on mountain sides are ground-water drains (i.e., they gain ground waters from both the sides and bottom). However, in a study of the interaction between the W Stream and ground water near the FS1 nest, Shattuck (1991) found that the stream does not act as a drain along its entire length. By constructing wells along six transects across the stream and contiguous uplands, Shattuck was able to examine the ground-water flow pattern in detail. At transects where the stream flowed on till, Shattuck found that the W Stream indeed gained ground water. However, at a bend in the W Stream where the entire drift section was sand, ground water enters the stream from the uphill bank, and stream water infiltrates into the ground along the downhill bank to flow toward Hubbard Brook. This finding indicates that a detailed knowledge of the geologic framework is essential to the understanding of ground-water movement on a mountain side.

STOP 4. SURFACE GEOPHYSICS. Open field 200 m southeast of Mirror Lake outlet. At this stop, we demonstrate the use of azimuthal seismic refraction method and azimuthal square-array direct-current (DC)-resistivity method for determining the predominant strikes of steeply dipping fracture sets in the bedrock, which underlies 3 to 10 m of glacial drift.

Azimuthal Seismic-Refraction Method. In a uniform rock containing a single set of closely spaced, steeply dipping fractures, the seismic-velocity maximum occurs in the same direction as the fracture strike, and the seismic-velocity minimum occurs at 90° to the strike. Azimuthal changes in seismic velocity can be determined by an azimuthal seismic-refraction method described by Park and Simmons (1982). At this site, we conducted an azimuthal seismic-refraction survey by rotating a seismic-refraction line in 22.5°-increments about a common center point. Twelve vertical displacement 7-Hz geophones were placed 3.1 m apart. For each line, a 5.7-kg sledge hammer served as the impulsive energy source at each shot location. The shot locations consisted of a center shot between geophones 6 and 7, a near-end shot 3 m from each end of the line, and a far-end shot 35.1 m from each end of the line (Figure 8). Elevations were recorded for each shot and geophone location to within 0.03 m.

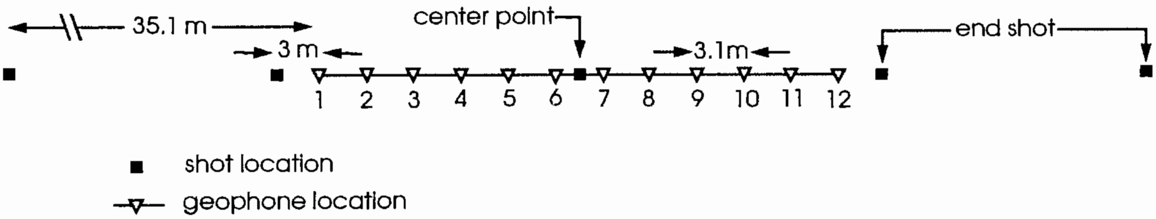

Figure 8. Locations of shot points and geophones on seismic refraction survey line.

We analyzed the seismic-refraction data for each line to determine the compressional (P)-wave velocity of the bedrock. The interpretation of fracture orientations from azimuthal refraction data can change depending on the type of velocity analysis used. In this study, the Hobson-Overton method, as implemented in the SIPT program (Haeni and others, 1987) and developed by Scott and others (1972) was used. The azimuthal plot of the bedrock seismic-velocities (Figure 10a) was interpreted to indicate a primary set of steeply dipping fractures and (or) foliation striking 22.5°, and possibly a secondary set of steeply dipping fractures striking 127°.

Azimuthal Square Array DC-Resistivity Method. In a uniform bedrock with closely spaced, steeply dipping, water-filled fractures, the maximum apparent (measured) resistivity occurs at 90° to the fracture strike. This anisotropic resistivity can be determined by the azimuthal square-array D-C resistivity method as discussed by Habberjam (1972, 1979). The method has not been in widespread use, but two applications are reported by Darboux-Afouda and Louis (1989) and Sehli (1990).

At this site, we conduct the DC-resistivity survey using a square array with the electrodes positioned at the corners. The array size (A) is the length of the side of the square. For depth sounding, the array is expanded about the center point in increments of $A \times \sqrt{2}$ (Habberjam and Watkins, 1967.) For each square, three measurements are made—two perpendicular measurements and one diagonal measurement (Figure 9). The two perpendicular measurements contain information on the variation of the resistivity in the subsurface. The diagonal measurement serves as a check on the accuracy of the perpendicular measurements.

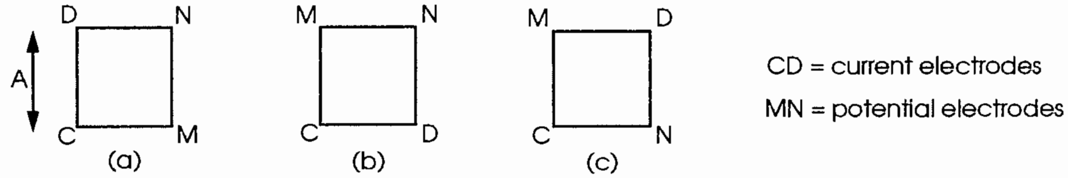

Figure 9. Electrode positions for square array measurements. (a) and (b) show perpendicular measurement. (c) shows diagonal measurement.

The survey conducted during the summer of 1992 consisted of six square-array soundings separated by a rotational angle of 15° about the array center point. For each sounding, the A-spacings of the arrays were expanded from 5 m to 50 m. A computer-controlled data acquisition system allowed a complete sounding at a given azimuth to be collected automatically via remotely accessed, addressable switches that connect the appropriate electrodes for a given measurement.

Square-array data can be interpreted graphically (using square-array data) or analytically (using crossed square-array data) to determine the fracture strike. In the graphic approach, the apparent resistivity is plotted against the azimuth of the measurement, and the fracture strike is perpendicular to the direction of maximum resistivity. In the analytical approach, crossed square-array data (two square arrays separated by an angle of 45°) are used. A method for analyzing crossed square-array data is described by Habberjam (1975).

The data collected at this site show a significant change in apparent resistivity for different azimuthal orientations for all A-spacings. Graphical interpretation of the individual square-array data can be made on a rosette diagram (Taylor and Fleming, 1988). The apparent resistivity data plotted as a function of azimuth is shown for the 50-m A-spacing (Figure 10b). The maximum resistivity occurs at 120°. The interpretation of this is that a primary set of steeply dipping fractures is present with a strike of 30°. A secondary maximum resistivity occurs at 60°, and assuming that these data do not reflect inhomogeneities in the bedrock, this peak could indicate the presence of another steeply dipping fracture set striking 150°.

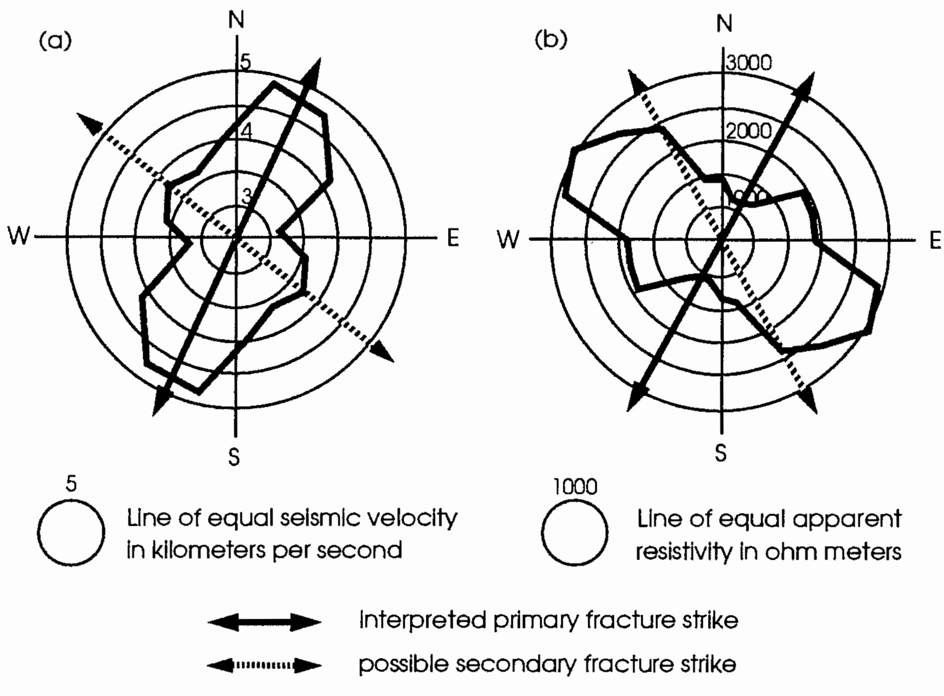

Figure 10. Plot of (a) seismic velocity and (b) apparent resistivity versus azimuth at Stop 4.

STOP 5. BOREHOLE GEOPHYSICS. FSE Well Field. At this stop, we demonstrate a four-step approach to characterizing fractures by borehole geophysical logging methods. The first step uses a suite of conventional geophysical logs to define the large-scale structure of the rock mass along the well bore. Next, downhole image logs are used to locate precisely the depth and orientation at which each fracture intersects the well bore. The third step uses high-resolution flow measurement techniques to determine which of the fractures intersecting the well bore produce flow when the well is pumped. The final step uses cross-borehole flow tests to determine the hydraulic connections between producing fractures identified in each of the separate boreholes.

Conventional Logs in Bedrock Wells (Step 1). Conventional geophysical logs such as caliper, gamma and resistivity logs show places in the well bore where there are major changes in background lithology or water quality, and "anomalous intervals" that may possibly signify the presence of fractures, fracture zones, and the associated alteration "halos". In borehole FSE5, the large deflection in the gamma log (B in Figure 11) corresponds to a change in rock type from granite (above 47 m depth) to pegmatite (below 47 m), and the single-point resistance log indicates an abrupt shift in water quality (F in Figure 11). There are several depths where the caliper log indicates local borehole enlargements (A in Figure 11). Since caliper arms are too large to fit into the apertures of natural fractures, these enlargements are indirect indications of fractures, and represent the local enlargement of the well bore where the drill bit encountered altered and fractured rock. Similar anomalies associated with the resistance, neutron, and gamma logs (C, D, and E in Figure 11) are assumed to indicate depths where the alteration around fractures and the mechanical enlargement of the borehole in the vicinity of the fracture are extensive enough to affect the geophysical measurement over the geophysical sample volume (Paillet, 1991b).

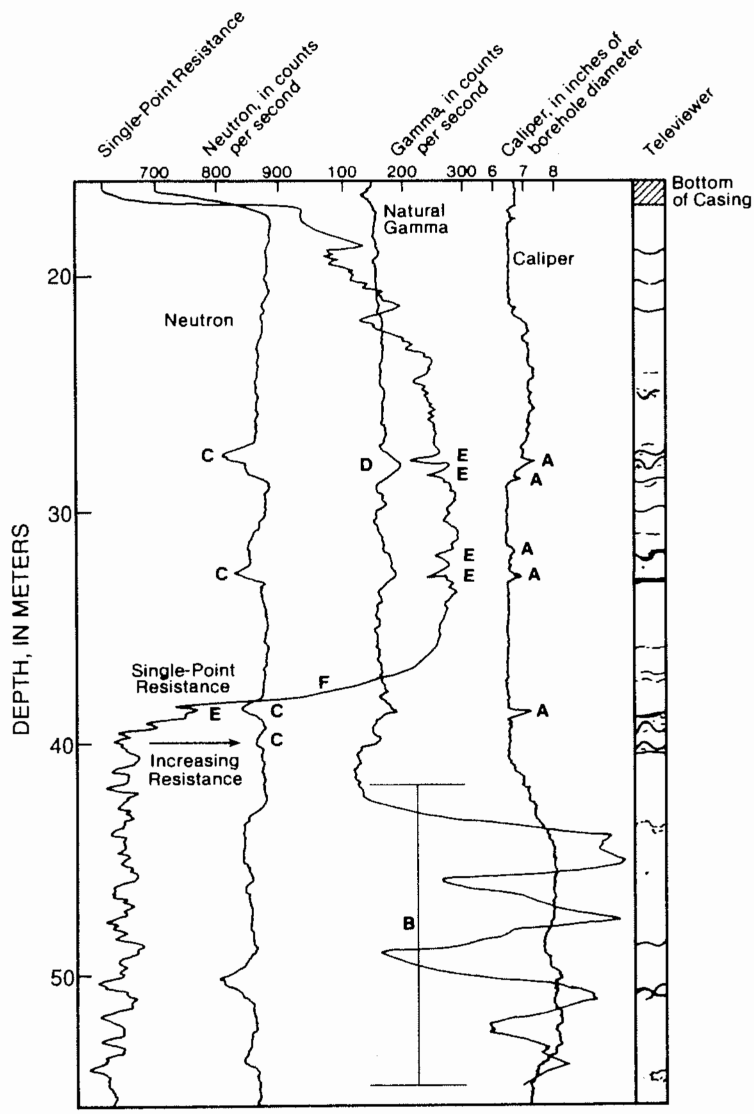

Figure 11. Single-point resistance, neutron, gamma, caliper, and borehole televiewer log of well FSE5.

Borehole Televiewer—A Downhole Image Log (Step 2). The borehole televiewer (BHTV) (Zemanek and others, 1970) is a tool that uses an acoustic signal to generate an image of the fractures that intersect a borehole. The BHTV scans the borehole wall with a 1.25 MHz source rotating at about 3 revolutions per second, and measures the intensity of the reflection of that acoustic energy. The signal is plotted as a photograph where the borehole wall is "split" along the magnetic north azimuth (Figure 12). Fractures are indicated by the characteristic "S" shaped line where acoustic energy is scattered by the fracture. This image can be used to compute fracture strike and dip by measuring the vertical distance over which the fracture intersects the well bore, and noting the azimuth of the high and low points of the fracture image. These measurements need to be corrected for borehole orientation, which can be determined through a borehole deviation survey.

A great deal of insight can be obtained by comparing the BHTV data, which gives the appearance of the fracture at the borehole wall, with the conventional logs, which average the properties of fractures with those of the surrounding rock. This comparison usually confirms that the anomalies given by the conventional log are associated with the largest fractures and most intensely fractured intervals, while isolated fractures are generally not indicated by the conventional logs. The relative "size" of fractures given by the BHTV logs also may be related to fracture permeability, but there are many complications and qualifications in relating the width of the fracture "line" on the BHTV log to fracture aperture. One simple approach is to assign a permeability score to each fracture ranging from 1 (probably closed) to 5 (a major open fracture zone or small cavern) (Paillet and Kapucu, 1989).

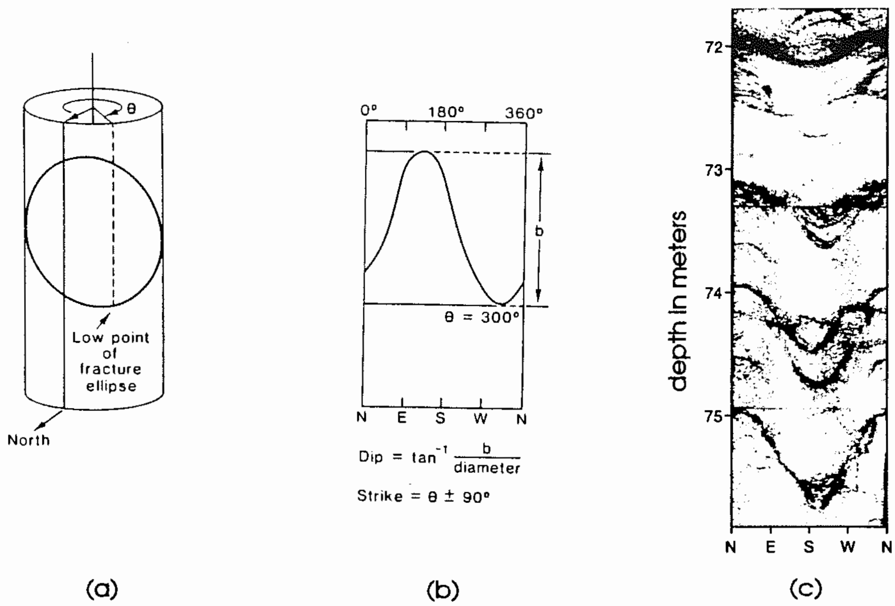

Figure 12. Schematic drawing of (a) fracture intersecting borehole, and (b) borehole televiewer display of fracture trace. (c) Example of borehole televiewer log.

Production Tests to Define Inflow (Step 3). We have found from experience that the "size" of fractures identified on borehole image logs like the BHTV can be a good representation of local fracture aperture, but may not indicate whether the fracture takes part in ground water flow through the rock mass. To identify those fractures that produce water to a well, we pump a well and measure the distribution of flow rate along the well bore. Where the flow rate stays uniform along the well, the rock is either unfractured or the fractures do not yield water to the well. In contrast, a location where the flow rate changes abruptly marks the presence of a water-productive fracture.

Because wells drilled in fractured rocks often do not yield significant amount of water, we generally pump at a low rate (several to tens of L/min). At these pumping rates, the distribution of inflow along the well bore cannot be accurately measured with a conventional impeller flowmeter. In a 15-cm diameter borehole, the most sensitive impeller flowmeter requires a flow rate of greater than 5 L/min to turn the impeller blades (Hess and Paillet, 1990). To improve the sensitivity, a number of high-resolution borehole flowmeters are being developed. We use the U.S. Geological Survey heat-pulse flowmeter (HPFM). This device uses a slight electrical discharge across a wire grid to heat a small parcel of water, and measures the time required for that parcel of water to travel about 2 cm up or down the borehole. The HPFM system has a resolution of about 0.04 L/min when the annular region between the tool measurement section and the borehole wall is blocked with a downhole-inflated packer.

In many situations, there is flow along the well even before the pump is turned on, because the well connects previously unconnected fractures that are at different ambient hydraulic heads. Although this borehole flow rate is extremely small (tenths to hundredths of L/min), it can be measured by the HPFM. The measurement of this flow rate under unpumped conditions provides additional information on the locations of water-productive fractures in the well.

For the Mirror Lake area, we generally find that most of the inflow to the bedrock wells enters at one or two specific fractures or fracture zones, while many other similar fracture zones produce little or no measurable inflow (Figure 13). With a few exceptions, the fractures found to produce flow in one borehole are not found to project to a similar fracture intersecting an adjacent borehole. So far we have not found anything unusual about the orientation or appearance of the producing fractures that would distinguish them from the much larger population of fractures that produce little or no flow during pumping. Perhaps a geomechanical approach to analyzing the relationship between the fracture patterns, rock stress, and geologic history may explain this observation.

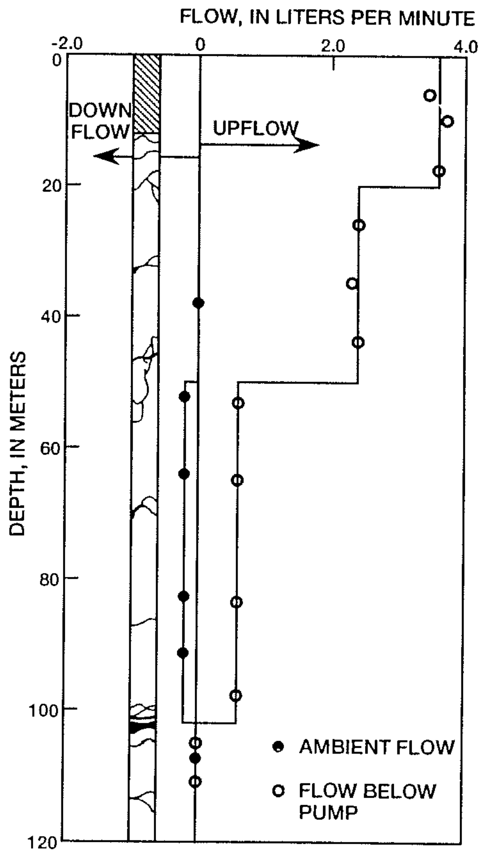

Figure 13. Borehole flow log in well FS1 under unpumped conditions and during pumping.

Cross-Borehole Flow Tests (Step 4). The identification of producing fractures in individual boreholes tells us little about how these fractures are connected into a larger-scale flow network. To help us infer how fractures are connected in the rock mass, we developed the cross-borehole flow test. In a cluster of open wells that penetrate a fracture network, pumping from one well will induce flow in the unpumped (observation) wells. The cross-borehole flow test measures the flow rate distribution in the pumped well and in the observation wells.

To illustrate the application of this method, we pumped well FSE4 and measured flow rates in the pumped well and in the observation wells FSE1, FSE2, FSE3, and FSE5. When pumping begins, water is drawn from the observation wells through the fractured rock into the pumping well. The flow measurements show that water exits each observation well through one or two fractures, and enters the pumping well through a single fracture (Paillet and others, 1987). Figure 14 shows a cross section through the center of the borehole array. Projected onto this cross section are the pumping and observation wells, the fractures intersected by the wells, and the inflow and exit points. Note that the overall flow paths in the rock appear to form a thin, near-horizontal, permeable zone. However, this permeable zone is composed of intersecting fractures with moderate dips.

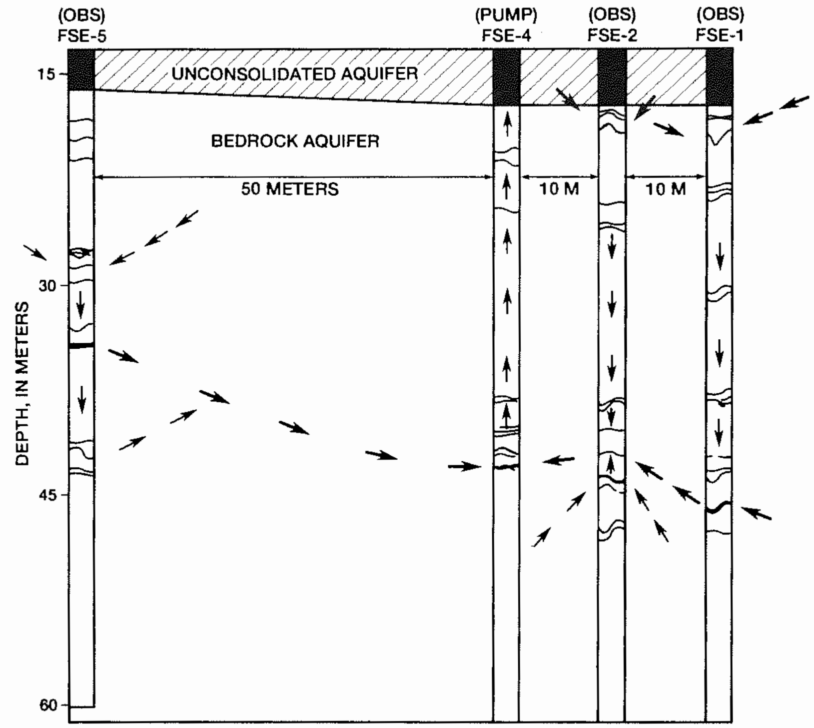

Figure 14. Borehole flow in wells FSE1, FSE2, and FSE5 during pumping of FSE4.

During pumping, flows in the well bores evolve as the drawdown propagates from the pumping well. The transient nature of the well-bore flow contains valuable information about the hydraulic properties of the fracture network. We are currently developing methods to analyze this transient flow, in ways that are similar to the traditional well test analysis. For simple settings such as that of a single fracture connecting a pumping and an observation well, we develop type curves that can be matched to the flow data to determine the hydraulic properties of the fracture. More complicated settings that involve multiple fractures and multiple observation wells will require analysis by a numerical model. For these complicated settings, the interpretation may not be unique. Nevertheless, the cross-borehole flow test appears to have real potential utility, especially for preliminary identification of important fractures. Such information is extremely valuable for the design of multiple-borehole hydraulic tests.

STOP 6. BOREHOLE VIDEO CAMERA LOGGING. FSE Well Field. At this stop, we demonstrate the use of a submersible color video camera to describe bedrock lithologies and fractures encountered in boreholes.

The use of a video camera was prompted primarily by a need to identify or verify rock types encountered in wells in the Mirror Lake area. These wells were drilled by air-percussion method, which produced drill cuttings measuring 1 to 2 mm in length. Although we can describe the mineralogy, texture, grain size and color of the drill cuttings, determining the rock types is a difficult task. The cuttings are often not large enough to exhibit features of the source rock, such as foliation or banding. If a cutting sample is derived from a mixture of two or more rocks, it is impossible to determine the relative positions of the rocks in the well. By using a video camera to observe the borehole wall, we improve our ability to identify the rock types and the locations of contacts.

Description of the Equipment. The equipment consists of the downhole camera and light source, and the uphole winch, control unit, and video tape recorder and monitor. The color video camera and light source are encased in a 9.2 cm diameter housing, which is suspended from a double-steel-wrapped coaxial cable. On land surface, a powered winch raises and lowers the camera in the borehole. A camera control unit encodes the depth of the camera, digitizes the camera's view of the borehole, and provides downhole control of the light intensity, focus, and iris (or lens aperture), all of which enhance the video image. The processed image, including a superimposed digital depth readout, is sent to a video tape recorder (VTR) and a high resolution monitor. This camera has two light attachments which allow for two different perspectives of the well: one looking down the well and the other looking at the side of the well. To adequately view and record the image, a high-quality VTR is used, with fast- and slow-forward and reverse speeds, freeze frame and real-time counter capabilities.

Video Survey of Borehole. Two surveys are made in every borehole. For the first survey, the camera is positioned to look down the borehole. From this perspective (Figure 15a), the borehole wall closest to the camera lens appears at the edge of the video image, while the bottom of the well should appear at the center. In the actual video image, however, the bottom of the well is blocked by the light attachment, which is supported by two rods. A planar feature (e.g., a fracture) that intersects the borehole at 90° appears as a circle, while a planar feature that intersects the borehole at less than 90° appears as an ellipse. During the first survey, we record the occurrence of foliation, fractures, zones of borehole enlargement, and major changes in rock type and texture. We also select portions of the well to be more closely viewed during the second survey.

The second survey uses a light attachment that has a 360° rotational mirror tilted at 45° to the camera lens to permit a side-looking view of the borehole wall. The resultant image is a composite of two views. The mirror view appears at the center of the image (Figure 15b). Surrounding the mirror view is the wide-angle view that looks beyond the edges of the mirror, and down the well, much like the perspective shown in Figure 15. The simultaneous presentation of side-looking and downward-looking views allows the viewer to see the borehole wall in perspective. This is especially helpful when trying to find individual fractures identified in the first survey, or when tracing a fracture that is connected to or in close proximity to other fractures. During the second survey, we view the rocks in greater detail, and we make more precise measurements of the locations and dips of major fractures noted during the first survey.

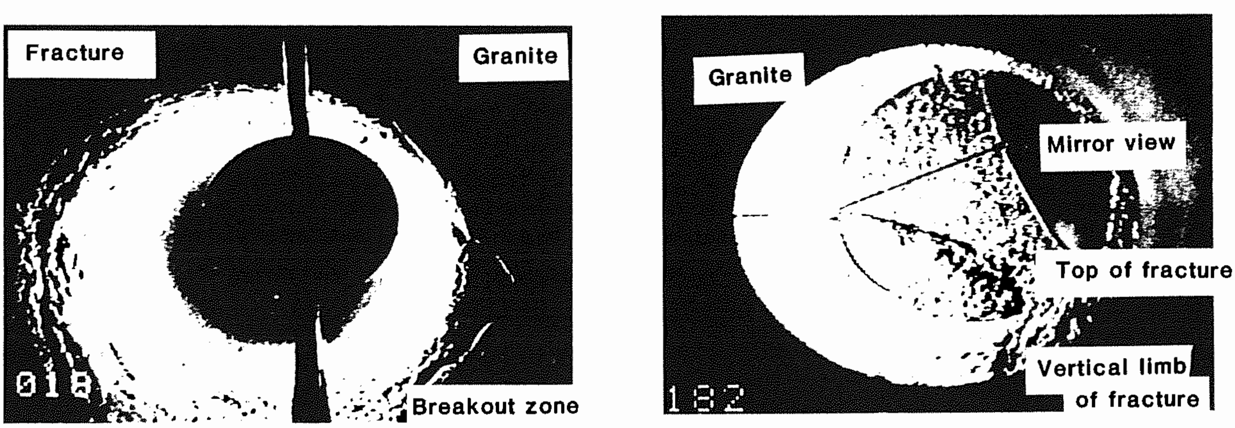

Figure 15. (a) Video image looking down the well. (b) Composite side-looking and down-looking video image.

Video Images of Rock Types. Typical images of rock types in the Mirror Lake area have been generalized from examining the video logs of 29 wells in the Mirror Lake area. Because of the very localized nature of the sampling, we have not assigned geologic names to the rocks. However, in the following descriptions, the schist and gneiss probably correspond to the metamorphic rocks of the Rangeley Formation. The granite probably corresponds to the Concord granite, and the basalt probably corresponds to the lamprophyre.

Schist and gneiss are easily identified by the foliated biotite, muscovite, and sillimanite. Some schist sections of the wells exhibit augens, banding, and/or large felsic sections. Metasedimentary rocks typically are black, brown, green, yellow or white. The coarse-grained biotites and muscovites reflect the light and appear shiny, whereas fine-grained schists are much darker in comparison. In general, the schists are much darker than the granites.

The granite is leucocratic, typically creamy white to gray with an occasional greenish tinge. Iron staining associated with fractures can be seen clearly in the some of the video images. These plutonic rocks are usually medium grained and have a sugary texture. They occasionally exhibit weak foliation of biotites and muscovites, and sometimes contain strongly foliated biotite schlieren. These linear features are easily visible in the video image, and can usually be differentiated from fractures. Local variations in the granite, such as increased biotite or quartz content, can darken the borehole wall. A few of the granites display phenocrysts of garnet that can be easily seen with the side-looking mirror attachment.

Pegmatite is usually the lightest and most reflective rock in the boreholes. The contacts between the pegmatite and their host rocks can be viewed with the mirror attachment. Some contacts are sharp and straight while others are graded or wavy. Individual crystals of muscovite, biotite, feldspar and quartz can be easily observed and their length measured.

Basalt is the darkest and least frequently encountered rock in the wells. Because of their extremely fine grained matrix and mafic minerals, these rocks reflect very little light. However felsic inclusions, including feldspar phenocrysts and cavity fillings, are highly reflective and discernible in the video image. Basalts crosscut both the granite and the schist, occur at a variety of depths, and have orientations ranging from sub-horizontal to sub-vertical.

Fracture identification. Fractures appear in the video image as dark lines. Fractures can be differentiated from other dark, planar features by a change in relief or the smoothness of the wall. When the light source is below the fracture, the fracture is in a shadow. In contrast, a dark, planar feature that is not a fracture (e.g., a thin basalt dike) appears smooth and continuous. Some fractures exhibit significant borehole enlargement and elongation. Other fractures have breakout zones only along a portion of the fracture.

During the first survey, fractures are identified individually or, when multiple fractures occurred over a short distance, as fracture zones. We note whether the fracture intersects the entire borehole or only part of the borehole. The fractures are recorded as horizontal, moderately dipping or steeply dipping.

The dip of fractures can be determined during the second survey, with the use of the side-looking mirror, by determining the vertical distance from the top of the fracture to the bottom of the fracture. This distance is measured at land surface by first marking the cable when the camera is pointed at the top of the fracture, then marking the cable again when the camera is pointed at the bottom of the fracture, and finally measuring the distance between the two marks. The division of this distance by the borehole diameter (obtained from the caliper log of the well) yields the tangent of the dip angle, as long as the borehole is vertical. Otherwise, one must correct for the deviation of the borehole. Because compass directions are not indicated on the video image, it is not possible to determine the fracture strike.

We have not attempted to measure the fracture apertures from the video images. Instead, fracture apertures are qualitatively described as "very tight", "narrow", "wide", or "fracture zone with breakout." In addition, we note the occurrence of mineralizations or coatings. These include iron (sometimes occurring within the rock matrix), grayish white clay, white calcite, or light white to brownish yellow quartz. It was impossible to differentiate black manganese coatings from shadows due to the lighting.

Effectiveness of Video Logging. The effectiveness of video logging can be assessed by comparing the video log interpretations with cores and borehole televiewer logs. We made such a comparison for two wells that were drilled first by coring a smaller hole and then enlarging the hole by percussion drilling. Interpretations of rock types using video logs and percussion drill cuttings agreed with the interpretations of the core. There was also general agreement between fractures identified by video logging and by the borehole televiewer. These results suggest that, for the purpose of rock-type and fracture identification, the choice of percussion drilling followed by video logging is a practical, low-cost alternative to coring. As an additional benefit of video logging, knowledge of the bore-hole wall condition, e.g., whether it is circular, enlarged, or jagged, provides valuable information for selecting the placement of packers for hydraulic and tracer tests.

STOP 7. CROSS-HOLE ELECTROMAGNETIC TOMOGRAPHY. FSE Well Field. At this stop, we demonstrate the use of electromagnetic tomography to map fractures in the bedrock. A tomogram is a spatial visualization of a rock property such as electromagnetic wave velocity, attenuation, or scattering. Because the presence of a fracture will alter the properties of a rock, pictures of rock property distributions can be interpreted as pictures of fracture distributions, superimposed on any lithologic inhomogeneities.

The U. S. Geological Survey has designed and built a high-speed system that can function as a hole-to-hole electromagnetic tomography system or alternatively as a single-hole reflection mode radar. When operating in the hole-to-hole tomography mode (Figure 16), short electromagnetic wavelets are radiated from a transmitter in one hole and received by a receiver in another borehole. The received wavelet is 1) delayed in time by propagation distance and relative dielectric permittivity (the square of the ratio of the speed of light in vacuum to the wave propagation velocity in the rock), 2) reduced in amplitude by geometric spreading and attenuation in the rock, and 3) broadened if frequency dependent velocity, attenuation, or scattering occurs. From each recorded wavelet one can deduce an average velocity, average attenuation, and average dispersion. If data are recorded with sufficient density at a variety of angles through the volume of rock under study, the spatial distribution of rock properties such as velocity, attenuation, or dispersion can be determined by a tomographic inversion algorithm.

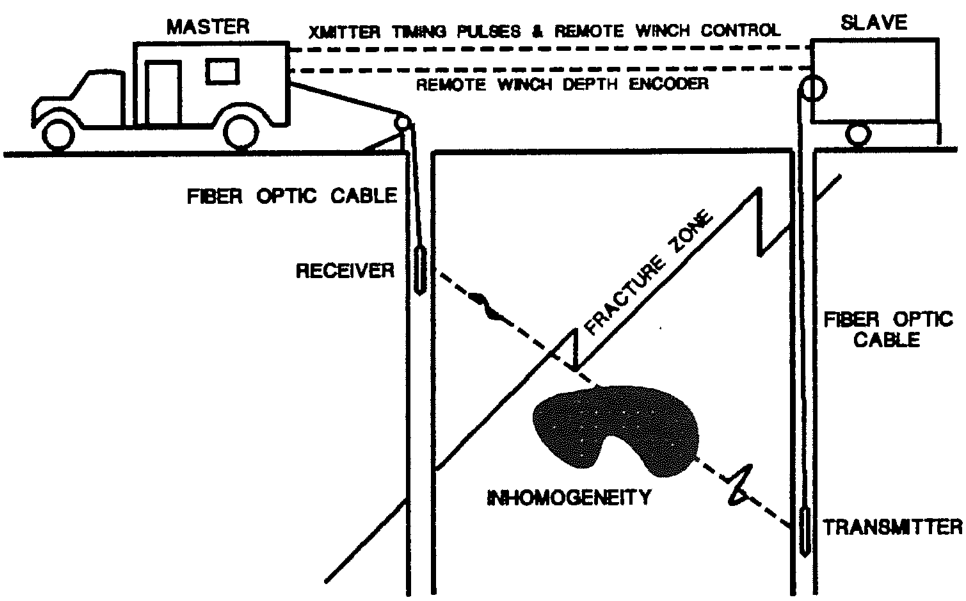

Figure 16. Equipment for hole-to-hole electromagnetic tomography

The resolution of a tomogram is limited by wavelength, spatial data density, and viewing angle. Two features cannot be resolved (determined to be distinct from each other) if the separation between them is smaller than about one third of a wavelength in the medium. For a 60 MHz center frequency, the wavelength in a typical granite is about 2 m, so the resolution limit is about 67 cm. A fracture with an aperture much smaller than the resolution limit may be detected if the lateral extent of the fracture is large, but two fractures closer together than the resolution limit cannot be resolved as distinct. Resolution can be further degraded if the data density is low, i.e., when the recording interval is larger than the wavelength used. In most geologic applications, the limited viewing angle resulting from placing the transmitter and receiver in boreholes is yet another factor that can degrade the resolution of the tomogram.

During the tomographic survey, both the transmitter and receiver are raised from the bottom to top of their respective boreholes at equal and uniform speeds, so that a constant vertical offset is maintained between the two units. To achieve good dynamic control over the relative depths of the transmitter and receiver, we designed and built a dual drawworks controller that can slave the motion of the transmitter winch to that of the receiver winch. This controller typically maintains the depth offset to within ±5 cm. To achieve a high spatial data density within a reasonable time, we designed and built a high speed digitizer/stacker that can record at an effective digitizing time interval of 1 ns while stacking signals to increase signal-to-noise ratio. Real-time display of the full wave forms is available either in wiggle trace or color map form. The acquisition, tomographic processing, and graphics visualization software are described by Olhoeft (1988). In the Mirror Lake area, we survey each well pair five times with five different transmitter-receiver offsets: -10 m, -5 m, zero offset, +5 m, and +10 m. We typically stack 512 repetitive wavelets, displaying and recording them while logging continuously at about 12 cm/s. At that logging speed we achieved a recording interval of about 17 cm. This spacing is considerably finer than the one-or-more-meter spacing in typical applications of tomography to geologic media.

An example of a velocity tomogram between wells FSE1 and FSE4 at the Mirror Lake site is shown in Figure 17, which is a gray scale reproduction of a color original. The region of low electromagnetic wave velocity corresponds to high transmissivity fractures determined by Paillet (1991b). The color original and computer data display will be available at the field demonstration.

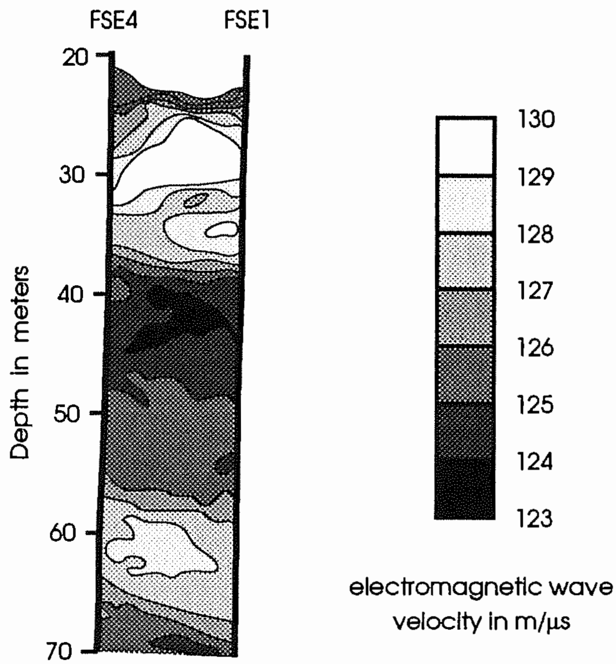

Figure 17. Velocity tomogram in vertical section between wells FSE1 and FSE4.

STOP 8. HYDRAULIC TESTING. FSE Well Field. At this stop, we demonstrate the techniques and equipment used to conduct single-borehole hydraulic tests.

The equipment for single-borehole hydraulic testing (Figure 18) consists of three main components: the straddle packers, the fluid injection system, and pressure transducers. A packer is a downhole device for sealing a borehole. When inflated, the flexible bladder of the packer expands to seat against the borehole wall. We use pneumatic packers, which are inflated by compressed air. For hydraulic testing, two packers are normally used to isolate the test interval in a borehole. Such a set up is often referred to as a straddle-packer configuration.

The fluid injection system consists of a pressurized water tank at land surface, flexible tubing (water line) that transmits water from the tank to the test interval, two in-line flow meters to measure the injection flow rate, and a downhole air-operated valve that starts and stops the fluid injection. The water tank is pressurized by regulated compressed air to achieve the desired downhole injection pressure. Depending on the flow rate, the injection water is routed through one of two in-line flow meters, one for higher rates and the other for lower rates. Together, the two flowmeters can accurately measure flow rates from 5 ml/min to 10 L/min.

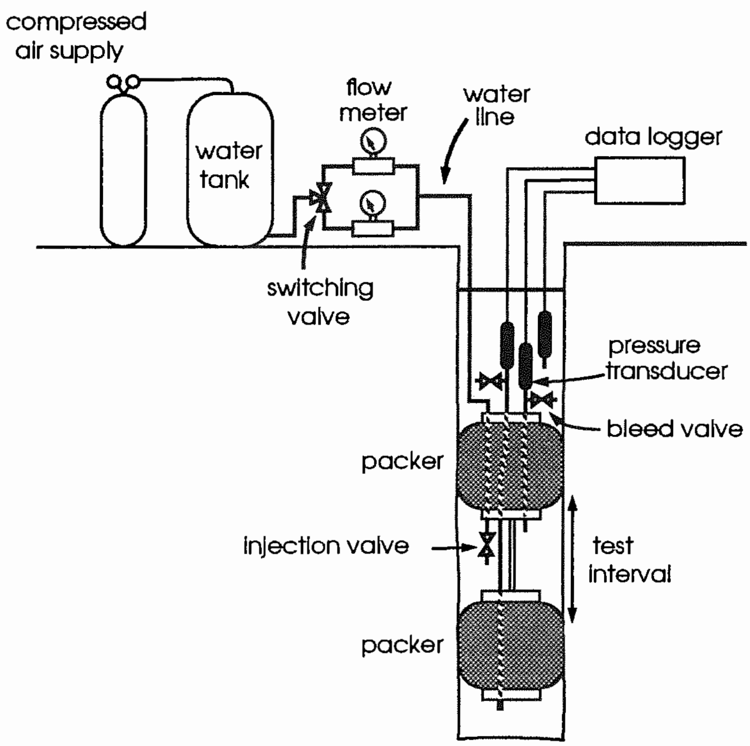

Figure 18. Equipment for single-borehole injection test.

Downhole pressures are measured by pressure transducers. To determine the hydraulic properties of the test interval, the most important pressure measurement is the pressure change in the test interval. However, we also measure the pressures above and below the test interval, which should remain constant under ideal conditions. A rise in the pressures above and/or below the test interval indicates possible fluid leakage, which can result from a poor packer seal or the presence of "short-circuiting" fractures between the test interval and the rest of the borehole. If a significant portion of the injection water leaks around the packers, the injection test would yield incorrect values of hydraulic properties.

Our test procedure consists of the following steps. (1) The straddle-packer assembly is lowered to the desired depth. (2) The packers are inflated. (3) When the test interval pressure has returned to its ambient value, the downhole valve is opened, and injection begins at a prescribed pressure. (4) When the flow rate has stabilized, the injection pressure is increased, causing the flow rate to also increase. (5) When the flow rate has once again stabilized, the downhole valve is closed, thus shutting off the injection. (6) We measure the pressure decay, and then deflate the packers. The test procedure requires approximately 45 minutes to complete.

Figure 19 illustrates schematically the history of pressure and flow rate at the injection interval. Inflating the packers will increase the fluid pressure as the packers enlarge to seat against the borehole wall (line segment AB in Figure 19). The decay of this pressure to its ambient value (segment BC) can require a long time in a low-permeability test interval, in which case the use of a "bleed" valve to release the pressure can significantly decrease the decay time. Line segment DE marks the start of injection. While the injection pressure is kept constant (segment EF), the injection rate is initially high but decreases with time to a stable value. Line segment FG marks the second pressure increase, while point H marks the end of injection, which is followed by a pressure decay (segment HI).

Our analysis of the injection tests is based on the assumption that the fluid injection establishes a radially diverging, steady-state flow from the test interval. Furthermore, we assume that the injection test influences the fluid pressure within a finite radial distance from the test interval, i.e., there is no pressure increase beyond a radius of influence. With these assumptions, we can calculate the transmissivity T of the rocks in the test interval by the Theim equation (as discussed by Bear, 1979): $T = (Q\rho g/2\pi\Delta p)\ln(R/r_w)$, where Q is the stabilized injection rate, ρ is the fluid density, g is gravitational acceleration, Δp is the pressure increase (injection pressure minus ambient pressure), R is the radius of influence, and r_w is the radius of the test interval. Because R appears in the argument of the logarithm, an approximate value is adequate for calculating transmissivity. For the Mirror Lake area, we assume R to be 3 meters. Dividing the transmissivity by the length of the test interval yields the hydraulic conductivity of the rocks in the test interval.

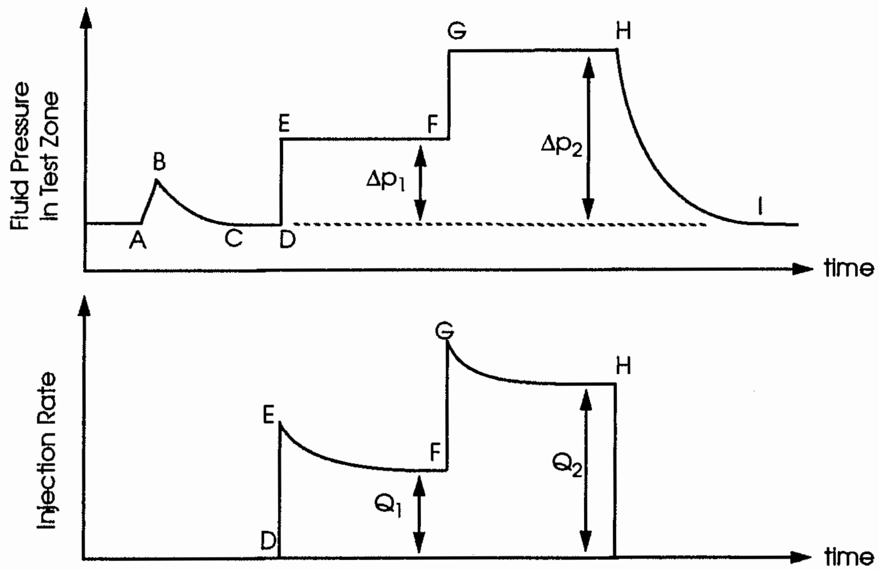

Figure 19. Pressure and flow rate history during single-borehole injection test.

The use of two different injection pressures provides a way of checking if injection pressures are forcing fractures to open, thus changing their transmissivities. For each injection pressure, an estimate of the transmissivity of the fracture in the test interval is made. If the two transmissivities are similar, we infer that fracture properties are not altered during injection. However, if the transmissivity computed with the higher injection pressure is significantly larger than that computed from the lower injection pressure, we consider this as evidence that the injection pressure is forcing open fractures and changing their hydraulic properties.

The results of the above steady-state analysis are subject to at least three sources of error. First, for tests of relatively short durations (tens of minutes), conditions may be far from steady state at the end of the test. Second, the concept of radius of influence is not rigorously defined but is made for mathematical simplification. Third, the analysis also ignores the effect of heterogeneities and possible presence of hydraulic boundaries. For these reasons, the hydraulic test results should be viewed as an order-of-magnitude estimate of the transmissivity or hydraulic conductivity of the fractured rock in the test intervals.

The lowest hydraulic conductivity that can be determined by injection testing is primarily controlled by the lowest measurable flow rate, highest injection pressure, and the longest test interval. At the Mirror Lake site, our flow meter can measure flow down to 5 ml/min. To prevent opening a fracture by high fluid pressure, we generally limit the injection pressure to less than 350 kPa (50 psi) above the ambient downhole pressure. To obtain an adequate resolution of hydraulic conductivity distribution along the borehole, we typically set the test interval at 5 meters. These values give the lower limit of detectable hydraulic conductivity at approximately 3×10^{-10} m/s. Because this value is substantially higher then the typical hydraulic conductivity of intact crystalline rock, we apply injection tests only to intervals of a borehole where there are fractures.

Selecting the test intervals in a borehole requires knowledge of fracture location and borehole wall condition. We use borehole televiewer logs and video camera images to identify the position of fractures along a borehole. To achieve a pressure-tight packer seal, the packers should be inflated against smooth sections of the borehole. Caliper logs, which makes a mechanical measurement of the average borehole diameter, and video images are extremely useful for locating sections of the borehole that are rough or broken. These sections are avoided for packer placement.

Figure 20 presents the results of single-borehole hydraulic testing in well FSE11 in the Mirror Lake area. The borehole televiewer log and the caliper log provided the necessary information for selecting the 5-m test intervals. Unfractured portions of the well were not tested. Note that the hydraulic conductivities of the rocks in the test intervals vary over 4 orders of magnitude, from 10^{-9} m/s to 10^{-5} m/s. Such a large variation is typical of fractured crystalline rocks.

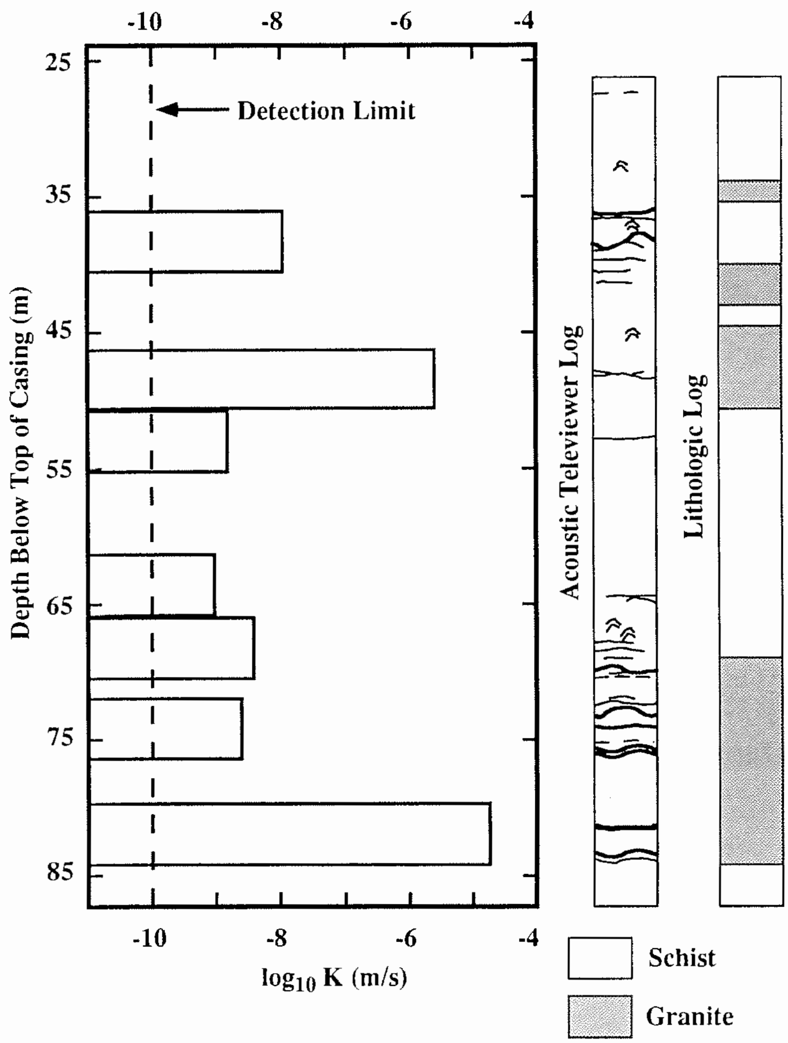

Figure 20. Hydraulic conductivity profile, borehole televiewer log, and lithology of well FSE11.

STOP 9. TRACER TESTING. FSE Well Field. At this stop, we demonstrate the equipment for conducting a converging-flow tracer test. In this test, water is pumped at a constant rate from a packer-isolated interval in a well. When a steady flow field is established, a pulse of tracer is injected into the flow field through a packer-isolated interval in a neighboring well. The arrival of the tracer from the tracer-injection interval to the pumped interval is monitored by measuring the tracer concentration in the pumped water. Plotting the tracer concentration versus time yields what is known as a breakthrough curve. Analysis of the breakthrough curve commonly yields the porosity and the dispersivity of the portion of rock through which the tracer has travelled.

A common practice of tracer injection is to first inject tracer solution into a packer-isolated interval and then inject tracer-free water, which is supposed to flush the tracer from the well bore into the fracture. Our field experience suggests that this method does not provide good control over how the tracer enters the flow system in fractured rocks. During tracer injection and the subsequent flushing, the tracer solution continuously mixes with tracer-free water in the well bore. At the end of flushing, some tracer remains in the well bore, and later diffuses into the fracture. As a result, a pulse injection is not achieved.

To improve the control over how the tracer enters the flow field, we designed a tracer injection system that utilizes three packers and two downhole valves that control an injection tube and a return tube (Figure 21a). The upper and lower packers (labelled A and C in Figure 21a) serve the normal function of isolating a well-bore interval. These packers stay inflated during the entire test. The middle packer B is positioned such that when inflated, it blocks off the fracture into which the tracer will be injected. The use of this middle packer allows us to mix the tracer in the well bore prior to injection, and to control the timing and amount of tracer that is injection into the fracture.

Our tracer injection procedure consists of three steps: the tracer-mixing step, the tracer-injection step, and the clean-up step. The tracer-mixing (Figure 21b) step begins with the inflation of the middle packer to block off the fracture from the well bore. In a surface reservoir, a known volume of tracer solution is prepared for mixing with the tracer-free water in the well bore between packers A, B, and C. Mixing is accomplished by opening the injection and return valves and pumping the tracer solution from the surface reservoir down the injection tube. At this stage, no tracer can enter the fracture, as it is blocked off by the middle packer. Instead, the tracer mixes with the water in the portion of the well bore between packers A, B, and C, and the mixture returns to the surface reservoir via the return tube. The tracer mixture is recirculated until a uniform tracer concentration is achieved in the well bore and in the surface reservoir. At this point the injection and return valves are closed, and the tracer-mixing step is complete.

The tracer injection step begins with opening the injection valve and deflating the middle packer (Figure 21c). The fracture is now in contact with the fluid in the well bore. The tracer mixture is pumped down the injection tube and enters the fracture. Because the waters in the well bore, tubing, and surface reservoir have been thoroughly mixed, the concentration of the tracer solution entering the fracture is identical to the concentration of the tracer solution in the surface reservoir. At the end of injection, the middle packer is again inflated to block off the fracture. Now, no more tracer can enter the fracture. The decrease in the volume of tracer solution in the surface reservoir is the volume injected into the fracture. Multiplying this volume by the tracer concentration (after mixing) gives the mass of tracer injected into the fracture.

During the clean-up step, the tracer remaining in the well bore is removed. With the middle packer still inflated, the injection and return valves are opened. Tracer-free water is pumped down the injection tube to flush the tracer solution out the return tube. The flushing is continued until the return water is essentially tracer free.

Although we have had good successes with our tracer injection method, it is not without drawbacks. The most stringent requirement is that the middle packer must block off all the transmissive fractures in the tracer-injection interval. This requirement is easily satisfied if the borehole wall is relatively smooth, and the interval contains no more that a few closely spaced fractures. In contrast, if the borehole wall is rough, or if the interval contains several transmissive fractures that span a distance longer than the bladder of the middle packer, then it is not possible to block off the fracture(s). In these situations, one will have to resort to the common, two-packer method of tracer injection.

To illustrate a converging-flow tracer test, we present the result from a test conducted during August 1992. In well FSE6, a 8.7-m long pumping interval straddled several transmissive fractures that intersect the well between depths of 33 m and 38 m. The interval was pumped at 10 L/min. After a day of pumping, 16 L of sodium bromide tracer solution at a concentration of 15.7 gm/L was injected over 2 minutes into a fracture at a depth of 43 m in well FSE9, located 36 m from well FSE6. Based on hydraulic response, we infer that the tracer-injection interval is directly connected to the pumped interval via highly-transmissive, interconnected fractures. The breakthrough curve is shown in Figure 22. The peak concentration at the pumped well was 22.5 mg/L and occurred 4.0 hours after tracer injection. We are currently analyzing these data to determine the transport properties of the rock.

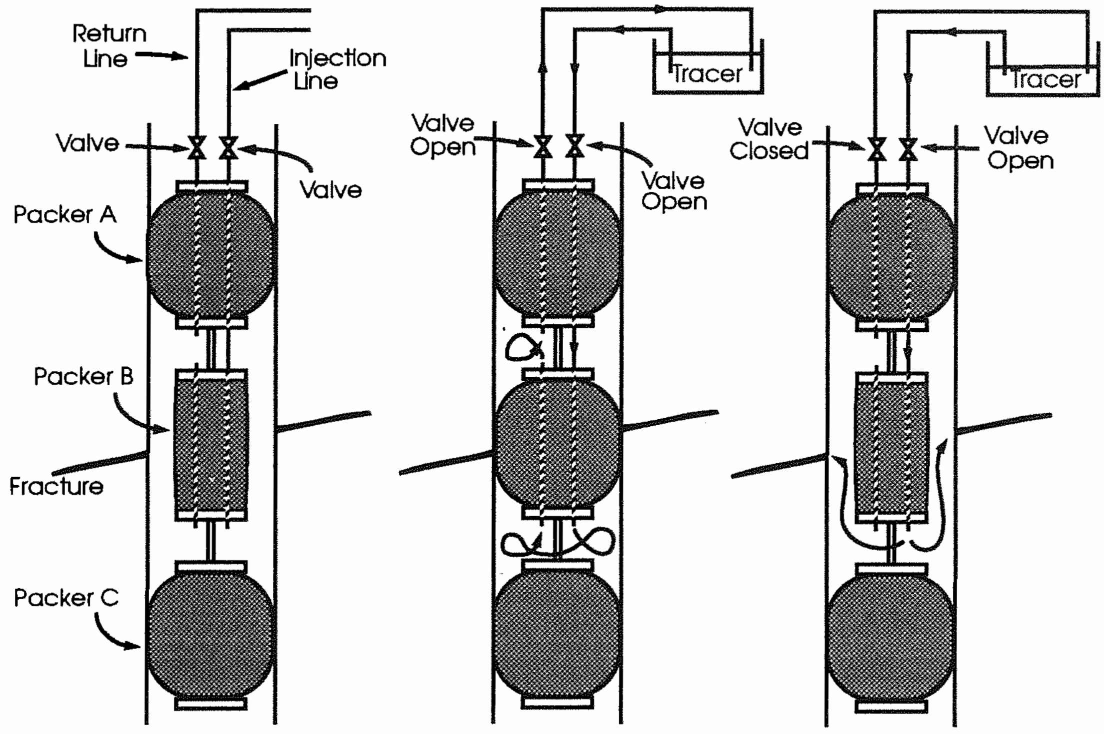

Figure 21. Schematic illustration of procedure for tracer injection. (a) Packer setup. (b) Tracer mixing step. (c) Tracer injection step.

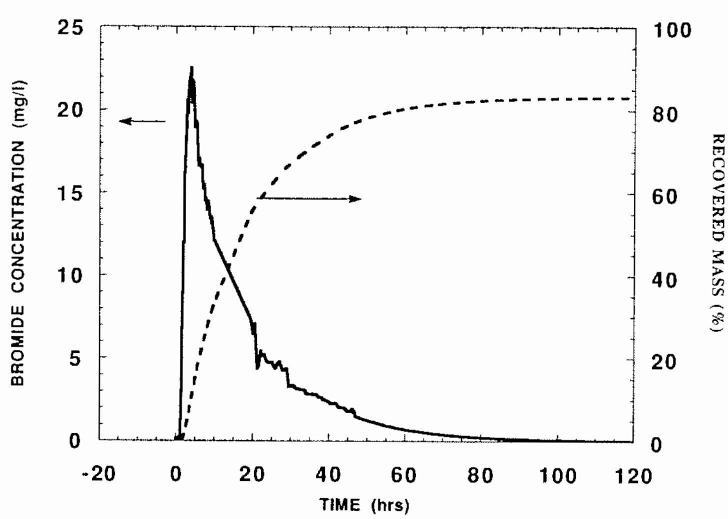

Figure 22. Breakthrough curve and percentage mass recovered from tracer test during which FSE6 was pumped and tracer was introduced in FSE9.

REFERENCE CITED

Barton, C. C., and Larsen, Eric, 1985, Fractal geometry of two-dimensional fracture networks at Yucca Mountain, southwest, Nevada, in Stephansson, Ove (ed.), Fundamentals of Rock Joints: Centek Publishers, Lulea, Sweden, p. 77-84.

Barton, C. C., and Hsieh, P. A., 1989, Physical and hydrologic-flow properties of fractures: Field Guide Book T385, 28th International Geological Congress, American Geophysical Union, Washington, D. C., 36 p.

Barton, N. R., and Choubey, Vishnu, 1977, The shear strength of rock joints in theory and practice: Rock Mechanics, v. 10, p. 1-54.

Bear, Jacob, 1979, Hydraulics of Groundwater, McGraw-Hill, New York, 567 p.

Busenberg, Eurybiades, and Plummer, L. N., 1992, Use of chlorofluorocarbons (CCl_3F and CCl_2F_2)as hydrologic tracers and age-dating tools: The alluvium and terrace system of central Oklahoma: Water Resources Research, v. 28, no. 9, p. 2257-2283.

Darboux-Afouda, R., and Louis, P., 1989, Contribution des mesures de l'anisotropic electrique la recherche des aquifres de fracture en milieu cristallin au Benin: Geophysical Prospecting, v. 37, p. 91-105.

Dines, K. A., and Lytle, R. J., 1979, Computerized geophysical tomography: Institute of Electrical and Electronics Engineers Proceedings, v. 67, no. 7, p. 1065-1073.

Forster, Craig, and Smith, Leslie, 1988, Groundwater flow systems in mountainous terrain 1. Numerical modeling technique: Water Resources Research, v. 24, no. 7, p. 999-1010.

Habberjam, G. M., 1972, The effects of anisotropy on square array resistivity measurements: Geophysical Prospecting, v. 20, p. 249-266.

Habberjam, G. M., 1975, Apparent resistivity, anisotropy and strike measurements: Geophysical Prospecting, v. 23, p. 211-247.

Habberjam, G. M., 1979, Apparent resistivity observations and the use of square array techniques, in Saxov, S., and Flathe, H. (eds.), Geoexploration Monographs, series 1, no. 9, p. 1-152.

Habberjam, G. M., and Watkins, G.E., 1967, The use of a square configuration in resistivity prospecting: Geophysical Prospecting, v. 15, p. 221-235.

Haeni, F. P., Grantham, D. G., and Ellefsen, Karl, 1987, Microcomputer-based version of SIPT—A program for the interpretation of seismic-refraction data: U. S. Geological Survey Open-File Report 87-103A (text), 13 p., and 87-103B (disk).

Harte, P. A., 1992, Regional ground-water flow in crystalline bedrock and interaction with glacial drift in the New England uplands: M. S. Thesis, University of New Hampshire, Durham, New Hampshire, 141 p.

Hess, A. E., and Paillet, F. L., 1990, Applications of the thermal-pulse flowmeter in the hydraulic characterization of fractured rocks, in ASTM STP 1101, p. 99-112.

Kak, A. C., and Slaney, Malcolm, 1988, Principles of computerized tomographic imaging: The IEEE Press, New York, 329 p.

Lewis, M. R., and Haeni, F. P., 1987, The use of surface geophysical techniques to detect fractures in bedrock—An annotated bibliography: U.S. Geological Survey Circular 987, 14 p.

Lieblich, D. A., Lane, J. W., Jr., and Haeni, F. P., 1991, Results of integrated surface-geophysical studies for shallow subsurface fracture detection at three New Hampshire sites, in Expanded Abstracts with Biographies, 61st Annual International Meeting, November 10-14: Society of Exploration Geophysicists, Houston, Texas, p. 553-556.

Lieblich, D. A., Haeni, F. P., and Cromwell, R. E., 1992a, Integrated use of surface-geophysical methods to indicate subsurface fractures at Tibbetts Road, Barrington, New Hampshire: U.S. Geological Survey Water-Resources Investigations Report 92-4012, 33 p.

Lieblich, D. A., Haeni, F. P., and Lane, J. W., Jr., 1992b, Integrated use of surface-geophysical methods to indicate subsurface fractures at Milford, New Hampshire: U.S. Geological Survey Water-Resources Investigations Report 92-4056, 38 p.

Likens, G. E. (ed.), 1985, An Ecosystem Approach to Aquatic Ecology, Mirror Lake and its Environment: Springer-Verlag, New York, 516 p.

Likens, P. C., 1991, 1991 Publications of the Hubbard Brook Ecosystem Study: Institute of Ecosystem Studies, Millbrook, N. Y., 109 p.

Lyons, J. B., Bothner, W. A., Moench, R. H., and Thompson, J. B., Jr. (eds.), 1989, unpublished Bedrock Geologic Map of New Hampshire, 1:250,000 scale.

McHone, J. G., 1984, Mesozoic igneous rocks of northern New England and adjacent Quebec: Summary, description map, and bibliography of data sources: Geological Society of America, Map and Chart Series, MC-49.

Olhoeft, G. R., 1988, Interpretation of hole-to-hole radar measurements: in Third Technical Symposium on Tunnel Detection Proceedings, Jan. 12-15, 1988, Colorado School of Mines, Golden, Colorado, p. 616-629.

Olsson, Olle; Anderson, Per; Carlsten, Seje; Falk, Lars; Niva, Borje; and Sandberg, Eric, 1992a, Fracture characterization in crystalline rock by borehole radar, in Pilon, J. (ed.), Ground penetrating radar: Geological Survey of Canada Paper 90-4, p. 139-150.

Olsson, Olle; Falk, Lars; Forslund, Olof; Lundmark, Lars; and Sandberg, Eric, 1992b, Borehole radar applied to the characterization of hydraulically conductive fracture zones in crystalline rock: Geophysical Prospecting, v. 40, p. 109-142.

Paillet, F. L., 1991a, Use of geophysical well logs in evaluating crystalline rocks for siting of radioactive waste repositories: The Log Analyst, v. 32, no. 1, p. 85-107.

Paillet, F. L., 1991b, Comparing geophysical logs to core and cross-hole flow logging in the Mirror Lake drainage basin, in Mallard, G. E., and Aronson, D. A. (eds.), U. S. Geological Survey Toxic Substances Hydrology Program—Proceedings of the technical meeting, Monterey, California, March 11-15, 1991: U. S. Geological Survey Water Resources Investigations Report 91-4034, p. 162-171.

Paillet, F. L., Hess, A. E., Cheng, C. H., and Hardin, E. L., 1987, Characterization of fracture permeability with high-resolution vertical flow measurements during borehole pumping: Ground Water, v. 25, no. 1, p. 28-40.

Paillet, F. L., and Kapucu, Kemal, 1989, Fracture characterization and fracture-permeability estimates from geophysical logs in the Mirror Lake watershed, New Hampshire: U. S. Geological Survey Water Resources Investigation Report 89-4058, 49 p.

Paillet, F. L., Novakowski, K. S., and Lapcevic, P. A., 1992, Analysis of transient flows in boreholes during pumping in fractured formations, in Transactions of 33rd Annual Logging Symposium: Society of Professional Well Log Analysts, Oklahoma City, Oklahoma, p. S1-21.

Park, Stephen, and Simmons, Gene, 1982, Crack induced velocity anisotropy in the White Mountains, New Hampshire: Journal of Geophysical Research, v. 87, no. 84, p. 2977-2983.

Pollard, D. D., and Aydin, Atilla, 1988, Progress in understanding jointing over the past century: Geological Society of America Bulletin, v. 100, p. 1181-1204.

Rosenberry, D. O. and Winter, T. C., 1993, The significance of fracture flow to the water balance of a lake situated in fractured crystalline rock terrane: in Hydrogeology of Hard Rocks, 24th Congress of the International Association of Hydrogeologists, Oslo, Norway.

Scott, J. H., Tibbetts, B. L., and Burdick, R. G., 1972, Computer analysis of seismic refraction data: U. S. Bureau of Mines Report of Investigations 7595, 95 p.

Sehli, A. S., 1990, Contribution of electrical prospecting to the geophysical study of discontinuous media, in International symposium on applications of geophysics to water prospecting in arid and semi-arid areas, Aug. 22- 24, 1990, Luzern, Switzerland.

Shapiro, A.M., and Hsieh, P.A., 1991, Research in fractured rock hydrogeology: Characterizing fluid movement and chemical transport in fractured rock at the Mirror Lake drainage basin, New Hampshire, in Mallard, G. E., and Aronson, D. A., eds., U. S. Geological Survey Toxic Substances Hydrology Program—Proceedings of the technical meeting, Monterey, California, March 11-15, 1991: U. S. Geological Survey Water-Resources Investigations Report 91-4034, p. 155-161.

Shattuck, P. C., 1991, Shallow water-table response to precipitation and evapotranspiration in an ephemeral stream valley, Woodstock, New Hampshire: M. S. Thesis, University of New Hampshire, Durham, New Hampshire, 113 p.

Solomon, D. K., Poreda, R. J., Schiff, S. L., and Cherry, J. A., 1992, Tritium and helium-3 as ground water age tracers in the Borden aquifer: Water Resources Research, v. 28, no. 3, p. 741-755.

Taylor, R. W., and Fleming, A. H., 1988, Characterizing jointed systems by azimuthal resistivity surveys: Ground Water, v. 26, no. 4, p. 464-474.

Ulriksen, P. F. 1982, Application of impulse radar to civil engineering: Ph.D. thesis, Lund University of Technology, Lund, Sweden, 179 p.

U. S. Department of Agriculture Forest Service, 1986, Hubbard Brook Experimental Forest: Northeastern Forest Experiment Station NE-INF-71-86, 15p.

U. S. Department of Agriculture Forest Service, 1991, The Hubbard Brook Ecosystem Study: Site Description and Research Activities: Northeastern Forest Experimental Station NE-INF-96-91, 61p.

Winter, T. C., 1984, Geohydrologic setting of Mirror Lake, West Thornton, New Hampshire: U. S. Geological Survey Water-Resources Investigations Report 84-4266, 61 p.

Zemanek, Joseph, Glenn, E. E., Norton, L. J., and Caldwell, R. L., 1970, Formation evaluation by inspection with the borehole televiewer: Geophysics, v. 35, no. 2, p. 254-269.

Chapter S

Highlights of Proterozoic Geology of Boston

By Nicholas Rast, J.W. Skehan, and S.W. Grimes

Field Trip Guidebook for the Northeastern United States:
1993 Boston GSA

Volume 2
Contribution No. 67, Department of Geology and Geography, University of Massachusetts, Amherst, Massachusetts

HIGHLIGHTS OF PROTEROZOIC GEOLOGY OF BOSTON
by

Nicholas Rast, Department of Geological Sciences, University of Kentucky, Lexington, KY, 40506;
J.W. Skehan, Weston Observatory, Department of Geology and Geophysics,
Boston College, Weston, MA 02193;
and
S.W. Grimes, Department of Geological Sciences, University of Texas, Austin, TX 78712

INTRODUCTION

In this guide we are concerned with the geology to the west of Boston, where in the last three to four years significant discoveries have been made. The basic geological mapping in the area (Fig. 1) has been made by geologists of the USGS, including Nelson (1975a & b), Castle (1965) and Castle and coworkers (1976), Hepburn and DiNitto (1978), and parts of it since have been reviewed and reinterpreted by Thompson (1985), Thompson and Hermes (1990), Thompson and Skehan (1992), Bailey and others (1989), and Rast and Skehan (1990). In the last few years a much more intensive program of field-work by Skehan and Rast (1990, 1991), and Rast and Skehan (1990a, b), and Grimes (1993) resulted in the establishment of a stratigraphic and intrusive sequence and stages of structural deformation (Table 1).

TABLE 1

EVOLUTION OF THE AVALON TERRANE

Sequence of Events in the Northern Appalachians
(Massachusetts), according to Rast and Skehan

14) Cambrian- - *rifting IV*

~~~~~~~~~~~~~~unconformity~~~~~~~~~~~~~~

Pan- African II

13) Westwood Granites (580 Ma)
12) Central Boston metasediments with tillite and basalts- - *rifting III*

~~~~~~~~~~~~~~unconformity~~~~~~~~~~~~~~

11) Lynn / Mattapan Complex (602 Ma)- - *subduction*

~~~~~~~~~~unconformity- - post-orogenic collapse~~~~~~~~~~

Pan- African I

10) Esmond Granite (621 Ma)
9) Dedham- Milford Granites- - *migmatization* of mylonites (630 Ma)
8) Mylonitization & Greenschist metamorphism and folding
   - - *transpression, compression*: Avalon Orogeny (main phase)
7) Mafic dikes - - *relaxation*
6) Mylonitization - - *transpression*
5) Mafic dikes - - *rifting II*
4) Intrusion of gabbro-diorites and granites
3) Volcanics (bimodal) Middlesex Fells Complex - - *continued rifting I*
2) Westboro Quartzite - Blackstone Fm. deposition and slumping
   (olistostrome) - - *rifting I*
1) Basement Gneisses - - *orogeny - metamorphism* (?750 Ma)

In part this scheme varies from that developed by the USGS that resulted in the formulation of the Geological Map of Massachusetts, 1983 by E-an Zen and a subsequent comprehensive description, edited by Hatch (1991) in which the area under consideration was discussed by Goldsmith. His synthesis, however, was prepared prior to our latest findings.
~~~~~~~~~~

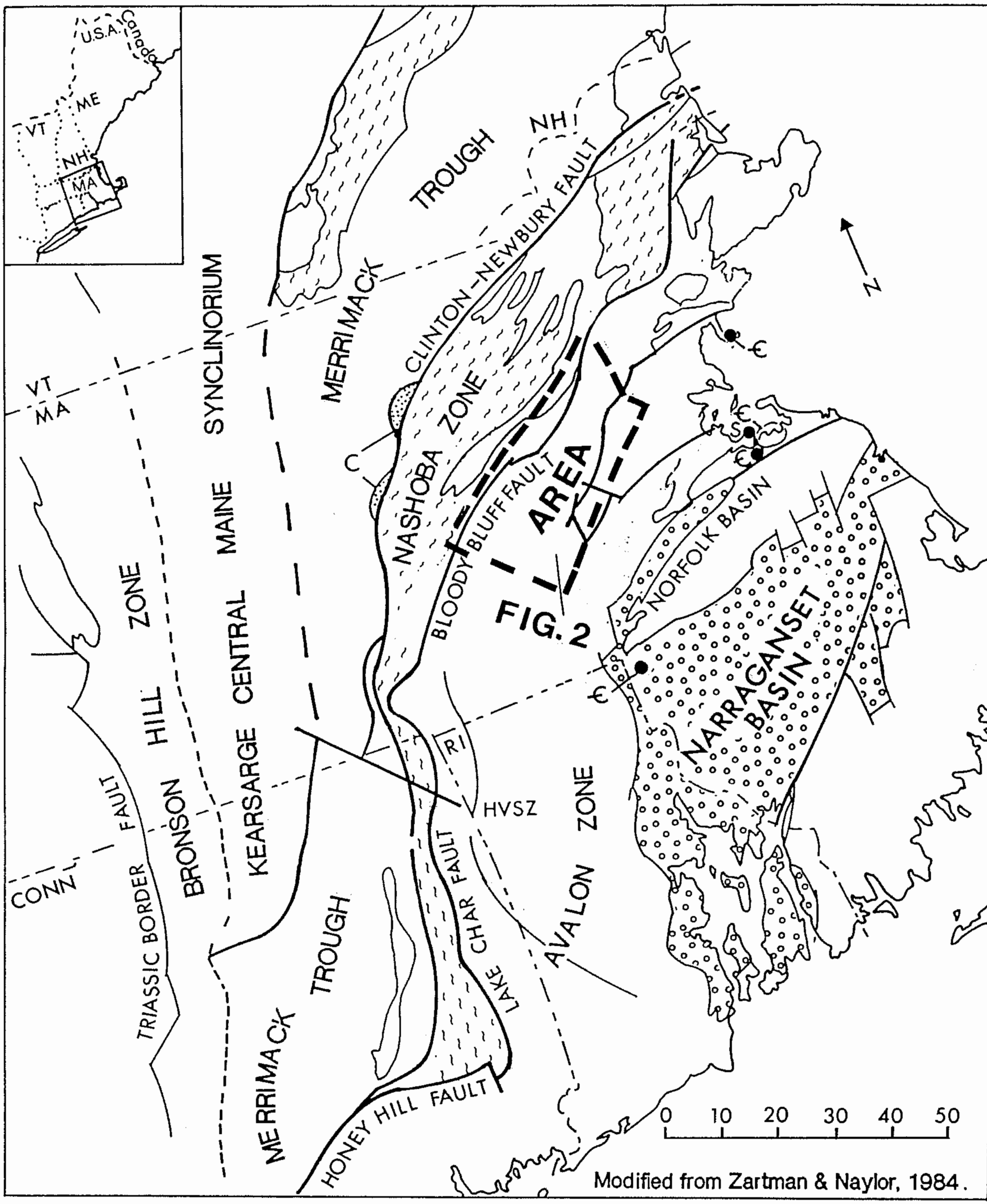

Figure 1. Generalized geological map of Boston region.

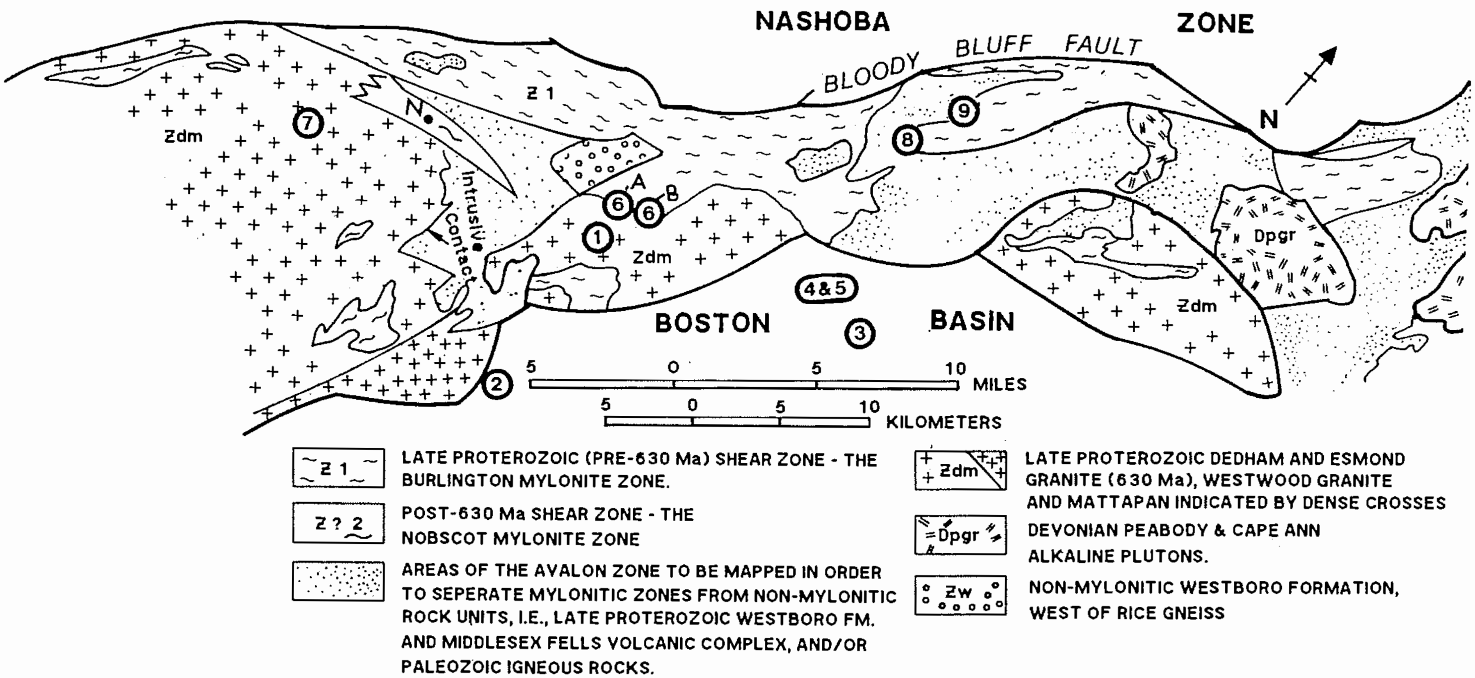

Figure 2. Outlines of the area under consideration. Modified after Castle et al (1976), Nelson (1976a and b), Grimes (1993), and Thompson and Skehan (1992). Positions of field-trip stops are shown and numbered in circles.

TIME SEQUENCE AND STRATIGRAPHY

The basement geology of southeastern Massachusetts is divided into three main belts, which are often assumed to be terranes. From west to east the three belts are: (1) the Merrimack Trough; (2) the Nashoba Zone, and (3) the Avalon of Massachusetts and Rhode Island (Fig. 1). The first was formerly considered to consist of Siluro-Devonian strata, the second was thought to be of unknown age, being possibly Precambrian or Lower Paleozoic, and the last, mainly of Precambrian stratified and intrusive rocks, injected by lower to middle Paleozoic intrusives and partly covered by Carboniferous strata.

It is now clear that the Merrimack Trough belt has been deformed in pre-Middle Ordovician and, therefore, is likely to be older and parts of it may be Late Proterorozoic. The Nashoba belt likewise is Lower Paleozoic to Precambrian, being invaded by the ca 450 Ma Andover Granite (Zartman and Naylor, 1984). Only the Avalon of Boston is incontrovertibly Proterozoic, consisting in Massachusetts of earlier, in part mylonitized, Westboro Quartzite, Cherry Brook Formation, and the associated deformed felsic and mafic igneous rocks, sometimes referred to as the Middlesex Fells Volcanic Complex. The ca 630 Ma Dedham Granite intrudes the mylonitized rocks and itself is intruded by a later Westwood Granite of a somewhat younger, but still Proterozoic age (ca 579 Ma;) determined by Kovach et al. (1977).

The Dedham and Milford granites cut the mylonitized Westboro Quartzite and the Middlesex Fells volcanic rocks (Fig. 1), and are, therefore, younger than them (Rast and Skehan, 1990). They are in places cut by narrower zones of mylonitization of E-W trend. Grimes (1993) mapped one of the most extensive and widest of such zones as the Nobscot Shear Zone. Thus two episodes of mylonitic shear are recognized, the first and most widespread resulted in major shear zones of pre-630 Ma age, such as the Burlington Mylonite Zone (Fig. 2), and the second occurring in narrower bands of post-630 Ma age. The total number of exposures of Dedham-Burlington Zone contacts is by now numerous (11) and therefore a chance of the granite from place to place being different is excluded. On the basis of these observations we suggest that the first episode of intense deformation represents what, in the northern Appalachians, is referred to as the Main Avalonian orogeny (Hepburn and others, 1987), while the second episode of mylonitization may represent a later phase of it, although until isotopic dating is done it is difficult to be certain. Both episodes are clearly earlier that the cataclastic deformation that affects many parts of the area.

The Proterozoic granites are in fault contact with the rocks of the so-called Boston Basin, where a 7000 ft-thick succession of sediments and associated volcanics is exposed. The sediments include a spectacular diamictite, claimed by some to be a tillite (Socci and Smith, 1990), while alternatively it is thought of as a sedimentary slump breccia by others. In addition, the lower conglomeratic part of the sedimentary succession appears to be unconformably lying on volcanic Mattapan ignimbrites, which Thompson and Hermes (1990) relate to a late Proterozoic caldera. In Westwood township the volcanic Mattapan ash-flow tuffs contain boulders of either Westwood or Dedham Granite indicating that unlike the view of Hepburn and others (1987) granites and proximate volcanic rocks are not necessarily coeval.

The southern part of the Boston Bay Group is widely affected by cleavage of debatable age. The cleavage is axial planar to the SSE-verging asymmetrical folds of possibly Late Carboniferous (Hepburn and others, 1987) or Proterozoic age (Rast and Skehan, 1990). The former view is based on the superficial similarity between this cleavage and that affecting Carboniferous strata of Rhode Island, while the latter is based on the fact that the admittedly small exposures of Cambrian rocks in the eastern part of the Boston area (Nahant, Weymouth, Braintree,) are uncleaved, while the diamictite exposed on the Squantum Peninsula to the north of these, is particularly strongly cleaved (Fig. 1).

Throughout this excursion the emphasis is laid on the nature of the structure of the basement metasedimentary and plutonic rocks, on aspects of the stratigraphy of the Boston Basin, and on the at present controversial interpretation of the area. It seems likely that the Boston Basin is not a depositional depression (Thompson and Skehan, 1992). If the isotopic age, as determined by Kaye and Zartman, is ca 600 Ma, then the Boston Bay Group constitutes a post-deformational deposit of conglomeratic molasse, slump conglomerates, and associated volcanic intercalations of bimodal, anorogenic type covering a deformed and granite-intruded basement. The absence of zones of mylonitization from the Boston Bay Group suggests that it was laid down entirely later that the deformation that has produced mylonites.

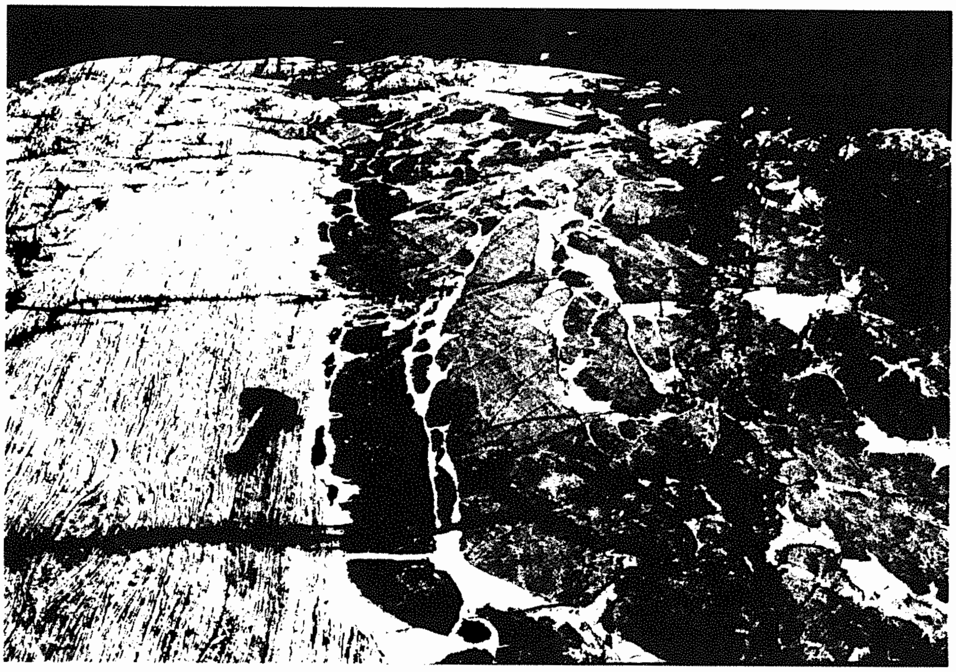

Figure 3. Foliated Rice Blastomylonitic Gneiss cut by undeformed Paleozoic, black veined gabbro-diorite. Note the indented margin. Hammer 15" long. Wayland Hills Rd., Wayland.

Figure 4. Mylonitized Milford Granite (Nobscot Shear Zone). Quartz ribbons are recrystallized. Feldspar porphyroclasts heavily altered, scale X30.

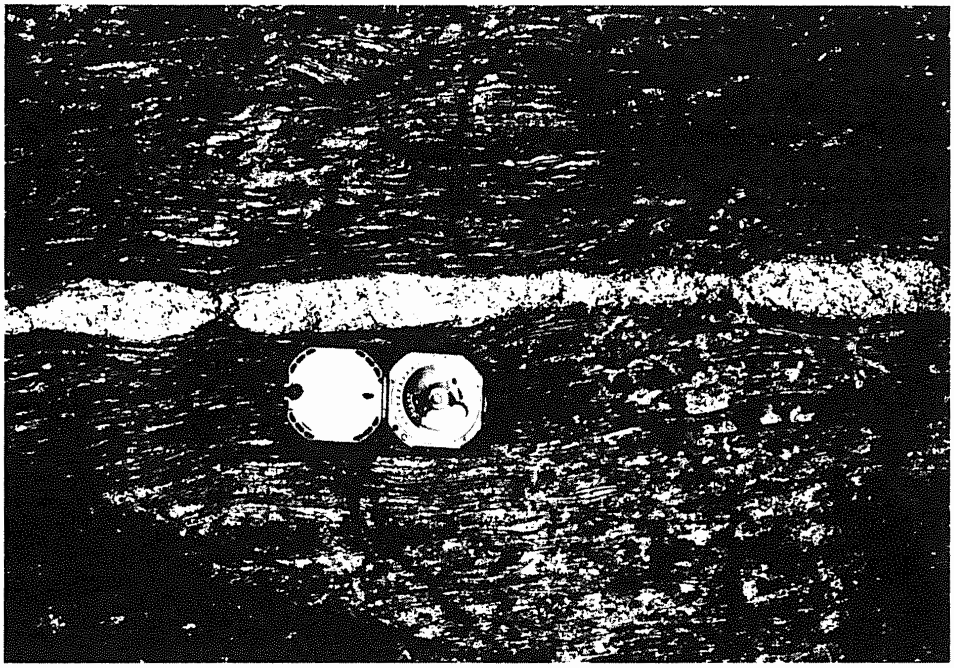

Figure 6. Boudinaged apilite vein in the Rice Blastomylonitic Gneiss of Wayland Hills Rd., showing superpostion of compressive strain on mylonite after the interusion of the Dedham Granite.

Figure 7. A micrograph of cataclastically deformed mylonite of the Burlington Mylonite Zone. Note psuedotachylite on the right side of the photograph. Scale X50.

THE STRUCTURE OF THE BURLINGTON MYLONITE ZONE

Castle and others (1976) have identified a major mylonite zone (Fig. 2) of variable width and irregular outlines. This mylonite zone has been in the last fifteen years widely accepted as the trace of the Bloody Bluff fault and a margin of the Avalon terrane *sensu stricto*. Although the general trend of the zone is NE-SW and it lies parallel with the Bloody Bluff fault, within, it commonly shows sharp trend deflection of the mylonitic schistosity. These deflections are particularly apparent at numerous bodies of gabbro-diorites that lie at the margins and penetrate the mylonite zone. These gabbro-diorites, frequently composed of associated basic pillow-like bodies and granitic veins, are not interpenetratively deformed and deflect and cross-cut the foliation (Fig. 3). The post-mylonitization bodies are undated, but provisionally can be correlated with Siluro-Devonian rocks of similar type outcropping north of Boston and in the Nashoba zone. It should be stated that there are also schistose and mylonitized bodies of gabbro-diorite type that can be recognized in the mylonite zone. These are clearly pre-mylonitic and in places are so badly deformed that they acquired the aspect of schistose mafic volcanic rocks and in the past were confused with the early volcanic bodies of the Middlesex Fells Volcanic Complex. The width of the Burlington zone also varies partly as a result of constrictions by gabbro-diortes, and partly because notheastward the zone as a whole narrows. In addition to gabbro-diorites a large number of diabase intrusions are emplaced into mylonites and some are partially or completely mylonitized.

THE NOBSCOT SHEAR ZONE

The Nobscot Shear Zone (Fig. 2) is a locus of mylonitization that affects the Milford Granite in Framingham. It extends, from Nobscot Village East and West for three miles on either side. Several outcrops of mylonite may be either splays or parallel, en echelon shear zones, of which the Nobscot shear zone is the best exposed. Progressive development of mylonitic textures occurs along Edgell Road, beginning one-third mile south of Nobscot and heading north.

TABLE 2

SENSE OF SHEAR DETERMINATION IN VARIOUS MYLONITES
According to Grimes, 1993

AREA/SAMPLE	LINEATION/ EXTENSION DIRECTION	SENSE OF MOVEMENT:	CRITERIA:
FRAMINGHAM:			
390	233,53 (ext.)	WEST SIDE DOWN	S-C fabric; Asymmetry of porphoclast tails
490	030,02 (ext.)	DEXTRAL*	"S-C type" fabric
590	030,02 (ext.)	DEXTRAL*	"S-C type" fabric; p-clast tail assym.
890	ambiguous	DEXTRAL	S-C fabric; p-clast tail assym.
791	099,14	DEXTRAL*	Muscovite fish; asymm. of epidote, trails
2392	060,09	DEXTRAL*	p-clast tail asymm; asymm. folding
KING PHILIP'S AREA:			
892	117,01 (ext.)	PURE SHEAR DEFORM	Quartz c-axis fabric
1092	ambiguous	DEXTRAL	Biot. fish; asymm. of opaques, epidote trails
1192	114,23 (ext.)	SINISTRAL	Biot. fish; "foliation cut-off";asymm.folding
2092	127,07	SINISTRAL*	Musc. fish, p-clast tail asymm.
NOBSCOT SHEAR ZONE:			
290	081,07	TOP-TO-WEST	S-C fabric, p-clast. tail asymm.
492	298,16	WEST SIDE DOWN	S-C fabric, p-clast. tail asymm.
692	281,18	TOP-TO-EAST	S-C fabric; biot., musc. tails
592	289,16	TOP-TO-EAST	S-C fabric; P-clast tail asymm.; biot. fish
792	079,12	TOP-TO-EAST	S-C fabric; P-clast tail asymm.; biot. fish
1392	081,51	TOP-TO-EAST	Musc., biot. fish
RICE GNEISS:			
Smoky Hill Rd., Mainstone Farm, Pine Street; Wayland		SINISTRAL	Asymm. folding (s-folds)

*- Weakly defined; may reflect last increment of complex deformation path

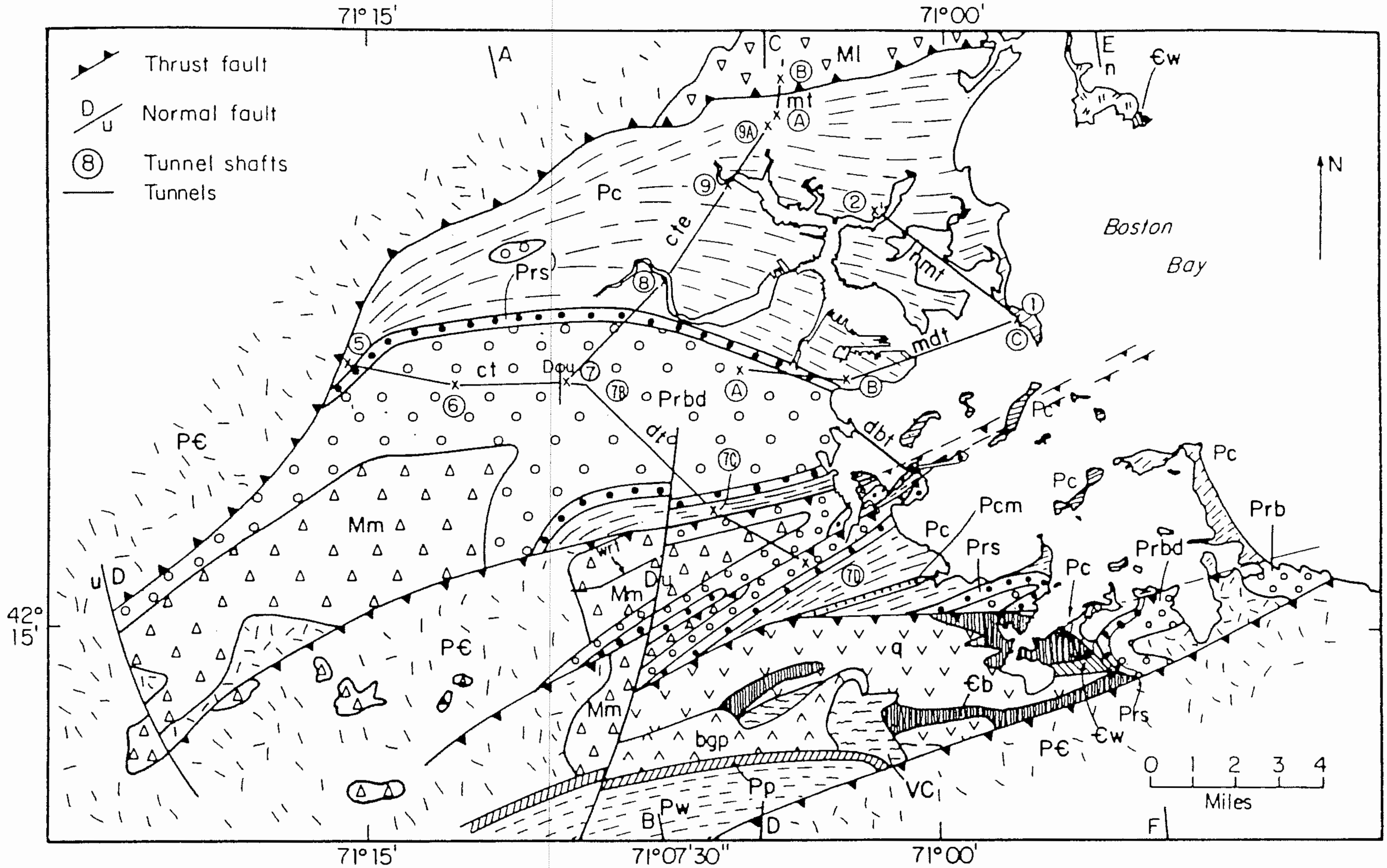

Figure 5. Sketch map and stratigraphy of the Boston Basin outlined by marginal faults. After Billings (1976a).

The granite mylonite generally has a fairly well-developed, sub-horizontal lineation, composed of quartz rods and altered feldspar; muscovite and biotite is commonly crystallized along the surface of the rods. Thin sections demonstrate pervasive alteration of feldspar porphyroclasts to muscovite and quartz (Fig. 4). Quartz shows granoblastic textures, with good "foam structure" (i.e. 120° angles at cell boundary junctions), and is almost entirely free of undulatory extinction. In hand sample, quartz typically shows the sort of "sugary" fine-grained texture typical of Milford Granite. Either these features were the products of syntectonic processes, or else the mylonite has been extensively altered and recrystallized subsequent to deformation. As a result, most of the grain-scale structural features typical of a granitic mylonite have been lost, obscuring much information on strain path. However, most of the samples still exhibit good S-C fabrics--an intragranular structure--and mica fish, and yield sense of shear information (see Table 2). Sense of shear is dextral (north wall--top to east) for all samples except one. In addition, angles between S and C planes are generally small (<20°), which indicates high shear strains (Simpson and Schmid, 1983). Dextral shear bands (i.e., normal microfaults that cut the foliation) are also common, but Lister and Snoke (1984) and Simpson and Schmid (1983) consider this feature of ambiguous significance.

Similar E-W trending, moderately north-dipping to vertical, relatively thin mylonitic shear zones have been noted in outcrops of Dedham Granite to the north (specifically in Burlington and Lexington) and in drill cores from Framingham.

STRATIGRAPHY AND STRUCTURE OF THE BOSTON BASIN

The intitial unravelling of the stratigraphy of the rocks of Boston Basin is due to Billings (cf. 1976a), who considered it both a geomorphic depression and a complex synclinorium that is separated from the surrounding uplands by a series of intersecting faults (Fig. 5). The evolution of the Basin terminology is briefly reviewed by Skehan (1976, 1979), Thompson and Skehan (1992). The rocks inside the Basin form a thick succession of conglomerates (Roxbury Conglomerate) at the bottom and finer grained clastic rocks (quartzites and argillites) at the top. The conglomeratic part is in places interbedded with volcanic rocks of both felsic and mafic character (Durfee-Cardoza et al., 1990) and known as Brighton Volcanics, which within the Boston Bay Group occupy two horizons. Fragments of volcanic rocks are found within the conglomerates.

The conglomerates consist of a varity of pebbles of quartzite and granite of Dedham type and contain at intervals unconformable channels, which cut into minor beds of argillite. The discontinuous beds, fairly high-energy cross-bedding and irregular lenses of conglomerate, suggest fluvial deposition (Bailey, 1987). The effectively subaerial conditions are confirmed by red, oxidized tops of basaltic horizons.

The thick conglomerate section is capped by interbedded argillites and sandstone-quartzites and conglomerates with, in places, considerable fissility and occasional ripple marks. Recrystallization precludes sedimentary assessment of the sandstones, but their occasionally feldspathic character suggests derivation from adjacent granitic basement and transportation in a shallow sea. The Dorchester Member rocks are covered by the Squantum "Tillite" (diamictite) which has a sandy to argillaceous matrix supporting clasts of up to 3 ft across and much finer debris and consisting of granite, quartzite, felsic volcanic fragments and basalt. Billings (1976b) reports it being in places just conglomeratic. In places Socci and Smith (1990) have observed drop-stones associated with channels, load casts, slump-folds and other features, which these authors attribute to "glacially influenced deposition on a slope." Because the "Tillite" is deformed and in places cleaved, it is difficult to be completely certain as to the reality of drop-stones.

The "Tillite" passess up into the Cambridge Argillite, which is a succession of bedded shaley and sandy claystone, in parts slightly calcareous, and with occasional intercalations of conglomerates and quartz sandstones. Rare grading and occasional rhythmic character of laminations has been reported by Billings (1976b).

The overall sedimentary character of the Boston Bay Group suggests a transition from fluvial Roxbury Conglomerate through shoreline facies of the Dorchester Member into an essentially marine sequence of the Squantum "Tillite" and Cambridge Argillite at the top. If so then the deposition is essentially basinal, although there is little evidence of the basinal nature of the exposed Boston Basin as such.

Thompson and Skehan (1992) have pointed out that even outside the bounderies of the Basin, as defined by faults projected by Billings (1976 a and b), both volcanic rocks and sedimentary strata normally associated with the Basin, can be recognized. Thompson and Skehan (1992) also point out that the Westwood Granite is related to a caldera structure that affects the Dedham Granite and was conducive to the eruption of the Mattapan ash-flow tuffs, ultimately emerging as a resurgent plug.

POST-DEDHAM DEFORMATION

There is considerable evidence for various stages of post-Dedham deformation, ranging from boudinage of Dedham aplites (Fig. 6) to brittle faulting and associated brecciation at times associated with pseudotachylite (Fig. 7). The detailed deciphering of such brittle fractures is a subject for the future, because such brecciation and shearing affects not only the older Proterozoic rocks of the area but younger Phanerozoic intrusions as well. For instance Kaye (1983) has reported a lenticle of Triassic sedimentary rocks caught within a trace of a branch of the Bloody Bluff fault suggesting that the brittle fault is either post-Triassic or has suffered a multiplicity of movements.

ACKNOWLEDGEMENTS

Much of the research of this study was stimulated by the landmark recognition and mapping of the Burlington Mylonite Zone by Castle (1965) and by Castle and others (1976) in what we have come to recognize as the Avalon Zone of Massachusetts. Skehan is grateful for having been introduced to the complexities of the Nashoba block and Merrimack Trough by his former thesis director, Marland P. Billings, who in 1960 invited him to engage in detailed mapping of the geology of the 8-mile long Wachusett-Marlborough Tunnel. In the course of that two-year project Skehan (1964) and Skehan and Abu-Moustafa (1976) had recognized mylonites and blastomylonites in the Nashoba Zone as had Castle in his 1965 study.

We have been encouraged by the careful observations of many other geologists, including students and faculty of Boston College, but especially by the late Professor W. O. Crosby of M.I.T., who near the turn of the last century mapped what we now recognize as the terrane boundary of the Nashoba with the Merrimack Trough. It was our good fortune to be made acquainted with Crosby's unpublished reports of 1898-1907 to the Metropolitan Water Commission on the geology of tunnel segments along the alignment of the aqueduct system across the Nashoba and Avalon terranes to Boston. These reports were entrusted to J.W. Skehan by his late mentor, Professor Robert R. Shrock upon the death of the late Irving Crosby, geologist son of W. O. Crosby. The expenses of N. Rast were defrayed by the Hudnall Endowment; J. W. Skehan gratefully acknowledges research support by the Jesuit Community of Boston College and by Weston Observatory; and S.W. Grimes acknowledges support of his research by the Linehan Fund of the Department of Geology and Geophysics and by Weston Observatory, both of Boston College. We acknowledge the assistance of Frances Ahearn, Thomas A. Davidson, Tracy S. Downing, and Patricia C. Tassia in the preparation of the manuscript.

ROAD LOG

Assemble at 8 am, for departure at 8:15 at an area to be designated and signposted in the lobby ofthe Copley Square Marriott Hotel, to be directed by S.W. Grimes and N. Rast to the bus. Note that in the forthcoming excursion the sequence of stops is determined by geologic rather than geographic considerations.

Milage

0.0 The log begins at a stop in front of the hotel and proceeds via Massachusetts Turnpike to the intersection of the Pike and Route 128.
11.3 Exit via interchange to Route 30 and turn West.
15.9 Turn left toward Natick into Oak St. at Rice Rd. intersection with Route 30.
16.7 Proceed to a modern office building labelled Hardinge. Stop by the entrance with an exposure to the left of it, and another exposure 30 yards to the south along Oak St.

STOP 1. DATED DEDHAM GRANITE. (30 MINUTES) From this locality Zartman and Naylor (1984) obtained a maximum Pb206/Pb207 age of 627$\pm$ 5 Ma. By combining their results from here with other sampled localities they obtained an overall age of the granite as 630$\pm$ 15Ma. In the first exposure the rock is pale biotite-hornblende granodiorite that is slightly foliated. We interpret this foliation as primary flow. It is vertical and strikes 032°. Reddish aplites and pegmatite veins that cross-cut it are entirely undeformed and are clearly coeval with the granite.

In the second, a somewhat coarser, unfoliated granite is cut by a diabase sill-like intrusion. It is possible that this locality--a site of an old quarry--supplied most samples for isotopic dating.

22.1 Return to Route 30 and Route 128 intersection; turn south.
33.5 Continue to the intersection with 109. Turn into 109 and proceed south past exposures of Westwood Granite until a fairly sharp

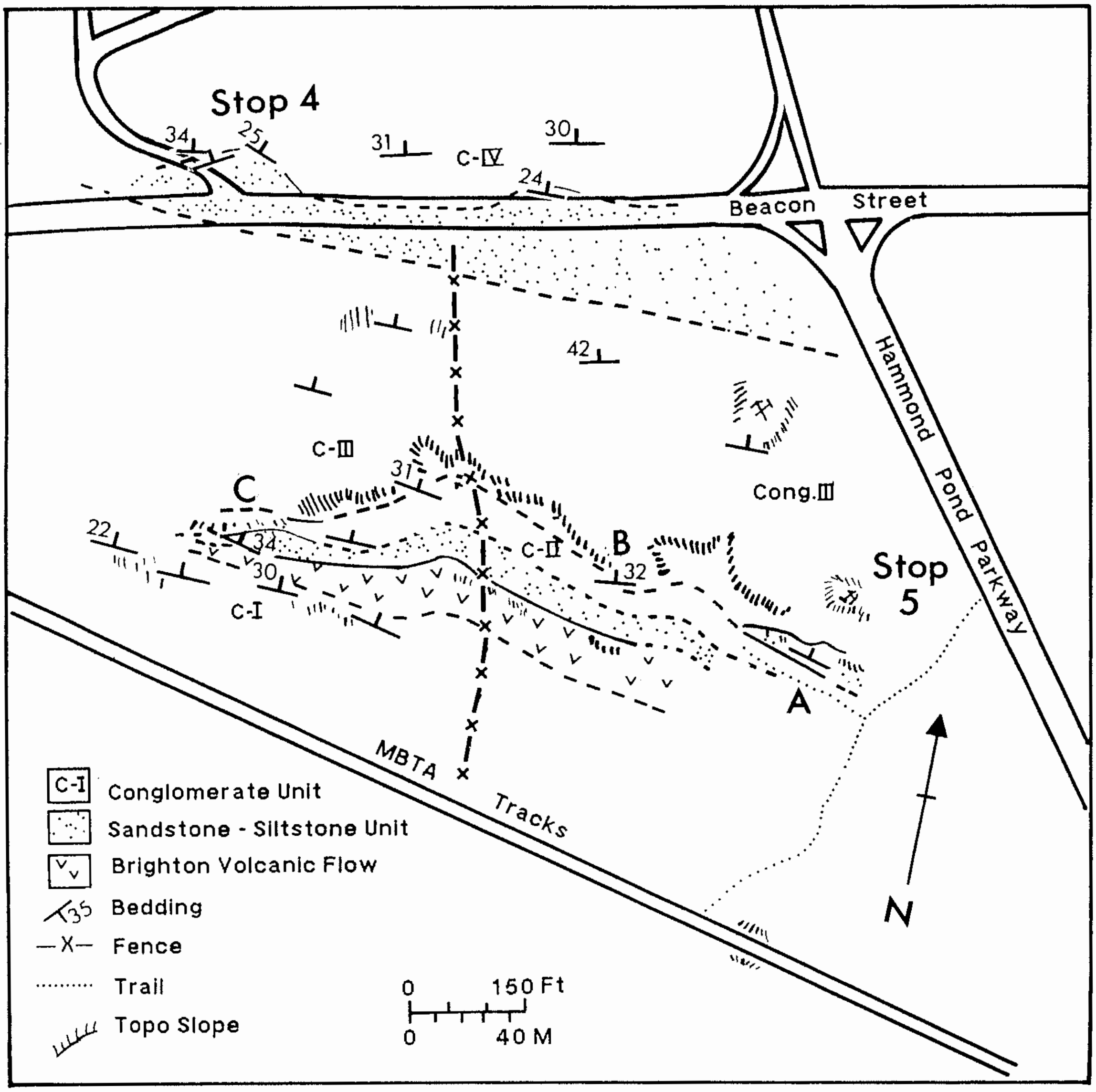

Figure 8. Sketch map showing the positions of stops 4 and 5, indicated by bold numbers and also outlines of local geology. Modified from Rehmer and Roy (1976).

corner that has a signpost Highland Glen. Turn right into Highland Glen and proceed to the top of the hill. Stop at any empty parking slot.

STOP 2. MATTAPAN VOLCANICS WITH INCLUSIONS OF DEDHAM GRANITE. (30 MINUTES) The low cliff at the back of the parking lot consists of a much brecciated Mattapan welded tuff which has at first a few, and then more numerous boulders of the pinkish, coarse Dedham Granite. At the northeastern end of the outcrop a fairly large exposure of the Dedham Granite also represents a fragment, because at the contact with the brecciated welded tuff there is no chilling of the granite.

45.4 Return to 109 and proceed north; cross 128 and then the Charles River. Immediately turn left onto the VFW Parkway. Proceed to the first rotary and continue past Joyce Kilmer Park to Walter St. Turn right onto Walter St. and park at the entrance to the Arnold Arboretum in a small parking lot. Descend and walk to Bussey St. Enter the park at the first set of gates on the right. Walk 100 yds up a slight incline to the top of the first prominence on the left. It has a large number of exposures and blocks of rock.

STOP 3. SQUANTUM "TILLITE." (30 MINUTES) The rock is a diamictite with fragments of variable dimension up to 3 ft long consisting mainly of quartzite, but also brecciated welded tuff, and Dedham-type granite, all set in an unsorted clastic matrix of variable grain size. In places the matrix is cleaved. Elsewhere it shows slump folds. Some fragments appear to be drop-stones. Some of the largest fragments, and in many blocks quartzite fragments are so closely broken up that the smaller pieces obviously were parts of a larger block.

49.8 Return to the parking place; exit onto VFW Parkway, turn left and proceed to the first rotary. Turn right onto Roxbury Parkway and continue across two rotaries and the interchange with Route 9 via Hammond Pond Parkway to Beacon St. Turn left and stop. This position will be used to examine stops 4 and 5 (Fig. 8).

STOP 4. BROOKLINE MEMBER OF THE ROXBURY CONGLOMERATE AND BRIGHTON VOLCANICS, BEACON STREET AT HAMMOND POND PARKWAY, NEWTON. (20 MINUTES) Rehmer and Roy (1976) have lauded localities at Stops 4 and 5 as being the best in the Boston Basin for examining the sedimentological features of the conglomerate facies of the Boston Bay Group. They have recorded an aggregate thickness of about 360 ft of section for these localities and have mapped out several intervals (Fig 8) of pebble and cobble conglomerate with beds of sandstone and shale, as well as a 40 ft-thick lava flow of the Brighton Volcanics. They indicate that conglomerate filled basal channels cut at least 50 ft deep and cut laterally a few hundred yards into finer-grained sedimentary rocks.

A 40 foot cliff along the north side of Beacon Street is formed of outcrops of the lower part of the Brookline Member of the Roxbury Conglomerate. A thick conglomeratic unit forms most of the rock cliff westward along Beacon Street to Bishopsgate Road (Fig. 8). The conglomerate, however, both at the east and west ends of the outcrop, abuts truncated beds of thinly laminated siltstone and fine sandstone. This unconformable contact is interpreted as a substantial channel filling of conglomerate cut into the finely bedded unit. Rehmer and Roy (1976) have interpreted this sequence as forming the upper part of the succession whose lower part will be seen at Stop 5 in the Webster Conservation Area. The laminated siltstone contains strata-bound, overturned to recumbent folds that have been interpreted to be the result of penecontemporaneaus deformation (Skehan and Barton, 1973, Fig. 8; Rehmer and Roy, 1976; Skehan, 1976, 1979) These are approximately E-W striking beds that dip about 25°-35°N and lie on the northern flank of the Central Anticline whose crest is 1.3 mi. to the south of these localities.

Cross Beacon Street and walk along the south-bound lane of Hammond Pond Parkway to the Trail on the map (Fig. 5).

STOP 5. BROOKLINE MEMBER OF THE ROXBURY CONGLOMERATE AND BRIGHTON VOLCANICS, WEBSTER CONSERVATION AREA, NEWTON. (45 MINUTES) The area of Stop 5 is shown in Figure 8. Large and abundant outcrops of the lower part of the Brookline Member of the Roxbury Conglomerate are well displayed. Entering the Conservation Area from Hammond Pond Parkway along the path (Fig. 8), outcrops can be examined at Localities A, B, and C (Fig. 8) for a variety of depositional and erosional features. Poison ivy flourishes here and even when it has lost its leaves it has not lost its ability to impart a nasty skin irritation.

Erosional unconformities occur at the base of the upper three conglomerate units (Fig. 8), each having several feet of relief. The sandstone-siltstone sequences underlying the upper conglomerates are clearly truncated at the unconformable contact. Well-rounded pebbles and cobbles of felsite, rhyolite, quartzite, intermediate and mafic volcanics, granite and pelite have been recorded, and most of the conglomerate is clast-supported in a medium- to coarse-grained lithic and feldspathic sandstone matrix. Sandstone lenses within the conglomerate, some of which are cross-bedded, are typically less than one-ft thick and are laterally discontinuous. These sandstone lenses have been used to subdivide conglomeratic units (Rehmer and Roy, 1976).

In Locality C (Fig. 8) the basaltic lava flow consists of a 33 ft-thick massive lower part, and amygduloidal, red fragmental top. It is overlain by red-brown volcanogenic sandstone containing blocks of lava. Rehmer and Roy (1976) interpret the flow as an aa-type with abundant rubble in its upper part.

50.1 Return to the bus; travel west on Beacon Street to Eliot Street and turn right
50.2 Travel North on Eliot Street.
50.5 Turn west (left) on Route 30 to its junction with Rice Road.
53.1 Park. Exposures form a low cliff on the north side of Route 30. So far we have considered the Dedham Granite and the rocks that are at a higher level; now we shall consider its relationships to the pre-existing rocks and particularly mylonites.

STOP 6A. RICE GNEISS AND ITS RELATION TO THE DEDHAM GRANITE. (30 MINUTES) This is the type locality of the Rice Gneiss as defined by Nelson (1975a), who considered it as metamorphosed tuffs and sandstones, while Goldsmith in the Bedrock Geology of Massachusetts, edited by Hatch (1991), included it in the unit Zv of the State Map (Zen, 1983), that is described as "metamorphic mafic and felsic volcanic" rock, a description usually applied to the Middlesex Fells Volcanic Complex. Grimes (1993) thus renamed it as the Rice Blastomylonitic Gneiss. At Rice Road intersection it should be studied from east to west along Route 30, where it is a quartz-rich foliated quartz-biotite-muscovite-feldspar mylonite with lenticles of amphibolite and a pronounced foliation, which contains schistose amphibolite, veins of granitic material and blocks of Westboro Quartzite. The foliation is commonly folded either into almost symmetrical or asymmetric folds with a few inches amplitudes and steep plunges. The foliation is cross-cut by undeformed veins of granite or aplite related to the Dedham Granite, outcrops of which occur on the north side of the nearby Massachusetts Turnpike. Some zones of the gneiss are hornfelsed and these zones show traces of former foliation although they are usually recrystallized. Intrusive, much less deformed diabase bodies are found within the gneiss. Westward the gneiss passes laterally into a migmatitic fragmental rock, in which large lozenge-shaped bodies of the migmatite "float" and which are sinistrally rotated in the gneissose matrix. We interpret this rock as the remobilized Rice Blastomylonite.

This lithology dies out up the hill to the north and appears to form an antiformal core of disturbed lithology with the Rice Blastomylonite deformed into sinistral parasitic, S-type folds on the eastern limb of the main fold and dextral, parasitic Z-type folds on the western limb of the main fold. The stage of generation of these folds is at present unknown, but may be contemporaneous with the intrusion of the Dedham Granite.

63.8 Mount the bus and proceed east and stop at the next prominent cliff at a convenient stopping place on Route 30.

STOP 6B. INTRUSIVE CONTACT OF THE DEDHAM GRANITE AND HORNFELSED MYLONITES. (20 MINUTES) At this roadside exposure traffic is heavy and dangerous; in examining the exposure keep off the road on the sandy curb. The generally continuous cliff shows an edge as well as intrusive veins of Dedham Granite both in intrusive and faulted contacts. The hornfelsed mylonite and associated intrusive diabase are cut by the granite. In the western part of the outcrop the aplitic (chilled?) edge of the granite shows xenoliths of the hornfelsed mylonite with occasional pseudotachylite at the contact. Late basaltic dikes cut both the mylonite and the granite. The hornfelses exhibit a residual trace of mylonitic foliation. This exposure constitutes a significant evidence that the Dedham Granite is later than the Burlington mylonitization.

72.6 Drive west on Route 30 to Framingham where it joins Route 9.
74.0 Continue on Route 9 and 30 through Framingham to where 30 and 9 separate; continue on Route 30.

75.3 Just after crossing the Mass Turnpike turn right into Mill Street and then left on Belknap Road. Millwood Street is the second right turn; follow it to the entrance of the Callahan State Park. Park in the parking lot and walk about 0.25 mile west to the end of the aqueduct.

STOP 7. SPILLWAY CUT; WEST END OF FLOOD CONTROL DAM, CALLAHAN STATE PARK, MILLWOOD STREET, FRAMINGHAM. (35 MINUTES) This set of outcrops consists prodominantly of a granite mapped as "Zgr" (Proterozoic Z "biotite granite") on the Massachusetts state map (Zen 1983; Wones and Goldsmith 1991). This granite is assumed by Grimes (1993) to have been coeval with the Dedham. These outcrops are distinctive as they display fabrics that appear systematically throughout the Milford, as well as remnants of other fabrics.

From the end of the access road along the aqueduct walk down the slope to the spillway. Here in the north end of the cuts there is a well-developed mylonite section enveloping a large, mylonitized xenolith of the Westboro Formation. The moderate northeasterly dip and NE to E strike of the mylonitic foliation, and the subhorizontal E-W quartz-feldspar stretching lineation in the granite mylonite is characteristic of shear zones developed throughout the Milford in the Framingham area. The best exposed of these shear zones is in the Nobscot village. Below the granite mylonite is a black phyllonite, assumed to be part of the Westboro Formation. Quartz veins within the phyllonite show dextral (top to the east) shearing. This is in accordance with the shear sense displayed by S-C fabrics within the Nobscot shear zone. Below the phyllonite are quartzitic and mafic mylonites.

The Milford Granite to the south, on both sides of the cut, is divided into undeformed to protomylonitic knots, 2 to 16 in in diameter, bounded by anastamosing bands of mylonite. Some of these knots, especially in the eastern outcrop, give dextral shear sense. However, some of the knots in the western outcrop contain an apparent sinistral S-C fabric, which has not been seen elsewhere. We suggest that this sinistral fabric is a remnant of an earlier deformation which, in most locations, has been erased by dextral shearing. This explains why the phyllonite fabric is ambiguous, while the late stage quartz veins within clearly show dextral motion.

A surface at the north end of the eastern outcrop displays a lineation, confined to a narrow layer, composed of thin quartz-feldspar rods that plunge 42°, bearing 324°. This lineation may correlate with NW-dipping, normal-motion shear zones that appear sporadically in the Framingham quadrangle, but are common in the Marlborough quadrangle to the west (Ashland 1991).

79.9 Return by the same route to the junction of Route 30 and 128. Turn north into Route 128 and I-95.
88.2 Continue on 128 to Exit 30A to Lexington.
89.6 Turn left and follow Lincoln Street to the parking lot of the Hayden Recreation Center on the right. Park and walk to the glaciated outcrop between the Center and Lincoln Street.

STOP 8. JUNCTION OF DEDHAM GRANITE AND OLDER ROCKS. (20 MINUTES) A well-exposed contact between the Dedham Granite and older foliated porphyritic amphibolite with a NW-SE strike, intruded by younger sheared but unfoliated diabase. The granite and associated aplites crosscut the amphibolite and the diabase, and granite shows a fine-grained margin at the contact. The granite, which is partly sheared, is epidotized. Its primary constituents are quartz, feldspar, biotite and hornblende. The porphyritic amphibolite is a part of the Burlington Mylonite Zone and is found elsewhere within it.

90.9 Exit to Lincoln Street and proceed northward (right) toward Worthen Road. Turn left and continue to Bedford Street (also Route 225). Turn left and continue along Bedford Street to Route 128 and I-95.
91.4 At Route 128 turn east to the Middlesex Turnpike interchange. Proceed north along the Turnpike to the third traffic light and turn left into the parking lot of Victoria Station Restaurant. Park at the northernmost corner.

STOP 9. DEDHAM-BURLINGTON MYLONITE ZONE CONTACTS. (30 MINUTES) In the cliffs behind the parking area Dedham Granite, which is only slightly deformed, intersects the 068° trending mylonite zone with sharp cross-cutting contacts. The mylonite zone at the top of the cliff shows folds with excellent dextral folds and occasional asymmetric feldspars. Within the mylonite there are slightly deformed diabases which are also cut by the granite.

The existence of little deformed diabase intrusions within the mylonite zone, although cross-cut by the granite, suggests that a considerable period of time separates mylonitization and emplacement of the Dedham Granite, implying that the Burlington Mylonite Zone is a product of pre-630 Ma structural orogenic events that can be correlated with the Pan-African I.

106.3 Exit right onto the Middlesex Turnpike and continue south beyond Route 128 to where it joins Massachusetts Avenue, which leads to the vicinity of the Hynes Auditorium and the Marriott Hotel.

REFERENCES

Ashland, F. X., 1991, Deformation histories across the Bloody Bluff Fault, eastern Massachusetts: Geological Society of America, Abstracts with Programs, v. 23, no. 1, p. 2.

Bailey, R. H., Skehan, J. W., Dreier, R. B., and Webster, M. W., 1989, Olistostromes of the Avalonian terrane of southeastern New England, *in* Horton, J. W. Jr., and Rast, N., eds., Mélanges and Olistostromes of the U.S. Appalachians: Geological Society of America Special Paper 228, 93-112.

Bell, K.-G., and Alvord, D. C., 1976, Pre-Silurian stratigraphy of northeasternMassachusetts. In Page, L. R., ed., Contributions to the Stratigraphy of New England: Geological Society of America Memoir 148, p. 179-216.

Billings, M.P., 1976a, Bedrock Geology of the Boston Basin. In Cameron, Barry, ed., Geology of Southeastern New England, New England Intercollegiate Geological Conference (NEIGC), p. 28- 45 Geological Society of America, Special Paper 146, p. 5-30.

Billings, M.P., 1976b, Geology of the Boston Basin, in Lyons, P.C. and Brownlow, A.H., eds., Studies in New England Geology: Geological Society of America, Special Paper 146, p. 5-30.

Castle, R. O., 1964, Geology of the Andover Granite and surrounding rocks, Massachusetts: U.S.Geological Survey, Open-file Report 64-33, 550 pp.

Castle, R.-O., 1965, A proposed revision of the subalkaline intrusive series of northeastern Massachusetts: U.S. Geological Survey Professional Paper 525C, 74-80.

Castle R. O., Dixon, H. R., Grew, E. S., Griscom, A., and Zietz, I., 1976, Structural dislocations in eastern Massachusetts: U.S. Geological Survey, Bulletin 1410, 39 pp.

Chute, N. E., 1966, Geology of the Norwood Quadrangle, Norfolk and Suffolk Counties: U. S. Geological Survey Bulletin 1163-B, 78 pp.

Durfee Cardoza, K., Hepburn, J. C., and Hon, R., 1990, Geochemical constraints on the paleotectonic settings of two late Proterozoic mafic volcanic suites, Boston-Avalon zone, eastern Massachusetts, *in* Socci, A. D., Skehan, J. W., and Smith, G. W., eds, Geology of the Composite Avalon Terrane of Southern New England, Geological Society of America, Special Paper 245, 113-131.

Goldstein, A. G., 1989, Tectonic significance of multiple motions on terrane-bounding faults in the northern Appalachians: Geological Society of America Bulletin, v. 101, p. 927-938.

Goldstein, A., 1991, The Sterling shear zone in eastern Massachusetts; evidence for complex Alleghanian motions along the western margin of the Avalon Zone in eastern Massachusetts: Geological Society of America, Abstracts with Programs, v. 23, no. 1, p. 36.

Grimes, S. W. 1993, Structure and Tectonics of the Bloody Bluff Fault Zone, Natick and Framingham Quadrangles, Eastern Massachusetts; M.S. Thesis, Chestnut Hill, MA, Boston College, 130.

Hatch, N. L.,Ed., 1991, The Bedrock Geology of Massachusetts: U.S. Geological Survey Professional Paper, 1366-E-J.

Hepburn, J. C., 1978, Preliminary reconnaissance bedrock geologic map of the Marlborough quadrangle, Middlesex and Worcester Counties, Massachusetts: U. S. Geological Survey Open-File Report 78-222, 29 p., 1 pl., scale 1:24,000.

Hepburn, J.C., M. Hill, and R. Hon, 1987, The Avalonian and Nashoba Terranes, Eastern Massachusetts, U.S.A.: An Overview: Maritime Sediments and Atlantic Geology, v. 23, p. 1-12.

Kaye, C. A., 1980, Bedrock geologic maps of the Boston North, Boston South, and Newton quadrangles, Massachusetts: U.S. Geological Survey, Misc. Field Studies Map MF-1241, scale 1:24,000.

Kaye, C. A., 1983, Discovery of a Late Triassic basin north of Boston and some implications as to post-Paleozoic tectonics in northeastern Massachusetts: American Journal of Science, v. 283, p. 1060-1079.

Kaye, C. A., 1984, Boston Basin restudied. In Hanson, L. S., ed., Geology of the Coastal Lowlands, Boston Ma to Kennebunk ME; 76th Annual New England Intercollegiate Geological Conference: Salem (MA) State College, p. 124-144.

Kaye, C. A., and Zartman, R. E., 1980, A late Proterozoic Z to Cambrian age for the stratified rocks of the Boston Basin, Massachusetts. In Wones, D. R., ed., The Caledonides in the U.S.A.; Proceedings, IGCP Project 27: Blacksburg, Virginia Polytechnic Institute and State University, Memoir 2, p. 257-261.

Kovach, Adam, Hurley, P. M., and Fairbairn, H. W., 1977, Rb-Sr whole rock age determinations of the Dedham Granodiorite, eastern Massachusetts: American Journal of Science, v. 277, p.905-912.

Lister, G.S. and Snoke, A.W., 1984, S-C Mylonites: Journal of Structural Geology, v. 6, (6), p.617-638.
Nelson, A. E., 1975a, Bedrock geologic map of the Natick quadrangle, Middlesex and Norfolk Counties, Massachusetts: U.S. Geological Survey Map GQ-1208.
Nelson, A. E., 1975b, Bedrock geologic map of the Framingham quadrangle, Middlesex and Worcester Counties, Massachusetts: U.S. Geological Survey Map GQ-1274.
Rast, N., and Skehan, S.J., J. W., 1990a, The Late Proterozoic Geologic Setting of the Boston Basin, *in* Socci, A. D., Skehan, J. W., and Smith, G.W., eds, Geology of the Composite Avalon Terrane of Southern New England, Geological Society of America, Special Paper 245, p. 235-247.
Rast, N., and Skehan, J. W., 1990b, Proterozoic mylonitization in eastern Massachusetts: Geological Society of America, Abstracts with Programs, v. 22, no. 2, 63.
Rast, N., Skehan, J. W., Hepburn, J. C., Myskowski, E. M., and Grimes, S. W., 1990, Proterozoic kinematics in the Avalon superterrane of southern New Brunswick, Canada, and eastern Massachusetts, U.S.A.: Geological Society of America, Abstracts with Programs, v. 22, no. 7, p. 263.
Rehmer, J. A., 1976, The Boston Bay Group: The Boulder Bed Problem. In Cameron, Barry, ed., Geology of Southeastern New England, New England Intercollegiate Geological Conference (NEIGC), p. 71 Geological Society of America, Special Paper 146, p. p. 71-91.
Simpson, C. and Schmid, S., 1983, An evaluation of criteria to deduce sense of movement in sheared rocks: Geological Society of America Bulletin, v.94, p.1281-1288.
Skehan, J. W., 1979, Puddingstone, Drumlins, and Ancient Volcanoes: A Geologic Field Guide along Historic Trails of Greater Boston; WesStone Press, Weston, MA, 63pp.
Skehan, J. W. and Barton, C.W., 1973, he Geology of Newton, The Newton Conservators, Inc., 27 pp.
Skehan, J. W., and Rast, N., 1990, Proterozoic Mylonitization in Eastern Massachusetts; Geological Society of America Abstracts with Program, v. 22, (2), p.63.
Skehan, J. W., and Rast, N., 1991, Pre-Mesozoic evolution of Avalon terranes of southern New England, *in* Socci, A. D., Skehan, J. W., and Smith, G. W., eds., Geology of the Composite Avalon Terrane of Southern New England: Geological Society of America, Special Paper 245, 13-54.
Smith, C. J., and Hon, R., 1984, Geology, petrology, and origin of the Precambrian igneous rocks located in the area north of Boston, *in* Hanson, L. S., ed., Geology of the Coastal Lowlands, Boston Ma to Kennebunk ME; 76th Annual New England Intercollegiate Geological Conference: Salem (MA) State College, p. 292-309.
Socci, A. D., and Smith, G. W., 1990, Stratigraphic implications of facies within the Boston Basin, *in* Socci, A. D., Skehan, J. W., and Smith, G.W., eds, Geology of the Composite Avalon Terrane of Southern New England, Geological Society of America, Special Paper 245, p. 55-74.
Thompson, M. D., Evidence for a late Precambrian caldera in Boston, Massachusetts: Geology, 13, 641-643.
Thompson, M. D., and Hermes, O. D., 1990, Ash-flow stratigraphy in the Mattapan Volcanic Complex, greater Boston, Massachusetts. In Socci, A. D., Skehan, J. W., and Smith, G.W., eds, Geology of the Composite Avalon Terrane of Southern New England, Geological Society of America, Special Paper 245, p. 13-53.
Thompson, M.D. and Skehan, J.W., 1992, Re-evaluating the Boston "Basin," Northeastern Geology, v. 14, (2 and 3), p. 102-107.
Zartman R. E., and Naylor, R. S., 1984, Structural implications of some radiometric ages of igneous rocks in southeastern New England: Geological Society of America Bulletin, 95, 522-539.
Zen, E-an, ed., 1983, Bedrock Geologic Map of Massachusetts, United States Geological Survey, scale 1:250,000.

Chapter T

Archaeological Geology on Long Island, Boston Harbor

By Barbara E. Luedtke and Peter S. Rosen

Field Trip Guidebook for the Northeastern United States:
1993 Boston GSA

Volume 2
Contribution No. 67, Department of Geology and Geography, University of Massachusetts, Amherst, Massachusetts

ARCHAEOLOGICAL GEOLOGY ON LONG ISLAND, BOSTON HARBOR

by
Barbara E. Luedtke, Department of Anthropology, University of Massachusetts, Boston, 02125
and
Peter S. Rosen, Department of Geology, Northeastern University, Boston, MA 02115

INTRODUCTION

The Boston Harbor Islands are a rich source of information for both archaeologists and geologists because they have been far less modified by urbanization and land filling than most other parts of Boston Harbor. Of the more than 30 islands in Boston Harbor, Long Island is the largest (86.2 ha) and the longest (2.9 km) (Fig. 1). In many ways it is geologically, archaeologically, and historically typical of the other Boston Harbor Islands, though it does have a number of unusual features.

The Boston Harbor Islands have been used by humans for various purposes throughout the Holocene. Although PaleoIndian sites have been found elsewhere in the Boston area (Carty and Spiess, 1992), no artifacts datable to this period have been found as yet on the Boston Harbor Islands. A single Early Archaic point from the HL-11 site on Long Island is the oldest artifact found on the islands thus far (Luedtke, 1984). Middle Archaic artifacts have been found at several sites (Luedtke, 1975, 1984, 1990) and Late Archaic sites are quite common. The Harbor area was primarily riverine or estuarine during most of this early period, and settlement patterns would have been oriented toward very different resources than in later periods. Shellfish beds became established by the Early Woodland period, and evidence suggests that from then on the Harbor Islands were used primarily as locations for temporary camps from which to procure and process coastal resources. During the later part of the Late Woodland period, farming hamlets were established on some of the islands (Luedtke, 1980). Year-round occupation of any of the islands during the prehistoric period is unlikely because of their small size.

The Islands were occupied by Europeans even before the establishment of the Massachusetts Bay Colony in 1630, and they have played an integral role in the history of the City of Boston from then to the present. Throughout the prehistoric and historic periods, geological factors have affected the ways in which people used the islands.

COASTAL GEOLOGIC FRAMEWORK

Boston Harbor

The sedimentary framework of Boston Harbor consists of drumlin topography resulting from two different age drifts. A pre-Wisconsinan drift is overlain by a thin layer of late Wisconsinan drift (Knebel et al, 1992). The topographic low, which now forms harbor bottom, is largely composed of late Wisconsinan glacio-marine clays (Boston Blue Clay), (Kaye, 1982) as is much of the adjacent Massachusetts Bay.

The Boston Harbor Islands consist of drowned drumlins often linked by tombolos and modified by other spit forms. The harbor was submerged at 5,630 yr BP during the Holocene transgression. However, modification of the drumlin shoreline by longshore processes probably was not significant until a slowing of the rate of sea level rise approximately 3,000 yr BP (Rosen et al, 1993; Kaye and Barghoorn, 1964). The topography of the pre-Holocene basement beneath the Harbor indicates that the position of tombolos is controlled by the underlying geology rather than modern coastal processes. Most tombolos are located along pre-existing basement highs, and major tidal channels occur where there are pre-existing drainage channels (Rendigs and Oldale, 1990).

Dunes are not common on barriers within the Boston Harbor region due to the coarseness of the sediment. The barriers occur in both transgressive and regressive forms; the emergent portions of both barrier types are most frequently composed of gravel storm ridges. The lack of dunes makes overtopping (non-channelized flow over the barrier surface) a common process during storm events. This results in

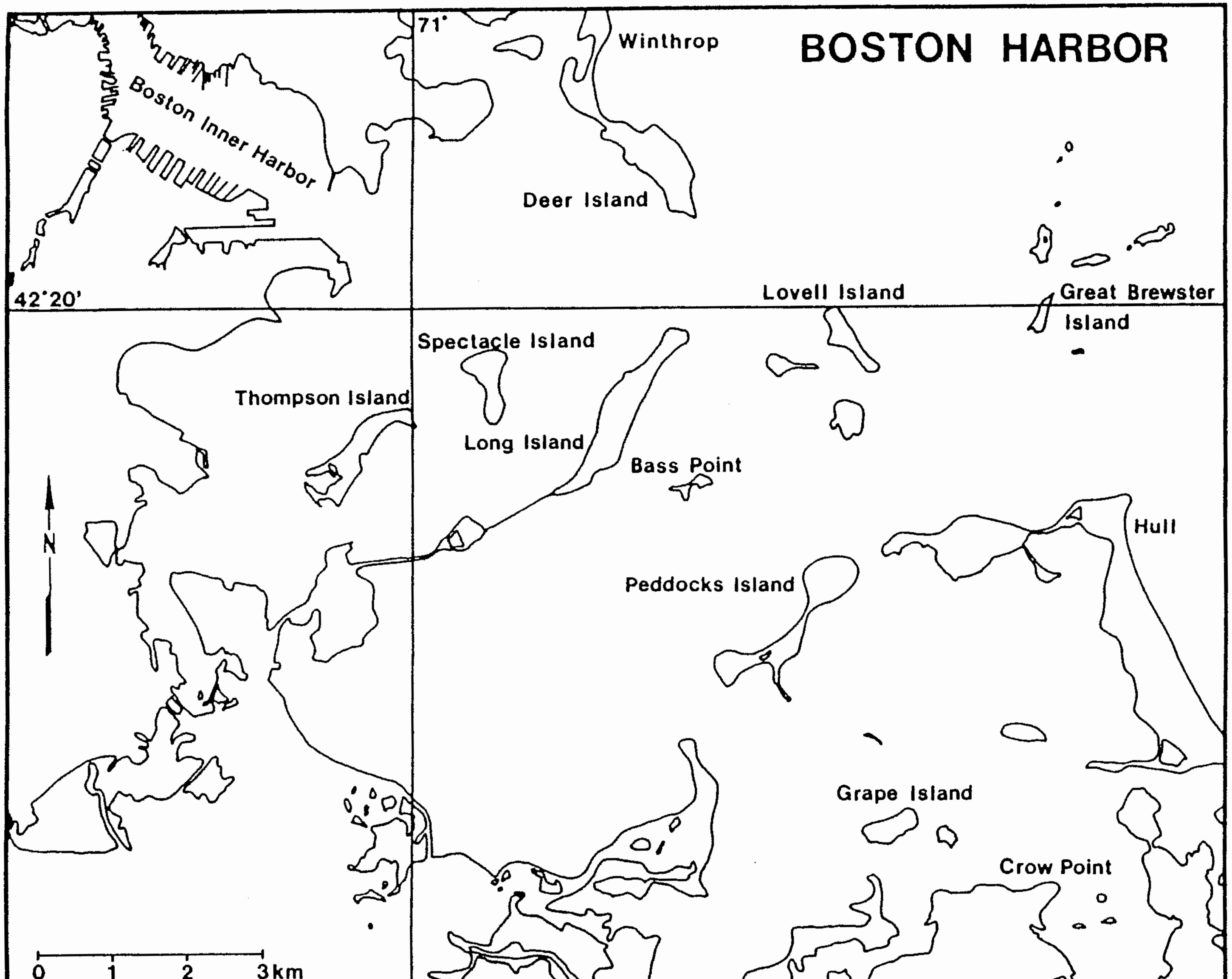

Figure 1. Location map showing Bass Point on Long Island.

transgressive barrier spits, consisting of a single asymmetrical overtopping ridge and a series of gravel overwash or overtopping lobes projecting into the backbarrier lagoon. Channelized flow over the gravel barrier crest is less common, but occurs as a process distinct from the process in sandy barrier spits. Due to the lack of dune vegetation, an overwash channel remains as a semi-permanent feature once it has formed. Overwash is not restricted to storm events, but can occur frequently at high tide during periods of higher wave energy or during spring tides. An overwash channel may migrate downdrift, similar to an inlet on sandy shorelines (Rosen and Leach, 1987).

As Boston Harbor opens to the northeast, waves refract around the islands and longshore drift typically converges at the leeward, or southerly ends of the islands. The resulting regressive cuspate spits form as series of preserved storm ridges if coarse sediment dominates, or less commonly, dune ridges.

Many of the cuspate spits in the harbor have common forms. North Spit on Thompson Island consists of gravel ridges (Rosen, 1984) indicating a reorientation of the shoreline since the formation of the barrier about 2,200 yr BP. Tracer studies have shown that longshore transport dominates these low wave energy gravel beaches during non-storm periods, while onshore gravel movement that forms the ridges occurs mainly during storms (Rosen and Brenninkmeyer, 1989). The northeast side of the spit is eroding at about 0.15 m/yr, due to exposure to higher wave energy and no longshore input of sediment. This results in the truncating storm ridges. The southwest side is accreting at roughly the same rate due to a local drift reversal. Therefore, this "traveling headland" is gradually migrating to the southwest, which is an updrift direction, by the addition of successive ridges to the shoreline.

South Cuspate Spit on Thompson Island is one of the few sandy accumulative features in Boston Harbor. A dearth of sediments to the south, and an abundance of longshore sand to the north (derived from an eroding delta foreset deposit; Caldwell, 1984) results in gradual accumulation of the spit northward. This trend is recorded in a succession of preserved dune ridges parallel to the northern shore. However, there has been no discernible change in shore position since 1847 (Rosen, 1984).

At least four of the cuspate spits on Boston Harbor Islands have known prehistoric sites associated with them. At this time it is unclear whether this is due to the fact that the spits provided an important resource such as shellfish, or simply to the fact that such spits tend to protect sites from the erosion that has been so destructive to other archaeological sites in the Harbor area.

Long Island And Bass Point

Geologic Setting. Long Island is composed of eight east- to southeast-trending drumlins that have been joined by tombolos (Fig. 2). The eroding faces of these drumlins provide evidence of the two superposed tills. North, or updrift of Bass Point, the tills are readily discernible on the basis of texture. The upper till is bouldery and separated from the lower till by a two-m-thick sand layer interbedded with till. The upper till averages 56% sand, while the lower till averages 35% sand. The lower till contains shell fragments in which chert has replaced most of the carbonate material (Newman et al, 1990; Newman et al, this volume).

Parts of the exposure of the till northeast of Bass Point are continuously wet, as evidenced by *Phragmites sp.* on the slope. The moisture is probably due to groundwater collecting in one of the sand layers and flowing out on the bluff, leaking stormwater sewerage systems, or both. This has lead to continual slumping and rapid erosion in this area.

Bass Point is a cuspate spit on the south side of Long Island that is migrating to the south. The dune ridges enclose a saltmarsh which is presently dominated by *Phragmites*, due to the lack of connection with the harbor. This landform has been classified as a looped bar (Johnson 1967), although this term appears to designate a fixed landform. The cuspate outline of Bass Point is asymmetrical, forming what is sometimes referred to as a "traveling headland". It is unlike most cuspate spits in Boston Harbor in that there is no evidence of a convergence of longshore drift at this point. Net longshore transport is to the southeast, with sediment carried around the point where it accumulates on the lee side of the feature. The northeast-facing

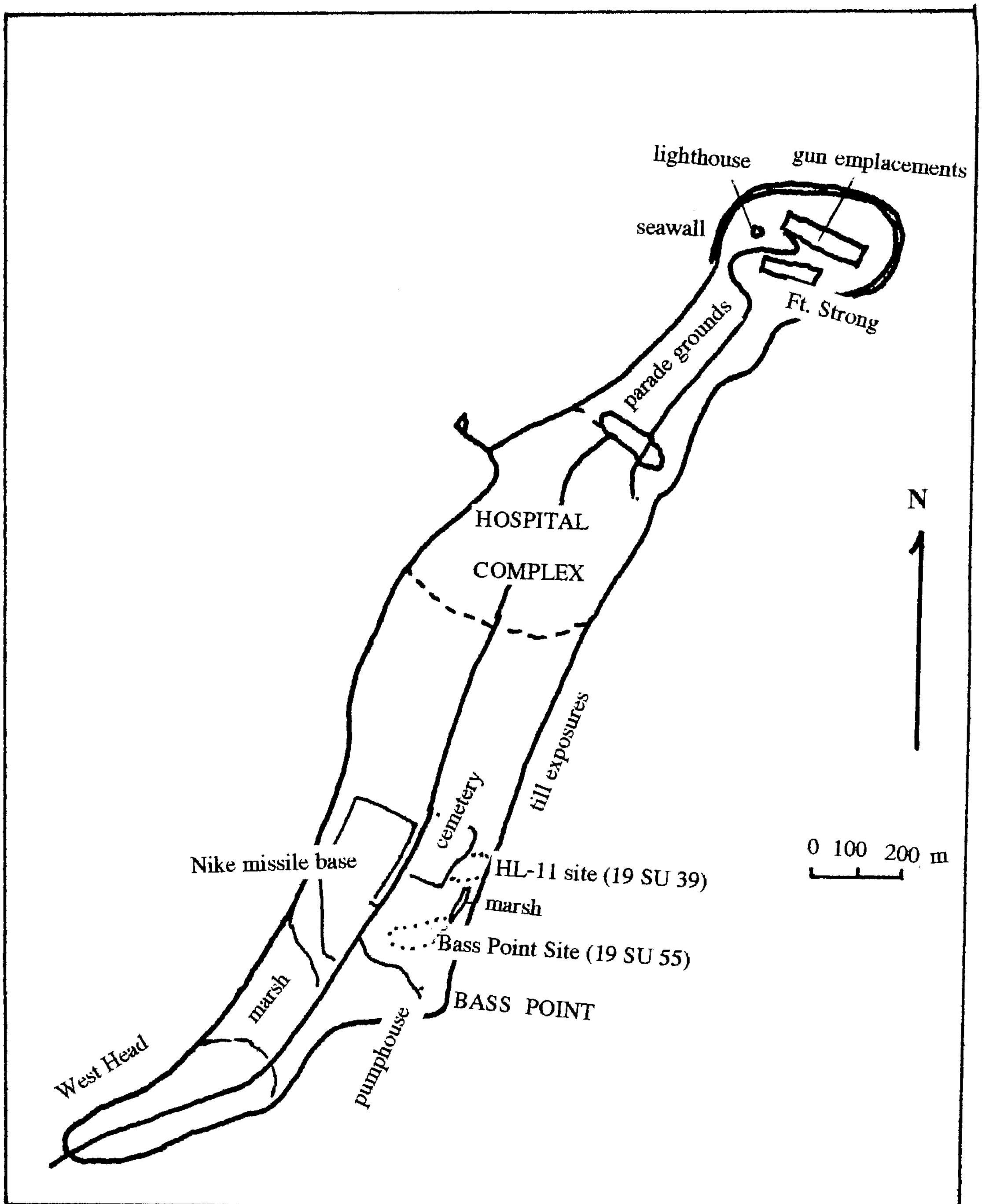

Figure 2. Long Island, showing major geological and cultural features.

(updrift) side of the spit consists of a single transgressive asymmetrical overtopping ridge composed of mixed sand and gravel. This form reflects the limited volume of sediment input to the system relative to wave energy. The southeast-facing (lee) arm of the spit consists of a ridge or ridges that tend to be symmetrical, indicative of an accumulative feature.

Analysis of historic shoreline change along Bass Point in the 91 year period from 1847 to 1938 indicates that the southwest-facing (lee) arm of the cuspate spit accreted at an average rate of 0.33 m/yr. The updrift side retreated an average of 0.5 m/yr over the same period. These trends are consistent with the ridge morphology. The eroding drumlin shorelines adjacent to Bass Point showed long term erosion rates on the order of 0.1 m/yr or less.

ARCHAEOLOGY ON LONG ISLAND

Although the northern half of Long Island has been heavily impacted by military and institutional users of the island, the southern half remains relatively undisturbed. This southern end of Long Island was first systematically surveyed for archaeological sites during the summer of 1984 by a University of Massachusetts, Boston, archaeological field school under the direction of Barbara Luedtke. Six sites were found, representing all periods from Early Archaic through Late Woodland (Luedtke, 1984).

Two of these sites are of special interest because of their unusually close proximity to each other and their association with Bass Point. HL-11 (19 SU 39) and Bass Point (19 SU 55) are both relatively large shell middens. The centers of the two sites are only about 200 meters apart, and their perimeters are much closer. We rejected the possibility that they are both part of a single very large site; our survey methods involved excavation of shovel test pits (STPs) at 10 meter intervals along transects spaced 10 meters apart, and this relatively close sampling revealed a definite barren zone between the sites in which no artifacts were found in shovel test pits. This barren zone does not correspond to an obvious geographical boundary. The site centers are located near either end of the linear saltmarsh, which has a few patches of cattail suggesting that it may be fed in part by freshwater springs. Both sites are located at about the same elevation, on gentle slopes facing the southeast, and both are on Newport silt loam soils (Peragallo 1989) . The only obvious difference in locational attributes is that HL-11 is located adjacent to the beach while the Bass Point site is located well inland behind the sand spit (Fig. 2).

We were also unable to detect any obvious functional differences between the two sites, based on analysis of data from eleven one meter square test pits at the HL-11 site and nine one meter square test pits at the Bass Point site. Both sites have a similar structure, consisting of a central area of fairly dense shell midden, ranging from 5 to 20 cm in thickness, surrounded by a less heavily utilized area with scattered shell, flaking debris, and occasional artifacts and features. There is considerable horizontal and vertical variation in both sites.

Both sites were occupied most heavily during Woodland times, and both appear to have been base camps rather than specialized processing camps. As Table 1 indicates, both have roughly the same kinds of artifacts, features, and food remains. Quantities in most categories are also similar. More biface reduction does appear to have taken place at HL-11, thus accounting for the greater number of both flakes and bifaces. The range of lithic raw materials is generally similar at both sites, with grey porphyritic rhyolite making up the bulk of both assemblages. Quartz, other rhyolites, quartzites, and argillites are also present in small quantities. Most of these raw materials are available locally in the form of beach cobbles. In addition, we discovered a large glacial erratic of the grey porphyritic rhyolite uphill from both sites that had clearly been flaked, almost certainly by prehistoric inhabitants of the island.

Faunal remains suggest that deer (*Odocoileus virginianus*) provided much of the meat eaten at both sites (most of the bones classified as "large mammal" represent deer). Dogs, other mammals, a few reptiles, and a variety of birds were also eaten. Coastal resources include large numbers of shellfish, primarily *Mya arenaria*, the softshell clam, and also fish, primarily cod (*Gadus morhua*). The apparent predominance of cod at the Bass Point site is probably due to sampling error; 72 of those fragments (representing a minimum of 3 individuals) came from a single STP. Excluding that STP, the remains of a minimum of 3 individual cod were recovered at each site. Finally, there are no obvious seasonal differences between the two sites. Hickory nuts (*Carya sp.*) were found in many squares at both sites and are available only in the fall. All of the faunal species represented would also have been available in fall, suggesting that this was the primary season of use for both sites.

TABLE 1: Comparison of artifacts, features, and food remains.

Archaeological remains	Bass Point site	HL-11 site
Lithic artifacts (#)		
Projectile points	2	5
Bifaces		7
Cores	4	4
Drills	1	1
Scrapers	1	1
Hammerstones	2	7
Pestles	1	
Worked slate		3
Steatitle bowl		1
Flakes	360	1996
Ceramic sherds	37	60
Fire cracked rock	148	592
Features		
Pits	1	2
Fire stains	3	7
Postmolds	3	2
# of fragments		
Hickory nuts	16	36
Acorn		3
# of bones		
Deer	9	12
Large mammal	26	97
Dog	3	2
Medium mammal	31	61
Beaver		1
Fox		2
Mustelid		2
Small mammal	1	7
Turtle	2	
Reptile	1	
Large bird	8	11
Medium bird	21	11
Small bird	1	
Common loon	1	
Cod	163	43
Tomcod		4
Dogfish		1

The most obvious difference between the Bass Point and HL-11 sites is chronological. A number of temporal indicators occur at one site but not the other, suggesting that the two sites may have been occupied in alternation. Calibrating this alternation is difficult because none of the available chronological data is ideal or precise, but the mutually exclusive distribution of several of the indicators is certainly striking. Five chronological indicators of varying degrees of specificity are available: 1) radiocarbon dates, 2) lithic artifact styles, 3) ceramics, 4) exotic lithic materials, and 5) shellfish types. Each will be discussed below.

Radiocarbon Dates

Three radiocarbon dates are available for these sites, one from Bass Point and two from HL-11. The first, on quahog (*Mercenaria mercenaria*) from level 4 (25-30 cm) of square 9 at the Bass Point site, produced a date of 2030 +/- 80 radiocarbon years BP, C-13 corrected (GX-10880). The second is on quahog from level 4 (20-25 cm) in square 9 at HL-11, with an age of 2165 +/- 90 radiocarbon years BP, C-13 corrected (GX-11234). The third, on softshell clam (*Mya arenaria*) shell from Feature 1 in square 11 at HL-1, produced a date of 1630 +/- 90 radiocarbon years BP, C-13 corrected (GX-11235). Since all dates are on shell, which is affected by the reservoir effect in this region, all have been calibrated using the correction factors in Stuiver et al. (1986) and are shown on Figure 3 with 2 sigma ranges. While there is considerable overlap between the two quahog dates, for reasons that will be discussed below, the third date does not overlap the others.

Lithic Artifacts

The Massachusetts Historical Commission's typology has been used here to define projectile point types and assign the time ranges given below and shown on Figure 3 (MHC, 1984). Not many projectile points were found at either site, but the ones found overlap little in time ranges, and it is notable that no points of the same type were found at both sites.

Bass Point produced only two fragmentary projectile points. The first is clearly a Levanna point of late Middle Woodland and Late Woodland age (1,300-400 BP), and the second is probably also this type. In addition, a small stemmed point of probable Late Archaic age (6,000-4,000 BP) was found on the surface of a road near the site and may or may not be associated with it.

Hl-11 produced five projectile points. The earliest is an Early Archaic bifurcate based point (9,000-8,000 BP), the oldest artifact found thus far in the Boston Harbor area. Because no other Early Archaic materials were found at the site and this point was found in a level which also contained younger artifacts, we cannot assume that there was an Early Archaic component at this site. The point may represent a stray find, or may even have been an artifact picked up as a curiosity by later Native Americans and then lost here. A Brewerton eared notched point (5,000-4,000 BP) represents the Late Archaic period, as do two points attributable to the Susquehanna tradition (4,100-3,600 BP), one probably a reworked Atlantic point and the other a fragment of a Mansion Inn blade. A small steatite bowl found at HL-11 also dates to the end of the Late Archaic and Terminal Archaic periods. Finally, a broken fragment of what is probably a Jack's Reef pentagonal point (1,600-1,100 BP) was found.

Ceramics

Ceramic styles changed more rapidly over time than did lithic artifact styles, and are probably more sensitive chronological indicators. Decoration, vessel shape, temper type and size, and vessel thickness all varied with time in this region (Luedtke, 1986). The first ceramics in New England belonged to the Vinette tradition, and their most distinctive attribute is cordmarking on both the interior and exterior of the vessel. Sherds from three different vessels of this type were found at Hl-11, and none at Bass Point. One vessel at HL-11 and two at Bass Point represent the very thick (greater than 1 cm) and grit tempered ceramics with smooth surfaces and punctations that are also apparently of Early Woodland age (Petersen and Hamilton, 1984) and may be slightly younger than the Vinette ware (Luedtke, 1986).

Both sites produced numerous sherds of the grit tempered ceramics usually attributed to the Middle Woodland period. Most did not have obvious decoration, although one sherd at HL-11 showed rocker-stamping, generally an earlier trait in this area, and two had dentate stamping (Luedtke, 1986). Perhaps more significantly, Middle Woodland vessels at Bass Point were thinner than those at HL-11. Here and elsewhere in North America, there appears to have been a progressive trend toward thinner vessels over time, perhaps reflecting changes in cooking or pottery production technology (Luedtke, 1986). Thus, the measurable Middle Woodland vessel lots at HL-11 have a mean thickness of .729 cm (R .675-.85, N=5) while those from Bass Point had a mean thickness of .635 cm (R= .6-.7 N=4). While sample sizes are small and the actual differences in thickness are not great, there is very little overlap in the ranges.

Use of shell as a tempering material is generally associated with the Late Woodland period, though there was undoubtedly a transition period during which both types of temper were used. In fact, one very thick (1.22 cm) shell tempered vessel with cordwrapped stick impressions was found at HL-11 in the feature which also produced the Middle Woodland radiocarbon date. Again, Late Woodland vessels became thinner over time, and this attribute helps compensate for the lack of surface decoration on most of these sherds. Bass Point produced shell tempered vessels with slightly thicker walls (mean= .670 cm, R= .6-.8, N= 7) while HL-ll produced slightly thinner and thus probably later vessels (mean= .622 cm, R= .55-.75, N= 8).

Exotic Lithic Materials

While most types of lithic raw materials were found at both sites, only the Bass Point site produced red and gold jasper, elsewhere suggested as a chronological marker for the later part of the Middle Woodland period (Luedtke, 1987). Three different test pits at Bass Point produced a total of six jasper flakes, representing 1.6% of the total flake assemblage. If jasper occurred at the same frequency at HL-11 we should have recovered 33 jasper flakes. However, none of the eleven test pits at HL-11 produced any jasper at all. Such a clear difference is unlikely to be due to sampling error.

Shellfish

Earlier researchers noted that the lower levels of some Boston Harbor shell middens contained shellfish species now rarely found in the Harbor and generally restricted to the area south of Cape Cod, while upper levels of the same sites invariably consisted almost exclusively of softshell clam, currently the most common shellfish in the Harbor. Braun (1974) documented this pattern and suggested that it was due to a shift in the Labrador Current that brought slightly warmer water to the Boston Harbor area. Thus, Early Woodland and early Middle Woodland shell middens in the Boston area often contain significant quantities of quahog (*Mercenaria mercenaria*), oyster (*Crassostrea virginica*), and bay scallop (*Aequipecten irradians*), in addition to softshell clam (*Mya arenaria*). Braun argued that use of the warm water species declined after about 2500 BP, with the ocean reaching modern temperatures about 1500 BP. His general conclusions have been supported by subsequent field work in the area.

While softshell clam made up the vast majority of both the HL-11 and Bass Point shell middens, each site produced squares with quahog, oyster, and scallop in their lower levels. Quahog shells from both early deposits were radiocarbon dated, as discussed above. Although their ranges do overlap at two sigma, the date from HL-11 may be slightly earlier.

Although any one of the indicators discussed above is obviously imperfect, when they are all put together a pattern of alternating site use emerges (Fig. 3). The occupation line shown on Figure 3 is not the only one that could be drawn, but it does account for all the data. According to this interpretation, HL-11 apparently was preferred when possible, and may have been the only one of these two site occupied during Archaic times. Sea levels were still rising in Boston Harbor through most of the Archaic period, and neither Bass Point nor HL-11 is likely to have been coastal during that time. In fact, it is quite possible that the Archaic materials we found only represent the inland edge of Archaic sites that were largely destroyed by erosion as sea levels rose.

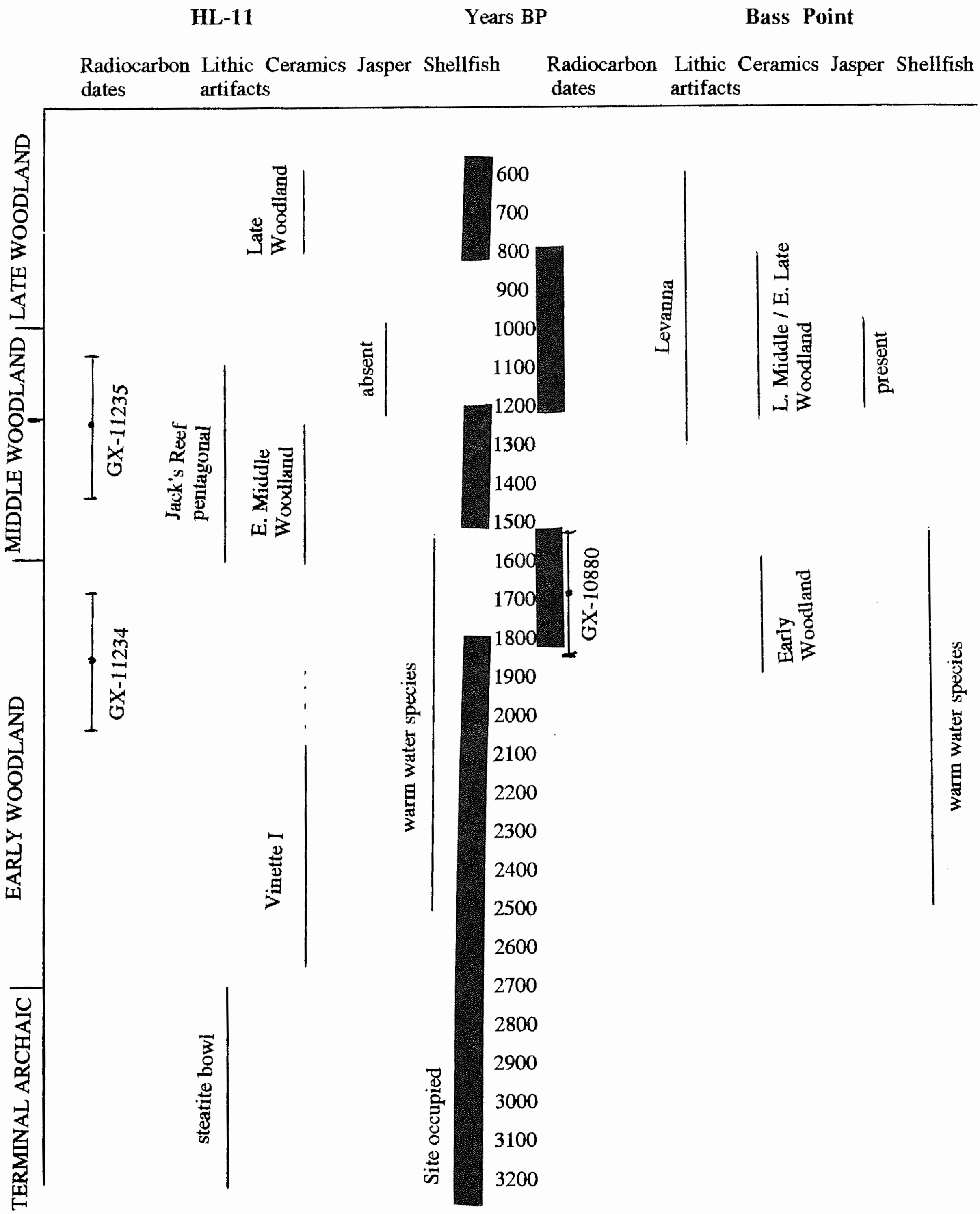

Figure 3. Chronological markers and proposed pattern of alternating occupations at the Bass Point and HL-11 sites, Long Island.

By Early Woodland times, sea level rise had slowed, shellfish beds had developed, and both of these sites were used regularly from then on. HL-11 was apparently occupied during the Terminal Archaic and into the Early Woodland; the presence of Susquehanna Tradition projectile point styles, a steatite bowl, several Vinette I ceramic vessel lots, warm water shellfish, and a radiocarbon date all support this interpretation. Later in the Early Woodland Period, settlement apparently shifted to the Bass Point site; a radiocarbon date, warm water shellfish, and the presence of thick grit tempered vessels with smooth surfaces and punctations all indicate this period. Settlement shifted back to HL-11 very early in the Middle Woodland Period, and a radiocarbon date, a Jack's Reef pentagonal point, and slightly thicker grit tempered and stamped ceramics are found. Bass Point was again the site of choice during the later part of the Middle Woodland and on into the early Late Woodland; thinner grit tempered vessels, slightly thicker shell tempered vessels, jasper, and two Levanna points all are appropriate to this period. Settlement shifted back to HL-11 for a few more centuries, and thinner shell tempered ceramics were left behind. Neither site appears to have been occupied after about 600 BP; it has been suggested that settlement patterns on the Boston Harbor Islands underwent considerable change at this time due to the introduction of farming into New England. (Luedtke, 1980).

Why did settlement shift back and forth between these sites? It is always possible that ideological or social factors were involved, but it seems more likely that some repeated ecological or geological shift caused this alternation. In the context of most Boston Harbor Island site locations, the present Bass Point site is not a desirable place to camp. Known sites on the other islands are most often close to the beach, probably to ensure easy access to shellfish beds and perhaps also so that the occupants of the sites could keep an eye on their canoes. In at least one other case, that of HL-7 on Grape Island, a site was abandoned once a sand spit built up and cut off access to the beach (Luedtke, 1975). It seems possible that some characteristic of the Bass Point spit and its changes over time played a role in this archaeological phenomenon.

HISTORIC ACTIVITIES ON LONG ISLAND

Like many of the other Harbor Islands and much of the mainland, Long Island was inhabited primarily by farmers and fishermen during the 17th and 18th centuries. However, certain characteristics of the islands set them apart from the mainland and resulted in a number of distinctive uses, most of which are represented on Long Island. The large number of people who lived and worked on Long Islands during some historic periods is especially impressive given the fact that all personnel and supplies had to be brought in by boat, to docks on the northwest side of the island, until the Long Island bridge was built in 1951.

First, the islands were recognized as both landmarks and hazards to navigation, and in 1794 a lighthouse was built on the northeast end of Long Island marking President Roads, the major shipping channel into Boston's Inner Harbor. The lighthouse present today at Long Island Head was built in 1819; it was moved several times when the nearby fort was enlarged, became automatic in 1929, and is inactive today (MAPC, 1972).

The Harbor Islands were also viewed as crucial to the defense of Boston Harbor, and fortifications were begun on Castle Island as early as 1634. Long Island has been used by the military for most of its history. Yankee troops fired cannons at the British fleet from Long Island in 1776, helping to drive the British from Boston. Camp Wrightman, a major conscript camp, was established on Long Island during the Civil War; several companies of heavy artillery and about 1,000 draftees were stationed there. In 1867 the north end of the island was taken by the federal government, renamed Fort Strong, and extensively renovated. Several batteries of six and eight inch guns were emplaced in 1899, and 1,500 men were stationed here during World War I (MAPC, 1972: 49). Although the guns had become obsolete by then, Fort Strong was still used as a mine operations center during World War II. The Fort was declared surplus property in 1946, but many of the buildings and gun batteries are still visible, adjacent to a flat area that was the parade grounds. A Nike missile base, built on Long Island in the 1950s, is the most recent military structure on the island (MAPC, 1972).

During the 19th century the Boston Harbor Islands enjoyed a brief period of popularity for resort hotels and summer homes, until better means of transportation allowed Bostonians to vacation further from the city. In the mid 1800's a large resort hotel, Long Island House, was built on top of the central drumlin. However, "adventurous young men" from the city persisted in staging illegal prize fights on the Island, tarnishing its reputation and contributing eventually to the failure of the resort (Sweetser,1988: 186).

The Boston Harbor Islands have also been perceived as ideal locations for activities that Bostonians wished to keep separate from the rest of society. Thus, the islands have served as sites for prisons, quarantine hospitals, prisoner of war camps, and trash dumps since the 17th century. In 1878 the City of Boston began work on a state-of-the-art sewer system focused on Moon Island but with additional facilities on Long Island, Nut Island, and Deer Island. The remains of four massive granite storage tanks are still visible on Moon Island just before the Long Island bridge. These once served as a reservoir for raw sewage, which was pumped through a brick sewer from Boston. Gates were opened twice daily, and sewage was released into the Harbor on the outgoing tide. The new wastewater treatment plant that will finally bring about the much-discussed clean up of Boston Harbor is also being built primarily on the Harbor Islands.

In 1882 the City of Boston acquired Long Island in order to consolidate several city poor houses there. By 1885, 650 paupers were quartered on the island, and there are estimated to be about 2,000 paupers' graves, some in the known graveyard areas and others unmarked. The poor house later became a home and hospital for unwed mothers, and later still a shelter for homeless men. A dormitory for 300 alcoholics was added in 1940. A chapel, a recreation hall, staff housing, a power plant, and other facilities were added to serve the hospital. This complex became the Long Island Chronic Disease Hospital in 1969, and was used as a homeless shelter during most of the 1980's. Many of the hospital/poor house buildings, which still dominate the center of the Island, are no longer in use, though a few drug rehabilitation programs are still located on the island.

Future plans for Long Island include its incorporation into the Boston Harbor Islands State Park, and recreation will then be the primary activity occurring there.

Although the intensive historic activities described here have undoubtedly destroyed some of the prehistoric archaeological sites that once existed on Long Island, erosion is probably the most important agent of site loss on this as on the other Boston Harbor Islands. Clifford Kaye studied erosion at West Head, on the southwest end of Long Island, and found that the cliff retreated an average of 0.1 m/yr during the period from 1958 to 1962, mostly as a result of direct rain wash and mass movement of saturated surface material produced by the spring thaw (Kaye, 1967). This slope is not exposed to winter storms as are others in the harbor, and erosion is far more severe on the exposed cliffs and beaches.

HISTORIC SEAWALLS

Throughout historic times, considerable efforts have been made to control erosion on the islands, most often with seawalls. Additional seawalls are presently being planned by the City of Boston to stabilize buildings northeast of Bass Point and to stabilize the roadway at West Head, Long Island, and on Moon Island. The earliest seawalls in the Boston region consisted of cobb cribs, consisting of an open wooden framework that could readily be floated into position and sunk with rock from local sources.

Stone seawalls date from the late 1700's in the region. Methods to efficiently cut, or hew, the stone weren't developed until 1803 and weren't widely used until about 1830. Some early stone seawalls used wood platforms as foundations, which sunk in the mud as weight was added. With cut stone, a vertical wall with fewer supports was possible. In the mid 1800's, the importance of the characteristics of the fill material behind the wall in reducing lateral forces and promoting drainage were recognized.

While forms of concrete had been utilized in construction in Roman times, with the fall of Rome this art was diminished until the mid 19th century, following the development of Portland Cement in 1824. This proved to be an immediate cost advantage over timber or stone walls. However, until the 1880's concrete technology had not developed to a level where it consistently provided a durable structure in the marine environment. The harsh environmental conditions in Boston may have resulted in the common practice of constructing a seawall of concrete, and continuing to face the structure in stone. It wasn't until well into the 20th century that concrete was used without stone in seawalls.

The seawall at North Head, Long Island is an example of this transitional design form (Fig. 4). It was constructed in 1870 with a cement foundation and backing, a cut granite facing, and a rip rap toe. It was then backfilled with porous material to promote drainage (Vine and Rosen, 1992).

ACKNOWLEDGMENTS

Both authors thank Ms. Meribah Stanton, past-Director of the Long Island Hospital, for permission to conduct research on Long Island. The archaeological research was supported in part by funding from the University of Massachusetts, Boston. The Long Island Archaeology Field Crew deserves special thanks, as does Shirley Hayden, the graduate assistant for the field school.

ROAD LOG

Assemble at Boston Marriott Copley Place, in downtown Boston.

Mileage

0.0 Road log begins at Exit 12 (Neponset/Quincy) off Rt. 93, the Southeast Expressway. Follow signs for Rt. 3A.
0.7 Cross the Neponset River bridge, bearing left onto Quincy Shore Drive toward Squantum.
1.6 At major traffic light at end of Quincy Shore Drive, turn left onto E. Squantum Street and proceed north, keeping salt marsh and harbor on your left.
3.0 Gate controlling access to Long Island.
3.8 End of causeway and beginning of Moon Island; bear right. You will pass the granite sewage holding tanks and the Boston Police Revolver Firing Range on your left.
5.0 West Head, where erosional studies were conducted by Clifford Kaye.
5.4 Trail leading to Bass Point is on your right; park on trail or off road.

STOP 1. BASS POINT. We will examine Bass Point as a geological feature, and also the Bass Point and the HL-11 sites as examples of archaeological sites which may have had differential uses because of geological processes. We will also examine the till exposed along the beach to the north of Bass Point.

5.7 Civil War memorial and paupers' graveyard. Park off road.

STOP 2. LUNCH.

6.0 Beginning of Long Island Hospital complex. Follow main paved roads, bearing left, until you leave the hospital grounds and drive onto the flat former parade ground.
7.0 Long Island Head. Park off road.

STOP 3. FORT STRONG, LONG ISLAND LIGHTHOUSE, SEAWALL. We will examine the construction technique for the Long Island seawall, which is well exposed at this point, as well as the Lighthouse and the remaining fortifications and buildings of Fort Strong. We will also have excellent views of the other Boston Harbor Islands, including Deer Island and Spectacle Island which are currently undergoing major alterations as a result of the Central Artery and Wastewater Treatment Plant construction projects.

Return to Boston via same route.

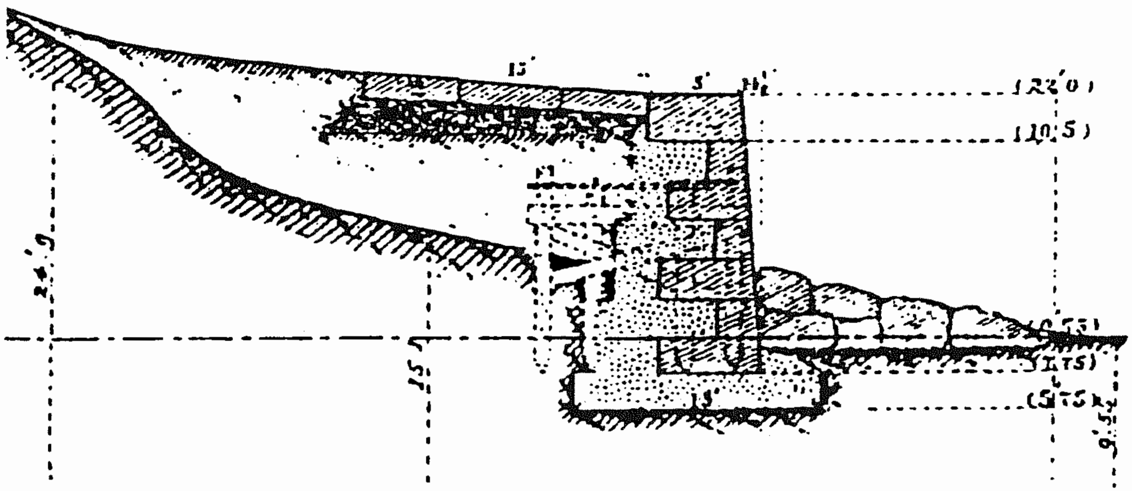

Figure 4. Cross section of the seawall on North Head, Long Island, Boston Harbor constructed in 1870 of concrete with a facing of dressed stone. Stippled pattern depicts cement.

REFERENCES CITED

Braun, D. P., 1974, Explanatory models for the evolution of coastal adaptation in prehistoric eastern New England: American Antiquity, v.39, p.582-596.

Caldwell, D. W., 1984, Surficial geology and archaeology on Thompson Island, Boston Harbor, Massachusetts: p. 402-416 *in* Hanson, L. (ed.), Geology of the Coastal Lowlands, Boston, MA to Kennebunk, ME, New England Intercollegiate Geological Conference, Salem, MA.

Carty, F. M., and Spiess, A. E., 1992, The Neponset Paleoindian site in Massachusetts: Archaeology of Eastern North America, v. 20, p. 19-37.

Johnson, D. W., 1967, The New England-Acadian Shoreline: Reprinted from 1925 edition by Hafner Publishing Company, NY.

Kaye, C. A., 1967, Erosion of a sea cliff, Boston Harbor, Massachusetts: p. 521-528 *in* Farquhar, O. C. (ed.), Economic Geology in Massachusetts, Univ. Mass. Graduate School, Amherst.

Kaye, C. A., 1982, Bedrock and Quaternary geology of the Boston area, Massachusetts: Geological Society of America, Reviews in Engineering Geology, v. 5, p. 25-40.

Kaye, C. A., and Barghoorn, E. S., 1964, Late Quaternary sea-level change and crustal rise at Boston, Massachusetts, with notes on the autocompaction of peat: Geological Society of America, Bulletin, v. 75, p. 63-80.

Knebel, H. J., Rendigs, R. R., and Bothner, M. H., 1991, Modern sedimentary environments in Boston Harbor, Massachusetts: Journal of Sedimentary Petrology, v. 61, N. 5, p. 791-804.

Luedtke, B. E., 1975, Survey of twelve islands in Boston Harbor: Report submitted to Massachusetts Department of Natural Resources (now Department of Environmental Management).

Luedtke, B. E.,1980, The Calf Island site and the late prehistoric period in Boston Harbor: Man in the Northeast, v. 20, p. 25-76.

Luedtke, B. E., 1984, Preliminary report on an archaeological survey of the southern half of Long Island, MA: Report submitted to the Massachusetts Historical Commission.

Luedtke, B. E., 1986, Regional variation in Massachusetts ceramics: North American Archaeologist v. 7, p. 113-135.

Luedtke, B. E., 1987, The Pennsylvania connection: jasper at Massachusetts sites: Bulletin of the Massachusetts Archaeological Society, v. 48, p. 37-47.

Luedtke, B. E., 1990, Report on an archaeological survey of World's End, Massachusetts: Report submitted to The Trustees of Reservations and to the Massachusetts Historical Commission.

Massachusetts Historical Commission (MHC), 1984, Guide to Prehistoric Site Files and Artifact Classification System: Massachusetts Historical Commission, Boston, MA.

Metropolitan Area Planning Council (MAPC), 1972, Boston Harbor Comprehensive Plan: Report prepared for Massachusetts Department of Natural Resources.

Newman, W. A., Berg, R. C., Rosen, P. S., and Glass, H. D., 1990, Pleistocene stratigraphy of the Boston Harbor drumlins, Massachusetts: Quaternary Research, v. 34, p. 148-159.

Peragallo, T. A., 1989, Soil Survey of Norfolk and Suffolk Counties, Massachusetts: U.S. Department of Agriculture, Soil Conservation Service, in cooperation with the Massachusetts Agricultural Experiment Station.

Petersen, J. B., and Hamilton, N. D., 1984, Early Woodland ceramic and perishable fiber industries from the Northeast: a summary and interpretation: Annals of the Carnegie Museum v. 53, p. 413-445.

Rendigs, R. R., and Oldale, R. N., 1990, Maps showing the results of a subbottom acoustic survey of Boston Harbor, Massachusetts: U. S. Geological Survey Miscellaneous Field Studies Map MF-2124, 2 sheets.

Rosen, P. S., 1984, Gravel spit processes, Thompson Island, Boston Harbor, Massachusetts: p. 25-38, *in* Hanson, L. (ed.) Geology of the Coastal Lowlands, Boston, MA to Kennebunk, ME, 76th New England Intercollegiate Geological Conference, Salem, MA.

Rosen, P. S., and Brenninkmeyer, B. M., 1989, Transport of coarse material in low energy beach environments: p. 1724-1737, *in* Magoon, O. T. et al. (eds), Coastal Zone 89; Sixth symposium on coastal and ocean management, v. 2, Amer. Soc. Civil Engineers, NY.

Rosen, P. S., Brenninkmeyer, B. M., and Maybury, L. M., 1993, Holocene evolution of Boston Inner Harbor, Massachusetts: Journal of Coastal Research, v. 9, p. 271-311.

Rosen, P. S., and Leach, Kenneth, 1987, Sediment accumulation forms, Thompson Island, Boston Harbor, Massachusetts: p. 233-259 *in* Fitzgerald, D. M., and Rosen, P. S. (eds.), Glaciated Coasts, Academic Press, San Diego.

Stuiver, Minze, Pearson, G.W., and Tom Braziunas, 1986, Radiocarbon age calibration of marine samples back to 9000 cal yr BP: Radiocarbon, v. 28, p. 980-1021.

Sweetser, M. F., 1988, King's Handbook of Boston Harbor: Reprinted from 1888 edition by Applewood Books, Boston.

Vine, D. B., and Rosen, P. S., 1992, Historic seawalls of the Boston Harbor, Massachusetts region: evolution, construction and repair: p. 849-867 *in* Ports '92, Amer. Soc. Civil Engineers, NY.

Chapter U

Pleistocene Geology of the Boston Basin and Its Adjacent Surroundings

By William A. Newman, David M. Mickelson, Richard C. Berg, Richard D. Rendigs, Robert N. Oldale, and Richard H. Bailey

Field Trip Guidebook for the Northeastern United States: 1993 Boston GSA

Volume 2
Contribution No. 67, Department of Geology and Geography, University of Massachusetts, Amherst, Massachusetts

PLEISTOCENE GEOLOGY OF THE BOSTON BASIN AND ITS ADJACENT SURROUNDINGS

by
William A.Newman, Department of Geology, Northeastern University, Boston, MA 02115
David M. Mickelson, University of Wisconsin-Madison, Madison, WI 53706
Richard C. Berg, Illinois State Geological Survey, Champaign, Ill 61820
Richard D. Rendigs, U. S. Geological Survey, Woods Hole, MA 02543
Robert N. Oldale, U. S. Geological Survey, Woods Hole, MA 02543
Richard H. Bailey, Department of Geology, Northeastern University, Boston, MA 02115

INTRODUCTION

This one day trip consists of 7 stops. Four are on Long Island, one at Squantum head, and two at Fourth Cliff, Scituate about 18 miles southeast of Long Island or 25 miles southeast of Boston. The purpose of this trip is to illustrate glacial and post glacial deposits of Boston Harbor and Fourth Cliff, Scituate and to discuss weathering profiles, drumlin formation, and Boston Harbor stratigraphy. To this end, 3 papers provide further discussion of these topics before the stop descriptions.

STRATIGRAPHY OF THE BOSTON HARBOR DRUMLINS

by
Richard C. Berg

Diamictons, interpreted to be tills, have been characterized through sampling of 15 profiles on eight islands and two peninsulas in Boston Harbor (Newman and others, 1990) (Figure 1). Approximately 500 g of material was collected for each of 237 samples. Texture, structure, color, sedimentary features, degree of compaction, presence of shell fragments and concretions, and degree of leaching and oxidation were noted at sampling stations. The clay-mineral composition for each sample was determined using an oriented aggregate settling technique. Quantification of all clay-mineral data was based on peak heights. Replication of analyses indicated a precision of 1- 2%. Particle-size analyses were performed on 134 samples using the standard hydrometer method (ASTM-422).

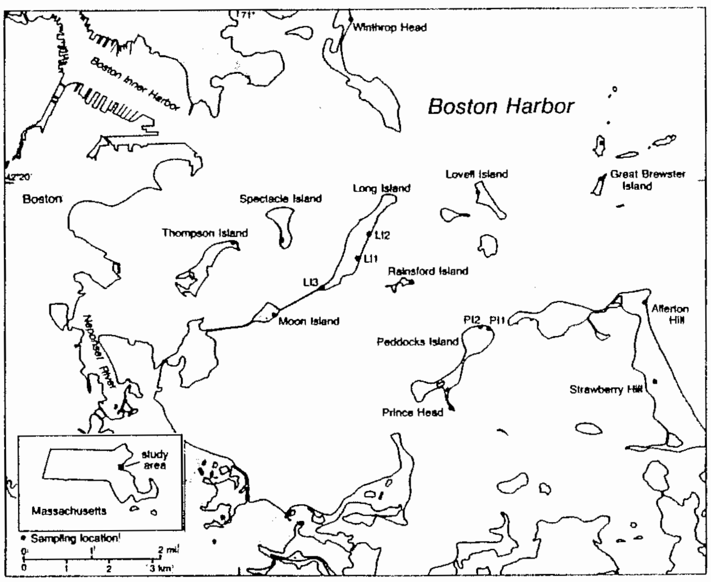

Figure 1. Map of study area showing drumlin sampling locations (from Newman and others, 1990)

In Boston Harbor, the lower till is compact, faintly stratified, and commonly exhibits horizontal fissility. Cobble- to boulder-sized clasts are generally smaller and more striated than those in the upper till. The unweathered lower till is olive gray (5Y 4/2) and contains marine shell fragments. In the weathered lower till, the depth of oxidation may extend below the depth of carbonate leaching (i.e., Long Island-1, -2, -3, Rainsford Island, Peddocks Island-1, -2, and Great Brewster Island) or may approximate the depth of leaching (i.e., Winthrop Head, Allerton Hill, and Strawberry Hill; (Figure 2).

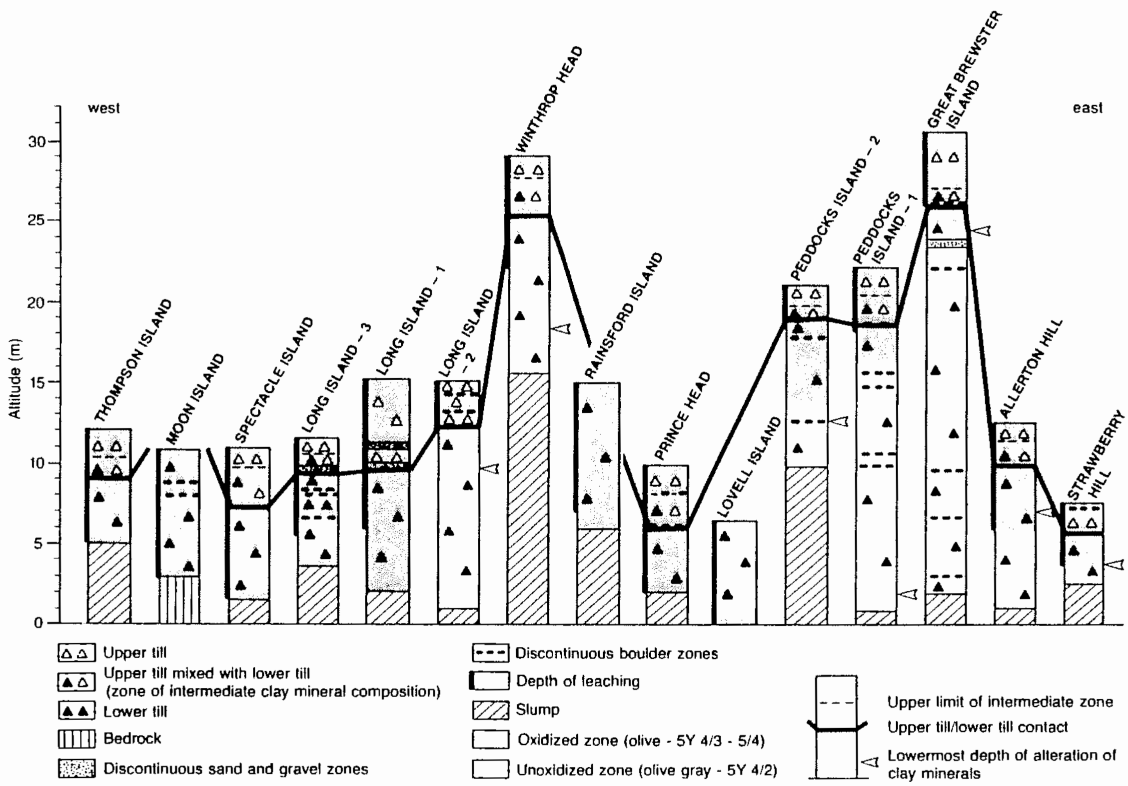

Figure 2. Correlation of stratigraphic sections of Boston Harbor drumlins (from Newman and others, 1990).

The upper till is olive (5Y 4/3-5/4), oxidized, compact, faintly stratified, contains more boulders than the lower till, and marine shell fragments are lacking. The upper and lower tills have about the same texture and lithologic composition. Clay minerals are a more diagnostic criteria for separating the upper from the lower till, and a more distinctive index of weathering than are color changes, presence of shells, or leaching depths. Buried soil profiles within drumlin sections are characterized by a progression of clay-mineral alteration from chlorite to high-charge vermiculite to low-charge vermiculite.

Regional characteristics of tills

The two tills of Boston Harbor are differentiated on the basis of five field and laboratory criteria, (1) standard deviations of particle sizes, (2) unaltered clay minerals, (3) a zone of intermediate clay-mineral composition at the base of the lower till, and (4) occurrence of weathering profiles, and observable stratigraphic breaks.

Table 1 shows that the mean texture of the two tills is a clay loam or loam. Although the upper till is slightly sandier and less clayey than the lower till, the sand and clay percentages exhibit a wider range of textures in the upper till. The silt component of both tills exhibits a relatively large standard deviation.

TABLE 1

Summary means and standard deviation of till textures and unaltered clay mineral components

	Upper Till	Lower Till
Texture samples N=	**20**	**97**
Sand	37.8 ± 9.2	34.8 ± 4.9
Silt	36.2 ± 5.4	37.1 ± 6.0
Clay	26.0 ± 6.1	28.1 ± 3.8
Unaltered clay mineral samples N=	**15**	**54**
Low-charge vermiculite	6 ± 1.3	13 ± 2.9
High-charge vermiculite	13 ± 3.2	11 ± 1.2
Illite	55 ± 2.2	48 ± 2.1
Chlorite	23 ± 1.8	23 ± 2.0
Kaolinite	3 ± 0.7	5 ± 0.7

The average clay-mineral compositions and standard deviations for the unaltered upper and lower tills are also shown in Table 1. Unaltered tills are those at the base of the units; they maintain relatively uniform percentages of clay minerals throughout the profile and lack significant chlorite weathering. The definition of unaltered clay minerals in the upper till is based on the chlorite percentage generally being 20% or more of the clay minerals. Standard deviations for all clay-mineral components of each unaltered till are small because of the uniformity of clay-mineral data for the two tills.

The amount of illite is an effective index that discriminates the two tills. The upper till averages 7% more illite than the lower till; it is best characterized by illite percentages of 55 to 58%, while values of 45 to 51% best characterize the lower till. Another discriminator differentiating the two tills is the quantity of vermiculite. The unweathered lower till always contains more low-charge vermiculite than the upper till. The weathering of chlorite under well-drained, acid, oxidizing conditions, such as exist in the harbor region, results in a predictable suite of clay-mineral alteration products. Deep weathering, represented by chlorite loss and development of low- and high-charge vermiculite, occurs in the uppermost portion of the lower till in Boston Harbor. Chlorite percentages decrease upward in the upper till due to postglacial weathering at the surface. At nine of the fifteen sampling profiles (Figure 2) is a 1- to 2-m-thick zone at the base of the upper till that contains lower chlorite values than those above, and considerably higher chlorite values than the upper portion of the lower till. This zone is believed to contain reworked sediment from the lower till. Profile 3 from Long Island (Figure 5) shows this phenomenon.

Although chlorite loss is evident in both tills, the lower till shows a much greater development of both low-charge and high-charge vermiculite than the upper till. Assuming that weathering intensity was similar for both tills, the loss of chlorite and the development of large amounts of both high-charge and low-charge vermiculite must reflect a longer weathering history for the lower till than the upper till. It is indicative of climatic conditions similar to the present and to those presumed to have persisted during the Sangamonian Interglacial. The depth of the weathering profile, the sequence of clay- mineral alteration products, and the presence of pedogenic features in the upper part of the lower till are comparable to such characteristics of Sangamonian weathering profiles in the midwestern United States (Follmer, 1983).

Long Island Sections

Long Island is composed of eight interconnected east- to southeast-trending drumlins. Two tills are readily discernible on the basis of texture at the southeastern-facing exposure on the southern portion of the island. Figure 3 shows textural and clay mineralogical data along sampled profile 1 (Figure 14, 119 m). The upper till is bouldery and separated from the lower till by a 2-m-thick sand layer interbedded with till. The sandy loam upper till averages 56% sand, while the clay loam lower till averages 35% sand. The upper part of the lower till is oxidized and leached, has stains on ped faces and in joints, and contains argillans (clay skins) and truncated, clay- filled fractures. These features are characteristic of a C horizon, above which the A and B horizons of the soil profile are missing.

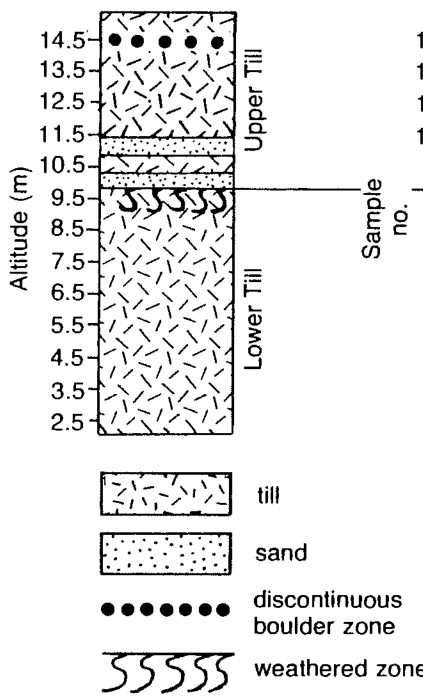

Sample no.	S	Sl	Cl	LCV	HCV	I	C	K
13	53	33	14	6	9	56	25	4
12				7	9	58	23	3
11	67	22	11	7	9	56	25	3
10				9	10	57	22	2
9	48	37	15	8	10	56	24	2
8	26	41	33	13	14	58	11	4
7	30	41	29	15	13	57	11	4
6	39	47	14	18	12	54	13	3
5				19	11	52	14	4
4	37	36	27	17	12	52	15	4
3				17	11	53	15	4
2				17	12	52	15	4
1	41	34	25	15	11	54	16	4

S - sand
Si - silt
Cl - clay
LCV - low charge vermiculite
HCV - high charge vermiculite
IZ - intermediate zone of clay mineral composition
I - illite
C - chlorite
K - kaolinite

Figure 3. Textural and clay mineralogical data from Long Island profile 1 (Newman and others, 1990).

Clay-mineral data (Figure 3) show that chlorite percentages decrease upward in the lower till from 16% at the base of the exposure to 11% just beneath the sand. Maximum weathering of chlorite therefore, occurs just below the contact. Above the sand, chlorite increases abruptly with a concurrent decrease in both high- and low-charge vermiculite.

At the southeastern-facing exposure on the northern portion of the island, the sandy loam upper till of profile 1 grades into a clay loam upper till. Figure 4 shows textural and clay mineralogical data along sampled profile 2 (Figure 1). The textural difference between upper tills at the two locations on the island is therefore lacking. However, profile 2 shows chlorite declining from 22% at the base of the exposure to 11% at an altitude of 12 m (Figure 4). Within the next half meter, a discontinuity in clay mineral composition exists where chlorite increases to 16%, and vermiculite decreases. This upward decrease of chlorite in the lower till, followed by an abrupt increase of chlorite in the upper till, is similar to the trend observed at profile 1 (Figure 3). The upper till at profile 2 however, exhibits lower chlorite percentages than at profile 1 because it is more weathered.

The northwestern-facing exposure at the southern tip of the island, exhibits a sand zone separating the two tills, as in profile 1. Figure 5 shows textural and clay mineralogical data along sampled profile 3 (Figure 1). The sand is a 40-cm-thick layer, the base of which lies 9.7 m above sea level. The texture of the upper till at profile 3 is loam to clay loam, similar to the upper till at profile 2.

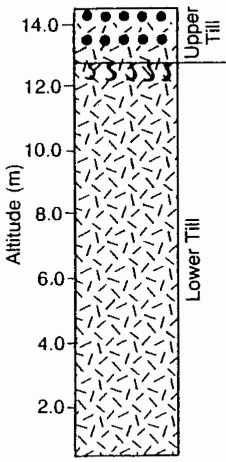

Sample no.	S	SI	Cl	LCV	HCV	I	C	K
14	34	39	27	5	13	60	18	4
13	33	35	32	8	11	61	16	4
12	35	36	29	14	13	59	11	3
11	34	34	32	14	11	54	17	4
10	29	40	31	15	10	53	18	4
9	33	36	31	14	10	51	20	5
8				14	10	50	22	4
7				14	11	50	21	4
6				14	10	53	19	4
5	32	36	32	14	10	51	19	6
4				14	10	52	19	5
3				14	10	52	19	5
2				13	10	51	21	5
1	34	32	34	10	9	54	22	5

Figure 4. Textural and clay mineralogical data for Long Island profile 2 (from Newman and others, 1990).

Chlorite values decrease from 14% at the base of the exposure to 9% at the till/sand contact. Maximum weathering of chlorite therefore, occurs just below the sand. The lack of high chlorite percentages at the base of the lower till is because unaltered lower till is not present. Above the sand contact clay, mineral data show higher chlorite and lower low-charge vermiculite percentages than below the contact. A zone which contains an intermediate percentage of chlorite (16%) occurs at the base of the upper till (sample 13 in Figure 5); the sample above (sample 14), in the upper till, contains 22% chlorite. This intermediate zone is believed to reflect the incorporation of eroded lower till into the upper till.

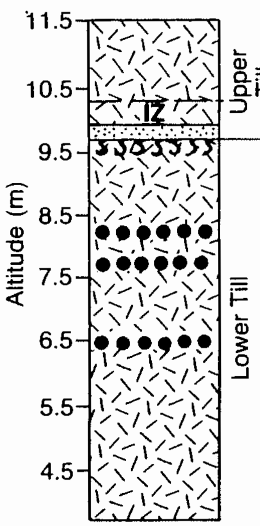

Sample no.	S	SI	Cl	LCV	HCV	I	C	K
14	40	33	27	4	16	54	22	4
13	40	30	30	11	15	53	16	5
12	36	33	31	16	15	55	9	5
11	42	30	28	20	13	54	9	4
10				21	12	54	9	4
9				23	12	53	8	4
8				22	11	55	8	4
7	47	26	27	22	10	55	10	3
6				20	10	54	12	4
5	42	29	29	16	9	60	12	3
4				23	12	52	11	3
3				16	11	55	14	4
2	46	34	20	22	10	51	13	4
1				20	11	52	14	3

Figure 5. Textural and clay mineralogical data for Long Island profile 3 (from Newman and others, 1990)

Summary

The Long Island sections display a consistent stratigraphic succession applicable to the entire study area. Long Island profile 1 shows two texturally distinct tills (upper is sandy loam, lower is clay loam) separated by a sand layer. Long Island profile 3 shows two tills separated by a sand layer; however, the tills are texturally similar (both are loam/clay loam). Long Island profile 2 shows neither a textural distinction between the tills (both are clay loam) nor a sand layer separating the two tills. Common to all profiles, however, are truncated soil profiles in the upper part of the lower till overlain by the upper till. The same diagnostic clay-mineral discontinuity defining the upper and lower till contact at profiles 1 and 3 exists at profile 2. Distinct differences in clay-mineral assemblages and weathering profiles observed at Long Island exist throughout the study area.

ORIGIN OF DRUMLINS IN THE BOSTON BASIN

by
David M. Mickelson

Introduction

About 200 drumlins are present in the Boston Basin and along the south shore of Massachusetts. They form a prominent part of the landscape and have figured in historic events and determined development patterns for over 200 years. Because of extensive urbanization, access to most of the drumlins is impossible. Wave erosion around the islands of Boston Harbor and along the shore south of Massachusetts to Plymouth provide excellent exposures of the internal composition of some of these drumlins.

Other papers in this guidebook focus on stratigraphy in the drumlins and more generally in Boston Harbor (Figure 1). This paper focuses on issues of drumlin genesis and, in particular, the conclusions that can be drawn from drumlin exposures in eastern Massachusetts (Figure 6). In parts of the basin drumlins form irregular, more-or-less coalescing groups. In other areas they form eneschelon clusters 2 to 3 kilometers long and elsewhere are scattered as single drumlins. Probably some are rock cored, although the majority of those exposed contain cores of till or sand and gravel. The average trend of the drumlins is about 100° (Crosby, I.B., 1934) and vary to about 30° either side of the mean. A longer paper on the drumlins in Boston Harbor is in preparation (Newman and Mickelson, in prep.).

Origin of Drumlins

The genesis of drumlins has been discussed in hundreds of papers published during the last 100 years, and these are not reviewed here. The early literature is referenced by Menzies (1984), a few more recent papers are referenced here.

Probably the reason that drumlin genesis is still a puzzle is that unlike many landforms their formation cannot be documented beneath modern glaciers. Although there are examples of linear forms being recognized beneath the Antarctic ice sheet using geophysical techniques, the ice is thick and the scale of the features is not clear. Thus, the origin of drumlins must be deduced from observations of drumlins that have already formed. Because drumlins contain fluvial sediment, lacustrine sediment, till and other diamictons, and bedrock, arguments for genesis that are based on the genesis of sediment within the drumlin form result in a broad diversity of opinions on their formation (Table 2).

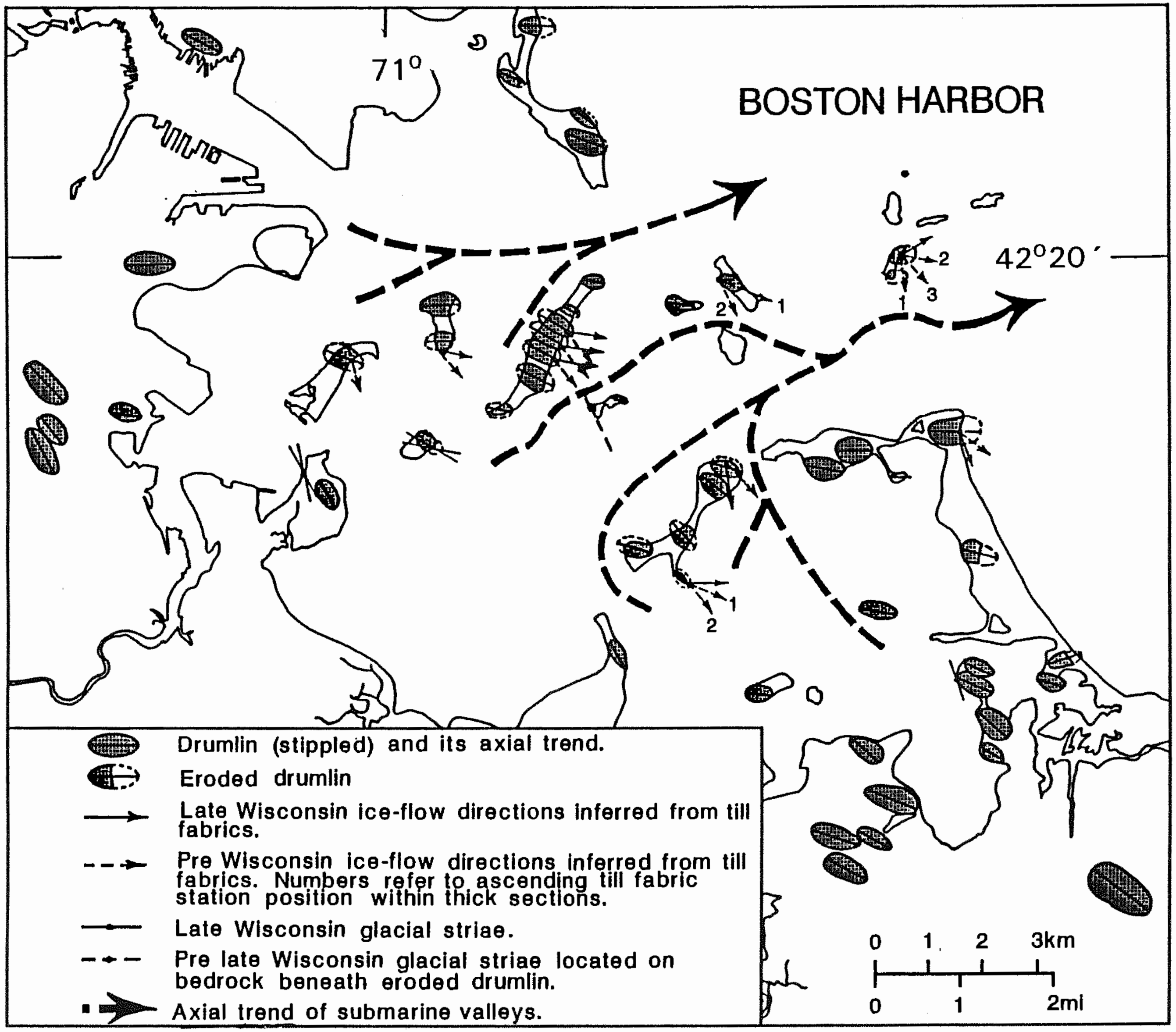

Figure 6. Trends of Boston Harbor Drumlins, till fabric and bedrock striations (from Newman and Mickelson, in review).

TABLE 2. OUTLINE OF PROCESSES OF DRUMLIN FORMATION PROPOSED IN THE LITERATURE

	Process and Materials		Product
Fluvial	Deposited in bedforms	Deposition of sand and gravel	Fluvial sediment in bedforms
	Cavities produced by water, then filled	Deposition of sand and gravel	Fluvial sediment conformable with cavity shape
	Shaping of pre-existing material	Erosion of sediment	Fluvial sediment or lag over pre-existing material
Glacial	Deposited in streamlined form	Deposition of basal debris rich ice (meltout, lodgement)	Basal till
		Deposition of wet deforming bed	Flow till
		Dropped into cavity	Flow and deformation structures in flowed diamicton
	Eroded into streamlined form	Relegation of basal debris rich ice	Basal till over preexisting material
		Rapid deformation of wet sediment	Flow till over preexisting materials

Most glacial geologists have argued that drumlins are formed by a flow of ice across the landscape although recently Shaw (for instance Shaw and others, 1989) has argued that drumlins are subglacial fluvial forms. For those composed of fluvial sediment he argues that the deposition of sand and gravel took place as bedforms in water flowing beneath the ice. For drumlins composed of diamicton he suggests that cavities beneath the ice are formed by flowing water and that diamicton was squeezed or otherwise transported into a cavity produced by flowing water.

Another body of papers suggests that drumlins are the product of direct glacial action although probably in the presence of water along a sliding bed or in a deforming layer. One end member of these glacial processes is the accumulation of sediment in the streamlined form. These sediments might be basal till deposited by some process of meltout or lodgement, flowed or otherwise modified diamictons deposited in a cavity, or flow till deposited by a wet subglacial deforming bed (Table 2). The other end member suggests that the streamlined form of drumlins is a result of erosion at the bed of the glacier. This erosion could be by freezing-on locally or by mobilization of sediment in a subglacial wet deforming bed. In either case, the streamlining is caused by erosion, and till or other sediment are deposited on the form later.

Drumlins that are composed primarily of diamicton or sand and gravel, some of which clearly predates the last glaciation, must have formed by this later process. Upham (1893a, b; 1894) described numerous sand and gravel cored drumlins in this area. He argued (1894) that drumlins here and in the vicinity of Madison, Wisconsin were both formed by the same process. He suggested that erosion of preexisting sand and gravel produced the drumlin shape and that this shaping was followed by deposition of till over a streamlined surface. Based on our observations in this area we arrive at basically the same conclusion.

Evidence for erosional drumlins

In this context, "erosional drumlins" is used to describe those whose streamlining was produced by erosion as opposed to accumulation of diamicton at the base of the ice. In most cases deposition also contributes to the present landform because basal till, small amounts of sand and gravel, and supraglacial diamicton were deposited over the streamlined erosional surface. Nonetheless, these drumlins are considered erosional because the erosion process was primarily responsible for producing the streamlined shape.

Newman and others (1990; Berg, this volume) document the presence of two diamicton units that they interpret as mostly basal till. They argue that because of the amount of weathering on the lower till it must be pre-Sangamonian age. They also recognize a younger, sandy, friable till that overlies the lower till and is sometimes separated from it by sand and gravel. The distribution of these units within the drumlins provides evidence of their erosional nature.

Figure 7 shows a cross section on the stoss (northwest) side of the drumlins on Long Island. Here the upper diamicton is fairly thin (3-4m) and overlies the older diamicton, which contains carbonate shells up to the contact. These shells indicate that the leached section of the weathering profile was removed by the ice that deposited the upper younger, sandy diamicton. Figure 8 shows the section on the distal side (southeast) of these drumlins and indicates that the weathering profile is thicker (though not complete) on the drumlin crests than in the interdrumlin areas. This indicates that the weathering profile has been preferentially eroded in the area between the drumlins. A detailed description of the Long Island site is given in the stop descriptions by Newman and Mickelson (this volume).

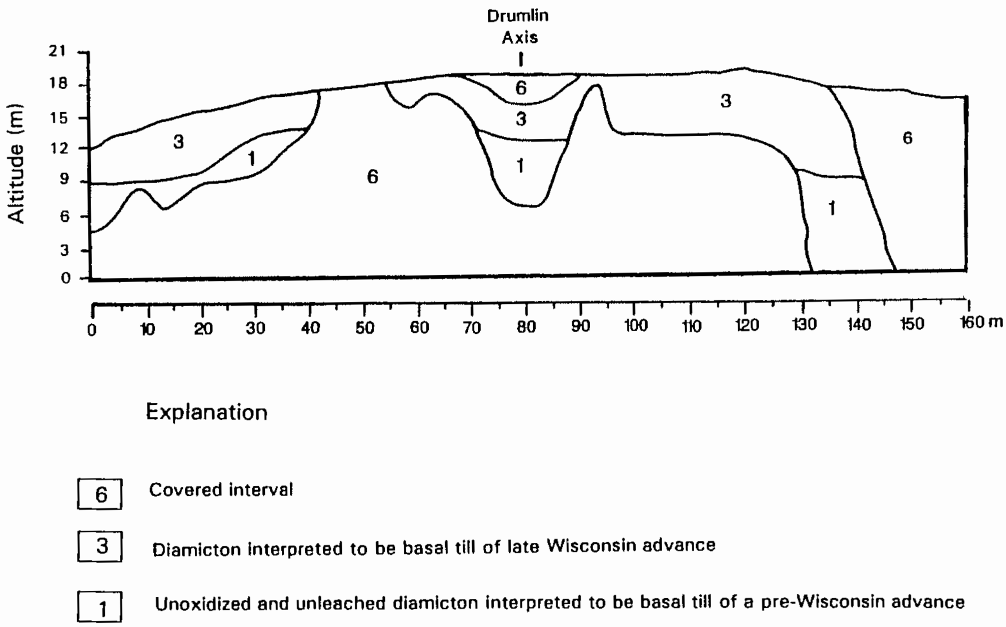

Figure 7. Stratigraphic section along the northwestern (stoss) side of the Long Island drumlin complex. Drumlin axis indicated is the same drumlin as one at 325 m on Figure 8. The same unit labels are used here as in Figure 8, although some of the units are not exposed in this section.

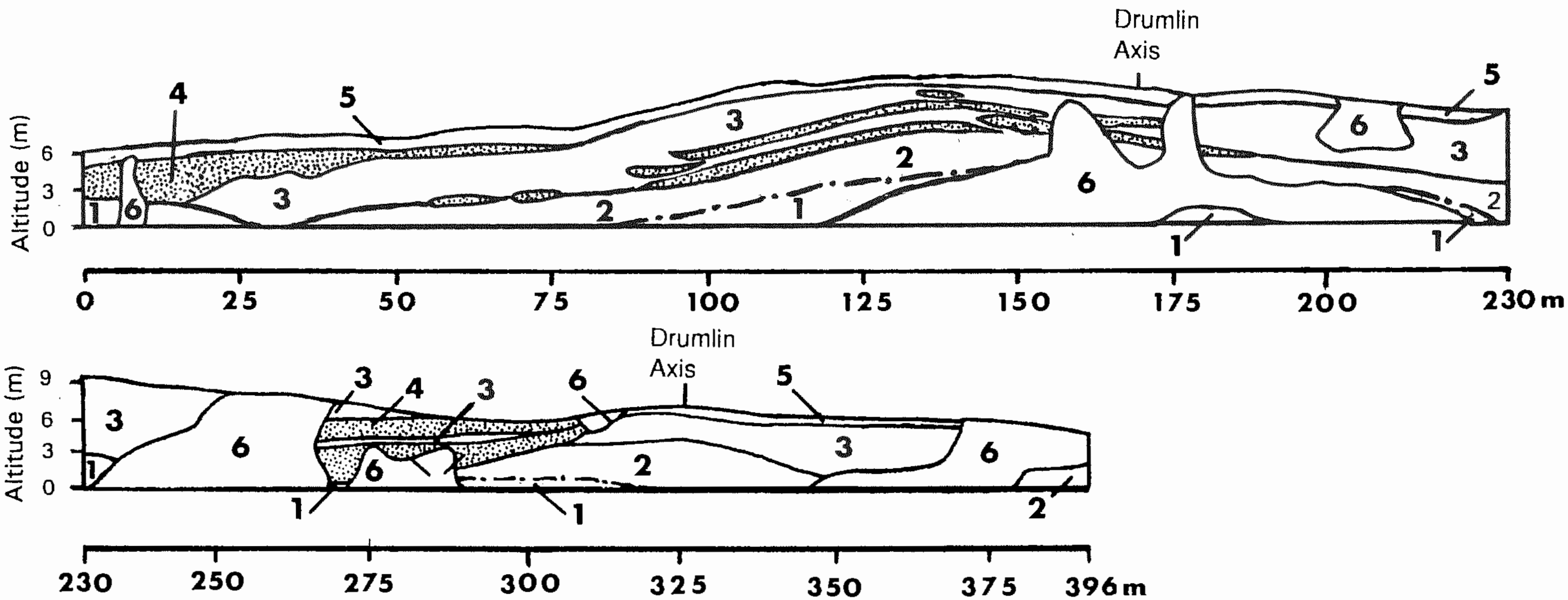

Explanation

- 6 — Covered interval
- 5 — Diamicton interpreted to be supraglacial till, flow and slopewash sediment
- 4 — Interbedded medium sand, coarse sand and sandy gravel
- 3 — Diamicton interpreted to be basal till of late Wisconsin advance
- 2 — Oxidized and leached diamicton interpreted to be basal till of pre-Wisconsin advance
- 1 — Unoxidized and unleached diamicton interpreted to be basal till of a pre-Wisconsin advance
- —•— Indistinct contact between weathered and unweathered diamicton

Figure 8. Stratigraphic section along the southeastern (lee) side of the Long Island drumlin complex.

Other islands examined in the harbor show exposures of either the upper diamicton, the lower diamicton, or both, sometimes with intervening stratified sediment. On Moon and Rainsford Islands (Figures 1 and 2) the crest of the drumlin has no cap of upper diamicton. At Moon Island the lower part of the section is covered with slumped material, but 6-8 m of older diamicton above the slumped sediment appears to be leached of carbonate. The Rainsford Island (Figures 1 and 2) section is more or less parallel to the drumlin axis and consists entirely of older diamicton based on its degree of consolidation and analysis of samples by Newman and others (1990). The older, lower part of the section contains shells. Both of these sites suggest that the depth of leaching was over 8 m in the older diamicton before the younger ice advance removed part of the weathering profile at many locations. Clearly some sediment was eroded even where the weathering profile is thick because an actual soil profile is not present even though the sediments are oxidized and carbonate has been leached.

Peddocks Island (Figure 1) has an exposure nearly 1 km long parallel to, and oblique to, the ice flow direction. The stratigraphy here is complex, with many sand lenses and boulder zones. Newman and others (1990) show a mixed zone between what they interpret as upper till and lower till. Carbonate is unleached in the section, suggesting that as much as 8 m of sediment was eroded by the last ice advance. Another exposure parallel to the drumlin axis is at Prince Head (Figures 1 and 2). In this 10 m high eroded face both diamictons are present and the lower diamicton is leached to the beach level.

Other drumlins in the Boston area, particularly those on the south shore, are cored with sand and gravel. Although many are not well exposed we have done detailed description of Fourth Cliff, a well-exposed wave-cut drumlin at Scituate, approximately 25 miles SE of Boston. This section is described in detail in the stop descriptions (Newman and Mickelson, this volume). The core of the drumlin is composed of extensively faulted and folded pre-Wisconsin diamicton and overlying sand and gravel. Blanketing this lower diamicton and faulted gravel is interbedded late Wisconsin diamicton and sand and gravel. We interpret the diamicton as basal till and suggest that the lower sand is either proglacial or subglacial.

Discussion

Although the drumlins described above contain a variety of sediment types, there is one unifying theme to their composition. All are composed of deposits from two different glacial events. All show evidence that streamlining took place on sediments of the earlier glacial event or by streamlining of proglacial fluvial sediment deposited with the advance of the ice that carved the drumlins. Thus, one might argue that instead of the genesis of the sediment within the drumlin core, what is important in interpreting the genesis of the drumlins is the streamlining process and cross-cutting relationships of late Wisconsin and pre-late Wisconsin deposits.

In all of the cases we have observed the older deposits appear to be streamlined by an erosional process that truncates bedding and weathering profiles. Shaping of the drumlins takes place before the deposition of the final late Wisconsin basal till. Thus, we argue that a process of erosion is fundamentally responsible for the streamlining of the drumlin form, and that late Wisconsin deposits have been draped over this streamlined landscape.

THE QUATERNARY STRATIGRAPHY OF BOSTON HARBOR

by
Richard R. Rendigs and Robert N. Oldale

Introduction

Boston Harbor is a glacially carved estuary located along the eastern coast of Massachusetts. The harbor and its associated islands lie within a triangular shaped lowland known as the Boston basin. The complex Quaternary history of the basin consists of multiple glaciations, a relatively high sea-level stand, marine regression as a result of isostatic rebound, and subsequent coastal submergence caused by the eustatic rise in sea level. The strata within the harbor record these geologic events that can be reconstructed from subbottom acoustic profiles and from sediment samples from cores. Approximately 130 km^2 of high-resolution, seismic-reflection and side- scan sonar profiles along with 12 vibracores were collected to reconstruct the shallow sedimentary framework of Boston Harbor (Figure 9).

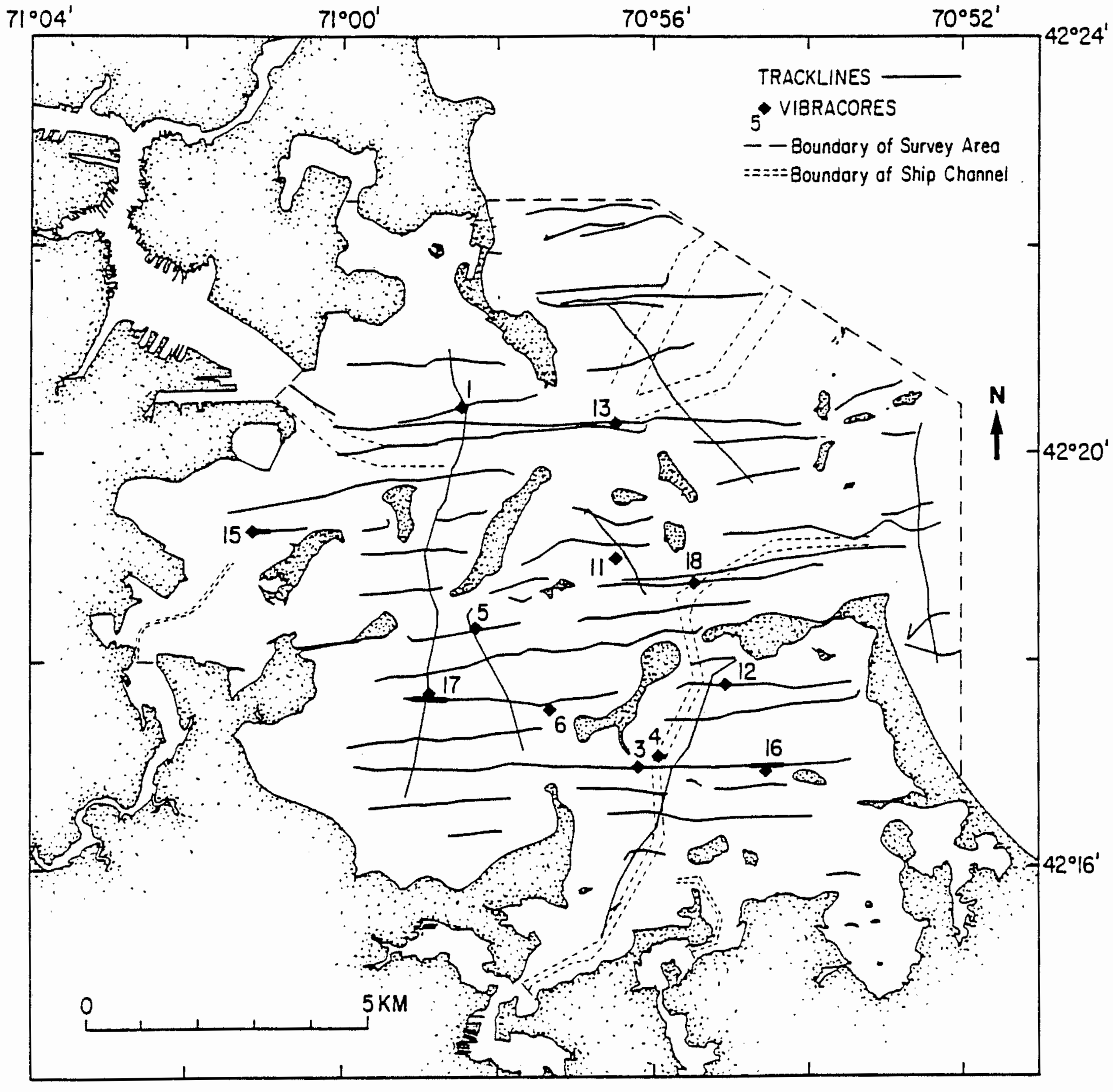

Figure 9. Tracklines and vibracore locations from a high-resolution seismic-reflection survey in Boston Harbor.

Geologic Setting

Boston Harbor lies within a fault-bounded structural basin known as the Boston basin. Basement rocks within the basin consist of a complex suite of granites and volcanic and sedimentary rocks thought to range in age from Middle Proterozoic to Middle Paleozoic age.

Glacial deposits within the basin record two major ice advances. The oldest advance most likely occurred during marine oxygen isotope stage 6 (Illinoian). The younger glacial sediment consists of terrestrial and marine deposits of Wisconsinan age.

Postglacial events in Boston Harbor include a rapid marine regression due to isostatic rebound (Oldale and others, in press) and a marine transgression that reworked glacial deposits and transported this material into the harbor. Many of the barrier islands, spits, along with the north tip of Cape Cod were formed as result of littoral drift. Estuarine mud is currently being deposited within sheltered areas of the harbor.

Sedimentary units and geologic history

The interpretative sections of the seismic-reflection profiles from sites 15, 16, and 17 and a description of geologic units from the Boston Harbor survey are shown in Figures 10a and 10b, respectively. The stratigraphically lowest reflector in the subbottom profiles is inferred to be underlain by either Proterozoic or Paleozoic age bedrock (Pz) or pre-Wisconsinan till (Qt), both of which can be correlated with outcrops on the seafloor and to exposures on the harbor islands and along the mainland shore (LaForge, 1932; Phipps, 1964; Kaye, 1978; Rendigs and Oldale, 1990; Knebel and others, 1992). Additional correlations of the material beneath the basal reflector is also provided by drilling logs (Metcalf and Eddy, Inc., 1989) and seismic-refraction data (Weston Geophysical Engineers, Inc., 1969; Weston Geophysical Corporation, 1989).

The next stratigraphically identifiable reflector is thought to be underlain by deposits representing the New England lower till (unit Qt) of pre- Wisconsinan age (Oldale and Colman, 1992). Analysis of weathering profiles and clay mineral alteration products of the lower till exposed in the Boston basin drumlins (Newman and others, 1990) suggest an Illinoian age (oxygen isotope stage 6) for this deposit.

The bedrock and lower till are overlain by a discontinuous seismic unit (Qdr) inferred to be glacial drift of late Wisconsinan age. Cores show the unit to be composed of ice proximal sand and gravel and till deposited in a submarine environment (Rendigs and Oldale, 1990).

The next seismic unit, (Qm) is characterized by rhythmically banded and draped reflectors that represent laminated glaciomarine deposits of clayey silt. The source of this glaciomarine mud, locally known as Boston blue clay, is thought to have been rock flour laden meltwaters discharged through englacial and subglacial tunnels from the retreating glacier (Oldale and others, 1990). Deposition of the mud was rapid (6 meters/1000 years) in Stillwagen basin just to the east of Boston Harbor (Tucholke and Hollister, 1973). On land, glaciomarine mud deposits as thick as 60 meters have been found near Beacon Hill and thicknesses as great as 75 meters underlie areas of the Charles River (Kaye, 1961; 1982). Deposits of glaciomarine mud as much as 25 meters thick are found within depressions in the bedrock surface or the lower till within the harbor (Rendigs and Oldale, 1990). Radiocarbon ages on barnacles in the Boston basin (Kaye and Barghoorn, 1964), and on foraminifera from Wilkinson basin in the western Gulf of Maine (Schnitker, 1988), indicates the glaciomarine mud was deposited between about 18 and 15 ka. As the glacier retreated north of Boston, concurrent marine submergence of the coastal area reached a maximum of about 18 meters above present levels (Kaye and Barghoorn, 1964).

Coastal emergence resulted from postglacial rebound during the late Wisconsinan and early Holocene (Oldale and others, in press). An unconformity represented by a discontinuous seismic reflector (ru) is located atop glacial deposits. The unconformity was cut when the glacial deposits were subaerially exposed and incised by streams. Heterogeneous deposits of fluvial gravel, sand, and mud (unit QF) were laid down within stream beds.

A rapid rise in sea level during the late Wisconsinan and Holocene (Oldale and others, in press) planed and truncated the glacial and post-glacial deposits and produced a transgressive unconformity (seismic reflector tu) atop these deposits. Fine-grained sediments were winnowed from coarser deposits by wave erosion and deposited discontinuously throughout the harbor (seismic unit Qpm).

As water depths increased across the area during the late Holocene, shallow water deposits of sandy mud (seismic unit Qb) which were derived primarily from wave erosion of the harbor islands and the mainland shore, were locally deposited within harbor channels and adjacent to inner harbor shorelines and islands.

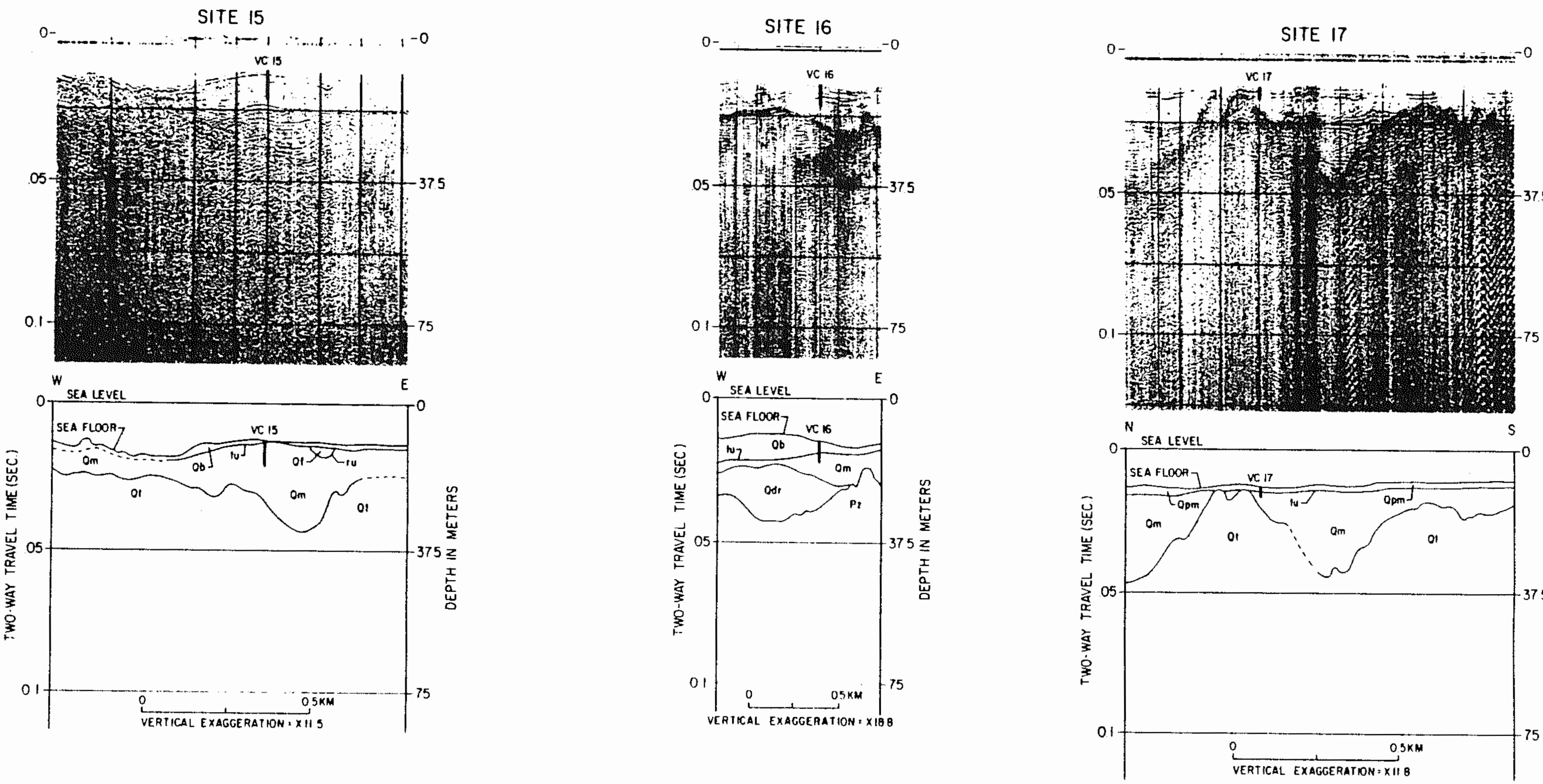

Figure 10a. Seismic profiles and matching interpretative line drawings of selected vibracord sites 15, 16, and 17 within Boston Harbor

Correlation of Geologic Units

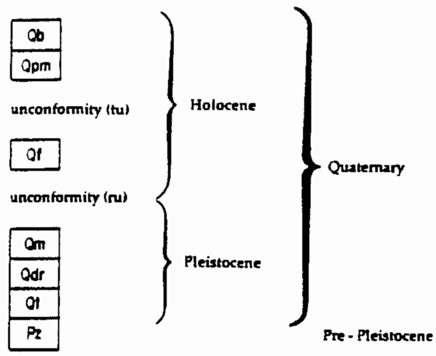

Description of Geologic Units

Qb Shallow Water Marine Deposits (Holocene) - A medium to fine - grained sandy mud; includes some gravel and shell hash and discontinuous layers of amorphous organic matter. Discontinuously overlies the transgressive unconformity (tu). Overlain in places by a veneer of modern estuarine deposits.

Qpm Deep Water Marine Deposits (Holocene) - A clayey - silt deposited in bathymetric lows derived from wave generated erosion of drift deposits. Primarily, horizontally bedded and less cohesive than the underlying glacial-marine deposits. Occurs discontinuously throughout the harbor.

Qf Fluvial Deposits (Holocene) - Mostly sand; may include some gravel, silt, and clay. Overlies the regressive unconformity (ru). Considered to be the subaerial stream / estuarine deposits formed during the late Wisconsinan to early Holocene lowstand of sea level.

Qm Glacial - Marine Deposits (Pleistocene) - Mostly rythmically bedded silts and clays with minor amounts of interbedded silty sands. Upper part oxidized where exposed during the lowstand of sea level. The unit was deposited by glacial meltwater laden with rockflour during the late Wisconsinan.

Qdr Submarine Glacial Drift (Pleistocene) - Ice contact and outwash deposits of sand, gravel, and till of Wisconsinan age. A thin and discontinuous unit that occurs below the glacial marine deposits (Qm). Unconformably overlies bedrock, coastal plain deposits, or older till deposits (Qt).

Qt Older Drift Deposits (Pleistocene) - The pre - Wisconsinan "drumlin till" of Boston Harbor. Forms the acoustic basement in most places. Overlain by outwash (Qdr), glacial marine deposits (Qm), or postglacial deposits. The till is oxidized up to a depth of 10 m. Outcrops discontinuously along the sea floor and unconformably overlies bedrock.

Pz Bedrock (Pre - Pleistocene) - Igneous, sedimentary, and volcanic rock. Locally outcrops on the harbor sea floor, islands, or adjacent shoreline.

Contact - Dashed where inferred or approximately located.

tu Transgressive unconformity

ru Regressive unconformity

Figure 10b. Description and correlation of geologic units inferred from seismic records and vibracores from Boston Harbor

Present day estuarine silt and amorphous organic material are found in subtidal flats and back-water sheltered areas where tidal currents are weak. These youngest sediments contain pollutants associated with hundreds of years of unabated disposal of sewage and industrial wastes into the harbor.

DROPSTONES (?) AND THE ORIGIN OF THE SQUANTUM "TILLITE"

by
Richard H. Bailey

One of the oldest controversies in Boston area geology is the supposed glacial origin of diamictites within the Late Proterozoic Boston Bay Group. More information about the Boston Bay Group, the Squantum Member of the Roxbury Formation, and the geology of Squaw Rock Park is given in Hepburn and others (1993) in this guidebook and in Bailey (1987).

In the earliest comprehensive study of the Squantum diamictites, R. W. Sayles (1914) evaluated several possible modes of origin. He favored glaciation as the best explanation for the poorly sorted matrix supported conglomerates, rare striated blunt-ended clasts, and boulders apparently isolated in slate. All of the above and subsequently published evidence for glaciation has been contested, and/or evaluated as supporting other depositional mechanisms. Pettijohn (1975, and older editions) and Dott (1961) reinterpreted the Squantum and associated strata as a sequence of non-glacial subaqueous mass flow deposits. More recently, Socci and Smith (1990) and Smith and Socci (1990) developed basin models for the Boston Bay Group involving glacial transport into a marine basin (by floating ice). They identified many supposed dropstones and stated that dropstones were present in all fine grained facies (Smith and Socci, 1990; p. 80; Socci and Smith, 1990; P. 63).

A clast dropped by floating ice onto a cohesive muddy bottom will bend, penetrate, or otherwise disrupt the primary stratification under the clast (Thomas and Connell, 1985). The clast may come to rest with the a/b plane at a high angle to bedding. If the clast falls on a firm bottom or is subjected to subsequent currents the a/b plane will frequently parallel or lie at a low angle to bedding. Clasts that have the above features occur in transitional strata below and above Squantum diamictites and they are found at a few localities in other Roxbury beds. The interpretation of an outsized or oversized clast or lonestone as a true dropstone requires careful consideration of the following relationships.

1. Dropstones are independent of facies because drifting ice may release clasts above any environment in the sedimentary basin. Material dropped from floating ice should be broadly distributed across facies, given certain limitations on hydrography, winds, and currents.

2. Dropstones are "exotic" with respect to bedding units that contain them. A convincing dropstone is a large outsized clast in a thinly bedded mudstone. An outsized clast is one whose diameter is greater than the precompaction thickness of the enclosing strata. Other geometrical considerations include clast orientation, evidence of penetration and rucking, clast size to bed thickness correlation, and the relationship of clasts to bed, scour, or bedding amalgamation surfaces.

3. Dropstones present a paradox of transport energy that must be considered in sedimentologic context. If bedding features and primary sedimentary structures indicate availability of energy and/or depositional mechanisms sufficient to move clasts laterally then an interpretation of vertical fall is seriously weakened.

I recognize 6 different types of outsized or oversized lonestones in strata of the Boston Bay Group. Four of these distinctive types are illustrated below (Figure 11) and may be seen on this trip. Based on clast/bedding relationships only rare Type 1 clasts closely resemble true dropstones (see 2 above). Despite their geometrical similarity to dropstones, I do not consider these clast to be convincing evidence of ice rafting because they are not truly isolated from coarse clastic facies, and their sedimentological context suggests possible emplacement by rolling, sliding, or transport in various sorts of sediment gravity flows. Other types of lonestones have also been identified as dropstones, but most fail to meet one or more of the criteria above. I find little evidence for widespread involvement of ice in the deposition of the Boston Bay Group. It is particularly difficult to reconcile the glaciomarine depositional models of Socci and Smith (1990) and Smith and Socci (1990) (where ice sheets and bergs drift into the basin) with the lack of isolated outsized clasts in the medial to distal facies of the Cambridge Formation and in most other fine grained facies of the Roxbury Formation. Definitive evidence for Proterozoic glaciation during deposition of the Boston Bay Group has Yet to be presented.

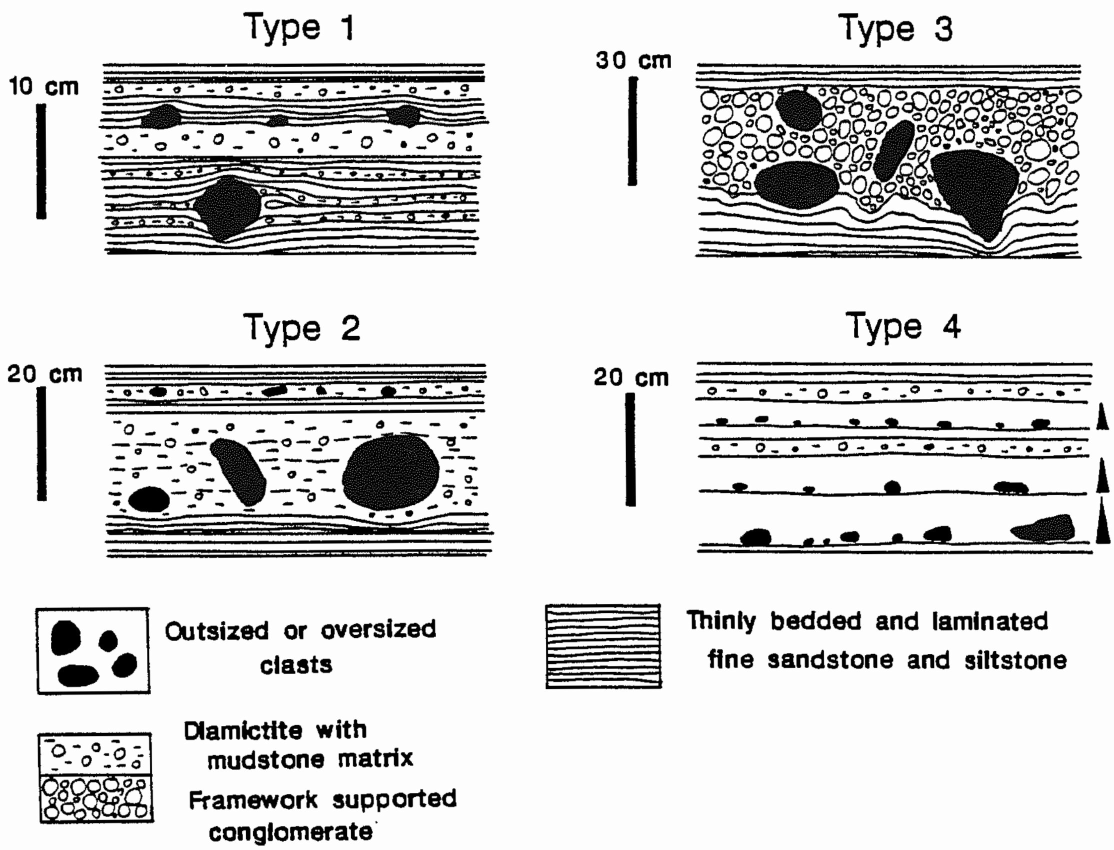

Figure 11. Four types of outsized or oversized lonestones in strata at Squaw Rock Park, Quincy, MA. Lonestones are shown in black.

ACKNOWLEDGEMENTS

We thank Alan Saiz for producing the computer graphics used in the figures.

FIELD TRIP ITINERARY

STOPS 1- 4. LONG ISLAND DRUMLIN COMPLEX (Long Island, Boston, MA; Leaders: W. A. Newman and D. M. Mickelson). We describe 3 sections on the southeast side of Long Island and one on the northwest. The purpose of the stops is to:

1) Illustrate the major stratigraphic units in the Boston Harbor area.
2) Illustrate two of the sites where clay mineralogy and texture of closely spaced samples supports field interpretations of a weathering profile on the lower diamicton.
3) Discuss the age and origin of diamicton units exposed in the bluffs.
4) Illustrate the relationship of sediments exposed in the bluff to drumlin topography on the land surface.

Figures 7 and 8 illustrate the distribution of sediments in section along the two sides of the island where sections will be examined.

The field trip begins at the Watertower parking lot of the Long Island Hospital, Boston, Massachusetts. Access to the Long Island drumlin exposures via the Long Island Bridge is granted seven to ten days after filing a written request to the Assistant Director of Operations, Long Island Hospital, Boston, Massachusetts.

From the parking lot walk eastward past a small gatehouse and toward the large smokestack in the distance. As you approach the building, follow the driveway to the bluff top and continue south along the bluff top to where you can access the beach. PLEASE EXERCISE EXTREME CAUTION ON YOUR DESCENT TO THE BEACH. THE SLOPE IS EXTREMELY DANGEROUS WHEN WET!!! When you reach the beach walk southward approximately 350 meters to Stop 1.

STOP 1 (Figure 8, 119 meters). The section (Figure 3) here is the most complete on the island. It is typical of many of the Pleistocene stratigraphic sections of Boston Harbor. The lower 7 m of the exposure consists of a very dense, compact, brown, oxidized, silty sand diamicton. The upper part of the diamicton is oxidized and leached, has stains on ped faces and in joints, and contains argillans (clay skins) and clay filled fractures. These features are characteristic of a C-horizion, above which the solum (the A and B horizons of the soil profile) is missing. The presence of pedogenic and weathering features just below the contact between the upper and lower diamictons indicates that this weathering profile is not an extension of the modern one from above, but the truncated portion of a weathering profile that developed on the land surface before the last glaciation formed the drumlin now at the surface. Marine shells and shell hash are present in the lower less oxidized, unleached, 3 m of the section.

Uncomformably overlying this is 1 to 2 m of sand and interbedded diamicton. The sharp contact between this unit and the lower diamicton at this location is marked by a line of vegetation rooted in the sand layer. This sand unit, interbedded with layers of pebbly gravel, stony till like diamicton and entrained lower till blocks contains small scale thrusts and folds.

The upper 5 m of the section is loose, friable, brown sandy oxidized diamicton containing abundant cobbles and boulders. Extending across the section approximately 1 m below the crest is a line of boulders. The upper 0.25 to 1 m of the section consists of postglacial soil development in eolian sand and silt, colluvium, and diamicton.

Here, on the lee side of the drumlin a weathering profile is preserved on top of the lower diamicton. The thickness of this weathering profile varies across the section and is thickest beneath the drumlin axes (Figure 8, 170 m) The significance of the buried weathering profile, and in particular the depth of carbonate leaching, is that it can be traced laterally in a section and is clearly thicker in the lower diamicton unit beneath the drumlin axes than in interdrumlin troughs (Figure 8, 270 m). In the low area to the south of the main drumlin on Long Island (Figure 8, 24 m) the thickness of the lower till unit that is leached is only about 0.3 m. Note that in the interdrumlin areas the top of the lower diamicton drops to beach level. (Figure 8, 30m and 270 m) and that it rises again at the south end and beneath the most northern drumlin crest (Figure 8, 325 m). At the south end of the section there appears to be no weathering profile on the lower diamicton unit, and carbonate is present immediately below upper contact with the upper diamicton.

The abrupt changes in clay minerals shown by Newman and others (1990), and presence of pedogenic and weathering features just below the contact between the upper and lower diamictons indicate that this weathering profile is not an extension of the modern one from above, but the truncated portion of a weathering profile that developed on the land surface before the last glaciation formed the present drumlins. Although in some cases the lack of a weathering profile could result from a locally high water table, the gradual thinning of the profile away from the drumlin crests argues for truncation. Also sand and gravel layers interbedded with the upper diamicton in the Long Island section parallel the erosion surface on the lower unit indicating that the form was there when these sediments were deposited.

Walk 100 m southward along the beach to Stop 2. As you walk along the beach take a moment and examine the thick Mercenaria shell fragments that have been winnowed out of the lower diamicton.

STOP 2 (Figure 8, 15 m). The lower diamicton, exposed in the lower 2- to 3-m of this section, contains Mercenaria mercenaria shell fragments throughout. Mercenaria shells found in the lower diamicton on Peddocks Island drumlin yielded initial AARE ages of 200 ka and 214 ka (Belknap, 1979). However, these ages have been reevaluated and the new AARE ages indicate a probable Sangamon age (Belknap, 1980).

The extensively leached zone, present at Stop 1, is missing here. Overlying an irregular contact is a 2- to 5-m thick zone of interbedded medium sand, coarse sand, and sandy gravel. A 0.5 to 1 m thick carapace of diamicton, covers the section.

Walk northward along the beach 640 meters to Stop 3.

STOP 3 (Figures 1 and 5). The lower diamicton comprises nearly the entire section, extending some 12 to 13 m above beach level. The upper part of this lower diamicton is oxidized to a depth of approximately 2 m. Although access is difficult we can demonstrate that carbonate is present to within 2 m of the contact and believe it to be present even higher. Carbonates including large Mercenaria shells extend up to the erosion contact. The upper diamicton is approximately 3 m thick in this section and is marked by a stone line or cobble concentration. These do not appear to form a pavement of cobbles that are bevelled and striated.

Retrace your steps to the Water Tower Parking Lot, cross to the northwest side of the island via the parking lot and road running along the south and then west sides of hospital building. Descend to beach level on the road, then walk south on beach about 100 m.

STOP 4 (Figure 7). On the stoss (northwest) side of the Long Island drumlins the upper diamicton (unit 3) is fairly thin (3 to 4 m) and overlies the lower diamicton unit with shells present up to the contact. This indicates that the leached and oxidized part of the weathering profile was removed by erosion before unit 3 was deposited. The loose, interbedded diamicton and sand of unit 5 on the lee side of the drumlin is missing in this section.

Discussion

Observations made on drumlins in Boston Harbor suggest the following sequence of events: advance of ice into the harbor area sometime before the late Wisconsin glaciation. This ice advanced into marine silt and clay that contained shells of Mercenaria mercenaria as well as many other species. After this glacial event a long period of weathering took place on the diamicton. Clay minerals were altered (Newman and others, 1990) and the lower diamicton was oxidized and leached of carbonate to depths in excess of 6 m. Ice advanced during late-Wisconsin time across this landscape and carved drumlins out of the underlying weathered diamicton. This produced thickness variations in the leached and oxidized lower diamicton in cross section at Long Island from about 4 m to being absent. Evidently this same glacial event deposited less consolidated diamicton with sand and gravel lenses as a blanket over this drumlinized unconformity that had developed beneath the ice.

We suggest that the drumlins formed by differential erosion of pre-existing diamicton, probably under wholly or partly frozen bed conditions. With warming climate, a wet sliding bed continued to shape the drumlins. Finally, till was deposited on the sculptured drumlin cores during the retreat phase of glaciation and the orientation of the drumlins was changed somewhat because of late changes in ice flow direction.

STOP 5. LATE PROTEROZOIC SQUANTUM DIAMICTITE (Squaw Rock Park, Quincy, MA; Leader: R. H. Bailey). See Bailey (1987) and Hepburn and others (1993), this guidebook, for location information and geologic map.

Station A (Bailey, 1987). Complex bedding relationships at the base of a diamictite bed are apparent in this portion of the cliff. Intricate soft sediment folds, large intraclasts, load structures, and boulders may be observed in the 15 m length of cliff illustrated in Figure . Evidence of sediment transport by debris flows, turbidity currents, and high concentration sand and gravel sediment gravity flows is present. Types 1-4 lonestones are present in unit 6 (Figure 11).

Station B (Bailey, 1987). Thinly bedded sandstone and siltstone strata beneath diamictites are exposed along the north facing cliff. These beds contain graded beds and conspicuous soft sediment folds but no lonestones.

Station C (Bailey, 1987). Interbedded conglomerates and sandstones near the base of the Squantum diamictite are exposed at the northeastern end of the headland. This is a good spot to study the poorly sorted felsite, granitoid, and quartzite clasts supported by a sandy mudstone matrix.

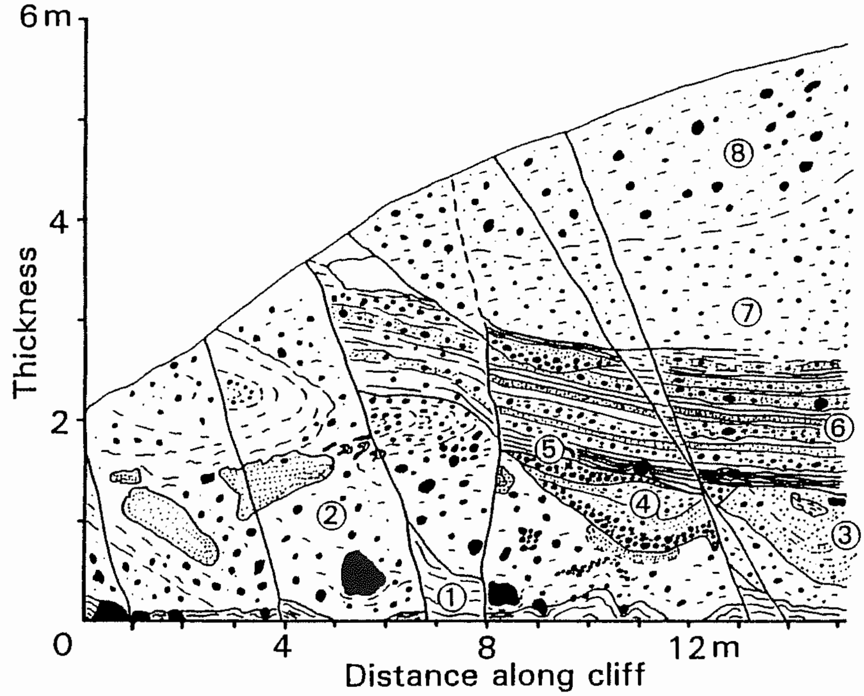

Figure 12. Detailed stratigraphic section along the cliff at station A. Note 2X vertical exaggeration. Plane of section oriented NE-SW, view is to south. Unit 1. thinly laminated deformed and loaded sandstone, Unit 2. diamictite with intraclasts and soft sediment folds, Unit 3. deformed pebbly/grannule sandstone, Unit 4. clast supported conglomerate and diamictite, Unit 5. clast supported conglomerate, Unit 6. interbedded graded sandstones and diamictites, both with lonestones, Unit 7. pebble diamictite, Unit 8. pebble and cobble diamictite.

From Squaw Rock return to route 3A south via Dorchester Street, East Squantum Street, and Quincy Shore Drive. Continue south on Route 3A to Humarock, Situate (Figure 13) located about 25 miles southeast of Boston and about 18 miles southeast of Long Island. At Humarock drive north on Central Avenue and bear left into the Air Force Recreational Area. Continue straight down the road until your approach the beach. Park on the left and descend down to the beach. (Permission can be obtained from the commander on duty at the Air Force Recreational Area before examining the exposures).

STOPS 6 AND 7. FOURTH CLIFF DRUMLIN (Scituate, MA; Leaders: W.A. Newman and D. M. Mickelson)

The purpose of this stop is:

1) to demonstrate that drumlin morphology is independent of underlying sedimentary structure.
2) to show that the drumlin core is an erosional form that is sculpted on deformed pre-Wisconsin diamicton, pre-Wisconsin or Wisconsin stratified sediment, or some combination of the two.

The morphology of the Fourth Cliff drumlin has been modified by extensive wave erosion and by the construction of a World War II observation tower along its northern crest. Other drumlins in the immediate vicinity (i.e., Second Cliff and Tilden Island located to the northwest and southwest respectively) trend approximately 330º. The trend of the axis of the undissected Fourth Cliff Drumlin probably closely approximated trends of adjacent drumlins.

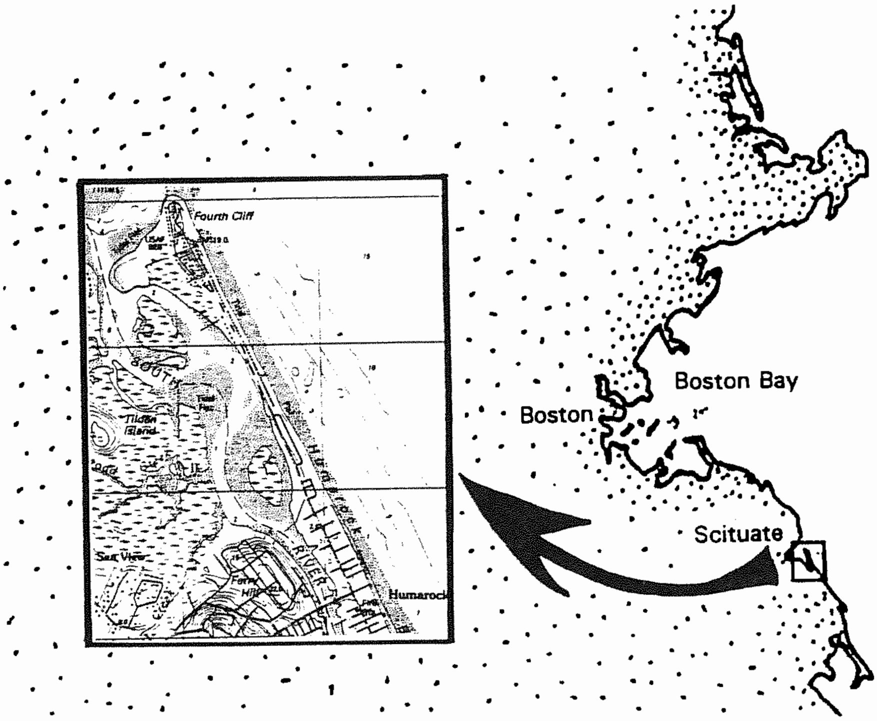

Figure 13. Location of Fourth Cliff drumlin, Scituate, MA

STOP 6 (Figure 15, 35m). An erosion surface that can be traced for about 220 m separates upper dark brown (10YR 4/4) sandy diamicton from a lower brown (10YR 5/4) sandy diamicton at this section. The lower diamicton is hard, compact, and oxidized. Numerous faults, joints, and partings filled with sand grains heavily coated with iron oxide extend to the erosion surface. We interpret this as basal till based on the structure of the sediment and well-developed fabric. Pods or blocks of oxidized sand, measuring up to 0.6 m x 0.3 m x 0.3 m, are frequently observed near beach level. Preserved just below the erosion surface are occasional truncated synclines of downfolded pebbly and cobbly gravel. To the south the surface of the lower diamicton becomes more bouldery and looser. Near the base of the exposure is unoxidized gray till that contains some reed-like plant remains that was determined to be more than 35,000 years old (Chute, 1965).

Above the erosion surface is an unoxidized, compact, dark brown (10YR 4/4) sandy diamicton containing irregular blocks of the oxidized lower diamicton. This unoxidized diamicton pinches out at approximately 268 m (Figure 14).

Beginning at 168 m and between the two diamictons there is a 0.10 m thick discontinuous layer of well sorted fine and coarse unoxidized sand that reveals in some locations fluvial cross-beds. To the south, these fine and coarse sands become interbedded with layers of diamicton and interbedded stratified sediments increase in thickness to more than 6 m.

Above the upper diamicton beginning at 154 m and extending to the south are thin units of well-sorted beds of unoxidized coarse and fine sand interbedded with unoxidized diamicton. To the south these beds also thicken and increase in apparent dip. A 1-to 1.5-m thick, carapace of loose sand, diamicton and eolian sediment covers the section.

STOP 7 (Figure 15, 350 m). The sediments here have an apparent dip to the south. The section consists of thick units of sand interbedded with coarse gravel lenses and diamicton. The upper surface of this diamicton is oxidized and the lower part is unoxidized. Above an angular unconformity at the top of the section is a loose, sandy, diamicton.

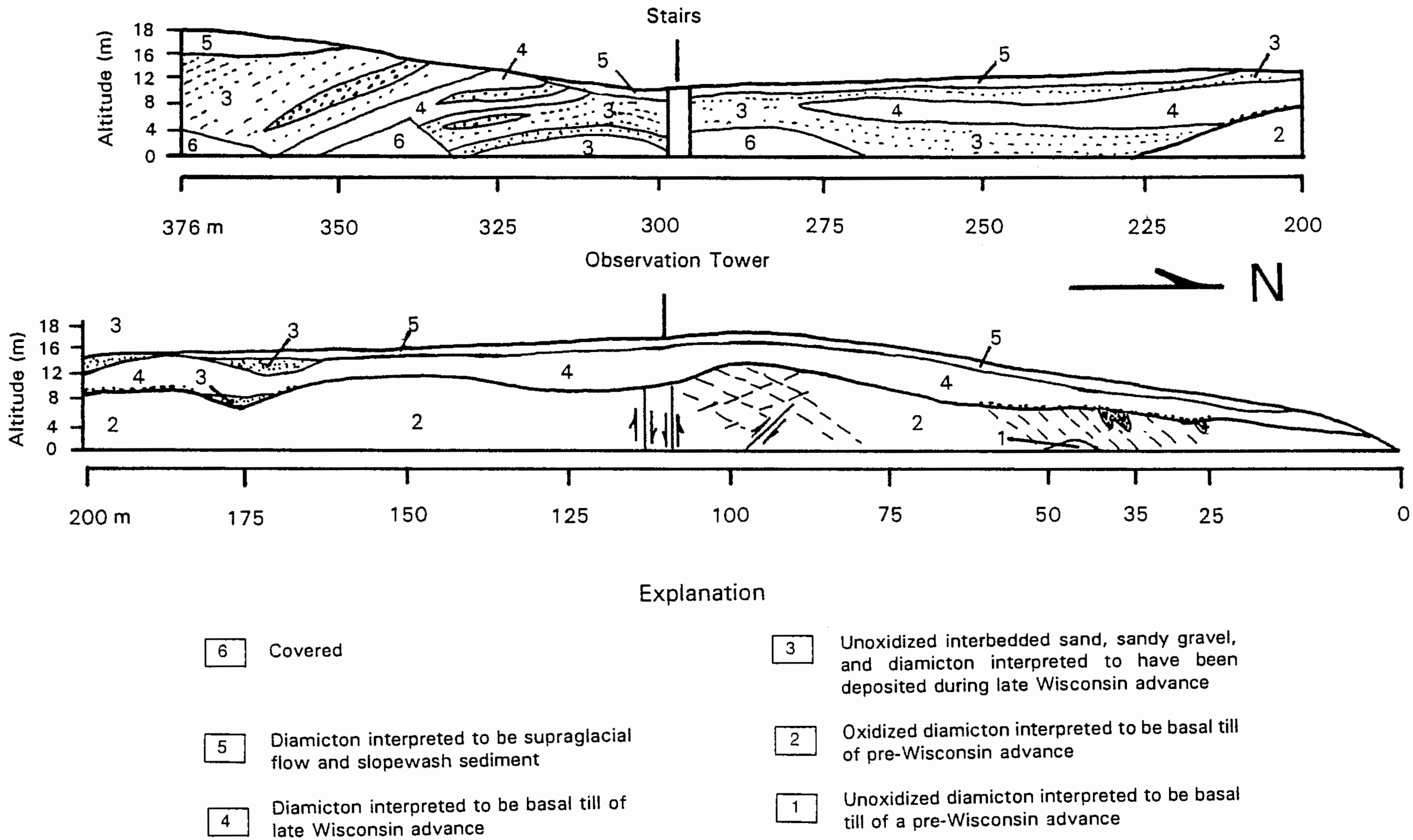

Figure 14. Stratigraphic section along the eastern side of Fourth Cliff drumlin.

Discussion

The core of the northern part of the drumlin (Stop 6) is extensively oxidized diamicton. Faults and joints extending through this unit are abruptly truncated at the erosion surface. We interpret the age of this diamicton as pre-Wisconsin based on the extent of oxidation as well as the presence of organic material dated greater than 35,000 C-14 years B.P. This unit plunges beach level at 221 m. The thin layer of well-sorted and stratified sand that occurs just above the erosion surface, and the overlying brown diamicton and beds of stratified sand interbedded with thin layers of diamicton are interpreted as late Wisconsin till and melt waterstream deposits, The carapace of loose sandy diamicton and eolian sediment are interpreted as colluvium and possibly supraglacial sediment.

The interbedded sand, gravel, and diamicton at the southern end of the section is essentially unoxidized. The top of the gray diamicton exposed at beach level at 343 m is oxidized but the profile is not extensive thus we cannot be sure of the age of this sediment. It has clearly been folded after deposition, then truncated by erosion. Based on our other observations we interpret this angular unconformity to be due to subglacial erosion during the drumlin forming process, but we cannot prove it here.

REFERENCES CITED

Bailey, R. H., 1987, Stratigraphy of the Boston Bay Group, Boston area, Masachusetts: Geological Society of America Centennial Field Guide, Northeastern Section, v. 5, p. 209-212.

Clark, P.V., and Lea, P.D., eds., The last interglacial-glacial transition in North America: Boulder, Colorado, Geological Society of America Special Paper 270, p. 163-170.

Chute , N. E., 1965, Geologic map of the Scituate Quadrangle, Plymouth County, Massachusetts: U. S. Geological Survey Geologic Quadrangle Map GQ-467, scale 1:24,000.

Crosby, I.B., 1934, Evidence from drumlins concerning the glacial history of Boston Basin: Bulletin of the Geological Society of America, v.45, p. 135-158.

Dott, R. H., 1961, Squantum "Tillite", Massachusetts, evidence of glaciation or subaqueous mass movement?: Geological Society of America Bulletin, v. 72, p. 1289-1306.

Follmer, L. R. (1983). Sangamon and Wisconsinan pedogenesis in the midwestern United States. *in* "Late Quaternary Environments of the United States" (H. E. Wright, Jr., Ed.), Vol. 1, "The Late Pleistocene" (S. C. Porter, Ed.), pp. 138-145. Univ. of Minnesota Press, Minneapolis.

Hepburn, J. C., Hon, R., Dunning, G., Bailey, R.H., Galli, K.G., 1993, The Avalon and Nashoba terranes (eastern margin of the Appalachian Orogen *in* southeastern New England), Field Trip Guidebook for the Northeastern United States: 1993 Boston GSA, edited by Jack T. Cheney and J. Christopher Hepburn, Department of Geology and Geography, University of Massachusetts, Amherst, Massachusetts, p. FF1 - FF30.

Kaye, C.A., 1961, Pleistocene Stratigraphy of Boston, Massachusetts, *in* Short papers in the geologic and hydrologic sciences: U.S. Geological Survey Professional Paper 424-B, p. B73-B76.

_____, 1978, Surficial geologic map of the Boston area, Massachusetts, U.S. Geological Survey Open File Report 78-111, scale 1:100,000.

_____, 1982, Bedrock and Quaternary geology of the Boston area, Massachusetts: Geological Society of America Reviews in Engineering Geology, v. 5, p. 25-39.

Kaye, C.A., and Barghoorn, E.S., 1964, Late Quaternary sea-level change and crustal rise at Boston, Massachusetts, with notes on the autocompaction of peat: Geological Society of America Bulletin, v. 75, p. 63-80.

Knebel, H.J., Rendigs, R.R., Oldale, R.N., and Bothner, M.H., 1992, Sedimentary framework of Boston Harbor, Massachusetts, *in* Fletcher, C.H., III, and Wehmiller, J.F., eds., Quaternary coasts of the United States: Society of Economic Paleontologists and Mineralogists Special Publication no. 48, p. 35-43.

LaForge, L., 1932, Geology of the Boston area, Massachusetts: U.S. Geological Survey Bulletin 839, 105 p.

Metcalf and Eddy, Inc., 1989, 1988 Marine Drilling Summary Report: Report to Massachusetts Water Resources Authority, v. 1. 27 p.

Menzies, John, 1984, Drumlins: A Bibliography: Norwich, GeoBooks, 117p.

Mickelson, D. M., and Newman, W. A. (1987). Till drumlins of the Boston Basin formed by subglacial erosion. Geological Society of America Abstracts with Programs 19, 771-772.

Newman, W. A., Berg, R. C., Rosen, P. S., and Glass, H. D. (1990). Pleistocene stratigraphy of the Boston Harbor Drumlins, Massachusetts. Quaternary Research, 34, 148-159.

Oldale, R.N., and Colman, S.M., 1992, On the age of the penultimate full glaciation of New England, *in* Clark, P.V., and Lea, P. D., eds., The last interglacial-glacial transition in North America: Boulder, Colorado, Geological Society of America Special Paper 270, p. 163-170.

Oldale, R.N., Colman, S.M., and Jones, G.A., in press, Radiocarbon ages from two submerged strandline features in the western Gulf of Maine off northeastern Massachusetts: Quaternary Research, v. 38, 24 p.

Oldale, R.N., Williams, R.S., and Colman, S.M., 1990, Evidence against a late Wisconsinan ice shelf in the Gulf of Maine: Quaternary Science Reviews, v. 9, p. 1-13.

Pettijohn, F. J., 1975, Sedimentary Rocks: New York, Harper and Row, 628 p.

Phipps, D., 1964, The geology of the unconsolidated sediments of Boston Harbor: Cambridge, Massachusetts, Massachusetts Institute of Technology, unpublished M.S. thesis, 53 p.

Rendigs, R.R., and Oldale, R.N., 1990, Maps showing the results of a subbottom acoustic survey of Boston Harbor, Massachusetts: U.S. Geological Survey Miscellaneous Field Studies Map MF-2124, 2 sheets, scale 1:50,000.

Sayles, R. W., 1914, The Squantum "Tillite": Bulletin of Harvard Museum of Comparative Zoology, v. 66, p. 141-175.

Schnitker, D., 1988, Timing and environment of deposition of the offshore equivalent to the Presumpscot Formation: Geological Society of America Abstracts with Programs, v. 20, no. 1, p. 68.

Shaw, J., Kvill, D., and Rains, B., 1989, Drumlins and catastrophic subglacial floods: *In*: Menzies, J. and Rose J., (eds.), Subglacial Bedforms - Drumlins, Rogen Moraine, and Associated Subglacial Bedforms: Sedimentary Geology, v. 62, p. 177-202.

Smith, G. W., and Socci, A. D., 1990, Late Proterozoic sedimentary geology of the Boston Basin, *in* Socci, A. D., Skehan, J. W., and Smith, G. W., Geology of the Composite Avalon Terrane of Southern New England: Boulder, Colorado, Geological Society of America Special Paper 245, p. 75-84.

Socci, A. D., and Smith, G. W., 1990, Stratigraphic implications of facies within the Boston Basin, *in* Socci, A. D., Skehan, J. W., and Smith, G. W., Geology of the Composite Avalon Terrane of Southern New England: Boulder, Colorado, Geological Society of America Special Paper 245, p. 55-74.

Thomas, G. S. P., and Connell, R. J., 1985, iceberg drop, dump, and grounding structures from Pleistocene glacio-lacustrine sediments, Scotland: Journal of Sedimentary Petrology, v. 55, p. 243-249.

Tucholke, B.E., and Hollister, C.D., 1973, Late Wisconsinan glaciation of the southwestern Gulf of Maine - new evidence from the marine environment: Geological Society of America Bulletin, v. 84, no. 10, p. 3279-3296.

Upham, W., 1893a, Drumlins near Boston, Appalachia, v. 7, p. 39-48.

______, 1893b, The origin of drumlins, (with discussion by W. M. Davis and G. H. Barton): Proceedings Boston Society Natural History, v. 26, p. 2-25.

______, 1894, The Madison type drumlins: American Geologist, v. 14, p.69-83.

Weston Geophysical Engineers, Inc., 1969, Seismic refraction investigations of Dorchester Bay: Report to Boston Redevelopment Authority, 6 p.

Weston, Geophysical Corporation, 1989, Marine geophysical investigation proposed inter-tunnel alignment, Nut Island to Deer Island, Boston Harbor, Massachusetts: Report to, Metcalf and Eddy, Inc., Westboro, Massachusetts, 13 p.

Chapter V

Ground-Water Contamination and Solute-Transport Research at the U.S. Geological Survey's Cape Cod Site

By Denis R. LeBlanc, Stephen P. Garabedian, and Kathryn M. Hess

Field Trip Guidebook for the Northeastern United States:
1993 Boston GSA

Volume 2
Contribution No. 67, Department of Geology and Geography, University of Massachusetts, Amherst, Massachusetts

GROUND-WATER CONTAMINATION AND SOLUTE-TRANSPORT RESEARCH AT THE U.S. GEOLOGICAL SURVEY'S CAPE COD SITE

by
Denis R. LeBlanc, Stephen P. Garabedian, and Kathryn M. Hess
U. S. Geological Survey, Marlborough, MA 01752

INTRODUCTION

The U.S. Geological Survey (USGS) Cape Cod Toxic-Substances Hydrology Research site is located in the northern part of Falmouth, Mass., on Cape Cod (fig. 1). This site is the focus of research on the geologic, hydrologic, chemical, and microbiological processes that affect the movement of contaminants in a sewage plume originating from Otis Air Base. It was selected for study as part of a nationwide program of the USGS to describe the fate of contaminants in the subsurface. The purpose of this paper is to review past research efforts at the Cape Cod site and to provide information for participants in the Geological Society of America (GSA) field trip to the site on October 29, 1993. Earlier summaries of research at the Cape Cod site can be found in reports by LeBlanc (1984b), Franks (1987), Ragone (1988), Mallard and Ragone (1989), and Mallard and Aronson (1991).

SITE DESCRIPTION

The study area is on a broad sand and gravel glacial outwash plain that was formed during the last Pleistocene glacial retreat. The outwash plain slopes southward to Nantucket Sound and is pitted with many kettle holes, some of which contain ponds. The area contains several valleys that transect the plain from north to south. Most of these valleys, which typically are 150 to 270 m (meters) wide and 10 m deep, do not contain streams but have wetlands at their southern ends.

A hydrogeologic section showing the vertical distribution of sediment types is shown in figure 2. The top 30 to 50 m of sediment are a glacial outwash composed of stratified, medium to coarse sand with some gravel. In the northern part of the study area, the sand and gravel overlies fine sand and silt. To the south, the outwash overlies fine sand, silt, and sandy till. The till contains lenses of clay, silt, sand, and gravel. These unconsolidated sediments overlie a crystalline (granodiorite) bedrock surface, which generally slopes from west to east through the study area.

On the basis of measured values for similar sediments on Cape Cod, LeBlanc (1984c) estimated that the horizontal hydraulic conductivity of the sand and gravel in the study area ranges from 60 to 90 m/d (meters per day). Results of an aquifer test conducted in the study area in 1984 indicate that the horizontal hydraulic conductivity of the sand and gravel may be locally as high as 120 m/d (Garabedian et al., 1988). The horizontal hydraulic conductivity of the underlying fine sand and sandy till is estimated to be about one-tenth that of the sand and gravel (LeBlanc, 1984a). The crystalline bedrock is assumed to have a very low hydraulic conductivity; therefore, the bedrock is considered to be the bottom of the regional ground-water flow system.

Ground water in the unconsolidated sediments is under unconfined (water table) conditions. The water table slopes toward the south at about 1.5 m/km (meters per kilometer) (fig. 1). Seasonal variations in aquifer recharge produce an annual water-table fluctuation of 0.3 to 0.9 m; the highest levels are in the spring and the lowest are in the fall.

Ground-water recharge to the study area occurs primarily from precipitation and underflow from upgradient areas. Little surface-water runoff occurs because the sandy soils are very permeable. Estimated recharge to the aquifer is 0.5 meters per year, about 45 percent of the total precipitation (LeBlanc, 1984a). Estimated rates of horizontal ground-water velocity in the sand and gravel range from 0.2 to 0.6 m/d. These estimates are based on an average hydraulic gradient of 1.5 m/km, a horizontal hydraulic conductivity of 60 to 120 m/d, and a porosity of 30 to 40 percent (LeBlanc, 1984c).

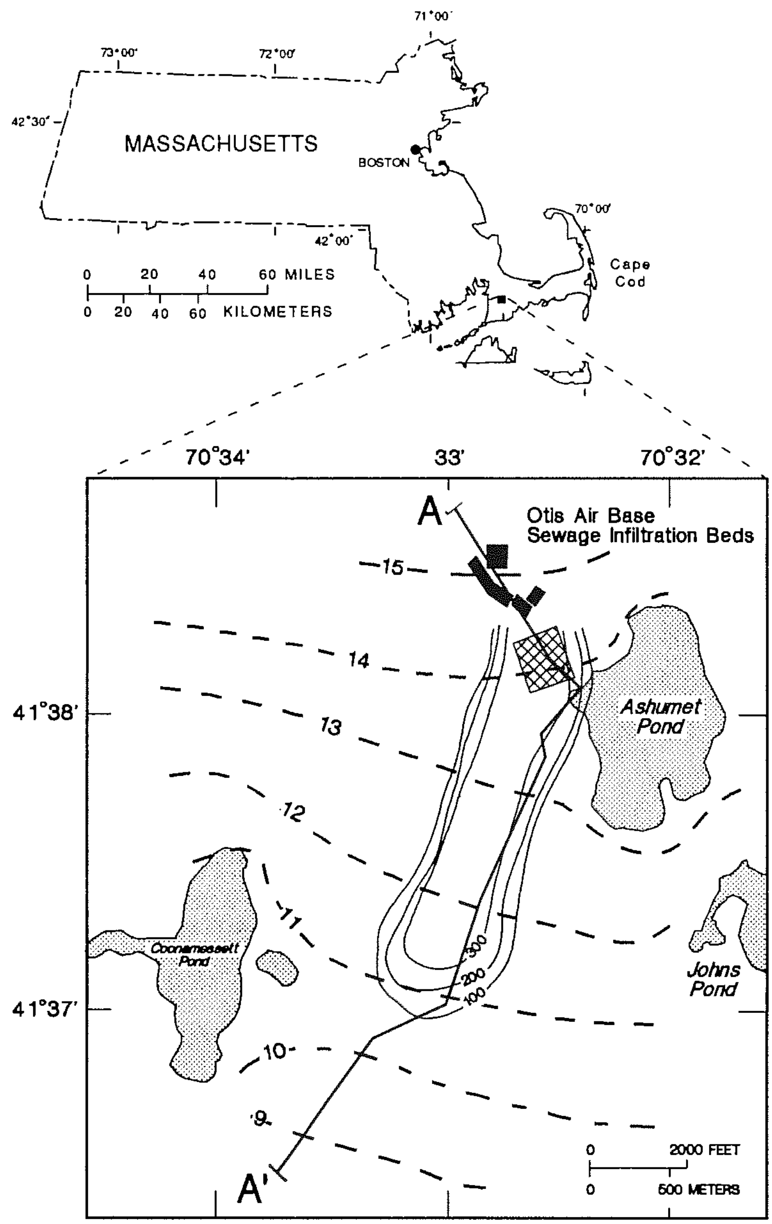

EXPLANATION

TRACER-TEST SITE -- Shows area in figure 3.

LINE OF EQUAL BORON CONCENTRATION, 1978-79-- Concentrations in micrograms per liter.

WATER-TABLE CONTOUR, NOVEMBER 1979-- Altitude of water table in meters. Datum is sea level.

A—A' LINE OF SECTION SHOWN IN FIGURE 2.

Figure 1. Location of study area, showing sewage plume and tracer-test site. (Modified from LeBlanc, 1984c, fig. 16.)

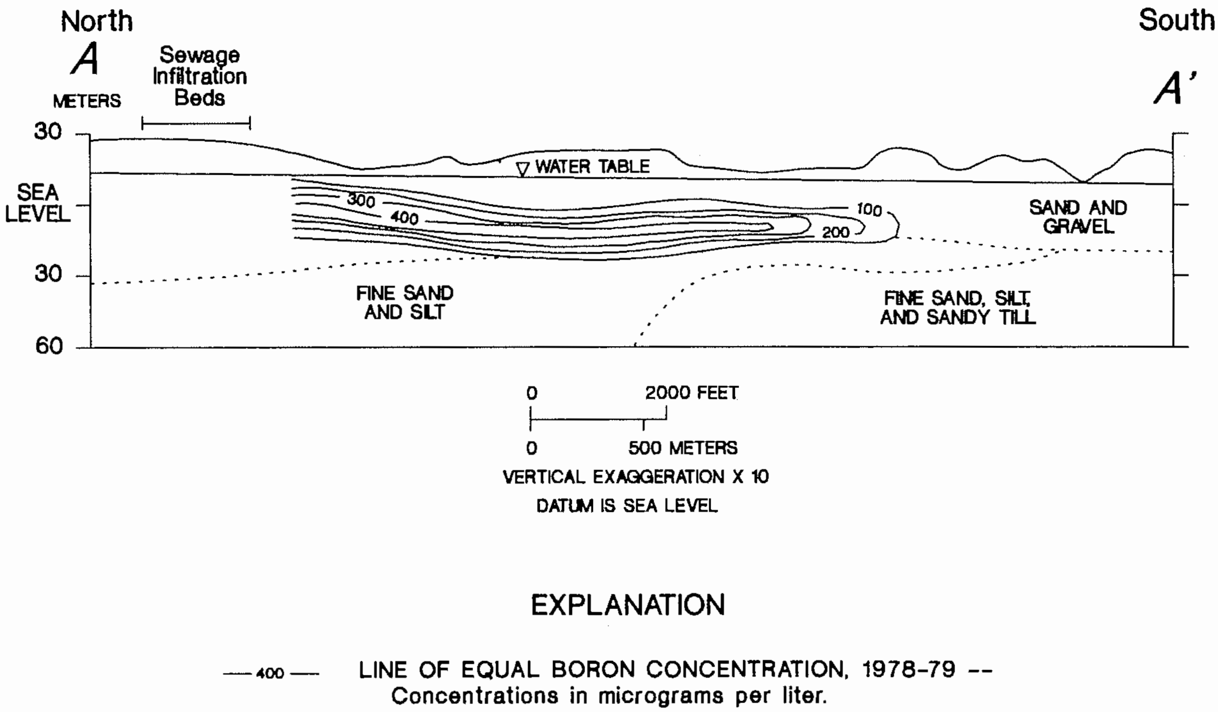

Figure 2. Vertical location of sewage plume and geohydrologic units. Line of section shown in figure 1. (Modified from LeBlanc, 1984c, figs. 9 and 17).

SEWAGE PLUME

LeBlanc (1984b,c) described the extent of contamination in the aquifer caused by the disposal of treated sewage onto infiltration beds at Otis Air Base (fig. 1). In 1979, the plume of contaminated ground water, formed by disposal since 1936, was 0.8 to 1.1 km (kilometers) wide, 23 m thick, and more than 3.4 km long (figs. 1, 2). The plume moves to the south in the direction of ground-water flow and is overlain by up to 15 m of uncontaminated ground water derived from precipitation that recharges the aquifer.

The plume of sewage-contaminated ground water is characterized by elevated concentrations of dissolved solids, boron, chloride, sodium, phosphorus, ammonium, nitrate, detergents (LeBlanc, 1984c) and, in some locations, volatile organic compounds (Thurman et al., 1984; Barber et al., 1988). Boron, chloride, and sodium appear to be conservative and nonreactive, and are attenuated primarily by hydrodynamic dispersion. Phosphorus movement is greatly retarded by colloidal precipitation (Gschwend and Reynolds, 1987; Backhus and Gschwend, 1990) and adsorption onto the sediments. Although a maximum nitrate concentration of 16 mg/L (milligrams per liter) (as nitrogen (N)) has been detected in the sewage effluent, the concentration in the center of the plume immediately downgradient from the disposal beds is below detection (Leblanc, 1984c; Ceazan et al., 1989) owing to microbially mediated denitrification (Smith, Howes, and Duff, 1991a). Within 1.5 km of the disposal beds, the predominant nitrogen species in the plume is ammonium. Beyond 1.8 km from the beds, the predominant nitrogen species changes to nitrate, with concentrations of about 3 to 4 mg/L. This distribution of ammonium is caused, in part, by adsorption onto the aquifer sediments (Ceazan et al., 1989), which retards the movement of ammonium. Detergent concentrations exceed 0.5 mg/L methylene-blue-active subtances (MBAS) from 0.9 to 3.0 km downgradient from the disposal beds. This distribution of detergents reflects the use of nonbiodegradable detergents during 1946-64 (LeBlanc, 1984c; Thurman et al., 1986; Thurman et al., 1987).

Elevated VOC concentrations are present in two zones in the study area, one of which is immediately downgradient from the disposal beds and the other 500 to 2,600 m downgradient from the beds. The source of the VOC zone immediately downgradient from the disposal beds may be unrelated to the sewage disposal because the VOC's are found beneath the sewage plume. However, the VOC zone that is farther from the disposal beds is thought to originate from the sewage-treatment facility because the VOC's are found within the sewage plume (Thurman et al., 1984; Barber et al., 1988). VOC concentrations in the downgradient zone exceed 50 μg/L (micrograms per liter), which suggests that the VOC's are mobile and not readily degraded in the sandy aquifer (Barber, 1988; Barber et al., 1988).

Bacterial population counts as large as 2×10^6/mL (per milliliter) are found in ground water near the disposal site; these counts decrease to about 2.5×10^5/mL farther than 1 km from the beds (Harvey et al., 1984). These numbers appear to correlate with the availability of degradable organic compounds; concentrations of dissolved organic carbon decrease from 12 mg/L to less than 2 mg/L over the same distance (Thurman et al., 1986). The decrease in bacterial numbers with distance, particularly bacteria smaller than 0.4 micrometers in diameter, also suggests that transport and filtering of bacteria is occuring (Harvey et al., 1989). Assays of microbial activity have been made for both ground water and aquifer sediments because more than 90 percent of the bacteria are attached to silt- and clay-sized particles (Harvey and George, 1987; Smith and Duff, 1988). These assays show that rates of microbially mediated denitrification are greatest in water and sediment collected from a 1- to 2-m thick zone near the top of the plume, demonstrating the need for close-interval vertical sampling (Smith, Harvey, and LeBlanc, 1991.)

RESEARCH ON TRANSPORT PROCESSES

Past research efforts at the Cape Cod Toxic-Substances Hydrology Research site have focused on defining and describing the extent of ground-water contamination in the sewage plume. Current research at the site includes efforts to characterize specific physical, chemical, and microbiological processes affecting the transport and fate of solutes and microorganisms in the aquifer. These processes are characterized using small-scale laboratory experiments such as batch and column tests, intermediate-scale field experiments such as natural-gradient tracer tests with transport distances of 1 to 280 m, and large-scale investigations of the sewage plume with specialized sampling methods.

A major objective at the Cape Cod site has been to relate the dispersion of solutes to the heterogeneity of aquifer hydraulic properties. A direct measure of the dispersion of solutes in the aquifer was obtained by a spatial-moments analysis of a large-scale natural-gradient tracer test conducted from 1985-87 (LeBlanc et al., 1991; Garabedian et al., 1991). Bromide, a nonreactive tracer, was monitored with a three-dimensional array of 9,840 sampling points in an abandoned gravel pit as it moved 280 m through the aquifer (fig. 3). The spatial-moments analysis indicates that the aquifer dispersivity is about 1.0 m in the direction of flow, about 0.02 m in the transverse horizontal direction, and about 0.002 m in the transverse vertical direction (Garabedian et al., 1991).

Hess et al. (1992) presented estimates of aquifer macrodispersivity using the statistical properties of the hydraulic-conductivity distribution in the theoretical stochastic transport equations of Gelhar and Axness (1983). The statistics were obtained from the analysis of nearly 1,500 measurements of hydraulic conductivity at the Cape Cod site that were made using borehole-flowmeter tests and permeameter analyses of cores (Wolf et al., 1991) near the location of the large-scale tracer test. The range of estimated asymptotic longitudinal macrodispersivity is 0.35 to 0.78 m; this range is similar to the longitudinal dispersivity observed in the large-scale tracer test.

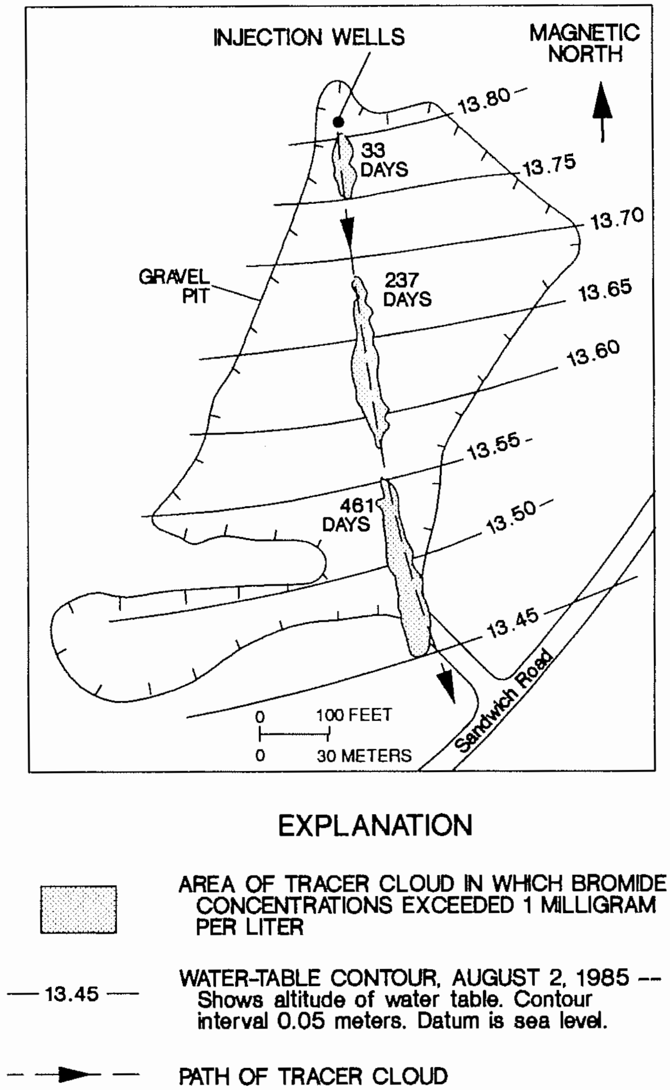

Figure 3. Tracer-test site in abandoned gravel pit, showing water table and path of bromide tracer cloud. Location of map shown in figure 1. (Modified from LeBlanc et al., 1991, fig. 4).

In addition to measuring dispersion in the aquifer, the large-scale natural-gradient tracer test was also conducted to determine geochemical controls on reactive transport in a heterogeneous aquifer. Two reactive tracers, lithium and molybdate, were monitored as part of the tracer test and were found to be significantly retarded relative to bromide (LeBlanc et al., 1991). For lithium, a cation, adsorption occurs on the mineral surfaces and, more significantly, inside the weathered grains (Wood et al., 1990), where adsorption is controlled by diffusion into micropores. The diffusion-controlled adsorption resulted in a skewed distribution of lithium, with highest concentrations near the leading edge of the solute cloud and lower concentrations in the trailing edge. Adsorption of molybdate (an oxyanion of molybdenum) was affected during the tracer test by the presence of the sewage plume, which caused variations with depth in pH and phosphate, an oxyanion that competes with molybdate for adsorption sites (Stollenwerk and Kipp, 1990).

The effect of hydrologic and geochemical processes on metal-ion transport was evaluated in a series of laboratory experiments and small-scale tracer tests conducted at the Cape Cod site (Kent et al., 1989). The results of the tracer tests with Zn (zinc), Cr (chromium), and Se (selenium) showed, in some cases, significant changes in speciation during transport. The reactions and processes that affected the observed test results include adsorption-desorption, aqueous complexation, and oxidation-reduction reactions. The results of additional studies to identify the geochemical parameters controlling metal-ion sorption and to describe their spatial variability are being used in conjunction with tracer-test studies (Davis et al., 1991) to develop coupled solute-transport and reaction models that incorporate the observed spatial variability in (1) geochemical parameters used to estimate sorbent abundance, (2) metal sorption coefficients, and (3) hydraulic conductivity

The microbial populations, activity, and transport in the aquifer have been characterized using several techniques. A method to measure microbial activity directly in the aquifer at a site where denitrification is occuring was tested using methane and a hexafluoroethane as tracers (Smith, Howes, and Garabedian, 1991). These dissolved gases were transported without retardation, but concentrations of methane apparently decreased because of biodegradation. Tracer tests conducted at two sites showed that transport of bacteria is affected by bacterial size and electrical charge on the surfaces of the bacteria (Harvey et al., 1989). In one test, the bacteria moved at the same rate as a nonreactive tracer, chloride, through about 7 m of the aquifer under a natural hydraulic gradient. Other tests included a series of small-scale, forced- and natural-gradient tracer experiments using labeled bacteria at sites in the contaminated and uncontaminated areas of the aquifer (Harvey and Garabedian, 1991). Results indicate that the magnitude of immobilization, retardation, and differential size exclusion of the bacteria from small pores can vary significantly within the aquifer. In some experiments, breakthrough patterns of bacteria closely matched that of the conservative tracers. However, earlier and later arrival (tailing) of peak microbial abundance relative to the conservative tracers has also been observed.

FIELD TRIP

The GSA field trip to the Cape Cod Toxic-Substances Hydrology Research site will visit several sites where field studies on the transport and fate of contaminants in ground water are being conducted by the USGS and several universities. At several stops along the path of the sewage plume, field methods such as tracer tests and closely spaced vertical sampling of ground water and aquifer materials will be demonstrated to show the effects of dispersion and geochemical processes on contaminant migration in the sand and gravel aquifer. The trip will include a stop in the gravel pit where more than 1,000 multilevel wells are being used in ground-water tracer experiments with inorganic, organic, and microbial tracers. The specific stops and demonstrations will highlight field efforts in progress during the trip.

REFERENCES

Backhus, D.A., and Gschwend, P.M., 1990, Fluorescent polycyclic aromatic hydrocarbons as probes for studying the impact of colloids on pollutant transport in groundwater: Environmental Science and Technology, v. 24, no. 8, p. 1214-1223.

Barber, L.B., II, 1988, Dichlorobenzene in ground water: Evidence for long-term persistence: Ground Water, v. 26, no. 6, p. 696-702.

Barber, L.B., II, Thurman, E.M., Schroeder, M.P., and LeBlanc, D.R., 1988, Long-term fate of organic micropollutants in sewage-contaminated groundwater: Environmental Science and Technology, v. 22, no. 2, p. 205-211.

Ceazan, M.L., Thurman, E.M., and Smith, R.L, 1989, Retardation of ammonium and potassium transport through a contaminated sand and gravel aquifer: The role of cation exchange: Environmental Science and Technology, v. 23, no. 11, p. 1402-1408.

Davis, J.A., Kent, D.B., Rea, B.A., Maest, A.S., and Garabedian, S.P., 1991, Influence of redox environment and aqueous speciation on metal transport in groundwater: Preliminary results of tracer injection studies, *in* Allen, H.E., Brown, D., and Perdue, E.M., eds., Metals in Groundwater: Chelsea, Mich., Lewis Publishers.

Franks, B.J., ed., 1987, U.S. Geological Survey Program on Toxic Waste--Ground-Water Contamination: Proceedings of the third technical meeting, Pensacola, Florida, March 23-27, 1987: U.S. Geological Survey Open-File Report 87-109, 214 p.

Garabedian, S.P., Gelhar, L.W., and Celia, M.A., 1988, Large-scale dispersive transport in aquifers: Field experiments and reactive transport theory: Cambridge, Mass., Massachusetts Institute of Technology, Dept. of Civil Engineering, Ralph M. Parsons Laboratory, Hydrology and Water Resources Systems Report No. 315, 290 p.

Garabedian, S.P., LeBlanc, D.R., Gelhar, L.W., and Celia, M.A., 1991, Large-scale natural-gradient tracer test in sand and gravel, Cape Cod, Massachusetts: 2. Analysis of spatial moments for a nonreactive tracer: Water Resources Research, v. 27, no. 5, p. 911-924.

Gelhar, L.W., and Axness, C.L., 1983, Three-dimensional stochastic analysis of macrodispersion in aquifers: Water Resources Research, v. 19, no. 1, p. 161-180.

Gschwend, P.M., and Reynolds, M.D., 1987, Monodisperse ferrous phosphate colloids in an anoxic groundwater plume: Journal of Contaminant Hydrology, v. 1, no. 3, p. 309-327.

Harvey, R.W., and Garabedian, S.P., 1991, Use of colloid filtration theory in modeling movement of bacteria through a contaminated sandy aquifer: Environmental Science and Technology, v. 25, no. 1, p. 178-185.

Harvey, R.W., and George, L.H., 1987, Growth determinations for unattached bacteria in a contaminated aquifer: Applied and Environmental Microbiology, v. 53, no. 12, p. 2992-2996.

Harvey, R.W., George, L.H., Smith, R.L., and LeBlanc, D.R., 1989, Transport of microspheres and indigenous bacteria in a sandy aquifer: Results of natural- and forced-gradient tracer experiments: Environmental Science and Technology, v. 23, no. 1, p. 51-56.

Harvey, R.W., Smith, R.L., and George, Leah, 1984, Effect of organic contamination upon microbial distributions and heterotrophic uptake in a Cape Cod, Massachusetts, aquifer: Applied and Environmental Microbiology, v. 48, no. 6, p. 1197-1202.

Hess, K.M., Wolf, S.H., and Celia, M.A., 1992, Large-scale natural gradient tracer test in sand and gravel, Cape Cod, Massachusetts: 3. Hydraulic-conductivity variability and calculated macrodispersivities: Water Resources Research, v. 28, no. 8, p. 2011-2027.

Kent, D.B., Davis, J.A., Maest, A.S., and Rea, B.A., 1989, Field and laboratory studies of transport of reactive solutes in groundwater, *in* Miles, D.L., ed., Water-Rock Interaction WRI-6 (proceedings of conference, Malvern, England, August 3-12, 1989): Rotterdam, The Netherlands, Balkema, p. 381-383.

LeBlanc, D.R., 1984a, Digital modeling of solute transport in a plume of sewage-contaminated ground water, *in* LeBlanc, D.R., ed., Movement and fate of solutes in a plume of sewage-contaminated ground water, Cape Cod, Massachusetts: U.S. Geological Survey Toxic Waste Ground-Water Contamination Program: U.S. Geological Survey Open-File Report 84-475, p. 11-45.

LeBlanc, D.R., ed., 1984b, Movement and fate of solutes in a plume of sewage-contaminated ground water, Cape Cod, Massachusetts: U.S. Geological Survey Toxic Waste Ground-Water Contamination Program: U.S. Geological Survey Open-File Report 84-475, 175 p.

LeBlanc, D.R., 1984c, Sewage plume in a sand and gravel aquifer, Cape Cod, Massachusetts: U.S. Geological Survey Water-Supply Paper 2218, 28 p.

LeBlanc, D.R., Garabedian, S.P., Hess, K.M., Gelhar, L.W., Quadri, R.D., Stollenwerk, K.G., and Wood, W.W., 1991, Large-scale natural-gradient tracer test in sand and gravel, Cape Cod, Massachusetts: 1. Experimental design and observed tracer movement: Water Resources Research, v. 27, no. 5, p. 895-910.

Mallard, G.E., and Aronson, D.A., eds., 1991, U.S. Geological Survey Toxic Substances Hydrology Program--Proceedings of the technical meeting, Monterey, California, March 11-15, 1991: U.S. Geological Survey Water-Resources Investigations Report 91-4034, 730 p.

Mallard, G.E., and Ragone, S.E., eds., 1989, U.S. Geological Survey Toxic Substances Hydrology Program--Proceeding of the technical meeting, Phoenix, Arizona, September 26-30, 1988: U.S. Geological Survey Water-Resources Investigations Report 88-4220, 651 p.

Ragone, S.E., 1988, U.S. Geological Survey Program on Toxic Waste--Ground-Water Contamination: Proceedings of the second technical meeting, Cape Cod, Massachusetts, October 21-25, 1985: U.S. Geological Survey Open-File Report 86-481, 174 p.

Smith, R.L., and Duff, J.H., 1988, Denitrification in a sand and gravel aquifer: Applied and Environmental Microbiology, v. 54, no. 5, p. 1071-1078.

Smith, R.L., Harvey, R.W., and LeBlanc, D.R., 1991, Importance of closely spaced vertical sampling in delineating chemical and microbiological gradients in groundwater studies: Journal of Contaminant Hydrology, v. 7, no. 3, p. 285-300.

Smith, R.L., Howes, B.L., and Duff, J.H., 1991, Denitrification in nitrate-contaminated ground water: Occurrence in steep vertical geochemical gradients: Geochimica et Cosmochimica Acta, v. 55, no. 7, p. 1815-1825.

Smith, R.L., Howes, B.L., and Garabedian, S.P, 1991, In situ measurement of methane oxidation in groundwater by using natural-gradient tracer tests: Applied and Environmental Microbiology, v. 57, no. 7, p. 1997-2004.

Stollenwerk, K.G., and Kipp, K.L., 1990, Simulation of molybdate transport with different rate-controlled mechanisms, *in* Melchior, D.C., and Bassett, R.L., eds., Chemical Modeling of Aqueous Systems II: Washington, American Chemical Society Symposium Series No. 416, chap. 19, p. 243-257.

Thurman, E.M., Barber, L.B., II, Ceazan, M.L., Smith, R.L., Brooks, M.G., Schroeder, M.P., Keck, R.J., Driscoll, A.J., LeBlanc, D.R., and Nichols, W.J., Jr., 1984, Sewage contaminants in ground water, *in* LeBlanc, D.R., ed., Movement and fate of solutes in a plume of sewage-contaminated ground water, Cape Cod, Massachusetts: U.S. Geological Survey Toxic Waste Ground-Water Contamination Program: U.S. Geological Survey Open-File Report 84-475, p. 47-87.

Thurman, E.M., Barber, L.B., II, and LeBlanc, D.R., 1986, Movement and fate of detergents in ground water: A field study: Journal of Contaminant Hydrology, v. 1, no. 1, p. 143-161.

Thurman, E.M., Willoughby, T., Barber, L.B., II, and Thorn, K.A., 1987, Determination of alkylbenzenesulfonate surfactants in groundwater using macroreticular resins and carbon-13 nuclear magnetic resonance spectrometry: Analytical Chemistry, v. 59, no. 14, p. 1798-1802

Wolf, S.H., Celia, M.A., and Hess, K.M., 1991, Evaluation of hydraulic conductivities calculated from multi-port permeameter measurements: Ground Water, v. 29, no. 4, p. 516-525.

Wood, W.W., Kraemer, T.F., and Hearn, P.P., Jr., 1990, Intragranular diffusion: An important mechanism influencing solute transport in clastic aquifers?: Science, v. 247 (March 30, 1990), p. 1569-1572.

Chapter W

A Geohistorical Boat Tour of Boston Harbor

By John Humphrey, Jutta Hager, and David Woodhouse

Field Trip Guidebook for the Northeastern United States:
1993 Boston GSA

Volume 2
Contribution No. 67, Department of Geology and Geography, University of Massachusetts, Amherst, Massachusetts

A GEOHISTORICAL BOAT TOUR OF BOSTON HARBOR

sponsored by
The Association of Engineering Geologists, New England Section
and
John Humphrey; Haley & Aldrich, Inc., 58 Charles Street, Cambridge, MA 02141
Jutta Hager; Hager GeoScience, Inc., 63 Gregory Street, Waltham, MA 02154
David Woodhouse; ECT, Inc., 9 Cedarwood Drive, Bedford, NH 03110

INTRODUCTION

Boston, affectionately called "The Hub" and plain old "Bean Town", is the capital of Massachusetts and the largest city in New England (Figure 1). Boston occupies the smallest land mass of any major city and is situated on Massachusetts Bay, a large body of water bounded by Cape Ann to the north and Cape Cod to the south. It sits in its sheltered bay and snug harbor with 38 islands that act as a buttress to the Atlantic Ocean (in 1621 the Pilgrims counted at least 50 islands).

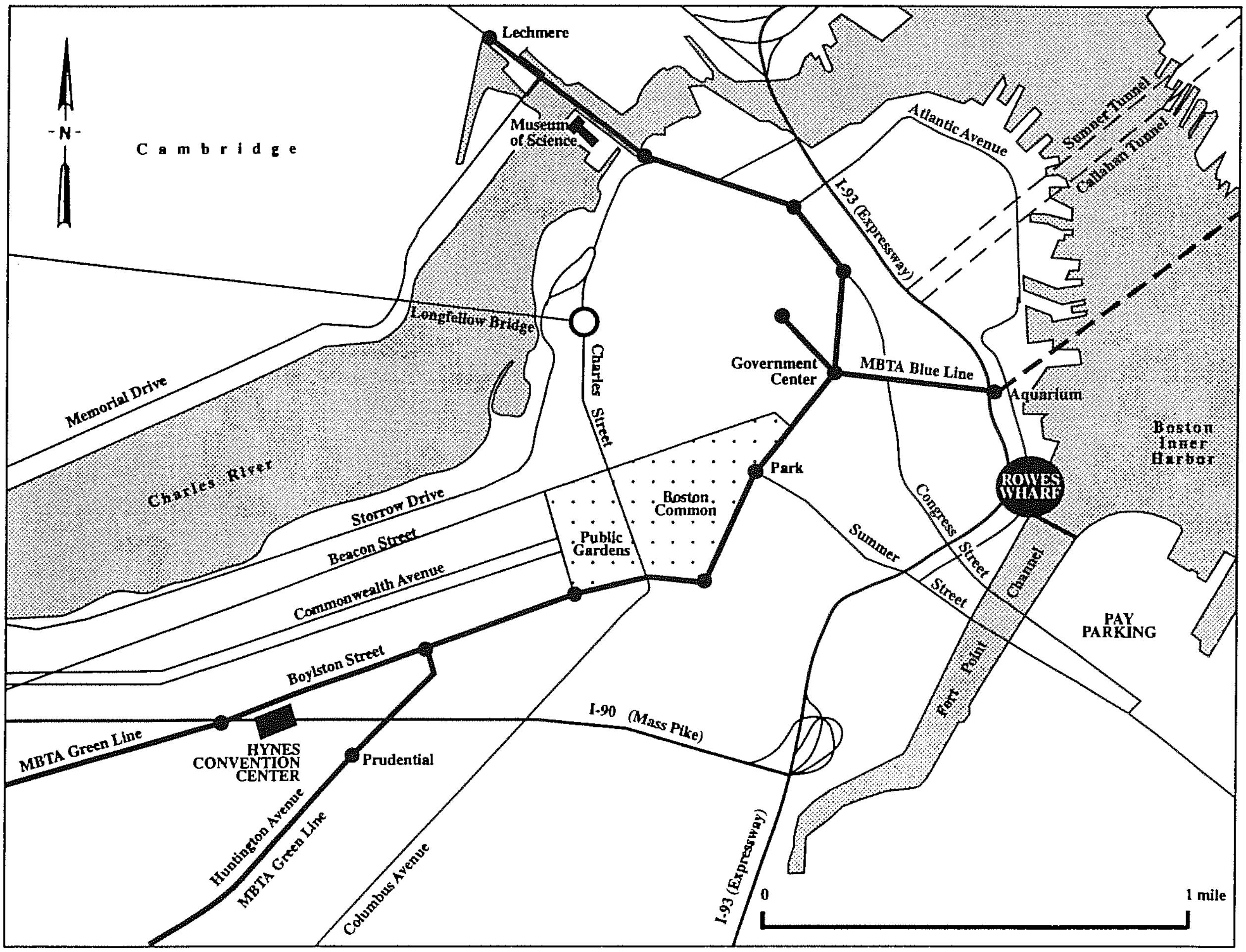

Fig. 1 DOWNTOWN BOSTON SHOWING SUBWAY STOPS FROM HYNES CONVENTION CENTER TO ROWES WHARF.

Boston Harbor is made up of the Inner and Outer Harbors. The Inner Harbor is a busy port in transition surrounded by the urban heart of Metropolitan Boston. The Outer Harbor is divided into three bays: Dorchester Bay, Quincy Bay and Hingham Bay. The two harbors encompass approximately 50 square miles, with 180 miles of coastline.

For many years Boston Harbor and its beautiful islands were neglected, misused and abused. Pollution, antiquated institutions, military activities and use as dumping grounds prompted then president-elect George Bush to draw national attention to the "most polluted harbor in the nation." In 1985, the Massachusetts Water Resources Authority (MWRA) was created and commenced the multi-billion dollar Boston Harbor Clean-up Project, which is now well underway. Additional public and private organizations, such as the Metropolitan District Commission (MDC) and the Friends of Boston Harbor, are also helping to return the harbor and its islands to their former beauty.

Our three-hour tour will follow the route outlined on Figure 2. During that time we will attempt to give you an overview of the geology of Boston and its attendant controversy, the mega-billion dollar construction projects, including the Third Harbor Tunnel, harbor-related clean up projects, and of course, its fascinating history and beauty.

Welcome aboard and enjoy the day.

HISTORY OF FOUNDING

The Indians settled in the Boston area around 2500 B.C. The Norseman Biarne visited the area in about 900 A.D., and many early traders and explorers came here during the 16th century. Captain Miles Standish with his small group of Pilgrims and Native American guides visited Boston Harbor on September 15, 1621.

The actual credit for the founding of Boston can be given to John Winthrop and his band of Puritan followers representing the Massachusetts Bay Company. On March 22, 1630, they sailed from England on their perilous journey to escape religious persecution and to found the "city upon a hill." Their destination was Salem, about 15 miles north of Boston, where more than 100 English settlers had been living for almost one year. One June 12, 1630, the hardy group reached Salem, where it was greeted by a landscape of barren rock and little soil, a brutal contrast to their native, fertile southern England. Pressured by his followers, Winthrop, after spending just five days in Salem, left for Charlestown (now a section of Boston), where a group of Englishmen had already settled.

Within a few weeks, the new settlers at Charlestown were nearly defeated by sickness, death and lack of water. Winthrop blamed their troubles on the one available source of water, a brackish spring that was exposed only at low tide. Help came in the person of the hermit William Blackstone, a retired Episcopal minister who had been living across the Charles River on Beacon Hill since 1625. Blackstone was the first English settler of what would become Boston (then called the Shawmut Peninsula), having built a cottage on the south side of Beacon Hill near the Common. Blackstone invited Winthrop and his group to share the abundant and refreshing spring water available on his land. Accepting Blackstone's invitation, Winthrop and his group moved across the river to the Shawmut Peninsula. The group settled near the North End, on Great Cove, at the head of what is now State Street.

Thus it was that Winthrop had founded his "city upon a hill." The "hill" was called the Trimountain for its three prominent peaks. The westernmost hill was Mt. Vernon, the central peak was Beacon Hill (or Sentry Hill) and the easternmost peak was Pemberton Hill. Boston was named after Boston,

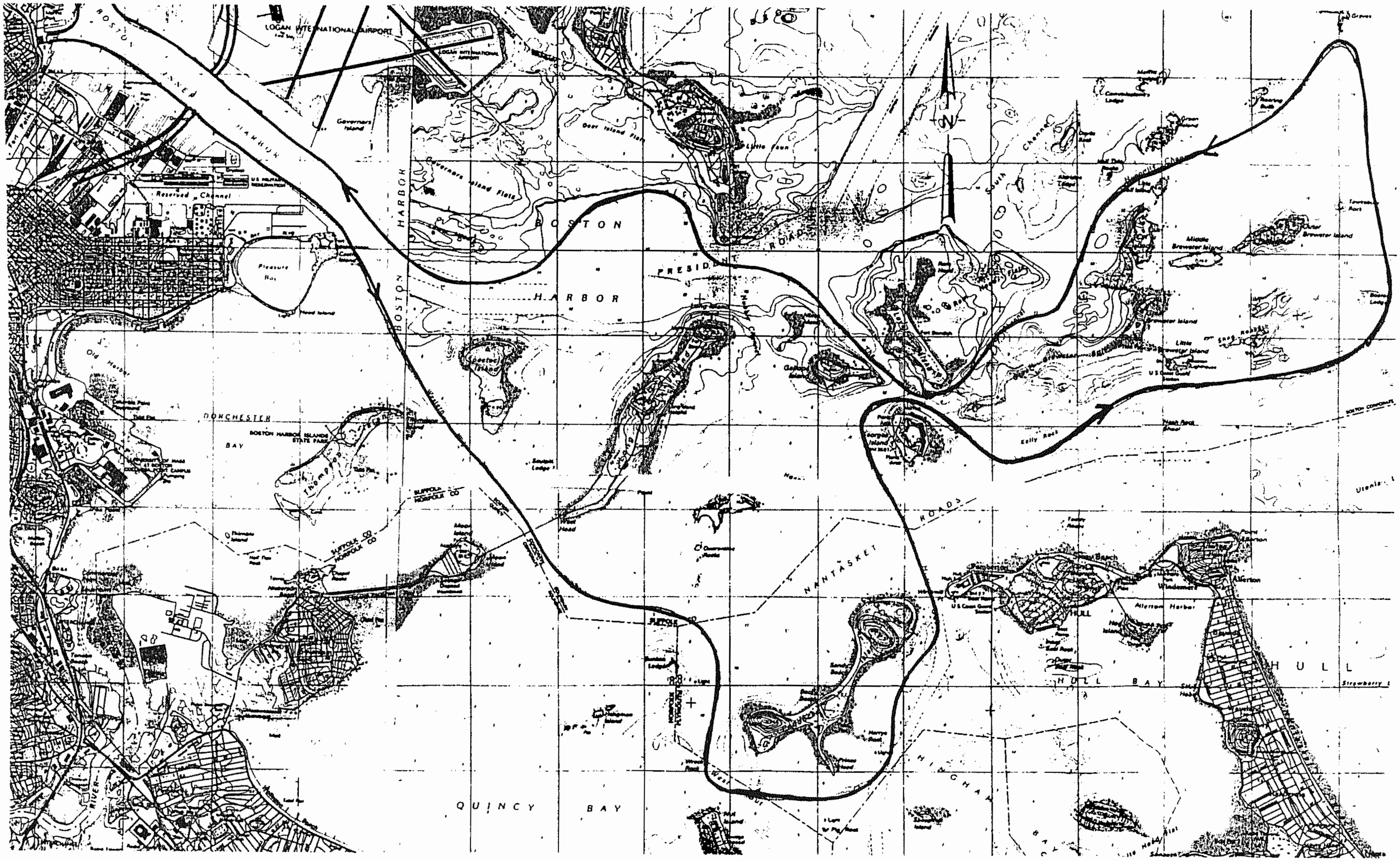

Fig. 2 NE-AEG BOSTON HARBOR TOUR ROUTE.

FIELD TRIP #24

England, which was located in the parish of St. Botolph. St. Botolph was the patron saint of fishing, thus establishing Boston's roots.

From its earliest beginnings, Boston flourished as a great port. In the eighteenth century, the Harbor Islands became popular resort areas. When a wave of social reform swept over Boston in the nineteenth century, the islands furnished a convenient place to establish hospitals, prisons, poorhouses, dumps and military installations. When the government withdrew its interests in the islands after World War II, unfortunately, so did almost everyone else. A long period of neglect began. The former locations of some of the country's most progressive hospitals and prisons became graveyards for outmoded institutions and desolate repositories for society's castoffs, including human waste.

GEOLOGICAL INFLUENCES AFFECTING THE FOUNDING OF BOSTON

Three major geological factors influenced the founding of Boston. First, it provided a safe harbor for the early settlers, who were a seafaring people. Boston's island-studded harbor is formed by a deep indentation in the coastline of Massachusetts. The indentation exists primarily because the sedimentary rock underlying Boston is softer and more easily eroded than the crystalline basement rocks surrounding it. Glacial ice eroded a depression in the softer rocks of the Boston Basin, as this large topographic and structural depression is called. Subsequent melting of the ice caused the sea level to rise and flood the depression forming Boston Harbor.

Second, the land of the Shawmut Peninsula provided the settlers with protection from their enemies. Boston was naturally situated for fortifications, with its Trimountain rising 150 ft. above the surrounding land. Further, the 789-acre Shawmut Peninsula was an island at high tide. The land to the south, called the Neck, that connected Roxbury and Boston, was very narrow and low, and at best served as a causeway for travelers.

The third primary geologic factor was the abundant fresh water available to the settlers. The Shawmut Peninsula became the Town of Boston because several good springs were found there, and the shallow dry wells produced water of good quality under artesian pressure.

These factors all contributed to a notable population increase and considerable development of the Shawmut Peninsula during the 17th and 18th centuries. In order to meet the needs of development and expansion, early land developers looked to the three hills of the Trimountain as a ready source of fill for the surrounding marshy lowlands.

In 1799, about 60 ft. of Mt. Vernon was excavated to fill in the cove at its base, creating Charles Street. The Mill Pond created in 1643 was the next area attacked in the enthusiasm for increasing the land area of Boston. John Hancock's heirs lowered the peak of Beacon Hill by 60 ft. and filled in the pond. The top of the last hill, Pemberton Hill, was shaved off in 1835 to produce new land north of Causeway Street and to develop Pemberton Square. The ridge connecting the former peaks of Pemberton and Beacon Hill was leveled in 1845.

Hills around Boston, including many of the harbor islands, consist of complex mixtures of overthrusted moraine and glaciomarine sediments representing multiple periods of glacial advances and retreats. Foundation excavations into Beacon Hill, the only remaining portion of Trimountain, have exposed deformed, faulted and folded units of clay, silt, sand and gravel overlying extensive fine-grained deltaic deposits.

The last major period of land expansion occurred during the latter half of the 19th century, when the Back Bay was filled with sand and gravel brought in by railroad. This filling of the bays around Boston has added character to the city, as well as creating a variety of engineering problems. It was a factor in social change and created a very peculiar patchwork street network, since each infilled area has its individual street pattern.

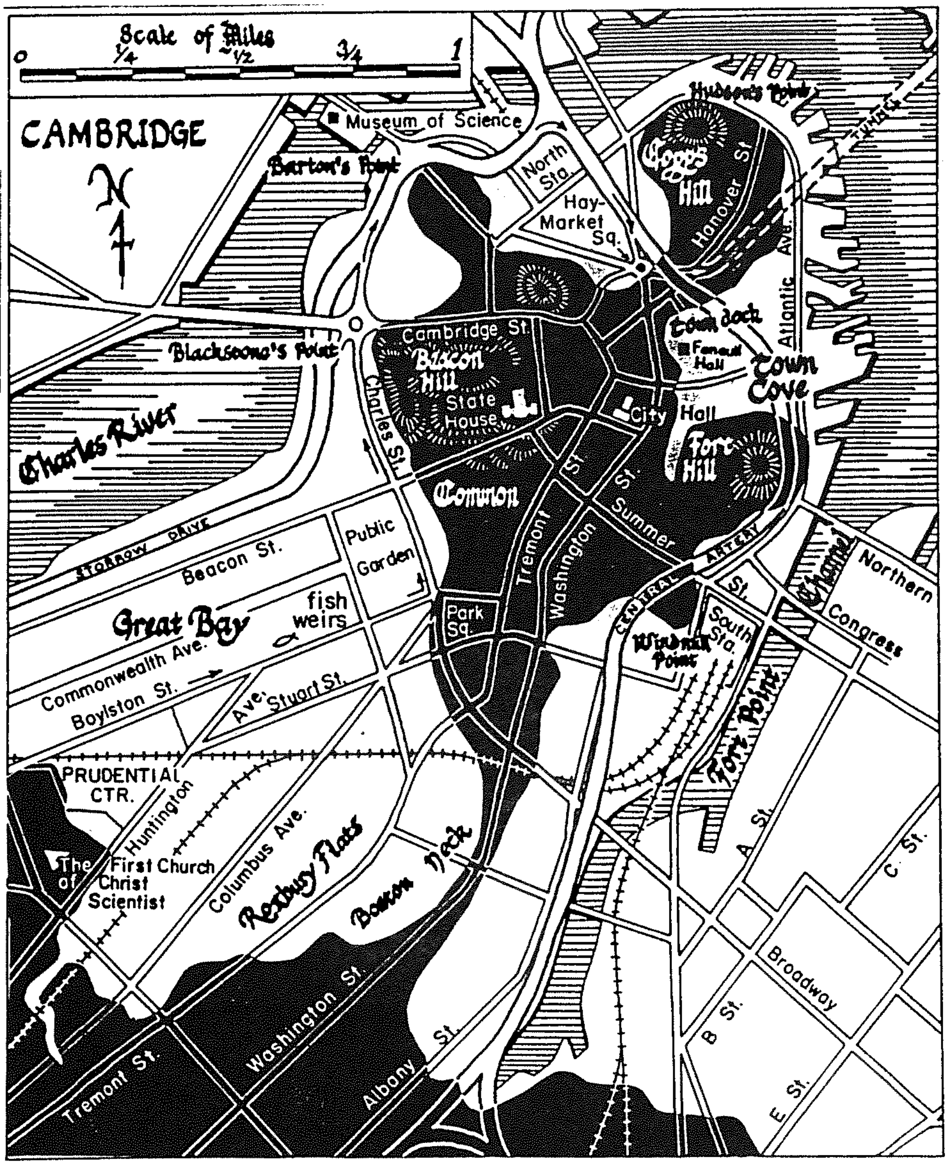

Fig. 3 1993 BOSTON SUPERIMPOSED ON 1632 BOSTON (BLACK).

HUMPHREY, HAGER AND WOODHOUSE

THE BOSTON HARBOR ISLANDS

Boston is entered from the sea via a broad bay dotted with many islands. Some of these islands consist of barren bedrock outcrops; many are tear-drop shaped hills called drumlins; a few may be erosional remnants of recessional moraines. All the harbor islands were wooded at the time of the first settlement, but they were soon cleared and converted to farmland.

Large vessels found the approach to Boston hazardous because of these islands and numerous shoals, particularly at low tide (the mean tidal range at Boston is almost 10 feet). Nevertheless, it was not until 1716 that a lighthouse was built on one of the rocky outermost islands. Although this lighthouse guided shipping to the entry of the harbor, it did little to help navigation through the tangle of natural obstructions inside. Hundreds of ships have been lost on the hidden rocks of Boston Harbor.

In a 1972 article in Yankee Magazine, Senator Edward M. Kennedy stated that "The Boston Harbor Islands are a rare combination of land and water resource - a resource that has a uniqueness not available in our parks and land preserves." Senator Kennedy went on to state that Boston Harbor and its islands should be restored and preserved as a parkland and recreation area. His views are shared by everyone who is familiar with the islands.

Because the Boston Harbor islands are accessible only by ferry or private boats, they are a relatively undiscovered paradise. Several million people live within a short drive of the Boston waterfront, but few realize the historical significance of the harbor, let alone the untamed beauty that awaits the adventurer beyond the crowded shoreline.

As the boat leaves Rowes Wharf in the Inner Harbor, you can look behind you up the Mystic River toward the former Charlestown Naval Yard and the Bunker Hill Monument. The historic U.S.S. Constitution is berthed there. The wooden masts of "Old Ironsides" can be seen nestled among new condominiums, boutiques and the headquarters of the MWRA.

LOGAN AIRPORT

As we travel to the islands, airplane traffic is very apparent. Logan International, the nation's eighth largest airport, is located to your left. The airport was constructed in the late 1940's by leveling a number of Inner Harbor islands and filling between them. Noddle, Bird, Governors, Apple and Hog Islands disappeared in the process. Governors Island had been one of the largest drumlin islands in the harbor. The island was granted to Boston's first Governor, John Winthrop, in 1632, and on it he planted a vineyard and the first apple and pear trees in New England. The Governor was reported to have taken great pride in his orchard, which had the reputation of being one of the finest in New England.

Today, the Inner Harbor is quite constricted. Mud flats and tidal marshes between Boston, South Boston and Charlestown, all once peninsulas, have been filled over the past two hundred years. Logan Airport alone occupies nearly 3000 acres of what was once harbor.

CASTLE ISLAND

Across the main harbor channel from the airport is a large crane used to unload containerized cargo from freighters. Located beyond the crane is Castle Island. Although it is now connected to the mainland, the connection was not constructed until the 1930's. Because of the island's key position, the fort located there played a major role in the defense of the Inner Harbor. Fort Independence, the venerable grandfather of all the Harbor's forts, is recognized as the oldest continuously used military

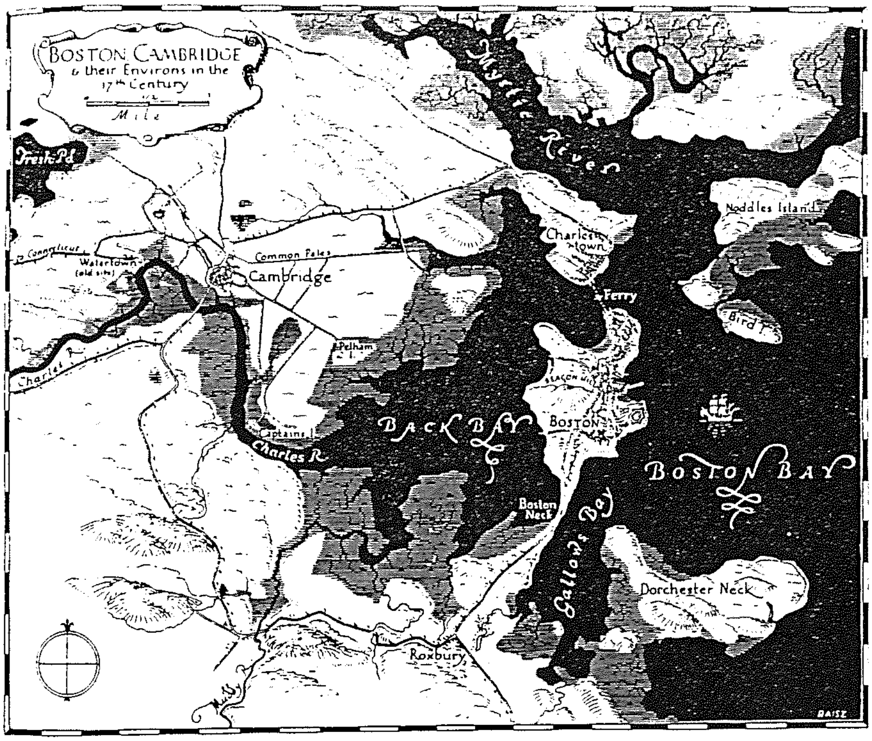

1690

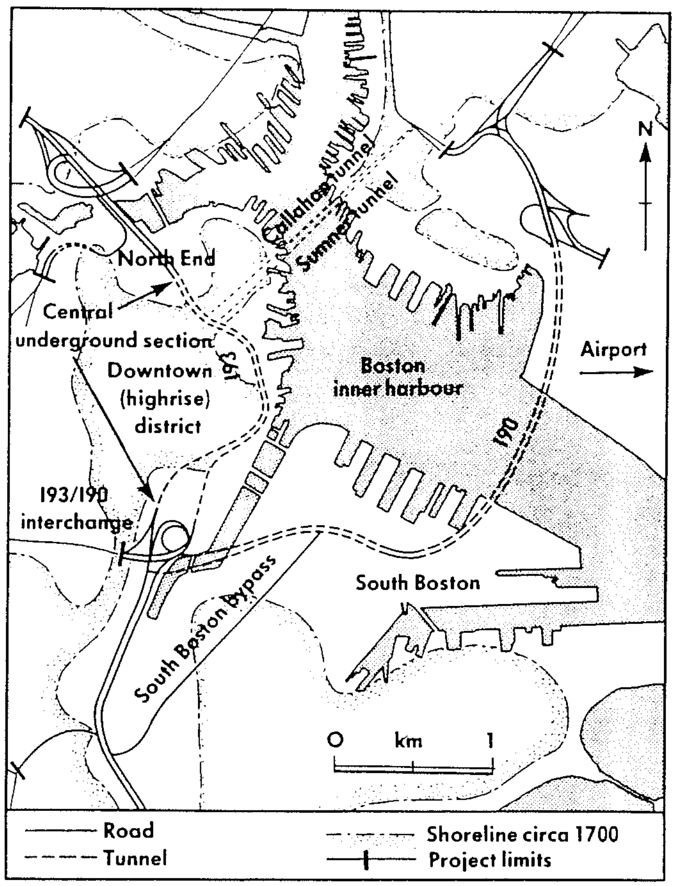

Fig. 4 BOSTON HARBOR 1990

fortification in the United States. The original stronghold, a "castle with mud walls," was replaced by a brick structure. After a fire destroyed this structure in 1673, it was replaced by a four-bastion stone fort named Castle William, in honor of England's king.

During the Colonial unrest, the Royal Governor and other Crown officials used the fort as a refuge from irate Bostonians. The British held Castle William until they evacuated Boston in March of 1776. Before the troops sailed, they blew up the fortification and destroyed its ordnance. The current fort was initiated by President John Adams in 1799 and named Fort Independence.

One of its more famous tenants was young Lt. Edgar Allen Poe, who used the fort for background in several of his novels. Over the years, Castle Island was the site of the first state prison and New England's first marine hospital, as well as an important observation post in both world wars. It is currently owned by the MDC and maintained by the Friends of Fort Independence as a popular historic and living history museum.

SPECTACLE ISLAND

Spectacle Island, on your left, has as diverse a history as any of the islands in the harbor. Lying between Castle and Long islands, the 97-acre Spectacle was originally formed by two drumlins connected by a low sandbar. Named for its resemblance to a pair of eyeglasses, the island was once covered by timber, which was used by early Bostonians for firewood. Through the years the island has been used for lumbering, pasturage, the site of two resort hotels, a rendering plant for dead horses, a plant which extracted grease from garbage, and until recently a dump for the City of Boston.

Today, Spectacle is littered with broken glass and rubbish. The island's shoreline is mostly rocky and in places is composed of cliffs of decomposing trash, an attraction for gulls and rats, the island's only occupants. As the steep banks of the dump area continue to erode, layers of rubbish are exposed, often to be washed away with the outgoing tide. Spectacle Island's future, however, looks much brighter. All the fill from the Third Harbor Tunnel and other Central Artery projects currently underway will be used to cover the "spectacle" in the harbor and create a new harbor island park.

THOMPSON ISLAND

If Spectacle Island is the ugly duckling of the Harbor Islands, Thompson Island, on your right, is the heralded beauty. Lying just off the Squantum section of Quincy, Thompson consists of 157 acres, some 50 acres of which are salt marsh. Trees, wild flowers and open fields cover the entire island. On the northeastern end is a fine beach. A long sandbar extends from the southern portion, nearly connecting the island with Squantum Head at low tide.

Thompson Island was used for farming until the 1880's when farming and education merged in a center for vocational training. The educational aspect of the island continues today at The Thompson Education Center with programs relating to the environment.

LONG ISLAND

A tall, red-and-white-checked tower marks Long Island, which with 213 acres is the largest island in the Boston Harbor and is the only true island accessible by bridge. When the Long Island Company purchased the island in 1849, the "Long Island House" and the "Long Island Hotel" were built with the intention of developing a summer resort area. However, with the onset of the Civil War, Union troops were quartered in these residences and the resort was never developed.

Fortifications on Long Island Head were started in 1863 and renovated for use during World War II. Some of Long Island's defenses reached the age of the guided missile with the installation of a Nike missile site, which is now abandoned.

Long Island eventually became the site of a chronic disease hospital operated by the City of Boston, and is now used as a shelter for Boston's indigent population.

MOON ISLAND

The boat passes under the steel bridge connecting the forested west end of Long Island to Moon Island. The extensive erosion at the base of the bridge supports is a dramatic illustration of the effects of the storms and tide that have been at work on all of the islands. Moon Island contains four huge granite storage tanks, constructed as part of Boston's sewer system in 1884. Capable of holding fifty million gallons of raw sewage, these tanks were connected to Boston by a 7-1/2-foot diameter brick sewer. The sewage was released with the outgoing tide. At the time it was constructed, this system attracted nation-wide attention as a solution to pollution in Boston's Inner Harbor!

RAINSFORD ISLAND

Rainsford Island, lying just southeast of Long Island has an area of only 11 acres. Its dominant feature, a drumlin at the eastern end, gives the island a gentle sloping profile toward the rocky western head. The island was originally granted to Edward Rainsford for use as a farm in about 1636.

Two quarantine fever hospitals were formerly located on Rainsford. In 1852, the entire island was converted into a pauper colony for the City of Boston. The women inhabited the structures on the eastern bluff, while the men resided in those on the western head.

Today, brightly-colored tents dot Rainsford Island's meadow and shores, during the summer. It is perhaps the favorite island in Boston Harbor for camping and picnicking.

NUT ISLAND

Once a four-acre island, Nut Island is now a man-made peninsula about 17 acres in size, attached to Quincy on the mainland. The Nut Island and Hull peninsulas form the pincers that separate Quincy Bay from Hingham Bay. In colonial times, cattle grazed on the island and were driven back to the mainland over a sandbar at low tide.

In 1876, a foundry company established a testing site for heavy ordnance on the island. Fifteen-inch guns fired projectiles weighing as much as 500 pounds at targets on Peddocks Island. In the 1890's the MDC took over the island and built a sewage treatment facility. In 1950 the MDC replaced this facility with a primary sewage treatment plant. Together with the Deer Island sewage treatment facility, the Nut Island plant handles Boston's sewage wastes. A deep tunnel is currently being drilled between Nut Island and Deer Island as part of the MWRA's harbor cleanup program. When it is completed, sewage will be transported to the Deer Island plant via the tunnel for treatment.

PEDDOCKS ISLAND

Peddocks Island is charmingly diverse. Behind the dock to the left is a pretty white clapboard chapel, and behind it rises a forested hill to 123 feet, the highest elevation on the harbor islands. To the right is one of the restored brick buildings of Fort Andrews, now a visitor's center operated by the MDC.

Peddocks has the distinction of being the site of the oldest human remains found around Boston Harbor. A male skeleton found on the island in 1971 has been determined by carbon-dating to be 4100 years old.

The interior of the 188-acre island contains a dense forest, salt marsh, small cottage community and the remains of Fort Andrews. This complex of handsome brick buildings was constructed around 1900 by the U.S. Government. During World War II, 2,000 Americans were stationed here, along with 1,000 Italian prisoners. A guided walk takes you past the barracks, stable, bakery, gymnasium and rows of compact officers' houses. Peddocks is a favorite camping site during the summer months.

GEORGES ISLAND

Georges is the most easily identifiable island in Boston Harbor because of its massive granite fortress. It is 28 acres in size and is one of the most historic sites in the City of Boston. The walls of this fort were constructed of granite brought by ship from Quincy and Cape Ann; they are approximately 70 feet high and 8 feet thick, enclosing an area of about 12 acres. The design of Fort Warren follows earlier French models using a star-shape, similar to that of Fort Independence on Castle Island. The fort originally held three hundred guns and is surrounded by a dry moat 50 feet wide, which is spanned by a drawbridge at the main entrance. Crude defenses were constructed on the island in 1778 to protect the French fleet of Count D'Estaing, anchored off Peddocks Island, from the British warships prowling the outer harbor.

The United States Government purchased the island in 1825 and shortly thereafter, in 1834 began construction of Fort Warren. The fort was named after Major General Joseph Warren, a physician as well as President of the Provincial Congress, who was killed in the Battle of Bunker Hill in Charlestown.

During the Civil War, a trooper stationed at Fort Warren composed the renowned song "John Brown's Body," more commonly known as "The Battle Hymn of the Republic." Many prominent Confederates were imprisoned at Fort Warren, including James M. Mason and John Slidell, both commissioners representing the Confederacy abroad and Alexander Hamilton Stephens, the vice-president of the Confederate States.

Georges Island is now owned by the MDC and operated primarily for recreational purposes. On May 31, 1972, Georges Island was designated a National Historic Site. Two years earlier, Fort Warren had been recognized as a National Historic Landmark by the United States Department of the Interior.

GALLOPS ISLAND

Like so many of the Boston Harbor Islands, Gallops Island was abandoned after World War II and entered into a period of decay. Today, the decay has been arrested and restoration has begun. Debris has been removed, old buildings demolished and the island's general appearance improved.

The 16-acre Gallops, which lies just west of Lovells and Georges Islands at the entrance to Quincy Bay, offers a pleasant outdoor experience with a sandy beach, a profusion of wild roses in summertime, and a grassy knoll that commands a fine view of the entire harbor, especially the Boston skyline and Boston Light on Little Brewster Island in the Outer Harbor.

The island was named after its first owner, Captain John Gallop, a harbor pilot. It was farmed extensively in the 18th and early 19th centuries. From the 1830's until the Civil War, the island was a popular resort, featuring an inn and restaurant famous for its good chowder.

During the Civil War, 3,000 soldiers were encamped on Gallops. The island subsequently became the site of a quarantine hospital with an immigration station added in 1916. Just before World War II, the U.S. Maritime Services established a radio school on the island. After the war, the buildings were dismantled and the island abandoned.

THE BREWSTER ISLANDS

Facing out toward the vast Atlantic like lonely sentinels, the stark, windswept Brewsters mark the easternmost boundary of Boston Harbor. These islands of the Outer Harbor include Great Brewster, Little Brewster, Middle Brewster, Outer Brewster, Calf, Little Calf, Green, Shag Rocks and the Graves.

Like many of the islands of the Inner Harbor, Great Brewster is a drumlin, composed of deposits of glacial till and clay. The other islands of the Outer Harbor are rocky outcrops, formed as the ice sheet tore away pre-glacial soils and ground down the hills to Precambrian bedrock. The Brewsters may once have been a single land mass the became separated into a series of smaller islands through continuous erosion by the wind and sea. At low tide, when the shallow water surrounding the islands recedes to reveal partially submerged boulders and sandbars, it is easy to see how that islands might have originally been connected.

This group of islands was named in 1621 after Elder William Brewster, a preacher at the church of the Plymouth Bay Colony. He had come to Boston Harbor on an excursion with Captain Myles Standish and Squanto, their Indian guide.

GREAT BREWSTER

The first recorded inhabitants of Great Brewster were a small colony of fishermen who established a settlement on the island in 1840. Fish and lobsters were caught in abundance among the craggy rocks just offshore. In 1871, Augustus Russ, founder of the Boston Yacht Club, purchased the island and built a summer villa there. He then leased several lots to other summer residents.

Today, the island is inhabited only by seagulls and rats. Traces of human habitation remain as stone walls and foundations of old summer homes.

OUTER BREWSTER

The most easterly of the Harbor Islands, 17.5-acre Outer Brewster is also the largest outcrop of solid bedrock in the Harbor. Its rugged terrain contrasts dramatically with the more protected and placid islands in the Harbor. Several acres of grass and brush grow on the island, but nary a tree.

The island was purchased in 1799 by Nathaniel Austin and remained in his family for many years. One of Austin's sons, Arthur, quarried diabase on the island for building purposes. Several roads and buildings still extant in Boston are believed to have been constructed with the rock from Outer Brewster. According to one report, Austin intended to turn the quarry site into a harbor. A cove on the northeast part of the island marks the site of the former quarry and proposed harbor.

In 1941, the U.S. Army took over the island and built Battery Jewell, a completely self-sufficient installation including a desalinization plant. Personnel were housed in three reinforced concrete barracks. The battery itself, which was bomb- and chemical-proof, was built into a manmade hill containing tunnels and ammunition storage rooms. After the war, the site was deactivated, and in the early 1950's, the island was sold as surplus property. The deserted concrete barracks and Battery Jewell still stand, silent testimony to the island's importance during World War II.

LITTLE BREWSTER

Little Brewster is a narrow elongated outcrop of rock known mainly for Boston Light, the oldest lighthouse in North America. As 18th-Century Boston became a booming port, merchants and shipowners realized the need for a powerful beacon at the Harbor entrance to guide incoming ships. From the time it was erected in 1716, Boston Light has played a strategic as well as navigational role.

During the Revolutionary War, British and American forces vied for control of Boston Light. In 1775, the Redcoats captured the Light and blocked entrance to the Harbor. When the British evacuated Boston in March 1776, British marines blew up Boston Light. Because of its strategic importance, however, the Light was rebuilt in 1783 by the State of Massachusetts. In 1790, the Federal Government took possession of both Little Brewster and the Lighthouse.

The War of 1812 found the British once again in Boston Harbor. Within sight of Little Brewster, the British ship Shannon engaged the American frigate Chesapeake. The Shannon won the battle, but immortality went to the Americans in the end, when wounded Captain James Lawrence of the Chesapeake shouted his famous command, "Don't give up the ship!"

Today, the 98-foot high granite lighthouse is operated by the U.S. Coast Guard. Accompanied by blasts from a foghorn, its beacon, flashing at 10-second intervals, shines 16 miles out to sea. Boston Light has been declared a National Historic Landmark.

THE GRAVES

The outermost light in Boston Harbor, Graves Light was built by the Federal Government in 1905 on an outcrop of diabase known as Graves Ledge. The light marks the main entrance to Boston Harbor and the most northerly point of the Brewsters. The gray, 93-foot high granite structure is manned. Its beacon, flashing twice every six seconds, shines 16 miles out to sea.

The island was named for Thomas Graves, a vice-admiral in the fleet of 17th century Massachusetts Governor John Winthrop. The name is appropriate, for it also evokes the shipwrecks that claimed so many lives in its vicinity. It has even been said that the rocks look like headstones, marking the watery graves of the drowned.

GREEN ISLAND

Green Island is a desolate two-acre rock outcrop covered with scrubby bushes and weeds. The island is named for Joseph Green, a well-known merchant who owned the island in Colonial times. The only human inhabitants of the island have been an occasional hermit. Since access is unsafe and the island is an active nesting area for gulls and cormorants, public use is discouraged. As we pass the island, however, note the erosion along its shore; this is in part due to the changing of patterns of ocean currents resulting from the dredging and filling of Boston Harbor.

CALF ISLAND

Directly north of Great Brewster is Calf Island, a flat 17-acre rock mass covered with weeds and high grasses. A shallow brackish pond surrounded by tidal marshes lies in the middle of the island, which supports wildlife consisting of gulls, rats and rabbits.

Calf Island is sometimes referred to as "the Home of the Lonely Grave." According to an old account, an unknown ship was wrecked and washed up on the island's shore. The unidentified crew members were buried by fishermen on the island in unmarked graves.

During the 19th century, Calf was inhabited by a small colony of lobstermen, and in 1883, the island was the site of illegal Sunday boxing matches.

Benjamin P. Cheney and his actress wife, Julia Arthur, purchased the island in 1902 and built a mansion on a cliff overlooking the southeastern shore of the island. The remains of these buildings - ruins of foundations and two stone chimneys, bearing the initials "B. P." (Cheney) - are still visible. The main house and boathouse were destroyed by fire after World War II. In 1971, vandals torched the remainder of the estate.

Archaeological explorations have turned up several artifacts - fragments of china, gold and silver buttons - which suggest that Calf Island may become an important historical site.

LOVELLS ISLAND

Lovells Island, situated directly north of Georges, is the flattest island in Boston Harbor. It covers an area of approximately 62 acres and is distinguishable by two long sandy beaches on both the harbor and ocean sides. The water on the eastern shore is deep, and popular with swimmers and boaters.

This island was named around 1630, after Captain William Lovell, a Boston merchant. Europeans used it for timber, fishing, as a residence for keepers of Boston Light and as a rabbit run.

Military use of Lovells began in 1643, when the island provided timber and firewood for the fort on Castle Island. Purchased by the Federal Government in 1825, Lovells provided a training ground for the 18th New Hampshire Volunteer Infantry. Construction of a major defense facility, Fort Standish (named for Pilgrim Myles Standish), began in 1900. The fort was expanded and used throughout World War II.

Two tragic shipwrecks have occurred off the treacherous shores of Lovells Island. In 1782 the "Magnifique," a French man-of-war under the command of Admiral Vaubaird, struck a protrusion of the "Ram Head Flats" on the northeast shore, now called the "Man-of-War Bar." The vessel sank almost immediately, carrying with it a cargo of gold and silver that has never been recovered.

Just four years later, during a severe winter storm in 1786, a passenger ship was hurled upon these same treacherous flats. The passengers fled to the summit of the island's only hill where they hid behind a huge boulder. The next morning all were found, dead from exposure, still huddled behind the rock. A young man and his bride were found frozen to death, still locked in each other's arms. Since then, this boulder has been appropriately named "Lover's Rock."

HUMPHREY, HAGER AND WOODHOUSE

NIX'S MATE

Located just northwest of Gallops Island is a huge black-and-white cement pyramid perched on a square granite base. This unusual looking structure, built in 1805, marks the location of a former island known as Nix's Mate. The island itself has been eroded away by the wind and the sea, leaving behind a rocky sandbar visible only in low tide.

During the 17th century, several pirates who had been convicted and executed in Boston were transported to Nix's Mate for burial. Two pirates, Samuel Cole and Henry Greenvill, were buried on Nix's Mate; a third, William Fly, was hung there in chains and left to die, serving as a warning to other pirates.

DEER ISLAND

Deer Island is a 210-acre peninsula extending southeast from Point Shirley in the City of Winthrop, overlooking President Roads, the main shipping channel into Boston Harbor. Formerly a true island, it was connected to the Town of Winthrop in 1936 by filling of a narrow channel called Shirley Gut. The island's name was derived from the deer that were found there during Colonial times. Until recently, Deer Island consisted of three drumlins, the largest of which in the center rising to approximately 120 feet.

In the past, Deer Island was best known for its prison. In 1676, during King Philip's War - that ferocious Indian uprising against Massachusetts colonists - captured Indians were imprisoned on the island. A reformatory was built in the mid-19th Century; the facilities included a piggery and cemetery. The reformatory was converted into the Suffolk County House of Correction in 1896. Hill Prison, a 5-story brick and granite structure, was built in 1904 and operated until it was razed in 1992.

At the beginning of the Second World War, the U.S. Army fortified the southern tip of Deer Island. This complex of bunkers and watch towers, known as Fort Dawes, served as the Harbor Entrance Command Post.

Today, the original landscape of Deer Island has been totally rearranged as a result of the construction activity associated with the expansion of the MWRA's Wastewater Treatment Facility, the lynchpin in the EPA-mandated Boston Harbor cleanup. Fort Dawes and Hill Prison are gone. The glacial material composing the central drumlin has been largely used to create "landforms" at the northern and southern ends of the peninsula to make the new sewage treatment facilities less visible to Deer Island's neighbors. Work is proceeding on both the inter-island deep rock tunnel to Nut Island and the nine-mile-long outfall tunnel that will carry treated sewage out into the Atlantic Ocean. As Deer Island rapidly approaches the status of a small city, the mega-billion dollar MWRA Wastewater Treatment Facility rises like a Phoenix from its ashes!

PRESIDENT ROADS

We have completed our whirlwind tour of Boston Harbor, with its complex of islands, and are now returning to the Inner Harbor by the main shipping channel, President Roads. If time allows, we will pass into the Inner Harbor for a quick look at "Old Ironsides."

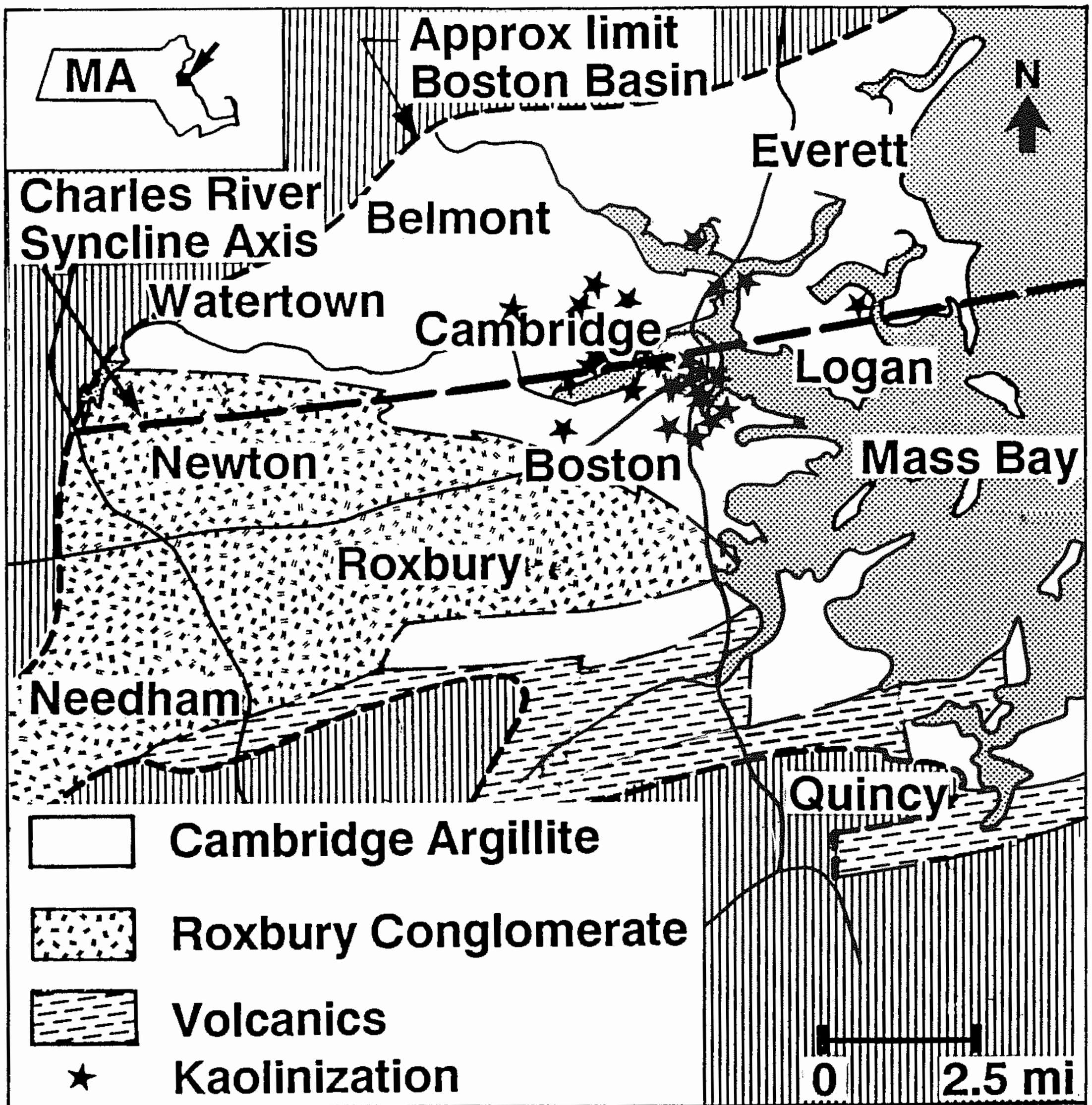

Legend:

Cambridge Argillite with minor sandstone, conglomerate and tuff

Roxbury Conglomerate with minor argillite and sandstone

Volcanic rocks, granites, diorites and gabbros

★ Areas of known kaolinization

GEOLOGIC MAP OF THE BOSTON BASIN

REFERENCES CITED

1. Barosh P., Kaye, C.A., and Woodhouse D., 1989, Geology of the Boston Basin and Vicinity: Journal of the Boston Society of Civil Engineers, v. 4., No. 1, p. 39-52.

2. Kales Emily and David, 1976, All About the Boston Harbor Islands: Herman Publishing Inc., 112 p.

3. Kaye C.A., 1976, The Geology and Early History of the Boston Area of Massachusetts, A Bicentennial Approach, Washington, D.C.: U.S. Government Printing Office, 77 p.

4. Mikal, A., 1973, Exploring Boston Harbor, N. Quincy: The Christopher Publishing House, 112 p.

5. Snow E.R., 1971, The Islands of Boston Harbor; New York: Dodd, Mead & Company, 251 p.

6. Woodhouse, D., 1989, The History of Boston: The Impact of Geology: Journal of the Boston Society of Civil Engineers, v. 4, No. 1, p. 33-38.

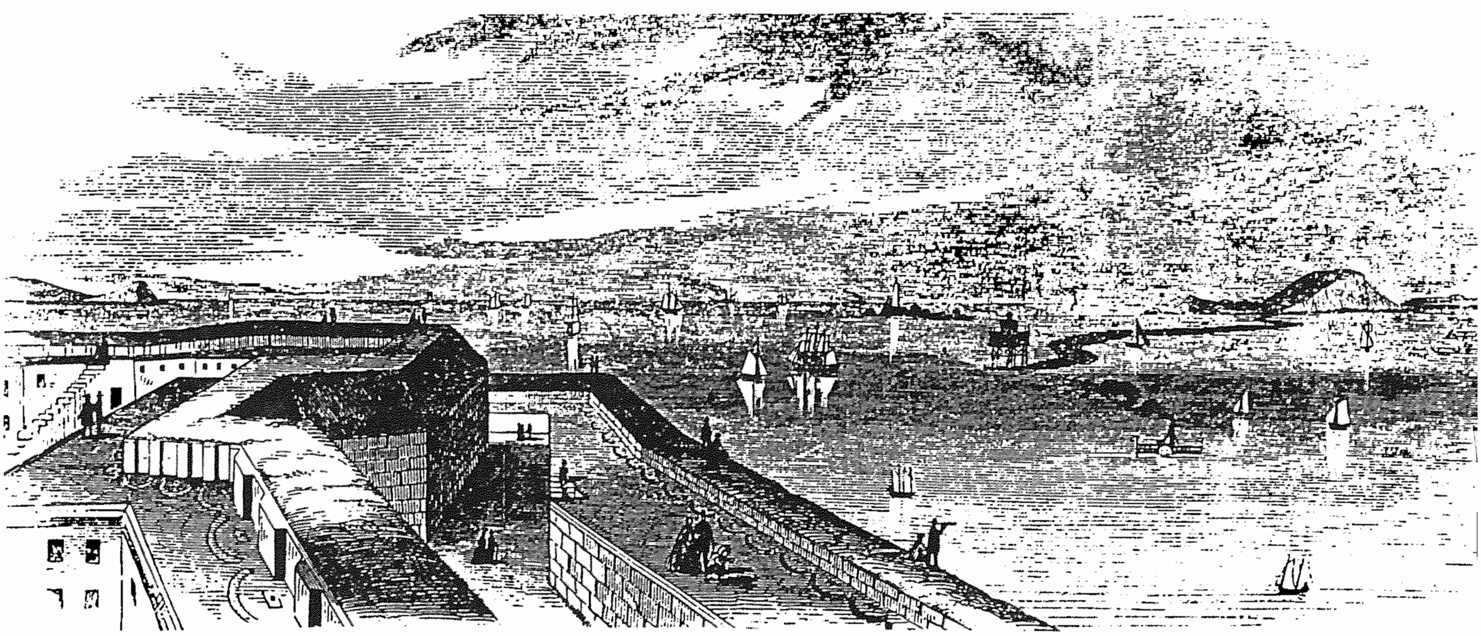

VIEW OF OUTER BOSTON HARBOR FROM FORT WARREN, 1857

Chapter X

The Avalon and Nashoba Terranes (Eastern Margin of the Appalachian Orogen in Southeastern New England)

By J. Christopher Hepburn, Rudolph Hon, Gregory R. Dunning, Richard H. Bailey, and Kenneth Galli

Field Trip Guidebook for the Northeastern United States: 1993 Boston GSA

Volume 2
Contribution No. 67, Department of Geology and Geography, University of Massachusetts, Amherst, Massachusetts

THE AVALON AND NASHOBA TERRANES (EASTERN MARGIN OF THE APPALACHIAN OROGEN IN SOUTHEASTERN NEW ENGLAND)

by

J. Christopher Hepburn,[1] Rudolph Hon,[1] Gregory R. Dunning,[2] Richard H. Bailey, [3] and Kenneth Galli[3]

1. Dept. of Geology & Geophysics, Boston College, Chestnut Hill MA 02167
2. Dept. of Earth Sciences, Memorial Univ. of Newfoundland, St. John's, Newfoundland, Canada A1B 3X5
3. Dept. of Geology, Northeastern University, Boston, MA 02115

INTRODUCTION

The Boston area contains one of the best examples of "Avalonian" geology outside of the type area in eastern Newfoundland and the Boston-Avalon Terrane, together with the Nashoba Terrane to the northwest, make up the eastern margin of the Appalachian orogen in southeastern New England. The outboard Meguma Terrane of Nova Scotia presumably lies off shore but is not present on land at this latitude. This excursion is designed to show participants the important features of the Boston-Avalon and Nashoba Terranes and to visit many of the "classic" exposures. In addition, we will discuss new work on geochemistry, sedimentology and particularly exciting, new U-Pb isotopic age determinations that are leading to revised interpretations and models for the geological history of this area.

The Boston area and its rocks have been visited by geologists for nearly as long as geologists have existed in the New World (see Rodgers et al., 1989), so that even the hammer marks on the outcrops must bear a distinct chronology. Dozens of guidebooks and hundreds of articles have been written over the last two centuries, yet despite this long history and the many geologists who have worked here (or perhaps because of it) few exposures are entirely without controversy, as we shall see. Given the scope of this guidebook it is impossible to adequately credit or discuss all the work that has led to our current understanding of the Boston area, and we apologize to those whose work we are too constrained to credit. Recent field guides pertaining to eastern Massachusetts with more complete descriptions of many of the exposures we'll visit include several (in 1964, 1981, 1984 and 1986) put out by the New England Intercollegiate Geological Conference (NEIGC), an organization dedicated to field excursions that is nearly as old as the Geological Society of America itself, and one prepared for the 28th International Geological Conference (Zen, 1989). The Bedrock Geological Map of Massachusetts (Zen et al., 1983) is the most recent regional compilation of the geology. U.S.G.S Professional Paper #1366 E-J (Hatch, 1991) accompanies this map and contains a thorough summary of the areal geology and an extensive bibliography on eastern Massachusetts. Geological Society of America Special Paper #245 (Socci et al., 1990) provides recent summaries of some of the specific geologic problems we face in the Boston area.

BOSTON-AVALON TERRANE

Overview

The Boston-Avalon Terrane contains many features similar to the type Avalon of eastern Newfoundland including those critical for establishing it as a fragment of "Avalonia," a 590-630 Ma calc-alkaline plutonic-volcanic event and Cambrian platformal sedimentation with an Acado-Baltic fauna. However, the Boston area has been eroded to a somewhat deeper level than eastern Newfoundland. Indeed, at current levels of erosion the most widespread rocks are plutonic (Zen et al., 1983). Late Proterozoic sedimentary rocks are only exposed in the Boston Basin itself, and a thin vestige of the Cambrian sediments is all that remains of the early Paleozoic sequence.

The most abundant of the plutonic rocks (Figure 1) are those associated with the late Proterozoic (ca. 630-600 Ma, Zartman and Naylor, 1984) arc magmatism of the main pulse of Avalonian igneous activity (Figure 2). They are so abundant that we tend to relate all other events in the area to these rocks, as either "pre-" or "post-" this magmatism. These magmatic rocks include the calc-alkaline Dedham (Stop 1-4), Milford, Westwood (Stop 3-3) and associated granites, which together reach batholithic proportions. The Lynn, to the north of Boston (Stop 1-3), and the Mattapan Volcanics, to the south (Stop 3-4), are co-magmatic extrusive equivalents. A poorly preserved record of quartzitic sedimentation (Westboro Fm., Stops 1-5,1-6) and mafic volcanism that pre-date the late Proterozoic magmatism (Middlesex Fells Volcanics, Stop 3-1) are preserved largely as blocks and pendants in the plutons (Figure 3). Their age is not well constrained other than that they pre-date the Avalonian magmatism. Geochemistry

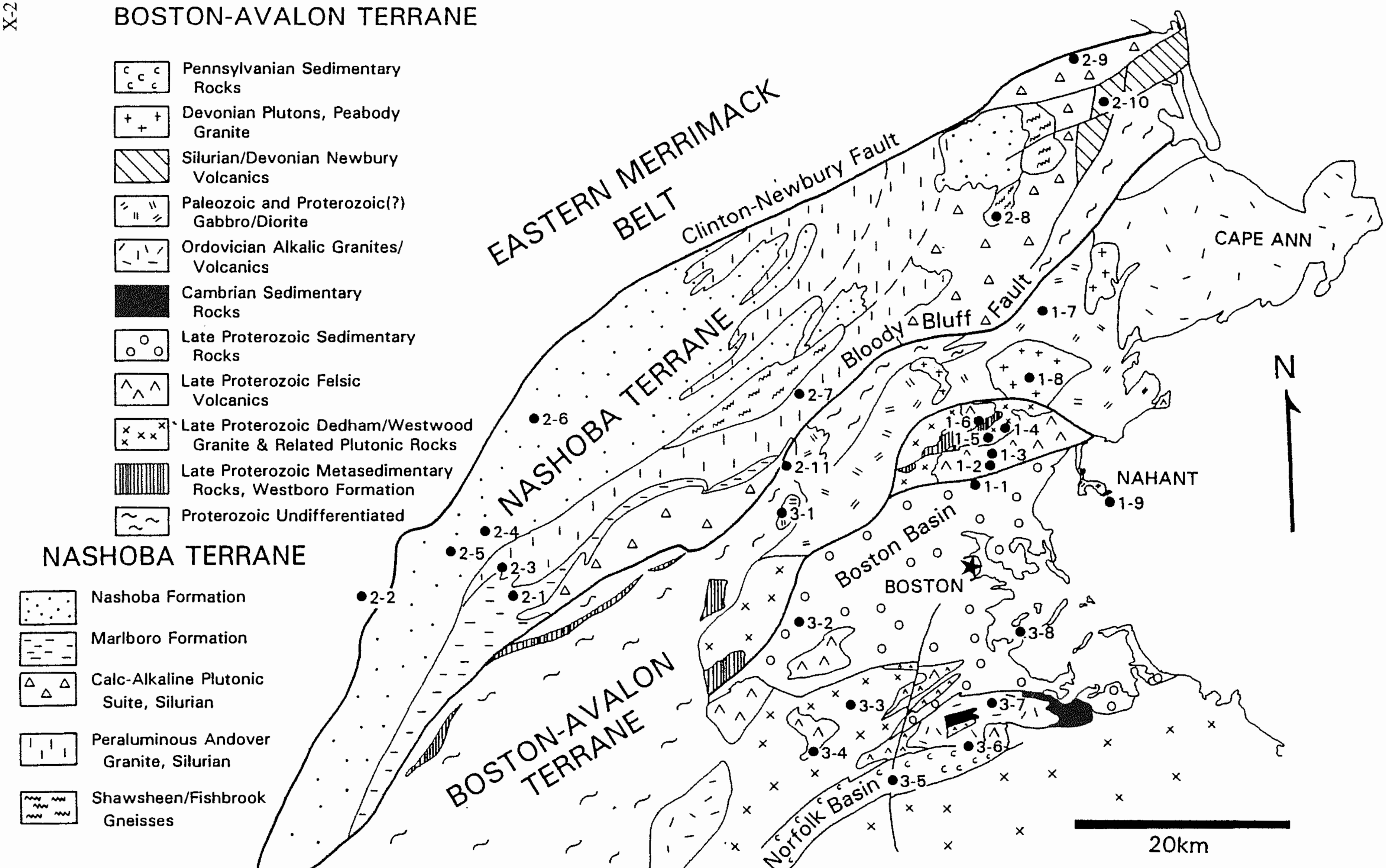

Figure 1. Geologic map of Boston - Avalon and Nashoba Terranes. Field trip stops are numbered dots.

indicates the Middlesex Fells Volcanics are alkalic (Cardoza et al., 1990) and likely formed in an extensional environment.

The Boston Basin developed as an intra-arc rift basin (Bailey, 1984; Nance, 1990; Socci and Smith, 1990) during the waning stages of the Avalonian arc magmatism. Acritarchs (Lenk et al., 1982) confirm the Late Proterozoic age of the Boston Bay Group sediments, which are of two principal types, conglomerates (Roxbury Fm., Stop 3-2) and shales (Cambridge Argillite, Stop 1-1). The depositional environment of the Boston Bay Group including the infamous Squantum Tillite or Tilloid (Stop 3-8) has long been debated. Terrestrial depositional models of glacial and/or fluviatile origin and those involving submarine mass-wasting are the leading contenders (Rehmer and Roy, 1976; Socci and Smith, 1990).

Following deposition of the Boston Bay Group, the area became a stable shelf or platform in the Early and Middle Cambrian (Figure 3) with deposition of the Weymouth (Stop 1-9) and Braintree Fms. (Stop 3-7). These units contain an Acado-Baltic trilobite fauna that allow correlation of the Boston area with the type Avalon and other Avalonian fragments (e.g., Rast and Skehan, 1983). There is no sedimentary record in the Boston-Avalon Terrane in Massachusetts with ages between Cambrian and Carboniferous (excepting for the Siluro-Devonian sediments within the Newbury Volcanic Complex; see below). During the Carboniferous, fossiliferous Pennsylvanian rocks (Stops 3-5, 3-6) formed as terrestrial deposits in rift basins.

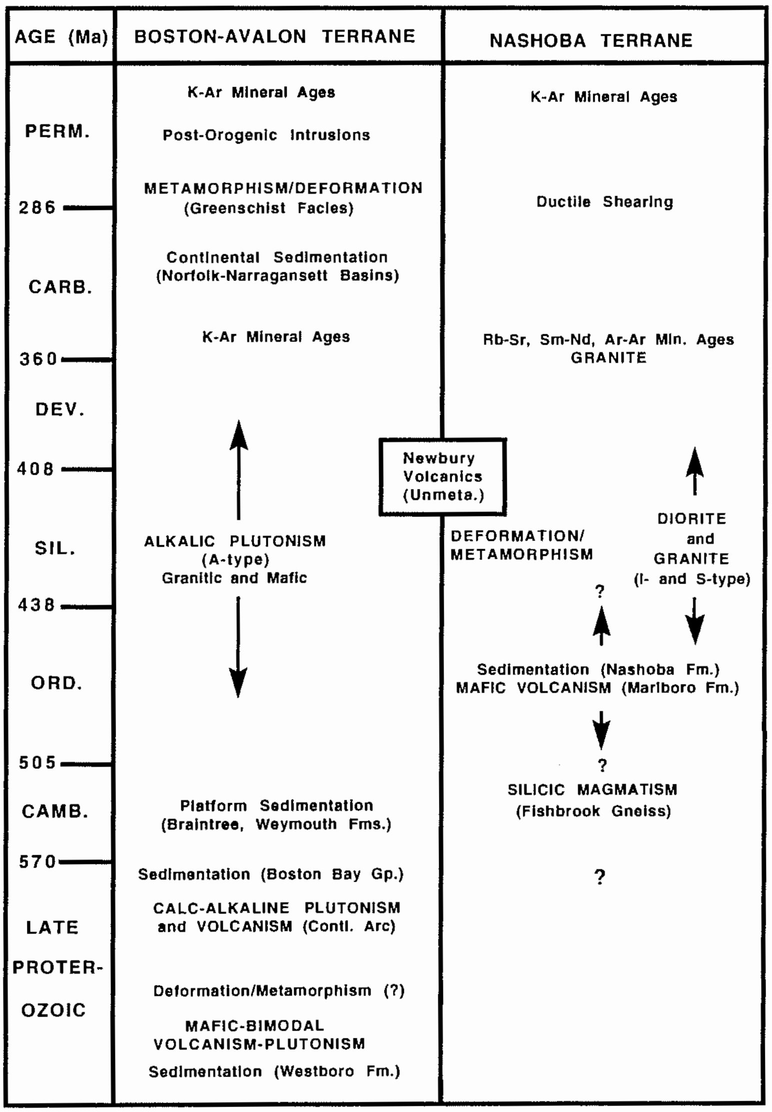

Figure 2. Comparisons of geologic events in the Boston-Avalon and Nashoba Terranes, Boston area, eastern Massachusetts.

From the Ordovician to the Devonian, the Boston-Avalon Terrane was broadly intruded by alkaline magmas quite different from the calc-alkaline ones associated with the earlier arc. These magmas, intruded in distinct pulses (Hermes and Zartman, 1985), include both granitic (Stop 1-8) and mafic plutons (Stops 1-7, 3-1) and local felsic volcanics (Hermes and Murray, 1990).

Metamorphism and Deformation

In the Boston area, the Boston-Avalon Terrane has experienced regional metamorphism no higher than the lower greenschist facies. Deformation, except along some of the major fault zones, is largely by brittle faulting. The metamorphism is generally thought to be largely Alleghanian in age. Alleghanian metamorphism clearly increases toward the south and the west. In southern Rhode Island, Pennsylvanian sediments in the Narragansett Basin are metamorphosed to upper amphibolite facies conditions (see Mosher et al., this volume, Chapt. BB). Evidence for Precambrian deformation and greenschist facies metamorphism preceding the Late Proterozoic arc magmatism is preserved in Rhode Island (Rast and Skehan, 1983; Skehan and Rast, 1983) but is difficult to decipher in the Boston area. Folded metasedimentary xenoliths found in the Dedham North Granite, north of Boston, are our best evidence for such an event.

Proterozoic and Paleozoic Sedimentary Rocks in the Boston-Avalon Terrane

Sedimentary rocks to be seen on this trip comprise the following four major depositional sequences:

1. Late Proterozoic Westboro Formation (Stops 1-5, 1-6)
2. Latest Proterozoic Boston Bay Group (Stops 1-1, 3-2, 3-8)
3. Early Cambrian Weymouth and Middle Cambrian Braintree Formations (Stops 1-9, 3-8)
4. Pennsylvanian Pondville and Wamsutta Formations (Stops 3-5,3-6)

Small amounts of fossiliferous Siluro-Devonian strata in the Newbury Volcanic Complex and areas of strongly deformed and metamorphosed Late Proterozoic metasedimentary rocks are also present but will not be examined on this trip.

Westboro Formation

Westboro strata are the oldest sedimentary rocks in the Boston-Avalon Terrane that have recognizable sedimentary structures and textures (Figure 3). The age of the Westboro is problematical, but must lie between 1500 Ma (the U-Pb age of contained detrital zircons, Olszewski, 1980) and the age of cross-cutting granitic plutons at 600 - 630 Ma (such as the Dedham North Granite at Stop 1-5). An age of 700 - 800 Ma is inferred for the Westboro based on possible correlations with better dated similar sequences in Newfoundland (O'Brien, et al., 1983). The Westboro is poorly exposed but is encountered as lenticular masses of quartzarenite, olistostromal mixtures of mudstone, quartzarenite and carbonate, quartzarenite turbidites and dark mudstones that generally have been subjected to no more than lower or middle greenschist facies metamorphism. Locally, these rocks are metamorphosed to the hornblende-hornfels facies immediately adjacent to plutons. Mafic Middlesex Fells Volcanics may be interstratified with the Westboro, but the relationship between these two formations is difficult to prove from field evidence. The Westboro has been interpreted as a platformal or cratonal sequence disrupted and subjected to gravity re-sedimentation during a ca. 750 Ma episode of ensialic rifting (Bailey et al., 1989).

Boston Bay Group

The Boston Bay Group consists of over 5 km of immature clastic sedimentary rocks and interstratified mafic Brighton Volcanics that rest unconformably on the Dedham Granite and/or Mattapan Volcanics (Figure 3). Of the two main units, the coarser clastics of the Roxbury Formation dominate the southern half of the Boston Basin, and finer clastics of the Cambridge Formation comprise most of the northern portion of the basin. The lower Cambridge is coeval and interstratified with the Roxbury, while the upper Cambridge onlaps the Roxbury to the south (Billings, 1976). The Roxbury is a heterogenous mixture of conglomerates, sandstones, and mudstones, capped by a thick diamictite or sequence of diamictites. The Cambridge Formation contains acritarchs that assign a Late Proterozoic age to the Boston Basin sediments.

Sediment compositions, facies relationships, and indicators of paleocurrent and paleoslope demonstrate that a rugged, largely granitic and felsic source terrain formed the southern and western margin of the Boston Basin. Inferred depositional environments and transport mechanisms include braided streams and fan deltas, submarine slopes

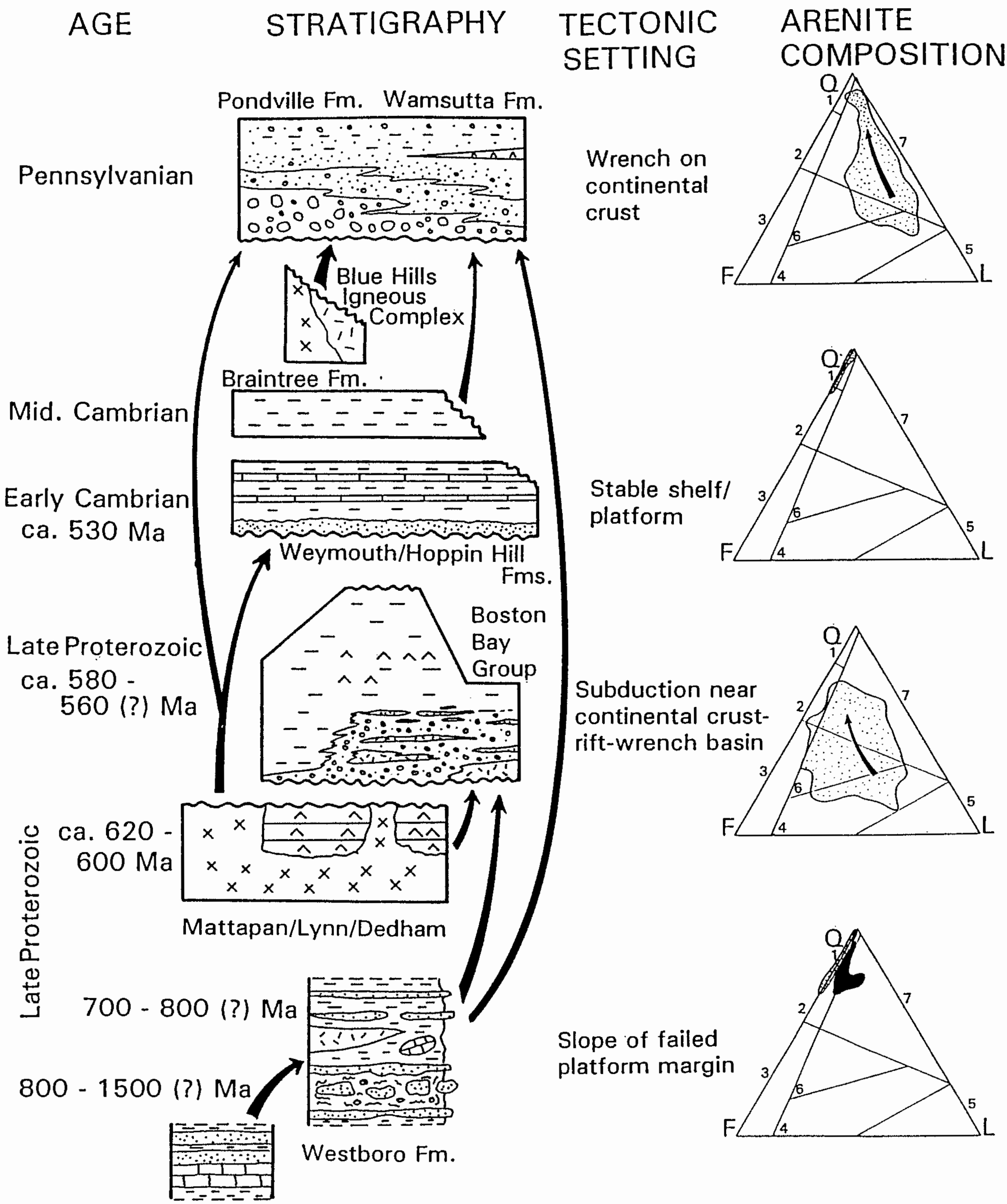

Figure 3. Summary of stratigraphy, tectonic setting, and sandstone composition of four sedimentary sequences in the northern part of the Boston-Avalon Terrane: Arrows link sedimentary sequences with primary source rocks. Q-F-L plots with tectonic discrimination fields, 1) craton interior, 2) transitional continental, 3) basement uplift, 4) transitional arc, 5) undissected arc, 6) dissected uplift, 7) recycled orogenic; black area in Westboro plot encloses Boston Bay Group quartzite cobbles; arrows show change in composition upsection.

and fans with debris and other sediment gravity flows, or a deep basin with distal turbidites. There is evidence that some facies may have formed on shallow shelves and glaciation may have played a role in the deposition of portions of the sequence. Geochemistry of the Brighton Volcanics (Cardoza et al., 1990) and compositions of detrital framework grains suggest that the Boston Bay Group formed in a tectonic regime where continental crust was involved with subduction (Figure 3). A fault bounded wrench or rift basin in a region of general crustal convergence would provide an appropriate depositional and tectonic setting for the Boston Bay Group.

Weymouth and Braintree Formations

The Early Cambrian Weymouth Formation consists of reddish to black thinly laminated mudstones, nodular mudstones, and reddish and white limestones. At the type area in Mill Cove, Quincy, MA, a mudstone and limestone interval with an Acado-Baltic small shelly fauna is overlain by mudstones bearing a *Callavia* zone trilobite fauna. Only the lower portion of the sequence is now exposed and the trilobite horizon has been covered for many years. Cambrian strata at East Point in Nahant, MA (Stop 1-9) correlate with the lower Weymouth of Mill Cove. At Nahant several 2 to 3 m thick limestones occur in at least 100 m of nodular, silty, trace fossil-bearing mudstone. Early Cambrian strata probably were deposited unconformably on the Boston Bay Group but are now isolated in structural blocks that were thrust over the Boston Basin. The Weymouth Formation and correlative fossiliferous strata at Hoppin Hill, North Attleboro, MA are shelf or platform facies deposited on stable crust. A more complete description and discussion of the Early Cambrian strata at Nahant, MA are given in Bailey and Ross in this volume (Chapt. Y).

The Middle Cambrian is represented by the gray mudstones of the Braintree Formation (Stop 3-7). The Braintree contains a low diversity trilobite assemblage including abundant specimens of the large species *Paradoxides harlani* (Green) and several species of inarticulate brachiopod and hyoliths. Middle Cambrian strata occur as roof pendants, xenoliths, and fault bounded blocks within or against the Quincy Granite.

Pondville and Wamsutta Formations

Pennsylvanian rocks of the Norfolk Basin (Figure 1) are an erosional outlier of the much more extensive Narragansett Basin in SE Massachusetts and Rhode Island. About 1500 m of strata are preserved in the Norfolk Basin in a tightly folded syncline. Along the NE margin of the basin, boulder conglomerates of the Pondville Formation (Stop 3-6) rest unconformably on the Blue Hills Igneous Complex or Mattapan Volcanics; but in most areas the basin is bounded by faults that juxtapose Pondville or Wamsutta Formations against older rocks (Figure 1). Plant fossil biostatigraphy suggests that deposition began in the early Middle Pennsylvanian (Westphalian B) in a local graben (preserved in part by the present Norfolk Basin) and extended south during the mid-Late Pennsylvanian (Stephanian) as the crust underwent further extension and general subsidence (Skehan et al., 1986; Mosher, 1983). Crustal extension and syntectonic deposition of immature clastics are attributed to wrenching along sinistral transcurrent faults that formed step-faulted pull-apart basins.

The Pondville Formation conglomerates and sandstones represent proximal to medial alluvial fan and braided stream deposits which intergrade upward into the reddish Wamsutta Formation sandstones and mudstones. The Wamsutta (Stop 3-5) is a sequence of fining upward braided channel cycles with intervals of red overbank mudstones. Abrupt crevasse splay deposits, broad gravel floored channels, abundant mudcracks, and poorly developed caliche nodule horizons suggest a monsoonal paleoclimate with a prolonged dry season.

Igneous Rocks of the Boston-Avalon Terrane

Most of the igneous rocks to be seen on this trip comprise two principal petrological suites that occur within three broad magmatic episodes:

1. Calc-alkaline arc magmatism associated with the late Proterozoic Avalonian event; 590 to 630 Ma: Dedham North Granodiorite/Granite (Stops 1-4; 1-5), Westwood Granite (Stop 3-3), Lynn (Stop 1-3) and Mattapan (Stop 3-4) Volcanics.

2a. Alkaline magmatism of the Late Ordovician (ca. 435 to 460 Ma) : Quincy Granite (Stop 3-7), diorite at Danvers (Stop 1-7).

2b. Alkaline magmatism of the Devonian (ca. 370 to 400 Ma): Peabody Granite (Stop 1-8); gabbro- diorite in Waltham (Stop 3-1)

Other plutonic episodes created the Cambro-Ordovician Nahant Gabbro (Stop 1-9) and the Jurassic Medford Dike north of Boston, while possibly other plutonic events remain to be identified.

Avalonian Calc-alkaline Magmatism

One of the defining criteria of the Avalon Terrane is the presence of extensive felsic volcano-plutonic complexes that yield emplacement ages between 590 and 630 Ma. Within the Boston-Avalon Terrane about a dozen or so separate plutonic bodies have been identified to date, and new ones are still being added to the list (Dillon and Hon, 1993; Hamidzada et al., 1993). Voluminous extrusive rocks are associated with this magmatism both north of the Boston Basin (Lynn Volcanics) and south of it (Mattapan Volcanics). These are co-magmatic or associated with the Dedham North (Smith and Hon, 1984) and Westwood granites (Kaye, 1984), respectively. The Brighton Volcanics (not visited on this trip) form flows and tuffs within the Boston Bay Group and likely represent the waning stages of arc magmatism (Cardoza et al., 1990).

Extensive calc-alkaline plutons both north and south of Boston have long been recognized and, although physically separated by the Boston Basin, have been commonly mapped together as the Dedham. We will be visiting only the Dedham north of Boston (Dedham North), a petrologically diverse suite that varies from granite to granodiorite, tonalite, and quartz diorite. An FMA plot and a Peacock diagram (Figure 4 A, B) illustrate the calc-alkaline nature of the rocks from the Dedham North suite. Chemical variations within the suite plot as a straight line (Figure 4 C, D) between felsic and mafic end members, implying a mixing of two magmas as the principal petrogenetic process. Fractionation would have produced a concave trend. Thus, the Dedham North formed largely by the mixing of two melts: (1) a leucogranitic magma formed by partial melting of Westboro Fm. sediments; and (2) an enigmatic mafic magma whose parental composition is not represented as part of the complex itself. Support for this model is seen in overlapping ages of the different rocks from this suite (see Figure 5) and the fact that inherited zircon components in the granite match detrital zircon ages in the Westboro (Olszewski, 1980). In addition, since the minimum granites cannot be the heat source for the anatexis of the sediments (because granites do not have high enough temperatures), the presence of a higher temperature mafic magma is required to drive the partial melting process. The mafic melt must have had a composition more mafic than that of the quartz diorite phase. It may be equivalent to some of the mafic dikes that cut the Dedham North (Stop 1-5) and that show "undulating" contacts, indicating both rocks were still liquid or partially so at the time of intrusion. These analyzed, apparently co-intrusive dikes tend to plot at the extrapolated end of variation diagrams (Figure 4 C, D). They have calc-alkaline geochemical signatures that suggest a convergent plate margin in continental arc or back arc setting.

Crystallization ages for the Dedham North suite fall between 606 and 609 Ma, while the geochemically similar dacites and rhyolites of the Lynn Volcanics are somewhat younger at 596 ± 3 Ma. Presumably the Lynn Volcanics formed a surficial cover over the slightly older volcano-plutonic suite, and most of the older volcanics were eroded away prior to the eruption of the somewhat younger Lynn. Away from the Northern Boundary Fault, where the Lynn Volcanics abuts abruptly against the Boston Basin (Figure 1) the Lynn goes from red into darker bluish and greenish shades and becomes a subvolcanic facies with a high (40-60%) phenocryst count. This suggests that a traverse away from the fault (Stops 1-3 to 1-2 to 1-4) is also a traverse deeper into the subvolcanic regime and eventually into the magma chamber itself.

Paleozoic Alkaline Magmatism

Granite Intrusions. There are two episodes of Paleozoic alkaline hypersolvus granitic intrusions into the Boston-Avalon Terrane (Hermes and Zartman, 1985): (1) in the Late Ordovician (Cape Ann Complex north of Boston; Quincy Granite/Blue Hills Complex south of it; and (2) in the Devonian. The Peabody Granite (Stop 1-6) belongs to this younger age and is one of several such plutons that approximately track the trend of the Bloody Bluff Fault north of Boston (Figure 1). Devonian granites also occur south of Boston (Hermes and Zartman, 1985; Wones and Goldsmith, 1991). Descriptions of the alkalic rocks we will see are given for the individual stops. Volcanics associated with the granites likely form part of the Blue Hills Igneous Complex (Wampatuck Volcanics; Billings, 1982) south of Boston (Hermes and Murray, 1990).

Diorite to Gabbro Intrusions. Northwest of the Dedham North Complex is a band of largely mafic rocks 5 to 10 miles wide and at least 50 miles long (Bell and Alvord, 1976; units "Zv" and "Zdigb" of Zen et al., 1983; subzone 2 of Hepburn et al., 1987a). Rocks within it have variously been assigned to the Precambrian, Cambrian, Ordovician or Silurian. While field evidence suggests several magmatic pulses of different ages, geochemistry has failed so far to distinguish any distinct magmatic fingerprints. All rocks so far analyzed geochemically fall between transitional continental tholeiites and alkali basalts. New dates on mafic samples from this belt (see below) give ages

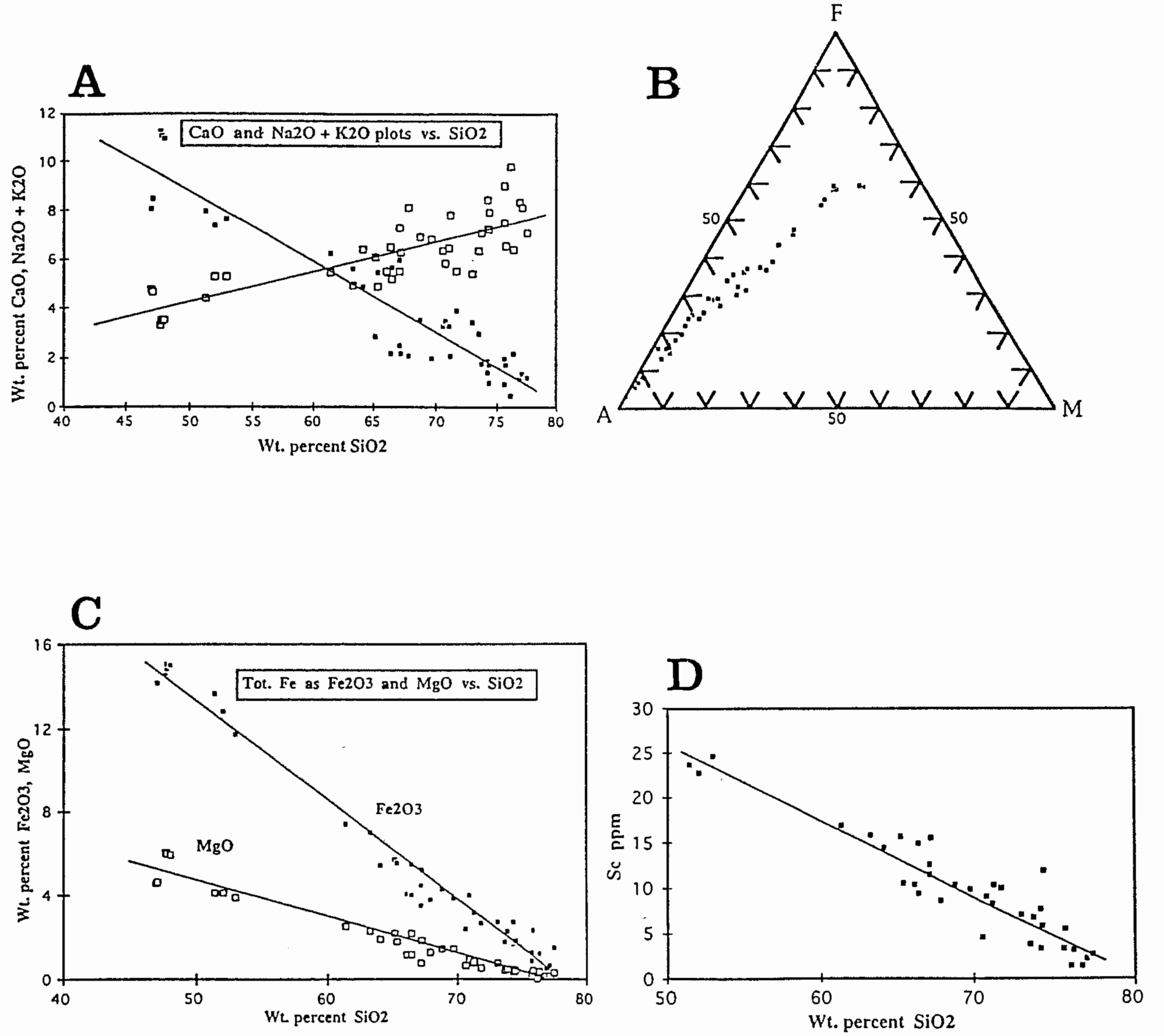

Figure 4. Harker variation diagrams and FMA plot for the Dedham North plutonic suite. Rocks with silica < 55% are mafic dikes.

A. CaO (solid squares) and $Na_2O + K_2O$ (open squares) vs. SiO_2 "standard" Peacock diagram, which defines calcic vs. alkalic affinity of a suite. The intercept at 62 wt.% SiO_2 is within the calc-alkaline domain.

B. FMA diagram. The distribution of rocks follows a calc-alkalic trend.

C, D. Geochemical plots suggest mixing (straight variation lines) between two end members (felsic and mafic) as opposed to concave trends (fractionation).

of 444 ± 3 and 373 ±4 Ma, indicating that extensive mafic magmatism was also present at the same time as the alkaline granitic plutonism. However, since field relations indicate that some of the mafic magmatism in this belt is related to the period of Dedham intrusion, younger ages cannot be uniformly extrapolated throughout it.

New U-Pb Geochronology of the Boston-Avalon Terrane

Six new U-Pb ages were determined by Dunning on rocks from the Boston-Avalon Terrane as part of our ongoing studies (Figure 5). (All these sample locations will be visited during the excursion). Four of the ages are from Late Proterozoic rocks associated with the main period of Avalonian magmatism: Lynn Volcanics, Dedham North Granodiorite, and the two samples from Sheffield Heights. These latter two samples are part of the Dedham North suite but reflect different compositional variations. The other two samples (Figure 5E-5F) are from the younger period of early to mid-Paleozoic alkaline magmatism.

Analytical Specifics

Samples were processed using the basic procedures as outlined by Dunning et al. (1990). All isotopic ratios were measured with a MAT 262 multicollector thermal ionization mass spectrometer, at Memorial University, operating in static multicollection mode with ^{204}Pb measured with an ion-counting secondary electron multiplier system. All error ellipses and uncertainties quoted on the ages are at the 2 sigma level. Linear regressions used the procedure of Davis (1982).

Lynn Volcanics. This rhyolite yielded abundant clear euhedral zircon. Three abraded fractions define a short mixing line anchored on concordia with a concordant fraction at 596.6 Ma. The regressed line yields a lower intercept age of eruption of 596 ± 3 Ma and a poorly defined upper intercept of 2672 +1700/-690 Ma (Figure 5A).

Dedham Granodiorite. This sample yielded both high quality euhedral zircon and titanite. Three abraded zircon fractions all clearly contain an inherited component and are not colinear, either due to Pb loss or variable ages of the inherited component. Two titanite fractions overlap with ^{206}Pb/^{238}U ages of 607 and 612 Ma. The regressed line through Z1, Z2 and T1 yields an intercept age of 607 ± 4 Ma, overlapping the titanite ages. The average age of the inherited zircon component is 1577 +130/-110 Ma (Figure 5B).

Sheffield Heights Diorite. This sample yielded abundant euhedral zircon and high quality titanite. Three fractions of abraded zircon prisms, and titanite concordant at 607 Ma, define a line that yields a lower intercept age of crystallization of 606 ± 3 Ma. The line gives an upper intercept average age of the inherited component of 1660 +150/-140 Ma (Figure 5C).

Sheffield Heights Granite. This granite yielded coarse euhedral to subhedral zircon. Four fractions of abraded euhedral grains show a minor but significant inherited older component. Fraction Z1 of lath-shaped grains touches the concordia curve with ^{206}Pb/^{238}U and ^{207}Pb/^{206}Pb ages of 608 and 617 Ma respectively. A regression line through all four fractions yields a lower intercept 609 ± 4 Ma age of crystallization with an average age of inherited zircon of 1780 +390/-260 Ma (Figure 5D).

Syenite Pod, Danvers. Three fractions of abraded clear coarse euhedral zircon from this rock define a mixing line with a lower intercept age of crystallization of 444 ± 3 Ma and a poorly constrained upper intercept of 2312 +1600/-570 Ma (Figure 5E).

Gabbro-Diorite, Waltham. This sample yielded high quality titanite and turbid high-U zircon. At the time of writing only one fraction of each has been analysed (Figure 5F). These yield an age of 373 ± 4 Ma from concordant titanite, supported by a ^{207}Pb/^{206}Pb age of 376 ± 3 Ma from 4% discordant, abraded zircon. Quite clearly, this is the age of igneous crystallization.

Interpretation

The 596 Ma date on the Lynn Volcanics finally ends the long standing debate about its age. Although, more recently a Precambrian age has been generally assumed for the Lynn because of its similar chemistry to the Dedham (Smith and Hon, 1984; Hermes and Murray, 1990), this marks the first time the Lynn has actually been dated. The date firmly establishes the Lynn as part of the Late Proterozoic Avalonian magmatic event in the Boston area.

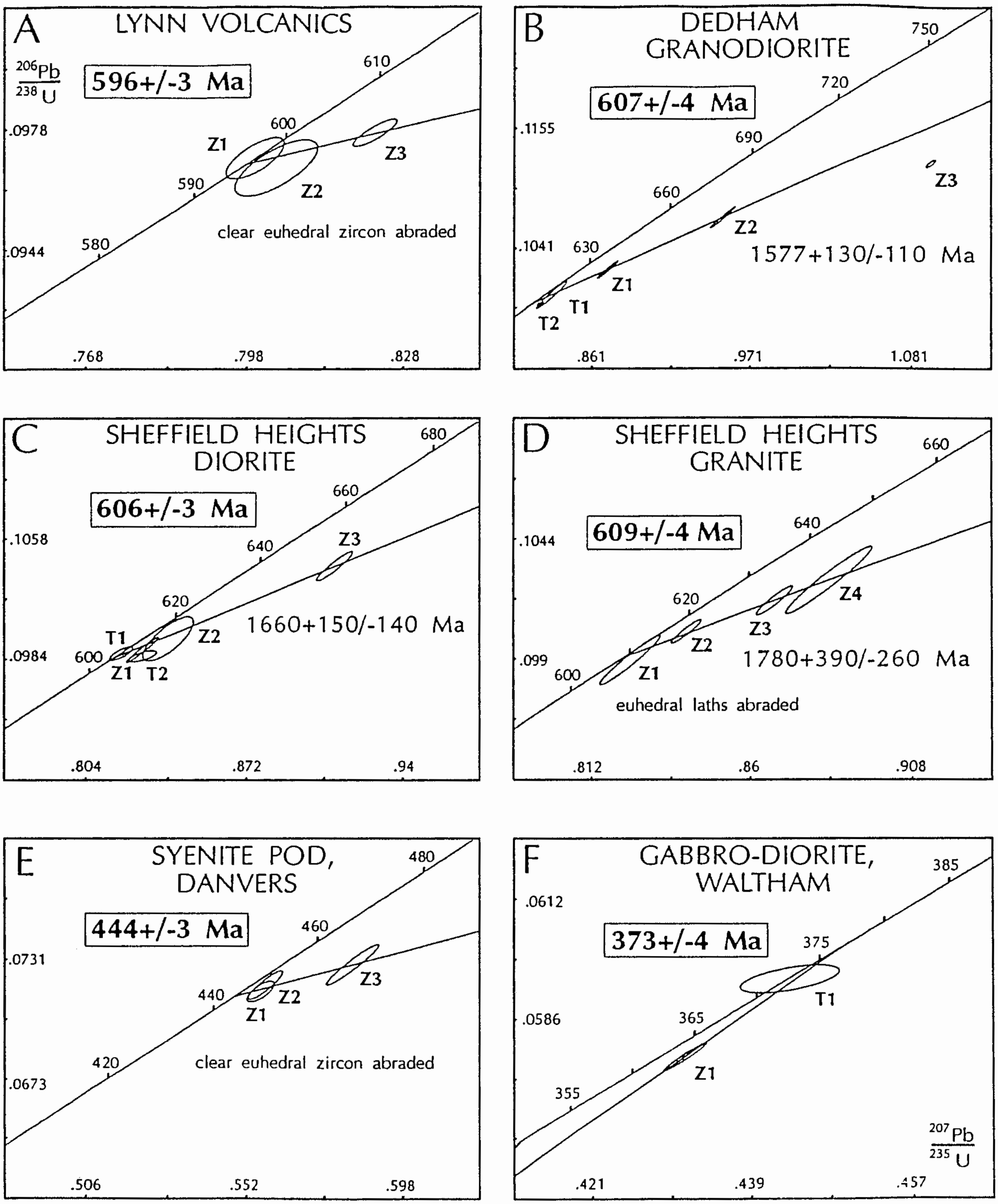

Figure 5. Concordia diagrams for new U-Pb data for rocks from the Boston-Avalon Terrane, eastern Massachusetts.

The Dedham Granodiorite north of Boston had not been dated previously by the U-Pb method (Zartman and Marvin, 1991). The 607 Ma age clearly indicates the Dedham North is part of the Late Proterozoic magmatic event, although it is somewhat younger than the 630 ± 15 Ma age obtained on the Dedham south and west of Boston (Zartman and Naylor, 1984). The dates on the two samples from Sheffield Heights indicate these samples are part of the Dedham North suite, despite their compositional variations and support the model for the origin of the Dedham North presented above and in the description for Stops 1-4 and 1-5. The age of the inherited zircon component in these plutonic samples is similar to that found by Olszewski (1980) for detrital zircons from the Westboro Fm.

The ages on the syenite pod from the gabbro-diorite in Danvers and from the gabbro-diorite in Waltham establish these rocks as having formed during the lower to mid-Paleozoic (Ordovician and Devonian) alkaline magmatism. They confirm that this event had a major mafic component in addition to the well known granitic magmatism of this period. It also means the ages of many of the mafic rocks in the western portion of the Boston-Avalon Terrane may need re-appraisal.

NASHOBA TERRANE

Overview

The Nashoba Terrane (Figure 1) lies west of the Boston-Avalon Terrane, across the prominent Bloody Bluff Fault Zone (Stop 2-11). It has a geological history distinct from that of the Boston-Avalon Terrane, and no geological units can be correlated between them. The stratigraphy of Nashoba Terrane (Figure 2) is dominated by a thick sequence of largely mafic volcanic rocks (Marlboro Fm., Stop 2-1) and volcanogenic sedimentary rocks (Nashoba Fm., Stops 2-4, 2-5, 2-6) of Ordovician age (which may also include some Cambrian or Early Silurian). These have been polydeformed and metamorphosed under sillimanite and sillimanite-K-feldspar zone conditions in the Silurian to amphibolites, various biotite-feldspar gneisses, schists and calc-silicate granulites (Bell and Alvord, 1976; Goldsmith, 1991a). Migmatites are developed in rocks of the appropriate compositions, particularly toward the northeast. Geochemistry of the Marlboro indicates the amphibolites were generally high-alumina basalts with trace element signatures compatible with an arc or marginal basin tectonic setting (DiNitto et al., 1984).

Dunning (Figure 6B) recently re-dated the Fish Brook Gneiss (Stop 2-8), a leucocratic feldspar-biotite gneiss once thought to represent Late Proterozoic basement for the terrane, on the basis of a 730 Ma date (Olszewski, 1980) and an unusual "swirled" foliation that suggested a possible earlier deformation (Bell and Alvord, 1976). The new date of 520 +14/-11 Ma establishes not only the age of this unit but constrains the age of the overlying Marlboro and Nashoba Fms. to the interval between 520 and 430 Ma, the younger age being that of the cross-cutting Sharpners Pond Diorite. The new date signifies that no Precambrian rocks have been found in the Nashoba Terrane. However, detrital zircons (Olszewski, 1980) and Nd isotopes in the Andover Granite (Hill et al., 1984) indicate the presence of Early Proterozoic crustal material in the terrane, at least as detritus.

The Nashoba Terrane experienced widespread plutonism from the mid-Ordovician through at least the Silurian (Figure 2) of contemporaneous calc-alkaline intermediate and granitic magmas (Zartman and Naylor, 1984; Hepburn et al., 1987a). The intermediate composition plutons, typified by the Straw Hollow Diorite (Stop 2-3) and the Sharpners Pond Diorite (Stop 2-9) are little deformed and range in composition from gabbroic cumulates to hornblende and hornblende-biotite diorites and tonalites that have sphene as a common accessory phase (Hill et al., 1984; Hon et al., 1986). The granites range in composition from metaluminous to peraluminous and vary from foliated biotite-muscovite granite to unfoliated garnet-bearing muscovite granite and pegmatite. They were likely intruded over at least a 50 Ma period (Zartman and Naylor, 1984; Hill et al., 1984). The Andover Granite (Figure 1, Stop 2-7) is thought to have been at least partially generated by anatexis of the Nashoba Fm. (Stop 2-6) during Silurian metamorphism. A new U-Pb date on the unfoliated, peraluminous younger phase of the Andover (Figure 6A) of 412 ± 2 Ma supports this conclusion. Magmatic pillows and other features (Stop 2-9; Hon et al., 1986; Hon et al., this volume, Chapt. Q) indicate the co-existence of at least some of the granitic and intermediate magmas. Geochemistry however, indicates they are not co-genetic. It is thought likely the intrusion of the calc-alkaline magmas contributed heat for the anatexis of the metasedimentary rocks that led to the granite formation.

During the Silurian, the Nashoba Terrane was polydeformed and metamorphosed. The 425 ± 3 Ma U-Pb age on monazite (Figure 6B) from the Fish Brook Gneiss dates the metamorphism. The metamorphism is generally of a lower pressure-higher temperature andalusite-sillimanite type, although early kyanite pseudomorphs replaced by sillimanite have been found in a few locations (Stop 2-3; Bober, 1989).

$^{40}Ar/^{39}Ar$ ages on hornblendes from amphibolites of the Nashoba Terrane give an age range of 354-325 Ma, and an Ar plateau age on biotite gives 308 Ma (Hepburn et al., 1987b). These indicate the time of uplift and cooling of the terrane. They also indicate the Nashoba Terrane in Massachusetts did not experience an Alleghanian thermal event sufficient to affect the Ar/Ar systematics of hornblende or biotite.

New U-Pb Geochronology of the Nashoba Terrane

Samples of the Nashoba Terrane were analyzed for U-Pb geochronology using the same procedures as noted previously for the Boston-Avalon Terrane samples, after the method of Dunning et al. (1990). Three geologically important ages were determined from the samples of the Andover Granite and Fish Brook Gneiss (Figure 6).

Analytical Specifics

Andover Granite. This coarse grained to pegmatitic muscovite-bearing S-type granite yielded zircon of a variety of morphologies and grain size and monazite. Much of the zircon is interpreted to be inherited from the source rocks, and the monazite is interpreted to be igneous, as is common in S-type granites. Three fractions of monazite analysed plot slightly above concordia with $^{206}Pb/^{238}U$ and $^{207}Pb/^{235}U$ ages of 412- 413 Ma and 410-411 Ma respectively. They indicate an age of 412 ± 2 Ma for this rock (Figure 6A).

Fishbrook Gneiss. The Fishbrook Gneiss yielded a large amount of zircon, much of which is virtually opaque, turbid and brown in color. There is also a significant amount of clear euhedral prism zircon and fine grained monazite. Three fractions of zircon and two of monazite have been analysed. Two abraded fractions of the clearest zircon have normal U concentrations of 150 - 200 ppm and plot near concordia with $^{207}Pb/^{206}Pb$ ages of 499 and 502 Ma, within error of each other, and one overlaps concordia. From these data, the igneous age of this rock could be 500 ± 5 Ma. The third fraction of abraded brown zircon contains 2000 ppm U and is very discordant. A line regressed through the three zircon fractions has an upper intercept age of 520 +14/-11 Ma and a lower intercept of 286 Ma (Figure 6B).

This 520 +14/ -11 Ma age would best represent the time of igneous crystallization if the low U clear zircons were affected by the disturbance (Alleghanian) that caused Pb loss in the high-U grains. But this need not be the case. If not, 500 ± 5 Ma is the better age. This will be resolved with further analyses underway at the time of writing.

Monazite yielded a reproduced unambiguous age of 425 ± 3 Ma, which is interpreted to represent a metamorphic event.

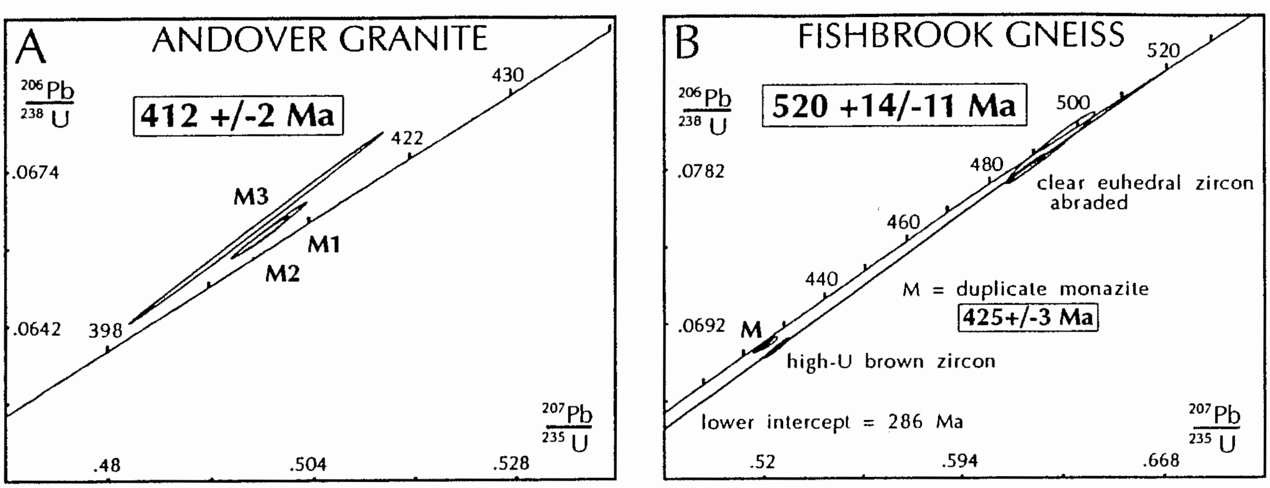

Figure 6. Concordia diagrams for new U-Pb data for rocks from the Nashoba Terrane, eastern Massachusetts.

Interpretation

The 520 Ma igneous crystallization age on the Fish Brook Gneiss establishes that this unit is Paleozoic and not Precambrian as previously thought (Olszewski, 1980). Two conclusions from this fact result: (1) the terrane has no (as yet) identified Precambrian basement, which supports the idea that it originated as an early Paleozoic arc, and (2) this age greatly restricts the possible age range of the overlying stratified rocks in this terrane (Marlboro Volcanics and Nashoba Fm.) to the interval between 520-430 Ma. Previously they were only known to be pre-430 Ma.

The date of 425 Ma on the monazite from the Fish Brook Gneiss clearly establishes the timing of the metamorphism in the Nashoba Terrane. Previously, this was only very approximately known through a series of, perhaps circular, arguments concerning the ages of poorly dated foliated plutons thought to have experienced the deformation and metamorphism vs. unfoliated plutons thought to post-date the metamorphism (Hepburn et al., 1987a). This date is of considerable importance for tectonic interpretations.

The date on the Andover Granite finally establishes the age for the younger phase of this complex pluton that has proved exceedingly difficult to date in the past (Zartman and Naylor, 1984; Hill et al., 1984). This age further confirms the timing of the deformation and metamorphism in the terrane as Silurian and supports the idea that the peraluminous Andover was at least partially generated by anatexis of sediments during the metamorphism.

EASTERN MERRIMACK BELT

Northwest of the Nashoba Block across the Clinton-Newbury Fault Zone is another potential terrane, the Merrimack Trough or Eastern Merrimack Belt (Figure 1). Since we will only be visiting one exposure in this terrane, it is beyond the scope of this guidebook to describe it in detail, particularly since the age of the rocks and their deformation are presently controversial. For detailed descriptions of these rocks refer to Lyons et al. (1982) and Robinson and Goldsmith (1991).

The rocks in this belt between the Clinton-Newbury Fault and approximately the Fitchburg Pluton (Zen et al., 1983) include a sequence of calcareous metasiltstones (Stop 2-2), pelites and impure quartzites. The metamorphic grade varies from lower greenschist facies near the Clinton-Newbury Fault Zone to the upper amphibolite facies westward in the belt. The rocks are either (1) Ordovician-Silurian in age (as shown by Zen et al., 1983) based on correlation with fossiliferous strata in Maine (Robinson and Goldsmith, 1991) or (2) pre-Middle Ordovician based on the ages of cross-cutting plutons (Lyons et al., 1982; Gaudette et al., 1984 ; Bothner et al., 1984; Hon et al., 1986). The age of the deformation and metamorphism in this belt depends to some extent upon the age assignment of the rocks and is either Acadian or from an earlier event.

NEWBURY VOLCANIC COMPLEX

The Newbury Volcanic Complex (Stop 2-10) occurs only within fault-bounded slivers (Figure 1) directly between the Boston-Avalon and Nashoba Terranes. It is not clear that it belongs to either of these terranes. For example, Zen (1989) included them within a separate terrane (Atlantica II) within his Atlantica Composite Terrane. The Newbury is composed of a series of andesitic and rhyolitic volcanics, shallow intrusions and interbedded sedimentary rocks that contain latest Silurian to Early Devonian fossils (Shride, 1976a). The rocks are essentially unmetamorphosed and, although tilted, not penetratively deformed. McKenna et al. (1993) indicate these rocks are calc-alkaline with trace element geochemical signatures indicative of formation in a continental arc environment. Hon and Thirlwall (1985) and Hon et al. (1986) note the similarity in the composition of the Newbury Volcanics to the intermediate and granitic magmas of the Nashoba Terrane and suggest that the Newbury may be the volcanic expression of this terrane preserved in a down-dropped fault block. Volcanic rocks similar in both composition and age also occur in the coastal volcanic belt in eastern Maine and may have once been continuous with the Newbury (Gates and Moench, 1981).

TECTONIC DISCUSSION

Differences in the geological history of the Boston-Avalon and Nashoba Terranes are shown in Figure 2. The Boston-Avalon Terrane was part of a continental arc during the Late Proterozoic, but by the early Paleozoic arc magmatism ceased and the area became a stable shelf or platform. It remained largely tectonically stable throughout the lower and middle Paleozoic, experiencing only intrusions by alkaline granitic and mafic magmas. In contrast, the Nashoba Terrane is interpreted to have formed in an arc or marginal basin setting in the Lower Paleozoic. Intruded extensively by calc-alkaline intermediate and granitic magmas during the Ordovician-Silurian it was deformed and metamorphosed to high grade during the Silurian. We interpret the Ordovician-Silurian calc-alkaline plutonism in the Nashoba and Eastern Merrimack Belt to be related to an east-dipping subduction zone beneath these terranes. The Newbury Volcanics may be preserved remnants of this magmatism. As the leading edge of the eastern terranes (Nashoba Terrane) impinged upon the Merrimack Belt (the whole Merrimack Belt of Zen et al., 1983, and not just the eastern portion described above) to the west during the Silurian, perhaps obliquely, it was deformed and metamorphosed. This initiated the final closure of the eastern terranes with those to the west. Thus, the Acadian orogenic cycle (if something at 425 Ma can be called Acadian) started earlier on the southeastern side of the belt and telescoped northwestward and westward during the late Silurian and early to mid-Devonian. In this interpretation, the rather extensive Ordovician to Devonian alkaline magmatism in the Boston-Avalon Terrane represents behind-the-arc magmas originating from the same east-dipping subduction zone and interacting with the mature crust of Avalonia (Paige and Hon, 1988; Hon et al., this volume, Chapt. Q). The Mississippian $^{40}Ar/^{39}Ar$ ages from the Nashoba Terrane represent the time of its final uplift and cooling in post-Acadian times.

The large faults within and between these terranes have clearly disrupted the original order of the crustal segments by foreshortening and strike-slip displacements of unknown magnitude. They have had a long and complex history of movement ranging from Precambrian to Mesozoic that is only now beginning to be understood (e.g., Skehan and Rast, 1991; Goldstein, 1992; Goldsmith, 1991b; Rast et al., this volume, Chapt. S).

ACKNOWLEDGMENTS

J.C.H. and R.H. would like to acknowledge the MIT Research Reactor and MIT Reactor Sharing Grant No. DE-FG07-80ER10770.A015 for the support that made possible the irradiations for INAA, which provided data for our geochemical interpretations. NSF Grant EAR-8212760 to J.C.H. and R.H. provided support during early stages of the work on the igneous rocks. Many thanks also to Sabrina for road-logging and for SuperPainting better than her father; and to Judy, who was still willing to keyboard and edit this manuscript even after taking on the onerous task of whittling down Chapter C.

ROAD LOG - DAY 1
BOSTON-AVALON TERRANE

STOP 1-1. CAMBRIDGE FM., LATE PROTEROZOIC, BOSTON BAY GROUP (Malden, MA; 30 minutes). From Boston proceed north on Rt. 1 to exit for Rt. 60 and Malden, follow signs for Rt. 60 west (Eastern Ave.) and proceed west for about 1.5 mi., left on Faulkner St., left on Lyme St., and park just before the next intersection. Climb to crest of hill to NE (Figure 7); hill is Tartikoff Park immediately to SW of former Daniels School (now Daniels Apartments) .

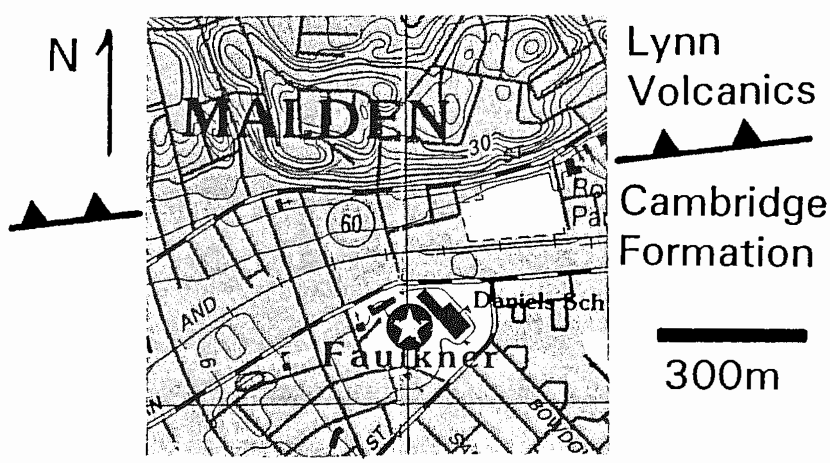

Figure 7. Location of the Cambridge Fm. about 0.7 km E of Malden Square, MA; USGS Boston North Quad. Cambridge outcrops occur on the hill (shown by star) SW of Daniels Apts. The position of the Northern Boundary Fault, inferred by topography and from strike projected from the Malden Tunnel data, is indicated along the sides of the figure.

This is the northernmost outcrop of the Cambridge Fm. in the Boston Basin; in fact, the Northern Boundary Fault of the Boston Basin is only about 300 m due north from the crest of the hill in the park (Figure 7). Hills to the north form a fault line scarp resulting from the differential resistance to erosion of the Lynn Volcanics relative to the softer sediments of the Boston Basin. The Cambridge at this locality strikes 230° and dips 78° to 82° to the north. Graded beds of very fine feldspathic sandstone and scour structures indicate that the beds are overturned and young to the south. The gray mudstone is thinly laminated and contains many soft sediment deformation structures including slump folds, load structures, pinch and swell bedding, and intrastratal microfaults. The outcrop north of the fence and above the church parking lot exposes many detailed sedimentary structures and 0.6 to 1.0 cm diameter ring-like structures (fossils?) on the soles of beds. A 4 m wide dolerite dike, striking 280°, cuts the Cambridge (cross-section is exposed north of the fence) and has been sheared parallel to strike. Much of the mudstone has also been tectonized.

The 1.6 km long Malden Tunnel, about 1.4 km to the west of this outcrop, crossed from the steeply dipping Cambridge to the Lynn Volcanics that form the upland topography to the north of the Boston Basin. Billings and Rahm (1966) described the fault in the tunnel as "knife-sharp and tight" and dipping 55° to the north. There is no doubt that the boundary fault in this area is a thrust as a borehole drilled during the tunnel project penetrated about 25 m of Lynn felsite along the edge of the thrust sheet before entering underlying Cambridge mudstones (Billings and Rahm, 1966). Projection from tunnel data suggests that the Tartikoff Park outcrop is probably the oldest exposed Cambridge and is about 300 m above the lowest Cambridge beds in the Malden Tunnel.

STOP 1-2. DEDHAM NORTH GRANITE, LATE PROTEROZOIC, SUBVOLCANIC - SHALLOW INTRUSIVE FACIES (Malden, MA; 20 minutes). From the Daniels Apartments (Stop 1-1) turn right onto Rt. 60 east (Eastern Ave.) for 0.8 mi toward an intersection with Rt. 99 north. Take left turn on Rt. 99 north (Broadway St.) and proceed for approx. 0.8 mi. At the intersection with Central St. to your right and Elwell St. to your left, turn left on Elwell St. Immediately behind the MOOSE club house at the corner of Elwell St. and Rt. 99 enter the parking lot on your left side. Exposures are on the sloping incline at the far right corner of the parking lot. NOTE: Eastern Ave. is parallel to and about 300 meters south of the Northern Boundary Fault. Rt. 99 then follows one of the younger faults that transects and offsets the Boundary Fault.

The Dedham North Granite is located north of the Boston Basin in contrast to the main body of Dedham Granite located to the south of the basin. Both plutons appear to have similar mineralogical and petrological characteristics, inspiring early workers to lump most of the eastern Massachusetts intrusives under one designation. The Dedham North intrusives are covered by the Lynn Volcanics on the south side and grade into more mafic compositions to the north.

This locality is only a few dozen yards away from a fault contact with the Lynn Volcanics, and the rocks exposed here are of a chilled, near contact facies. The rock is composed of 30 to 60% micrographic (granophyric) matrix and 1 to 5 mm phenocrysts of plagioclase (zoned andesine-oligoclase), quartz, hornblende, and biotite. The alkali feldspar-quartz micrographic matrix is colored pink; the euhedral plagioclase is white; quartz is transparent glassy; and hornblende and biotite are dark. Approx. half way up the outcrop is a 2 ft. wide greenish colored dike of rhyodacite that is compositionally similar to the Dedham North suite. The present day erosional levels at this locality are near the upper contact of the pluton.

STOP 1-3. LYNN VOLCANICS, LATE PROTEROZOIC, EXTRUSIVE FACIES (Saugus, MA; 25 minutes). Return to Rt. 99 (Broadway St.), turn left on Rt. 99 north, and continue north for approx. 0.5 mi. Immediately past the Malden-Saugus town line make a left turn into the entrance of TRIMOUNT quarry. Stop at the office on your left and ask for permission to enter the quarry area.

The quarry offers an amphitheater view of several members of the volcanic sequence, intruded by stoping pockets of the Dedham North or compositionally alike magmas, all cut by a prominent set of younger mafic dikes. Three different types of the Lynn Volcanics are represented here: (1) reddish colored, (2) dark bluish or greenish colored, and (3) a resurgent dome-like facies with up to 50% phenocrysts in the very fine-grained matrix.

The red colored facies occurs only in the regions immediately adjacent to the Northern Boundary Fault. It has been informally suggested that the reddish color of the volcanics is a result of intense surficial oxidation/weathering during the late Precambrian, shortly after their deposition. A sample of the reddish colored facies, collected at this locality, was dated by the zircon U-Pb method at 596 ± 3 Ma (Figure 5A). This is about 10 million years younger than the age of the underlying Dedham North intrusives. Similarity of geochemical composition and the presence of an older zircon population in both suites suggests a similar mode of origin. At present there is no geochronological evidence for volcanics exactly coeval with the Dedham North. However, field evidence suggests otherwise for some of the volcanics. Perhaps the reddish member seen here is a distal facies from a different caldera system.

STOP 1-4. DEDHAM NORTH GRANITE, LATE PROTEROZOIC, GRANODIORITIC FACIES (Saugus, MA; 15 minutes). Re-enter Rt. 99 north (Broadway St.) and continue north for approx. 0.5 mi. At this point Rt. 99 north will end by merging with Rt. 1 north. Proceed approx. 0.9 mi on Rt. 1 north passing Essex St. and Main St. exits. After the Main St. overpass and Grossman store on your right, enter the large parking area of the Kowloon Restaurant, just before Rt. 1 reaches the crest of the road. Exposures are at the far end of the parking lot.

This locality is very near a temporary blasting site from which we collected a sample for age determination. Based on data obtained from titanites and zircons (Figure 5B), the age is 607 ± 4 Ma. The age is approx. 10 million years older than the age of the Lynn Volcanics. A strong zircon inheritance component is present in this sample, pointing to an averaged age population of 1577 +130/-110 Ma. Similar inheritance is also seen in leucogranitic and quartz dioritic compositions within the Dedham North.

The Dedham North Granite has a compositionally highly variable suite ranging from leucogranites to granodiorites, tonalites, and quartz diorite. Mineralogy varies correspondingly from that of a minimum granite composition of 30 to 35% quartz, 25 to 30% plagioclase, 30 to 35% alkali feldspar, and 2 to 8% biotite to a quartz diorite modal composition of 10 to 15% quartz, 35 to 40% plagioclase, 10 to 15% alkali feldspar, and up to 25% hornblende and biotite. At this location the Dedham is of the typical granodiorite variety with partially saussuritized plagioclases of greenish white color, pinkish alkali feldspar, quartz, and partially chloritized biotite and hornblende.

Geochemical and isotopic evidence (Hill, pers. comm.; Figure 4) supports the conclusions that the Dedham North igneous suite is largely a result of mixing between a mafic magma not represented in the complex and an anatectic crustal melt, along with a smaller degree of concurrent fractional differentiation. The origin of the anatectic melt will be examined and discussed at the next stop (Stop 1-5).

STOP 1-5. DEDHAM NORTH GRANITE, LEUCOGRANITIC FACIES AND PARTIALLY MELTED WESTBORO FM. (Saugus, MA; 45 minutes). After returning to Rt. 1 north continue for approx. 1 mi. and take the first exit, the Lynn Fells Parkway. You will loop over Rt. 1. After making a left turn on the Lynn Fells Parkway south, continue for approx. 1.2 mi., crossing Main St. at 0.9 mi. Watch on your left side for the entrance with a guard house to Sheffield Heights Condominiums and turn left. Follow Lewis O. Gray Drive uphill. On your right you will pass exposures of the quartz diorite facies, the zircon dated locality (Figure 5C). As you reach the ridge line, turn left on Sheffield Way and continue all the way to the end. Turn around at the cul-de-sac and park on your left. Exposures are a ridge that forms a median between Sheffield Heights and Hammersmith Village developments. Please, be careful when crossing the landscaping, this is private property!!!

We are standing at the northeast tip of a large pendant consisting of gneisses and quartzites of the Westboro Formation. Entirely engulfed within the Dedham North suite, this pendant is approx. 900 ft. long and 200 to 300 ft. wide and is aligned in a northeasterly direction, which is also the direction of the foliation. The exposures show extensive migmatization of the pendant by partial melting of layers with a suitable geochemical composition. Geochemistry of the melts that surround the pendant are minimum granites, but a short distance from the pendant the composition rapidly changes to granodiorite, tonalite and quartz diorite. A sample of the "leucosome" leucogranite taken from this exposure was dated by zircon U-Pb and yielded an age of 609 ± 4 Ma (Figure 5D). A sample of the quartz diorite only 800 ft. to the north from this locality gave an age of crystallization at 606 ± 3 Ma (Figure 5C). Both samples contain a similar inheritance with the upper intercept of the concordia plot at 1780 +390/-260 Ma and 1660 +150/-140 Ma, respectively. These ages are statistically the same and show similar inheritance as in the sample of the Dedham North granodiorite taken at Stop 1-4.

In summary, the Dedham North suite consists of granites and rocks of intermediate compositions. The granites originated by partial melting of a sedimentary protolith, while the intermediate members show a mixing between this granitic magma, as evidenced by the zircon inheritance, and a mafic magma. In addition, since the granites cannot be the heat source, the presence of a mafic magma is required as a heat source to drive the partial melting process. The mafic melt that contributed to the Dedham North Complex presumably may be equivalent in composition to some of the mafic dikes at this exposure that show "undulating" (mafic magma intruding felsic magma) contacts. The geochemical character of these dikes suggests a convergent plate margin setting, although not the main arc environment. Perhaps, they reflect a setting transitional between the main arc and back-arc(?).

STOP 1-6. WESTBORO FM., LATE PROTEROZOIC (Saugus, MA; 45 minutes). North on Rt. 1; exit onto Lynn Fells Parkway and follow the parkway about 1 mile to intersection with Main St., turn right on Main and proceed about 1.2 miles to point where powerline crosses Main St. Park under powerline and take dirt road on northwest side of powerline to the south about 1.2 km. Hike over hill and down to the point where the road turns sharply left and descends a rocky scarp. Stop here and walk back through the section to the north (Figure 8).

This is the only known outcrop of the Westboro Fm. that displays common primary sedimentary structures and has a relatively unmodified sedimentary texture. These are low grade metamorphic rocks with metamudstones and muddy meta-arenites rich in chlorite, actinolite, epidote and quartz. Quartz-rich meta-arenites contain muscovite but are often not very recrystallized. Locally higher grade metamorphic mineral assemblages developed adjacent to the

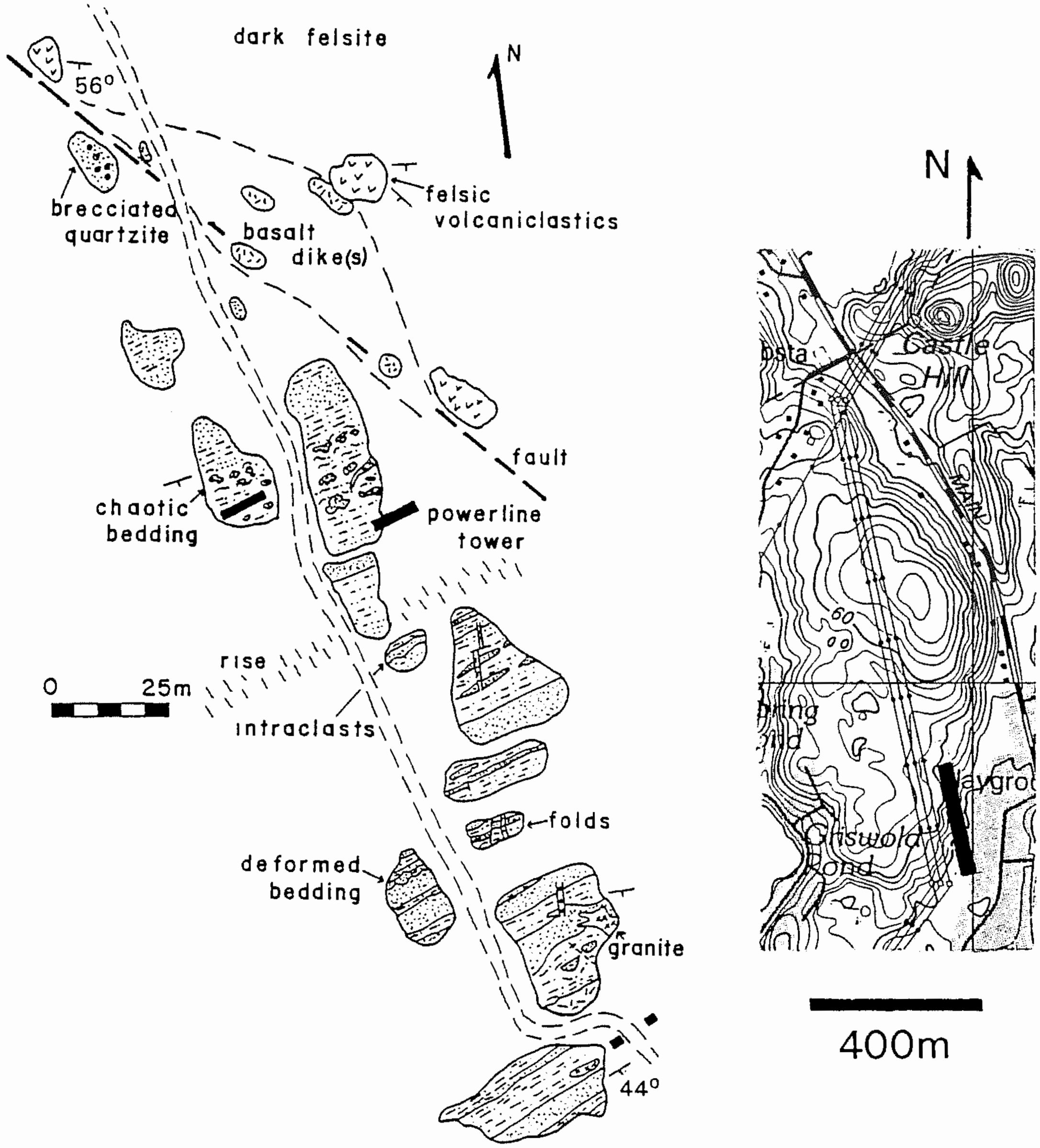

Figure 8. Location map (inset) and generalized sketch map of Westboro Fm. at Stop 1-6. Heavy bar on inset topographic map shows interval represented in detailed map.

Dedham intrusives. In the following discussion sedimentary protolith terms are used. Dark reddish brown siltstones and mudstones are interbedded with gray fine sandstones and 0.3 to 2 m thick beds of white quartzarenite. The sequence dips about 45° to the south and on the basis of load structures and cross-lamination is right-side up. Several arenite beds grade from medium sand upward to very fine sandstone and siltstone. Many of these arenites contain rounded, highly deformed or intricately embayed siltstone, mudstone and sandstone intraclasts. The uppermost portion of one graded bed has ripple cross-lamination and several beds have irregular, scoured and loaded lower contacts. These sandstones are interpreted as turbidites formed by a highly concentrated, cohesionless, sandy gravity flows.

Some of the beds are lenticular and deformed, and there is a 14 m thick interval (beneath the powerline towers) of highly irregular sandstone and mudstone intraclasts in a dark brown mudstone matrix. In thin section some of the sandstone masses have diffuse margins with escaping quartz grains and mudstone embayments. The megascopic features and microscopic texture suggests that this material was mixed together while soft. Bailey et al. . (1989) interpreted this and similar outcrops as olistostromes.

Dedham North Granite forms the first knob to the south of the sedimentary section, and veins and pods of presumably Dedham North intrude parts of the Westboro. A pegmatitic vein occurs in the road where it descends the rocky scarp. North and east of the sedimentary sequence are outcrops of crystal/lithic/vitric felsic tuff. Brecciated quartzites along the contact and the strike of the Westboro into the volcanics suggest that a fault separates the metasediments from the volcanics (Figure 8). As you hike back across the hill to the vehicles you pass through outcrops of dark to light gray recrystalllized felsite, and on the SW flank of the hill to the NE of the powerline, a diorite intrusion cuts the felsite.

STOP 1-7. DANVERS ALKALI GABBRO AND SYENITIC CUMULATES, ORDOVICIAN (Danvers, MA; 25 minutes). Retrace your way back to Rt. 1 north and continue north for approx. 7 mi. passing along the way exits to Rt. 129, Rt. 128, and Interstate 95 north. 0.8 mi. north of the Rt. 114 exit, follow the exit ramp to Centre St. CAUTION. This interchange serves Rt. 1, Centre St., and I-95 S and is somewhat disorienting! (Figure 9). On the completion of the ramp loop, turn right onto Centre St. and go under Rt. 1. At the T intersection turn left, and then left again into the parking area of a strip mall along Rt.1 south. Walk back under Rt. 1 and proceed to exposures on both sides of the ramp to Rt. 1 N and I-95 S from Centre St.

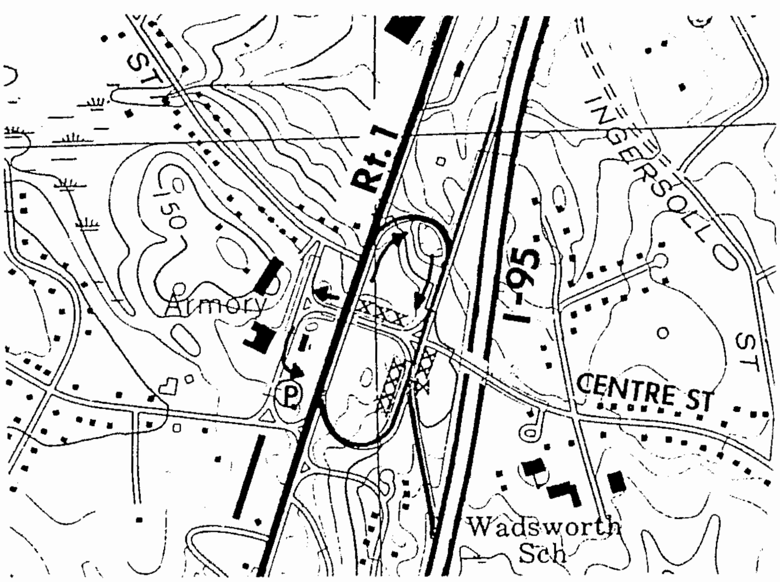

Figure 9. Location for Stop 1-7. Follow arrows to parking (P). The location of exposures is shown by strings of x's. Enlargement from U.S. Geol. Survey Topographical Map of the Salem Quadrangle, 1:24,000.

The rocks at these exposures prove both the presence of Late Ordovician mafic magmatism within the Boston-Avalon Terrane and a younger tectonic deformation. The principal rock type is a mildly alkalic gabbro (Ne normative) with phenocrysts of alkali feldspar. These phenocrysts are typically 0.5 to 2 cm in size and occasionally form pods and layers of syenite by accumulation of alkali feldspar (flotation and/or flow fractionation). A sample from one of these syenitic pods was dated by the zircon U-Pb technique and yielded an age of 444 ± 3 Ma (Figure 5E). This age is similar to the emplacement age of Cape Ann Granite (452 ± 10 and 446 ± 15; Zartman and

Marvin, 1971, and Zartman, 1977, respectively) suggesting that the origin of the Cape Ann Granite Complex is related to mafic alkali basalt magmatism.

Walk back toward the Rt. 1 overpass and examine the exposure on the north side of Centre St. just before the Rt. 1 overpass. The same rocks here are sheared and mylonitized (striking 45° to 50° E and dipping 60° NW), indicating post-Ordovician deformation.

STOP 1-8. PEABODY GRANITE, DEVONIAN (Peabody, MA; 15 minutes). Return to Centre St., proceed under Rt. 1, and take the exit ramp on your right to I-95 S to Boston. After the turn onto the exit ramp bear left at the fork and follow I-95 S toward Waltham for approx. 2.5 miles. Take Exit #45 to Rt. 128 north toward Gloucester. After 1.2 mi leave Rt. 128 N via Exit #28 to Centennial Drive. At the end of the exit ramp turn right on the cross road and immediately right again on Centennial Drive. Proceed 0.1 mi and turn left, crossing Centennial Drive into the parking lot of Hyde Opportunity manufacturing facilities. Exposures are at the far end on your right.

Throughout the Boston-Avalon Terrane are occurrences of mid-Paleozoic intrusions (Figure 1) of undeformed hypersolvus granites that belong to one of two discrete age groups: an Ordovician group of plutons emplaced during the 450 to 460 Ma interval, and Devonian plutons crystallized around 380 ± 20 Ma (Zartman, 1977; Hermes and Zartman, 1985). The chemical composition of both sets of plutons ranges between metaluminous to mildly alkaline granites with the corresponding agpaitic indices ranging from 0.85 to 1.15. Mineralogy in general is dominated by perthitic alkali feldspars, quartz, ferrous micas, ferrous amphiboles and pyroxenes.

Here, the Peabody granite is a homogenous, medium- to coarse-grained, hypersolvus granite with 20 to 30% quartz, 65 to 75% perthitic alkali feldspar, 5 to 10% ferrohastingsite and common accessories. Grain size is typically 5 to 10 mm, somewhat finer near the contacts. At these exposures we can observe common mafic enclaves that are virtually absent elsewhere in the pluton.

STOP 1-9. WEYMOUTH FM., LOWER CAMBRIAN (Nahant, MA; 60 minutes). From Rts. 1 or 128, or I-95, proceed south on Rt. 129 to Lynn Shore Drive, then south on Lynn Shore Drive to a rotary. From the rotary proceed south down the causeway on Nahant Rd. and follow Nahant Rd. to the gate at Northeastern University Marine Science Center at East Point. Proceed through the gate and park in front of MSC. You must obtain permission from the director of the Marine Science Center before your visit. From Boston or points south proceed north on Rt. 1A to rotary, then follow directions above.

In the rugged sea cliffs around East Point Early Cambrian nodule-bearing mudstones and limestones dip about 40° to the northwest. The limestones contain a diagnostic upper Placentian Series, Acado-Baltic small shelly fauna, but no trilobites. Cambrian strata are intruded by the Ordovician Nahant Gabbro and by numerous mafic dikes and sills. Details of igneous petrology, stratigraphy, and paleontology are given in Bailey and Ross, this volume, Chapt. Y. Please refer to this description for completeness.

ROAD LOG - DAY 2
NASHOBA TERRANE, EASTERN MERRIMACK BELT, BOSTON-AVALON TERRANE

STOP 2-1. MARLBORO FM., ORDOVICIAN?, NASHOBA TERRANE (Marlborough, MA; 20 minutes). Exit I-495 to Rt. 20 west, immediately turn right onto Felton St. toward the Radisson Inn. In 0.1 mi., turn left on Landry St. and follow (0.2 mi.) to junction with Rt. 20. Turn left (east) onto Rt. 20. In 0.1 mi. turn right into the parking lot of the DBM Corporation (just beyond gas station) and park. Walk SE to exposures along the entrance ramp from Rt. 20 to I-495 South and to exposures along Rt. 20 just west of the gas station by the "blue building." Beware of poison ivy and traffic!

Exposures here are typical amphibolites in the Sandy Pond Mbr. of the Marlboro Fm. (Bell and Alvord, 1976; DiNitto et al., 1984). Cross-cutting granitic dikes are tentatively assigned to the Andover Granite. The amphibolites are fine to medium-grained, massive to foliated hornblende-plagioclase ± quartz, biotite or epidote amphibolites and layered amphibolites. The metamorphic grade here is the sillimanite zone.

The Marlboro Fm. forms the major stratified unit on the eastern side of the Nashoba Terrane and consists of amphibolites, felsic gneisses and interbedded schists. It has generally been interpreted as a metamorphosed volcanic complex. Geochemistry on the amphibolites indicates that they were originally basalts and include high-alumina types with trace element signatures consistent with formation at a convergent plate margin or in a marginal basin setting (DiNitto et al., 1984).

STOP 2-2. OAKDALE FM., EASTERN MERRIMACK BELT (Boylston, MA; 20 minutes). From junction I-290 and Rt. 140 in Shrewsbury, proceed north on Rt. 140, 1.7 mi. to junction of Rts. 140 & 70. Continue NW on Rt. 140 for 0.3 mi. to outcrops on both sides of the road. Pull off on right and park.

The purpose of this stop is to examine exposures typical of the sedimentary sequence in the eastern part of the Merrimack Belt (Figure 1; Zen et al., 1983) and to contrast them with the Nashoba Terrane just to the east. The region immediately west of the Clinton-Newbury Fault Zone is characterized by a variety of calcareous metasiltstones, impure quartzites and pelitic rocks metamorphosed to only the lower greenschist facies, quite different from the high grade schists and gneisses in the Nashoba Terrane just to the east. The grade of metamorphism in the Merrimack Belt rises gradually westward. The age of the rocks and of the metamorphism and deformation in the eastern part of the Merrimack Belt is controversial. The rocks are either Siluro-Devonian as shown by Zen et al. (1983) and the deformation Acadian; or the rocks are pre-Middle Ordovician the the deformation possibly as old as Precambrian (Bothner et al., 1984)

The Oakdale Fm., here near its type locality, is typical of the rocks in this belt. It consists of light-gray to purplish-weathering calcareous metasiltstone and interbedded gray to gray-green phyllite. The siltstone beds range in thickness up to about 10 cm and are separated by thin partings of micaceous phyllite, or else they are interlaminated with paper-thin phyllite partings on a scale of a few mm. Ankerite causes the characteristic purplish-brown weathering spots (Hepburn, 1976). The beds dip moderately to the NW and are folded by small, tight folds with axial surfaces approximately parallel to bedding.

STOP 2-3. STRAW HOLLOW DIORITE & ANDOVER GRANITE, SILURIAN, NASHOBA TERRANE (Marlborough, MA; 40 minutes). From interchange of I-495, I-290 and "To 85" continue on "To 85" just beyond (east of) the point where the ramp from I-495 North joins it. Park with care on the right shoulder, past the electrical box. Or continue on "To 85" to the first intersection, turn around and retrace the route until just east of the cloverleaf and park on the shoulder.

We could spend hours at this series of exposures, but since time is limited we will restrict ourselves to three main features. First, proceed to exposures on the south side of "To 85" just east of junction with ramp from I-495 North along the south side of the cloverleaf. Here blastomylonite associated with a splay of the Assabet River Fault Zone is exposed. Later faulting at shallower depths produced fault breccia with a carbonate matrix, visible near the west end of the cloverleaf.

Next proceed with caution to the north side of the ramp from "To 85" to I-495 West, the center ramp in the interchange. Exposed along the north side of this ramp are examples of the two principal plutonic rock types in the Nashoba Terrane: intermediate composition diorites and peraluminous granites. The Straw Hollow Diorite is typical of the calc-alkaline dioritic to tonalitic bodies in the terrane. Most are hornblende or hornblende-biotite bearing and have sphene as an accessory mineral. The Straw Hollow contains at least two phases; a finer grained, more foliated phase has been intruded by a coarser grained, lighter colored, less foliated rock (Hill et al., 1984). The Straw Hollow is assumed to be similar in age to the Sharpners Pond Diorite to the northeast, dated at 430 Ma by Zartman and Naylor (1984). Granitic rocks in the Nashoba Terrane vary from two-mica foliated granites to unfoliated, garnet-bearing muscovite granites and pegmatites. Here, a coarse-grained phase of the Andover Granite is seen intruding the diorite. It has been sheared and deformed, likely at the same time that the blastomylonite seen on the other side of the cut was created. Note the Andover here for comparison with that we will see at Stop 2-7. At the east end of the outcrop, the Straw Hollow intrudes high grade pelitic schists containing kyanite pseudomorphs that have been replaced by sillimanite. (Please do not hammer on these.) Return to bus with care.

STOP 2-4. NASHOBA FM., ORDOVICIAN?, GNEISSES AND SCHIST, NASHOBA TERRANE (Berlin, MA; optional, 30 minutes). From Stop 2-3 proceed north on I-495. Exit at Rt. 62. Park along Rt. 62 at the bottom of the ramp from I-495 N. Examine the exposures along the east side of this ramp. <u>Beware of poison ivy!</u>

These exposures show some of the diversity within the Nashoba Fm., particularly among the gneisses. The gneisses commonly consist of biotite, quartz and plagioclase with varying percentages of these minerals in the different layers. K-feldspar may be an additional phase. More schistose beds may contain local garnet and/or sillimanite. Large muscovite flakes are likely retrograde. Minor amphibolite, calc-silicate granulite and dioritic sills are also present. Upper amphibolite facies metamorphic conditions prevail with granitic "sweats" starting to appear. The percentage of migmatitic melt generally increases to the NE in the Nashoba Terrane, as we will see at Stop 2-6. Note the multiple fold generations.

STOP 2-5. NASHOBA FM., ORDOVICIAN?, CALC-SILICATE GRANULITE AND AMPHIBOLITE (Berlin, MA; 50 minutes). From Stop 2-4 continue west on Rt. 62 for 2.1 mi. to flashing light in Berlin. Turn left onto Linden St. and continue for 0.5 mi. Park just before railroad tracks on the north side of the road. Walk north along dirt path adjacent to RR tracks and across the Corp of Engineers Flood Control Dam over North Brook, proceeding to the spillway at east end of the dam.

Calc-silicate granulite and marble occur at several horizons in the Nashoba Fm. This outcrop is likely correlative with calc-silicates in either the Beaver Brook or the Fort Pond Member of the Nashoba Fm. (Bell & Alvord, 1976). The calc-silicate granulites here contain diopside, actinolite, phlogopitic biotite, plagioclase, tourmaline and opaques. The deformation has been largely by flow in the more calcareous layers, and tectonic "fish" of originally more dolomitic or shaly layers (Hepburn and Munn, 1984) are readily observed . Garnet-bearing schistose rocks and amphibolites are present at the north end of the cut, and garnet-bearing amphibolites are present in outcrops 150 meters south along the spillway.

Return to I-495 and proceed north. <u>Note large exposures of biotite gneiss and schist of the Nashoba Fm. along I-495 between Rt. 62 and Exit #28.</u>

STOP 2-6. NASHOBA FM., ORDOVICIAN?, MIGMATITES (Harvard, MA; 30 minutes). Leave I-495 at Exit #28, Rt. 111 West. Turn right (west), cross over I-495 on Rt. 111 and stop 0.1 mi. beyond the bridge adjacent to large exposures on the right (north), opposite the entrance to I-495 South.

This large outcrop contains an excellent example of the migmatized Nashoba. Here biotite gneisses are interlayered with migmatitic gneisses and pegmatites. Sillimanite is commonly present with biotite in selvages along the rims of melted material. Muscovite is present in large, retrograded? flakes. Two generations of pegmatites are present here, the earlier having been deformed. It is believed that most of the pegmatite and granite in this outcrop is locally generated by anatexis of layers with the appropriate composition. Observe how the percentage of melt changes with the composition of the original layer. It is believed, although not yet firmly established, that when melting in the Nashoba reached sufficient proportions for the magma to coalesce and move, it formed the younger phases of the Andover Granite (Hepburn and Munn, 1984). Late brittle faults with gouge cut the outcrop.

LUNCH STOP. NORTH BRIDGE OVER THE CONCORD RIVER, MINUTE MAN NATIONAL HIST. PARK, CONCORD, MA. (40 minutes). Site of "the shot heard 'round the world" where the colonists first fired upon the British troops, April 19, 1775, starting the American Revolution.

STOP 2-7. ANDOVER GRANITE, SILURIAN, NASHOBA TERRANE (Bedford, MA; 25 minutes). From Concord continue on Rt. 62 east until junction with Rt. 3 in Bedford. Park on south side of Rt. 62 and examine exposures along the east side of the entrance ramp from Rt. 62 to Rt. 3 South.

The characteristic pink to white, unfoliated, muscovite-rich granite and granitic pegmatites of the Andover Granite are exposed here. This is the location from which the sample dated by Dunning gave the 412 ± 2 Ma age (Figure 6A). The dated rock represents the youngest granite in the outcrop and is believed to be one of the youngest phases in the Andover complex. It cross-cuts, or contains within it fragments to blocks of foliated Andover Granite, a more mafic granodiorite or diorite, and biotite gneiss of the Nashoba Fm.

STOP 2-8. FISH BROOK GNEISS, CAMBRIAN, NASHOBA TERRANE (North Andover, MA; 45 minutes). From junction of Rt. 114 and 62 in Middleton, proceed west on Rt. 114 approx. 4 mi. to the North Andover town line. In 0.2 mi. turn right onto Sharpners Pond Rd. and go straight to the end (approx. 1 3/4 mi.) to the entrance of Boxford State Forest. Park at the guard rails blocking the continuation of the road and walk the dirt path straight ahead for approx. 1/4 mi. to a large, semi-cleared area to the right of a small pond.

The Fish Brook Gneiss is a gray, fine- to medium-grained biotite-bearing felsic gneiss with a particular "swirled" foliation (Bell and Alvord, 1976). Biotite schist, biotite gneiss and amphibolite are present in minor amounts as inclusions. Granitic and pegmatitic dikes cutting the Fish Brook are believed related to the Andover Granite.

The origin of the Fish Brook Gneiss and particularly its unusual foliation have been variously interpreted. Is the foliation an original, perhaps volcanic, feature enhanced by tectonism? Or has this unit experienced greater deformation (and an additional deformational event?) compared to the rest of the Nashoba Terrane, indicating that it is an older basement? Bell and Alvord (1976) included the Fish Brook as part of the stratigraphic sequence of the Nashoba Terrane and interpreted its origin as a waterlaid tuff. Olszewski (1980) obtained zircons from this and other Fish Brook localities which yielded a zircon Pb-U upper intercept age of 730 ± 26 Ma, which he interpreted to represent a crystallization age of an original volcanic protolith. New analyses from rocks at this site gave the concordia plot shown in Figure 6B and an age of 520 +14/-11 Ma for the original crystallization of the Fish Brook. This makes the Fish Brook Gneiss early Paleozoic, not Precambrian basement. Consequently, it is unlikely that it was separated from the other stratified units of the Nashoba Terrane by a major unconformity. The 425 ± 3 Ma age on monazite (Figure 6B) from this exposure is interpreted to represent the time of metamorphism for the Nashoba Terrane.

STOP 2-9. SHARPNERS POND QUARTZ DIORITE, SILURIAN, NASHOBA TERRANE (Newbury, MA; 30 minutes). Exit from I-495 N at Exit #56, Scotland Rd., Newbury-Newburyport. At the end of the exit ramp turn left, pass under I-495 and park on right shoulder. Walk to exposures on the north side of Scotland Rd., just west of I-495, and along the entrance ramp to I-495 South, near where it joins I-495.

The Sharpners Pond Pluton (approx. 60 sq. mi.; Hon et al., 1986) is the largest of the intermediate calc-alkaline plutons in the Nashoba Terrane. It is dated at 430 ± 5 Ma from zircons (Zartman and Naylor, 1984) and consists largely of hornblende diorite, hornblende-biotite tonalite and biotite tonalite (Castle, 1965). Much of the pluton is rather homogeneous with these rock types grading gradually into one another. Sphene is a characteristic accessory phase. Near its eastern border, as seen here along the ramp to I-495 S, the Sharpners Pond Pluton exhibits complex brecciation, "pillowing" and magma mixing of the more mafic rocks within a granitic matrix. Geochemical study indicates that the granite and the mafic to intermediate rocks are not co-genetic. The granitic rocks likely represent anatectic melts formed in response to higher temperatures that resulted from the intrusion of the more mafic magmas. These two magmas interact to form a variety of structures, as shown in these exposures (Hon et al., 1986).

Turn around, follow Scotland Rd. east to Park St. and Rt. 1 in Newbury. Go south on Rt. 1.

STOP 2-10. NEWBURY VOLCANIC COMPLEX, LATE SILURIAN-EARLY DEVONIAN, PORPHYRITIC ANDESITE (Rowley, MA; 25 minutes) From Newbury continue south on Rt. 1, crossing the Parker River. 1.5 mi. south of the river turn left (east) onto Central St. and park along the road as soon as possible. Outcrops are on both sides of Central St. near the intersection with Rt. 1.

The Newbury Volcanic Complex consists of a series of andesitic and rhyolitic volcanic rocks and associated sediments that lie entirely within fault slivers along the Bloody Bluff Fault Zone, directly between the Boston-Avalon and Nashoba Terranes (Figure 1). It is well dated as latest Silurian to possibly Early Devonian on the basis of shelly fossils found in associated sediments at this locality (but hidden beneath the pavement today) as well as other nearby sites (Shride, 1976b). The exposures here, at the so-called Glen Mills site, are tuffs and flows of the porphyritic andesite member (Shride, 1976a, b). The top of each flow is recognizable by the presence of a vesicular band. Note the differences in the phenocryst content between the flows.

Tectonically the Newbury, while tilted, is important because it demonstrates the lack of penetrative deformation and metamorphism higher than the lowermost greenschist facies during the Acadian or subsequent orogenies. Notice the undeformed nature of the plagioclase phenocrysts and the filled amygdules in the outcrop. (Contrast this to the Silurian deformation seen earlier in the adjacent Nashoba Terrane).

Geochemically the Newbury Volcanic Complex consists of a volcanic suite of andesites and rhyolites (Shride, 1976a). The andesites are high-alumina calc-alkaline rocks with trace element signatures indicative of formation on a continental margin above a subduction zone (McKenna et al., 1993). The Newbury Volcanic Complex is similar in age and overall composition to volcanic rocks in the Coastal Volcanic Belt of eastern Maine (Gates and Moench, 1981). Hon et al. (1986) suggested that the similarity in the chemistry between the Newbury and the plutonic rocks of the Nashoba Terrane could indicate the Newbury are preserved volcanic remnants of this terrane.

STOP 2-10A. NEWBURY VOLCANIC COMPLEX, RHYOLITE (Newbury, MA; optional, 20 minutes). From Stop 10 turn around, then turn right onto Rt. 1 and proceed north 0.9 mi. Turn left onto Elm St. (toward Governor Drummer Academy). Almost immediately pull off and park by a small outcrop on the right. The rock is a purplish flow-banded rhyolite in the Newbury (Member 6 of Shride, 1976 a, b).

STOP 2-11. BLOODY BLUFF FAULT ZONE, NEAR THE BOUNDARY BETWEEN BOSTON-AVALON AND NASHOBA TERRANES (Minute Man Natl. Hist. Park, Lexington, MA; optional, 30 minutes). From Stop 10 return to Rt. 1 south, follow to Rt. 133 west and take I-95 south and west to junction of Rt. 2A in Lexington, Exit #30B. Exit on 2A west, toward Concord. At the end of the exit ramp turn right and proceed 0.2 mi. to Massachusetts Ave. (just past the hotel entrance on right, opposite the road to Minuteman Tech. on the left). Turn right onto Mass. Ave. Proceed 0.2 mi. to curve at the south end of Fiske Hill. Park along the right side of the road. Walk across the road to the lighter colored outcrops. <u>No hammers. This is a National Park.</u>

Exposures along the north side of the road consist of mylonitized granite (Dedham Granite?) and mafic rocks within the Bloody Bluff Fault Zone in its type area. The Bloody Bluff Fault Zone separates the Nashoba Terrane on the west from the Boston-Avalon Zone on the east and has had a long and complex history of movement. See Nelson (1987) for a more complete description of this exposure. The fault zone here is on the order of a kilometer wide. The rocks have a well-developed mylonitic foliation dipping to the northwest. Differences in the response of the granitic and mafic rocks to the shearing are evident here.

Continue on Mass. Ave. for another 0.1 mi. until the intersection with the first road on left (Do not cross over I-95). Turn left onto Wood St., proceed 0.1 mi. and turn left onto Old Mass. Ave. Follow this for 0.5 mi. to junction with Rt. 2A. Park in the lot at left and walk to the outcrop to the right of the road junction. <u>The small rusty-weathered exposure is "the" Bloody Bluff</u>. The rock is an altered and shattered granite (again, likely Dedham). Bloody Bluff and Fiske Hill were sites of skirmishes between the colonists and the retreating British troops on April 19, 1775, following the outbreak of hostilities at North Bridge earlier that day. Due to casualties (and not the rusty coloration), the rock and consequently the fault zone received its sanguine name.

Follow Rt. 2A east to I-95, then back to the hotel.

ROAD LOG - DAY 3
BOSTON-AVALON TERRANE

STOP 3-1. IGNEOUS COMPLEX, WESTERN BOSTON-AVALON TERRANE (Waltham, MA; 30 minutes). From the hotel proceed north on I-95 to exit for Wyman St.-Winter St., Waltham. At end of exit ramp (0.3 mi), turn right. In 0.2 mi. turn right again and follow Winter St. west across I-95. In 0.4 mi. stay straight and follow Winter St. around the Cambridge Reservoir. In 1.2 mi. turn left into the Bay Colony Corp. Center. Follow road uphill past outcrops for 0.25 mi. Park in the turnout opposite the entrance to 950 Winter St. and walk back along entrance road to outcrops.

The westernmost portion of the Boston-Avalon Zone, to the west and north of Boston, is underlain by a complex series of largely mafic plutonic and volcanic rocks shown on the Massachusetts Geologic Map as Zdigb and Zv (Zen et al., 1983). Clearly, several ages of plutonic rocks are present in this area (subzone 2 of Hepburn et al., 1987a) but few details on their ages or chemistries have yet been firmly established. The purpose of visiting this locality is to demonstrate the complexity of the igneous rocks found throughout this belt, as well as to see the diorite recently dated as Devonian (373 ± 4 Ma; Figure 5F). Compare this rock with the gabbro-diorite seen further north in this belt (Stop 1-7) from which the syenitic pod yielded the 444 Ma date. These dates indicate that the Boston-Avalon Terrane experienced a major, prolonged period of mafic magmatism spanning the Ordovician to Devonian, in addition to the well recognized peralkaline granitic plutonism of the same time period (Cape Ann, Peabody, Quincy, etc.).

The rocks seen here include xenolithic blocks of pre-630 Ma Westboro Fm. (quartzite) and Middlesex Fells Volcanics (fine-grained epidotitized mafic rocks), the dated medium-grained diorite, finer grained gabbro-diorites and several generations of granitic dikes. One granitic dike contains spectacular, elongated, magmatic pillows of diorite.

STOP 3-2. ROXBURY FM., LATE PROTEROZOIC, BOSTON BAY GROUP (Wellesley, MA; 30 minutes). South on I-95 (Rt. 128), take exit #20 for Rt. 9 east. After about 0.25 miles bear right onto 1st exit road. Park beside old stone building, an 18th century nail factory, on the right (south) just before crossing the Charles River. Take trail on west side of the river to Hemlock Gorge and outcrops along river. You can continue up the trail to the top of the gorge where Echo Bridge, designed by Boston's famous 19th century architect H.R. Richardson, carries a water aqueduct across the river. Turn right (west) to see outcrops along the grade of the aqueduct. You can return to vehicles by the same trail or by crossing the aqueduct and descending stairs at east end of bridge. The latter will give you a chance to try out your echo.

The polymictic clast-supported conglomerates in the outcrops near the Charles River are typical of the Brookline Mbr. of the Roxbury Fm. Dominant clast lithologies are felsites, granites, and well rounded to subrounded quartzites (similar to the Westboro seen at Stop 1-6). Conglomerate matrix and interbedded sandstones are feldspathic litharenites; silicified felsite fragments are the dominant detrital framework sand grains (Figure 3). Most outcrops of Roxbury are apparently homogeneous. At some localities where sandstone and siltstone interbeds are common, large conglomerate-filled channels may be discerned. This lack of sedimentary structures within most of the Roxbury makes it difficult to infer mechanisms of transport and environments of deposition. Some outcrops have bedding characteristics and structures indicative of braided streams and fan deltas, while other outcrops are best explained by subaqueous gravity flow processes. It is possible that the unit was deposited in a variety of basin marginal environments.

STOP 3-3. WESTWOOD GRANITE, LATE PROTEROZOIC (Dedham, MA; optional, 30 minutes). From Stop 3-2 proceed south on I-95 and exit at Rt. 109, Westwood. At end of ramp turn left (east) on Rt. 109, cross I-95 and park opposite the entrance ramps to the northbound lane of I-95. Walk north, along the curved exit ramp from I-95 N to Rt. 109.

The Westwood Granite intrudes the Dedham Granite and is likely co-magmatic with the Mattapan Volcanics (Stop 3-4) (Wones and Goldsmith, 1991). The 603 ± 3 Ma U-Pb zircon date on the Mattapan (Kaye and Zartman, 1980) likely gives the best age estimate for the Westwood. The Westwood is characteristically light-colored, often pink to salmon weathering, notably finer grained than the Dedham, lacks hornblende and has a lower color index (Wones and Goldsmith, 1991). Also present in this exposure are a number of mafic dikes, as well as various intermediate to mafic inclusions.

STOP 3-4. MATTAPAN VOLCANICS, LATE PROTEROZOIC, BRECCIA (Westwood, MA; 25 minutes). From Stop 3-3, turn around and head SW on Rt. 109 to Westwood. At junction of Hartford St. in Westwod Center, stay to the left on Rt. 109, note the mileage. Continue on Rt. 109, 0.8 mi. to exposures on the right (north) side of Rt 109 (High St.) opposite the junction of Lake Shore Drive and the Westwood Veterans Memorial.

The Mattapan Volcanic Complex likely formed a co-magmatic volcanic-plutonic complex with the Westwood Granite, similar in many ways to that seen on Day 1 between the Lynn Volcanics and Dedham North Granite (Kaye, 1984). The Mattapan is thought to be the source of many of the felsic pebbles in conglomerates of the Boston Basin. Here, a volcanic breccia in the Mattapan is exposed. Most of the fragments in the breccia are felsite from the Mattapan itself or pieces of Dedham Granodiorite (Chute, 1964). Thompson and Hermes (1990) have interpreted this breccia as originating during collapse of a caldera.

STOP 3-5. WAMSUTTA FM., PENNSYLVANIAN, NORFOLK BASIN (Canton, MA; 30 minutes). South on I-95, take Exit #62 onto University Ave. Proceed for about 1 mi. and turn left at stop sign onto Dedham St. Proceed for about 0.7 mi. and turn right just beyond interstate overpass into Shawmut Industrial Park. Follow Shawmut Rd. to SW corner of park and turn right (toward railroad tracks) at back end of warehouses. Outcrop is a blasted face adjacent to tracks and a series of natural exposures to north. <u>Danger - these tracks are heavily travelled by high speed commuter trains - keep off tracks.</u>

About 90 m of Pennsylvanian strata form a large scale, upward coarsening sequence that lies approximately 940 m above the basal unconformity (Stop 3- 6). The lower portion of the section consists of black and red shale with dark interbedded feldspathic litharenites (Figure 10). A caliche horizon of small carbonate nodules occurs in one

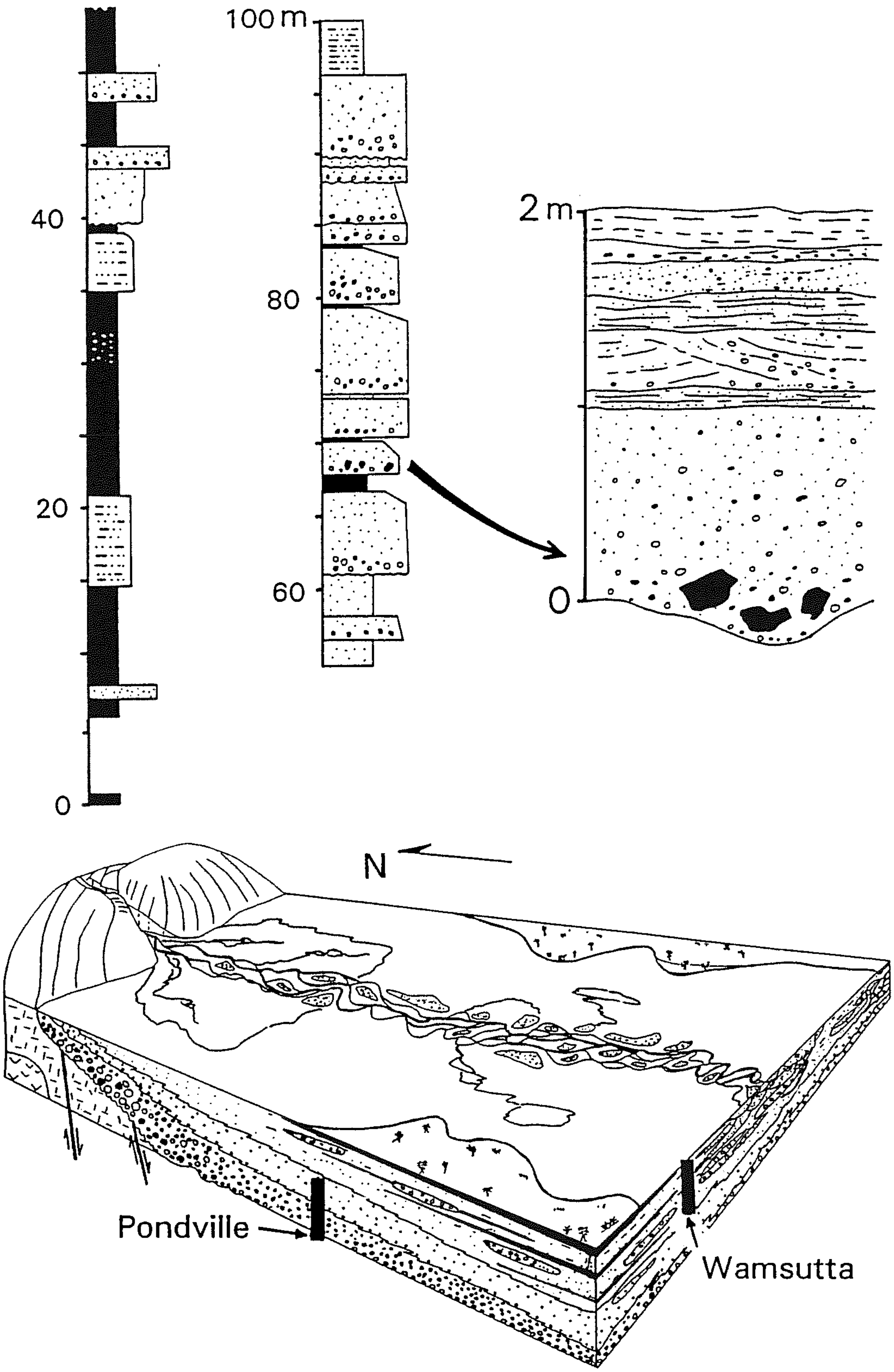

Figure 10. Stratigraphic section of Wamsutta Formation at Shawmut Industrial Park, Stop 3-5. Small inset section shows detail in one fining upward cycle. Block diagram shows facies relations and paleoenvironmental setting of the northern margin of the Norfolk Basin.

sequence of red mudstones (Figure 10), and portions of the black shales are carbonaceous. The upper part of the section is a sequence of polymictic conglomerates, sandstones, thin mud drapes and thin interbeds of dark mudstone organized in fining upward cycles. This part of the section may be interpreted as a series of flood cycles in a broad, shallow, braided stream system. The abrupt occurrence of mudstones beneath the conglomerate floored channels and large angular mudstone intraclasts in these conglomerates probably resulted from channel avulsion and lateral migration of the braided stream onto overbank deposits. Planar bedded and trough cross-bedded sandstones were probably deposited on tops of longitudinal bars migrating downstream. The lower portion of the section represents overbank environments or possibly large muddy intrachannel islands. Sandstones in this lower sequence probably represent tributary channel or channel avulsion deposits.

This outcrop is unusual because it has both the highest proportion of mudstone and the coarsest conglomerates of any measured Wamsutta section in the Norfolk Basin. This textural paradox might be the result of tectonic rejuvenation or wet climatic cycles that increased the competence of rivers.

The Alleghanian deformation in the Boston area is demonstrated by this exposure. It has folded these strata into vertical to slightly overturned beds, introduced a well-developed fracture cleavage into the mudstones and produced tension gashes filled with quartz, carbonate or chlorite. However, the rocks in this part of the Norfolk Basin are still submetamorphic (diagenetic zone; based on illite crystallinity from this exposure, Hepburn and Rehmer, 1981).

STOP 3-6. UNCONFORMITY AT BASE OF PENNSYLVANIAN PONDVILLE FM. AND PONDVILLE - WAMSUTTA TRANSITION (Quincy and Randolph, MA; 45 minutes). South on I-95. Take exit for Rt. 28 north, proceed north under I-95, make U-turn and park on the west side of Rt. 28 in a small pull-off that is just before the on-ramp for the northbound lane of I-95. Walk down the on-ramp toward the northbound lane of I-95 and cross over to large roadcut. Watch for speeding vehicles on roadway. To see the transition of the lower and upper members of Pondville walk back around on-ramp and south under I-95, enter gate between north and south bound lanes and walk down old road for about 100 m. To see the transition of the upper member of Pondville with overlying Wamsutta walk or drive to off-ramp of south bound lane of I-95. Pondville/Wamsutta transition is at north end of the cut along the off-ramp.

This spectacular roadcut exposes the southerly dipping (about 70^{o}) nonconformity between the Ordovician Blue Hills Igneous Complex (Blue Hills Porphyry) and the lower member of the Pondville Formation. Starting from the unconformity, about 94 m of the Pondville boulder conglomerate (lower member) is overlain by 91 m of pebbly granule and coarse sandstone (upper member),which grades upward into 45 m of Wamsutta red sandstones and mudstones. Moving northward from the nonconformity and into the Blue Hills Complex there is a thin zone of dense reddish aphanitic material with quartz phenocrysts. This is underlain by an interval of greenish porphyry spheroids (10 to 30 cm in diameter) in a phenocryst-bearing aphanitic groundmass. Below this the porphyry has been fractured, but the blocks have not been transported; and this zone grades into more typical homogeneous porphyry with quartz and microperthite phenocrysts.

A great deal of entertaining debate has focused on the origin of the "spheroidal zone" below the unconformity. A popular early interpretation was that the spheroids represent a Pennsylvanian paleosol developed on the exposed Blue Hills Igneous Complex. Other explanations have utilized magmatic and/or volcanic processes. The mineralogy and geochemistry of the spheroidal zone is a very close match with that of the rest of the Blue Hills Porphyry, which is co-magmatic with the Quincy Granite, so we do have some constraints on our speculation. Entertain us with your hypotheses.

The environment of deposition of the Pondville boulder conglomerate is intriguing. A likely geomorphic setting for such a coarse deposit could be the bedrock-floored mouth of a canyon at the apex of an alluvial fan. This extremely coarse conglomerate is restricted to a region less than 1 km broad along the northern margin of the Norfolk Basin. Clasts in the Pondville are mostly from the Blue Hills Igneous Complex; but curiously, typical Quincy Granite is very rare or not present. It is possible that during the Pennsylvanian the deeper portion of the igneous complex was still not exposed by erosion. Slate, basalt, and quartzite clasts are also present.

The Wamsutta outcrop south of I-95 is a sequence of upward-fining sandstone-mudstone fluvial cycles that exhibits an overall upward-fining megacycle. Sandstone beds are typically capped by a zone of mud cracks or mud curls. The entire I-95/Rt. 28 outcrop belt is a retrogradational "gigacycle" deposited in environments of diminishing transport energy. As the early rift topography was subdued by erosion more sluggish braided streams buried the source terrain. This retrogradation of sediments over a bedrock surface is reminiscent of pediment formation and burial in modern dry climates. Stream gradients would be re-established with subsequent tectonism and basin margin uplift (Cazier, 1987).

STOP 3-7. QUINCY GRANITE (ORDOVICIAN) AND BRAINTREE ARGILLITE (MIDDLE CAMBRIAN), IN THE QUINCY QUARRIES (Quincy, MA; 45 minutes). Take I-95 south to Rt. 3 north, exit for Furnace Brook Parkway but stay on ramp (rotary) to north and exit right onto Willard St., if you miss the turn go around the rotary and try again. Proceed north on Willard St. and turn left at stop sign. Go under Rt. 3 overpass and turn right onto Ricciuti Dr. at "Mr. Tux." Proceed about 0.5 mi. and park at sign indicating the trail to Quincy Quarries.

Quincy Granite. The Quincy Granite is characteristic of the early to mid-Paleozoic peralkaline intrusions into the Boston-Avalon Terrane (recall also the Peabody Granite, Stop 1-8) and forms the Blue Hills Igneous Complex along with the Blue Hills Porphyry. The Wampatuck Volcanics of the Blue Hills (Billings, 1982) may be an extrusive phase (Hermes and Murray, 1990). The Quincy Granite intrudes the Middle Cambrian Braintree Argillite, and although difficult to date (Naylor and Sayer, 1976) it has yielded a 450 ± 25 Ma (Ordovician) date by U-Pb methods (Zartman and Marvin, 1991). Typically the rock is a dark gray to green-gray, medium-grained, hypersolvus microperthitic granite with hypidomorphic texture. Riebeckitic amphiboles and acmitic pyroxenes are present (Wones and Goldsmith, 1991). While difficult to see from our stop at the top of the quarries, riebeckite can be found coating joints and slickenside surfaces (Wones and Goldsmith, 1991).

The Blue Hills Porphyry (not present at this stop) contains microperthite and quartz phenocrysts in an aphanitic matrix. Major and trace element chemistry indicate that the Blue Hills Porphyry and Quincy Granite are likely co-magmatic. Coarse-grained phenocryst-rich phases of the porphyry grade into true Quincy granite, and in some cases it is difficult to distinguish between the two. It is likely the Blue Hills Porphyry represents a hypabyssal, chilled border phase of the Quincy (Naylor and Sayer, 1976). At Stop 3-6 we saw a very fine-grained, matrix-rich version of the porphyry that might represent quenched magma at or near the margin of the pluton.

As evidenced by these large, abandoned quarries, the Quincy Granite has been used extensively as a building stone in the Boston area (e.g., Quincy Market) and elsewhere. The rock takes a good polish and has a distinctive gray to dark gray-green color. Quarrying began in 1815 but did not become extensive until the building of the Bunker Hill Monument. The first commercial narrow-gauge railroad in the United States was built to haul granite from Quincy to the monument's site in Charlestown (Skehan, 1975). Since there is no longer any commercial quarrying, many of the quarries have been preserved as public parks and reservations (to the delight of geologists, rock climbers and graffiti artists).

Braintree Argillite. A small pile of spoil excavated at or very near the original site of the famous Hayward Creek "trilobite" quarry in the Braintree Formation is about 5 m into the woods on the south side of the road, and about 50 m west down Ricciuti Dr. from the quarry trail parking area.

This spoil was produced when a drydock that now occupies a perfectly good trilobite locality was enlarged in the early 1970's. There are no extant collecting localities in the Braintree so the shipyard company dumped some of the spoil here for collecting. (When was the last time you searched for trilobites in a granite quarry?) The material in this pile is fresher and much more fossiliferous than any natural exposures that can be seen at present. The rock is a gray, brittle, silicified mudstone or argillite. Disseminated pyrite and small vugs filled with euhedral pyrite are commonly associated with the black trilobites. Bedding is obscure except where it is defined by fossils. There is no shortage of pieces of *Paradoxides* in the pile, but with individual trilobites up to 45 cm long, you are unlikely to recover more than a pygidium, a genal spine, or a piece of a cephalon. Correlative Middle Cambrian strata in Newfoundland were deposited on a deep water muddy shelf, and the Braintree Fm. probably accumulated in a similar environment.

STOP 3-8. SQUANTUM "TILLITE" MBR. OF THE ROXBURY FM., LATE PROTEROZOIC, BOSTON BAY GROUP (Squaw Rock Park, Quincy (Squantum) MA; 45 minutes). Go north on Rt. 3, exit at Granite Ave. Proceed north on Granite Ave. to intersection with Gallivan Blvd. Turn right on Gallivan Blvd. and proceed to Neponset Circle (intersection with Rt. 3). Follow signs for Rt. 3A to Quincy, stay in left lane and bear left onto Quincy Shore Drive after crossing Neponset River. Proceed on Quincy Shore Drive for 0.9 mi. and turn left at light onto Squantum St. Proceed on Squantum St. and bear left, following shoreline, onto Dorchester St. Just before causeway, turn left into parking area for VFW post. Follow trails to north then west along shoreline to outcrop A (Figure 11).

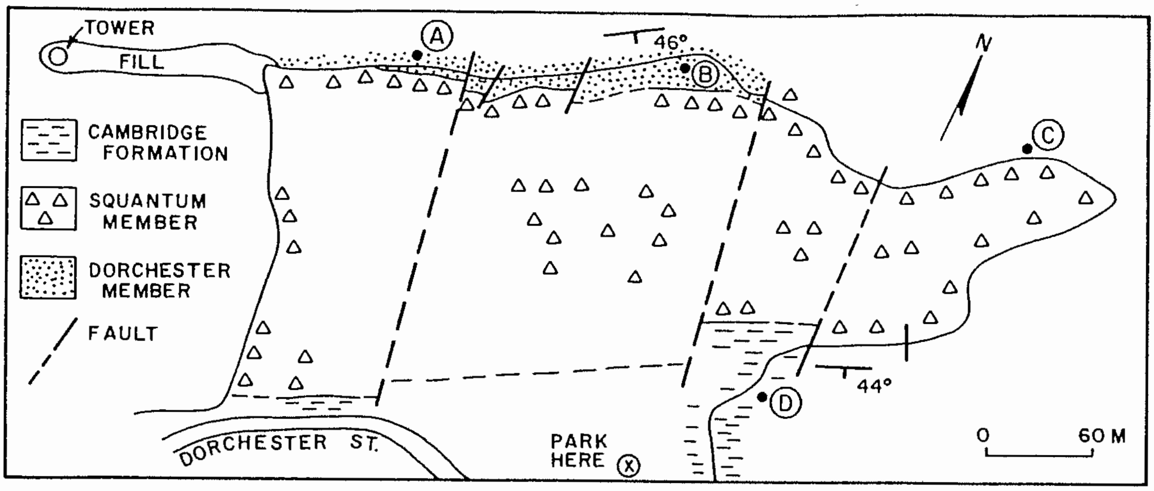

Figure 11. Simplified geologic map of Squantum Head, Squaw Rock Park, Quincy MA.

A 130 m sequence of polymictic diamictite beds, sandstones, and conglomerates comprise the heterogeneous unit mapped as the Squantum "tillite" or Squantum Member. The rocky headland known as Squaw Rock has the best and most extensive exposure of the Squantum in the Boston Basin. A unit of thinly laminated gray sandstones with graded beds and several scales of slump folds (mapped as the Dorchester Member of the Roxbury Fm.) underlies the diamictite sequence . Purple to gray mudstones with extensively deformed beds and pods of pebbly and granule sandstone overlie the diamictite (mapped as the Cambridge Argillite). The interbedded contacts of all units are fully exposed.

The base of the diamictite sequence is a chaotic interval of cobbles and boulders and intraclasts up to 2 m long in a purple-gray muddy matrix. Clasts in the diamictite are predominantly felsites and granites with some well rounded pebbles and cobbles of quartzite. This heterogeneous interval resulted from a spectrum of gravity mass transport processes ranging from low density cohesionless flow to high density plastic flow. See Bailey, in Newman et al., this volume, Chapt. U, for more details on the question of glaciation during the deposition of the Boston Bay Group.

Numerous faults cut the headland and offset the stratigraphy. Fine sandstones and mudstones have a strong cleavage that strikes nearly parallel to bedding and dips to the north at 60° to 70° degrees. This cleavage is also well expressed in the mudstone matrix of the diamictites but is deflected around clasts in the matrix.

End of Field Excursion

Return to Rt. 3 North and proceed to Logan Airport.

REFERENCES CITED

Bailey, R.H., 1984, A Precambrian continent margin sequence (slope deposits and olistostromes): Boston North quadrangle, Massachusetts: *in* Hanson, L.S., ed., Geology of the Coastal lowlands: Boston, MA to Kennebunk, ME, 76th New England Intercollegiate Geological Conference, Salem State College, Salem, MA, p. 145-164.

Bailey, R.H., Skehan, J.W., Dreier, R.B. and Webster, M.J., 1989, Olistostromes of the Avalonian terrane of southeastern New England, *in* Horton, J.W. and Rast, Nicholas, eds., Melanges and Olistostromes of the U. S. Appalachians: Geological Society of America Special Paper 228, p. 93-112.

Bell, K.G. and Alvord, D.C., 1976, Pre-Silurian stratigraphy of northeastern Massachusetts: *in* Page L.R., ed., Contributions to the Stratigraphy of New England, Geological Society of America Memoir 148, p. 179-216.

Billings, M.P., 1976, Geology of the Boston Basin, *in* Lyons, P.C. and Brownlow, A.H., eds., Studies in New England Geology, Geological Society of America Memoir 146, p. 5-30.

Billings, M.P., 1982, Ordovician cauldron subsidence of the Blue Hills Complex, eastern Massachusetts: Geological Society of America Bulletin, v. 93, p. 909-920.
Billings, M.P. and Rahm, D., 1966, Geology of the Malden tunnel, Massachusetts: Journal of the Boston Society of Civil Engineers, v.. 53, p. 116 -141.
Bober, Roman, 1989, Metamorphism of the Nashoba Block and the Tadmuck Brook Schist, east-central Massachusetts: Unpubl. M.S. thesis, Boston College, Chestnut Hill, MA, 194 p.
Bothner, W.A., Boudette, E.L., Fagan, T.J., Gaudette, H.E., Laird, J. and Olszewski, W.J., Jr., 1984, Geologic framework of the Massabesic Anticlinorium and the Merrimack Trough, southeastern New Hampshire: *in* Hanson, L. ed., Geology of the Coastal Lowlands: Boston, MA to Kennebunk, ME, 76th New England Intercollegiate Geological Conference, Salem State College, Salem, MA, p. 186-206.
Cardoza, K.D., Hepburn, J.C. and Hon, R., 1990, Geochemical constraints on the paleotectonic setting of two late Proterozoic mafic volcanic suites, Boston-Avalon zone, eastern Massachusetts: *in* Socci, A.D., Skehan, J.W. and Smith, G.W., eds., Geology of the Composite Avalon Terrane of Southern New England, Geological Society of America Special Paper 245, p. 113-131.
Castle, R.O., 1965, A proposed revision of the subalkalic intrusive rocks of northeastern Massachusetts: U.S. Geological Survey Professional Paper 525-C, p. 74-80.
Cazier, E.C., 1987, Late Paleozoic tectonic evolution of the Norfolk Basin, southeastern Massachusetts: Journal of Geology, v. 95, p. 55-73.
Chute, N.E., 1964, Geology of the Norfolk basin Carboniferous sedimentary rocks and the various igneous rocks of the Norwood and Blue Hills quadrangles: *in* Skehan, J.W., S.J., ed., Guidebook to Field Trips in the Boston Area and Vicinity, 56th New England Intercollegiate Geological Conference, Boston College, Chestnut Hill, MA p. 91-114.
Davis, D.W., 1982, Optimum linear regression and error estimation applied to U-Pb data: Canadian Journal of Earth Sciences, v. 19, p. 2141-2149.
Dillon, Peter, Dunning, G.R. and Hon, R., 1993, Geochemical and geochronological evidence for two distinct Late Avalonian magmatic suites, eastern Massachusetts: Geological Society of America Abstracts with Programs, v. 25, no. 2, p. 12.
DiNitto, R., Hepburn, J.C., Cardoza, K.D. and Hill, M., 1984, The Marlboro Formation in its type area and associated rocks just west of the Bloody Bluff Fault Zone, Marlborough area, Massachusetts: *in* Hanson, L. ed., Geology of the Coastal Lowlands: Boston, MA to Kennebunk, ME, 76th New England Intercollegiate Geological Conference, Salem State College, Salem, MA, p. 271-291.
Dunning, G.R., Barr, S.M., Raeside, R.P. and Jamieson, R.A., 1990, U-Pb zircon, titanite and monazite ages in the Bras d'Or and Aspy terranes of Cape Breton Island, Nova Scotia: Implications for igneous and metamorphic history: Geological Society of America Bulletin, v. 102, p. 322-330.
Gates, Olcott and Moench, R.H., 1981, Bimodal Silurian and Lower Devonian volcanic rock assemblages in the Machias-Eastport area, Maine: U.S. Geological Survey Professional Paper 1184, 32 p.
Gaudette, H.E., Bothner, W.A., Laird, J., Olszewski, W.J., Jr. and Cheatham, M.M., 1984, Late Precambrian/Early Paleozoic deformation and metamorphism in southeastern New Hampshire -- confirmation of an exotic terrane: Geological Society of America Abstracts with Programs, v. 16, p. 516.
Goldsmith, Richard, 1991a, Stratigraphy of the Nashoba Zone, eastern Massachusetts: an enigmatic terrane: *in* Hatch, N.L. Jr., ed., The Bedrock Geology of Massachusetts, U.S. Geological Survey Professional Paper 1366 E-J, p. F1-F22.
Goldsmith, Richard, 1991b, Structural and metamorphic history of eastern Massachusetts: *in* Hatch, N.L. Jr., ed., The Bedrock Geology of Massachusetts, U.S. Geological Survey Professional Paper 1366 E-J, p. H1-H63.
Goldstein, A., 1992, Motion on the Clinton-Newbury and related faults and multiple deformation of the Merrimack Group in eastern Massachusetts: Aspects of the Alleghanian Orogeny in southeastern New England: *in* Robinson, P. and Brady, J.B., eds., Guidebook for Field Trips in the Connecticut Valley Region of Massachusetts and Adjacent States, 84th New England Intercollegiate Geological Conference, p. 120-131.
Hamidzada, N.A., Hermes, O.D. and Murray, D.P., 1993, Multiple mafic and felsic magma interaction as exhibited in the Dartmouth Pluton, Avalon Zone, southerastern Massachusetts: Geological Society of America Abstracts with Programs, v. 25, no. 2, p. 21.
Hatch, N. L., Jr., 1991, ed., The Bedrock Geology of Massachusetts: U.S. Geological Survey Professional Paper 1366-E-J.
Hepburn, J.C., 1976, Lower Paleozoic rocks west of the Clinton-Newbury Fault Zone, Worcester area, Massachusetts: *in* Cameron, B., ed., Geology of Southeastern New England, 68th New England Intercollegiate Geol. Conference, Boston University, Boston, MA, Science Press, Princeton, NJ, p. 366-382.
Hepburn, J.C. and Munn, B., 1984, A geologic traverse across the Nashoba block, eastern Massachusetts: *in* Hanson, L.S., ed., Geology of the Coastal lowlands: Boston, MA to Kennebunk, ME, 76th New England Intercollegiate Geological Conference, Salem State College, Salem, MA, p. 103-114.

Hepburn, J.C. and Rehmer, J.R., 1981, The diagenetic to metamorphic transition in the Narragansett and Norfolk Basins, Massachusetts and Rhode Island: *in* Boothroyd, J.C. and Hermes, O.D., eds., Guidebook to Geologic Field Studies in Rhode Island and Adjacent Areas: 73rd New England Intercollegiate Geologic Conference, Univ. of Rhode Island, Kingston, RI, p. 47-65.

Hepburn, J.C., Hill, M. and Hon, R., 1987a, The Avalonian and Nashoba Terranes, eastern Massachusetts, USA: an overview: Maritime Sediments and Atlantic Geology, v. 23, p. 1-12.

Hepburn, J.C., Lux, D.R. and Hill, M., 1987b, $^{40}Ar/^{39}Ar$ Carboniferous cooling ages from the Nashoba Terrane, eastern Massachusetts: Geological Society of America, Abstracts with Programs, v. 19, no. 1, p. 18.

Hermes, O.D. and Murray, D.P., 1990, Geochemical distinctions of late Proterozoic and Paleozoic volcanism in the Avalon zone of New England: *in* Socci, A.D., Skehan, J.W. and Smith, G.W., eds., Geology of the Composite Avalon Terrane of Southern New England: Geological Society of America Special Paper 245, p. 97-112.

Hermes, O.D. and Zartman, R.E., 1985, Late Proterozoic and Devonian plutonic terrane within the Avalon Zone of Rhode Island: Geological Society of America Bulletin, v. 96, p. 272-282.

Hill, M., Hepburn, J.C., Collins, R.D. and Hon, R., 1984, Igneous rocks of the Nashoba Zone, Eastern Massachusetts: *in* Hanson, L., ed., Geology of the Coastal Lowlands: Boston, MA to Kennebunk, ME, 76th New England Intercollegiate Geological Conference, Salem State College, Salem, MA, p. 61-80.

Hon, R. and Thirlwall, M.F., 1985, Newbury Volcanics - a Late Silurian island arc (?): Geological Society of America Abstracts with Programs, v. 17, p. 25.

Hon, R., Hepburn, J.C., Bothner, W.A., Olszewski, W.J., Gaudette, H.E., Dennen, W.H. and Loftenius, C., 1986, Mid-Paleozoic calc-alkaline rocks of the Nashoba Block and Merrimack Trough: *in* Newberg, D.W., ed., Guidebook for Field Trips in Southwestern Maine, 78th New England Intercollegiate Geological Conference, Bates College, Lewiston, ME, p. 37-52.

Kaye, C.A., 1984, Boston Basin restudied: *in* Hanson, L., ed., Geology of the Coastal Lowlands: Boston, MA to Kennebunk, ME, 76th New England Intercollegiate Geological Conference, Salem State College, Salem, MA, p. 124-144.

Kaye, C.A. and Zartman, R.E., 1980, A late Proterozoic Z to Cambrian age for the stratified rocks of the Boston Basin, Massachusetts, USA: *in* Wones, D.R., ed., Proceedings, The Caledonides in the USA, International Geological Correlations Project 27, Blacksburg, VA, Virginia Polytechnic Institute and State University Memoir 2, p. 257-261.

Lenk, C., Strother, P.K., Kaye, C.A. and Barghoorn, E.S., 1982, Precambrian age of the Boston Basin: new evidence from fossils: Science, v. 216, p. 619-620.

Lyons, J.B., Boudette, E.L. and Aleinikoff, J.N., 1982, The Avalonian and Gander Zones in central New England: *in* St.-Julien, P. and Beland, J., eds., Major Structural Zones and Faults of the Northern Appalachians: Geological Association of Canada Special Paper 24, p. 43-66.

McKenna, J.M, Hepburn, J.C. and Hon, R., 1993, Geochemistry of the Newbury Volcanic Complex, northeastern Massachusetts: Geological Society of America Abstracts with Programs, v. 25, no. 2, p. 63.

Mosher, Sharon, 1983, Kinematic history of Narragansett Basin, Massachusetts and Rhode Island: constraints on late Paleozoic plate reconstructions: Tectonics, v. 2, p. 327-344.

Nance, R.D., 1990, Late Precambrian-early Paleozoic arc-platform transitions in the Avalon terrane of the Northern Appalachians; review and implications: *in* Socci, A.D., Skehan, J.W. and Smith, G.W., eds., Geology of the Composite Avalon Terrane of Southern New England, Geological Society of America Special Paper 245, p. 1-11.

Naylor, R.S. and Sayer, S., 1976, The Blue Hills Igneous Complex, Boston area, Massachusetts: *in* Cameron, B., ed., Geology of Southeastern New England, 68th New England Intercollegiate Geological Conference, Boston University, Boston, MA: Science Press, Princeton, New Jersey, p. 135-146.

Nelson, A.E., 1987, The Bloody Bluff fault zone near Lexington, Massachusetts, *in* Roy, D.C., ed., Decade of North American Geology Centennial Field Guide, vol. 5, Geological Society of America, p. 205-208.

O'Brien, S.J., Wardle, R.J. and King, A.F., 1983, The Avalon Zone: A Pan-African terrane in the Appalachian orogen of Canada: Geological Journal, v. 18, p. 195-222.

Olszewski, W.J., Jr., 1980, The geochronology of some stratified metamorphic rocks in northeastern Massachusetts: Canadian Journal of Earth Sciences, v. 17, p. 1407-1416.

Paige, M.L. and Hon, R., 1988, Use of granitic types in tectonic analysis: Mid-Paleozoic magmatism, eastern Massachusetts (USA): [Abstract] 8th International Conference on Basement Tectonics, p. 29.

Rast, N. and Skehan, J.W., S.J., 1983, The evolution of the Avalonian plate: Tectonophysics, v. 100, p. 257-286.

Rehmer, J.A. and Roy, D.C., 1976, The Boston Bay Group: the boulder bed problem: *in* Cameron, B., ed., Geology of Southeastern New England, 68th New England Intercollegiate Geological Conference, Boston University, Boston, MA, Science Press, Princeton, NJ, p. 71-91.

Robinson, Peter and Goldsmith, Richard, 1991, Stratigraphy of the Merrimack Belt, central Massachusetts: *in* Hatch, N.L., Jr., ed., The Bedrock Geology of Massachusetts. U.S. Geological Survey Professional Paper 1366 E-J, p. G1-G37.

Rodgers, John, Grasso, Thomas and Jordan, W.M.,1989, eds., Boston to Buffalo, in the Footsteps of Amos Eaton and Edward Hitchcock: Field Trip Guidebook T169, 28th International Geological Congress, American Geophysical Union, 99 p.

Shride, A.F., 1976a, Stratigraphy and correlation of the Newbury volcanic complex, northeastern Massachusetts: *in* Page, L.R., ed., Contributions to the Stratigraphy of New England, Geological Society of America Memoir 148, p. 147-177.

Shride, A.F., 1976b, Stratigraphy and structural setting of the Newbury Volcanic Complex, northeastern Massachusetts: *in* Cameron, B., ed., Geology of Southeastern New England, 68th New England Intercollegiate Geological Conference, Science Press, Princeton, NJ, p. 291-300.

Skehan, J.W., S.J., 1975, Puddingstone, Drumlins and Ancient Volcanoes: A Geologic Field Guide Along Historic Trails of Boston: Boston College Bicentenniial Publication, Chestnut Hill, MA, 63 p.

Skehan, J.W., S.J. and Rast, N., 1983, Relationship between Precambrian and Lower Paleozoic rocks of southeastern New England and other North Atlantic Avalonian terranes: *in* Schenk, P.E., ed., Regional Trends in the Geology of the Appalachian-Caledonian-Hercynian-Mauritanide Orogen, NATO Advanced Science Institutes Series, D. Reidel Publishing Co., Dordrecht, p. 131-162.

Skehan, J.W., S.J. and Rast, N., 1991, Tectonic lithologies in the Boston Avalon -- mylonites, pseudotachylites and migmatized mylonites: Geological Society of America Abstracts with Programs, v. 23, p. 128.

Skehan, J.W., Rast, N. and Mosher, S., 1986, Paleoenvironmental and tectonic controls of sedimentation in coal forming basins of southeastern New England, *in* Lyons, P.C. and Rice, C. L., eds., Coal Forming Basins in the United States: Geological Society of America Special Paper 210, p. 9 - 30.

Smith, C. and Hon, R., 1984, Geology, petrology and origin of the Precambrian igneous rocks located in the area north of Boston: *in* Hanson, L. ed., Geology of the Coastal Lowlands: Boston, MA to Kennebunk, ME, 76th New England Intercollegiate Geological Conference, Salem State College, Salem, MA, p. 292-309.

Socci, A.D. and Smith, G.W., 1990, Stratigraphic implications of facies within the Boston Basin: *in* Socci, A.D., Skehan, J.W. and Smith, G.W., eds., Geology of the Composite Avalon Terrane of Southern New England, Geological Society of America Special Paper 245, p. 55-74.

Socci, A.D. Skehan, J.W. and Smith, G.W., 1990, eds., Geology of the Composite Avalon Terrane of Southern New England: Geological Society of America Special Paper No. 245, 254 p.

Thompson, M.D. and Hermes, O.D., 1990, Ash-flow stratigraphy in the Mattapan Volcanic Complex, greater Boston, Masssachusetts: *in* Socci, A.D., Skehan, J.W. and Smith, G.W., eds., Geology of the Composite Avalon Terrane of Southern New England, Geological Society of America Special Paper 245, p. 85-95.

Wones, D.R. and Goldsmith, Richard, 1991, Intrusive rocks of eastern Massachusetts: *in* Hatch, N.L., Jr., ed., The Bedrock Geology of Massachusetts, U.S. Geological Survey Professional Paper 1366 E-J, p. I1-I61.

Zartman, R.E., 1977, Geochronology of some alkalic rock provinces in eastern and central United States: Annual Review of Earth and Planetary Sciences, v. 5, p. 257-286.

Zartman, R.E. and Marvin, R.F., 1971, Radiometric age (Late Ordovician) of the Quincy, Cape Ann and Peabody granites from eastern Massachusetts: Geological Society of America Bulletin, v. 82, p. 937-958.

Zartman, R.E. and Marvin, R.F., 1991, Radiometric ages of rocks in Massachusetts: *in* Hatch, N.L., Jr., ed., The Bedrock Geology of Massachusetts, U.S. Geological Survey Professional Paper 1366 E-J, p. J1-J19.

Zartman, R.E. and Naylor, R.S., 1984, Structural implications of some radiometric ages of igneous rocks in southeastern New England: Geological Society of America Bulletin, v. 95, p. 539-552.

Zen, E-an, 1989, Tectonostratigraphic Terranes in the Northern Appalachians: 28th International Geological Congress Field Trip Guidebook T 359, American Geophysical Union, 68 p.

Zen, E-an, ed., Goldsmith, R., Ratcliffe, N.M., Robinson, P. and Stanley, R.S., compilers, 1983, Bedrock geologic map of Massachusetts: Reston, VA, U.S. Geological Survey, scale 1:250,000.

Chapter Y

Geology of East Point, Nahant, Massachusetts

By Richard H. Bailey and Martin E. Ross

Field Trip Guidebook for the Northeastern United States:
1993 Boston GSA

Volume 2
Contribution No. 67, Department of Geology and Geography, University of Massachusetts, Amherst, Massachusetts

GEOLOGY OF EAST POINT, NAHANT, MASSACHUSETTS

by
Richard H. Bailey and Martin E. Ross
Department of Geology, Northeastern University, Boston, MA 02115

INTRODUCTION

The sea cliffs surrounding the eastern tip of Nahant, MA are a favored destination for many dozens of geologists and geology students every year. The prime geological attractions are faulted, fossiliferous, Lower Cambrian strata and numerous mafic sills and dikes that cut the Cambrian rocks. Rugged cliffs, embayed with pocket boulder and cobble beaches, also offer the opportunity for study of interesting coastal geomorphology and sedimentology. This is a place where you can see coastal geomorphic features and the processes that created them, huge waves crashing into sea cliffs.

Geomorphology and Geologic Setting

Nahant is a rocky "island" about 9 miles (14 km) northeast of Boston, jutting into Massachusetts Bay (see Figure 1 in Hepburn and others, 1993, this volume, chapter X). Nahant was originally connected to the mainland by a 2 km long tombolo, upon which the modern causeway was built. Much of the island is surrounded by cliffs, up to 15 m high, and coastal bedrock exposures. The cliffs are cut by prominent narrow vertical walled chasms produced by wave plucking of mafic dikes and/or fault zones. Some of the more homogeneous outcrops of igneous rocks have glacial striae and some have glacially sculpted forms.

Most of Little Nahant and Nahant are underlain by Ordovician gabbro, with Cambrian rocks exposed only at the East Point area and in a smaller area in Little Nahant. The local geological setting is somewhat enigmatic, in as much as the "island" of Nahant is surrounded by water. Its relationship with surrounding geology may be similar to that of Cambrian strata and igneous rocks south of Boston where the Cambrian sequence is intruded and surrounded by the Blue Hills Igneous Complex which is in turn faulted against older and younger rocks. Although Nahant is geologically isolated, both the igneous and sedimentary rocks can be related to rocks on the mainland.

On a clear day you can gain an appreciation of the regional setting of Nahant by walking to the top of the highest hill above the cliffs. Looking to the northeast you can see the rocky granite peninsula of Cape Ann. To the southwest (250°) you can see the skyline of Boston, and in the distance to the left of the city (220°) the highest peak on the horizon is Great Blue Hill of the Blue Hills "range" (underlain by the Blue Hills Igneous Complex) which forms the southern margin of the Boston Basin. Looking due south you see Boston Harbor and Massachusetts Bay which are underlain by Late Proterozoic sedimentary rocks of the Boston Bay Group. In the distance to the south you can see the drumlins of the Boston Harbor Islands.

Mapping and Locality

The maps and data presented in this guide resulted from two coordinated, but separate efforts. Mapping, and studies of petrology and geochemistry of igneous rocks were performed by M. E. Ross. R. H. Bailey mapped sedimentary rocks and studied stratigraphy, sedimentology, and paleontology. Bailey and Ross combined their work to analyze structure, geomorphology, and regional tectonic setting. Mapping in the project was done on enlargements of aerial photographs at a scale of 1 inch = 50 feet (2.54 cm = 15.2 m). We first present discussions of sedimentary and igneous rocks and then describe aspects of the geology of the separate structural blocks comprising East Point. This latter section, with the accompanying maps constitutes the field guide for this trip.

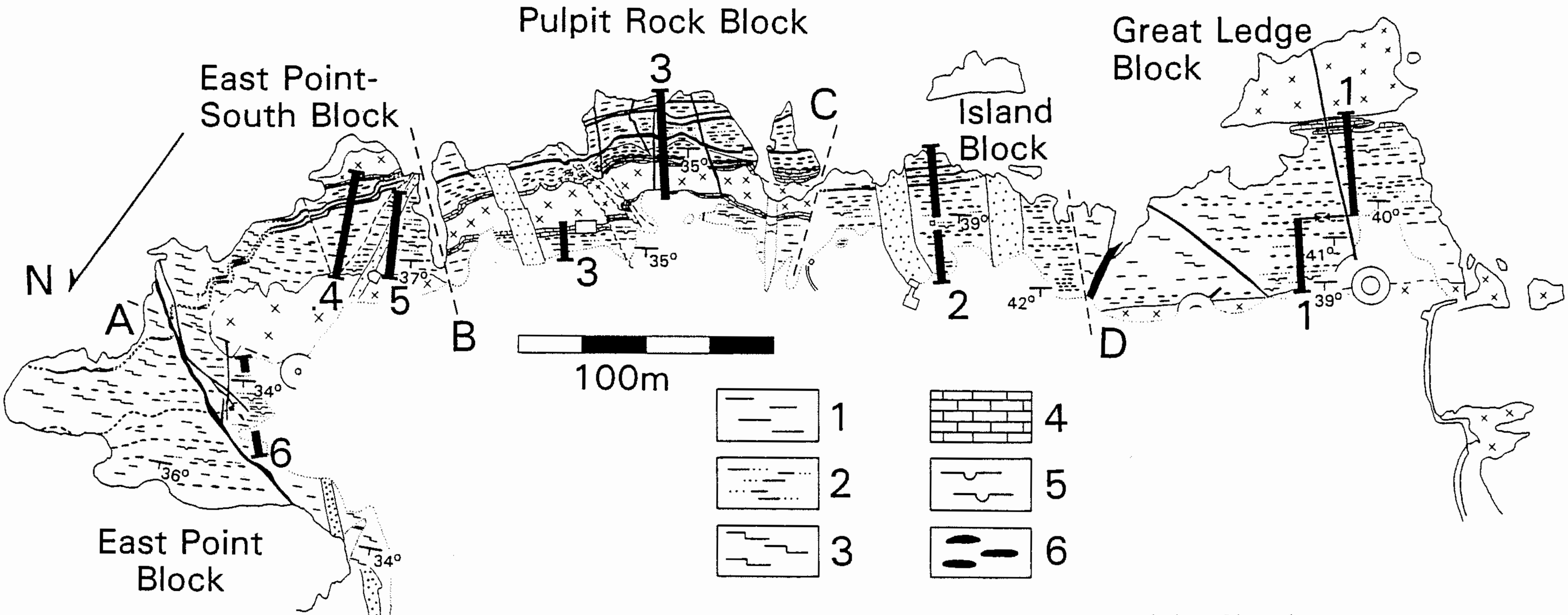

Figure 1. Geologic map of East Point, MA. This map presents relationships of sedimentary strata of the Weymouth Formation. Thick sills (x - pattern), thick dikes (heavy stipple), thinner sills and dikes (black), are from Figure 2. Heavy dashed lines (A - D) are major faults bounding structural blocks. Rectangular, circular, and other linear features are gun emplacements, pillboxes, walls, stairs, walkways, and other human features shown for reference. The lightly stippled line shows the limit of bedrock exposure.

Heavy bars with crossed ends labeled 1 - 6 are positions of measured stratigraphic sections shown in Figure 3.

Description of legend:

1. Laminated mudstone
2. Silt/very fine sand laminated mudstone
3. Fractured and tectonized mudstone
4. Limestone and nodular limestone
5. *Teichichnus* trace fossil
6. Altered carbonate nodules

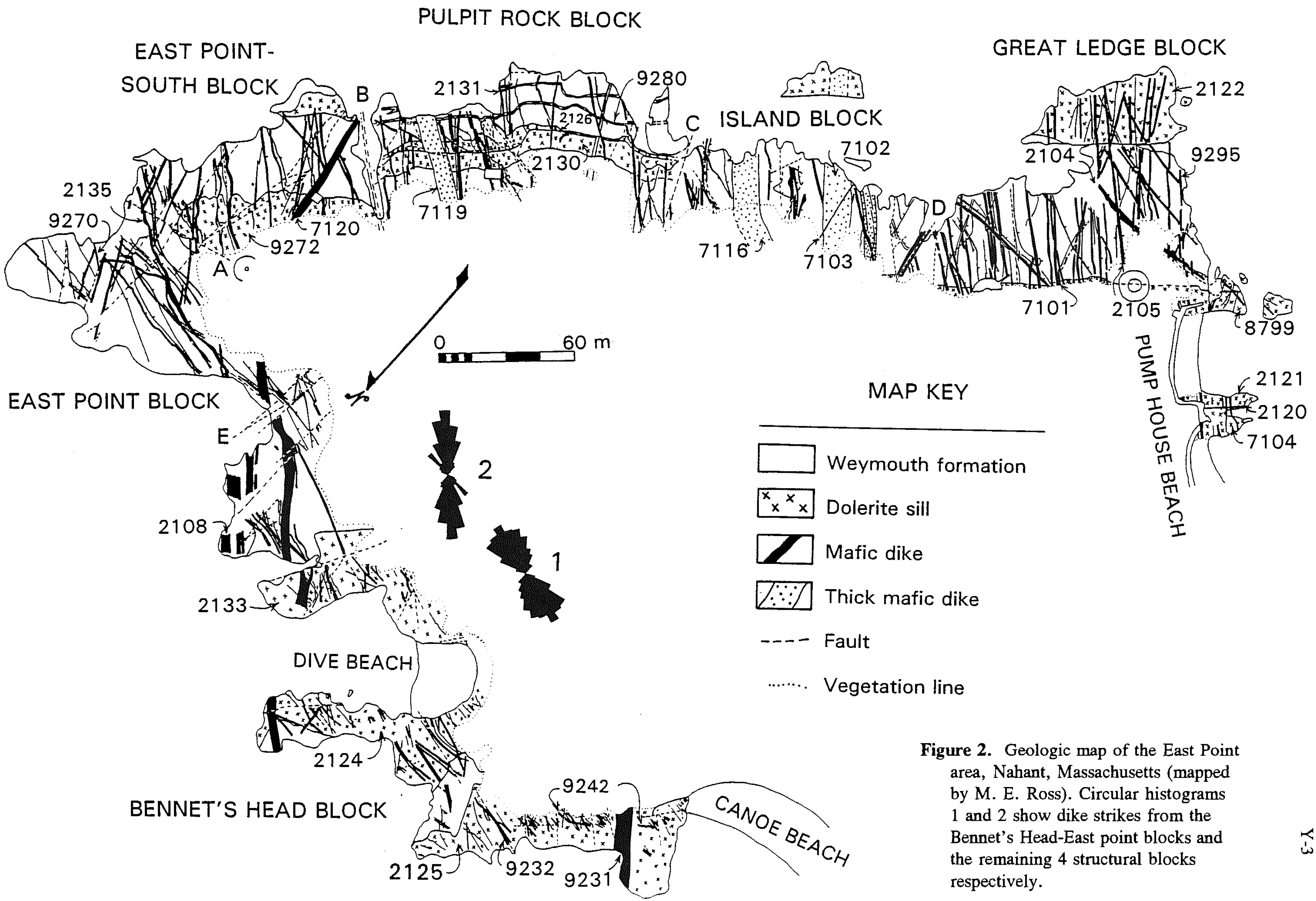

Figure 2. Geologic map of the East Point area, Nahant, Massachusetts (mapped by M. E. Ross). Circular histograms 1 and 2 show dike strikes from the Bennet's Head-East point blocks and the remaining 4 structural blocks respectively.

To reach East Point from Boston and points south follow Rt. 1A north to Lynn Shore Drive, proceed on Lynn Shore Drive to rotary at north end of Lynn Beach, and from rotary go south on Nahant Rd. across causeway and through Nahant to the gate at the Northeastern University Marine Science Center. From points north and west take I-95 north or south to Rt. 129; follow Rt. 129, carefully noting route signs, through Lynn to Lynn Shore Drive, follow Lynn Shore Drive south to rotary at north end of Lynn Beach, and follow instruction above. Enter the gate and park in front of the MSC. You must get permission in advance from the Director of the Marine Science Center to park and to visit portions of the cliffs. Do not park outside the gate as you will be quickly ticketed and/or towed.

CAMBRIAN SEDIMENTARY ROCKS

Regional and Local Stratigraphy

Lower Cambrian rocks are exposed in three primary areas in eastern Massachusetts, Nahant, the Mill Cove area of Weymouth, and the area around Hoppin Hill, North Attleboro. In addition, there are very small areas of outcrop near Sheldonville, MA and near Newport, Rhode Island, and a number of boulders and cobbles with Lower Cambrian fossils have been collected along the coast of Massachusetts.

Strata at Nahant are correlated with green and red nodular mudstones and white limestones at the type locality of the Weymouth Formation at Mill Cove. The section at Hoppin Hill, named the Hoppin Formation (Emmerson, 1917), consists of pebbly feldspathic arenite and quartzarenites nonconformably overlying the Hoppin Granite (ca. 600 to 620 Ma) (Billings, 1929; Dowse, 1950). The arenite beds are in turn overlain by red and green mudstones and fossiliferous reddish nodular limestones (Anstey, 1979). This section was recently restudied by Landing (1988) who proposed abandonment of the term Hoppin Formation and correlated the Hoppin strata with the Weymouth Formation. In addition, Landing (1988) named the North Attleboro Formation to encompass the basal quartzarenite which he inferred on the basis of reworked quartzite pebbles, to be separated from overlying strata by an unconformity. We prefer to retain the term Hoppin Formation because the basal arenites appear to grade upward into overlying strata.

Regional Biostratigraphy

Early paleontologic studies revealed that at both Mill Cove and Hoppin Hill a fauna dominated by small tubular and conoidal fossils (hyoliths) was overlain by a trilobite bearing assemblage (Burr, 1900; Shaler and Foerste, 1888; Grabau, 1900; Foerste 1899). The *Callavia*-zone trilobites of both areas are typical of the Acado-Baltic faunal province, and may be correlated with similar horizons in New Brunswick, Newfoundland, England, and Morocco (Theokritoff, 1968; Anstey, 1979; Landing, 1992).

The excellent work by Landing and co-workers (Landing, 1988; Landing and others, 1989; Landing, 1989; Landing, 1991, 1992, 1993) on the Lower Cambrian of the Avalonian Terranes has established a biostratigraphic zonation based on calcareous and phosphatic small shelly species and assemblages. The upper trilobite bearing beds at Mill Cove and Hoppin Hill comprise the Branchian Series, upper Lower Cambrian, (= Brigus Formation) of Newfoundland (Landing, 1992). The underlying upper Placentian Series is based on a sequence of small shelly species in the Bonavista Group of Newfoundland (Landing and others, 1989) which characterize an older *Sunnaginia imbricata* zone and a younger *Camenella baltica* zone. The lower beds of the Hoppin Formation were assigned to the *S. imbricata* zone (Landing, 1988). The lower Weymouth at Mill Cove contains a sparse fauna possibly representing the *C. baltica* zone and Weymouth limestones at Nahant contain a characteristic *C. baltica* zone calcareous shelly assemblage.

Distribution of small shelly faunas in Lower Cambrian rocks is often highly uneven, as at Nahant, with abundantly fossiliferous limestones interbedded with thick clastic sequences devoid of shelly species. Because of

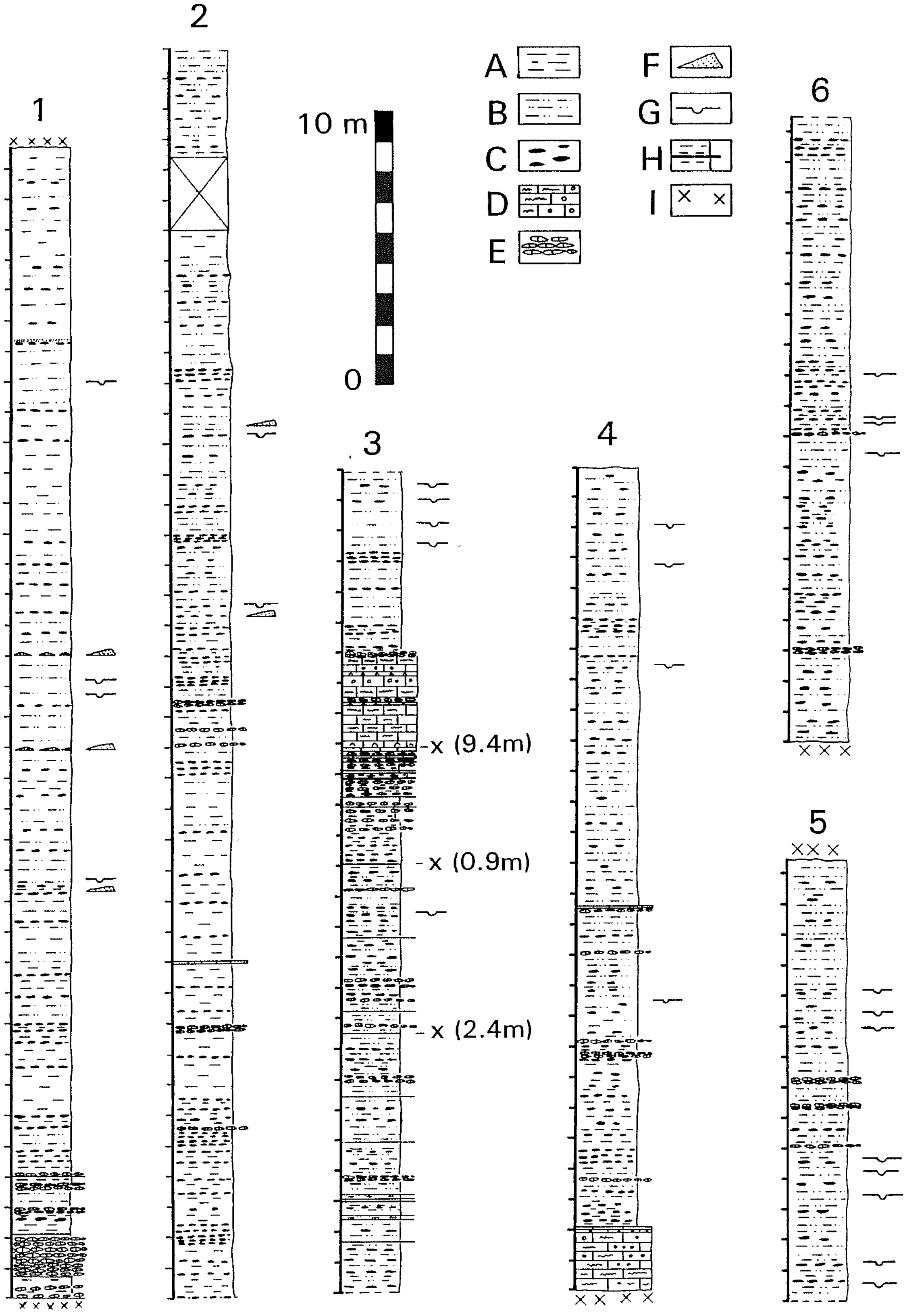

Figure 3. Measured stratigraphic sections of Weymouth Formation at East Point. See Figure 1 for section locations. Descriptions for legend: A. laminated mudstone, B. silt/sand laminated mudstone, C. nodules, D. limestone (cherty, fossiliferous), E. nodular limestone, F. ripple cross-laminated silt/sand intervals, G. *Teichichnus* traces, H. thin micritic limestones (not nodular), I. mafic sills (thickness), sill thickness is removed from sedimentary section.

this sudden introduction of taxa with a particular lithofacies one must interpret Lower Cambrian biostratigraphy with care.

Nahant Stratigraphy

Six measured sections from Nahant are presented in Figure 3. The total thickness of exposed strata cannot be ascertained due to offsets on major faults. No single bed or package of beds could be correlated with certainty between the mapped structural blocks. Assuming there is no duplication of strata due to overlap of sections, a total cumulative thickness of at least 167m is exposed.

Facies and Petrography

The 3 primary lithofacies recognized in Nahant strata 1) mudstone, 2) nodular mudstone, 3) limestone (Bailey, 1984) may be divided into a number of facies sub-types.

Laminated Mudstone. Most of Nahant strata is a dark grey to black (on freshly broken surface) faintly laminated argillite or claystone to mudstone, with altered carbonate nodules. In thin section, sparse lenses and stringers of quartz silt and rare very fine sand grains are present. Trace fossils (*Teichichnus*) and scour surfaces occur but are not abundant.

Silt Laminated Mudstone. Tan to purple-grey weathering mudstones have very distinctive, millimeter scale, silt laminae. Some graded very fine sand laminae overlie irregular scoured surfaces and grade up to silt/clay and silt laminated bedding. Isolated ripple cross-laminated lenses of very fine sand and silt occur sparsely and a horizon of 2-3 cm sandstone hummocks(?) is present in section 1 (Figure 4).

Nodular Mudstones. Mudstones similar to facies above may contain ovoid (2-3 cm x 4-8 cm) or planar (0.5-1 x 3-6 cm) nodules. Ovoid nodules are more common in faintly laminated mustone, and planar nodules are more common in silt laminated mudstone. The ovoid nodules may represent patches of primary carbonate and the planar nodules probably result from early diagenetic processes in coarser laminations (Landing, 1988; Landing and Myrow, 1993). Both types of nodules may be so abundant on single bedding planes or on closely spaced bedding planes that they coalesce to form nodular pseudobeds or nodular limestones.

Virtually all of the nodules in any type of mudstone have been altered from carbonate to chert and epidote, and near sills and dikes to Ca-silicates and Ca-garnet (Bingham, 1977). Nodules are often zoned with Ca-silicate interiors and chert rims. The chert rims may extend well beyond the original core of the nodule into adjacent stratification. Many of the nodules at Nahant have the core dissolved. The high degree of alteration, and the subsequent dissolution render interpretation of nodule development and diagenesis somewhat problematical. Shelly fossils have never been observed in either type of nodule.

***Teichichnus* Mudstone.** Purple to grey weathering mudstones, often associate with silt laminated intervals, contain common to very abundant traces of the burrow *Teichichnus* (Figures 4 and 5, and discussion in paleontology section). Some horizons have been intensively bioturbated (Figure 5).

Nodular Limestone. Intervals of numerous irregular or discontinuous micrite nodules constitute thin limestone beds.

Limestones. Limestone strata range from 0.5 - 1 cm thick laminae to 3 m thick beds. Thicker limestones are made up of a sequence of amalgamated beds dominated by micrite (almost always recrystallized to microspar or very fine sparry calcite). Thick limestones also contain hyolith packstone, wackestone, and small patches (3-4 cm long) of hyolith grainstone. Peels from limestones slabbed parallel to bedding show nests or pockets of hyoliths. Many of the individual hyolith cones are oriented at high angles to bedding and nested (cone-in-cone) conchs are common. Burrow like pockets in micrite and the interstices of intraclasts(?) are often filled with packstone (Figure 4).

All of the thicker limestones have laminated irregular, greenish or tan chert layers and fine networks of chert "veins". These laminated cherts have been interpreted to be planar stromatolites, but diagnostic forms and fabrics are lacking (Bailey, 1984; Landing 1988). Some of the chert beds extend irregularly into the limestone and contain fossils. These layers represent silicified limestones.

Environments of Deposition

Muddy and thinly laminated beds at Nahant are best explained by deposition, in low energy mid shelf environments, generally below fair weather wave base. Periodic storm currents or storm surges could produce starved ripple trains (cross-laminated silt/very fine sand patches) and scour surfaces. Myrow (1992) noted somewhat similar thin graded sand/silt couplets that might have resulted from sediment deposited during decelerating storm flow. Nahant examples of such beds are very thin (1-3 cm) indicating that they are probably distal tempestites.

Limestones represent shallower shelf conditions than mudstones. Moderate energy levels are indicated by limited fragmentation of fossils, little sorting of bioclasts, and abundant micrite matrix. Well winnowed shell lags are not present and conical/tubular fossils do not show a strong preferred orientation (Figure 4). Stromatolitic structures and/or fabrics typical of very shallow water peritidal limestones are not present (as they are in red nodular limestone horizons in the Hoppin Formation). I interpret the Nahant limestones to represent shallow subtidal shelf environments rather than peritidal settings (Bingham and Bailey, 1985).

Stratigraphic section 3 (Figure 3) represents a shoaling upward cycle with shallowest water depths represented by limestone strata. Upward through the section, nodular mudstones are interbedded, with nodular limestones, which in turn grade into the primary limestone bed with thick micrite intervals. The thick limestone bed is composed of the various microfacies discussed above. The thin centimeter scale micritic limestone "microbeds" and the decimeter scale limestones may represent the distal edges of seaward prograding carbonate sheets (Myrow and Landing, 1991; Landing, 1992).

Intensely burrowed intervals could represent deepest water conditions (but not anoxic) where lack of storm disturbance allows infauna to thoroughly churn sediment, and destroy many of the sedimentary structures. The intensity of burrowing in some of these strata (Figure 5) contradicts the idea that bioturbation was not an important process in the early Paleozoic. Much of our knowledge of sediment disturbance by burrowing was gained by the study of carbonate dominated cratonal sequences, which may contain an atypical sample of affects of earliest Paleozoic infauna.

PALEONTOLOGY

Early Cambrian shelly fossils represent an important phase in the history of life. Although many of these small fossils were described by the turn of the century, the detailed study of faunas near the Proterozoic/Phanerozoic boundary in North America has advanced substantially in the last decade. Louis Agassiz in 1850 was the first person to note fossils in Nahant limestones, and by 1900 a number of species had been described (Foerste, 1889). Landing (1988) reviewed the Nahant fauna and restudied all other extant localities of Lower Cambrian in eastern MA. All of the fossils discussed below except for trace fossils are from the thicker limestone strata.

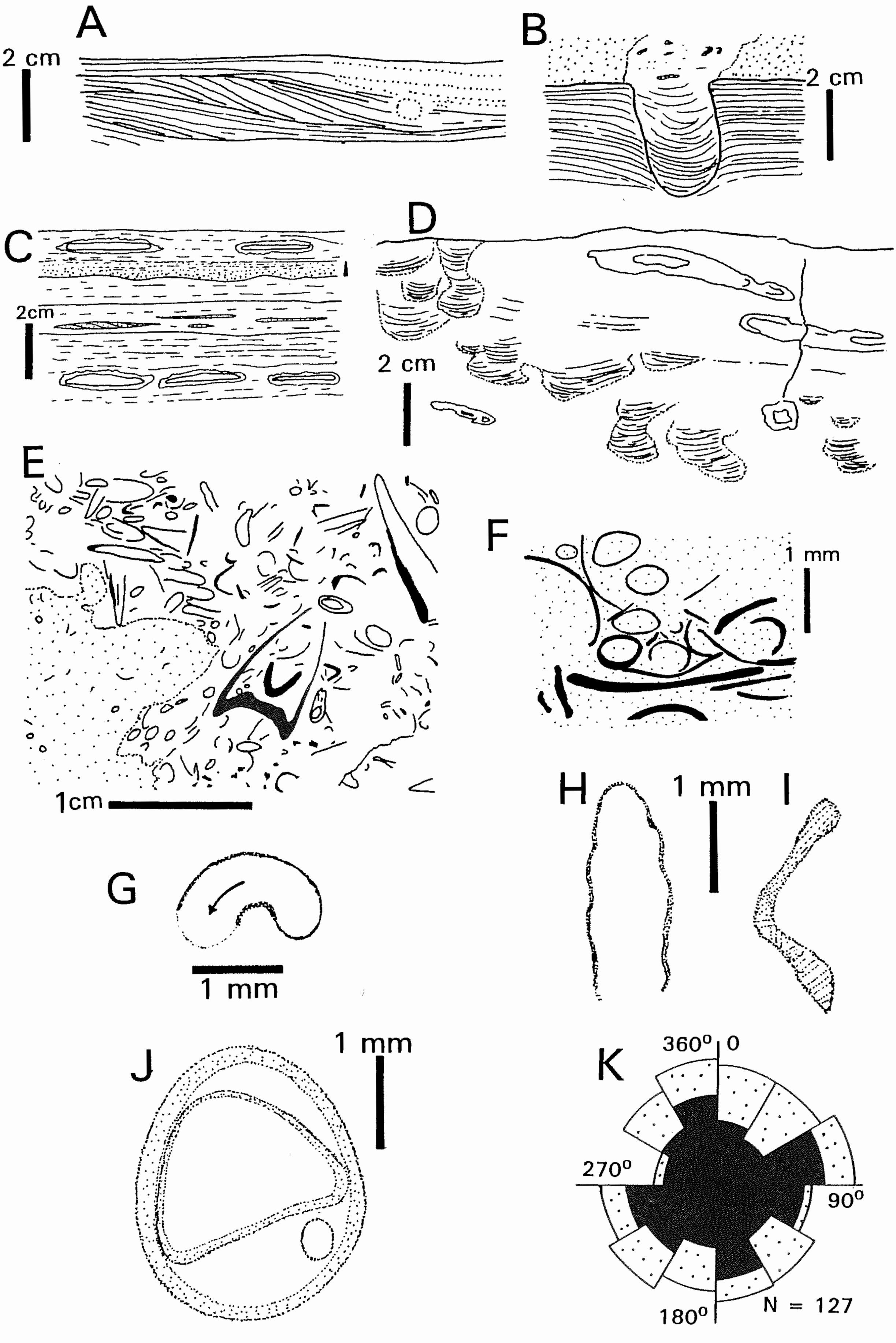
A
2 cm
B
2 cm
C
2cm
D
2 cm
E
1cm
F
1 mm
G
1 mm
H
1 mm
I
J
1 mm
K
360° 0
270°
90°
180°
N = 127

All species known from Nahant are small calcareous cones, tubes, coiled conchs, and cap-like specimens that were almost certainly originally aragonitic (James and Klappa, 1983). All skeletal microstructure has been destroyed by recrystallization and shells are now calcite spar.

Orthothecid hyoliths are typically long conical tubes, nearly straight or slightly curved, with rounded triangular, circular, or elliptical cross-sections. These are what you see when you look at the Nahant limestones up close. The apertural end of the hyolith conch was closed by an operculum. Hyoliths are usually interpreted as mollusks (Marek and Yochelson, 1976) or annelids (Runnegar and Pojeta, 1974). Among the more abundant hyoliths or hyolith-like conchs are *"Allatheca" degeeri*, *Hyolithes tenuistriatus*, *"Ladatheca" cylindrica* and *Gracilitheca bayonet* (Figure 4).

The small snail *Aldanella attleborensis* is one of the earliest gastropods. Specimens are common in Nahant limestones (Figure 4). Broad to narrow, rugose curved conchs, such as *"Ginella" acutacosta* may represent monoplacophorans, gastropods, or other taxa.

Other phosphatic sclerites, spines, and plates from an assortment of Early Cambrian problematica have not been recovered from Nahant (Landing, 1988). Trilobites have never been reported from Nahant strata, but Bailey (1984) described a poorly preserved pygidium-like segmented fragment from the top of the 3 m limestone bed in section 3 (Figure 3). The specimen has not improved with age and it looks as enigmatic now as it did 10 years ago.

Large numbers of burrows typical of the ichnogenus *Teichichnus* occur in Nahant mudstones. In plan view a *Teichichnus* burrow is 1-2 cm wide, and slightly sinuous or curved. The spreite or laminated infill of the burrow, appears as concentric tan or purple-grey silt and sand laminae. Burrows can usually be recognized by the marked color contrast between the mudstone substratum and the burrow fill. In some cases the burrow fill is weathered into relief on a bedding plane. Burrows may branch and cut one another. (Figure 5).

In cross-section *Teichichnus* appears as a series of stacked or nested concave upward silt laminae (Figure 4). In most cases the trace rises vertically through 2 - 5 cm of sediment and it often migrates obliquely across stratification as it rises.

Teichichnus has a long range, through almost all of the Phanerozoic. The trace maker is unknown and may be a different creature at different intervals of geologic time. Annelid worms and arthropods are potential candidates for the burrower. In life the animal dug an elongate tube into the mud and then moved back and forth, moving the burrow backward and upward as it mined the ceiling and walls for particulate organic detritus. The concave up laminae represent the winnowed spoil under the animals feet (foot?).

Figure 4. Sedimentary structures and fossils from the Weymouth Formation Nahant: A. cross-laminated very fine sand lens (section 1), B. *Teichichnus* burrow in silt laminated mudstone (section 4), C. graded sand/silt bed with planar nodules (section 3), D. *Teichichnus* cross- sections, E. irregular pods of biomicrite surrounded by hyolith packstone, sketch made from peel parallel to bedding (upper limestone, section 3), F. cross-sections of *"Allatheca"*(?) and hyolith fragments with micrite matrix, wackestone, this specimen and G - J sketched from photomicrographs (upper limestone, section 3), G. section through 0.3 whorl of *Aldanella*, arrow points towards aperture, H. section through *"Ginella"*(?), I. hyolith operculum, J. nested hyoliths, *Gracilitheca* in *"Allatheca"*(?), K. Equal area circular histogram of tubular and conical fossils in upper limestone bed (section 3), black area shows orientation of cones with paleocurrent azimuth toward aperture; stippled area represents elongate tubes without current sense plotted in both opposite quadrants.

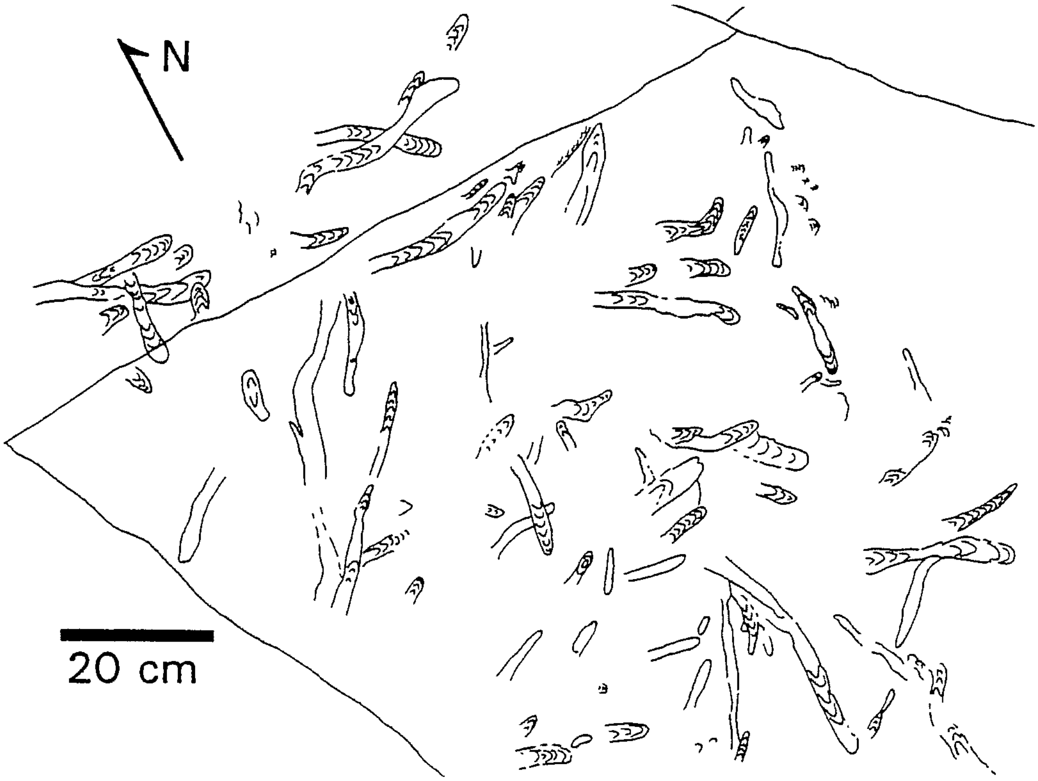

Figure 5. Map of bedding surface (section 6) with abundant *Teichichnus* traces.

IGNEOUS PETROLOGY

Field Relationships and Ages of Igneous Rocks

The Weymouth Formation in the East Point area of Nahant has been intruded by at least 13 sills and a mafic dike swarm consisting of approximately 240 dikes (Figure 2). Although some of the dikes and sills have been mapped previously (Kaye, 1965; Verma, 1973, Bailey; 1984, Ross, 1990), Figure 2 is the first detailed map of all of the dikes and sills. Previous mapping within the study area (Bailey, 1984, Verma, 1973, Kaye, 1965) included the outcrops in the Dive Beach-Bennet's Head area, along Pump House Beach, and at Great Ledge (Figure 2) as part of the main body of the Nahant Gabbro which lies immediately west of Figure 2 and underlies the remainder of Nahant. This investigation shows that these outcrops are dolerite sills within the Weymouth and that their petrography and major and trace element composition are distinct from those of the Nahant gabbro. Since the contacts of these sills with the Weymouth Formation are not Nahant Gabbro-Weymouth Formation contacts, the relationship of the gabbro and Cambrian strata is thrown into question. Present mapping shows that the contact between the Weymouth Formation and the Nahant Gabbro must lie to the west, passing through Canoe Beach and Pump House Beach and is inferred to strike NNE. Because this contact is covered, it cannot be determined whether or not it is an intrusive or fault contact.

The sills range in thickness from 125 cm to at least 9.4m, strike between N36°-50°E, and dip 30°-57°NW. They are generally concordant with bedding in the Weymouth Formation but locally may be slightly discordant. To the west of the East Point area, Nahant and Little Nahant are underlain by the Nahant Gabbro and tonalite respectively. Rb-Sr dates of 493 $\pm$31 Ma and 461 $\pm$35 Ma were reported by Zartman and Marvin (1971) on biotite from the gabbro. The tonalite has yet to be dated. The age of the sills can only be inferred from the field data and the fact that, as shown below, they were not derived from the Nahant gabbro magma. The following evidence suggests the sills are older than the Nahant Gabbro: they are cut by a northwest-trending dike swarm of probable Paleozoic age (see below); they intrude the Early Cambrian Weymouth Formation, which, with the sills, appears to have been intruded by the Nahant Gabbro.

The dikes range in thickness from less than 5 cm to 13.6 m. Over 95 percent of the dikes strike northwest with all of the remainder striking between azimuth 70° and due east (Figure 2). Approximately half of the dikes trend between azimuths 300° and 330°. This dominant northwest trend is typical for Paleozoic swarms elsewhere in the Avalon terrane in eastern Massachusetts (Ross, 1990) but is markedly more pronounced. Mesozoic dikes and structures elsewhere on the Avalon terrane, and New England in general, have dominant northeast trends (Ross, 1992). The absence of northeast-trending dikes at Nahant and cross-cutting relationships suggest none of the Nahant dikes in Figure 2 are Mesozoic.

Dike frequency within the Nahant swarm is 179 dikes/km which is the densest concentration of dikes yet reported in eastern Massachusetts. Pine Hill, Medford, for example, contains only 37 dikes/km yet has one of the denser dike concentrations in the region.

Petrography

Nahant Gabbro and Tonalite. Two modal analyses of the gabbro (one from west Nahant and one from outcrops just west of Canoe Beach) are included in Table 1 and the following description is based on examination of these 2 samples. The gabbro is medium- to coarse-grained, hypidiomorphic, equigranular, and ophitic. The sample from Fort Rock in west Nahant contains local intergranular patches. The plagioclase is zoned from labradorite in grain cores to oligoclase-andesine at grain margins. The rock is fresh to slightly altered (sausuritization of plagioclase). Magnetite, ilmenite, pyrite, and apatite occur as accessory minerals. Biotite, pennine, and smectite are present as secondary minerals. The tonalite of Little Nahant is texturally similar to the gabbro in handspecimen. The one sample examined in thin section is plagioclase-phyric and consists of plagioclase (63.5%, 17.2% as phenocrysts), hornblende (11.4%), quartz (11.4%), granophyre (4.2%), microcline (3.5%), biotite (2.6%), magnetite (2.7%), pyrite (trace), apatite (trace), epidote (trace), and possibly a trace of orthopyroxene. Chlorite and some of the biotite are also present as secondary minerals altering hornblende.

Sills. Modal analyses of the sills are presented in Table 1. The sills are classified as dolerites and leuco-dolerites with one being a leuco-quartz-dolerite (IUGS system used with "dolerite" substituted for "gabbro"). The modes in Tables 1 and 2 do not total 100 percent because they do not include the nonopaque accessory minerals. Most of the sills are equigranular but can contain up to 11.9 volume percent plagioclase phenocrysts typically less than 5 mm in diameter. A trace to 25.9 volume percent augite phenocrysts up to 3 mm in diameter are present in 4 of the sills (Table 1). In addition to pyroxene phenocrysts, sill 2126 (mode 2126 is from chilled margin and mode 2127 is 93 cm from the base of the sill) and the lower portion of sill 2130 at Pulpit Rock (Figures 2 and 8) also contain severely chloritized olivine phenocrysts that average about 5 mm in diameter. The aphyric sills and the groundmasses of the porphyritic sills are generally hypidiomorphic and commonly subophitic to ophitic.

Plagioclase anorthite contents (estimated by the Michele-Levy method on a flat stage) fall predominantly in the andesine to labradorite range. Plagioclase phenocrysts in the 5 porphyritic sills were too altered to allow determination of anorthite contents but probably equal or exceed those of the groundmass grains. Accessory minerals include magnetite, ilmenite, apatite, and occasionally pyrite, quartz, and biotite. The leuco-quartz-dolerite sill forming Great Ledge (sample 2122) contains 3.6 percent myrmekite.

Dikes. Ninety-five of the dikes have been examined in thin section. Modal analyses of 14 representative dikes are summarized in Table 2. The vast majority recognized are dolerites and leuco-dolerites (IUGS system as modified above for sills), 11 of which contain olivine. Forty-five of the 95 dikes examined contain a trace to nearly 49 percent phenocrysts with most containing less than 10%. Phenocryst assemblages include plagioclase (17 dikes), pyroxene (3 dikes), olivine (2 dikes), plagioclase + pyroxene (20 dikes), and plagioclase + pyroxene + olivine (3 dikes). One dike (sample 9270, Table 2) contains 10.4 volume percent quartz in interstices and as granular, microscopic amygdales. Two dolerite dikes rich in plagioclase-bearing, olivine pyroxenite xenoliths (modes in Table 2) have also been identified. These will be described in more detail in a

TABLE 1. MODAL ANALYSES OF NAHANT SILLS

Petrographic group and map station	whole-rock or groundmass					phenocrysts		
	plag.	aug.	oliv.	op.	qtz.	plag.	aug.	ol.
dolerite (*indicates altered)								
8799	54.6	31.4		10.4		2.8	0.2	
9280	46.6	32.8		11.6		7.4	1.6	
2133*	28.8	37.8		3.1		4.4	25.9	
2124	50.3	37.8		8.1	2.5			
2126	41.0	49.0		9.6			0.4	
2127	42.2	33.2		7.0			7.6	10.0
9272	53.7	34.5		7.3	3.7			
olivine-dolerite								
2120	54.4	33.5	6.1	4.0				
2130*	37.6	35.0		7.4			4.2	15.0
leuco-dolerite								
7104	65.4	24.2		9.0				
2122	58.0	22.0		8.0	7.0			
2125	57.2	21.0		8.0	0.4	11.4	0.4	
2131	60.2	22.1		4.0		11.9		
Nahant gabbro (main pluton, not sill)								
7123	61.9	28.3		9.8				
2141	65.0	26.1		7.6				

TABLE 2. SELECTED MODES OF NAHANT DIKES

Petrographic group and map station	whole-rock or groundmass					phenocrysts		
	plag.	aug.	oliv.	op.	qtz.	plag.	aug.	oliv.
Pyroxenite xenoliths								
7101	4.7	77.8	12.8	4.3				
2105		13.6				1.6	48.6	13.5
Dolerites (* indicates altered)								
2104	54.4	16.8		13.2		13.6	2.0	
7102*	39.2	52.2		4.4				3.8
7103*	35.4	58.3		6.0			tr	
7116*	41.4	52.4		3.0				
7118*	44.8	39.4		8.4		6.0	0.6	
2108*	56.2	32.8		8.4				
9232	50.8	28.2	16.0	5.0				
9270	52.0	33.0		4.6	10.4			
2135*	45.8	33.4		9.6			3.6	7.2
9295*	54.3	26.4		6.3		1.4	6.3	5.3
Leuco-dolerites								
7119	59.2	31.8		8.8	tr			
7120	63.6	25.7	1.9	8.6	tr			
9231	63.6	20.4	6.2	10.0	tr			tr

TABLE 3. MAJOR AND TRACE ELEMENT XRF ANALYSES OF NAHANT GABBRO AND DOLERITE SILLS, NAHANT

Rock unit	Nahant gabbro		alkaline dolerite sills						subalkaline dolerite sills					
Sample	7123	2141	2131	7104	2121	8799	2125	2126	9272	2124	2130	2133	9280	2122
SiO_2	46.00	47.10	54.98	50.95	49.96	50.25	49.39	50.73	50.10	49.84	49.58	47.49	50.82	52.73
TiO_2	4.15	3.29	1.92	3.22	3.79	3.24	3.34	3.03	2.70	3.16	2.44	2.53	2.98	3.20
Al_2O_3	19.01	19.33	16.79	15.04	14.28	14.65	15.58	14.01	15.10	14.04	12.60	10.87	15.36	13.67
FeO	11.51	10.90	9.05	11.07	11.81	11.26	10.99	11.39	10.00	10.88	10.81	11.59	10.69	12.11
MnO	0.17	0.12	0.22	0.17	0.16	0.19	0.15	0.20	0.16	0.19	0.17	0.22	0.18	0.19
MgO	4.54	3.82	2.29	4.77	4.29	4.26	4.31	5.92	5.37	6.80	10.29	12.45	4.82	3.59
CaO	10.10	10.58	4.90	7.69	7.30	6.84	8.18	7.68	9.38	9.23	9.48	9.18	8.11	6.83
Na_2O	2.10	3.07	4.71	4.65	4.44	4.79	3.59	5.00	2.69	3.42	2.07	1.77	2.87	3.60
K_2O	2.42	0.86	3.57	1.34	2.17	1.66	1.79	0.46	1.80	0.92	1.21	1.24	1.70	2.10
P_2O_5	0.09	0.13	0.71	0.57	0.64	0.57	0.58	0.44	0.39	0.43	0.35	0.38	0.45	0.63
Total	100.10	99.20	99.14	99.47	98.84	97.71	97.90	98.86	97.69	98.91	99.00	97.72	97.98	98.65
Ni	11	3	0	46	18	33	30	44	45	104	251	323	30	0
Cr	25	22	5	87	19	54	57	82	91	240	381	640	53	5
Sc	34	22	17	21	22	25	21	28	26	33	28	30	25	21
V	468	421	56	242	277	242	246	247	218	255	212	225	247	245
Ba	607	226	1190	506	762	824	667	180	312	215	259	433	424	502
Rb	62	18	79	19	27	25	29	12	54	22	44	29	68	34
Sr	522	659	630	725	678	845	812	448	603	628	426	360	603	541
Zr	91	110	433	246	295	269	287	215	205	207	174	177	228	309
Y	14	13	43	31	30	30	27	27	24	24	23	23	26	36
Nb	16.5	14.4	59.0	43.6	40.0	42.0	36.0	31.9	27.0	30.9	25.2	27.6	28.6	41.0
Ga	22	27	25	23	23	22	25	20	16	21	19	19	24	23
Cu	32	49	44	39	42	56	100	131	55	73	83	77	68	13
Zn	92	93	96	109	124	186	128	100	94	122	104	162	118	141
Pb	nd	8	9	nd	11	25	10	9	8	5	4	13	19	3
La	nd	1	38	nd	6	33	24	3	5	25	8	2	0	35
Ce	nd	27	103	nd	65	69	69	47	63	50	39	58	59	87
Th	nd	0	5	nd	0	3	3	2	2	1	0	2	2	3

TABLE 4. MAJOR AND TRACE ELEMENT XRF ANALYSES OF DIKES AT EAST POINT, NAHANT

Suite	Alkaline dikes								Subalkaline dikes				Xenoliths	
Sample	2104	2108	2135	7116	7119	7103	9231	9232	9270	9295	7120	7102	2105	7101
SiO_2	50.38	47.23	46.14	46.57	45.93	47.43	44.45	47.07	51.50	47.71	48.25	48.71	42.92	43.43
TiO_2	3.25	3.26	2.80	2.23	2.97	3.28	3.48	2.20	3.64	2.04	2.50	2.21	1.93	2.45
Al_2O_3	15.84	14.28	13.75	13.21	15.20	14.08	14.17	14.30	16.51	13.63	15.50	12.81	7.83	9.14
FeO	12.35	12.02	12.75	10.10	14.28	11.36	15.25	11.26	10.27	11.75	13.04	10.60	13.04	15.94
MnO	0.20	0.22	0.23	0.15	0.22	0.18	0.25	0.16	0.12	0.17	0.20	0.18	0.26	0.25
MgO	3.42	6.15	8.76	9.71	6.72	6.02	7.60	9.49	5.48	8.07	6.74	9.12	18.71	16.00
CaO	7.52	8.05	8.37	10.72	8.77	9.39	9.00	8.86	4.61	9.22	8.94	9.98	10.31	8.39
Na_2O	3.41	3.36	2.67	2.51	2.58	3.10	2.80	2.44	2.40	2.20	2.60	2.53	0.32	0.69
K_2O	1.93	1.15	1.31	1.00	1.59	1.72	0.61	1.56	1.75	1.57	1.00	0.98	0.18	1.20
P_2O_5	0.36	0.52	0.37	0.34	0.39	0.44	0.29	0.30	0.68	0.19	0.34	0.29	0.23	0.14
	98.66	96.24	97.15	96.54	98.65	97.00	97.90	97.64	96.95	96.55	99.11	97.41	95.73	97.63
Ni	0	79	128	240	74	68	72	196	20	131	84	195	542	309
Cr	7	170	142	498	153	151	142	358	81	372	73	466	971	496
Sc	25	20	26	25	30	25	34	27	21	28	29	30	28	29
V	283	249	230	195	299	252	396	196	238	211	275	202	185	236
Ba	422	295	241	303	238	395	167	335	57	226	179	242	20	216
Rb	56	33	59	27	60	45	15	43	78	54	19	27	5	29
Sr	500	429	348	516	500	474	484	456	84	357	432	374	135	221
Zr	202	234	192	199	164	216	130	158	303	115	161	170	132	90
Y	33	28	27	20	24	25	20	20	44	20	26	25	17	15
Nb	32.2	41.0	32.3	32.1	22.6	37.0	17.9	25.6	71.0	14.2	22.5	27.4	23.7	18.7
Ga	27	24	23	20	21	23	22	20	31	22	25	19	18	15
Cu	33	70	57	87	47	80	57	55	68	99	63	94	94	23
Zn	141	182	140	98	112	159	104	99	154	108	121	192	159	231
Pb	15	8	3	2	nd	3	1	5	5	10	nd	36	11	6
La	17	19	6	18	nd	12	0	0	38	4	nd	18	19	0
Ce	62	57	59	50	nd	52	35	35	125	20	nd	54	40	17
Th	3	2	4	2	nd	0	0	2	1	0	nd	3	1	3

Figure 6. Alkalies-SiO_2 diagram with symbols as follows: triangles = sills; plusses = dikes; boxes = Nahant gabbro diamond = tonalite dots = xenoliths

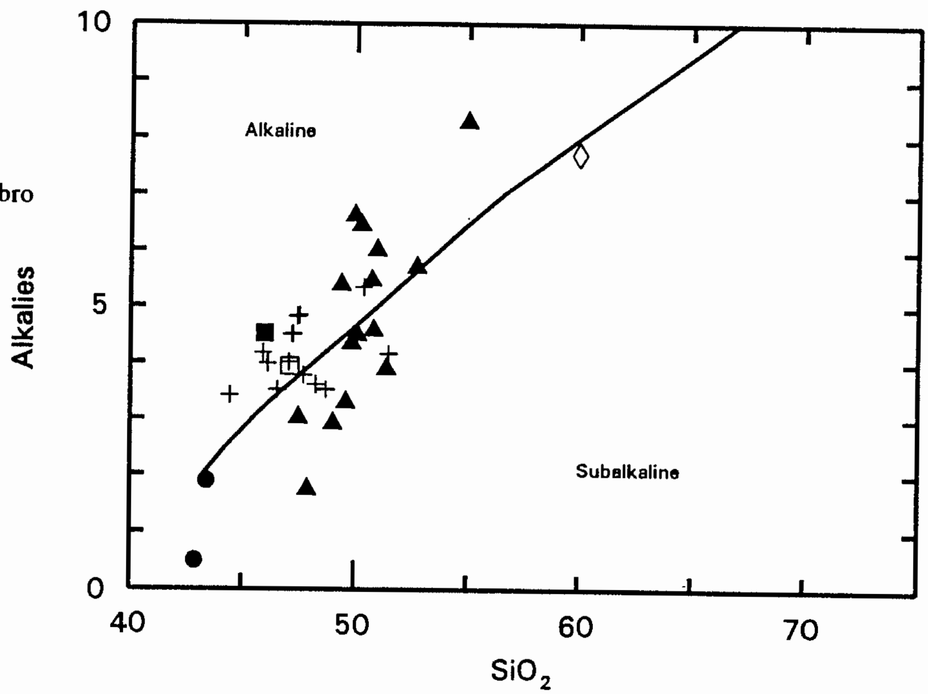

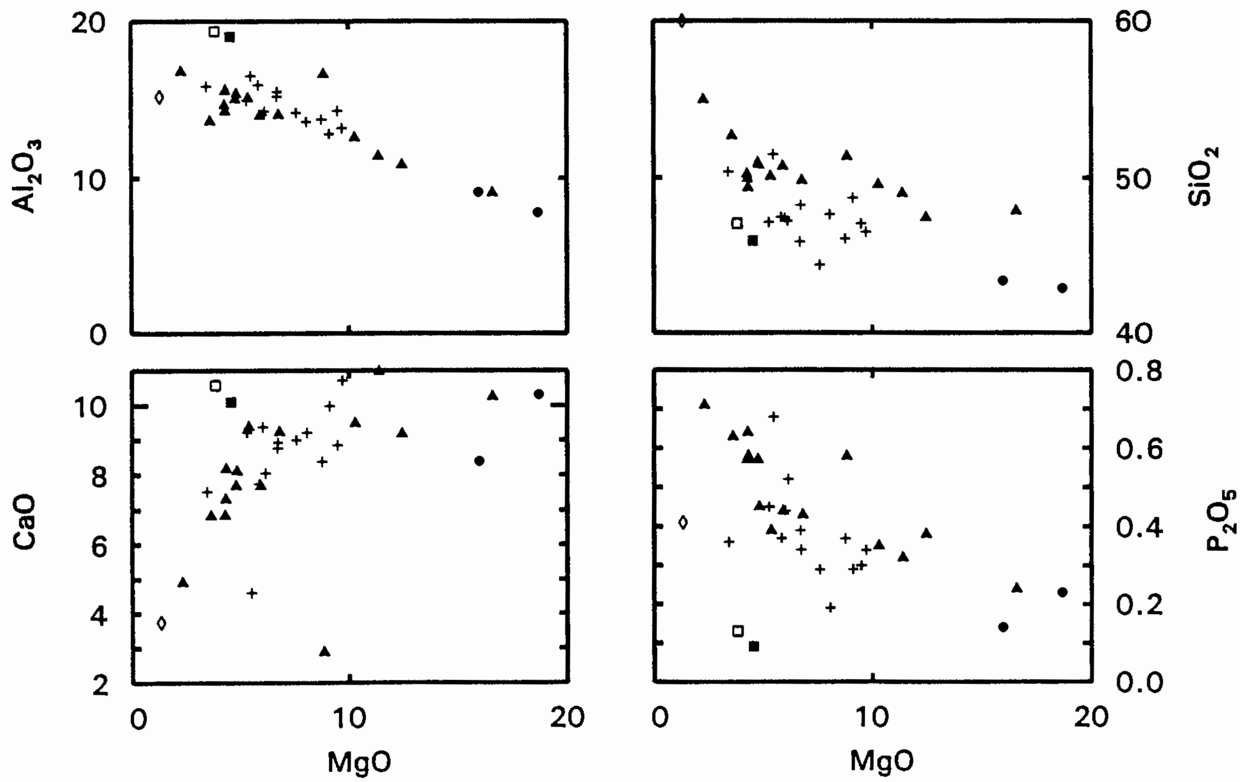

Figure 7. MgO variation diagrams for Nahant dikes and sills. Symbols as in Figure 6.

later section. The one diorite dike identified (9283, Figure 8) exhibits trachytic texture in its groundmass which contains 60.0 percent plagioclase, 14.4 percent hornblende, and 6.2 percent opaque oxides. It contains 6.6 percent andesine phenocrysts and 12.8 percent hornblende phenocrysts.

Alteration. The sills and dikes range from fresh to severely altered with alteration products including saussurite, sericite, uralite, chlorite (often pennine), biotite, carbonate, opaque oxides, and leucoxene. The alteration appears to be of at least two origins as follows: deuteric alteration (saussurite, sericite, uralite, chlorite) and hydrothermal (chlorite and calcite). This distinction is based on the presence of chlorite and carbonate in veins as well as in interstices and altering primary minerals. Calcite and quartz are commonly present in breccias and gouge along faults in the area that may have acted as the main conduits for siliceous or carbonate-rich hydrothermal solutions. Chloritization may in part be related to low grade regional metamorphism and/or to contact metamorphism adjacent the Nahant Gabbro pluton.

PETROCHEMISTRY

Nahant Gabbro and Tonalite

Major and trace element compositions were determined by XRF analyses of 2 samples of the Nahant gabbro (Table 3; analyses by the Basalt Research Laboratory of Washington State University). One sample of the tonalite of Little Nahant was also analyzed (not listed in Table 3) and contains the following oxide weight percents: 59.98 SiO_2, 1.12 TiO_2, 15.19 Al_2O_3, 8.22 FeO, 0.21 MnO, 1.31 MgO, 3.75 CaO, 5.04 Na_2O, 2.67 K_2O, and 0.41 P_2O_5. It also contains the following trace elements (ppm): 6 Ni, 10 Cr, 23 Sc, 27 V, 951 Ba, 57 Rb, 379 Sr, 348 Zr, 45 Y, 66.0 Nb, 24 Ga, 24 Cu, 68 Zn, 1 Pb, 48 La, 123 Ce, and 9 Th. Both gabbro samples plot in the alkaline field of the alkalies-silica diagram of Irvine and Baragar (1971)(Figure 6). The gabbro is olivine-normative and the tonalite is quartz-normative. Compared to the sills and most of the dikes, the Nahant Gabbro is enriched in Al_2O_3, TiO_2, and V and depleted in P_2O_5, MgO, Zr, and Nb (Figures 6 and 7, Tables 3 and 4). These data clearly indicate that the Nahant Gabbro and tonalite were not sources for the sill and dike magmas.

Sills

Thirteen major and trace element XRF analyses were completed for the Nahant sills (Table 3). Sill 2120 (not shown on Table 3) contains the following oxide weight percents: 47.89 SiO_2, 1.76 TiO_2, 9.06 Al_2O_3, 11.21 FeO, 0.17 MnO, 16.61 MgO, 10.24 CaO, 0.72 Na_2O, 1.02 K_2O, and 0.24 P_2O_5. It contains the following trace elements (ppm): 531 Ni, 892 Cr, 29 Sc, 181 V, 202 Ba, 25 Rb, 289 Sr, 119 Zr, 15 Y, 17.0 Nb, 17 Ga, 61 Cu, 131 Zn, 6 Pb, 6 La, 41 Ce, and 0 Th. Seven of the sills are tholeiitic to borderline calc-alkaline with the remaining 6 samples being alkaline (Figure 6). Three of the sills (2131, 2124, and 2130) are weakly quartz-normative, two (2125 and 9280) are clearly quartz-normative, and the remainder are olivine-normative.

All but sill 2120 are highly enriched in TiO_2 with seven samples containing over 3.00 weight percent TiO_2 (Table 3). Three of the sills (including 2120 listed above) are very enriched in MgO ($>$ 10 weight percent).

Dikes

Major and trace element XRF analyses of 12 of the dikes are presented in Table 4. Eight of the analyzed dikes are alkaline and 4 are tholeiitic (Figure 6). Only two of the dikes are weakly quartz-normative (2104, 9270) with the remaining 10 being olivine-normative. Pyroxenite xenoliths (7101 and 2105) from 2 dolerite dikes are both clearly ultramafic in chemical composition (Table 4). These are the first reported analyses of ultramafic rocks from the Avalon terrane in eastern Massachusetts. A suite of ultramafic xenoliths from a Mesozoic camptonite dike in Cambridge, Massachusetts (Ross and others, 1983, Ross, 1992) are substantially lower in Al_2O_3 and TiO_2 and richer in MgO than the Nahant pyroxenites (Ross, unpublished data). The dikes overlap the sills in composition (Figures 6 and 7) but no physical connection between any sills and possible feeder dikes were observed in the field. Like the sills, the dikes do not resemble the Nahant Gabbro and tonalite in composition (Figures 6 and 7; Tables 3 and 4). As a group, they resemble some of the Nahant sills and the high TiO_2 dikes of probable Paleozoic age present in swarms elsewhere in the Avalon terrane of Massachusetts (see Ross, 1990).

MAGMATIC SEQUENCE AND TECTONIC SETTING

Magmatic Sequence

Mafic magmatism began with several episodes of sill intrusion into the Early Cambrian Weymouth Formation. A small number of the dikes in Figure 2 may also have been emplaced at this time (some are cut by at least one sill). Emplacement of the Nahant Gabbro, occurred as late as the Ordovician. The northwest-tilting of the Weymouth Formation may pre-date or post-date intrusion of the Nahant Gabbro. Kaye (1965) described a northeast-trending zone of folded sheeting joints in the Nahant Gabbro which he related to a possible hidden, west-dipping thrust fault. The relationship of this folding and possible faulting event to the tilting of the sills and the Weymouth beds is unclear.

Cross-cutting relationships indicate at least 4 episodes of mafic dike intrusion are represented as follows from oldest to youngest: older ENE dikes, NW main phase, younger ENE, and NNW. The NW-trending main phase dikes account for approximately 95 percent of the swarm and may represent more than one intrusive episode.

The possibility that some dikes were intruded between the tilting of the Weymouth Formation (and sills) and emplacement of the Nahant Gabbro cannot be determined until investigation of the dikes within the gabbro is completed. Reconnaissance mapping in the main body of the Nahant Gabbro suggests that most of the dikes post-date it. The dikes in Figure 2 show no evidence of having been folded. However, their trend is very nearly perpendicular to the strike of the Weymouth beds and presumably more-or-less parallel to the principal compressive stress direction and so would remain vertical or nearly so during tilting. The older, more easterly-trending dikes strike more obliquely to bedding and, if present during tilting, should exhibit southeasterly dips. This is indeed the case, especially in the Great Ledge block where they dip as low as 55° SE (Figure 2). In contrast, dikes trending more northerly and oblique to the bedding should exhibit shallow northeast dips if present during the tilting event. A thick, younger, northerly-trending dike in the East Point-south block (7120, Figure 2) dips 79° NE but other thinner, similarly-trending dikes to the north are vertical. This suggests these younger dikes post-date most, if not all, of the northwest tilting of the beds. It appears, then, that dike emplacement may have pre-dated and post-dated the tilting of the sediments and sills. Radiometric dating of these dikes will eventually provide a bracket for the age of the tilting event.

Tectonic Setting

The two Nahant Gabbro analyses plot in the within-plate-basalt field on the Zr-Zr/Y diagram of Pearce (1983) and the Zr-TiO_2 diagram of Pearce and others (1981) but does not plot in any of the fields on the Zr-Ti/100-Y*3 diagram of Pearce and Cann (1973). All of the dikes and sills plot in the within-plate-basalt fields on all three of the above diagrams with the exception of sill 2131 which plots outside of all fields on the Zr-Ti/100-Y*3 diagram. Whether or not this within-plate magmatism occurred during a single episode of continental rifting (or failed rifting) is problematic. In any case, the prominent northwest dike trend indicates that during their emplacement, the area was undergoing northeast-southwest extension.

FIELD DESCRIPTIONS OF STRUCTURAL BLOCKS

Faults

The East Point area is cut by many faults, some of which are shown in Figures 1 and 2. Five of the faults (faults A, B, C, D, and E, Figure 2) divide the area into the following 6 structural blocks with significant stratigraphic displacements occurring across bounding faults: Bennet's Head block, East Point block, East Point-south block, Pulpit Rock block, Island block, and Great Ledge block (Figure 2). The East Point-south block includes a small sub-block bounded by fault B and the fault just north of dike 7120 (Figure 2) mentioned earlier, no stratigraphic correlations are possible between the 6 structural blocks. The precise amount of movements on the bounding faults cannot be determined but estimates of possible minimum strike-slip offsets required are in the magnitude of several hundred meters. Dip-slip components would require minimum offsets of only several tens of meters.

Although some faulting appears to have pre-dated dike and sill emplacement, the main faulting post-dates most of the igneous activity within the study area. This faulting could be associated with either the Alleghanian Orogeny (latest Carboniferous and Permian) or adjustments during Triassic rifting of Pangea. The faults are commonly mineralized with calcite and/or quartz. Three dikes in the East Point block cross fault A without offset and must post-date it. Many of the dikes appear to parallel a northwest-trending set of faults. In some cases faulting has occurred within dikes and parallel to their trends, representing minor post-dike-emplacement movement or reactivation of earlier faults along which the dikes were intruded. A preliminary survey of 140 joints reveals no clear correlation between jointing and dike trends, although Verma (1973) reported steeply dipping, northwest-trending sets at Great Ledge and East Point. Additional work is needed before jointing can be proved or disproved as a control of dike orientations.

The Bennet's Head and East Point blocks show 30° of counter-clockwise rotation of dike trends relative the other blocks (Figure 2). The mechanism of this rotation is unclear at present but appears to be related to movement along fault A, although other faults such as E, F, and G (Figure 2) may also have been involved.

Bennet's Head Block

Sedimentary Rocks. Much of the poorly exposed sedimentary rock in this block has been heavily sheared and intruded, hence it is not shown in Figure 1. One feature of particular significance is abundant quartzite xenoliths found in dike 9241 (Figure 2). These 10 to 50 cm, rounded to angular xenoliths, are thoroughly recrystallized, meta-quartzarenites. As there are Cambrian quartzarenites at the base of the Hoppin Formation, it is possible that these xenoliths were derived from a similar basal quartzarenite sequence below the presently exposed strata. There are also Late Proterozoic quartzarenites and these rocks cannot be excluded as a potential source of the xenoliths.

Igneous Rocks. The outcrops immediately east and west of Dive Beach and east of Canoe Beach (2133, 2124, and 2125 on Figure 2) were mapped previously (Kaye, 1965; Verma, 1973; Bailey, 1984) as part of the Nahant Gabbro. As discussed earlier, these three bodies differ from each other and markedly from the Nahant Gabbro in chemistry and petrography. New mapping (Figure 2) has also shown them to be discrete sills. The exposed sill-argillite contacts in the Bennet's Head block are all conformable. The best exposure of a contact is at the base of sill 2125. The top surface of the underlying argillite at this contact is grooved and slickensided roughly parallel to the dip of the beds and sill. A series of minor, non-plunging folds trending N45°E are also present in the argillite beneath this contact and may represent drag folds related to sill intrusion or subsequent faulting along the contact, or folding associated with the westward tilting of the strata.

A dolerite dike containing abundant, large, rounded quartzite xenoliths is exposed in en echelon segments along the cliffs between Bennet's Head and Canoe Beach (dike 9241, Figure 2). The host dike is a dolerite highly contaminated with quartz.

East Point Block

Sedimentary Rocks. Some of the best *Teichichnus* traces at Nahant are present on the dip surfaces about 15 m north of the circular gun emplacement, note iron rod anchored into rock (10 to 12.5m interval in section 6, Figure 4). On several bedding planes it is possible to see *Teichichnus* in both plan view (Figure 5) and cross-section (Figure 4) (**PLEASE DO NOT HAMMER ON, DEFACE, OR REMOVE ANY OF THE TRACE FOSSILS**). Stratigraphy seems to be continuous from the west end of the block across the east-trending chasms, dikes, and faults, to the easternmost point.

Igneous Rocks. The East Point block is separated from the East Point-south block by fault A and from the Bennet's Head block to the west by fault E (Figure 2). See the above description of the Bennet's Head block for a discussion of the faulting and rotation of it and the East Point block. Several thin dikes at East Point occur in en echelon segments with complex terminations. Dike 2135 contains a minor fault along its entire length. It cannot be determined if this fault entirely post-dates the dike or was merely reactivated after the dike intruded along it (both dip 53°S).

East Point - South Block

Sedimentary Rocks. A 2 m thick limestone bed (interval 0 to 2.1m, section 4) occurs at the base of the block, just above high tide level. This very well exposed bed has irregular greenish to tan laminated chert horizons and numerous pods and lenses of hyolith packstone to grainstone. Several cross-sections of the distinctive hyolith *Gracilitheca bayonet* were observed. Three thin limestone beds (bases at 7.6m, 11.0m, 12.4m, section 4) are present and may be traced with difficulty possibly as far as East Point. A wedge shaped sub-block, bounded by a fault oblique to dike 7120 (the thick brick-red dike under the pillbox) and fault B, offsets beds about 2.5 m. A separate section (section 5, Figure 3) is presented for this sub-block. Excellent sediment structures (Figure 4) and cross-sections of *Teichichnus* may be seen between the concrete pillar beside the chasm and the outcrop a few m to the SW of the pillbox (interval 3.5 to 10.2m, section 5).

Igneous Rocks. The most interesting igneous feature within the East Point-south block is the faulted termination of sill 9272 by fault A at the northern boundary of the block (Figure 2). What appears to be the tip of the sill is present locally along the north side of the fault. Thin sills extend about 2 meters northward from it into the Weymouth Formation. This appears to be the intrusive terminus of sill 9272 and places constraints on the amount of offset possible along fault A. There are also several complex faulting and intrusive cross-cutting relationships present in this area of the block that offer significant challenges to mapping.

Pulpit Rock Block

Sedimentary Rocks. An interval of nodular mudstone with very thin, 1-3 cm micritic limestones occurs near the base of the section (interval 1.0 to 4.0m, section 3). No fossils were seen in these limestones. Where these limestones have been dissolved, thin bedding plane "slots" are present in the outcrop. Thinly bedded and laminated mudstone contains abundant diagenetic/metamorphic nodules. Most of the Ca-silicate and carbonate cores of these nodules have been dissolved. Thinly laminated nodular mudstone contain detailed sedimentary structures between sills 2131 and 9280 at the south end of Pulpit Rock (interval 12.0 to 13.5m, section 3). Below the thick sill (2130) is an interval of contact metamorphosed nodular mudstone, nodular limestone, and marble (= recrystallized micrite and hyolith packstone). The thickest limestone exposed at Nahant (interval 17.5 to 20.8m, section 3) occurs just above sill 2130. Beneath and to the east of the pillbox, the full thickness

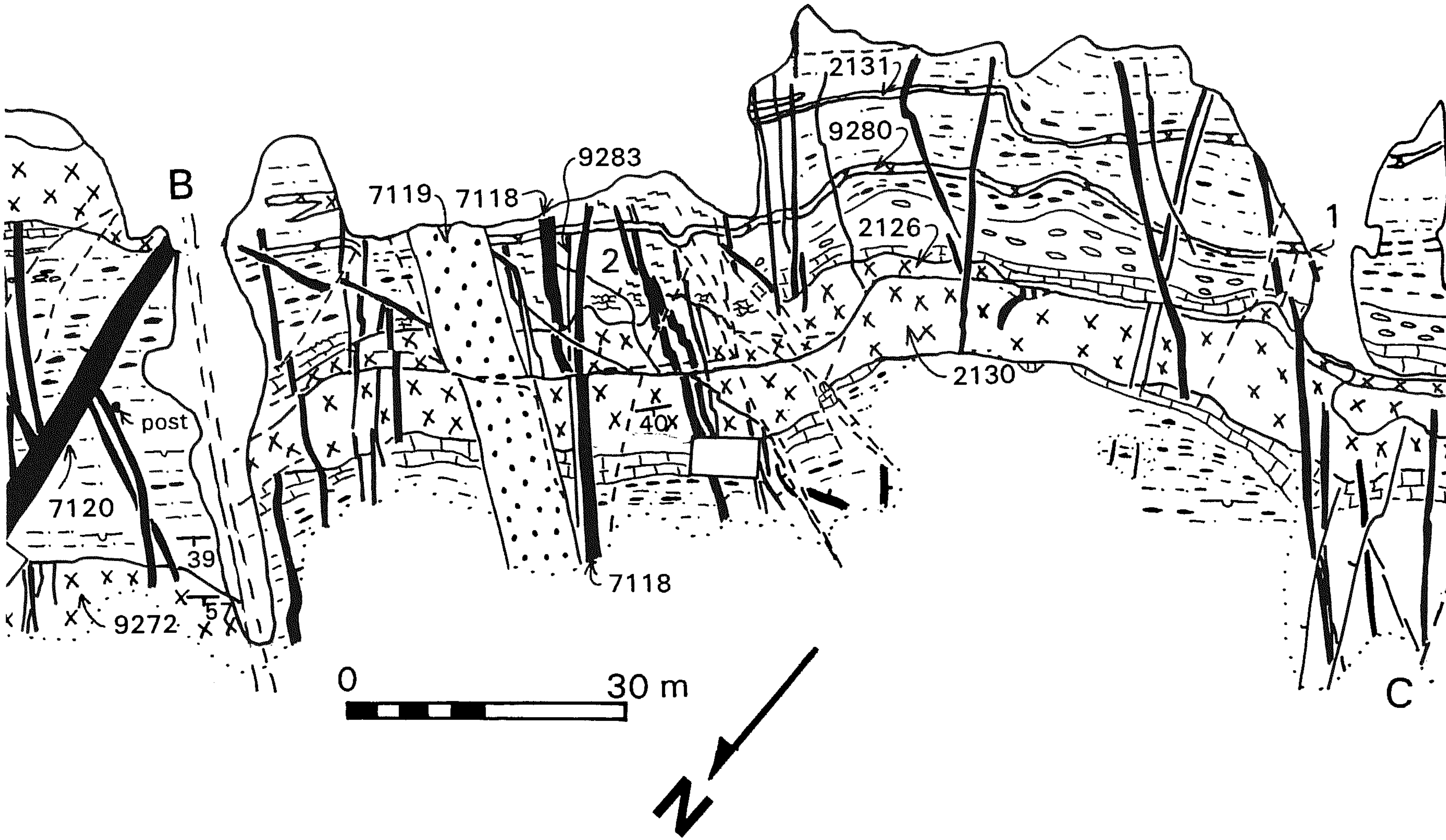

Figure 8. Geologic map of the Pulpit Rock block, Nahant. See keys to Figures 1 and 2 for map symbols.

of this limestone is preserved (**AS THESE LIMESTONES AT NAHANT ARE RARE AND SPECIAL PLEASE DO NOT COLLECT FROM OR HAMMER ON THE OUTCROPS**; there are numerous float specimens in the rubble). Details of the paleontology and petrography of this limestone are given in preceding sections.

Igneous Features. The Pulpit Rock block was intruded by 40 dikes and 4 sills and is bounded by faults B and C (Figures 2 and 8). The lower 2 thin sills (2131 and 9280, Figure 8) are best exposed in the prominent sea cliff in the central portion of Pulpit Rock. The lower sill shows en echelon offset at the northeast end of Pulpit rock (Figure 8). This is an alkaline, plagioclase-phyric, leuco-dolerite (2131 in Tables 1 and 3) that is weakly quartz-normative. It has the highest SiO_2, Al_2O_3, and total alkalies content of any of the sills and contains the least MgO, TiO_2 (other than 2120), and CaO (Table 3).

The next sill up in the section (9280, Figure 8) is a tholeiitic (borderline calc-alkaline), plagioclase-phyric dolerite containing small, fresh augite phenocrysts and microphenocrysts up to 1 mm in diameter. An interesting feature of this sill is the presence of several irregular-shaped to rounded granite xenoliths near its upper contact (Locality 1, Figure 8). These resemble Dedham Granite and the possibility of them having floated to the top of the sill is intriguing. By walking a few meters northwest the eroded fault bounding the south margin of the Pulpit rock block can be seen.

The next sill up-section (2126, Figure 8) is restricted to the Pulpit Rock block, reaching its maximum thickness of 3.5 m near the center of the block. Its contact with the thick, overlying sill appears to be faulted and has retreated deeply due to erosion by storm waves to form an overhang. Close examination of this contact reveals that the overlying sill is chilled against it, indicating the fault is merely following an igneous contact. Minor, left-lateral offsets of dikes have occurred along this faulted contact and several dikes terminate within sill 2126 (Figure 8). At Locality 2 (Figure 8) a 16 cm thick slab of limestone, still connected to the underlying Weymouth Formation, projects obliquely up into the base of the sill. A thin wedge of the sill penetrates 85 cm along the bedding beneath the slab in such a way that suggests magma flowed in a general northeast direction. In outcrop the sill contains reddish-brown, weathered spots corresponding to severely chloritized olivine phenocrysts and glomeroporphyritic clusters averaging about 5 mm in diameter.

The overlying, 9.4m thick sill is an olivine-pyroxene-phyric, altered, tholeiitic dolerite (weakly qz-normative)(Tables 1 and 3). The most striking field feature of this sill is its relatively well-developed columnar jointing forming columns up to 2.6 m in diameter. The columns are best seen in the overhanging cliff formed by the sill where its basal contact is undermined by wave erosion near Locality 2 (Figure 8). A large, intact column lies on its side near the base of the cliff and its hexagonal cross section can readily be observed. The columnar jointing appears to be best developed at this locality within this sill and has not been observed in any of the other sills in the area. The pitted, oxidized-looking spots in the lower portion of this sill are due to alteration of ferro-magnesian minerals, mainly olivine.

Numerous examples of cross-cutting dikes, dikes cutting sills, and a sill cutting dikes can be observed in the Pulpit Rock area (Figure 8). Dike 9283 is a hornblende-plagioclase-phyric diorite (Table 2) showing trachytic texture and evidence of flow differentiation and dike-parallel layering. The margins of the dike appear bleached to a light tan color, especially where in contact with the Weymouth Formation. Several high-angle, northwest-trending minor faults cut the rocks here, as well as a low-angle, bedding-parallel fault (Figure 8). One of the high angle faults a few meters southwest of Locality 2 (Figure 8) offsets the Weymouth Formation and sills 2126 and 2130. The limestone beneath these two sills shows intense faulting that nearly completely obliterates bedding in the vicinity of the above mentioned, high angle fault.

Both sills can be followed to the northeast where they are truncated by Fault B. Another thick sill (9272, Figure 8) and the underlying bedded sediments are visible across the fault. This is not the same sill you have been following and note that no sill or fault underlies it as they do sill 2130. Examination of Tables 1 and 3 shows that sills 2126, 2130, and 9272 differ in mineralogy and chemistry. It can also be seen that sill 9272 is slightly discordant to the bedding in the Weymouth at Fault B.

Island Block

Sedimentary Rocks. Several thin limestones are exposed in the lower part of the section (interval 8.0 to 11.5m, section 2) and excellent trace fossils and sedimentary structures are present near the old steps to the west of dike 7116. Densely nodular mudstones at the western edge of the block are truncated by fault D.

Igneous Rocks. The Island block contains the two thickest dikes in the study area (Figure 2). Dike 7116 is an alkaline, altered dolerite and dike 7102 is a tholeiitic, altered dolerite and contains abundant, small, dark, ultramafic-looking xenoliths and epidote bodies as well as xenoliths of the Weymouth formation, pink felsites, and dioritic xenoliths.

Great Ledge Block

Sedimentary Rocks. An altered nodular limestone (interval 0.7 to 2.1 m, section 1) occurs immediately above sill 2122 (Great Ledge). The rest of the section is laminated and nodular mudstone with excellent examples of lamination and isolated patches and lenses of cross-laminated siltstone and very fine sandstone (intervals 12-14.7 and 17.5 to 21.1 m, section 1). Cross-sections of *Teichichnus* are moderately common in the upper portion of the section.

Igneous Rocks. The Great Ledge block is noteworthy for its high number of dikes as well as their variety of types and trends compared to the other blocks. It contains more ENE-trending dikes (approximately 10) as well as a large number of NW-trending, parallel dikes (Figure 2). The ENE-trending dikes appear to be in two sets, one set older and one set younger than the NW-trending dikes (Figure 2). Great Ledge itself, consists almost entirely of sill 2122. This sill is unique within the area by containing abundant quartz and 3.6 percent myrmekite (Table 1). It is second only to sill 2131 in its SiO_2 content (Table 3). Though considered by previous workers to be part of the main body of the Nahant Gabbro, the chemistry and petrography of this sill preclude that correlation.

Two dolerite dikes are present (7101 and 2105, Figure 2) that contain abundant ultramafic xenoliths (7101 and 2105, Tables 2 and 4). A third, unsampled dike between these two also contains a few similar xenoliths locally. The dikes are clogged with xenoliths which make up an average of about 75-80 percent of the dikes, especially dike 7101. The xenoliths are medium-grained, up to at least 70 cm in diameter, and are rounded, ovoid, or irregular in shape. They weather deeply and appear oxidized and pitted on weathered surfaces. Dike 7101 and the unsampled dike cut sill 8799 but the junction of dike 2105 with the sill is covered. Peridotite (Kaye, 1965) and rocks approaching pyroxenite (Verma, 1973) are present within the main body of the Nahant Gabbro but their mineralogies and chemical compositions are unknown, so no conclusions regarding their possible relationship to the xenoliths can be made at this time.

The two headlands along Pump House Beach (Figure 2) represent four sills with one of the contacts and/or interbedded Weymouth covered. Like Dive Beach (Figure 2), the re-entrant occupied by the small beach between these headlands may owe its location to wave erosion along the contact (and Weymouth Formation if present). The western headlands along Pump House Beach contains an interesting sill problem that can be debated in the field. Three sills are present at this locality in the following stratigraphic sequence: sill 2121, sill 2120, sill 7104 (Figure 2). Rather than a sill, 2120 could be a dike locally intruded along the contact between the two thicker sills. Sills 2121 and 7104 have similar major and trace element compositions (Table 3) but 7104 is coarser and lacks the plagioclase and augite phenocrysts present in sill 2121. Sample 2120 is from an erosional remnant of a 15-20cm thick tabular body that is concordant (Az 44°, dip 39° NW) along the contact of two thicker sills (2121 and 7104, Figure 2). In spite of being thin, it is markedly medium-grained with euhedral olivine and pyroxene grains commonly as large as 4-5 mm. The top of the underlying sill is chilled against 2120. A thin dike cutting sill 2121 is truncated by sill 2120 (Figure 2). Sill 2120 also has a chemistry and petrography distinct from the overlying and underlying sills (Tables 1 and 3). For these reasons 2120 is not believed to be a layer of crystal accumulation at the base of the overlying sill. With its high MgO content (16.61 percent) it resembles the ultramafic xenoliths in dikes 7101 and 2105 described above.

ACKNOWLEDGEMENTS

We are very grateful to Alan Saiz for his help in figure preparation and computer operations. His advice and assistance allowed timely completion of this guide.

REFERENCES CITED

Anstey, R. L., 1979, Stratigraphy and depositional environments of the Early Cambrian Hoppin Slate of southeastern New England and its Acado-Baltic Fauna: Northeastern Geology, v. 1, p. 9-17.

Bailey, R. H., 1984, Cambrian rocks of East Point, Nahant, Massachusetts: *in* Hanson, L. S., ed., Geology of the Coastal Lowlands Boston, Massachusetts to Kennebunk, Maine, 76th Annual New England I Intercollegiate Geologic Conference Guidebook, Salem, Salem State College, p. 249-269.

Bingham, M. P., and Bailey, R. H., 1985, Depositional environments of Lower Cambrian limestone, Nahant, MA: American Association of Petroleum Geologists Bulletin, Abstracts for Annual Meeting, v. 6, P. 238.

Billings, M. P., 1929, Structural geology of the eastern part of the Boston Basin: American Journal of Science: v. 18, p. 97-137.

Bingham, M. P. 1977, Petrographic and paleontologic study of the Nahant Cambrian strata, Massachusetts: unpublished undergraduate research project, Northeastern University, 19 p.

Burr, H. T., 1900, A new Lower Cambrian fauna from eastern Massachusetts: American Geologists, v. 25, p. 42-50.

Dowse, A. M., 1950, New evidence on the Cambrian contact at Hoppin Hill, North Attleboro, Massachusetts: American Journal of Science, v. 248, p. 95-99.

Emmerson, B. K., 1917, Geology of Massachusetts and Rhode Island: U. S. Geological Survey Bulletin 597, 289 p.

Foerste, A. F., 1889, The paleontological horizon of the limestone at Nahant, Mass.: Proceedings of the Boston Society of Natural History, v. 24, p. 261-263.

Foerste, A. F., 1899, The Cambrian strata of the Attleboro district, p. 386- 393, in Shaler, Woodworth, J.B., and Foerste, A.F., Geology of the Narragansett Basin, U.S. Geological Survey Monograph 33.

Grabau, A. W., 1900, Paleontology of Cambrian terranes of Boston Basin: Boston Society of Natural History Occasional Papers, v. 4, p. 601-694.

Irvine, T. N., and Baragar, W. R. A., 1971, A guide to the chemical classification of the common volcanic rocks: Canadian Journal of Earth Sciences, v. 8, p. 523-548.

James, N. P., and Klappa, C. F., 1983, Petrogenesis of Early Cambrian reef limestones, Labrador, Canada: Journal of Sedimentary Petrology, v. 53, p. 1051-1096.

Kaye C. A., 1965, Folding of the Nahant gabbro, Massachusetts, United States Geological Survey Professional Paper 525-C, p. C12-C19.

Landing, E., 1988, Lower Cambrian of eastern Massachusetts: stratigraphy and small shelly fossils: Journal of Paleontology, v. 62, p. 661-695.

Landing, E., 1989, Paleoecology and distribution of the Early Cambrian rostrochonch *Watsonella crosbyi* Grabau: Journal of Paleontology, v. 63, p. 566-573.

Landing, E., 1991, Upper Precambrian through Lower Cambrian of Cape Breton Island: faunas, paleoenvironment, and stratigraphic revision: Journal of Paleontology, v. 65, p. 570-595.

Landing, E., 1992, Lower Cambrian of southeastern Newfoundland: epirogeny and Lazarus faunas, lithofacies-biofacies linkages, and the myth of global chronostratigraphy, in Lipps, J., and Signor, P.W., eds., Origins and Early Evolution of Metazoa, Plenum Press, New York, p. 283-309.

Landing, E., 1993, In situ earliest Cambrian tube worms and the oldest metazoan-constructed biostrome (Placentian Series, southeastern Newfoundland): Journal of Paleontology, v. 67, p. 333-342.

Landing, E., Myrow, P., Benus, A.P., and Narbonne, G.M., 1989, The Placentian Series: appearance of the oldest skeletalized faunas in southeastern Newfoundland: Journal of Paleontology, v. 63, p. 739-769.

Marek, L., and Yochelson, E.L., 1976, Aspects of the biology of the Hyolitha (Mollusca): Lethaia, v. 9, p. 65-82.

Myrow, P.M., 1992, Bypass-zone tempestite facies model and proximality trends for an ancient muddy shoreline and shelf: Journal of Sedimentary Petrology, v. 62, p. 99-115.

Myrow. P.M., and Landing, E. 1991, Mixed siliciclastic-carbonate deposition in an Early Cambrian oxygen-stratified basin, Chapel Island Formation, southeastern Newfoundland: Journal of Sedimentary Petrology, v. 62, p. 455-473.

Pearce, J. A., 1983, Role of the subcontinental lithosphere in magma genesis at active continental margins, *in* Hawksworth, C., and Norry, M. J., eds., Continental basalts and mantle xenoliths: Nantwich, England, Shiva, P. 230-249.

Pearce, J. A., and Cann, J. R., 1973, Tectonic setting of basic volcanic rocks determined using trace element analysis: Earth and Planetary Science Letters. v. 19. p. 290-300.

Pearce, J. A., Alabaster, T., Shelton, A. W., and Searle, M. P., 1981, The Oman ophiolite as a Cretaceous arc-basin complex: Evidence and implications: Royal Society of London Philosophical transactions, ser. A, v. 300, p. 299-317.

Ross, M. E., 1992, Petrology and tectonic significance of Mesozoic mafic dikes of the Coastal New England Igneous Province, Massachusetts: *in* Puffer, J. H. and Ragland, P. C., eds., Eastern North American Mesozoic magmatism, Geological Society of America Special Paper 268, p. 63-74.

Ross, M. E., 1990, Mafic dikes of the Avalon Boston terrane, Massachusetts: *in* Socci, A. D., Skehan. J. W., and Smith, G. W., eds., Geology of the composite Avalon terrane of Southern New England, Geological Society of America Special Paper 245, p. 133-153.

Ross, M. E., Knowles, C. R., and Chamness, J. S., 1983, Megacrysts, xenocrysts, and ultramafic xenoliths from a camptonite dike in Cambridge, Massachusetts: Geological Society of America Abstracts with Programs, v. 15, p. 174.

Runnegar, B. and Pojeta, J., 1974, Molluscan phylogeny: the paleontologic viewpoint: Science, v. 186, p. 311-317.

Shaler, N.S., and Foerste, 1888, Preliminary description of North Attleboro fossils: Harvard Museum of Comparative Zoology Bulletin, v. 16, p. 27-41.

Theokritoff, G., 1968, Cambrian biogeography and biostratigraphy in New England, in Zen, E., White, W.S., Hadley, J.B., and Thompson, J.B. Jr., eds., Studies of Appalachian Geology Northern and Maritime, Interscience Publishers, New York, p. 9-22.

Verma, P. K., 1973, Contributions to the geology and petrology of Nahant and Weymouth areas, Massachusetts: Ph.D. thesis, Harvard University, Cambridge, Massachusetts.

Zartman, R. E., and Marvin R. F., 1971, Radiometric age (Late Ordovician) of the Quincy, Cape Ann, and Peabody Granites of eastern Massachusetts: Geological Society of America Bulletin, v. 82, p. 937-958.

Chapter Z

Building Blocks of Boston

By Dorothy Richter and Gene Simmons

Field Trip Guidebook for the Northeastern United States:
1993 Boston GSA

Volume 2
Contribution No. 67, Department of Geology and Geography, University of Massachusetts, Amherst, Massachusetts

BUILDING BLOCKS OF BOSTON

by
Dorothy Richter and Gene Simmons
Hager-Richter Geoscience, Inc.
8 Industrial Way - D10
Salem, NH 03079

INTRODUCTION

During today's trip, we will examine modern and historic uses of building stone in Boston. The trip is divided into two parts. Figures 1 and 2 are maps showing the locations of the stops in each part of the trip. The first portion of the trip includes the walk from the Marriott Copley Place Hotel lobby through Copley Square. We will hop on the subway at Copley Square and travel downtown for the second part of the trip, where we will make a walking loop through the Financial District, examining both modern and historic uses of stone on the way. All of the buildings will be examined from the public right-of-way, so the trip can be run as a self-guided tour at any time.

There are several references that provide information that we will use today. The following list is not designed to be comprehensive, but indicates the sources to which we turn when we have questions. The architecture of Boston is well described in the AIA Guide to Boston (Southworth, 1992) and Miller and Morgan (1990). Boston buildings are most commonly clad with granite, and information about specific sources of granite on old buildings can be gleaned from Brayley (1913) and Dale (1923). For newer buildings, we learned about quarry sources from stone suppliers and trade journals, such as Stone World, Dimensional Stone, and Building Stone.

HISTORIC BASIC USES OF STONE IN BOSTON

Boston has a rich heritage in the use of natural stone as a building material. There are few places in the City where stone is not used in at least some way. Streets were formerly paved with cobblestones and cut granite paving blocks, still visible in the historic districts and, in places, at the bottoms of potholes.

Unlike many areas outside of the northeast, stone has been, and is currently, used routinely for street curbing. Most curbing in Boston is granite, but in places, sandstone and slate curbing can be found. Prior to the Great Depression, granite curbing and paving blocks were supplied from New England quarries, most commonly from quarries located near the coast. Granite curbing wears well, and when streets with granite curbing are re-paved or widened, the old granite curbing often is simply re-set. Currently active sources of granite curbing for the Boston market are quarries in the Chelmsford granite (quarries located in Westford, Mass.), the Milford Granite of Milford, New Hampshire, the Concord Granite in Concord, New Hampshire, and a grey granite near Otis, Massachusetts.

Stone was also used for sidewalks. We will walk on various types of granite as well as "bluestone," a fine-grained arkose from the Catskill Mountains, during our trip today. And, of course, stone was used for building foundations, bridges, walls, and monuments.

STONE IN OLDER BUILDINGS

Prior to the use of steel framing for buildings, massive stone blocks of local building stones were used for load-bearing walls of buildings. The proximity of Boston to several sources of granite has made this a granite-rich city, at least in the commercial districts. The most common granites on older buildings in Boston are Quincy Granite, Milford Granite, Rockport Granite, Stony Creek Granite, and various granites from the coast of Maine (Deer Isle Granite is probably the most abundant). The dark blue-grey Quincy granite, a peralkaline riebeckite granite quarried south of Boston, was very popular for buildings and monuments (including the Bunker Hill Monument, begun in 1825). The pink gneissic Milford Granite, quarried southwest of Boston, blended well with the brick structures of the City. Grey, and greenish grey Rockport Granite, a hornblende granite quarried on Cape Ann north of Boston, has a fairly distinctive texture. Stony Creek Granite is a pink gneissic granite from near Branford, Connecticut. The Maine coastal granites are commonly pink and tan in color, and porphyritic or relatively coarse grained.

As in New York, brownstone flourished as a fashionable facing for townhouses during the peak construction in Back Bay in the 1870's and 1880's. Most of the brownstone is arkosic sandstone from quarries in the Mesozoic Connecticut Valley redbeds. Most of the brownstone buildings exhibit deterioration of the facing, particularly in blocks laid perpendicular to bedding.

The use of building stone as purely decorative cladding only began when steel framing became the structural support of buildings. The market for building materials also changed when rail transportation became more available, and materials such as Indiana Limestone could compete in the Boston market. As in cities all over the country, there are numerous institutional and commercial buildings clad with Indiana Limestone in Boston and Cambridge (MIT's main buildings, for example). Prior to the late 1960's and early 70's, granite and marble cladding was generally at least 2 inches thick, limestone cladding was generally about 8 inches thick, and most of the stone used on buildings in Boston came from North American sources.

MODERN STONE CLADDING

Developments in stonecutting technology during the last 20 years or so have produced a revolution in the use of building stone in cities throughout the world, and Boston is no exception. Modern stone cladding is thin (to 1 inch or even less) and hung from buildings by complex anchorage systems.

Today's building stone market is truly worldwide in scope. Major stonecutting centers, particularly those in Italy, buy rough stock (quarry blocks) from quarries throughout the world, do the cutting and finishing, and then ship the finished stone panels all over the world. The Italian fabricators have dominated the world market for several years. Architects and designers have a wide spectrum of colors and textures from which to choose. But, since there are now hundreds of different building stones marketed under nondescript trade names, it is commonly difficult to determine where in the world the stone on a local building was originally quarried.

ACKNOWLEDGEMENTS

We gratefully acknowledge the following individuals and companies that have provided information about the sources of stone on several of the buildings that we examined today. Mr. Richard Merrill, Building Manager for Trinity Church, kindly spent time explaining the preservation history of the Trinity Church. We also thank Mr. Gerry Rousseau of Rock of Ages Corporation, Mr. Stephen Gulyas of Stone Tech, Inc., Ms. Christina Ramos of New England Stone Industries, Inc., and Mr. William Lazar of Castellucci Stone Industries for providing information about quarry sources for several buildings in Boston. Rock of Ages Corporation loaned us a copy of Brayley (1913).

TRIP LOG

We assemble in the front lobby of the Marriott Copley Place Hotel. The Copley Place development was constructed in the air space above the Massachusetts Turnpike in 1980-1984 after much controversy between developers, government agencies and community groups.

Since we are on foot, no mileages are given in the log. The locations of the first four stops are shown in Figure 1.

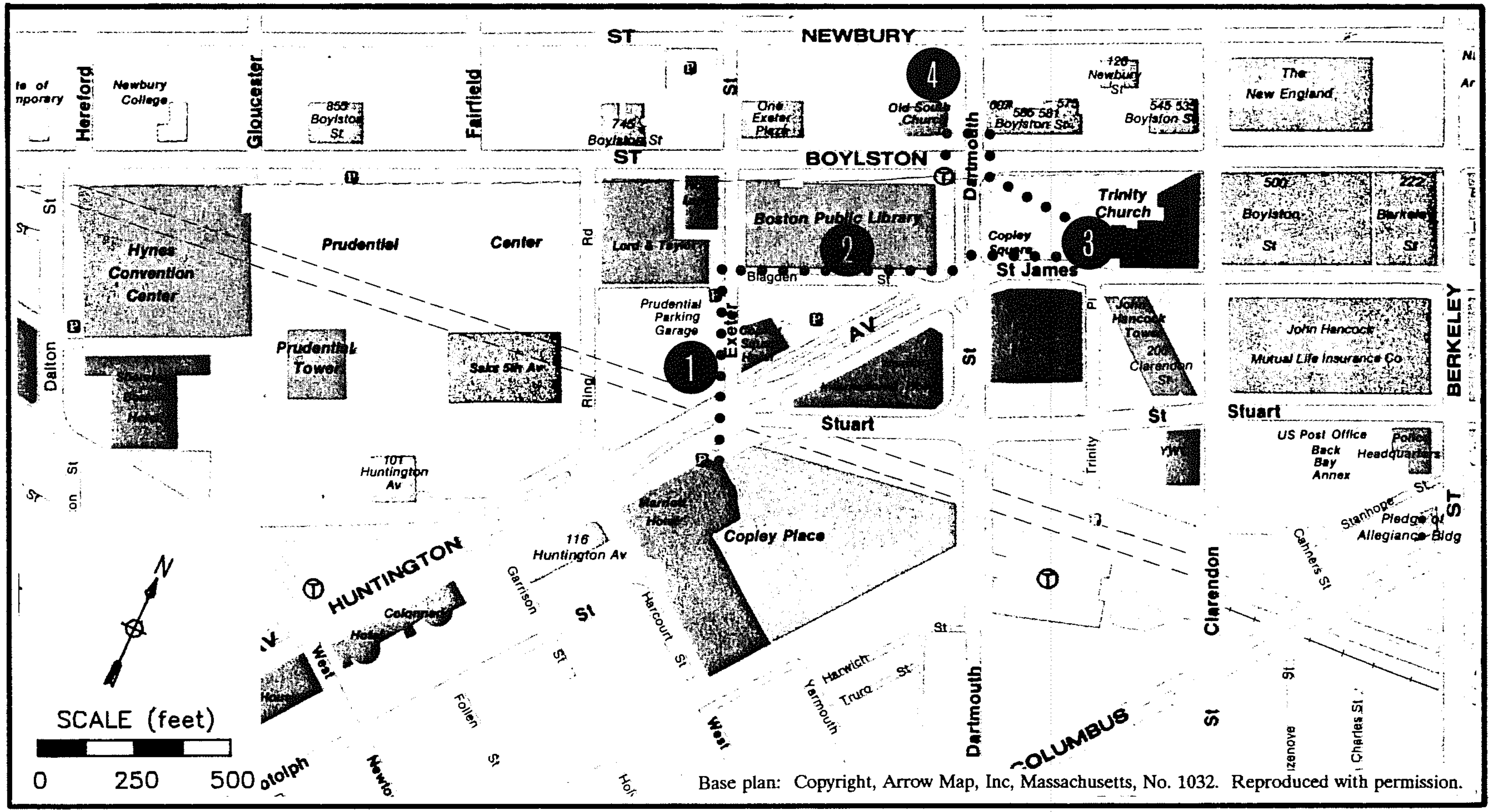

Figure 1. Map showing the locations of Stops 1 - 4.

Exit the lobby of the Marriott Copley Place Hotel at street level, near the entrance to the parking garage. The exterior trim on the hotel and the rest of the Copley Place complex is Stony Creek Granite, a pink Precambrian gneissic granite from Connecticut. The granite panels have a thermal finish. This granite is widely used in Boston, and we will see several other examples of it today.

Cross Huntington Avenue.

STOP 1. RETAINING WALL AT PRUDENTIAL CENTER COMPLEX. The Prudential Center complex, Boston's first major attempt at urban renewal, was constructed in the early 1960's and is now largely considered a poor design from several standpoints. The retaining wall, lifting the complex above the street level, is regarded as part of the problem because it isolates the complex rather than inviting the public in. In some places, the retaining wall has been removed as part of recent renovations.

The granite facing of the retaining wall is Swenson Green, quarried from the Cape Neddick igneous complex in York, Maine. The Maine Geological Survey Mineral Resources Index No. 2 (1958) describes this material as an alkaline syenite containing accessory arfvedsonite, aegirine-augite, and biotite. The granite has a honed finish on Huntington Avenue, and most of the large panels along Exeter Street have a thermal finish. Note the contrasting appearance of the thermal finished panels with the honed finished panels. This project was constructed in the early 1960's, and the granite is relatively thick by current standards; it is 2¾ inches to 3¾ inches thick.

When the wall was erected, the granite was considerably darker green in color. The color has faded and the panels appear now exhibit varying shades of greenish grey. Note the highly variable textures, veining, and rusty pits in the surface of the granite. The stone is no longer quarried.

Proceed down Exeter Street to Blagden Street. Turn right on Blagden Street.

STOP 2. BOSTON PUBLIC LIBRARY. The Boston Public Library consists of two wings occupying the block between Exeter Street and Dartmouth Street. The original building, facing Dartmouth Street in Copley Square, was designed in the Italian Renaissance style by Charles Follen McKim of McKim, Mead and White and opened in 1895. The new wing was designed as an understated modern addition by Philip Johnson to complement the old wing; it opened in 1971.

The granite on both the old and new portions of the library is the Milford Granite, a pink foliated Precambrian biotite granite quarried at Milford, Massachusetts. In the old wing, the granite is used in load-bearing walls with rusticated rock-pitch surfaces. In the new wing, the granite has a thermal finish and is at least 2 inches thick. Massive monolithic slabs are used to form a distinctive wall around the new wing at street level.

The color and texture of the granite are quite distinctive. As a massive local granite, Milford Pink was used for many buildings in Boston prior to WWII. In later years, the stone was not very popular, and most of the quarries operated intermittantly. We understand that one quarry was re-opened to produce the granite for the new wing of the library, and it is the last major building project produced from the Milford Granite.

Cross Dartmouth Street and the plaza at Copley Square to Trinity Church.

STOP 3. TRINITY CHURCH. Trinity Church was designed by Henry Hobson Richardson in the Romanesque style and opened in 1877. The portico and front tower peaks were added in 1898. Since the church is constructed on fill in the former Back Bay, the building is supported by 4500 wooden piles, of which over 2000 are in an area of 90 feet by 90 feet to support the foundation of the front tower. Four granite pyramids, each measuring 35 feet square at the base, 17 feet high, and 7 feet square at the top sit on the piles for the tower. The wood piles must be kept saturated, and the water table under the church is constantly monitored.

The stone on the exterior of the church is light colored granite liberally trimmed with brownstone. According to information provided by Mr. Richard Merrill, the building supervisor, the granite is Dedham Granite and the trim is Longmeadow sandstone. Southworth (1992) states that the granite was quarried in Dedham, Quincy, Westerly RI, and the Maine coast. Perhaps the Quincy and Maine coast granites, generally coarser grained than the stone visible at street level, were used for the granite piers discussed above.

Dedham Granite is known geologically as the late Precambrian Dedham granodiorite. Dale (1923) lists quarries in the Dedham at Wrentham, Stoughton, and Cohasset, but they are described as medium to coarse grained grey granites. The quarry at Wretham opened in 1884, after Trinity Church was opened.

We think the fine grained pinkish grey granite on the exterior of the church might be Westerly Granite from Rhode Island. Westerly Granite is a fine grained biotite granite noted for its uniformity. The USGS geochemical standard G-1 is Westerly Granite.

The red arkosic sandstone quarries at East Longmeadow, Massachusetts are located in the redbeds of the Mesozoic Connecticut Valley. The quarries, no longer active, produced the most durable of the so-called brownstones that were enormously popular building stones in the last quarter of the 19th Century. The demand for replacement stock for historic preservation purposes is so high that blocks from old bridge abutments and stone from other structures are salvaged and re-sold. According to Mr. Merrill, four replacement pieces from such salvaged stone were recently installed on the Trinity Church tower.

Trinity Church is a landmark structure that is carefully maintained. Reportedly, some of the brownstone on the front portico was re-cut during restoration work in 1915. The exterior of the building was cleaned in 1974 with a dilute acid wash, and the freshly revealed contrasting colors of the granite and brownstone drew much comment. The most recent historic preservation activities have been on the tower, where patching mortar has been used and a "stone strengthener" or consolidant has been injected into selected pieces.

> Cross over the Copley Square plaza toward the corner of Dartmouth and Boylston Streets and cross both streets.

STOP 4. OLD SOUTH CHURCH. This building is actually the "new" Old South Church constructed in 1875. Cummings and Sears were the architects and the style is described as Italian Gothic. The "old" Old South Meeting House, built in 1729, still stands at the corner of Washington and Milk Streets in downtown Boston.

The building blocks of this church are Roxbury Conglomerate, Boston's famous "puddingstone." The Roxbury Conglomerate is from the Boston Basin, now generally considered a late Precambrian Avalonian structure. The conglomerate used in this structure is well indurated and has weathered well.

Two contrasting sandstones are used extensively as trim on the Old South Church. The reddish sandstone is likely the Longmeadow sandstone from the Connecticut Valley. We are not certain where the buff colored sandstone was quarried.

> Cross Boylston Street toward the Boston Public Library and enter the Copley Square station for an INBOUND train on the Green Line of the MBTA. The current fare is $0.85 each way. Take any Green Line train to the Government Center stop and get off. Go upstairs to the street level. Granite gutters on the Government Center station building are cut from Rockport Granite.

The locations of the stops for this portion of the trip are shown in Figure 2.

The Sears Crescent Building near the subway station is a remnant of Scollay Square, the predecessor of Government Center, another major "urban renewal" project. Brownstone sills and lintels on the Sears Crescent have been extensively patched with a mortar that simulates the appearance of the brownstone pretty well. At the Court Street end of the Sears Crescent is a small grey granite (not sure of the source) building, known as the Sears Block, that dates from 1848.

Cross Court Street and proceed down Tremont Street.

6 Tremont Street. The Bay Bank building at the corner of Tremont and Court Streets is faced with polished Stony Creek Granite.

10 Tremont Street. The doorway trim is Carrara Marble.

16 Tremont Street. Stony Creek Granite facing.

18 Tremont Street. Bethel White Granite, quarried in Bethel, Vermont, facing in the doorway. Not sure of the source for the pink granite pilasters along the street.

STOP 5. KINGS CHAPEL. Kings Chapel was designed in 1749 by Peter Harrison. The AIA guide (Southworth, 1992) calls the style of this building American Georgian.

The exterior walls of Kings Chapel are blocks of Quincy Granite trimmed from boulders, not from bedrock. Kings Chapel is reportedly the oldest cut granite building in the US. Brayley (1913) contains a description of the splitting of the boulders for this building: first, the boulders were heated by building a fire on top, and second, a heavy iron ball was dropped on the boulder. The famous Quincy Granite quarries were started several decades later. The granite blocks exhibit varying colors due to the varying degrees of weathering of the original boulders.

Cross School Street and proceed down Tremont Street.

Parker House Hotel. Polished Rockport Granite facing. Not sure of the identity of the newer inset polished green granite on School Street facade.

73 Tremont Street. Across the street. Milford Granite load-bearing walls. Note the structural cracks at the corners of the building.

Old Granary Burying Ground. Across the street. Resting place of Paul Revere, Samual Adams, John Hancock, Robert Treat Paine, and Benjamin Franklin's parents. The Eqyptian-style Quincy Granite gate was designed by Solomon Willard, architect for the Bunker Hill Monument.

88 Tremont Street. Indiana Limestone in the doorway.

94 Tremont Street. Rockport Granite sidewalk slabs.

120 Tremont Street. Indiana Limestone facing.

Park Street Subway Station. Deer Isle Granite on both the original building across the street and on the recently renovated kiosks on the same side of the street.

128 Tremont Street. Carnelian (trade name) granite polished storefronts. This granite is quarried

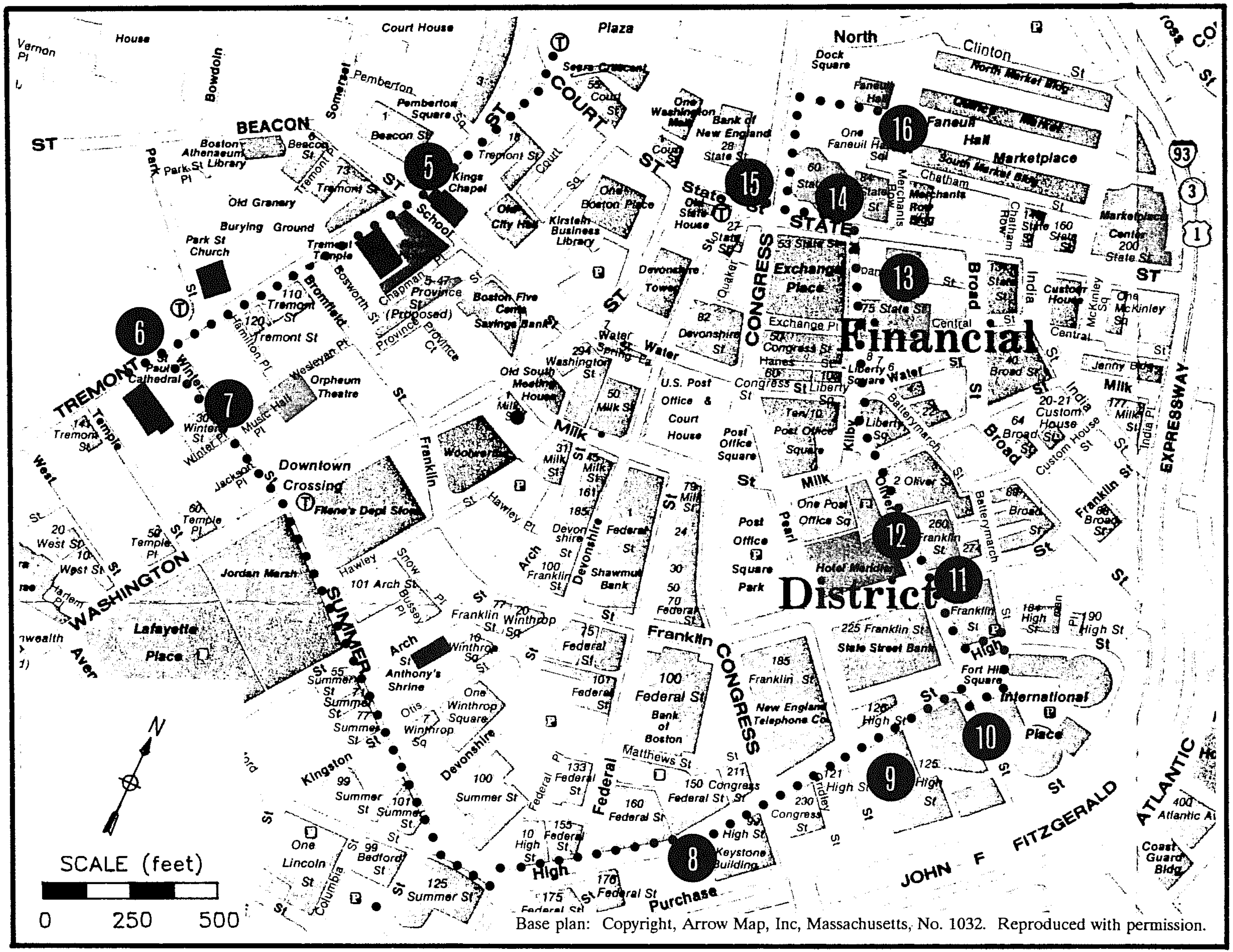

Base plan: Copyright, Arrow Map, Inc, Massachusetts, No. 1032. Reproduced with permission.

Figure 2. Map showing the locations of Stops 5 - 16.

in Milbank, South Dakota in the Minnesota River valley. The granite is also known as Dakota Mahogany. Note the "clear" uniform texture on the Dunkin Donuts storefront and the "wavy" gneissic texture on the Boston Five Cent Savings Bank on the corner of Winter and Tremont Streets.

Cross Winter Street and continue ½ block to next stop.

STOP 6. ST. PAUL'S CATHEDRAL. Designed by Alexander Parris and opened in 1820. The style is described as Greek Revival, an Ionic Greek temple. If you step back from the building, you can see blank stones in the pediment, intended for bas-relief carvings that were never executed.

The walls are light Quincy Granite, much more uniform appearing than those of Kings Chapel because they were quarried from fresh bedrock.

The 32-foot high columns are Acquia Creek Sandstone, a Cretaceous sandstone from Stafford County, Virginia. This is the same stone used for the White House and several other structures in Washington, but its use here in Boston is something of a surprise. According to a brochure published by the Church, a stone from Valley Forge in Pennsylvania was also included as a demonstration of patriotic fervor, but we do not know which one it is. Interesting features of the sandstone in the columns are the pronounced crossbedding, the bluish tint of the quartz clasts, and rusty nodules. The Acquia Creek sandstone is notorious for its poor weathering properties, and extensive repairs are visible on the columns here.

Retrace your steps to Winter Street and turn right on to Winter Street.

58 Winter Street. Handsome brownstone entry and bluestone sidewalk.

STOP 7. 30 WINTER STREET. Built for the Provident Institution for Savings in 1973 and now occupied by the Shawmut Bank, this is a typical commercial highrise building constructed before very thin granite cladding was widely available. The granite is likely at least 2 inches thick and has a thermal finish.

The granite is Charcoal Grey, quarried near Cold Spring, Minnesota. Note the scattered ovoid dark xenoliths, termed "knots" in the granite industry.

Proceed down Winter Street. Across Washington Street, the name changes to Summer Street. Continue down Summer Street.

Jordan Marsh Department Store. Polished grey granite store front in the older section near Washington Street is Concord NH granite, a two-mica granite. On the addition to the store, after Window 2, the polished grey granite is Chelmsford MA granite.

55 Summer Street, New World Bank. Foliated granite from Milbank, South Dakota. The stone for this building came from either the Carnelian quarries or the Sequoia quarry, also in Milbank, but known for its pronounced foliation.

99 Summer Street. Polished pinkish grey granite, Rosa Gamma, from Sardinia.

100 Summer Street. Across the Street. Texas Rose granite from the Llano Uplift in central Texas on the new tower.

125 Summer Street. A large complex incorporating the facades of several old commercial buildings at the base and a central new tower. Stony Creek Granite is used in the new portions of the complex.

Cross Summer Street and proceed down High Street.

10 High Street. Deer Isle Granite facing.

155 Federal Street, corner of High and Federal Streets. Indiana Limestone with interesting grooved textures.

STOP 8. KEYSTONE BUILDING, 99 HIGH STREET. This highrise office building was built in the late 1960's or early 70's, during which there was a mercifully brief period when Italian travertine was popular for thin exterior cladding on precast concrete walls on buildings in northern climates. The approximately 1-inch thick travertine is attached to the precast concrete panels by "hairpin" anchors inserted in holes on the back side of the stone, and the loop of the hairpin was embedded in the uncured concrete at the time of fabrication. A sheet of polyethylene is commonly used as a bond-breaker between the stone and the concrete for this type of construction. The travertine at the base of the building is attached by anchors inserted in sawn kerf slots at the top and bottom of each piece.

Look carefully at the travertine on this building, and you will see that every stone on the building has been re-anchored from the exterior by sets of bolts. Some stones have several sets of bolts, implying that the stone was severely cracked. In addition, some stones have been cut and replaced, and numerous cracks have been repaired. Half-moon cracks (now repaired) on the column covers are widespread and mark the locations of the kerfs used for anchorage. The repairs, which are nicely camouflaged, were completed about 3 years ago, and took about 2 years to complete.

150-160 Federal Street, across High Street from the Keystone Building, is clad with thermal finished Spanish Pink Granite.

Proceed down High Street, crossing Congress Street and Pearl Street. The New England Telephone Building has Indiana Limestone cladding. Not sure of the quarry origin for the pink granite at the base.

STOP 9. 125 HIGH STREET. Built in 1991, this building was designed by the Boston firm of Jung/Brannen. This building is a fine example of modern thin granite cladding, probably attached to a steel truss backup. The granite at the base is Deer Isle granite from Maine, and the balance of the building is Stony Creek granite from Connecticut. Note the effective use of contrasting polished and thermal finishes and false joints in single stone panels, giving decorative geometric designs and the appearance of several smaller stones.

Proceed down High Street, crossing Oliver Street.

STOP 10. INTERNATIONAL PLACE. Designed by Philip Johnson and John Burgee, the two towers were built in 1985 and 1992. The older tower with its palladian windows drew so much criticism that the second tower was redesigned. The extravagant lobby was said to have the largest amount of marble in a single lobby in the US, all imported, of course.

The granite on the exterior is Balmoral Red, a beautiful, uniform, fine grained red granite quarried in Taivassalo, in the southwestern part of Finland. The blocks quarried in Finland were shipped to Italy for fabrication, and the thermal finished slabs were shipped to the US. The granite is siliceous (33% quartz), and the quartz is somewhat smoky.

Cross High Street and proceed down Oliver Street.

STOP 11. 265 FRANKLIN STREET. The building was completed in 1984, Goody, Clancy & Associates architects.

Two imported granites are used on this building. The darker reddish granite with a thermal finish is Carmen Red, a coarse grained rapakivi granite quarried at Virolahti, on the southeastern coast of Finland. Note the large round red perthite crystals and the smoky quartz in the granite. The finer grained pale pink granite is known as Spanish Pink and is quarried in Spain.

Cross Franklin Street and proceed down Oliver Street.

STOP 12. 260 FRANKLIN STREET. This building dates from 1985, and The Stubbins Associates were the architects.

The stone on the exterior of this building is polished Spanish Pink Granite, and it is attached to a precast concrete backup with hairpin anchors. This granite is inexpensive compared to many other granites that were on the market in the late 70's and early 80's, and many structures all over the US have been clad with it. The granite has an extremely prominent rift, i.e., direction of easy splitting, so the physical properties of this granite are strongly anisotropic.

Proceed down Oliver Street. Cross Liberty Square, and proceed down Kilby Street.

STOP 13. 75 STATE STREET. Graham Gund Architects and Skidmore, Owings & Merrill were the architects of this Art Deco style post-modern building, erected in 1988. Reportedly, there is 3600 square feet of gold leaf applied to the building. The lobby contains dramatic marble tiling.

Five types of imported granite were used on the exterior of this building. They are called Gamma Pink, Napoleon Red, Imperial Mahogany, Biritiba, and Maritaca Green. All of the stone was fabricated in Italy. Gamma Pink is also know as Rosa Gamma and is quarried in Sardinia. Napoleon Red and Imperial Mahogany are quarried in Sweden. Biritiba is quarried in Brazil(?), and we do not know where Maritaca Green is quarried.

The granite at the base of the building appears to be massive, like the rusticated granite on older buildings. But if you look carefully, you will find epoxied miter joints at the corners of all blocks, a sure sign that the walls are not massive.

Across Kilby Street is Exchange Place, another example of facade preservation. The granite on the old facade is Stony Creek Granite.

Cross State Street and turn left. 84 State Street has Deer Isle Granite on the exterior.

STOP 14. 60 STATE STREET. Skidmore, Owings & Merrill designed this highrise office building in 1977.

The granite is Red Vånga, quarried in Vånga, Sweden and fabricated in Italy. The stone has a thermal finish and is attached to a steel truss backup. The granite has a uniform, faintly foliated texture.

Cross Congress Street.

STOP 15. 28 STATE STREET. This former bank headquarters building was designed by Edward Durrell Stone and erected in 1969.

The granite on the exterior is Carnelian Granite from Milbank, South Dakota. The stone is 2 inches thick, has a thermal finish, and on the main tower is attached to a precast concrete backup. At the lower levels, the granite was hand set. Look closely at the granite on the tower, and you will see that every piece of granite has been re-anchored to the backup by bolts applied from the exterior. This major repair work was done about 5 years ago. Note also that several corner cracks have been repaired on the tower, and that some repaired cracks start at the edge of the stone and stop in the middle of the panel. We suspect, but do not know because we have not examined the granite at close distance, that some of the "cracks" repaired in this operation are natural mineralized features in the granite that do not impair its strength.

Cross Congress Street and turn left. Walk to Faneuil Hall and Quincy Market.

STOP 16. FANEUIL HALL/QUINCY MARKETPLACE. This is where we terminate our walking tour. There is a wealth of stone to examine in the Marketplace while you have your lunch.

The main Quincy Market building was designed by Alexander Parris, the same architect for St. Paul's Cathedral, in 1824. Benjamin Thompson and Assoc. were the architects for the hugely successful renovations in 1976. According to Brayley (1913), the foundation of the Quincy Market building is Quincy Granite. Chelmsford Granite probably makes up most of the balance of the building, although Brayley also states that Hallowell Granite from Maine was used in part. The columns, single shafts of granite 20 feet 9 inches long, were quarried in the town of Chelmsford and were brought to Boston by canal.

The granite slab pavers between Quincy Market and Faneuil Hall are Chelmsford Granite. The 50-inch diameter round granite stools near the flower market are calyx cores from the Chelmsford Granite quarries. The cores were drilled for installation of quarry wire saws.

New buildings in the Marketplace are: One Faneuil Hall Square (housing The Limited), Graham Gund Architects, 1988, faced with Stony Creek Granite; and, at the far end of the complex, Marketplace Center, WZMH Group architects, 1983, faced with Deer Isle Granite.

To return to the Hynes Convention Center, cross Congress Street and walk across the Government Center Plaza to the Government Center subway stop. Take any INBOUND Green Line train (Boston College, Cleveland Circle, Riverside, or Arborway) to Copley Square, and walk up Boylston Street to the Convention Center. The exterior granites on the Hynes Convention Center are Rockville Grey from Rockville, Minnesota and Osage, a red granite quarried near Granite, Oklahoma.

To return the Marriott Copley Place Hotel, walk back up Congress Street to State Street. Cross State Street and enter the State subway station in the basement of the Old State House. Watch the signs in the subway station, because they are a bit confusing. Take a FOREST HILLS VIA DOWNTOWN CROSSING Orange Line train to the Back Bay/South End Station. Go upstairs, cross Dartmouth Street, and enter the Copley Place mall. The hotel is at one end of the mall. The fountain in the center atrium of the mall makes effective use of "skin cuts," the ends of quarry blocks. The "black granite" in the fountain is Belfast Black, a quartz norite from the Bushveld Complex in South Africa. The red granite is from India(?).

REFERENCES CITED

Brayley, A. W., 1913, History of the Granite Industry of New England: National Association of Granite Industries of the U.S., Boston, 2 vols, 170 p and 123 p.

Dale, T. N., 1923, The commercial granites of New England: U. S. Geological Survey Bulletin 738, 488p.

Maine Geological Survey, 1958, Maine granite quarries and prospects: Mineral Resources Index No. 2, 50p.

Miller, Naomi, and Morgan, Keith, 1990, Boston Architecture 1975-1990: Prestel Verlag, Munich, 248p.

Southworth, Susan and Michael, 1992, AIA Guide to Boston, 2nd ed.: The Globe Pequot Press, Chester, Conn., 552p.

Chapter AA

Coastal Geologic Hazards and Management Strategies Along a Complex Microtidal Coastline

By Jon C. Boothroyd, Christopher W. Galagan, and Denis E. Newcomer

Field Trip Guidebook for the Northeastern United States:
1993 Boston GSA

Volume 2
Contribution No. 67, Department of Geology and Geography, University of Massachusetts, Amherst, Massachusetts

COASTAL GEOLOGIC HAZARDS AND MANAGEMENT STRATEGIES ALONG A COMPLEX MICROTIDAL COASTLINE

by
Jon C. Boothroyd, Department of Geology, University of Rhode Island, Kingston, RI 02881,
Christopher W. Galagan, Applied Science Associates, Inc., 70 Dean Knauss Drive, Narragansett, RI 02882
and
Denis E. Newcomer, Baker Environmental, 29 Emmons Drive, Building C, Princeton, NJ 08540

INTRODUCTION

The microtidal coastline of Rhode Island is comprised of: 1) open coast barrier spits, lagoons and glacial headlands, and 2) a complex of estuarine coves, small barriers, and varied headlands in Narragansett Bay. The coast is hurricane dominated, but is also influenced by winter storms and a 30 cm/100 yr sea-level rise. The trip illustrates geologic processes and the resulting geomorphic and sedimentologic changes and their impact on people. Various management strategies designed to lessen the impact of geologic processes can be effective; a discussion of the usefulness of those strategies with regard to the goal stated is an important goal of this trip. Another important part of the trip is a discussion of geologic hazards resulting from accelerated sea-level rise due to global warming. We will visit selected environments both on the open barrier/lagoon shoreline and on Narragansett Bay.

SOUTHERN SHORELINE

The 33 km long microtidal shoreline of southern Rhode Island is a natural shoreline laboratory that is being used to track the effects of storm-fairweather cycles and extreme storm events, and to model the effects of accelerated sea-level rise due to global warming on barriers and headlands. Thirty years of beach profile monitoring (10 stations) indicates seasonality at some stations, mixed on-off seasonality at others, and five and ten year patterns of variation at most locations. The last ten year cycle reached peak accretion in 1989 with berm widening, eolian dune deposition, and the development of a temporary storage feature termed the backshore reservoir. Most beaches and associated barrier or headland cores have had a net loss of sediment since 1989, with erosion and removal of backshore reservoir material.

Mapping from vertical aerial photos indicates that erosional retreat of barriers ranges from 0.4-1.0 $m \cdot yr^{-1}$ (1939-85), and headlands from 0.2-0.9 $m \cdot yr^{-1}$, accomplished during sou'easter storm cycles and major hurricanes. Field mapping of barrier and headland changes after storm events (5-20 year storms) indicates that frontal erosion combined with washover sand accumulation have been underestimated as agents of change, particularly on headlands. Trimming of headland bluff and eolian foredune zone profiles allows a more dissipative supratidal zone, enhancing sedimentation in those areas. This effect was particularly pronounced during Hurricane Bob (1991), the Halloween Nor'easter (1991), and the Great December Storm of 1992. We have modified the standard FEMA/NAS storm erosion configuration to better reflect actual changes.

ACCELERATED SEA-LEVEL RISE

Data from the long-term monitoring allows us to better forward-model the effects on the shoreline resulting from projected sea-level rise due to global warming. We are using an isostatic subsidence of 15 cm 100 yr^{-1} based on Newport, RI tide gauge records, and two accelerated eustatic sea-level rise predictions, Hoffman (1984) and Houghton and others (1990), that give rises by 2100 of 1.75 m and 1.45 m respectively. Three methods are used to forward-model nine surveyed transects (four headland and five barrier). The historical erosion method (HEM) models horizontal migration by multiplying the site-specific historical erosion rate by the number of years from 1990. The National Academy of Sciences (NRC, 1990) NAS method determines shoreline response based on the historical erosion trend with respect to the local sea-level changes during that time interval. The sediment conservation method attempts to combine the HEM method with an analysis of change of barrier configuration that models past changes in geomorphology.

Based on observations of local coastal processes during storm events and on beach monitoring studies, 100-year storm event erosional profiles were constructed to develop FEMA wave envelopes along the nine coastal transects. We used the wave envelopes to model the location of FEMA flood zones for 2020, 2050, and 2100. Dramatic changes to transect configurations are projected to occur as barriers migrate and headlands retreat landward up to 345 m by 2100. The present-day East Beach barrier will have "rolled over" itself as the ocean transgresses 50 to 175 m landward by 2100. Average barrier migration for 2100 is 75 and 265 m, respectively, using HEM and NAS migration projections. Average retreat of headlands comprised of glacial deposits by 2100 is 44 m using HEM projections and 114 m using NAS projections. Preliminary modeling results using the sediment conservation method indicate very important overwash-generated sedimentation on headlands (a sink) and serious sediment deficits in beach and shoreface areas (sources).

The change in transect configuration will result in extreme changes in flood zone configuration. Over the next century (2100), FEMA A-zones are projected to shift landward up to 345 m. Most houses on the surveyed barriers and headlands will be flooded by that time.

NARRAGANSETT BAY

Depositional environmental mapping has been carried out for the entire 800 km shoreline of Narragansett Bay, including tidal rivers. This work was in support of a multidisciplinary study to identify and inventory critical habitats of the Bay; the geologic maps formed the base for mapping macrophytes and identifying habitats for wildlife, finfish, lobsters, and benthos. Eighty-five types of depositional features were mapped in open estuarine bay, cove, and upland environments. Features were separated as to major environment (i.e., barrier spit), as to subenvironment (i.e., backbarrier flat), and as to location (supratidal, intertidal, or subtidal). The mapped area extended landward from mean low water a minimum of 100 meters or to the landward limit of the contiguous feature; the mapped area extended seaward to a depth of 3-4 m, the limit of visibility on the photos. An important aspect of this work was to identify human-altered segments of the shoreline and map them as habitats. Approximately 25 percent of the shoreline is human altered.

Historic erosion/deposition rates for the period 1938-1988 were determined for 913 shoreline segments (segment length 100-800 m) by updating coverage from Dein (1981) using 1975 and 1988 vertical aerial photographs. Change in dune or bluff lines was mapped directly from the photos. The most highly erodible areas include barrier spit and glacial delta plain and ice marginal deposits exposed on east and south-facing coasts in the western part of the Bay. Most areas of significant deposition are human-altered sites of dredged-material disposal or filling of the Bay to install docks and piers.

ACKNOWLEDGEMENTS

The trip guide is abbreviated because the senior author (Boothroyd) suffered major injuries in a fall in early May, 1993, was hospitalized, and has had limited use of both arms forthwith. GSA requested that the trip be run and we will have a limited trip guide available in October. Boothroyd expects to be recovered sufficiently to be able to co-lead the trip at that time.

REFERENCES CITED

Hoffman, J.S., 1984, Estimates of future sea level rise, in Barth, M.C., and Titus, J.G., eds., Greenhouse effect and sea level rise - A challenge for this generation: Van Nostrand Reinhold co., p. 79-103.

Houghton, J.T., Jenkins, G.J. and Ephraums (eds.), 1990, Climate change: Cambridge University Press, New York.

National Research Council, 1990, Managing coastal erosion: Committee on Coastal Erosion Zone Management, Water Science and Technology Board, Marine Board, Commission on Engineering and Technical Systems, National Research Council: National Academy Press, Washington, D.C., 182 p.

Chapter BB

Alleghanian and Avalonian Tectonism in Southeastern New England

By Sharon Mosher, Daniel P. Murray, O. Don Hermes, and Peter L. Gromet

Field Trip Guidebook for the Northeastern United States: 1993 Boston GSA

Volume 2
Contribution No. 67, Department of Geology and Geography, University of Massachusetts, Amherst, Massachusetts

ALLEGHANIAN AND AVALONIAN TECTONISM IN SOUTHEASTERN NEW ENGLAND

by

Sharon Mosher, Department of Geological Sciences, University of Texas at Austin, Austin, TX 78712
and
Daniel P. Murray and O. Don Hermes, Department of Geology, University of Rhode Island, Kingston, RI 02881
and
Peter L. Gromet, Department of Geological Sciences, Brown University, Providence, RI 02912

The Alleghanian orogeny in southeastern New England represents the final amalgamation of Avalonian terranes against Laurentia during the collision between Laurentia and Africa. Recent geochronological, petrologic and structural work has better defined the relationships among the various terranes and the timing of juxtaposition. This trip will make a transect across southeastern New England looking at the effects of this diachronous orogeny and at the diverse Avalonian stratigraphies comprising the different terranes.

INTRODUCTION

Although the Alleghanian orogeny has long been recognized as the major mountain-building event in the central and southern Appalachians, only during the last ten years has it been shown that this orogeny also played a major role in the evolution of the northern Appalachians. Previously, most of the metamorphism and deformation of rocks east of the Connecticut River was considered to have occurred during the Acadian orogeny. Structural and metamorphic studies of Pennsylvanian-age rocks comprising the Narragansett basin of Rhode Island and Massachusetts first provided unequivocal evidence of post-Devonian deep-seated, high-grade collisional deformation (Mosher, 1983; Murray, 1988) Within the 15 million years following deposition, Pennsylvanian sediments were multiply deformed by large-scale, recumbent, nappe-like folds concurrent with upper amphibolite facies metamorphism and were intruded by a peraluminous, S-type granite (Zartman and Hermes, 1987; Reck and Mosher, 1989; Mahler and Mosher, in press). Subsequently, geochronological and structural investigations of the surrounding basement has documented the effects of this high-grade collisional deformation as far east as the Triassic Hartford rift basin (O'Hara and Gromet, 1983, 1985; Wintsch and Sutter, 1986; Getty and Gromet, 1992 a, b). Deformation increases dramatically in intensity from central Rhode Island westward and is manifested by ductile shear zones in western Rhode Island and by completely penetrative gneissification of basement rocks in eastern Connecticut (O'Hara and Gromet, 1985; Getty and Gromet, 1992 a, b). Metamorphic grade generally decreases northward and eastward, but appears to be strongly influenced by structrual level (e.g. Gromet, 1989; Getty and Gromet, 1992 a, b; Murray, 1988). For a detailed overview of the Alleghanian orogen in the northern Appalachians, see Snoke and Mosher (1989) and references therein; for more recent work see Getty and Gromet (1992a, b) and Goldstein (1989). A brief overview is given below.

Terranes or tectonic blocks

In southeastern New England, the Devonian Acadian metamorphic belt structurally overlies ~600 Ma (Avalonian?) basement gneisses (Stops 1-3) and is adjacent to a series of Avalonian 'terranes' or tectonic blocks that do not show evidence of an Acadian orogenic event (Fig. 1). Each Avalonian terrane has a distinct stratigraphy and tectonic history and is bounded by Alleghanian-age ductile shear zones. For a complete discussion, see Gromet (1989), Secor and others (1989) and references therein; a brief synopses of each terrane is given below.

The largest block is the easternmost Esmond-Dedham terrane that consists of 600-650 Ma granitic plutons (Stop 4), latest Proterozoic to Cambrian volcanic/volcaniclastic and marine sedimentary rocks containing an Acado-Baltic fauna (Stops 9, 10), a suite of alkalic lastest Precambrian to Devonian plutons (Stops 4, 5, 12) and associated volcanic and volcaniclastic rocks, and overlying Carboniferous nonmarine basins (Stops 7, 8, 11, 14, 15). Many of the basement rocks only show evidence of Avalonian and Alleghanian tectonic events. The ductile, Alleghanian-age Hope Valley shear zone (Stop 5) separates this terrane from strongly tectonized, *ca.* 600 Ma leucocratic metaigneous gneisses of the Hope Valley terrane in eastern Connecticut. A relative paucity of late Proterozoic intermediate to mafic rock types and

Paleozoic stratigraphy and magmatic history in the Hope Valley terrane suggests that this block may be unrelated to the Esmond-Dedham terrane. Similar rocks crop out in the cores of structural culminations such as the Pelham and Willimantic domes (Stops 1-3), indicating that these rocks underlie an extensive area in eastern Connecticut and eastern Massachusetts. Recent mapping in the New Bedford area of eastern Massachusetts (Stops 12, 13) has identified similar rocks east of the Narragansett Basin. If these rocks prove to be correlative, rocks of the Hope Valley terrane may underlie at least the southern margin of the Esmond-Dedham terrane.

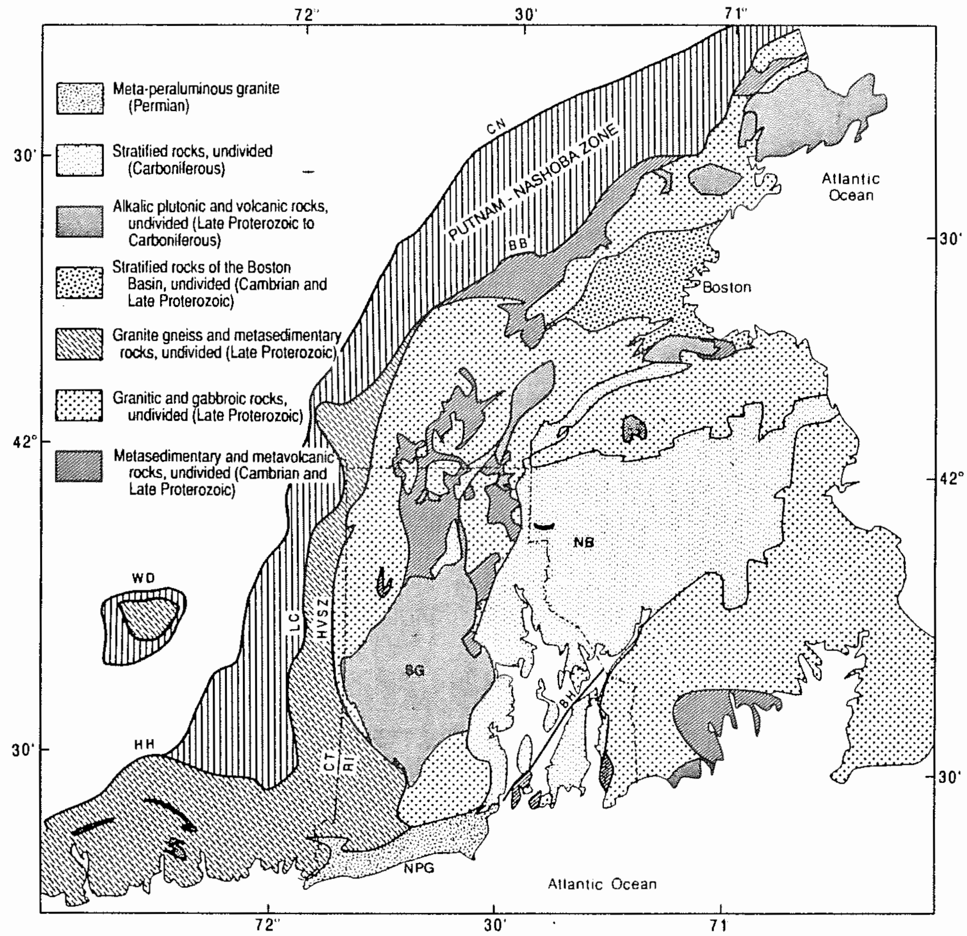

Figure 1. Generalized geologic map of southeastern New England (after Hermes and Zartman, 1992). The composite Avalon zone lies to the south and east of the Honey Hill-Lake Char-Bloody Bluff fault system (HH-LC-BB). The Hope Valley Shear zone (HVSZ) divides the zone into the Hope Valley terrane to the west, and the Esmond Dedham terrane to the east. A small outlier of the Avalon is exposed to the west as a window within the Willimantic Dome (WD). Major elements of the Avalon zone here include: (a) Late Precambrian granitoids intruded into older metasedimentary rocks, and overlain by Cambrian strata, (b) alkalic plutonic and volcanic rocks of latest-most Precambrian and Paleozoic ages, (c) Carboniferous metasedimentary rocks of the Narragansett (NB) and Norfolk basins, and smaller outlying basins of probable Carboniferous age to the west, and (d) peraluminous Narragansett Pier Granite (NGP) of Permian age in southern Rhode Island that intrudes rocks of both terranes. (Vertical ruled lines - Putnam-Nashoba zone; white area west of Putnam-Nashoba zone represents the Acadian metamorphic belt. CN - Clinton-Newberry fault; BH - Beaverhead shear zone; SG Scituate Granite.)

In southern Connecticut, the Hope Valley rocks structurally underlie the Acadian metamorphic belt and are separated from them by the Honey Hill ductile shear zone. In eastern Connecticut and eastern Massachusetts, the Putnam-Nashoba zone appears between the Acadian metamorphic belt and the Avalonian basement terranes (Hope Valley and Esmond-Dedham terranes). The Putnam-Nashoba block contains Ordovician or older metavolcanic and metasedimentary rocks, some of which are Proterozoic, but which are otherwise of uncertain affinity (Avalonian? Laurentian?). The Putnam-Nashoba zone is a tectonic fragment, being bound beneath by the Lake Char and Bloody Bluff faults and above by the Clinton-Newbury fault. Metamorphism is considered Silurian or older.

Timing of tectonothermal events

The Alleghanian orogeny apparently involved collision of one or more terranes caught between colliding Laurentia and Africa, transcurrent motion between terranes and/or Laurentia and Africa, and extensional collapse of the resultant orogenic welt. Because of late structural modifications associated with extension, the metamorphic grade, timing, and type of deformation commonly varies greatly over short distances. An overview of the overall timing of events is given below, but further details are given with each stop description.

The first evidence of the Alleghanian orogeny in New England is the formation of Pennsylvanian-age nonmarine basins filled with primarily fluviatile sediments (Mutch, 1968; Skehan and others, 1979, 1986). The larger Narragansett and Norfolk basins, as well as two smaller ones of probable Pennsylvanian age (the Scituate and Woonsocket basins), are floored by the Esmond-Dedham terrane (Fig. 1). The only other outcrops in southeastern New England are isolated deposits within the Clinton-Newbury fault zone at the southeastern boundary of the Acadian metamorphic belt. Sediments in the Narragansett and Norfolk basins were deposited on wet alluvial fans formed along uplifted and tectonically active basin margins (Severson, 1981; Mosher, 1983; Cazier, 1987) (Stops 7, 11). Early in the evolution of the basins, clastic sediments were interspersed with bimodal alkalic volcanics (Mutch, 1968; Maria, 1990) (Stop 14). Plant fossils range in age from Westphalian A or B to Stephanian B or C (Skehan and others 1979; Murray and others, 1981; Lyons, 1984), establishing the timing of deposition as ~310-290 Ma.

Essentially synchronous with deposition of the sediments, upper amphibolite grade, highly penetrative ductile deformation in eastern Connecticut and western Rhode Island occurred within the gneisses beneath the Honey Hill-Lake Char faults, in the cores of the Willimantic (Stops 1-3) and Pelham domes, and along Hope Valley shear zone (Stop 5) (Gromet, 1991; Getty and Gromet, 1992a, b). These integrated geochronological and microstructural investigations have established the timing of formation of the gneissic and mylonitic foliations as 290-305 Ma.

Sometime after 290 Ma but prior to the intrusion of the Narragansett Pier Granite at 275 Ma, the nonmarine basin sediments underwent regionally extensive, polyphase folding under mid-amphibolite to lowest greenschist facies (Murray and Skehan, 1979; Mosher, 1983; Reck and Mosher, 1989) (Stops 7, 8, 11). Highest grades are found in the southwestern Narragansett basin. Some of the adjacent basement rocks west of the basin also were affected by this folding (Dreier, 1985).

Felsic magmatism occurred from 270-280 Ma across the Avalonian basement resulting in extensive pegmatitic/ granitic dikes and several larger plutonic bodies (Zartman and Hermes, 1987; Wintsch and Aleinikoff, 1987; Aleinikoff and others, 1975; Getty and Gromet, 1991). The Narragansett Pier granite (275 Ma; Zartman and Hermes, 1987) cuts across the Hope Valley and Esmond-Dedham terranes and intrudes polydeformed Pennsylvanian-age metasedimentary rocks (Stop 6) and forms an essentially undeformed 'stitching' pluton.

Synchronous with intrusion of the Narragansett Pier Granite (275 Ma), a major N-trending sinistral transcurrent shear zone formed within the Narragansett basin (Reck and Mosher, 1989; Mahler and Mosher, in press) (Stop 8). After intrusion of the granite, dextral transcurrent shearing on the NE-trending Beaverhead shear zone further deformed the basin rocks (Mosher and Berryhill, 1991) (Stop 8). The upper time limit on this deformation is provided by $^{40}Ar/^{39}Ar$ biotite plateau ages of 250-240 Ma (Dallmeyer, 1982).

During the same time interval (265-280 Ma), localized NW-SE ductile stretching affected the uppermost structural levels of Avalonian basement in eastern Connecticut. Mylonitic amphibolites along the basement-cover contact were totally recrystallized during low to mid-amphibolite facies extension. In some locations (e.g. Willimantic Dome, CT;

Stops 1-3), the contact with the overlying Acadian metamorphic belt is a detachment characterized by extensional structures.

In the New Bedford area (Stops 12, 13), preliminary argon release patterns for hornblende from an amphibolite (Murray and Dallmeyer, 1991) suggest that the E-trending foliation and hornblende lineation formed ~270 Ma. Further work (in progress) is necessary to delineate the extent and nature of this Alleghanian deformation and metamorphism.

STOP DESCRIPTIONS

Background Information (Stops 1-3)

The first 3 stops provide views of three different structural levels in the Willimantic dome, a major structural culmination in eastern Connecticut. Much controversy has surrounded the processes involved in the origin of the dome, and the relative and absolute timing of the deformational/metamorphic events represented in the rocks about the dome (e.g., Snyder, 1964; Wintsch, 1979; Wintsch and Fout, 1982). Prior to detailed structural and geochronological studies across different structural levels exposed in the dome, it was thought that the metamorphism of the basement and cover were coeval, and that the basement-cover contact was a thrust. Getty and Gromet (1992 a, b) argue that the present contact is contained within a major extensional shear zone by demonstrating that: 1) cover rocks underwent their primary high grade metamorphism during the Devonian Acadian orogeny, 2) the basement gneisses underwent their primary high grade metamorphism/deformation approximately 100 m.y. later in the Pennsylvanian, and 3) a complex system of ductile to brittle Permian extensional shears overprint earlier structures in both basement and cover. The Permian extensional shears attenuated the crustal section, bringing cover rocks from higher crustal levels into contact with previously deep-seated basement gneisses. The extensional shears created a distinctive zone of pinch-and-swell deformation along the basement-cover boundary. Progressive exhumation of basement along the shears led to the warping and doming of the basement-cover boundary.

Structures present at different structural levels in the dome are shown schematically in Figure 2. Stop 1 at a deep structural level provides for examination of Late Precambrian granitoid gneisses and the Pennsylvanian penetrative ductile deformation that they suffered. Stop 2 is in the lower part of the overlying cover unit (Tatnic Hill Formation), where extensional pinch-and-swell structures are spectacularly developed, and later ductile-to-brittle normal faults can be observed. Stop 3 is at the basement-cover boundary itself, and displays the intense, penetrative mylonitization imposed on the rocks along this boundary.

DIRECTIONS TO STOP 1. From parking lot of Best Western Regent motel on Rt. 195 in Mansfield Center CT, exit right on to 195 south. Follow signs to Rt. 6, eventually entering highway section of Rt. 6 (abandoned Interstate I-84). Take exit at Rt. 32, turning right at end of exit ramp. Park immediately on right shoulder.

Stop 1: Willimantic Dome — Core gneisses at intersection of Rts. 6 and 32

Field Description

The roadcuts on both sides of the exit/entrance ramp contain excellent exposures of plagioclase gneisses making up the outer core of Willimantic dome. This location is on the SW flank of the dome, approximately 500 meters structurally below the contact with overlying cover units. The gneiss here is a fairly homogeneous hornblende-biotite gneiss, and was likely derived from an igneous protolith. U-Pb ages on relict sphene (Getty and Gromet, 1992a) and preliminary $^{207}Pb/^{206}Pb$ direct evaporation ages on zircon indicate a latest Precambrian age for the protolith. This gneiss protolith is believed to be part of extensive exposures of similar Avalonian assemblages to the south and east of the Honey Hill and Lake Char faults.

The gneiss is strongly recrystallized and contains a prominent SW dipping foliation, consistent with a position on the SW flank of the Willimantic dome. Examination of structures and fabrics in the walls of the roadcut reveals that the dominant foliation is overprinted by thin zones of shearing that are parallel to, or very slightly discordant to, the dominant foliation. Together these fabrics impart a slabby, almost layered, character to the outcrops. The gneiss contains some amphibolite layers, which are boudinaged along NW-SE axes. The asymmetry of deflected fabrics internal to one boudin (located NW of the exit/entrance ramps), and external shapes displayed in a train of boudins (located SE of the exit/entrance ramps) indicate normal-sense, tops=>SE shear (present reference frame). Pegmatitic segregations or vein quartz are common at many necks between boudins and at boudin ends. The pegmatitic segregations attest to the high metamorphic grade associated with at least a portion of this ductile deformation. Pegmatitic segregations/dikelets also appear as stringers more or less concordant to the dominant foliation, and in various stages of disruption by shearing along the foliation. A distinct set of late (post-shearing), steep-walled, coarse pegmatite dikes with a NE-SW strike are well displayed in the roadcut SE of the exit/entrance ramps. Coarse pegmatite dikes with a similar orientation are common in other nearby basement exposures, and suggest continued late NW-SE stretching (dilation) of the basement gneisses (Getty and Gromet, 1992b).

This outcrop has been described previously by Wintsch and Fout (1982) and Wintsch (1992), and was the subject of isotopic study by Getty and Gromet (1992a) and by Wintsch (1992). Getty and Gromet (1992a, b) found that the gneiss consisted of a penetratively deformed, recrystallized assemblage in which only zircon and augen of sphene appear to be relict from the original late Precambrian igneous crystallization. Various size fractions of clear sphene euhedra produced during the formation of dominant (early) recrystallized assemblage gave concordant U-Pb ages of 304+/-2Ma. The dominant gneissic fabric was overprinted by a lower-grade, less penetrative (on thin section scale) deformation, which produced thin zones with strong grain size reduction in less competent minerals (quartz, feldspar).

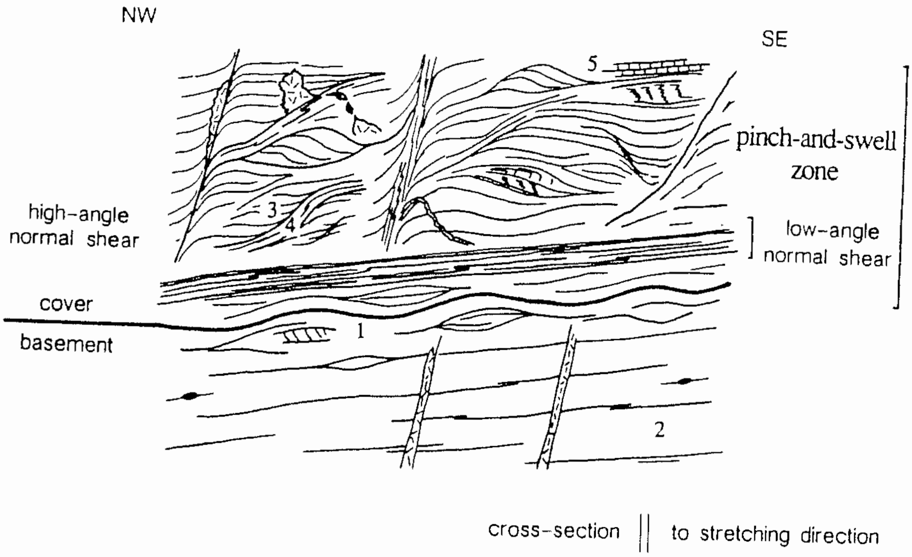

Figure 2. Schematic structural cross-section of Willimantic dome oriented parallel to NW-SE stretching direction (from Getty and Gromet, 1992b). The basement-cover contact is an abrupt lithological boundary with aluminous schist of the Tatnic Hill Formation above and granitic and amphibolite gneisses below. From bottom to top, the structures shown correspond to those of a NW-SE transect with increasing structural level from the core to the flank of the dome. Two dominant phases of deformation are characterized by distinct structural styles. Early phase ductile structures include the pinch-and-swell zone developed within the cover and uppermost basement, and a penetrative subhorizontal foliation in the basement gneisses. Later overprinting structures include steep, NW-dipping, planar normal sense shears that offset pinch-and-swell lozenges in the cover, and sharp-walled, NE-striking pegmatite dikes in the basement. A ductile to brittle progressive deformation is shown by strain localization in the high-angle shears, which locally evolve into brittle normal faults. Some high angle shears are intruded by pegmatites. A major low-angle, top=>NW normal shear (observed on the west flank of the dome) truncates all structures and appears to have acted as a detachment. Shear sense indicators at the outcrop scale include the sigmoidal deflection of foliations and veins upon entering shears, intrafolial folds in shear zones, and the displacement of early dikes. High-angle normal shears are not observed to overprint the low-angle detachment.

Significance

The dominant penetrative gneissic fabrics here are part of the widespread Pennsylvanian gneissification that affected Avalonian basement rocks exposed throughout eastern Connecticut and adjacent parts of Rhode Island. This deformation is ~100 m.y. younger than the dominant metamorphism of the overlying cover units. This deformation was overprinted by a lower grade, non-penetrative shearing that is parallel to, and probably coeval with, Permian extensional strain within the cover and along the basement-cover contact.

DIRECTIONS TO STOP 2. From intersection between Rts. 32 and 6, enter on ramp to Rt. 6 westbound, and continue through extensive roadcuts in spectacularly deformed schists of the Tatnic Hill Formation. Continue to just past the intersection with Rt. 66, and enter the Park-and-Ride lot on the right. Walk back up median to Rt. 6, to large roadcuts

Stop 2: Willimantic Dome — Cover schists near unfinished interchange of abandoned I-84

Field Description

These roadcuts were made in preparation for an interchange on the now defunct I-84, and were subsequently abandoned. The outcrops have been described in several other publications (e.g., Wintsch, 1979; Wintsch and Fout, 1982; Getty and Gromet, 1992b; Wintsch, 1992) so detailed descriptions are not duplicated here.

Schists of the Tatnic Hill Formation are deformed into "tectonic blocks" (Wintsch, 1979) or a "Pinch-and-Swell" zone (Getty and Gromet, 1992b). Inspection of the outcrops reveals that the early high grade metamorphic fabrics of the schists are cut by somewhat lower grade (lower amphibolite to uppermost greenschist) subhorizontal anastomosing ductile shear zones that are extensional in character (Getty and Gromet, 1992b). This style is developed over a range of scales. These ductile fabrics are progressively overprinted by steeper, ductile-to-brittle normal sense shears and faults.

The anastomosing shears contain a strong NW-SE mineral lineation, which defines the transport direction. A normal sense of shear is characteristic of the anastomosing shears (e.g., tops=>NW for NW-dipping shears, tops=>SE for SE-dipping shears), and is best observed in exposures permitting a view perpendicular to the NW-SE transport direction. The nature of the abandoned highway ramp cuts affords an opportunity to observe exposures at a variety of angles relative to the transport direction. The large scale of most structures favors viewing from a distance.

The age of the metamorphism and later shearing has been constrained by the U-Pb systematics of metamorphic monazites from the core of one boudin and a surrounding anastomosing shear (Getty and Gromet, 1992a). These results indicate that the original high grade metamorphism of the schists occurred during the Devonian Acadian orogeny, and that the retrogressive metamorphism in the extensional shears developed during the Permian.

Significance

The pinch-and-swell structures provide evidence for the Permian tectonic thinning of the base of the Tatnic Hill Formation, and that this thinning occurred during NW-SE oriented extension and through a range of temperatures spanning the ductile-to-brittle transition. It is emphasized that the dominant metamorphism of the Tatnic Hill rocks, as preserved in the centers of boudins, is 100 m.y. older than that of the immediately underlying basement rocks. Because these cover rocks lack the penetrative Pennsylvanian deformation present in the basement, they must have been at a much higher structural level than the gneisses at that time. Therefore, the extensional shears of the pinch-and-swell zone appear to be part of a system of structures with normal sense displacements that resulted in the thinning of the crust and the Permian juxtaposition of these different structural levels.

DIRECTIONS TO STOP 3. From Park-and-Ride lot, take Rt. 66 east, which shortly joins with Rt. 32 south, into the town of Willimantic. Before entering the heart of downtown Willimantic, make right turn to stay on Rt. 32 south. Follow signs to stay on Rt. 32 south until intersection with Rt. 289 (Mountain St). Continue straight through the intersection, which places you on Rt. 289 (do not take Rt. 32, which continues with a left), and proceed up Mountain St. about one half mile. Park on thin shoulder on right.

Stop 3: Willimantic Dome — Basement-cover boundary at Hosmer Mt.

Field Description

This roadcut displays the contact between mylonitized uppermost basement gneisses and overlying schists of the Tatnic Hill Formation. Although the exposure here is becoming terribly overgrown, it is still possible to see the structural character of the basement-cover contact. The most abundant basement rock type is a penetratively deformed amphibolite mylonite displaying a very strong NW-SE-trending lineation (oblique to the N-S orientation of the road). At road level, a small boudin of the dioritic gneiss can be observed within the amphibolite mylonites. The diorite gneiss appears to be the protolith to the amphibolite mylonites.

At the highest levels of the outcrop (at and to the south of the power line), the mylonitic basement rocks pass upward into rusty weathering mylonitic schists and gneisses mapped as the lower part of the Tatnic Hill Formation. Small-scale structures become complex as this contact is approached, with zones of lower-grade shearing and retrogression (especially chloritization of the more mafic rock types) locally overprinting the higher-grade ductile mylonitic fabrics.

The amphibolite mylonite was subject to an isotopic study by Getty and Gromet (1992a). Sm-Nd and Rb-Sr isochrons on completely recrystallized (uppermost greenschist to lowermost amphibolite grade) assemblage of plag-hb-sphene-epidote-apatite yielded ages of 272+/-7 Ma and 274+/-15 Ma, respectively, dating development of the strong stretching fabric.

Significance

The ages of intense mylonitic deformation at this outcrop define a zone of younger shearing between the older deformational/metamorphic events at both higher and lower structural levels. These shears and their young age indicate that the contact between the Tatnic Hill Formation and the basement gneisses is tectonic, and that final juxtaposition of basement and cover across the contact occurred as a result of Permian extensional shearing.

DIRECTIONS TO STOP 4. Retrace route back to intersection of Rts. 32 and 66. Turn right on to Rt. 66 east, to Rt. 6 east. Continue on Rt. 6 east into Rhode Island and intersection with I-295 (approx 40 mi.). Take I-295 north to intersection with Rt. 44, Exit 7. As you leave the exit ramp to I 295 there will be a small parking lot followed by a Mobil gas station on your left. Park in the area—the stop consists of the roadcuts on the entrance ramp to I 295 (south).

Stop 4: Relationship of Precambrian Esmond and Devonian Scituate igneous rocks, Route 44-295.

Background Information

Much of central and northern Rhode Island is dominated by rocks of the Esmond Igneous suite. The suite consists mainly of granite, granodiorite, and tonalite, with subordinate amounts of diorite, gabbro, and volcanic rock. The rocks represent a metaluminous, orogenic suite, dated by zircon U-Pb isotopes at 620 Ma (Hermes and Zartman, 1985). The Esmond suite, and the metasedimentary and mafic metavolcanic Blackstone Group rocks which they intrude, represent the Avalon basement of the Esmond-Dedham terrane. Rocks of the Esmond suite are variably deformed, but generally are more massive to the east, and progressively more deformed to the west near the Hope Valley shear zone.

In Rhode Island, the Precambrian basement rocks are intruded by Devonian and Carboniferous anorogenic plutons of alkalic affinity (Hermes and Zartman, 1985) (Fig. 1). In adjacent Massachusetts and the Gulf of Maine, similar kinds of plutons intruded the Avalon basement in the Latest-most Precambrian, Ordovician, Silurian, and Devonian. These suites are dominated by hypersolvus and subsolvus granites, including peralkaline varieties that contain accessory reibeckite, aegerine, astrophyllite, and fluorite. Lesser amounts of monzonite, monzodiorite, diorite, and gabbro occur. Locally, felsic rocks contain abundant mafic enclaves, some of which exhibit cuspate, quenched pillow-like features, demonstrating that mingling and mixing of felsic and mafic magmas were important igneous processes.

Field Description

Recent mapping by Hamidzada (1988) provides a useful framework for understanding the geology of this part of Rhode Island. The dominant rock at this stop is medium-grained, two-feldspar subsolvus granite of the Esmond Igneous suite. This leucocratic rock contains accessory biotite, sphene, apatite, zircon, and calcite; secondary epidote, chlorite, and muscovite impart a characteristic greenish sheen to the rock. The Esmond Granite is cut by numerous narrow mylonites at the western end of the outcrop, imparting a distinct foliation; to the east, the granite is relatively more massive. At the eastern end of the entrance ramp, the Esmond Granite contains several large xenolithic blocks of darker-colored, more mafic material. The more schistose xenoliths most likely are fragments of Blackstone Group rocks which commonly occur as stoped fragments included in rocks of the Esmond Igneous suite. The more massive, but fine-grained xenoliths probably are relatively older dioritic rocks of the igneous suite that subsequently were intruded and engulfed by younger pulses of more felsic granite magma. One 0.5 meter, late-stage dike of fine-grained Esmond Granite cuts coarser-grained Esmond Granite at the east end of the exposure. The nearly vertical dike exhibits parallel, but wavy walls, and contains flow-banded mafic segregations and schlieren parallel to the contacts.

Two relatively massive granitic dikes (ranging from 20-40 meters wide) related to the Devonian Scituate Igneous suite cut the Esmond Granite at this outcrop. The Scituate rocks consist of medium- to coarse-grained, porphyritic more mafic granite, compared to Esmond Granite. Distinguishing characteristic are the large K-spar phenocrysts, and ovid-shaped, glomeroporphyritic mafic clusters that contain hornblende, biotite, opaque minerals, sphene, allanite, and zircon. In some cases, the contact border zones of the dikes are leucocratic, and exhibit finer-grained non-porphyritic textures that may indicate chilling during emplacement; in other cases, the contact is coarse-grained and unchilled, and locally may consist of pegmatitic material. The western-most dike is cut by a late-stage fine-grained dike of Scituate Granite near its western contact with Esmond Granite.

Earlier geologic studies in Rhode Island, prior to new road cuts made during interstate highway construction, had interpreted Scituate rocks to be older than Esmond rocks. This outcrop, and others similar to it, show the relative age relationships are opposite, and these have been confirmed by radiometric dating. The Scituate Igneous suite is 370 Ma (Hermes and Zartman, 1985). At this locality, and in much of central Rhode Island, rocks of the Scituate suite are relatively massive and not extensively deformed; this character is in sharp contrast to Scituate rocks to the west in closer proximity to the Hope Valley shear zone, where they have been pervasively deformed and recrystallized to granite gneiss.

Significance

1. This stop provides the opportunity to observe the most common variety of basement granite (Esmond Granite) in the Esmond-Dedham terrane, and representative mid-Paleozoic plutonic rock of anorogenic and alkalic affinity intrusive into basement rock. Several compositionally and texturally distinct varieties of Esmond rocks occur, which intrude large blocks or pendants of schist of the Blackstone Group.

2. Both Precambrian and Devonian igneous rocks are relatively massive at this locality, with the exception of localized, small scale mylonitic shear zones; such fabric will contrast with more intense degrees of deformation exhibited by the rocks to the southwest at the next stop, near the Hope Valley shear zone.

DIRECTIONS TO STOP 5.

Return to cars and proceed south on I 295.

From Exit 7 (Rt. 44) to Exit 4 (Rt. 14) you are within, for the most part, the Scituate Granite. Continuing south, you will pass back into the Esmond Granite, and then into a long roadcut, approximately one mile north of Exit 3 (Rt. 37). This spectacular set of outcrops represents a section through the follwoing lithologies: 1) the Esmond Granite; 2) a complex contact zone between the Esmond Granite and the Blackstone Group; 3) the polydeformed Blackstone Group; and 4) the Carboniferous Narragansett Basin.

Continue south, thorugh an area of little outcrop, until I 295 merges with I 95. Proceed south on I 95, passing by outcrops of Devonian to Carboniferous (?) volcaniclastic and clastic metasedimentary rocks. Keep to the right at the junction with Rt. 4, so as to stay on I 95. As you drive southward on I 95 you will cross the Hope Valley shear zone. Take exit for Rt. 102 south, continuing to the intersection with Rt. 3 south. Make right turn on to Rt. 3 south and continue several miles, parallel to I-95 on the right. Pass under I-95, continue one half mile and park on right, on wide section of Rt. 3.

Stop 5: Hope Valley shear zone, including Ponaganset and Scituate granite gneisses

Background Information

This outcrop provides the opportunity to observe some of the typical rock types of the Esmond-Dedham terrane (O'Hara and Gromet, 1985) where they are strong sheared within the Hope Valley shear zone. This is also an opportunity to reexamine unit assignment problems faced by early workers. Prior to the 1980s, there has been considerable confusion concerning the assignment of the various gneisses exposed in southern Rhode Island to formations, and many units were viewed as gradational. U-Pb zircon ages by Hermes and Zartman (1985) tightly defined the ages of the major units, and demonstrated a Devonian age for the Scituate granite gneiss (Fig. 1). Thus it became obvious that the Scituate granite gneiss and the Hope Valley alaskite could not be gradational. O'Hara and Gromet (1985), and later Getty and Gromet (1988), exploited Rb-Sr whole rock systematics to separate Precambrian Hope Valley alaskite from Devonian Scituate granite gneiss in western Rhode Island and eastern Connecticut. The resulting distribution led to the recognition of the truncation of units against a major dextral shear zone, the Hope Valley shear zone, between rather distinctive groups of Avalonian rocks (the Esmond-Dedham and Hope Valley terranes) (Fig. 1). The significance of the Hope Valley shear zone has been challenged by some other workers.

Field Description

Outcrops are present on the east and west side of the road. East of the road, a lens of strongly deformed augen gneiss (microcline-quartz-plagioclase-biotite-sphene-oxide) occurs between amphibolite gneiss and leucocratic equigranular granitic gneiss (low in outcrop). The leucocratic gneiss is better exposed on the west side of the road. In the augen gneiss, a strong foliation (125°/25°NE) and a weaker lineation (140°N/10°N) are defined by biotite streaks and deformation tails developed about feldspar porphyroclasts. The augen gneiss develops mylonitic fabrics against the amphibolite gneiss, and the amphibolite gneiss had suffered some boudinage. The deformational fabric of these rocks is transected by pegmatoid dikes, and all are finally cut by a steeply dipping dike of granite aplite containing a discontinuous pegmatoid core.

The augen gneiss is typical of the Ponaganset gneiss, a widespread Late Precambrian metaplutonic unit of western Rhode Island and adjacent Massachusetts. On a lithic basis, the leucocratic gneiss could be assigned to either the Precambrian Hope Valley alaskite or the Devonian Scituate granite gneiss. The leucocratic gneiss was originally mapped as Hope Valley, but whole rock Rb-Sr analysis of a sample of the leucocratic gneiss from the west side of the road (Getty and Gromet, 1988) indicate that the protolith for this gneiss is Devonian in age. The pegmatite is typical of the late Paleozoic dikes that occur throughout Rhode Island and eastern Connecticut, and are believed to be related to the Permian Narragansett Pier Granite.

Significance

This stop is the southwesternmost occurrence of Devonian Scituate granite and the Ponaganset gneiss, which are part of a distinctive assemblage of rocks that occur throughout central and western Rhode Island. The highly tectonized nature of the Scituate and older lithologies along the Hope Valley shear zone, and their regional and small scale truncation against it (e.g., see Getty and Gromet, 1988), are considered strong indications that the Hope Valley shear zone is a major tectonic contact and that it is no older than Devonian. There are no units older than the Permian Narragansett Pier Granite (and related pegmatites) that tie these rock together, although the Precambrian rocks in both appear to have originated as part of the group of rocks known as Avalonian.

DIRECTIONS TO STOP 6. Reverse direction on Rt. 3, and enter I-95 south. Take Rt. 138 east to Rt. 1. Continue east, through the intersection, to Rt. 1A. Notice that the road on which you are traveling is no longer Rt. 138, it is now Bridgetown Road. Take Rt. 1A (Boston Neck Road) south until you are approximately .1 mile north of the Narrow River, at which point a secondary road branches off to the right. Take the secondary road .75 mile and park. The shore line exposures of Cormorant Point (Fig. 3) are just north of the inlet for the Narrow River (into the ocean) and may be reached by a .25 mile walk along a private driveway. The outcrops are entirely on private land, and permission to visit them must be obrained from the people living in nearby houses. This is a " no hammer" stop (there is plenty of loose material available for collecting) and is unsuitable for large groups without prior permission.

Stop 6: Injection contact zone of Narragansett Pier Granite and Pennsylvanian metasedimentary rocks, Cormorant Point.

Background Information

The Narragansett Pier Plutonic Suite consists of post-tectonic granitic rocks of Permian age that intrude a variety of country rocks from the Hope Valley and Esmond-Dedham terranes; thus, it is a stitching pluton (Fig. 1). U-Pb dating of monazite and zircon yields a radiometric age of 275 +/- 2 Ma (Kocis, 1981; Zartman and Hermes, 1987); a Ar^{40}/Ar^{39} mineral cooling age of 238 Ma was reported by Dallmeyer (1982). Interestingly, zircon U-Pb isotopics exhibits a pronounced inherited Pb component identified as Late Archean; such old relict zircon is absent in pre-Permian rocks of southeastern New England, and has led Zartman and Hermes (1987) to interpret the Archean crustal component to be derived by underplating of old material in the late Paleozoic during collision of Gondwana with Avalonia. The age of the granite is also constrained by megafloral data, as roof pendants contain *Annularia stellata* plant fossils, which are considered to be of Stephanian B or younger in age (Brown and others, 1978). The roof pendents contain a crenulated foliation that is truncated by the granite, implying that regional metamorphism and deformation(s) occurred in the interval between cessation of deposition (Stephanian B or younger; ~290 Ma) and granite emplacement (275 Ma). Taken together, these dates place tight constraints on the timing of the Alleghanian orogeny in New England.

Rocks of the pluton trend west to east from southeastern Connecticut across southern Rhode Island to the eastern boundary of the Narragansett basin. Most of the pluton consists of pink-colored, medium- to coarse-grained, equigranular to porphyritic, two-feldspar granite. Common accessory minerals include biotite, muscovite, magnetite, ilmenite, apatite, garnet, monazite, sphene, zircon, allanite, and pyrite. The rocks typically are slightly peraluminous, containing 1-3% corundum in their norms (Hermes and others, 1981); high Ba contents ranging from 1,000-3,000 ppm Ba distinguish the rocks from older plutonic rocks in Rhode Island. Local hornblende-bearing varieties occur at several localities in eastern Connecticut (Goldsmith, 1985). Cross-cutting aplites and pegmatites are abundant. In western Rhode Island, some aplites are 10-30 meters thick, and occur as gently south-dipping, east-west trending dikes (formerly called Westerly Granite). Mineralogy of these aplites is similar to coarser-grained granite varieties, and they are considered to be a late-stage, but comagmatic facies of the plutonic suite.

A leucocratic granite variety (white facies) occurs along the eastern margin of the pluton, where the rock is intrusive into carbonaceous- and graphite-rich layers of metasedimentary rocks that comprise the Narragansett basin. Essential minerals include microcline, plagioclase, and quartz, with accessory muscovite, garnet, biotite, monazite, zircon, and apatite. Compared to pink varieties of the suite, the leucocratic granite lacks opaque minerals, contains locally abundant Mn-rich spessartine garnet, and exhibits a higher muscovite/biotite ratio. Commonly, muscovite is euhedral, and clearly a primary igneous mineral. The leucocratic nature, and absence or scarcity of magnetite and biotite may reflect interaction of the magma with the carbonaceous-rich country rock such that reducing conditions kept iron mainly in the Fe^{+2} state. Thus, the presence of the white phase, with its xenoliths and roof pendants of carbonaceous material, preserves the record of fluid circulation between relatively oxidized fluids emanating from the granitic magma and reducing fluids in the country rock, which were buffered by the decomposition of carbonaceous material.

Field Description

The shoreline exposures at Cormorant Point straddle the contact between the leucocratic facies of the Narragansett Pier Granite and the Rhode Island Formation. The granite varieties exposed here can be subdivided into four field units that define a crude igneous layering: pegmatite; aplite; garnetiferous granite; and massive, equigranular, medium-grained granite. The best places to observe the igneous layering are on the small island (accessible at low tide), and along the southwest exposure of the point. A map showing the distribution of all these varieties is included in Hermes and others (1981), and a simplified version of it is given in Murray (1987). Variations in granite fabric and mineralogy reflect local and temporal variations in activity of water leading to variable rates of nucleation and crystalization, and to a lesser extent assimilation of the surrounding metasedimentary rocks.

Abundant lenses of Pennsylvanian metasedimentary rocks are prevalent throughout the area, consisting of pelitic and psammitic schist plus subordinate metaconglomerate. These lenses are characterized by a uniformly NE-trending schistosity (S_1) and pebble elongation direction that roughly coincides with both the orientation of the layering within the granite and with the regional tectonic fabric in the country rock. This suggests that the metasedimentary rocks are roof pendants and that the current erosion surface is close to the top of the magma chamber. Conformity of structure within the inclusions and the country rock suggests that granite magma was injected gently into this zone as a series of pulses that passively invaded the country rocks, preserving screens of largely unrotated metasedimentrary rock. Some pendants and xenoliths contain biotite enriched zones adjacent to the granite, and in some cases, garnet in these zones can be traced away from xenolith tails to form diffuse garnet trains in the granite. Such features suggest at least localized reaction and assimilation processes in the contact zone. Locally, the granite truncates both the dominant schistosity (S_1) as well as a crenulation cleavage (S_2) in the schist, demonstrating that the schists were deformed prior to granite emplacement. About 1 km north, large pegmatites are folded by late-stage (F_4) folds. This relationship plus the orientation of sheeted aplites and pegmatites led Reck and Mosher (1989) to propose that intrusion began during D_3. The time of intrusion is well constrained by a U-Pb age of 275 Ma from igneous monazite and zircon (Kocis, 1981; Zartman and Hermes, 1987), and by the presence of Stephanian B or younger (i.e., Late Pennsylvanian) plant fossils in one of the lenses (Brown and others, 1978).

Significance

1. Granite intrusive relationships clearly cut, and locally rotate previously deformed inclusions of Pennsylvanian sedimentary rocks, demonstrating that intrusion occurred after peak-stages of metamorphism and deformation.

2. Age Constraints: Permian age of intrusion documented by U-Pb dating of monazite; zircon shows Archean inherited component that may reflect interaction of Avalonia and Gondwana in the Late Paleozoic. Xenolithic inclusions contain Stephanian B plant fossils. Incremental argon measurements demonstrate relatively rapid simple cooling since time of emplacement.

3. Concordance of large screens of included schists with adjacent country rock indicates a passive mode of granite emplacement.

4. Leucocratic character of granite and absence or paucity of mafic and opaque minerals may relate to reducing conditions induced by high carbonaceous content of the country rocks in the contact aureole.

5. Great diversity of granite textures reflect variability of fluid content within the contact zone; flow fabrics demonstrate large scale fluid transfer and dynamic character in development of contact zone.

DIRECTIONS TO STOP 7. (See Fig. 3). Return to Rt. 1A and turn right. Go about 6 miles north to interesection with Rt. 138. If going directly to Stop 7, turn left on Rt. 138 west. If going to the motel, turn right on Rt. 138 and cross the Jamestown bridge. Continue on Rt. 138 following signs for the Newport Bridge. Cross the toll bridge and take second exit (Rt. 114 north). The Main Stay Inn is on the left coming off the Newport Bridge ramp. To reach stop 7 from motel, retrace route to intersection of Rt. 138 west and Rt. 1A. Proceed on Rt. 138 west for 1.3 miles to large road cuts. We will stop at one or two road cuts along Rt. 138 depending on access restrictions at that time. Recent road construction has added and removed some exposures. Construction was still underway when this guide was written.

Stop 7: Polyphase deformation and upper amphibolite facies metamorphism of Pennsylvanian age rocks, Narragansett basin, Stook Hill/Plum Beach

Background Information

In the southern portion of the Narragansett basin in Rhode Island, the first deformation consists of two nearly coaxial sets of NNE-trending, tight to isoclinal folds (F_{1a}, F_{1b}) accompanied by two pervasive foliations (S_{1a}, S_{1b}) at slight angles to one another (Henderson and Mosher, 1983: Reck and Mosher, 1989; Mahler and Mosher, in press). Vergence, where it can be determined, is westward. Refolding nearly coaxial (NNW to NNE-trending) to F_1 followed, but with an overall eastward vergence (Farrens, 1982). F_2 folds are generally broad, regional-scale folds with a pronounced axial planar crenulation cleavage. The two events affect all the sedimentary rocks and are accompanied by a prograde Barrovian metamorphism that varies both spatially and temporally across the basin with respect to the two deformations (Thomas, 1981; Farrens, 1982; Henderson and Mosher, 1983). The highest grade rocks are preserved in the western part of the basin (Fig. 3), where metamorphism is synchronous with D_1. Rocks at lower grades in the eastern and northcentral portions of the basin reached peak metamorphic conditions after D_1 and in places synchronous with D_2. In the southwestern portion of the basin, a later phase of deformation (D_3) formed a pervasive, metamorphic foliation (S_3) that is axial planar to both mesoscopic and megascopic isoclinal folds (F_3). S_3 and all previous structures are folded by large-scale, open folds (F_4). All structural information given below is from Mahler and Mosher (in press).

Field Description

Stook Hill. These outcrops represent upper amphibolite facies rocks with extremely well preserved primary structures. Lithologies present are metaconglomerate, metasandstone, carbonaceous schist, garnet amphibolite, and pegmatitic granite. The predominately overturned metasedimentary rocks contain a variety of relict textures such as graded bedding, cross bedding, erosional contacts, pebble lag deposits, and cut and fill channel structures indicative of a fluviatile origin.

The schist on the south side of the road contains the assemblage kyanite-staurolite-garnet-biotite-muscovite-quartz-ilmenite-graphite and rare fibrolite (Grew and Day, 1972; Murray, 1987). Geothermometry and geobarometry by Jones (1987) found temperatures must have exceeded 600°C and pressures reached 6.5 kb.

Along the northern side of the road, sedimentary structures indicate that the rocks lie on the overturned limb of a recumbent refold (Fig. 4a). Prior to road construction, the hinge and part of the right-side-up limb was exposed at the western edge of the outcrop. The pervasive foliation, S_{1b}, is axial planar to the regional folds and to tight minor NE-trending folds. S_{1b} is defined by ductilely deformed, elongate quartz grains and by aligned micas in the finer grained rocks. In coarser grained sediments, oblate pebbles and cobbles are aligned parallel to S_{1b} and are elongate NE parallel to F_{1b}. Within the schists, S_{1b} is axial planar to small floating intrafolial fold hinges of quartz veins that lie along S_{1a}. A biotite lineation plunging NE occurs frequently on the S_{1b} surface and is probably associated with F_{1b}.

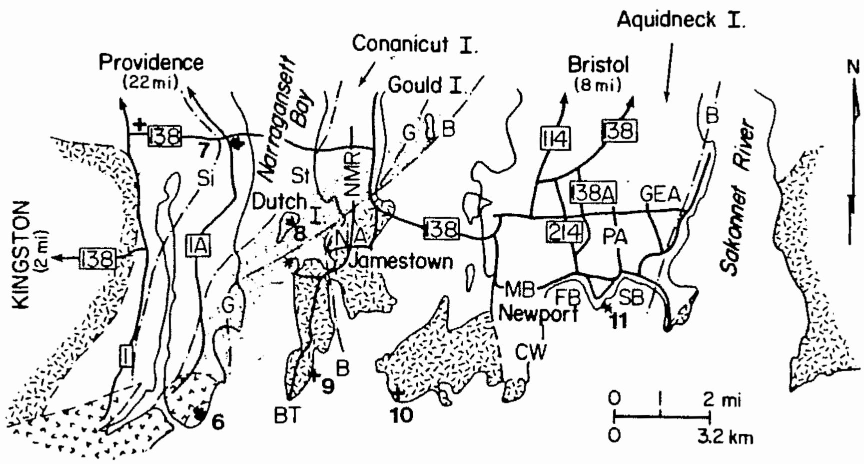

Figure 3. Location map for southern RI stops showing local roads. Geologic features shown: Beaverhead Shear Zone-shaded; basement-random dashes; Narragansett Pier Granite-v pattern; isograds-dash-dot lines (Si-sillimanite; St-staurolite; G-garnet; B-biotite). Roads and places referred to in text: NA-Narragansett Ave., NMR-North Main Rd., MB-Memorial Blvd., GEA-Green End Ave., PA-Paradise Ave., BT-Beavertail, CW-Cliffwalk, FB-First Beach, SB-Second Beach.

In thin section, inclusion trails in porphyroblasts clearly demonstrate that S_{1b} is a crenulation of S_{1a}. Staurolite and garnet porphyroblasts show sigmoidal inclusion patterns that curve into parallelism with S_{1b} near the porphyroblast margins and orthoclase contains inclusion trails at high angles to S_{1b}. Pressure shadows on the ends of the porphyroblasts are parallel to S_{1b} and are warped by the later S_3 foliation.

A second predominant foliation, S_3, is defined by aligned muscovite and biotite. The tails of sand pods, conglomerate cobbles, and ductilely deformed, elongate quartz grains of S_{1b} curve into parallelism with S_3. Little or no elongate quartz is associated with S_3, which helps distinguish S_3 from S_{1b}. Additionally, the spacing between individual S_3 foliation planes is generally larger than that between S_{1b}. No F_3 hinges have been recognized in the field, though they must be present because the angular relationship between S_{1b} and S_3 changes over short distances throughout the area.

Both bedding and all foliations strike EW and dip gently to the north. This orientation is in contrast with most of the rest of the basin where planar structures strike northerly and dip east or west. In this area the basin margin changes trend from N to WNW. Planar structures are generally moderately east-dipping along the coast parallel to the NE-trending basin margin (e.g. Plum Beach and further south) and gently north-dipping adjacent the WNW-trending basin margin (e.g. Stook Hill and outcrops in nearby woods):

Two or three superposed, noncoaxial crenulation cleavages affect the S_{1b} surface in some locations. The cleavages commonly affect only part of the outcrop and are localized in north-trending zones. Dikes and small masses of pegmatitic granite cross cut the foliations; dikes are boudinaged with E-trending axes.

DIRECTIONS TO NEXT OUTCROP. The next outcrop is near the Jamestown Bridge on Rt. 138 east of Stook Hill. To turn around, drive west to interchange with Rt. 1 and re-enter highway going east on Rt. 138. Turn right on Rt. 1A south and park in Park-and-Ride lot on left. Walk along highway to outcrops along southside of Rt. 138 east of Rt. 1A.

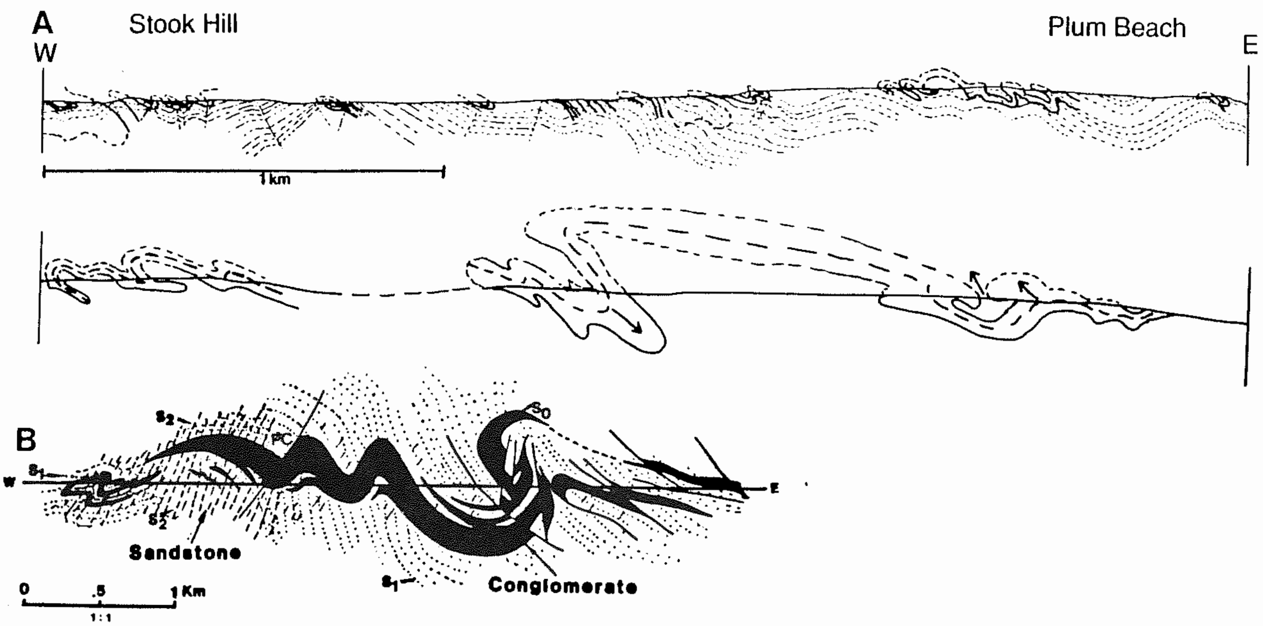

Figure 4. A) Profiles from Stook Hill to Plum Beach after Mahler and Mosher (in press). Top profile - solid lines represent S1b, dashed lines S3; bottom profile - solid lines represent bedding; arrows show directions of sedimentary younging. B) Profile from eastern basin margin to First Beach after Mosher (1981) and Farrens (1982). Location of Purgatory Chasm-PC.

Plum Beach. The predominate lithologies are a carbonaceous schist interlayered with metasandstone. Metamorphic grade is lower (staurolite) than at Stook Hill. The same structures (S_{1b}, S_3, and crenulations) are observable as at Stook Hill. Along the length of the outcrop, S_{1b} and S_3 are folded by open, NE-trending F_4 folds (Fig. 4a).

The prominent foliation (S_{1b}) is axial planar to asymmetric, W-verging F_{1b} folds defined by light-colored metasandstone layers in carbonaceous schist. The hinges of the folds are recognizable by connecting the sandstone pods. The long dimensions of the pods are axial planar to the folds, and several form floating parasitic fold hinges. This style of folding with transposition in the fold hinges is common in this area. The more competent sandstones, interlayered with the ductile shales, form boudins or lens-shaped "pods" in the hinge region of the folds; on the limbs (such as Stook Hill), the beds maintain their continuity. In the hinges, the less competent shale has flowed between these pods so the apparent sandstone/shale contact is not a true bedding orientation. In thin section, these structures fold a metamorphic foliation (S_{1a}).

Significance

These outcrops show that the Pennslyvanian sediments underwent upper amphibolite facies metamorphism synchronous with polyphase deformation that produced large-scale, recumbent, nappe-like folds. This deep-seated, high-grade, collisional deformation occurred between 290 and 275 Ma, somewhat later than the high grade deformation further west. Despite multiple deformations and high grade metamorphism, these rocks still preserve excellent primary structures characteristic of a fluviatile depositional environment.

DIRECTIONS TO STOP 8. (See Fig. 3). Return to intersection of Rt. 1A and Rt. 138. Turn right on Rt. 138 crossing the Jamestown Bridge. Take North Main Road south from Rt. 138, cross Narragansett Ave. and continue south past beach at Mackeral Cove. Take the first right onto Fort Getty Road. Follow road past gatehouse and campground to northern pier, keeping right on unpaved roads. We will be ferried to Dutch Island on a small motor boat. While waiting to go over or for others to come back, we will look at structures at Beaverhead.

Stop 8: Sinistral and dextral transcurrent shear zones, Pennsylvanian metasedimentary rocks, Beaverhead and Dutch Island

Background Information

The south-central portion of the Narragansett Basin in Rhode Island is cut by numerous zones of intense deformation that reorient or obliterate D_1 and D_2 structures and contain penetrative D_3 and D_4 structures. The zone containing the most intensely deformed rocks, the Beaverhead shear zone, trends approximately NE across the south-central basin (Figs. 1, 3) and results from shearing along a series of short, interconnected, NNE-, NE, and ENE-trending segments. D_3 structures occur in numerous discrete, N- and NE-trending sinistral strike- and oblique-slip shear zones. Structures include en echelon folds; E- and NE-trending open, chevron and box folds within NE- and NNE-trending zones, respectively; superposed, noncoaxial folds and crenulation cleavages that young in a clockwise direction and are in an appropriate orientation to have formed as a result of progressive rotation in a sinistral noncoxial strain field; sheath folds, tension gashes, and N-trending faults with sinistral offset (Mosher, 1983; Burks, 1985; Mosher and Berryhill, 1991). D_4 structures are generally restricted to the Beaverhead shear zone and include NE-trending dextral strike- and oblique-slip shear zones that reorient all previous structures (including sinistral shear zones and associated structures) into a NE orientation; en echelon folds; N-to NE-trending open folds within NE-trending shear zones; superposed noncoaxial folds and crenulation cleavages that young in a counterclockwise direction and are in an appropriate orientation to have formed as a result of progressive rotation in a dextral noncoaxial strain field; kink bands; tension gashes; large-scale boudinage with a north-south extension direction; and NE- to ENE-trending faults with a dextral oblique-slip offset (Mosher, 1983; Burks, 1985; Mosher and Berryhill, 1991). For NE-trending zones that underwent both sinistral and dextral motion, sinistral movement always preceded dextral movement. These zones apparently represent NNE-trending sinistral zones that were rotated into a NE-trend by subsequent dextral shearing. The most pervasive ductile deformation is that related to sinistral movement, however dextral motion on NE-trending zones was significant causing ductile reorientation of all earlier structures and formation of new minor structures. Oblique-slip dextral motion on ENE-trending zones, which occurred last, caused the least ductile deformation and the most brittle offset. For more discussion, see Mosher and Berryhill (1991).

Field description

Beaverhead. This outcrop lies within the Beaverhead shear zone and displays the effects of D_3 deformation. The main lithologies are graphitic biotite schist, chloritic quartzite, quartzite metaconglomerate, and graphitic slate. Units are generally overturned, forming the lower limb of a large recumbent, upward facing F_{1b} isocline. All outcrops show a pervasive bedding-parallel, S_{1b} schistosity, which generally strikes NE and dips 30-40°SE. Metamorphism to biotite grade was syn-D_1 and pre-D_2. Outcrops start 20 m west of the northern pier along the beach. A description of the entire exposure is given in Mosher and others (1987). At the southern end of the exposure (not visited today), D_4 shear zones cross cut the D_3 structures.

At the northern end of Beaverhead, a penetrative S_1 foliation is axial planar to several minor F_1 isoclinal folds in thin quartzite layers. Small amplitude (1-10 cm), NE-verging F_2 folds and an associated S_2 crenulation cleavage (striking NNW and dipping steeply SW) are also observable. Several generations of D_3 and D_4 crenulations and small folds are visible on S_1. At the end of this small cove near the broad, planar rock face, S_1 is folded by ENE-trending, F_3 chevron and box folds. Depending on tide level, the interference of large-scale orthogonal F_2 and F_3 folds can be observed.

At low tide continue along the outcrops, or return to the top by retracing your steps. Go down a few meters and take the first steep path. At path base, large ENE-trending, E-plunging F_3 chevron and box folds deform S_1 and a rarely visible NNW-trending S_2 crenulation. Several thin, pyrite-replaced layers are isoclinally folded by F_1.

Dutch Island. The main lithology is a gray phyllite with minor interlayered metasandstone, metaconglomerate, and carbonaceous phyllite and local calcsilicate pods. All rocks exhibit metamorphic mineral assemblages within the almandine zone. The pronounced foliation (S_{1b}) generally strikes N to NNE. Although early folds are observable on the island, the majority of the folding is the result of D_3 and D_4 deformation. Discrete shear zones containing D_3 and D_4 structures are observed on the west and south side of the island. We will be landing on the east side where the structures are best preserved although the unsheared parts are not. A very detailed discussion of structures, superposed relationships, and kinematic history is given in Mosher and Berryhill (1991) and has not been repeated here; structural maps that also show locations of specific structures can be found in the provided reprint. Along the coastline the following structures generally can be observed:

Sinistral shear-related structures: Three, superposed, flexural-slip fold generations with consistent younging in a clockwise manner. F_5 - S to SSW-trending, 2-10 cm amplitude, open to tight chevron folds; upright, recumbent or downward facing depending on position with respect to F_6 and F_7 folds. F_6 - SSW-trending 15 cm to > 5 m amplitude, open to tight, upright to recumbent folds. F_7 - SW-trending, extremely broad, upright folds. Axes are best defined by mapping the reorientation of F_5 and F_6 axial planes and axes. Twisted F_6 axes and axial traces result from interference with F_7 folds. Up to four superposed, clockwise younging crenulation cleavages can be observed although not all are present everywhere.

Dextral shear-related structures: D_3 structures can be seen to swing into wide NE-trending dextral zones. Up to four generations of superposed, 2-5 cm amplitude, doubly plunging, open folds (F_{8-11}) show a consistent counterclockwise younging. These folds are only found on E-dipping S_{1b} surfaces and therefore only on one limb of many D_3 folds. Overprinting relationships are subtle. As many as four (southern tip of the island) superposed, counterclockwise younging crenulation cleavages can be observed. These cleavages overprint the D_3 crenulations but are less abundant. Narrow ENE-trending brittle/ductile shear zones cut all structures and show oblique-slip offset and slickensides. Large scale foliation boundinage with N-S extension directions affect all structures.

Significance

These stops show the intensity of deformation caused by motion on late-stage, essentially post-metamorphic, sinistral and dextral strike- and oblique-slip shear zones. The style and intensity of deformation is in marked contrast with that found outside the shear zones (e.g. Stops 7, 11). These transcurrent shear zones apparently formed after collision as a result of interaction between terranes and/or Africa and Laurentia.

DIRECTIONS TO STOP 9. From the previous stop (Beaverhead) return to the entrance to Fort Adams at Mackeral Cove, and then proceed south on Beavertail Road into Beavertail State Park. Continue south, along the western side of the island, to the southern tip of island and the lighthouse. Follow the road northward to parking area #4 (the second parking area on your right, after you have passed the lighthouse; additional .5 miles). The shoreline exposures may be reached from trails branching off from the parking area (Fig. 5).

STOP 9: Fossiliferous Cambrian metasedimentary rocks at Beavertail, Conanicut Island, RI

Background Information

The stop consists of fossiliferous phyllites that display multiple phases of folding and faulting. These Cambrian-aged shallow water marine sedimentary rocks represent a sedimentary carapace that was deposited upon Proterozoic Z volcanic and granitic rocks. The outcrops visited at this stop are typical of the more or less continuous outcropping of Proterozoic Z to Cambrian (and ? younger) sedimentary and volcaniclastic rocks that occur along the southern half of Conanicut Island (Fig. 3) as well as directly to the east of this stop, along the western shore of Aquidneck Island. The occurrence of fossiliferous Cambrian rocks in southeastern New England with Acado-Baltic affinties has been known for over a hundred years (Skehan and others, 1978, and references therein) and they represent a crucial piece of evidence in support of the classification of the region as part of the Avalon terrane. Unfortunately most of these occurences are no longer accessible, and even at the time of maximum exposure revealed little about the paleogeographic or structural setting. The section exposed in southern Rhode Island represents by far the most extensive and informative record of Cambrian sedimentation in the New England Avalon terrane. This stop has been written up in several guidebooks, and the following description is culled from them (Murray and Skehan, 1979; Skehan and others, 1981, 1987).

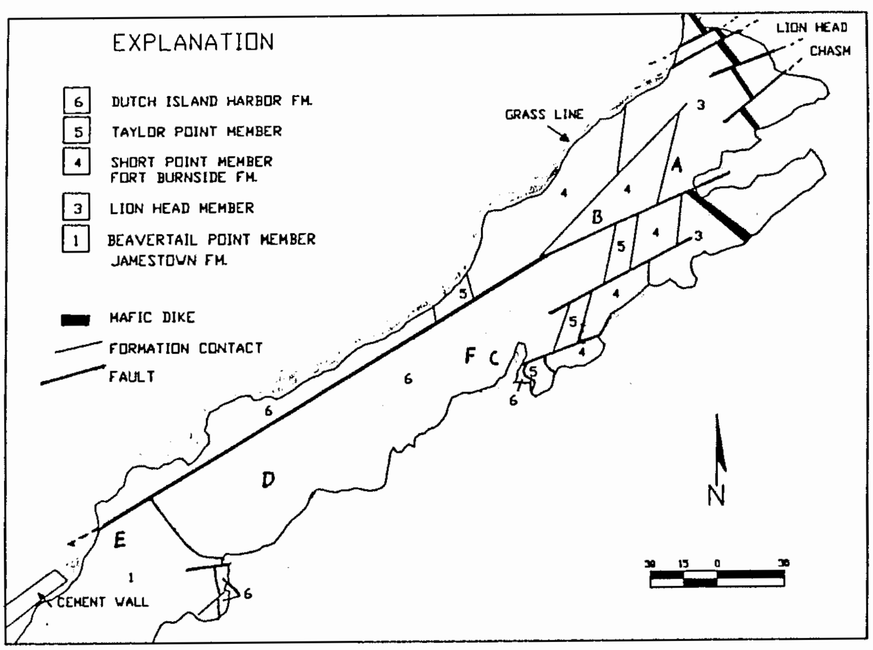

Figure 5. Sketch map of the field relationships in the vicinity of Lion Head Chasm, southeastern coast of Conanicut Island near Beavertail. Letters A-F indicate field stations that are discussed in the text. Modified and simplified from Skehan and others (1981, 1987); Murray and Skehan, (1979).

Stratigraphy. These strata consist of interbedded calcereous shales, siltstones, and fine-grained sandstones in which, despite the complexity of deformation, primary sedimentary structures are well preserved. One or more phases of lower greenschist facies metamorphism has produced various combinations of chlorite, white micas, quartz, carbonates, and pyrite. Differences in color and primary sedimentary structures permit the establishment of an informal stratigraphy, and its development and rationale are covered in the aforementioned references. The Cambrian section outlined below is a minimum of 350 meters thick. Brief descriptions are provided for those units present at this stop:

1. Dutch Island Harbor Formation (youngest). This formation consists of rhythmically bedded phyllite and is characterized by Bouma sequences and concretions.

2. Fort Burnside Formation
   a. Short Point member : Alternating gray phyllite and black phyllite plus siltstone. Dewatering structures and/or burrows are common in the lower portion of the unit.
   b. Taylor Point member: Consists of alternating siltstone, in which cross stratification is well preserved, and gray phyllite.

3. Jamestown Formation (oldest)
   a. Lion Head member: Massive gray to pale green phyllite in which bedding is difficult to discern. Abundant trilobite hash plus more complete trilobite specimens, which formed the basis for establishing the age and Acado-baltic affinity of the region, occur within this unit.
   b. Beavertail Point member: Relatively massive unit, which consists of approximately 90% pale green phyllite and 10% light brown siltstone.
   c. Hull Cover member: not present at this stop

Structure. Because of the structural complexity and restriction of outcrop to a narrow strip along the coast, the tectonic history of these rocks has not yet been completely deciphered and the extent to which these Cambrian rocks record pre-Alleghanian tectonism remains unclear. The following deformational events are recognized, going from oldest to youngest.

1. Tectonic slides: Skehan and others (1981) used the term "tectonic slides" to describe pre-S_1 cleavage faults which juxtapose various Cambrian-aged units against one another. They suggest these slides may have formed during lithification, and hence be of Cambrian age.

2. D_1 deformation is preserved as open to tight folds of variable orientation plus faults. An axial planar foliation is intermittently developed, and when observed is defined by a slaty cleavage usually filled by fibrous quartz veins. The age of D_1 is in dispute, with estimates ranging from Lower Paleozoic (roughly contemporaneous with the tectonic slides) to Alleghanian.

3. D_2 deformation is the dominant event in the area, and is responsible for the pervasive flat-lying S_2 slaty cleavage, mineral lineations, and the most of the easily recognized folds. Moreover, D_2 reorientates all previous structures, resulting in abundant evidence for refolding. At this locale D_2 folds are subhorizontal and trend north. Where interference patterns between F_1 and F_2 folds are observed, they most closely approximate Ramsay Type 3 refolds. D_2 folds best correlate with the most intense phase of folding recorded in the Carboniferous rocks.

4. Post-D_2 folding is relatively minor at this locale and consists of kink bands and large-scale, open folds. However, D_3 folds increase in intensity to the north.

5. Subsequent deformation consists of normal faults of unconstrained age.

Field Description

The stop consists of five stations along a traverse that begins at Lion's Head Chasm and proceeds southwestward. These stations are located on Figure 5, briefly described below, and discussed in more detail in the references.

1. Station A: Lion Head member - Trilobite fragments; deformed minette dike; kink bands.

2. Station B: Short Point and Taylor Point members - F_1 and F_2 folds; primary sedimentary structures; Ichnofossils; post-D_3 faults.

3. Station C, D, & E: Dutch Island Harbor Formation - F_1 and F_2 folds; primary sedimentary structures.

4. Station F: Tectonic slide, separating Beavertail Pt. member & Dutch Island Harbor Fm.

Significance

The Middle Cambrian trilobites with Acado-Baltic affinities which were discovered at this stop were critical for: 1) establishing the age relationships; and 2) classifying the region as part of the Avalon terrane (Skehan and others, 1978). Additionally, structural features are unusually well displayed and provide not only important constraints on the tectonic evolution of the region but also insights into structural processes. In particular, if pre-Alleghanian deformation is present (i.e., F_1 and tectonic slides), they represent the only documented post-Precambrian/pre-Alleghanian folding in the region (Esmond-Dedham terrane).

DIRECTIONS TO STOP 10. From the last stop return to Rt. 138 and head east across the Newport bridge to Aquidneck Island. Upon leaving the bridge go south, following the signs to Newport and scenic Ocean Drive. Continue south through Newport until you reach the northwest terminus of both Ocean Drive and Brenton Point State Park. Continuous shoreline exposures, along Ocean Drive, occur for the next several miles. Time permitting, we will make one or more stops along the road.

STOP 10: Proterozoic Z rocks at Brenton Point, Aquidneck Island, RI

Background Information

The southwest portion of Aquidneck Island is characterized by an unusually complete, though polydeformed, Proterozoic Z to Lower Cambrian stratigraphic section that is intruded by ~600 Ma porphyritic granite and unconformably overlain by Carboniferous sedimentary rocks. The purpose of the stop is to examine this stratigraphy and its associated structural features. All lithologies have been metamorphosed to the chlorite grade, with sporadic and localized contact metamorphism along the contact between granite and metasedimentary rocks. At present it is unclear to what extent, if any, these rocks were regionally metamorphosed prior to the Alleghanian orogeny. The description of this stop is summarized from several recent fieldguides, in which more detailed discussions and references may be found (Murray and Skehan, 1979; Rast and Skehan, 1981a; Skehan and others, 1987)

Stratigraphy. Brief descriptions are provided for those units present at this stop:

1. Pirate's Cave Formation: This ~20 meter thick unit consists of a basal limestone overlain by variously colored phyllites. It is of early Cambrian age, based upon the occurrence of hyoliths (references in Skehan and others, 1987).

2. Newport (i.e., Lilly Pond) Granite; ~595 Ma (Smith, 1978). The rock ranges from granite to adamellite in composition, and is typically porphyritic. Mafic minerals (hornblende and biotite) plus feldspar have been largely altered to chlorite, epidote, and white mica. It is invariably laced with mineralized fractures and locally contains well-developed arrays of en echelon quartz veins.

3. Price's Neck Formation: Purple volcaniclastic and turbidic rocks; thickness unspecified.

4. Newport Formation: Turbidic metagraywackes, metasiltstones, slates, and olistoliths; mimum thickness of 519 m (Bailey and others, 1989, Fig. 13).

Structure. As with the Cambrian phyllites at Beavertail, these rocks record multiple phases of folding plus syn- and post-folding faults. The following discussion is drawn from structural anlyses of the stop in Rast and Skehan (1981a; 1981b) and Skehan and others (1987). The first phase of folding produced variably oriented, tight to isoclinal folds with an intermittently developed slaty cleavage; most folds seen in outcrop are F_1. Because F_1 folds are present only in the Newport and Price's Neck Formation, and because they are truncated by the Newport Granite, they must represent Avalonian or older structures. The second phase of folding is manifested as relatively small folds plus a pervasive, flat-lying slaty cleavage, and is observed in the Newport, Price's Neck, and Pirate's Cave Formations. It is considered to be

Alleghanian, and correlative with the second phase of folding at Beavertail. Relatively open F_3 folds and F_4 box folds are also present. $F_{2\text{-}4}$ folds plus brittle deformation of the Newport Granite is considered to be Alleghanian.

Field Description

The stop begins at the northwestern edge of Brenton Point State Park (A), and proceeds south and east approximately a mile to the other end of the park (B).

A - Brenton Point State Park, north entrance: Pirate's Cave Formation, unconformable upon Newport Neck Fm. See Skehan and others (1987) for geologic map.

B - Brenton Point State Park, south entrance: Newport Formation. Unusually well displayed F_1 folds refolded by F_2 folds and cut by S_2 cleavage.

C - Continue east approximately 2 miles, passing outcrops of Price's Neck Formation and Newport Granite until the road becomes Bellevue Ave.

D - A right turn onto Ledge Ave. brings you to the beginning of the Cliffwalk. This scenic two mile walk begins in the Newport Granite, passes across the tectonized intrusive contact with the Price's Neck Formation, and then crosses the unconformity separating it from fossiliferous Carboniferous metasedimentary rocks.

Significance

The shoreline exposures along southern Aquidneck Island are important for the following reasons:

1. They display the most complete section of Proterozoic Z to Cambrian stratigraphy south of Boston. Because of the distinctiveness of the section, including the presence of olistostromes, the geology displayed here has played a major role in the long-range correlations of at present disconnected Avalonian terrains (Rast and Skehan, 1981b).

2. The truncation of F_1 structures by the radiometrically dated Newport Granite provides documentation of Avalonian tectonism.

3. The later structures provide further insights into Alleghanian tectonism, and contrasting responses of basement and Carboniferous cover to this event

DIRECTIONS TO STOP 11. (See Fig. 3). Continue east along road (becomes Bellevue Ave.) and turn right on Memorial Blvd. Continue past First Beach to Paradise Ave. Turn right into Second Beach parking lot. Purgatory Chasm State Park is just west of Second Beach along coast. Outcrops can be reached either from Second Beach parking lot at the southern end of Paradise Ave. or from Purgatory Chasm parking lot located on the road which parallels the coast west of Second Beach. This is a "no hammer" stop.

Stop 11: Purgatory Conglomerate of the Narragansett Basin, Purgatory Chasm State Park

Background Information

The Pennsylvanian-age Narragansett Basin is a composite graben filled with wet alluvial fan sediments that were deposited during active faulting. The Purgatory Conglomerate is a massive boulder to pebble conglomerate that interfingers with sandstones and siltstones that form the more distal portions of the alluvial fan complex. Cross beds, pebble lag deposits, and fining upward sequences are abundant. Structures in the lower grade portion of the basin consist of NNE-trending, tight to isoclinal, west-verging folds (F_1) with an axial planar foliation (S_1) and thrusts with a west-directed sence of motion (Fig. 4b). S_1 is defined by pressure solution seams and new white micas and/or chlorite. Rare thin sections show an earlier foliation suggesting that S_1 is correlative with S_{1b} elsewhere in the basin. No evidence of earlier folding (F_{1a}) in the massive Purgatory conglomerate has been found. The rocks have been refolded by nearly coaxial, regional to outcrop-scale, east-verging folds (F_2) with a pronounced axial planar crenulation cleavage.

For more information, see Mosher (1981, 1987). The description below is taken from Mosher and others (1987).

Field Description

At this outcrop the approximately 135 m thick, massive, clast-supported Purgatory Conglomerate units are interbedded with thin sandstones and magnetite-rich sandstone lenses. The conglomerate represents a proximal to very proximal facies of a wet alluvial fan that formed off the southeastern block-faulted margin of the basin. Clasts are generally prolate triaxial ellipsoids and range from pebbles to boulders in size (majority are cobbles). Clasts are predominatly quartzite, although rare granite and schist cobbles are present. The outcrop forms part of one of several elongate, N-trending ridges which mark the positions of major F_1 and F_2 fold limbs (Fig. 4b). Long cobble axes trend N10°E parallel to fold axes. Most deformation was caused by D_1 and D_2; only minor indications of D_3 and D_4 are observed. Metamorphism to chlorite grade was syn- to post-D_2.

Cobble deformation was achieved by pressure solution. Cobbles have tangential, almost planar, and deeply embayed contacts. Thin sections of cobble contacts show no evidence of quartz or mica deformation in either cobble; internal cobble bedding shows no distortion at such contacts. Some cobbles contain numerous microstylolitic seams parallel to long axes which give cobbles an internally deformed appearance in the field. Large fibrous pressure shadows of quartz can be seen at long axis terminations of most cobbles. Where cobbles are in close contact, matrix is 1-3 mm thick, depleted in quartz (<3%) and enriched in residual material remaining after pressure solution. Shear fractures offset margins of some cobbles. Substantial redistribution of cobble volume (V) has been measured for the conglomerate throughout the southeastern basin (23%, hinges; 55%, overturned limbs). Much strain is apparent because of original cobble shapes; intercobble rotation during D_1 and D_2 realigned already ellipsoidal sedimentary cobbles into their present position. Real strains are constrictional (Cobble strains - Percival Quarry (0.5 km north along Paradise Ave.): e_X=0%, e_Y=-20%, e_Z=-11%, V=-23%; west Easton's Point (0.2 km west along coast): e_X=0%, e_Y=-28%, e_Z=-26%, V=-41%). Although pressure solution features can be observed anywhere on this outcrop, best localities are: Second Beach near large out-of-place conglomerate block, hilltop near Chasm, and just east of Chasm parking lot along N-trending gravel pathways.

On hilltop near Chasm parking lot, conglomerate beds interfinger with sandstones (bedding: N10°E, 55°SE), showing right-side-up cross bedding and both flat-lying (N4°E,22°E) S_1 and steep (N24°E, 70°NW) S_2 foliations.

Purgatory Chasm is the result of weathering of closely spaced, quartz filled, 'joints' which may mark edges of large rectangular-shape boudins. Similar features, in the same orientation, crop out along northern Cliffwalk (Fig. 3) where conglomerate forms rectangular, sharp-ended boudins separated by quartz. (The most spectacular boudinage outcrops can be seen on Gould Island from a boat.) Exposed in the northern Chasm face is a N-trending fault. Faults and the Chasm boudin are the only evidence of D_3 and D_4 events.

Significance

This stop shows the style of early, low grade deformation of the Pennsylvanian sediments. Deformation is apparently correlative with that at Stop 7, but probably occurred a higher structural level. This outcrop is an excellent example of the coarse-grained alluvial fan sediments filling the Pennsylvanian nonmarine basins. This classical outcrop of Purgatory Conglomerate at Purgatory Chasm is significant, in itself, because the conglomerate has only been deformed by pressure solution and intercobble rotation.

DIRECTIONS. From here we will return to the motel. The easiest route is to take Paradise Ave. north to Green End Ave. and turn left (west). Follow this road across the island to the motel; it becomes Rt. 138 before the motel. If proceeding from Stop 11 to Stop 12, turn north (right) on Rt. 114 before reaching the motel and follow directions to Stop 12.

BACKGROUND INFORMATION FOR THE NEW BEDFORD AREA

Although there has been a great deal of interest and research into the geological history of southeastern New England during recent years, surprisingly little is known about the region south and east of the Narragansett Basin. The next two stops examine the results of recent work (Murray and others, 1990; Murray and Dallmeyer, 1991) that provides insights into the structural, petrographic and geochemical relationships in this area.

The region may be divided into two suites of rocks (Fig. 6). Group I includes granitoids which bear close resemblance to the Proterozoic to Devonian aged granitic basement of the Esmond-Dedham terrane. Of particular interest is the Dartmouth Pluton, a newly recognized unit of slightly deformed alkalic granite plus diorite (Murray and others, 1990; Dunham, 1989; Hamidzada and others, 1993) (Stop 12). In contrast, Group II consists of alaskitic and banded gneisses and schist that are reminiscent of gneissic rocks in western Rhode Island and adjacent Connecticut (Hope Valley terrane).

The dominant structural feature in the New Bedford area is a steeply dipping to vertical, east-trending foliation that becomes more pervasively developed to the south, and which is commonly geometrically identical to brittle and ductile shear zones in the region; it is this fabric that bears many similarities to the pervasive foliation of southwestern Rhode Island and southern Connecticut, that was seen on Day 1. Preliminary kinematic analysis of these shear zones (Murray and Hamidzada, unpub. data; Dunham, 1989) indicates north side down coupled with dextral motion. Variations in the style of deformation associated with this fabric can be used to divide the map area into "BRITTLE" and " DUCTILE" regimes (Fig. 6). Note that the boundary between these two structural regimes does not coincide with the contact between Groups I and II, implying that it represents younger strain gradient superimposed on the two lithotectonic suites, nor is it in general parallel to the east-trending foliation. The fabric is strongly oblique to the NE-trending schistosity of the southern Narragansett Basin and geometrically more comparable to relatively younger ENE-trending folds found in the Carboniferous rocks of the northern Narragansett Basin. In Group I rocks this fabric formed under metamorphic conditions that range to upper greenschist facies, with feldspars responding brittley to deformation in all cases. In contrast, Group II gneisses completely recrystallized under upper amphibolite facies conditions, with annealing and recovery mechanisms dominating. Moreover, banded gneisses in Group II display at least two generations of ductile deformation, the latest of which is correlated with the E-trending foliation seen in Group I rocks; thus, the shear zones and associated foliation are the second fabric (D_2) in Group II gneisses, and the sole fabric (D_2) in Group I lithologies. Preliminary argon release patterns from hornblende from an amphibolite (Murray and Dallmeyer, 1991) characterized by a strong D_2 foliation indicate an age of formation for hornblende lineation of ~270 Ma, supporting an interpretation of the D_2 fabric as Alleghanian.

This trip will examine these rocks at two locales. The first consists of two closely spaced stops in the Dartmouth Pluton, a Group I lithology, where examples of magma mingling will be seen, as well as evidence for evaluating the relative timing of igneous activity and tectonism. The second locale will be in Group II gneisses, where they are intruded by pegmatitic granite. At this stop we will have an opportunity to evaluate the hypothesis that these rocks may be correlative with gneissic rocks of the Hope Valley region and the Narragansett Pier Granite respectively.

DIRECTIONS TO STOP 12. From motel (Newport, RI) take Rt. 138 east to Rt. 114. Turn left and take Rt. 114 north to Rt. 24, and take that road to I 195 in Fall River, MA. Take I 95 to Exit 12, and proceed south to Dartmouth, MA. Continue south to Potomska Point, which is across a small inlet (to the east) from Demerest Lloyd State Park. The Cowyard is just to the east of Potomska Point. You will probably need to use the New Bedford South 7.5' topographic map to find these locales. The stop consists of two sets of shoreline exposures, one along Potomska Point and the other at the Cowyard. Both are on private land, and permission is required.

Stop 12: Dartmouth Pluton — Mixing and mingling relationships between mafic and felsic alkalic magmas.

Background Information

The composite Dartmouth Pluton includes a diverse variety of granitic to dioritic rocks that are intrusive into older granites and gneisses of the Avalon basement. A variety of mingling and mixing features caused by felsic and mafic magma interactions are well preserved, and are responsible in part for rocks of intermediate composition. Recent mapping and petrologic study (Dunham, 1989; Hamidzada and others, 1993) has permitted the rocks of the pluton to be subdivided into a relatively older group of bimodal granites and diorites, and a younger, compositionally more gradational suite of quartz monzonite to diorite rocks that include a variety of intermediate composition hybrid rock types.

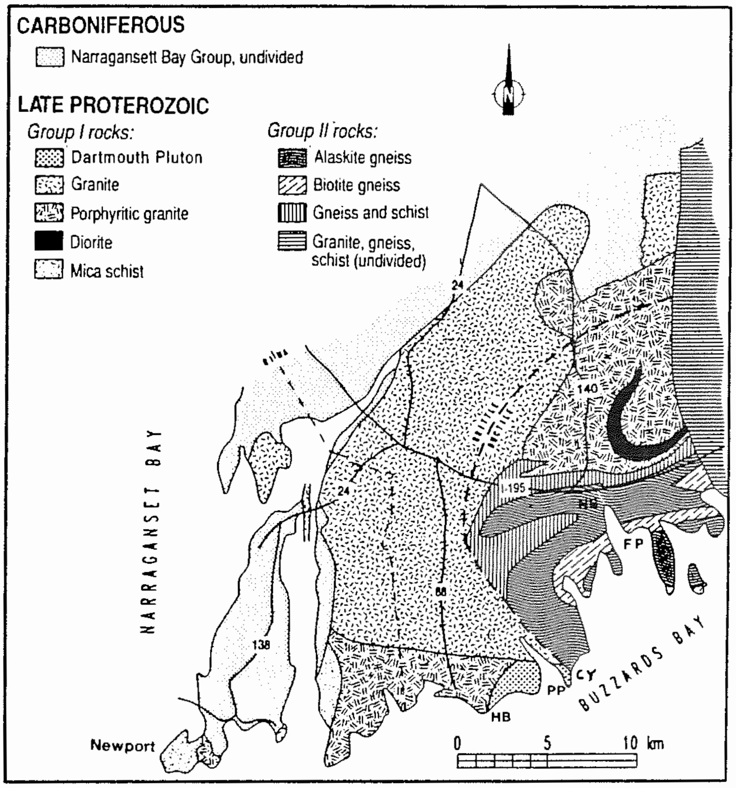

Figure 6. Geologic map of the New Bedford area. From Murray and others (1990) with modifications from Hermes and Zartman (1992) and Hamidzada and others (1993). Abbreviations: FP - Fort Phoenix; HB - Horseneck Beach; PP - Potomska Point; CY - Cowyard. Figure 7 consists of sketch maps of field relations at Potomska Point and immediately to the east.

Petrography and geochemistry indicate that the older and younger suites that comprise the pluton are not directly related petrogenetically. The alkali-feldspar granite from the older suite, which is petrologically similar to alkalic granites of diverse Paleozoic ages in the southeastern New England Avalon zone, yielded a U-Pb zircon age of 595 Ma (Hermes and Zartman, 1992). Thus, the range of ages for the alkalic igneous suites in the Avalon extends from the latest-most Precambrian to Carboniferous. The younger quartz monzonite suite of the Dartmouth Pluton has not been radiometrically dated; it, and related dioritic rocks, cut the 595 Ma alkali feldspar granite, thus constraining its maximum age, but leaving its minimum age unknown. Overall, the rocks of the Dartmouth Pluton are massive to feebly deformed. Local mylonitic shear zones that cut some of the rocks may represent both Alleghanian as well as Late Precambrian deformation.

Field Description

The eastern part of the Cowyard locale is dominated by hypersolvus alkali-feldspar granite (Fig. 7a) similar to the variety that yielded a 595 Ma U-Pb zircon age. The granite contains K-spar + quartz + biotite, with accessory plagioclase, zircon, sphene, and apatite. Numerous dikes and veins of quartz monzonite and fine-grained diorite intrude the alkali-feldspar granite in this area. Compared to the granite, the quartz monzonite contains substantial plagioclase, typically in rapakivii or anti-rapakivii texture; the diorite consists of plagioclase + hornblende + biotite +quartz +K-spar, with accessory sphene and apatite. To the west, quartz monzonite with abundant enclaves of porphyritic to equigranular, fine-grained diorite dominate. In some cases the diorite forms cuspate, "pillow-like" blobs within the granite exhibiting the classic features of magma comingling. At one locality, a diorite dike cutting quartz monzonite has been progressively pulled apart along strike to grade from offset dike fragments into a mass of disrupted, rounded pillow-like masses

(Fig. 7b), demonstrating that monzonitic and dioritic magmas were coeval, and that the felsic magma was not completely solidified upon injection of the more mafic magma. Significantly, the dike is disrupted by a series of left-lateral, steeply dipping, E-W ductile shear zones that impart an E-W fabric in the host monzonite; toward the southern termination of the dike, shearing has fully disrupted the dike to form comingled relict tails. Such features can be interpreted to have formed before final consolidation of the comingled monzonite and diorite, and therefore be contemporaneous with the age of intrusion, and pre-Alleghanian. A larger left-lateral mylonite zone, several meters in width separate the main mass of monzonite-diorite from the alkali feldspar granite to the east (Figure 7b).

Varieties of quartz monzonite dominate the coast line of Potomska Point (Fig. 7c), a short distance west of the Cowyard locale. Several large xenoliths or pendants of older two-feldpar granite are intruded by monzonitic rocks. The western end of Potomska Point contains swarms of enclave-rich quartz monzonite that preserves a variety of mafic-felsic magma mingling and mixing features, and hybrid rocks of intermediate compositions, including monzonite, quartz monzodiorite, and monzodiorite. Well preserved mingling and mixing features include: (a) cuspate and crenulated enclaves ranging in size from a meter downward to cm mafic clots, (b) hybrid inter-enclave material with intermediate color indicies, flow fabric, and disaggregated enclave material, (c) a variety of petrogrphic disequilibrium features, including rapakivii and anti-rapakivii textures, quartz ocelli with hornblende rims, xenocrystic feldspar megacrysts, and acicular quenched apatite.

Significance

1. The Dartmouth Pluton is the only alkalic plutonic complex found to the east of the Narragansett Basin.

2. At least some of the alkalic rocks of the pluton are Late Precambrian, demonstrating that alkalic igneous activity characteristic of post-collisional and anorogenic settings began abruptly and quickly after the preceding Avalonian orogeny in southeastern New England.

3. Older rocks of the pluton mainly are bimodal. In the younger suite, magma mingling and mixing features locally are abundant and well preserved; in some areas mixing has led to extensive hybridization, and to the widespread development of rocks of intermediate compositions.

4 Some mylonitic structures in the pluton appear to be generally coeval with stages of emplacement, and probably are pre-Alleghanian. Limited Ar release patterns fail to demonstrate a thorough, high temperature Late Paleozoic thermal event here, as is indicated to the west of the Narragansett Basin.

DIRECTIONS TO STOP 13. Take I 195 east to New Bedford, and take the first exit after you cross over the harbor (Exit 18). Go south on Rt. 240. You will shortly cross Rt. 6. Continue through the intersection, and drive south until you reach the end of the road. This is the entrance to Fort Phoenix. The stop is in the town of Fairhaven, at the east end of the hurricane storm barrier; it consists of shoreline exposures, at Fort Phoenix State Park, which form the base of the remains of a revolutionary war naval fortification.

STOP 13: Group II banded gneisses at Fort Phoenix

Background Information

This set of outcrops in New Bedford harbor consists of Group II banded gneiss intruded into alaskitic gneiss (Fig. 6). Ongoing mapping indicates at least two phases of folding in the banded gneiss, in which earlier, variably oriented isoclinal folds and foliation are overprinted by an axial planar foliation (S_2) which is geometrically identical to the east-trending shear zones observed in the Group I rocks. The gneisses are intruded by pegmatitic S-type granite reminiscent of the Narragansett Pier Granite observed on the west side of Narragansett Bay, apparently synchronous with the development of the S_2 foliation.

Field Description

The exposures consist of east-trending, north-dipping gneisses that parallel the coast. Proceeding northward (i.e., landward) one encounters:

1. Medium grained biotite-quartz-feldspar gneiss

2. Massive to alaskitic gneiss: This unit is intrusive into the next unit.

3. Banded gneiss: The unit consists of roughly equal amounts of millimeter- to centimeter-thick layers of biotite-quartz-feldspar gneiss, and quartz-alkali feldspar gneiss. Although migmatitic in appearance, layers have compositions that are inappropriate for anatexis, suggesting that the layering reflects original inhomogeneities and/or subsequent solid state modification. This unit contains the best evidence for multiple phases of ductile deformation.

4. Garnet-muscovite-quartz-microcline-plagioclase pegmatitic granite is intrusive both along and across the S_2 foliation, and where parallel to the foliation, the granite is boudinaged. Apparently the granite was emplaced during the waning stages of the development of the S_2 fabric. Although the granite is undated (and may not be datable), it is tempting to compare it to the white phase of the Narragansett Pier Granite that was seen on Day 1, for petrologically and macroscopically they are similar.

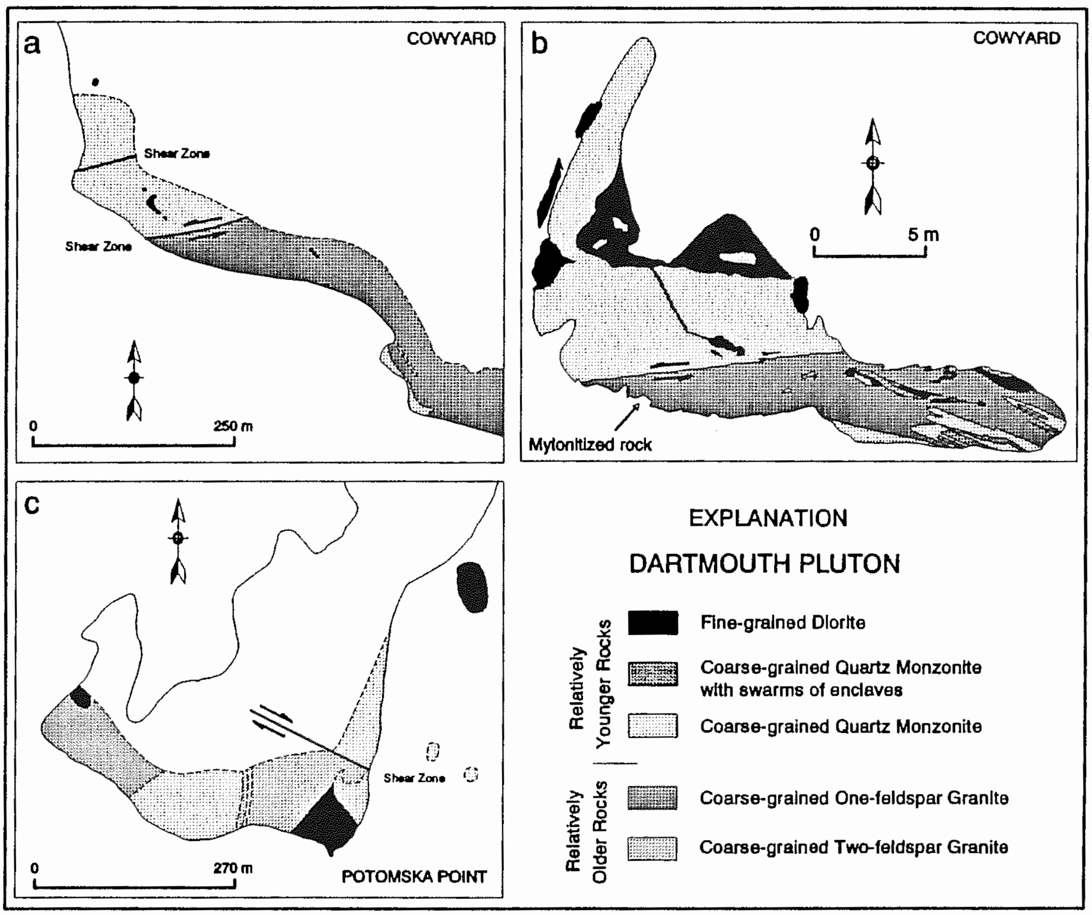

Figure 7. Field relations at Potomska Point and the Cowyard locale, within the Dartmouth Pluton. (a). The eastern part of the Cowyard consists of one-feldspar granite and is in fault contact to the west with quartz monzonite (b) The large scale map shows mafic enclaves within quartz monzonite, and a mafic pull-apart dike with left-lateral offsets. The northern part of dike displays cuspate margins and brittle fractures, whereas the southern portion consists of a large globular body (e.g., mafic enclave) that is flattened in the plane of the foliation, implying deformation synchronous with solidification. (c) Map shows the generalized geology of Potomska Point, characterized by quartz monzonite intrusive into two-feldspar granite, and areas of mafic-felsic comingling and enclave swarms.

DIRECTIONS TO STOP 14. From the last stop, retrace your route to I 195. Take I 195 west to Exit 13, Rt. 140. Take Rt. 140 north until you reach Rt. 24. Take Rt. 24 to I 495, and then go west on I 495 to I 95. Take I 495 south to I 295, and then take I 295 west to the first exit, Rt. 1. Take Rt. 1 south two miles to the Grossmans Lumberyard, (on your right) and park in the lot. The stop consists of rather tawdry exposures behind the lumberyard and nearby chopshop.

Stop 14: Bimodal volcanics of the Carboniferous Wamsutta Formation, northern Narragansett basin.

Background Information

The Wamsutta Formation overlies the basal Pondville Conglomerate within the Narragansett basin of northern Rhode Island and adjacent Massachusetts and the Norfolk basin of Massachusetts. The formation is dominated by conglomerate with lesser amounts of siltstone and sandstone. The depositional environment has been described as a system of streams flowing over humid alluvial fans (Severson, 1981; Cazier, 1987); the typical reddish color of the formation is attributed to alteration of accessory iron oxides to hematite under oxidizing conditions, possibly indicating well-drained environments (Lidback, 1977). Plant fossils estimated to be about Westphalian C in age (Knox, 1944; Lyons and Darrah, 1977; Hermes and Murray, 1990) have been collected and described from some of the sedimentary rocks. Interbedded within the sedimentary rocks are bimodal volcanic rocks (Figure 8). Recent mapping (Maria, 1990) recognized two discrete flows of rhyolite, and at least 4 flows of basalt. The two younger basalt flows contain inter-granular to subophitic clinopyroxene, whereas the older flows lack clinopyroxene. Both basalt types contain sparse plagioclase phenocrysts in a pilotaxitic groundmass of plagioclase, opaque minerals, apatite, and pseudomorphed olivine microphenocrysts. In most cases groundmass minerals are largely replaced by chlorite, epidote, granular sphene, and turbid clay-like alteration products. Amygdules are filled by calcite, chlorite, epidote, and/or chalcedony. The rhyolite consists of Carlsbad twinned anorthoclase phenocrysts immersed in a fine-grained devitrified or recrystallized matrix of mainly quartz and alkali feldspar. Minor accessories include riebeckite, sphene, and opaque minerals. In some samples the groundmass exhibits perlitic and patchy textures indicative of devitrification of glass matrix. Locally, the rhyolite is highly vesicular, now containing chalcedony in the vesicles. A conspicuous field characteristic of the rhyolite is the abundance of subparallel quartz seams, especially near the base, generally concordant to contacts; these features appear to be late-stage infilling of cooling cracks (possibly lithophysae) permeated by hydrothermal fluids at subsolidus conditions. Field and petrographic features indicate that the rhyolite is a lava flow, and not of pyroclastic origin.

Both the rhyolites and the basalts exhibits alkalic geochemistry, and along with their bimodal character, are supportive of extensional, rift-tectonics during the Wamsutta stage of basin development. Many similar geochemical features, as well as mafic-felsic magma interactions, are exhibited by the alkalic plutonic rocks of the southeastern New England Avalon zone that range in age from Late Precambrian to Carboniferous (Hermes and Zartman, 1992).

Field Description

This stop will examine contact relationships of a rhyolite lava flow with clastic sedimentary rocks of the Wamsutta Formation, and one of the basalt flows that outcrops nearby to the south. Maria (1990) has mapped the Wamsutta Formation, and the interstratified volcanic flows, as a gently folded syncline that plunges to the northeast; the stratigraphy is cut and offset by a series of high angle, NE-trending stike-slip faults. The base of the rhyolite consists of anorthoclase microphenocrysts, and typically exhibits subparallel stringers of late-stage quartz bands that probably represent lithophysae. The upper part of the flow is not exposed at this or other localities. The conglomeratic units adjacent to the rhyolite contain clasts of quartzite, granite, basalt, rhyolite, and metamorphic rocks. Some of the felsic volcanic clasts may represent pyroclastic volcanic materials erupted prior to extrusion of the apparently passive rhyolite flow.

Significance

1. The presence of bimodal lava flows of alkalic affinity interstratified with clastic sedimentary rocks of the Wamsutta Formation within the Narragansett basin indicate an extensional, rift-tectonic setting during early stages of basin development.

2. Bimodal volcanic suites containing rocks with compositions similar to those of the Wamsutta suite are found in Carboniferous basins along much of the northern extent of the Appalachian/Caledonide belt with volcanics of similar

age and compositions occuring in the Canadian maritimes (Dostal and others, 1983; Blanchard and others, 1984; Barr and others, 1985; Fyffe and Barr, 1986), and in the Variscan of Europe (Francis, 1988). However, these rocks are the only documented Carboniferous volcanic rocks in the USA Appalachians.

DIRECTIONS FOR STOP 15. Continue south on Rt. 1 to the intersection with Rt. 123. Take Rt. 123 northeast to the intersection with I 95. Take I 95 north to the intersection of I 95 and Rt. 140 in Foxborough, MA. The stop consists of roadcuts along the entrance ramps and along Rt. 140, where it passes underneath the interstate.

STOP 15: Rhode Island Formation

Background Information

The stop displays approximately 1400 meters of the Rhode Island Formation, the dominant formation of the Narragansett Bay Group of the Narragansett basin. It has previously been described by Lyons and Chase (1976) and the following text is adapted from their description as well as from unpublished data of the Narragansett Basin Coal Exploration Project (DPM, J. Skehan, and students). Here the Rhode Island Formation consists of interbedded granule conglomerate, sandstone, siltstone, shale, and coal, and is representative of the relatively fine-grained parts of the Carboniferous section.

Field Description

Based upon detailed mapping plus information from drillcores (Skehan and Murray, 1976; Lyons and Chase, 1976) the stratigraphic secion at this locale is interpreted to represent fluviatile sedimentary rocks in which the coal seams formed on flood plains. The beds are folded into open to tight, upright ENE-trending folds which at this site occur on the northern limb of the Manfield syncline. Brittle structures include a NW-trending fault that continues northward to offset the basin margin, plus other more localized faults (Figure 8). Heading north from the interchange on I 95, within

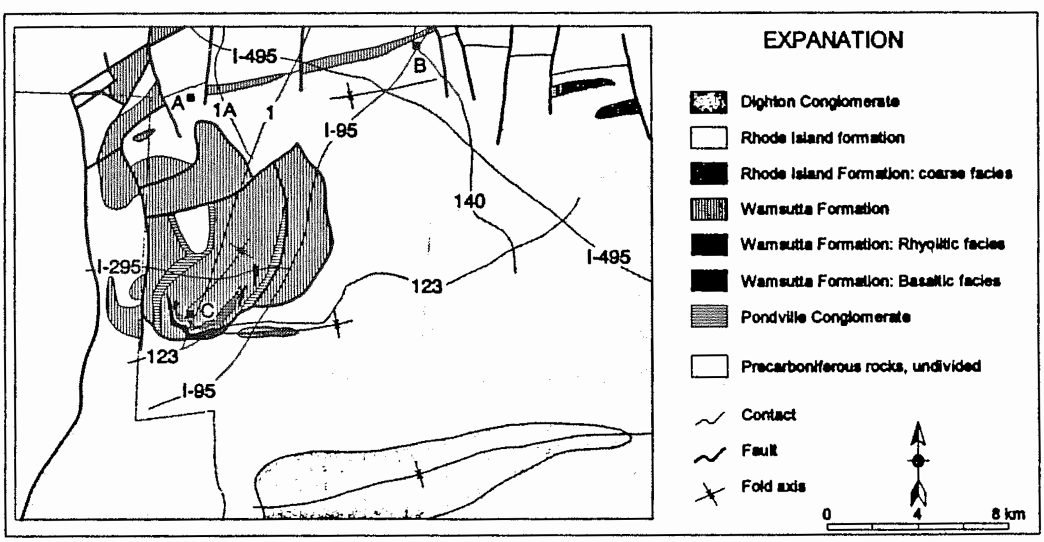

Figure 8. Simplified map of the geologic relationships in the northwest corner of the Narragansett basin. The numbered lines are roads and interstate highways. A Masslite Quarry; B Intersection of I 95 and Rt. 140, Stop 15 of this trip; C Outcroppings west of Rt. 1, Stop 14 of this trip. Compiled from the Massachusetts State Map (Zen, ed., 1983); Rhode Island State map (Hermes and others, compilers, in press); Skehan and others (1979); Maria (1990).

500 meters one crosses the contact between the Narragansett basin and faulted, ~600 Ma granodiorite. Despite the prevalence of fractures and faults in the area, it can be shown that the Narragansett Basin is autochtonous and is separated from the basement by a highly weathered zone.

Significance

The site is important because:

1. It contains a relatively accessible and representative stratigraphic section that includes all lithotypes of the Rhode Island Formation.

2. Westphalian C megafloral specimens collected here provide important age constraints on this part of the basin.

3. Thirteen thin coal beds (now covered) occur in the cloverleaf. They are on the north limb of the Mansfield syncline and have been correlated with mined seams to the south.

4. Drillcore and outcrop data from this site are important for understanding the nature of the margin of the Narragansett basin.

REFERENCES

Aleinikoff, J. N, Moench, R. H., and Lyons, J. B., 1985, U-Th-Pb geochronology of the Massabesic Gneiss and the granite near Milford, south-central New Hamphsire; New evidence for Avalonian basement and Taconic and Alleghanian disturbances in eastern New England: Contributions to Mineralogy and Petrology, v. 71, p. 1-11.

Bailey, B. H., Skehan, J. W., Dreier, R. B., and Webster, M. J., 1989, Olistostromes of the Avalonian terrane of southeastern New England: in J. W. Horton, Jr. and N. Rast, eds., Melanges and olistostromes of the U.S. Appalachians: Geology Society of America Special Paper, v. 228, p. 93-112.

Barr, S. M., Brisebois, D., and MacDonald, A. S., 1985, Carboniferous volcanic rocks of the Magdalen Islands, Gulf of St. Lawrence: Canadian Journal of Earth Sciences, v. 22, p. 1679-1688.

Blanchard, M., Jamieson, R. A., and More, E. B., 1984, Late Devonian - Early Carboniferous volcanism in western Cape Breton Island, Nova Scotia: Canadian Journal of Earth Sciences, v. 21, p. 762-774.

Brown, A., Murray, D. P., and Barghorn E., 1978, Pennsylvanian fossils from metasediments within the Narragansett Pier Granite, Rhode Island. Geological Society of America Abstracts with Programs 10, 35-6.

Burks, R. J., 1985, Incremental and finite strains within ductile shear zones, Narragansett Basin, Rhode Island [Ph.D. dissertation]: University of Texas at Austin, 138 p.

Cazier, E. C., III., 1987, Late Paleozoic tectonic evolution of the Norfolk Basin, southeastern Massachusetts: Journal of Geology, v. 95, p. 55-73.

Dallmeyer, R. D., 1982, $^{40}Ar/^{39}Ar$ ages from the Narragansett Basin and southern Rhode Island basement terrane: Their bearing on the extent and timing of Alleghanian tectonothermal events in New England: Geological Society of America Bulletin, v. 93, p. 1118-1130.

Dostal, J., Keppie, J. D., and Dupuy, C., 1983, Petrology and geochemistry of Devono-Carboniferous volcanic rocks in Nova Scotia: Maritime Sediments and Atlantic Geology, v. 19, p. 59-71.

Dreier, R. B., 1985, The Blackstone Series: Evidence for Precambrian Avalonian and Permian Alleghanian tectonism in southeastern New England [Ph.D. dissertation]: University of Texas Austin, 249 pp.

Dunham, T. S., 1989, The lonely alkalic pluton of southeastern Massachusetts: Geological Society of America Abstracts with Programs, v. 21, p. 12.

Farrens, C. M., 1982, Styles of deformation in the southeastern Narragansett Basin, Rhode Island and Massachusetts [Master's thesis]: University of Texas at Austin, 66 p.

Francis, E. H., 1988, Mid-Devonian to early Permian volcanism: Old World: in Harris, A. L. and Fettes, D. J., eds., The Caledonian-Appalachian orogen: Geological Society Special Publication No. 38, p. 573-584.

Fyffe, L. R., and Barr, S. M., 1986, Petrochemistry and tectonic significance of Carboniferous volcanic rocks in New Brunswick: Canadian Journal of Earth Sciences, v. 22, p. 1679-1688.

Getty, S.R., and Gromet, L.P., 1988, Alleghanian polyphase deformation of the Hope Valley shear zone, southeastern New England: Tectonics, v. 7, p. 1325-1338.

_____, and Gromet, L. P., 1991, Late Paleozoic tectonism in Avolanian basement rocks: a view from beneath the Devonian (Acadian) metamorphic belt: Abstracts with Program, Geological Society of America 23(1), p. 34.
_____, and Gromet, L.P., 1992a, Geochronological constraints on ductile deformation, crustal extension, and doming about a basement-cover boundary, New England Appalachians. American Journal of Science, v. 292, p. 359-397.
_____, and Gromet, L.P., 1992b, Evidence for extension at the Willimantic dome, Connecticut: Implications for the Late Paleozoic tectonic evolution of the New England Appalachians. American Journal of Science, v. 292, p. 398-420.
Goldsmith, R., 1985, Bedrock geologic map of the Old Mystic and part of the Mystic Quadrangles, Connecticut, New York, and Rhode Island: U. S. Geological Survey Map I-1524, scale 1:24,000.
Goldstein, A., 1989, Tectonic significance of multiple motions on terrane-bounding faults in the northern Appalachians: Geological Society of America Bulletin, v. 101, p. 927-938.
Grew, E.S., and Day, H.W., 1972, Staurolite, kyanite and sillimanite from the Narragansett Basin of Rhode Island: U.S. Geological Survey Professional Paper 800-D, p. 151-157.
Gromet, L. P., 1989, Avalonian terranes and late Paleozoic tectonism in southeastern New England: Constraints and problems. Geological Society of America Spécial Paper 230, p. 193-211.
_____, 1991, Direct dating of deformational fabrics: Short Course Handbook on Applications of Radiogenic Isotope Systems To Problems in Geology, Mineralogical Association of Canada, May, 1991, Chapt. 5, p. 167-189.
Hamidzada, N., 1988, Petrology, geochemistry and structure of the northeastern part of the Scituate Pluton, Rhode Island [Master's thesis]: University of Rhode Island.
_____, Hermes, O. D., and Murray, D. P., 1993, Multiple mafic and felsic magma interaction as exhibited in the Dartmouth pluton, Avalon zone, southeastern Massachussetts: Geological Society of America Abstracts with Program, v. 25, p. 21.
Henderson, C. M., and Mosher, S., 1983, Narragansett Basin, Rhode Island: role of intrabasinal horsts and grabens in Alleghanian deformation: Geological Society of America Abstracts with Programs, v. 15, p. 129.
Hermes, O. D., Gromet, L. P., and Zartman, R. E., 1981, Zircon geochronology and petrology of plutonic rocks in Rhode Island: in Boothroyd, J. C. and Hermes, O. D., eds., Guidebook to Geologic Field Studies in Rhode Island and Adjacent Areas, New England Intercollegiate Geologic Conference, 73rd Annual Meeting, p. 315-338.
_____, and Zartman, R.E., 1985, Late Proterozoic and Devonian plutonic terrane within the Avalon zone of Rhode Island: Geological Society of America Bulletin, v. 96, p. 272-282.
_____ and Murray, D. P., 1990, Geochemical distinctions of late Proterozoic and Paleozoic volcanism in the Avalon zone of New England: in Socci, A. D., Skehan, J. W. and Smith, G. W., eds., Geology of the composite Avalon terrane of southern New England: Geological Society of America Special Paper 245, p.97-112.
_____, and Zartman, R. E., 1992, Late Proterozoic and Silurian alkaline plutons within the southeastern New England Avalon Zone: Journal of Geology, v. 100, p. 477-486.
Jones, D. E., 1987, Phase equilibria and conditions of metamorphism in the southwest portion of the Narragansett Basin [Master's thesis]: Universtiy of Rhode Island, 210 p.
Kocis, D. E., 1981, The contact relationships of the Narragansett Pier Granite in the Narragansett Basin Area [Master's thesis]: University of Rhode Island.
Knox, A. S., 1944, A Carboniferous flora from the Wamsutta Formation of southeastern Massachusetts: American Journal of Science, v. 242, p. 130-138.
Lidback, M. M., 1977, Areal geology of the Attleboro quadrangle Massachusetts - Rhode Island [Ph.D. dissertation]: Boston University.
Lyons, P.C., 1984, Carboniferous megafloral zonation of New England, in P. K. Sutherland and W. L. Manger, eds., Neuvieme Congres International de Stratigraphie et de Carbonfere, Compte Rendu, v. 2, Biostratigraphy: Carbondale, Illinois, Southern Illinois University Press, v. 2, p. 503-514.
_____, and Chase, H. B., 1976, Coal stratigraphy and flora of the northwestern Narragansett Basin: in Cameron, B., ed., A guidebook of field trips to the Boston area and vicinity: New England Intercollegiate Geologic Conference, 68th Annual Meeting, Boston University, Boston, MA., p. 405-427.
_____, and Darrah, W. C., 1977, Floral evidence for Upper Pennsylvanian in the Narragansett Basin, southeastern New England: Geological Society of America Abstracts with Programs, v. 9, p. 297.
Mahler, J. P., and Mosher, S., (in press), Late-stage Alleghanian wrenching of the southwestern Narragansett Basin,

Rhode Island: American Journal of Science.

Maria, A., 1990, Petrology and significance of Carboniferous volcanics, South Attleboro, MA [Master's thesis]: University of Rhode Island, 172p.

Mosher, S., 1981, Pressure solution deformation of conglomerates from Rhode Island: Journal of Geology, v. 89, no. 1, p. 37-55.

Mosher, S., 1983, Kinematic history of the Narragansett Basin, Massachusetts and Rhode Island: constraints on late Paleozoic plate reconstructuions: Tectonics, v. 2, p. 327-344.

_____, 1987, Pressure solution deformation of the Purgatory Conglomerate, Rhode Island: quantification of volume change, real strain, and sedimentary shape factor: Journal of Structural Geology, v. 9, no. 2, p. 221-232.

_____, Burks, R. J., Reck, B. H., 1987, Alleghanian deformation in the southern Narragansett Basin, Rhode Island, in Roy, D. C., ed., Geological Society of America Centennial Field Guide — Northeast Section: Geological Society of America, v. 5, p. 191-194.

_____, and Berryhill, A. W., 1991, Structural analysis of progressive deformation within complex transcurrent shear zone systems: southern Narragansett Basin, Rhode Island: Journal Structural Geology, v.13, p. 557-578.

Murray, D. P., 1987, The Alleghanian Orogeny in the Narragansett Basin area, southern Rhode Island: in Roy, D., ed., Geological Society of America Centennial Field Guide — Northeast Section: Geological Society of America, v. 5, p. 187-190.

_____, 1988, Post-Acadian metamorphism in the Appalachians: in Harris, A. L., and Fettes, D. J., eds., The Caledonian-Appalachian orogen: Geological Society of London Special Publication 38, p. 597-609.

_____, and Skehan, J. W., 1979, A traverse across the eastern margin of the Appalachian-Caledonide orogen, southeastern New England: in Skehan, J. W., and Osberg, P. H., eds., The Caledonides in the U.S.A.; Geological excursions in the northeast Appalachians: International Geologic Correlation Program Project 27, Weston, Massachusetts, Boston College Department of Geology and Geophysics, p. 1-32.

_____, Raben, J. D. Lyons, P. C., and Chase, Jr., H. B., 1981, Geologic setting of coal and carbonaceous materials, Narragansett Basin, southeastern New England: in Boothroyd, J. C. and Hermes, O. D., eds., Guidebook to geological field studies in Rhode Island and adjacent areas: New England Intercollegiate Geologic Conference, 73rd Annual Meeting, p. 265-284.

_____, Hermes, O. D., and Dunham, T. S., 1990, The New Bedford area: A preliminary assessment: in Socci, D., Skehan, J. W. and Smith, G. W. (eds.), Geology of the composite Avalon Terrane of southern New England: Geological Society of America Special Paper 245, p. 155-170.

_____, and Dallmeyer, R. D., 1991, Polyphase tectonothermal evolution of basement in southeasternmost New England; evidence from $^{40}Ar/^{39}Ar$ hornblende ages: Abstracts with Programs, Geological Society of America v. 23, p. 107.

Mutch, T.A., 1968, Pennsylvanian nonmarine sediments of the Narragansett Basin, MA-RI: Geological Society of America Special Paper 106, p. 177-209.

O'Hara, K.D., and Gromet, L.P., 1983, Textural and Rb-Sr isotopic evidence for late Paleozoic mylonitization within the Honey Hill Fault Zone, southeastern Connecticut: American Journal of Science, v. 283, p.762-779.

_____, and Gromet, L.P., 1985, Two distinct late Precambrian (Avalonian) terranes in southeastern New England and their late Paleozoic juxtaposition: American Journal of Science, v. 285, p. 673-709.

Rast, N., and Skehan, J. W., S. J., 1981a, The geology of the Precambrian rocks of Newport and Middletown, Rhode Island: in Hermes, O. D., and Boothroyd, J. C. (eds.), Guidebook to Field Stations in Rhode Island and Adjacent Areas: New England Intercollegiate Geologic Conference, 73rd Annual Meeting, pp. 67-92, University of Rhode Island, Kingston, RI.

______ and Skehan, J. W., S. J., 1981b, Possible correlation of Precambrian rocks of Newport, Rhode Island with those of Anglesey, Wales: Geology, v. 9, p. 596-601.

Reck, B. H., and Mosher, S., 1989, Timing of intrusion of the Narragansett Pier Granite relative to deformation in the southwestern Narragansett Basin, Rhode Island: Journal Geology, v. 96, p. 677-692.

Secor, D. T., Jr., Murray, D. P., and Glover, III, 1989, Geology of the Avalonian rocks: in Rankin, D. W. et. al., Pre-orogenic terranes: in Hatcher, R. D., Jr. Thomas, W. A., and Viele, G. W., (eds.), The Appalachian-Ouachita Orogen in the United States: Boulder, Colorado, Geological Society of America, The Geology of North America, V. F-2, p. 57-85.

Severson, R. H., 1981, Depositional environments, facies relationships, and coal occurrence in Carboniferous sediments of the Narragansett Basin [M.A. thesis]: Kingston, University of Rhode Island, 105 p.

Skehan, J. W., Murray, D. P., Belt, E. S., Hermes, O. D., Rast, N., Dewey, J. F., 1976, Alleghanian deformation, sedimentation, and metamorphism in southeastern Massachusetts and Rhode Island: in Cameron, B., ed., Geology of Southeastern New England, New England Intercollegiate Geologic Field Conference, 68th Annual Meeting, Boston, Mass., p. 447-471

_____, Murray, D. P., Palmer, A. R., Smith, A. T., and Belt, E. S., 1978, Significance of fossiliferous Middle Cambrian rocks of Rhode Island to the history of the Avalonian microcontinent: Geology, v. 6, p. 694-698.

_____, Murray, D. P., Hepburn, J. C., Billings, M. P., Lyons, P. C., and Doyle, R. G., 1979, The Mississippian and Pennsylvanian (Carboniferous) Systems in the United States - Massachusetts, Rhode Island, and Maine: U. S. Geological Survey Professional Paper 1110-A, 30 p.

_____, Rast, N., and Logue, D. F., 1981, The geology of Cambrian rocks of Conanicut Island, Jamestown, Rhode Island: in Boothroyd, J. C., and Hermes, O. D., eds., Guidebook to geologic field studies in Rhode Island and adjacent areas: New England Intercollegiate Geologic Conference, 73rd Annual Meeting, Kingston, University of Rhode Island, p. 237-264.

_____, S. J., Rast, N., and Mosher, S., 1986, Paleoenvironmental and tectonic controls of sedimentation in coal-forming basins of southeastern New England: in P. C. Lyons and C. L. Rice, eds., Paleoenvironment and tectonic controls in coal-forming basins of the United States: Geological Society of America Special Paper 210, p. 9-30.

_____, Webster, M. J., and Logue, D. F, 1987, Cambrian stratigraphy and structural geology of southern Narragansett Bay, Rhode Island: in Roy, D.C (ed.), Geological Society of America Centennial Field Guide - Northeastern Section: Geological Society of America, v. 5, p. 195-200

Smith, B. M., 1978, The geology and Rb-Sr whole-rock age of granitic rock of Aquidneck and Connanicut Islands, Rhode Island [Master's thesis]: Brown University, Providence, Rhode Island, 94 p.

Snoke, A. W. and Mosher, S., 1989, The Alleghanian orogeny as manifested in the Appalachian internides: in Hatcher, R. D., Viele, G. W. and Thomas, W. A., eds., The Appalachian Ouachita Orogen in the United States: Geological Society of America, v. F-2, p. 288-318.

Snyder, G.L., 1964, Bedrock geology of the Willimantic Quadrangle, Connecticut: U. S. Geological Survey Quadrangle Map GQ-335.

Thomas, K.J., 1981, Deformation and metamorphism in the central Narragansett Basin of Rhode Island [Master's thesis]: University of Texas at Austin, 96 pp.

Wintsch, R.P., 1979, The Willimantic fault: a ductile fault in eastern Connecticut: American Journal of Science, v. 279, p. 367-393.

_____, 1992, Contrasting P-T-t paths: thermochronology applied to the identification of terranes and to the history of terrane assembly, southeastern New England: in Robinson, P. and Brady, J.B., eds., Guidebook for Field Trips in the Connecticut Valley Region of Massachusetts and Adjacent States: New England Intercollegiate Geological Conference, 84th Annual Meeting, Amherst College, Amherst, p. 48-66.

_____, and Sutter, J.F., 1986, A tectonic model for the late Paleozoic of southeastern New England: Journal of Geology, v. 94, p. 459-472.

_____, and Aleinikoff, J. N., 1987, U-Pb isotopic and geologic evidence for late Paleozoic anatexis, deformation, and accretion of the Late Proterozoic Avalon terrane, southcentral Connecticut: American Journal of Science, v. 287, p. 107-126.

_____, and Fout, J. S., 1982, Structure and petrology of the Willimantic dome and the Willimantic fault, eastern Connecticut: in Joesten, R. and Quarrier, S.S., eds., Guidebook for Field Trips in Connecticut and south central Massachusetts: New England Intercollegiate Geologic Conference 74th Annual Meeting, The University of Connecticut, Storrs, p. 465-482.

Zartman, R. E., and Hermes. O. D., 1987, Archean inheritance in zircon from late Paleozoic granites from the Avalon zone of southeastern New England: An African connection: Earth and Planetary Science Letters, v. 82, p. 305-315.

Zen, E-an, 1983, Bedrock geologic map of Massachusetts, United States Geological Survey, scale 1:250,000.

Chapter CC

Geology and Geomorphology of the Acadian Orogen, Central Maine

By Lindley S. Hanson, Dwight C. Bradley, and D.W. Caldwell

Field Trip Guidebook for the Northeastern United States:
1993 Boston GSA

Volume 2
Contribution No. 67, Department of Geology and Geography, University of Massachusetts, Amherst, Massachusetts

Trip #31
GEOLOGY AND GEOMORPHOLOGY OF THE ACADIAN OROGEN, CENTRAL MAINE

Lindley S. Hanson, Department of Geology, Salem State College, Salem, MA 01970
Dwight C. Bradley, U.S. Geological Survey, Anchorage, AK 99508
D. W. Caldwell, Department of Geology, Boston University, Boston, MA 02215

INTRODUCTION

This field trip will introduce you to the regional geology and geomorphology of central Maine (fig. 1), an area that includes some of the most spectacular scenery in New England. Over the course of three days, we will focus on rock units that are central to the interpretation of the Acadian orogeny, which, despite being the main orogenic event in much of the Northern Appalachians, remains the most controversial major episode. Central Maine plays a key role in the study of Acadian tectonics because, in this area, Acadian-deformed Silurian and Devonian strata are at least sparsely fossiliferous and are amenable to sedimentological analysis. In contrast, equivalent rocks along strike in New Hampshire and Massachusetts have been so strongly deformed and (or) metamorphosed that few sedimentological details have survived. Many prevailing stratigraphic concepts in these highly-studied areas are extrapolated from studies in Maine. Throughout the trip we will also illustrate how the local geomorphology is controlled by structure and lithology of Acadian features.

OVERVIEW OF REGIONAL GEOLOGY

ANTICLINORIAL BELT OF NORTH-CENTRAL MAINE

We will spend Day 1 in the anticlinorial belt of north-central Maine. This belt, which extends northeastward from western Maine through central Maine, includes a number of anticlines (e.g. Lobster Mountain and Caribou Lake anticlines in fig. 1) locally separated by synclines (e.g. Moose River and Roach River synclines). The anticlines are cored by a basement complex that was accreted to North America during the Ordovician Taconic orogeny. The lithology of the basement varies from one anticline to the next and includes Precambrian gneiss of the Chain Lakes Massif, a Cambrian ophiolite (Boil Mountain Complex), and Cambrian melange of the Hurricane Mountain Formation. Although the present structures within the anticlinorial belt are largely Acadian, the belt contains rocks deformed during the Cambrian Penobscottian orogeny (Boone and Boudette, 1989; Boone and others, 1989), which occurred within the Iapetus ocean prior to the Taconic collision. Ordovician volcanic rocks that crop out along the anticlinorial belt are generally attributed to Taconic arc magmatism. An example of these will be viewed at Stop 2.

Silurian strata along the anticlinorial belt were deposited in relatively shallow water (fig. 2). The Ripogenus Formation in the Caribou Lake anticline (Stop 2) is probably the best exposed and least tectonized of a series of correlative shallow-marine units (mostly quartzose sandstone, siltstone, and impure limestone) that were deposited along the anticlinorial belt from Maine to Massachusetts. These units, which include the well known Clough Quartzite and Fitch Formation in New Hampshire, are tectonically significant because they record an interval of shallow-marine deposition at slow to moderate subsidence rates along the Taconic-modified margin of North America (Bradley, 1983). This implies, in turn, that subsequent rapid subsidence, which was soon to follow in the Devonian (Stop 3), must have resulted from something other than an initially thin crust.

Another key feature of the anticlinorial belt is the presence of volcanic rocks representing all four stages of the Silurian and the first three of the Devonian. These volcanic rocks are part of what we have called the Piscataquis magmatic belt (Hanson and Bradley, 1989), which includes Silurian as well as Devonian volcanic rocks, plus related plutonic rocks. The name "Piscataquis volcanic belt" was originally applied by Rankin (1968), in a much more restricted sense, to a suite of Early Devonian volcanic rocks along an 80-km-long segment of the belt in central Maine. Silurian shallow-marine facies and volcanic rocks along the anticlinorial belt contrast sharply with the Silurian deep-water turbidites of the Kearsarge-Central Maine basin. We have attributed the volcanism to a magmatic arc that formed during northwest-directed subduction of the Kearsarge-Central Maine basin that eventually resulted in Acadian collision (Bradley, 1983; Hanson and Bradley, 1989). Stop 2 will feature outcrops of a Silurian volcanic rock unit, the West Branch volcanics (of Griscom, 1976).

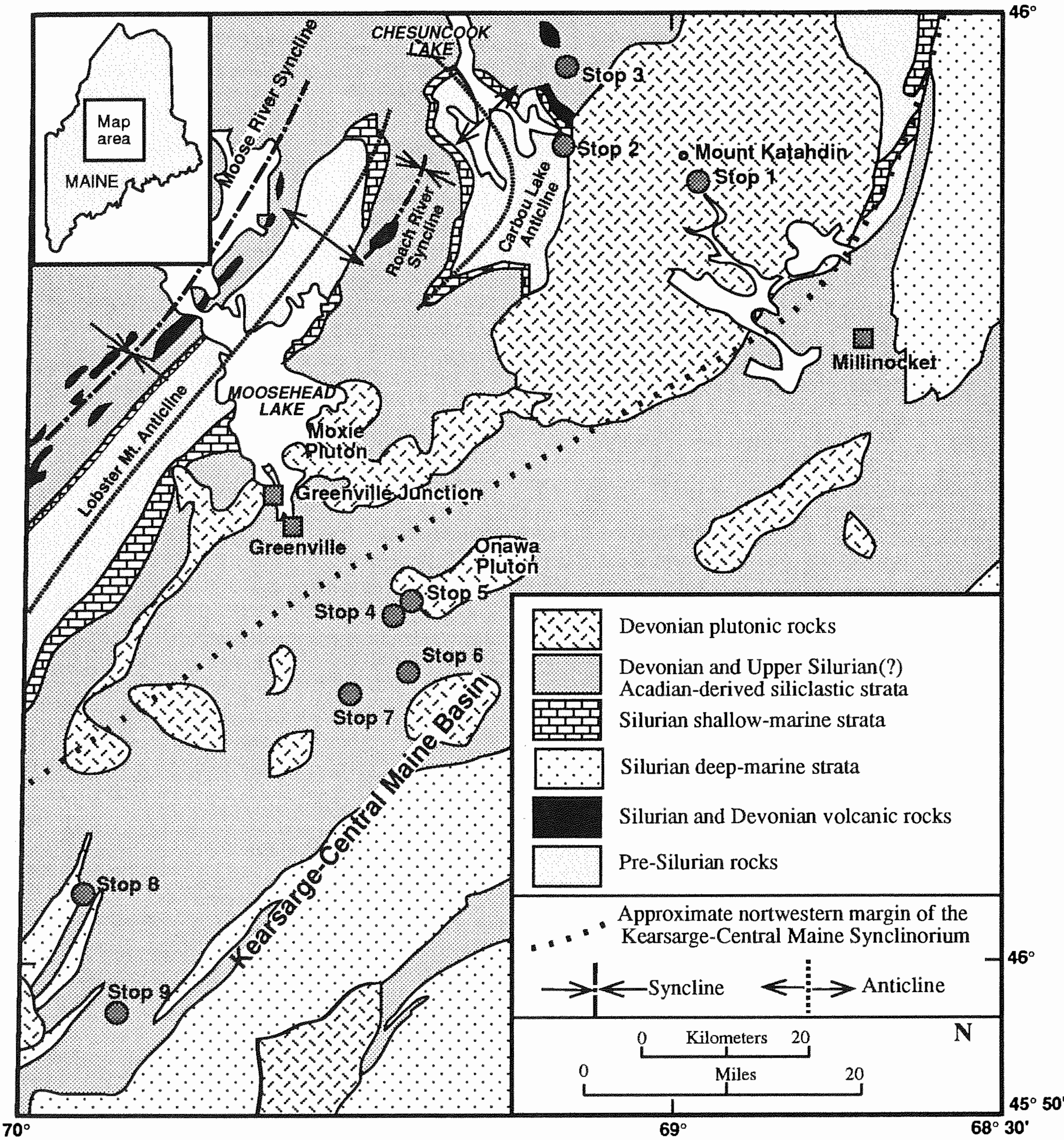

Figure 1. Geologic map of central Maine showing locations of field trip stops and major features discussed in this guide. Modified from Osberg and others, 1985.

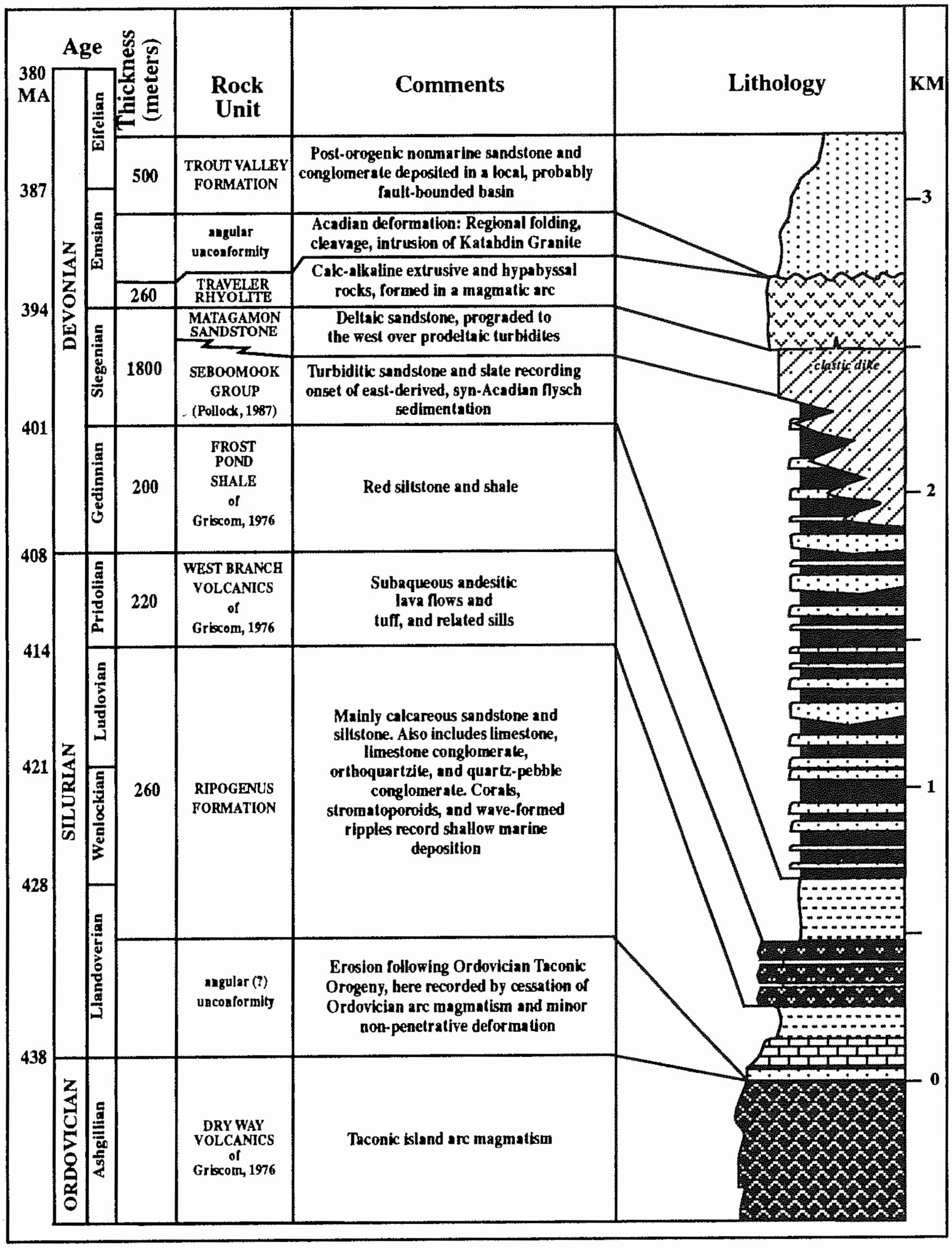

Figure 2. Stratigraphy of the Harrington Lake quadrangle. Adapted from Griscom (1976). Thicknesses reflect those mapped in this area only. Frost Pond shale, West Branch volcanics, and Dry Way volcanics are informal units defined in Griscom (1976).

Shallow-marine deposition along the anticlinorial belt was succeeded by deeper-water flysch sedimentation during Devonian time. The Devonian succession consists of turbidites (Seboomook Group of Pollock, 1987)[1] in Maine, Littleton Formation in New Hampshire) and in places, a younger succession of deltaic deposits (the Tarratine Formation and Matagamon Sandstone in Maine) that prograded over the turbidites. These Devonian clastic rocks are interpreted as part of an ancestral Acadian foreland basin. Acadian plate convergence caused this flexural depression to migrate cratonward to its final position in New York (the Catskill "delta"), but deformed, earlier incarnations of the Acadian foredeep are still preserved within the orogen (Bradley, 1983, 1987). Along the axis of the Piscataquis magmatic belt, foredeep deposits are partly younger than, partly coeval with, and partly older than magmatic rocks. Furthermore, foredeep deposits occur on both sides of the arc, as well as along its axis. Hence, we believe that the foredeep was superimposed on an active arc, and that subsidence was the result of flexure of the arc caused by a thrust load that lay outboard (southeast) of the arc (Bradley, 1983).

In the anticlinorial belt, the Acadian orogeny is manifested by regional-scale open folding, greenschist-facies metamorphism, cleavage development in suitable rocks, and intrusion and contact metamorphism by two large plutons, the Katahdin and Moxie. Evidence for Early Devonian age Acadian deformation will be discussed at Stop 1.

KEARSARGE-CENTRAL MAINE BASIN (DAYS 2 AND 3)

Days 2 and 3 will focus on strata within the Kearsarge-Central Maine basin that were deposited just prior to and during the earliest stages of the Acadian orogeny. This basin has been called the Merrimack trough in some publications, (e.g., Bradley, 1983; Osberg and others, 1989), but because Lyons and others (1982) have also applied this name to a distinctly older, different feature in southern Maine and New Hampshire, it has become more confusing than useful, and probably should be abandoned altogether. Many workers have called it the Merrimack synclinorium or Kearsarge-Central Maine synclinorium (KCMS), but these terms imply a relatively simple structure that is at odds with evidence that the basin is site of a closed ocean. By whatever name, this belt of Upper Ordovician through Lower Devonian deep-marine strata is one of the main sources of controversy regarding Acadian tectonics. The rocks were isoclinally folded, metamorphosed, and intruded by Devonian plutons. Various workers have suggested that the depositional basement was oceanic, continental, or transitional. Alternative interpretations for the mode of basin closure include subduction beneath the northwestern margin, subduction beneath the southeastern margin, subduction beneath both margins, or deformation of the basin fill without true (B-type) subduction of the basement. Hanson and Bradley (1989) reviewed the various alternative tectonic models.

Figure 3 is a generalized stratigraphic section of the Kearsarge-Central Maine basin based on the type sections in the Rangeley and Stratton quadrangles (~50 km southwest of the field trip area). The stratigraphy is broadly divisible into: (1) a lower sequence that was derived from the Taconic-modified margin of North America, that lay to the northwest, and (2) an upper sequence that was derived from outboard sources.

Lower Sequence

During this trip we will observe only the topmost part of the lower sequence, but the older units are inferred to extend beneath most of the trip area. In the Rangeley area, the lower sequence consists, from base to top, of four units: the Greenvale Cove, Rangeley, Perry Mountain, and Smalls Falls Formations. All are submarine fan deposits. Of these, only the Rangeley is *unequivocally* derived from the northwest, on the basis of plutonic conglomerate clasts that match the Ordovician Attean Quartz Monzonite in the Boundary Mountains anticlinorium (Moench and Pankiwskyj, 1988). Regional stratigraphic arguments summarized by Moench and Pankiwskyj (1988) suggest that the Perry Mountain and Smalls Falls Formations also are part of the northwest-derived sequence, and our limited, unpublished paleocurrent data from these two units tentatively support that interpretation. The three available paleocurrent studies show approximately southerly, southeasterly, and easterly paleoflow for the Smalls Falls Formation. At Stop 8, we will see the Smalls Falls Formation and discuss some of the uncertainties of paleocurrent analysis in this part of the Kearsarge-Central Maine basin.

---

1 The Seboomook Group (Pollock, 1987) includes most formations composing the Lower Devonian clastic wedge deposited in the Kearsarge-Central Maine basin (e.g., Carrabassett Formation), as well as in the anticlinorial belt and Connecticut Valley-Gaspe basin (e.g., Seboomook Formation of Boucot, 1961).

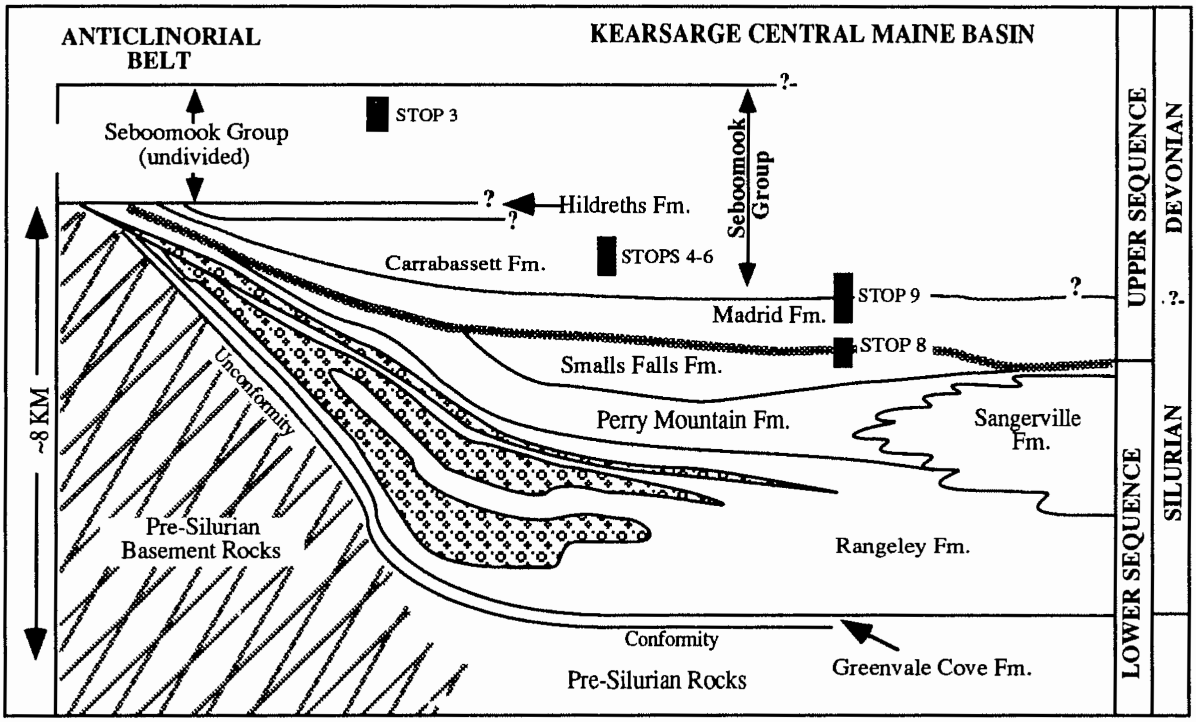

Figure 3. Stratigraphy of the Kearsarge-Central Maine basin in western Maine, modified from Hatch and others (1983). The Carrabassett Formation is only locally overlain by younger pre-Acadian rocks. Relative strati-graphic positions of rocks at field trip stops are indicated filled rectangles.

Upper Sequence

In the field-trip area, rocks assigned to the upper sequence of the Kearsarge-Central Maine basin include the Madrid and Carrabassett Formation, plus two younger informal units of local distribution that probably correlate with the Hildreths Formation and the undivided realm of the Seboomook Group (Hanson and Bradley, 1989) shown in Figure 3. On Day 2 (Stops 1-4), we will concentrate on the Madrid and Carrabassett Formations. The terminology used to describe sedimentary lithofacies is outlined in the Appendix to this guide. For a more detailed discussion see Hanson, 1984.

Madrid Formation.—The Madrid Formation (Day 3, Stops 8 and 9) is interpreted as an outer-fan deposit composed of thick bodies of B- and facies-C sandstones, and less abundant facies D. Sandstone framework grains are predominantly quartz and plagioclase. Three observations indicate derivation — or at least transport — from the northeast: (1) Paleocurrent data from the Madrid Formation show a remarkably consistent pattern of southwesterly paleoflow, parallel to the basin axis. (2) From northeast to southwest, the ratio of facies-B to facies-D turbidites decreases. (3) The Madrid ranges in thickness from 600 to 1500 meters in various parts of the field trip area and consists entirely of siliciclastic turbidites; 50 km to the southwest in the Rangeley region, the type Madrid consists of 100 m of calcareous siltstones (lower member) and only 200 m of siliciclastic turbidites (upper member). The Madrid is believed to mark the beginning of a transition in the Kearsarge-Central Maine basin from inboard to outboard provenance (Bradley and Hanson, 1989). The exact timing of the inferred provenance reversal is difficult to pinpoint because the Madrid lacks age-diagnostic fossils. The base of the Madrid has been placed in the Upper Silurian (Pridolian).

Carrabassett Formation.— The youngest regionally extensive unit in the Kearsarge-Central Maine basin is the Carrabassett Formation, which conformably overlies the Madrid Formation. It was deposited immediately prior to Acadian contractional deformation, and accordingly, was probably deposited in a convergent tectonic setting. It has been assigned an Early Devonian, probably Gedinnian age, but has not yet yielded age-diagnostic fossils. The sedimentary lithofacies comprising the Carrabassett Formation (Hanson, 1988, 1989; Hanson and Bradley, 1989) suggest an active slope environment characterized by local slope-basins and debris fans that were locally traversed by narrow channels (fig. 4).

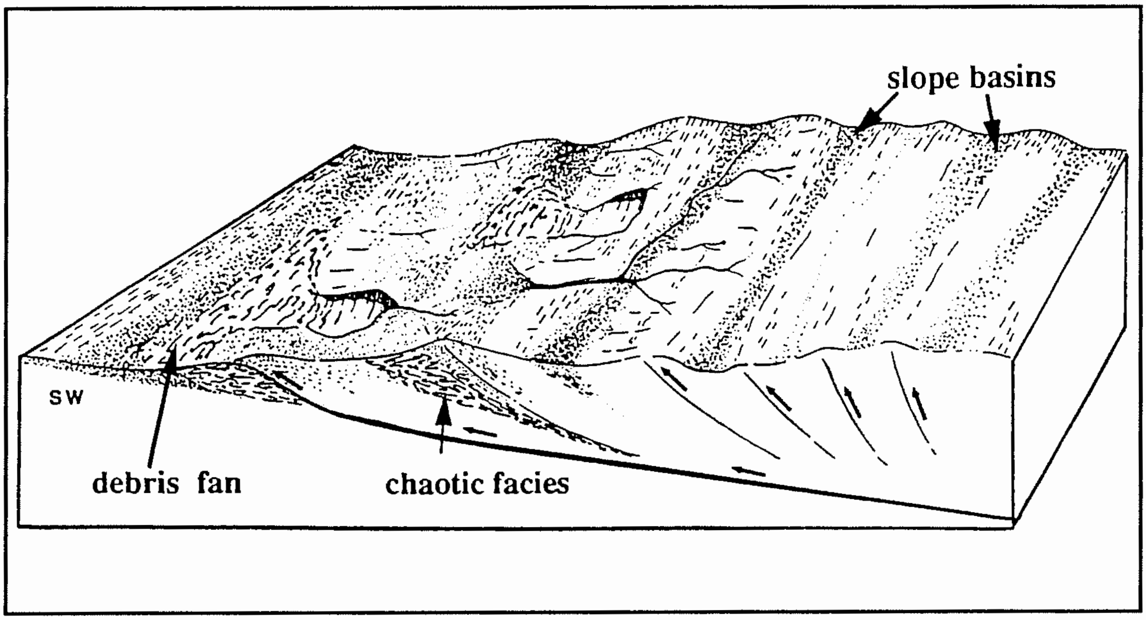

Figure 4. Depositional model for the Carrabassett Formation (inner trench slope) and the Madrid Formation (trench or foredeep axis).

The Carrabassett Formation is an ancient mud-rich turbidite system with an internally complex stratigraphy. Coarse sandstone and conglomerate are noticeably absent. At stops 4-6 you will see sedimentary features and facies associations that are typical of the formation. Disrupted facies are a major component of the Carrabassett Formation; exposures at Tobey Falls (Stop 6) clearly illustrate the abundance of these facies. We use the term *chaotic* for disrupted facies that were disturbed by sedimentary rather than tectonic processes. Chaotic strata consist of slumps and debris flows, the latter of which we loosely refer to as *olistostromes*. The chaotic strata of the Carrabassett Formation are typically composed of pelitic turbidites and hemipelagites typical of a slope setting.

The olistostromal nature of at least some disrupted rocks is unequivocally demonstrated at a number of excellent exposures (e.g. Hanson, 1983; and Hanson and Bradley, 1989), where debris flows occur at distinct horizons that have depositional upper contacts. We will see two good examples of debris flow deposits on Big Wilson Stream (Stop 4) and another on Borestone Mountain (Stop 5). The abundance of chaotic strata demonstrates that rapid sedimentation and active, unstable slopes prevailed throughout the deposition of the Carrabassett Formation.

Also contained in the formation are disrupted units that exhibit a fragment foliation defined by stretched and broken bedding (facies F2-3; see Appendix). Most of these disrupted beds contain multiple cleavages that yield phacoid-shaped clasts that may reflect in part, a premetamorphic tectonic fabric. A combination of soft-sediment and early tectonic deformational processes may have operated during the formation of these disrupted rocks. Side-scan sonar imaging of the lower slope of the Sunda arc accretionary prism has revealed mass movement of material extruded upward along thrust faults (Breen and others, 1986). The extruded material forms linear mud ridges that are over-ridden with further thrusting. Processes similar to these could explain some of the disrupted strata in the Carrabassett Formation.

Interbedded with and subordinate to disrupted units and pelitic turbidites, are two sandstone/siltstone-rich facies associations that we believe are submarine channel deposits; these are, (1) an upper-slope channel association, typically less than 25-meters thick and containing laterally discontinuous, thick, massive sandstones, and (2) a lower-slope-channel or fan-channel association (Stop 4), typically between 100 and 200 meters thick, and containing thinning-upward turbidite sequences with subordinate debris flow deposits. Channels suggested by the latter association probably traversed both the lower-slope and fans extending into slope basins as well as the principal foredeep.

Paleocurrent data are now fairly abundant for the Carrabassett Formation (Hanson and Bradley, 1989). As shown in Figure 8, they reveal overall northerly flow directions, although there is considerable scatter from one site to the next. Variations in paleocurrent directions result from (1) the complexities of the depositional environment where slope-channel, overbank, inter-channel, and basin flows are characteristically different and facies dependent, (2) the effects of emerging structures during the early stages of orogenesis, and (3) late-stage, local strike rotation of Acadian fold belts. Facies, paleocurrents, and stratigraphic relations together suggest that the Carrabassett Formation was deposited on an irregular submarine slope that descended to the north into the Madrid depositional basin (fig. 4). The slope, which was locally interrupted by slope basins, was extremely unstable. Because of high sedimentation rates and earthquakes generated by early orogenic tectonic activity, large quantities of sediment, mainly mud, were remobilized and deposited in a variety of slumps and debris flows. These chaotic deposits, along with turbiditic and hemipelagic sediments, formed the foundations of large, pelitic debris fans that covered the slope and filled local basins. Thick sandstone deposits were restricted to axial channels in basins and channels carved across the slope by turbidity currents. We will visit four localities on Day 2 (Stops 4-7) that have been instrumental in unraveling some of the complexities of Acadian flysch sedimentation in the Kearsarge-Central Maine basin.

GEOMORPHOLOGY

The topography in both the anticlinorial belt and the Kearsarge-Central Maine basin is controlled by the resistance of local metasedimentary and igneous rocks. Rock units vary greatly in their topographic expression as a result of internal variations in mineral composition and texture, both of which are greatly influenced by metamorphism. The more resistant rocks such as hornfels, massive sandstone, granophyre, and felsite form highlands that tower over lowlands underlain by weaker plutonic rock and strongly cleaved metasedimentary rocks.

Most mountains south of Katahdin, such as Borestone, Barren, Big Squaw, White Cap, and Saddleback, surround dioritic or gabbroic intrusions, and are composed of hornfels created by contact metamorphism of the Carrabassett Formation. Where the neighboring plutons are exposed, broad, irregular valleys have developed. Borestone Mountain (Stop 5), is an excellent example of a hornfels mountain. Beyond the influence of plutons, Acadian structures and their concomitant lithologies control the grain of the topography. Within the Carrabassett Formation ridges and valleys are often related to differential erosion of sedimentary facies associations. Thin sandstone units in the Carrabassett Formation are well jointed and easily excavated, forming narrow valleys, like those occupied by Little Wilson Stream and James Brook (Day 2, Stop 4). With a few exceptions, the ridge formers in the Carrabassett Formation are not sandstones, but chaotic units. Bedrock controls on geomorphic features will be emphasized at Stop 1 (Day 1), where we will show how granitic textures in the Katahdin pluton control topography in the Katahdin area, and Stop 5 (Day 2) where we will see how contact metamorphism has transformed mechanically weak slates to resistant, mountain-forming hornfels.

A SHORT HISTORY OF LOGGING IN THE WEST BRANCH REGION

By 1630, only twenty years after the Pilgrims arrived in New England, sawmills were being operated in York and Berwick in southern Maine. From these earliest days of Maine logging until about 1875, the principal wood harvested was pine. Pine was cut for lumber, and tall straight pine was used for masts; the best were saved for the King's navy. The King's pine was branded with the letter "A" and cutting one for private use was a capital offense.

The lumber industry moved northward during the 18th Century; loggers moved into the Androscoggin and Kennebec watersheds from Portland, and finally into the Penobscot watershed from Bangor, which became the lumber capital of Maine. Logging operations spread into the headwaters, both the East Branch and West Branch, of the Penobscot River in the 1830's. The West Branch River Driving Company sent long pine down the Penobscot to the navigable waters of Bangor. The loggers lived in the woods, from summer to late winter, then took the logs down river with them during the spring snow melt. At the end of the drive, they raised hell in Bangor until their money was gone, and they were dragged back into the woods by the crew bosses for another winter. Paper and pulpwood replaced lumber and pine by the last quarter of the 19th century. Great Northern Paper Company bought out the West Branch River Driving Company and their dams and built some of the largest paper mills in the country, in Millinocket and East Millinocket.

By the early 1900's a few all-weather roads began to penetrate the wilderness and to replace the seasonal tote roads that provisioned the woods camps. One was built from Moosehead Lake to the proposed site of the Ripogenus Dam for hauling material for that project. Later a steamboat, the Tethys, was hauled over the same road. This and other boats were used to haul pulp logs down the 20 mile-long Chesuncook Lake to Ripogenus Dam. Log drives ended on the West Branch and other rivers in Maine in the 1970's and all logs are now trucked or carried by rail to the mills.

In the early fall of 1846, on the first of his three trips to the Maine woods, Henry David Thoreau reached Abol Crossing (Day 1, Stop 1) in the company of some loggers who were repairing dams and booms for the drive the following spring. He came up the river in a bateau poled by his companions. Thoreau planned to climb Katahdin (he spelled it Ktaadn) from the south side by the Abol Slide, which formed in 1816. Dr. C.T. Jackson used this trail up the mountain in 1835 during the first geological survey of Maine, and Thoreau was quite familiar with his report, which he discussed several times in his *Maine Woods* (Thoreau, 1964). Thoreau climbed alone and reached the Tableland at the top of Abol Slide, but clouds and concern about being left behind by his companions forced him down the mountain before he reached the summit.

The Abol Slide is still much in evidences, a vertical gash toward the left side of the mountain as seen from Abol. Many other slides are also visible on Mount Katahdin itself and on the smaller mountains to the west, such as Owl Mountain, Barren Mountain, Mount OJI, and Doubletop Mountain. All of these slides involved the movement of a thin cover of regolith with its overlying vegetation and snow, all of which lie precariously on steeply-jointed, bedrock surfaces.

FIELD TRIP LOG

DAY 1

The road log starts from the Heritage Motor Inn in Millinocket. Some mileages are estimates from road maps. Drive east on Rte. 11 through Millinocket and turn right (northwest) on the state road, following signs to Baxter State Park. Drive 8.6 miles. At Millinocket Lake turn left onto the parallel Golden Road (a private logging highway) and drive approximately 1.5 miles to the Great Northern/Bowater gatehouse. Continue on the Golden Road 8.5 miles and park on either end of Abol Bridge, which spans the West Branch Penobscot River.

STOP 1. THE KATAHDIN PLUTON AS SEEN FROM ABOL CROSSING. The nearly horizontal skyline of Mount Katahdin, as seen from Abol, was believed to be a remnant of the so-called New England peneplain, a Cenozoic erosion surface that extended from here to Mt. Washington in New Hampshire (Goldthwait, 1914). The Tableland of Katahdin, which slopes quite steeply to the north, marks the upper surface of the Katahdin pluton (Griscom, 1976; Hon, 1980).

Mount Katahdin and its neighboring peaks, north of Abol Bridge, are underlain by the Katahdin Granite, a shallow-level pluton consisting mostly of biotite granite. The following considerations suggest that magmatism partly predated but largely postdated Acadian deformation: (1) the pluton truncates regional folds that deform rocks as young as the Traveler Rhyolite (Emsian, 394-387 Ma according to the DNAG time scale); (2) the Traveler Rhyolite, however, constitutes the volcanic carapace of the pluton (Hon, 1980); (3) the pluton itself displays little evidence of tectonic deformation; (4) deformation within the contact aureole appears to be less intense than outside the aureole (Hanson, 1988; Donley, 1993), and (5) isotopic ages from the pluton are widely scattered and inconsistent with stratigraphic constraints. Loiselle and others (1983) reported ages of 414±4 Ma ($^{207}Pb/^{206}Pb$ zircon) and 388±5 Ma (Rb/Sr whole rock). Denning and Lux (1990) reported an age of 400.1±1.0 Ma ($^{40}Ar/^{39}Ar$ biotite).

Differential uplift following Acadian orogenesis resulted in a regional tilt of 5° toward the northeast (Hon, 1980). Consequently, the map reveals an oblique cross-section (fig. 5) in which the Katahdin pluton can be seen as a shallow-level component of an extensive plutonic-volcanic complex. The volcanic carapace, the Traveler Rhyolite, is exposed along the northwest end of the pluton. Hon (1980) has shown that the Katahdin is also comagmatic with the deeper-level Moxie pluton (a calc-alkalic suite of diorite, gabbro, and minor ultramafic rocks) exposed in a 80-km-long tract extending southwest from the Katahdin. The Katahdin pluton, Moxie pluton, Traveler Rhyolite, and other Silurian and Devonian volcanic rocks along the anticlinorial belt, together comprise what we call the Piscataquis magmatic belt. Geochemistry suggests that magmatism was the product of subduction (e.g., Hon, 1980); regional geologic relations suggest to us that the subduction zone was more likely in the Kearsarge-Central Maine basin than in the Connecticut Valley-Gaspe basin, which lay to the northwest (Hanson and Bradley, 1989).

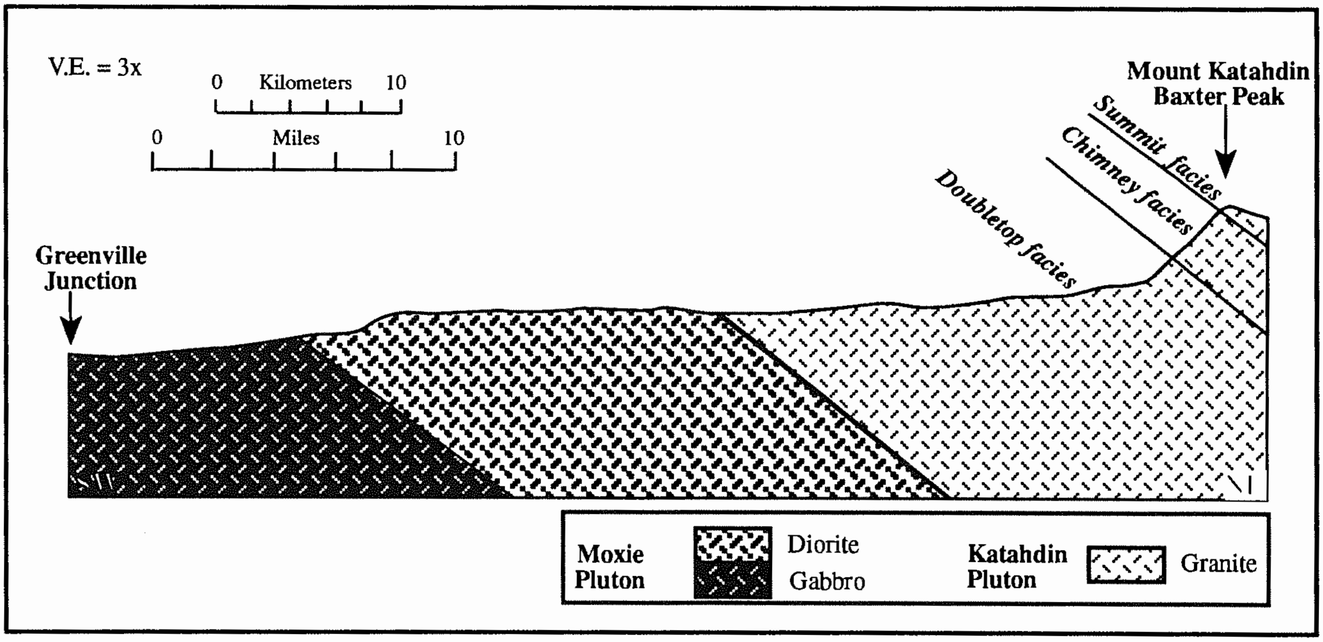

Figure 5. Profile along the Moxie-Katahdin trend between Mount Katahdin and Greenville. The top of Mount Katahdin still retains its resistant granophyric caprock (Summit facies).

To a geomorphologist the Katahdin pluton may seem somewhat enigmatic because of its extreme relief of nearly 1500 meters (4800 feet). Locally the pluton underlies both the highest peaks and the lowest basins. This contrast in topographic expression is the result of variations in the pluton's texture and the time of unroofing. The Katahdin pluton, a laccolith approximately 40 km in diameter and 5 km thick, is composed of seven different textural facies determined by cooling environment (Hon 1980). Two principal facies make up the bulk of the pluton and determine its geomorphology. The *Summit facies*, formed in the chilled zoned along the upper surface of the pluton, is a resistant granitic granophyre with a fine-grained interlocking texture; the *Doubletop facies* is a medium- to coarse-grained phaneritic granite formed deep within the pluton. Grain boundaries in the Doubletop facies are non-interlocking and straight; this facies therefore has little mechanical resistance to granular disintegration. The plateau-like summit of Mount Katahdin, at 5267 feet, is held up by the Summit facies, which dips northward beneath a cover of metasedimentary and resistant volcanic rocks. Once the Summit facies has been removed, erosion of the underlying Doubletop facies proceeds rapidly. Regional tilting resulted in early removal of the resistant rocks from along the higher southeastern margin of the pluton (fig. 5). The subsequent disintegration of the underlying Doubletop facies created the lowlands that now characterize the southern part of the pluton. As we stand here on Abol Bridge, underlain by the Doubletop facies, we can look northward to the steep south-facing slope of Mount Katahdin. The slope retreats to the north as the Summit facies is removed. Like a resistant sandstone on a high butte, the Summit facies is the caprock that protects the weaker rocks beneath it.

Also seen from this vantage point is a high terrace at approximately 1100 m. This terrace is part of a large lateral moraine formed during the last major stillstand of the late Wisconsinan Laurentide ice sheet. During this time, around 12,700 years ago, the ice margin was positioned along the Maine coast and the higher interior mountains stood out as nunataks above the ice surface (Shreve, 1985). On the north side of Mt. Katahdin are a number of glacial cirques. During deglaciation these cirques contained active glaciers that locally contributed to the continental ice mass (Caldwell, 1972).

Drive west on the Golden Road about 10 miles. Turn right andfollow gravel road about 0.3 mile past Pray's Store to a right fork, which leads in about 0.1 mile to Ripogenus Dam. Park at south side of the dam, then walk down dirt road to outcrops at foot of dam. Plan on being away from the bus for 2-3 hours.

Please use caution in the gorge below the dam. *Some of the outcrops are only exposed at low water, and the floodgates may or may not be open. A siren will sound shortly before they are opened.*

STOP 2. ORDOVICIAN AND SILURIAN ROCKS AT RIPOGENUS GORGE. This stop will involve a fairly rough traverse that focuses on the Silurian history of shallow water deposition and volcanism along the anticlinorial belt. Figure 6 shows the geology, based on mapping by Boston University's Geology Field Camp, and figure 2 shows the local stratigraphy, adapted from a Ph.D. study by Griscom (1976). Griscom's dissertation provides much background information on the three formations we will see.

Locality A, Dry Way Volcanics (of Griscom, 1987). The Dry Way volcanics consist of basalt in pillows and massive flows. Griscom (1976) estimated the stratigraphic thickness at greater than 1.5 km. These volcanic rocks, and a related nearby gabbroic pluton (Bean Brook pluton), are regarded by many workers as part of an arc terrane that collided with North America in mid-Ordovician time, causing the Taconic orogeny.

Follow "Dry Way" downstream ~100 m to pool.

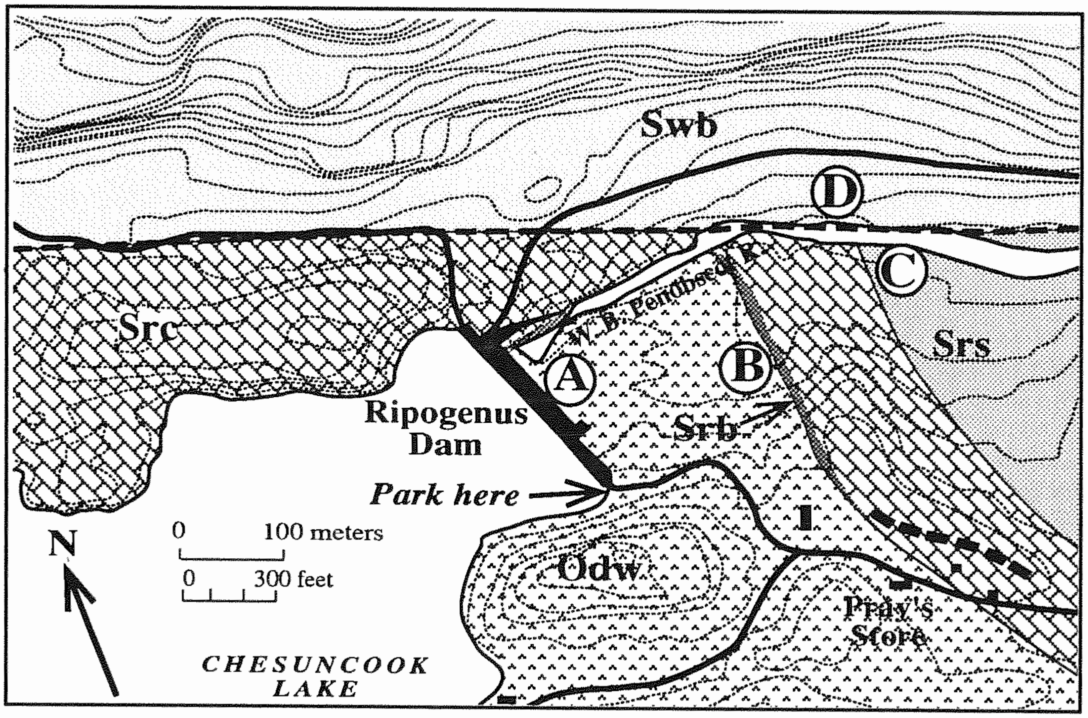

Figure 6. Geologic map of the Ripogenus Gorge area. Key to map units: **Odw**, Dry Way Volcanics (Ordovician); **Srb**, basal clastic member of the Ripogenus Formation (Silurian); **Src**, calcareous sandstone member of the Ripogenus Formation (Silurian); **Srs**, calcareous siltstone member of the Ripogenus Formation (Silurian); **Swb**, West Branch Volcanics (Silurian).

Locality B, Basal clastics and calcareous Sandstone member of the Ripogenus Formation.--Basal quartzose clastics (sandstone, pebble conglomerate) of the Ripogenus Formation overlie the Dry Way Volcanics (of Griscom, 1976) along a sharp contact. Hematite is locally present along the contact, and in thin fissures just below it, suggesting that an interval of subaerial erosion (corresponding to the time of Taconic orogenesis across strike in Quebec) preceded deposition of the Ripogenus (Griscom, 1976). Although an angular discordance is not obvious here, there is an angular unconformity exposed at the base of the dam. The 4- to 5-meter-thick basal clastic unit of the Ripogenus Formation is overlain by several tens of meters of calcareous sandstone. Weathered exposures display conspicuous rows of elliptical pits (typically 10-20 cm thick) at the more calcareous horizons. Shallow marine fossils, which commonly are found within these pits, include tabulate corals, rugose corals, brachiopods, and stromatoporoids. In nearby exposures, two polymict conglomerate horizons have been identified in the calcareous sandstone member. The conglomerates contain rounded, intraformational pebble- to cobble-size clasts of calcareous sandstone, calcareous siltstone, and limestone. In addition, one bed (~7 m thick) of light gray orthoquartzite occurs partway up the calcareous sandstone member. Griscom (1976) estimated the thickness of the Ripogenus Formation at about 260 m.

Traverse perpendicular to strike through woods for ~100 m to large outcrops along the river.

Locality C, Siltstone Member of the Ripogenus Formation.--The upper part of the Ripogenus Formation consists mainly of thin-bedded, green and white, calcareous siltstone. A horizon of pitted calcareous sandstone occurs near the base of the siltstone, suggesting an intertonguing relationship between the siltstone and calcareous sandstone members. Several hundred meters downstream along the south bank, the siltstone is conformably overlain by the West Branch volcanics (of Griscom, 1976). The siltstone has been contact metamorphosed by the Katahdin granite and (or) sills associated with the overlying West Branch Volcanics.

Go upstream 50-100 m and cross river on stepping stones above large pool.

Locality D, West Branch Volcanics (of Griscom, 1976).--The river here follows a vertical oblique-slip fault with a component of north-side-down dip-slip displacement. The West Branch Formation of Griscom (1976) is exposed on the north bank. It consists of prominent, cliff-forming outcrops of intermediate volcanic flows and sills, plus less resistant, slope-forming tuff and siltstone. At this stop, two sills sandwich a ~10 m interval of siltstone. Pillows and wave-formed ripple marks together indicate shallow-water deposition. The West Branch Volcanics are a calc-alkaline series with "transitional" affinities on various discriminant plots (Fitzgerald, 1991). The West Branch Volcanics form part of the Silurian and Devonian Piscataquis magmatic belt that lies along the northwestern margin of the Kearsarge-Central Maine basin. As mentioned in the regional geology section, this magmatic belt is regarded as the product of subduction that led to the Acadian collision.

Scramble uphill ~50 m through woods to dirt road that leads back to the north end of the dam. Return to bus. Depending on time and interest, there are two fairly quick, optional stops that can be made. (1) Very nice exposures of stromatoporoid-bearing calcareous sandstone of the Ripogenus Formation can be seen by descending the sluice at the north side of the dam. Below a 20-foot cliff at the base of the sluice, the basal clastic unit of the Ripogenus unconformably overlies the Dry Way Volcanics. (2) Follow the road that crosses the dam north for about one-half mile until the road begins to follow the lakeshore. There you can view a cliff of West Branch Volcanics that comes down to the road.

Here we will take a short detour for lunch at the Chesuncook Dam Boom House, about 2 miles west of the dam along the shore of Chesuncook Lake. The Boom House was a logging camp formerly used on the great log drives down the Penobscot. The log drives on the Penobscot ended in 1973. That same year a house of ill repute in Bangor closed and was being demolished when some loggers rescued an iron support beam from the house and moved it to the Boom House, where tools of the trade were welded to it. This totem pole is the Woodsman's Memorial that now sands in front of the Boom House. In front of the memorial is block of Lucerne Granite that once served as a door step to whore house. Although not a scheduled stop on the trip, Cambrian melange of the Hurricane Mountain Formation can be observed in shoreline exposures at the Boom House.

To continue the road log from stop 2 to stop 3, return to the Golden Road. Drive east about 1.5 mile, then turn left onto Telos Road. Follow Telos Road about 5 miles to north the end of Harrington Lake. Continue on another 0.5 mile to turnoff for Nesourdnahunk Gatehouse (now closed). Turn right, go another 0.5 mile to crossing of Soper Brook. Park. Follow brook downstream to lakeshore about 0.5 mile, then turn right and go a short distance to large outcrop along shore.

STOP 3. UNNAMED ROCKS OF THE SEBOOMOOK GROUP, HARRINGTON LAKE. This stop will involve a possibly wet traverse to a superb exposure of turbidite and slump deposits of the Seboomook Group, part of the Acadian foredeep described in the introductory text. The Seboomook (Pollock, 1987) is a name applied throughout most of Maine to a flysch sequence that blanketed the area during Early Devonian time. In the Harrington Lake quadrangle, Griscom (1976) estimated its thickness at about 1500 m. The Seboomook is overlain by prograding deltaic deposits of the Matagamon Sandstone (Hall and others, 1976). Overall sediment transport was toward the west.

Turbidites at this outcrop belong to facies D of Mutti and Ricci-Lucchi (1972). Foreset cross laminae indicate that paleocurrents were dominantly toward the west (fig. 7). Sedimentary structures are seldom preserved this well in the Acadian Orogen of Maine. None of the typical problems that have thwarted paleocurrent analysis in Maine are serious here (for example, tilt-correction of steeply plunging folds, correction for strain, 2-D exposures, obliteration by deformation or metamorphism, and poor fossil control).

A spectacular example of a stratabound, contractional slump deposit overlies the coherent turbidites (fig. 7). This slump illustrates a classic, recurrent problem in paleoslope analysis (Woodcock, 1979), which we will discuss on the field trip. The problem is: which of two fold geometries is appropriate — rumpled rug or sheath fold. If the rumpled rug model applies as is likely in this case, then the paleoslope (toward 075° or 255°) is normal to the tilt-corrected strike of axial planes and to the trend of fold axes. Considering the westerly paleocurrents, 255° would be the clear choice.

Return to Golden Road. Turn right (west) and drive 8-10 miles to fork in road. Bear left following sign to Greenville. Drive south 20-25 miles to the River's Inn, Greenville. End of Day 1.

DAY 2 (Figure 8)

From the center of Greenville travel south on Rte. 15 approximately 13 miles. Just before entering Monson, take a sharp lefthand turn onto the Elliotsville Road. Travel north, then northeast, approximately 8 miles to Big Wilson Stream. Park on the west side of the bridge.

STOP 4. CARRABASSETT FORMATION, TURBIDITE SECTION ON BIG WILSON STREAM, ELLIOTSVILLE. At this stop we will see a remarkably well-preserved section of turbidites in the Carrabassett Formation. The exposure is located just beyond the contact aureole of the Onawa pluton and displays greenschist-facies regional metamorphism. The section illustrated in figure 9 was measured from a series of excellent exposures between James Brook and Big Wilson Cliffs. This north-topping, 1.5-km-thick homoclinal section of well-bedded strata is sandwiched between disrupted strata having a composite thickness of several kilometers. The Stop 4 exposure is located near the base of the section.

Exposed here is a sequence of sandstone-rich turbidites with well preserved Bouma sequences. There are two channel sequences, each beginning with a broadly-channeled base followed by amalgamated sandstones and debris flows. The whaleback just south of the bridge is a debris flow that marks the base of the second major channel sequence. The sandstone-rich turbidites with thick-bedded sandstones are followed by more pelitic turbidites with progressively thinner sandstone/siltstone beds. Concomitant with this transition is a change from top-cut-out to base-cut-out turbidite sequences. The exposed bottoms of many sandstone beds contain scour marks, tool marks, and a variety of trace fossils. This section on Big Wilson Stream is interpreted to be a well-organized lower-slope-channel or fan-channel association. Grazing trails, such as *Paleodictyon*, suggest a bathyal to abyssal submarine environment. The presence of thick facies-D sandstones, exhibiting Tbc and Tc Bouma sequences, indicates that

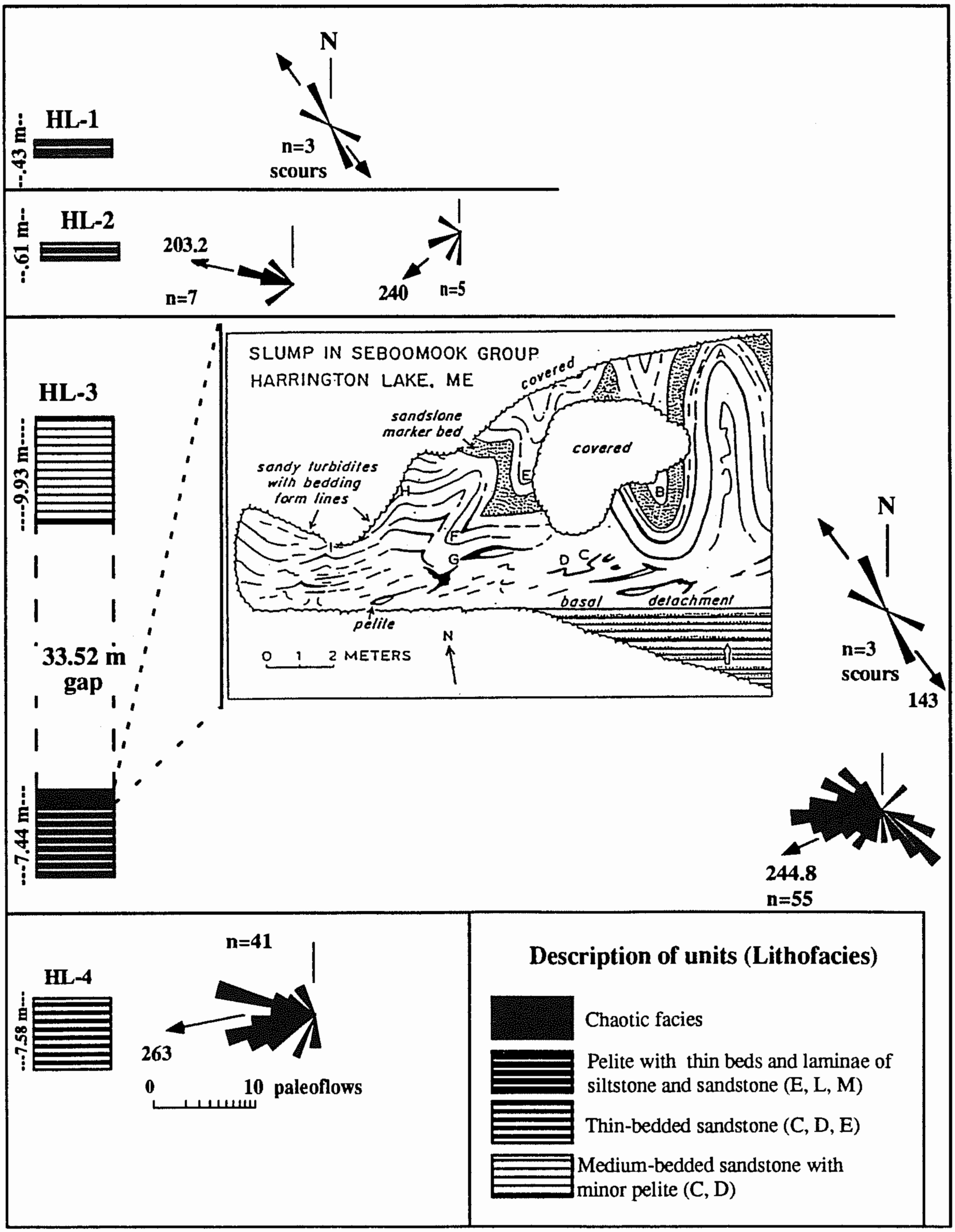

Figure 7. Generalized sections from exposures on Harrington Lake. Sections are arranged in relative stratigraphic order with their accompanying paleocurrent roses. All roses are from ripple foreset unless otherwise stated. The slump deposit that we will visit is detailed in the inset diagram to section HL-3.

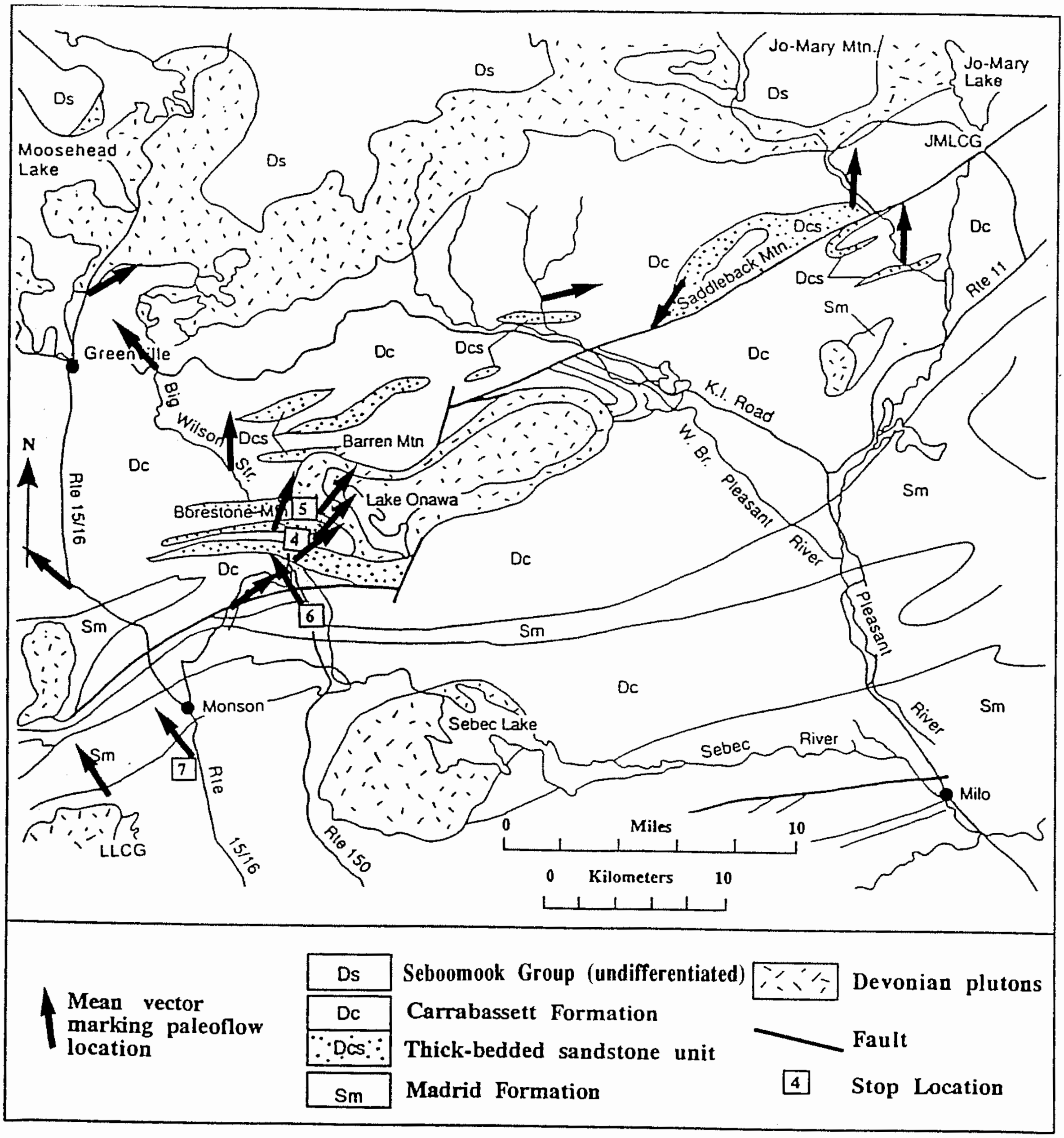

Figure 8. Geologic map of the northwestern margin of the Kearsarge-Central Maine basin in central Maine, showing field trip stops for Day 2 and paleocurrent directions in the Carrabassett Formation.

channel walls were shallow, allowing for a greater spread of overbank sands. The repetitive upward-thinning cycles suggest that the channel was free to migrate laterally and was not restricted between narrow canyon walls. A simple tilt-correction of paleoflow indicators gives southeasterly flow directions. However, regional mapping has shown that tectonic strike has been strongly deflected around the Onawa Pluton. After correcting for this deflection, the paleoflow directions are northeasterly.

From the east side of the bridge over Big Wilson Stream, follow Elliotsville Road north about half a mile to the well-marked trailhead for Borestone Mountain, shortly beyond the railroad crossing. The name "Borestone" has two spellings. Originally spelled "Borestone", the name was changed to "Boarstone" by the U.S.G.S. surveyor who mapped the quadrangle. Although the mountain is spelled "Borestone" on most maps, the original spelling is locally retained.

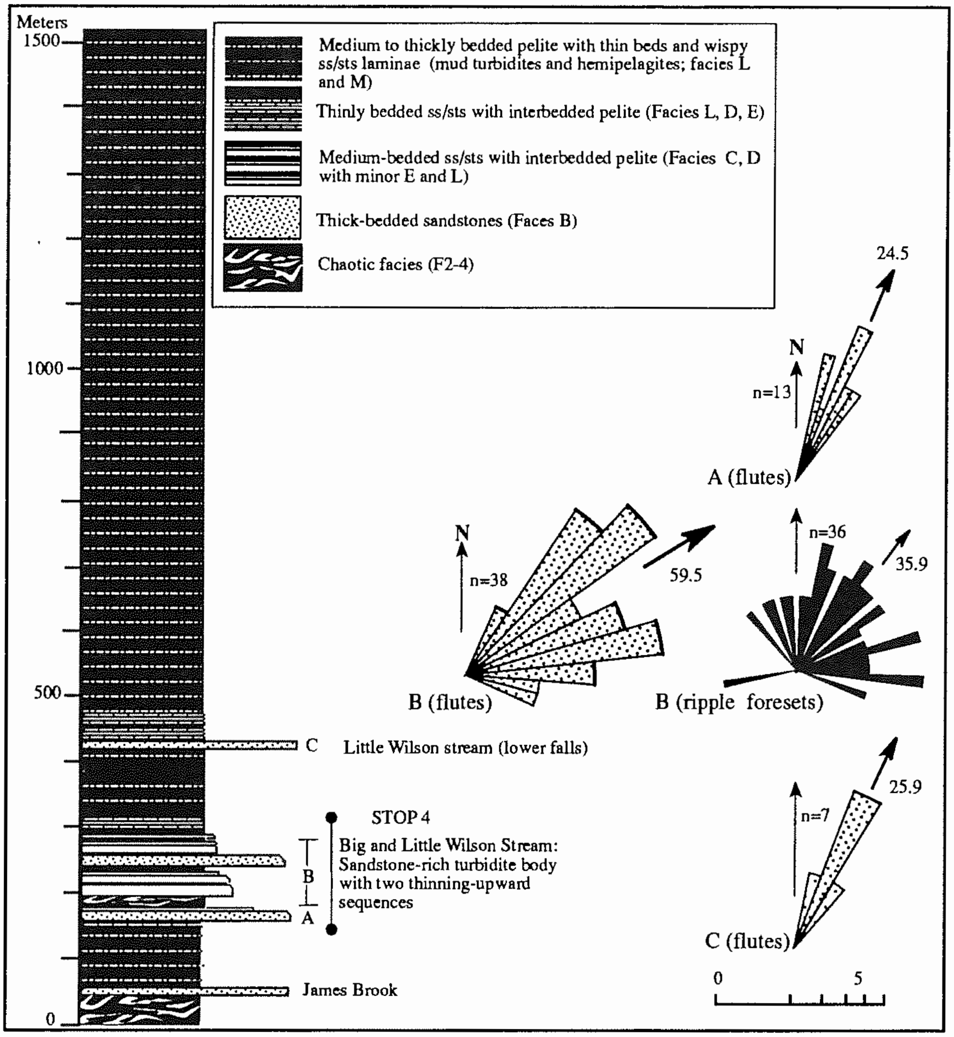

Figure 9. Homoclinal sequence, from James Brook to Big Wilson Cliffs, of sandstone-rich and pelitic-rich turbidites in the Carrabassett Formation. This bedded section is overlain and underlain by thick dissrupted assemblages.

Walk leisurely up the mountain. ***Please, do not bring rock hammers and stay on the trail and do not trample the vegetation.*** *The trail is maintained by the Audubon Society. You may wish to make a donation when you reach the visitors area at Midday Pond.*

STOP 5. PROGRESSIVE METAMORPHIC SEQUENCE AND SEDIMENTARY SLOPE ASSOCIATION OF THE CARRABASSETT FORMATION, BORESTONE MOUNTAIN.

Borestone Mountain, a mere 1970 feet (567 m), is underlain by contact-metamorphosed Carrabassett Formation in the aureole of the Onawa pluton (fig. 8). The contact aureole was originally mapped by Shailer Philbrick in 1936 and is a classic locality to observe progressive contact metamorphism. The Onawa pluton is a steep-sided, normally-zoned, dioritic stock (70 km^2). The outer margin of the stock ranges in composition from diorite to gabbro, whereas the inner region contains both granodiorite and granite. Being much less resistant than the surrounding hornfels, the plutonic rock has been excavated, forming the basin occupied by Lake Onawa. Philbrick (1936) noted that the resistance of rocks composing the mountain is related to metamorphic grade; the highest and most resistant rock is the migmatite, adjacent to the pluton. Therefore, the crest of the mountain lies near, and parallels, the contact. While walking from the base of the mountain to the top, you can observe an increase the metamorphic grade.

Philbrick subdivided the 1000-meter-wide contact aureole into four concentric zones:

(1) Spotted slate (not encountered along the trail).

(2) Andalusite "schist" (near beginning of trail). Fine-grained assemblage of quartz, chlorite, andalusite, biotite, and sericite. The texture is primarily microscopic with the exception of a few small andalusite porphyroblasts. The rock exhibits a faint relict cleavage, but nothing like the pervasive cleavage seen on Big Wilson Stream.

(3) Andalusite-biotite hornfels (along most of the trail). Medium-grained hornfels containing biotite, andalusite, quartz, orthoclase, and some muscovite. The rock has been thoroughly recrystallized; all relict foliation has been annealed and crystals are larger.

(4) Migmatite (crest of the mountain): Philbrick called this inner zone "injection hornfels". The rock is composed of a mixture of highly metamorphosed country rock and granitic-aplite veinlets. The veinlets appear to have been produced by the partial melting of the more quartzose-feldspathic layers within the country rock. The dominant mineral assemblage is quartz-perthite-biotite-muscovite; tourmaline, cordierite, andalusite, sillimanite, and sodic plagioclase occur locally. As seen along the trail, the boundaries between these metamorphic zones are gradational.

The sedimentary facies associations encountered along the lower half of the Borestone Mountain trail (fig.10) comprise an upper-slope facies assemblage with deeply incised, narrow sandstone channels, and abundant slump and debris flow deposits. The associations that compose the slope assemblage are listed below and can be easily located by following the trail map:

(1) Thick, laterally discontinuous, massive channel sandstones (Locality A) with minor associated medium- to thin-bedded, C- and facies-D sandstones. In contrast with the strata seen at Stop 4, thick facies-D sandstones are generally lacking, which suggests that channel walls were high enough to prevent lateral spreading of overbank sands and to inhibit channel meandering.

(2) Interchannel deposits (Locality C) containing thinly-bedded D-, and E-facies sandstones (composed of T_c sandstone only), and laminated-pelite facies (T_0 to T_5 of Stow and Shanmugam, 1980). We interpret facies D and E as occurring more proximal to channel margins than facies L.

(3) Slump and debris deposits (F2-1, F2-2 and F2-4). The rounded bedrock knob at the scenic overlook (Locality B) is a debris flow. The exposure at the overlook is a massive featureless pelite that offers few clues to its origin. However, the base the debris flow is well exposed between the overlook and the main trail, and here we can see that the flow overlies thin-bedded turbidites that were locally deformed by the movement of the overlying flow.

At the top of the mountain, if you make it that far, you will have a 360° panoramic view of central Maine. The summits of Borestone and Barren Mountains are held up by resistant hornfels in the contact aureole of the Onawa pluton. The basin between Borestone and Barren Mountains, including Lake Onawa, is underlain by the pluton itself. Sediment carried by Long Pond Stream is in-filling the northwest end of the basin. The stream flows across a thick deposit of alluvium (Bodfish intervale) before entering Lake Onawa where it forms an elongate delta showing well-defined subaerial and subaqueous levee deposits. The broad valley of Big Wilson Stream is visible to the southwest. Striking southeast, and curving tangentially toward the valley, are ridges of slate and sandstone of the Carrabassett Formation, which lie beyond the contact aureole. Most of the ridges are composed of chaotic strata; some of the intervening streams, such as James Brook and Little Wilson Stream, are located on bedded turbidite sections. The sandstone assemblage at Big Wilson Stream forms a ridge that can be traced westward where it intersects Little Wilson Stream, forming Little Wilson Falls. Most of Barren Mountain from the base, near Long Stream Pond, to the 1900-foot contour is composed of chaotic strata.

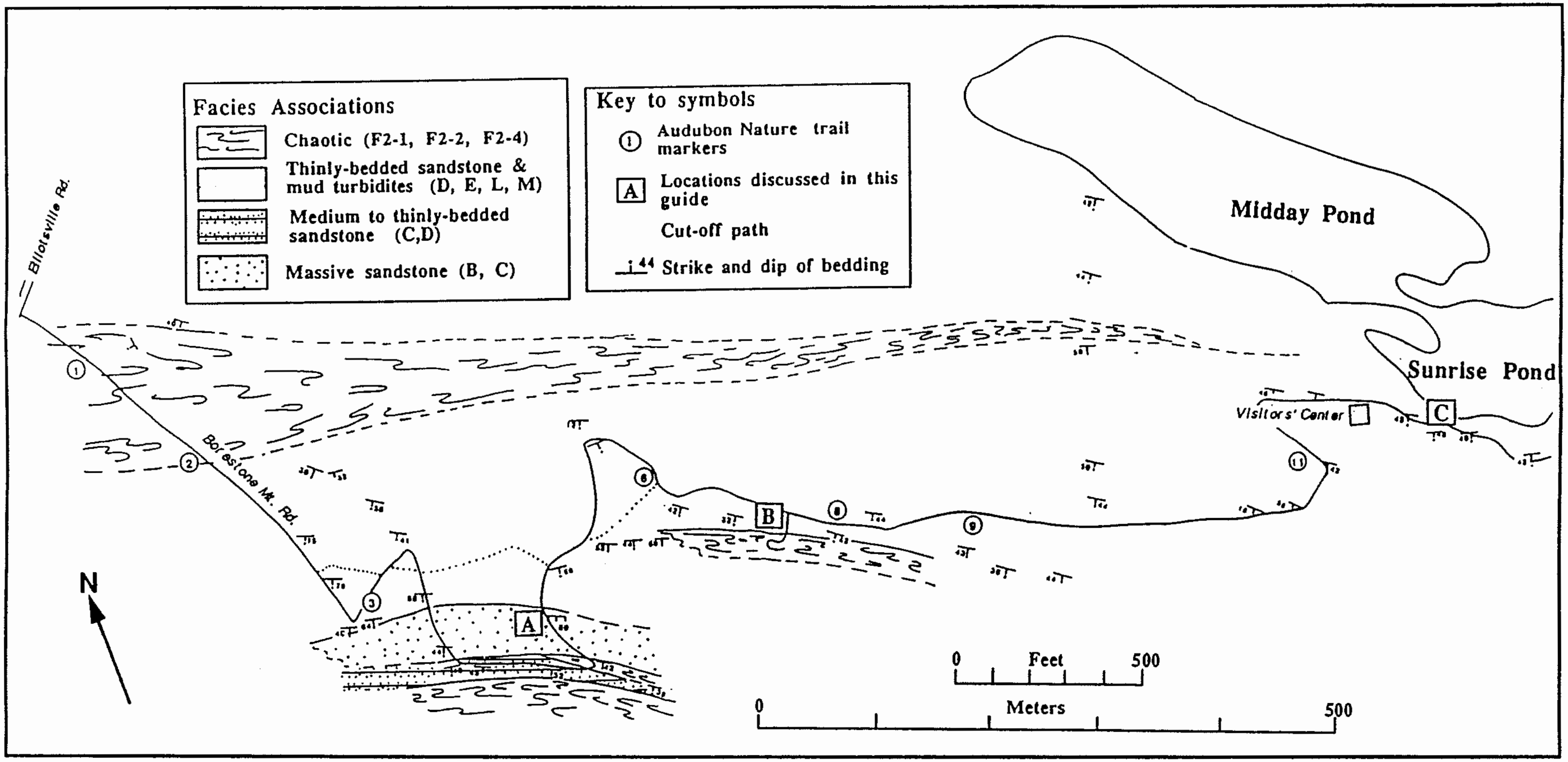

Figure 10. Geologic map of the Borestone Mountain trail, between the Elliotsville Road and the Audubon Visitors Center on Sunrise Pond. These strata comprise an upper-slope facies assemblage, characterized by pelitic turbidites/hemipelagites, laterally-discontinuous massive channel sandstones, slumps, and debris flows.

Drive south 0.8 miles to "Y" in road, bear left on the Willimantic road and continue about 4.5 miles. Cross Big Wilson Stream. The outcrop exposed in the stream is a lens of the Madrid-like rocks that may be in fault contact with the Carrabassett Formation. This outcrop contains an excellent example of a strataform debris flow. Continue approximately 0.8 miles until reaching a dirt road on left. Turn left and drive toward Leeman Brook. Park, cross brook and follow path to picnic area on Big Wilson Stream.

STOP 6. CARRABASSETT FORMATION, CHAOTIC ASSOCIATION AT TOBEY FALLS ON BIG WILSON STREAM, WILLIMANTIC. Over 400 meters of the Carrabassett Formation is exposed along Big Wilson Stream, both upstream and downstream from Tobey Falls. Unlike the exposures at Stop 4, strata here are predominantly disrupted. Disrupted units like these are typical and may compose up to 80 percent of the formation (fig. 11). On the eastern shore, sandstone beds that are somewhat reminiscent of the Madrid Formation are packaged between thick disrupted units. A preliminary analysis of paleoslope indicators suggests sediment transport to both the northeast and northwest (fig. 11). Yet to be determined is the relative importance of soft-sediment versus early tectonic deformation in the formation of the disrupted units. Not all units can clearly be identified as olistostromes, and some exhibit multiple (scaly?) cleavages reminiscent of those observed in accretionary prisms.

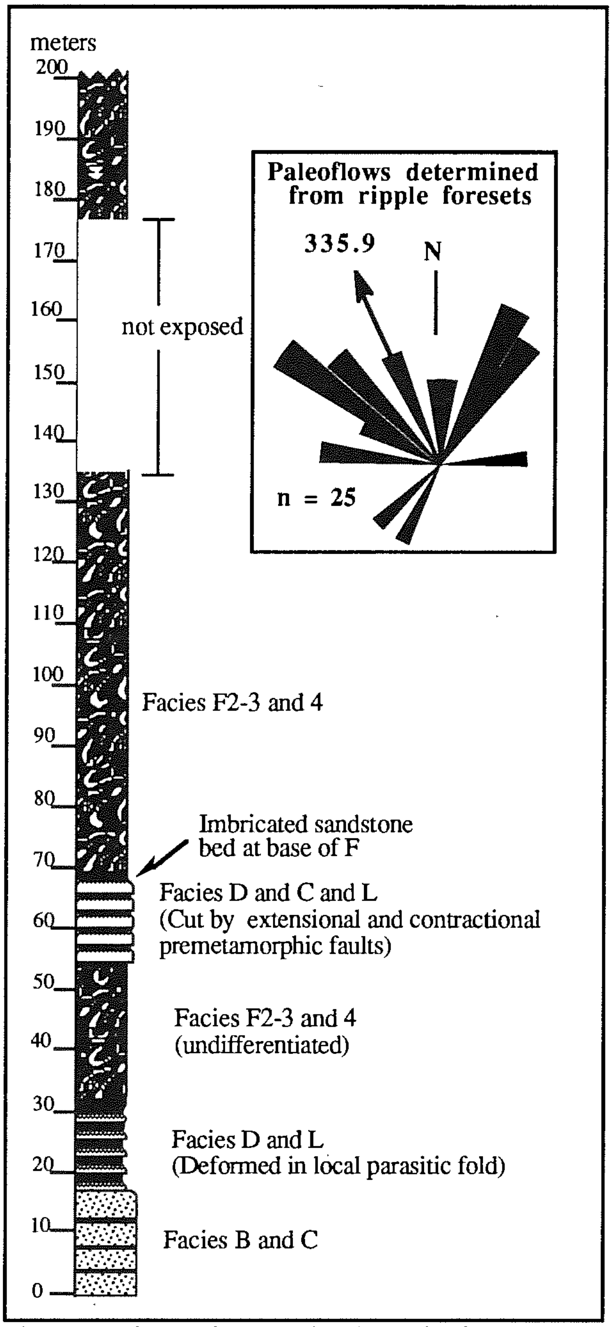

Figure 11. Generalized section (Stop 6) of the Carrabassett Formation at Tobey Falls.

Continue towards Monson on the Willimantic road for approximately 5 miles, turn left onto North Guilford Road. Drive approximately one mile to slate-paved road leading to the processing plant of the Portland-Monson Slate Company.

STOP 7. CARRABASSETT FORMATION, PORTLAND MONSON SLATE COMPANY, BURMAN QUARRY #6. Since the 1800's slate has been mined from a number of quarries in the Carrabassett Formation. The quarries lie in a northeasterly belt that extends from Blanchard to Brownville. The Portland-Monson Slate Co. owns a number of quarries in Monson, which lies in the center of this belt. The Burman Quarry #6, located south of Monson on the Guilford road, is the only one active at present. Most slate from this quarry is used for floor tile; however, some is also used for memorials, electrical switch boards, and a variety of specialty items. The "vein" of high-quality slate that is being mined is a 2- to 3-meter thick bed of "massive" pelite that is underlain by thin-bedded turbidites and hemipelagites and overlain by a sequence of thick turbiditic sandstones. The slate vein itself is not accessible for close inspection, but milled pieces from it are available. Thin, wispy chaotic stringers of siltstone are widely spaced throughout the milled stock. Some pieces (called "speckled slate") contain numerous 1-2 mm vertical burrows. These features suggest that the high-quality slate is composed of pelitic turbidites and hemipelagites, some of which have been disrupted.

The quarry pit follows the trend of an underground mine that was excavated in the 1800s. The current quarry operator (John Tatko, Portland-Monson Slate Co.) widened the excavation and removed the overburden, forming the present open quarry.

Return to Greenville.

DAY 3

Drive south on Rte. 15 to Abbott, then west on Rte. 16 through Bingham. Immediately after crossing the Kennebec River in Bingham, turn right (north) on an unnumbered road that follows the west bank of the river. Drive 1.2 miles to a pullout on the right. From here walk about 200 m down a small dirt road, going around a locked gate, to enormous outcrops below Wyman Dam.

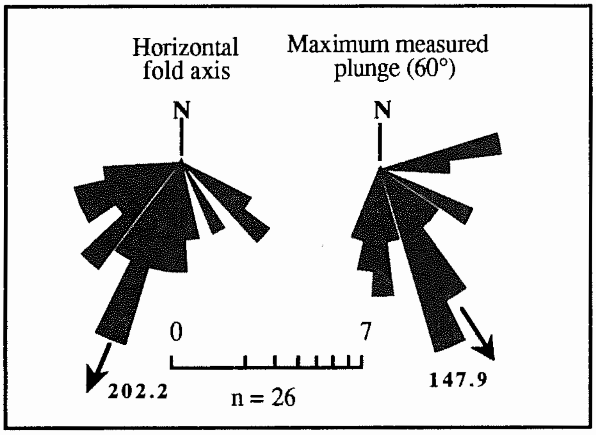

Figure 12. Paleocurrent roses for Smalls Falls Formation at Wyman Dam showing single-tilt and double-tilt (using 60° plunge) corrections. The true current flow probably falls somewhere between these two extremes.

STOP 8. SMALLS FALLS AND MADRID FORMATIONS AT WYMAN DAM

Beautiful exposures of sedimentary and structural features of the Smalls Falls and Madrid Formations (fig. 3) are exposed below Wyman Dam. This is one of the largest outcrops in Maine, and also one of the few clean exposures of the Smalls Falls Formation where paleocurrent indicators are present. The overlying Madrid Formation consists of amalgamated sandstones that commonly display low-angle laminations that may correspond to antidune "backsets", or to scour fills. Pitted horizons of deformed brachiopod molds are present and intensive search by field trip participants is encouraged because it might yield the first biostratigraphically useful fossils from the Madrid. As noted in the section on regional geology, the Smalls Falls-Madrid contact probably marks a transition from inboard to outboard provenance.

The upper part of the Smalls Falls Formation consists of rusty-weathering, thinly-bedded, cross-laminated turbidites. Paleocurrent indicators are present in greater abundance than in any other known exposure of the Smalls Falls Formation (fig. 12). However, structural corrections here are ambiguous, a problem that is widely encountered in orogenic belts and will be addressed at this stop. Depending on the structural correction employed ("single tilt" versus "double tilt" versus "incremental plunge"), paleocurrents are between SSE and SSW.

Retrace path to Bingham, then drive south on US 201 to Solon. Before reaching the center of town, turn right on Falls Rd. Drive 0.3 miles. Park at a large cleared area overlooking a dam and what is left of Caratunk Falls on the Kennebec River. A plaque commemorates the portage of Benedict Arnold's fleet of leaky bateaux here in October, 1775, during his campaign against Quebec in the early days of the Revolutionary War. This episode is brought to life in Kenneth Roberts' classic historical novel, Arundel. Walk downstream about 500 feet along a dirt road. Where it ends, follow a rough path to the right (watch for poison ivy) about 100 feet to large exposures along the river. Initials carved in the outcrop near its downstream end read "BA 1775".

STOP 9. MADRID AND CARRABASSETT FORMATIONS AT ARNOLD'S LANDING

This stop features excellent exposures of the uppermost Madrid and lowermost Carrabassett Formations, and their conformable contact. Figure 3 shows the stratigraphic position of this stop. Figure 13 shows a detailed measured section (beginning at river's edge) across the contact; it records a transition from submarine fan to slope

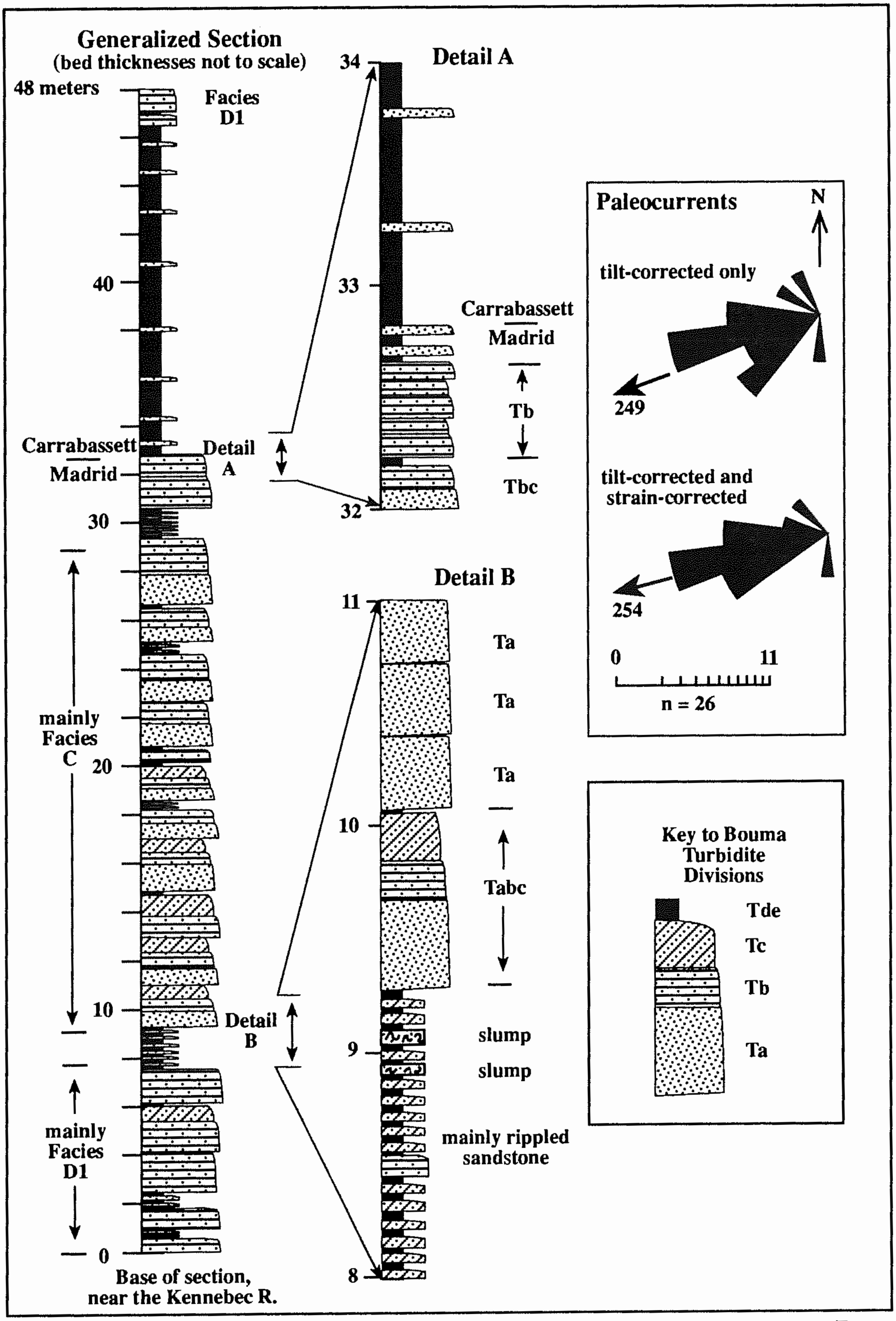

Figure 13. Detailed measured section across the conformable contact between Madrid and Carrabassett Formations at Arnold's Landing, Kennebec River. Column and paleocurrent roses (N=26) for the cross laminae in the Madrid Formation: (A) Based on single-tilt correction. (B) Based on strain-correction of data in A. Most direction shows only a small clockwise shift as a result of unstraining.

facies. The upper Madrid Formation consists of partial to complete Bouma sequences (facies C and D) and amalgamated sandstones showing erosive bases (facies B). Channeling suggests a relatively proximal (e.g. mid-fan) depositional setting, in contrast with inferred outer fan facies elsewhere in the Madrid to the southwest (Bradley and Hanson, 1989). A contractional slump horizon can be seen about 10 meters from the water's edge. Near the water's edge, an early fault showing ramp-on ramp and flat-on-ramp geometries is interpreted as a contractional structure that probably predated or accompanied regional deformation. The abrupt depositional contact between the Madrid and overlying Carrabassett Formation is poorly exposed in the woods along the access trail. Good exposures of the lowermost Carrabassett Formation are found near the river's edge a few tens of meters downstream. Bedding in these metapelites is marked by thin siltstone laminae, some of which are graded. They are interpreted as mud turbidites deposited on a submarine slope.

Cross laminae are abundant in facies D turbidites at Arnold's Landing and indicate flow toward the west-southwest (vector mean 249°) by single-tilt (fig. 13). This is typical of the Madrid Formation. Structural plunge, deduced from bedding-cleavage intersections, is gentle and thus negligible for paleocurrent analysis here. Elliptical calcareous concretions in some of the thicker facies-B sandstone bodies, however, show that the rocks have been penetratively strained, and this casts doubt on the accuracy of the paleocurrent directions cited above. On the bright side, these strain markers provide a rare opportunity to measure errors in paleocurrent directions that would be introduced by ignoring strain (in general, this is what we are forced to do, since strain markers are rare). Strain correction using a new orthographic technique yields results that are only about 10° more westerly than the trend prior to strain correction.

Return to Rte. 201 and drive south about 25 miles, through Skowhegan, to I-95. Follow I-95 back to Boston.

Acknowledgements

Research on the Carrabassett Formation was supported by the Maine Geological Survey and by the National Science Foundation (Grant #EAR87-20915: Lindley Hanson, Principal Investigator; Co-Investigator, Dwight Bradley). We are grateful for the assistance and hospitality of John Tatko, General Manager, Portland-Monson Slate Co., and Jack Dunstan, Manager, Borestone Mountain Wildlife Sanctuary.

APPENDIX
SEDIMENTARY LITHOFACIES

LITHOFACIES CATEGORIES

The lithofacies we used to describe Silurian and Devonian turbiditic formations fall into three principal categories (fig. 14); (a) sandstone/siltstone-rich turbiditic facies (Table 1), (b) pelitic-rich turbiditic facies (Table 2), and (c) disrupted facies (Table 3) respectively. A facies association is a combination of facies from one or more categories that occur together and that characterized a particular depositional environment.

A. Sandstone/siltstone-rich turbidite and related facies. This facies category is relatively sandstone-rich, typically containing greater than 40% sandstone. The sands were deposited by turbidity currents, grain flows, or some other related mechanism. With the exception of certain thick sandstone beds, strata in this category can be described using the Bouma (1962) divisions (Figure 15). The lithofacies classification used for these strata was adapted from Mutti and Ricci Lucchi (1972) and is outlined in table 1.

B. Pelitic facies. These facies include pelitic strata deposited by mud turbidites and hemipelagic settling. They may also occur as distal deposits and overbank deposits of more sand-rich turbidity currents. Pelitic strata are subdivided into two general facies (Hanson, 1988); laminated pelite (L), and massive pelite (M). Beds and laminae composing these facies are described (Hanson 1988, Hanson and Bradley, 1989) using the terminology of Stow and Shanmugam (1980). Poor preservation of sedimentary features in most pelitic rocks of the Carrabassett Formation has hindered attempts to use the original facies classification of Stow and Shanmugam (1980).

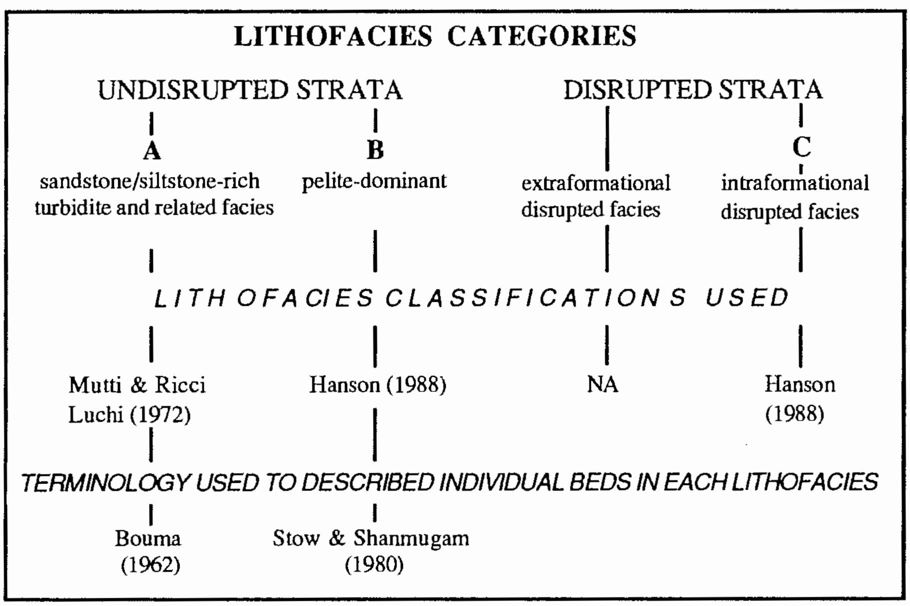

Figure 14. Outline of lithofacies classifications and references used in this guide.

C. Intraformational disrupted facies. These facies include any strata characterized by premetamorphic or synsedimentary disruption, such as submarine slump and landslide deposits, mud diapirs, and strata disrupted by premetamorphic or synsedimentary faulting. Intraformational disrupted units are composed of strata that are derived locally from within the same basin. Extraformational disrupted units contain exotic blocks that have been transported into the basin from some other terrane. All disrupted units of the Carrabassett Formation are intraformational.

SEDIMENTARY LITHOFACIES

Sandstone-rich turbidites facies. Sandstone-rich turbidite facies are primarily classified by the sequence of Bouma units composing each bed. Bouma (1962) noted that the sedimentary structures with a turbidite bed, deposited during a single event, occur in a predictable pattern or sequence. The complete sequence is shown in Figure 15. The sequence of Bouma units present reflects the strength and sand content of the turbidity current, and the distance traveled. Turbidite beds are described using *T* (standing for turbidite) followed by the small letters (a,b,c,d and e) indicating the divisions present in the bed.

Facies A	**Arenaceous-Conglomeratic Facies**
Description	Conglomerates, pebbly sandstones and medium- to very coarse-grained sandstone; Bouma sequence not applicable. Internal sedimentary structures such as grading, imbrication, large-scale cross-stratification, etc. may be present or entirely lacking.
Comments	*Generally absent from the Carrabassett Formation,* but common in the Rangeley Formation.
Facies B	**Arenaceous Facies**
Description	Laterally pinching, thick-bedded, medium-fine to coarse-grained massive or laminated sandstones. Dwatering structures are common along with flutes and load casts.
Comments	Present, but not a major facies of the Carrabassett Formation. Sandstones in the Carrabassett Formation are medium-fine to medium grained and generally lack dish structures. Commonly indistinguishable from facies C unless lateral continuity is observable.
Facies C	**Arenaceous-Pelitic Facies**
Description	Interbedded sandstone and pelite: complete Bouma sequences often represented; high sandstone to pelite ratio.
Comments	Subfacies of Mutti and Ricci Lucci, 1975; or Walker and Mutti, 1973 are not applied here.
Facies D	**Pelitic-Arenaceous Facies I**
Description	Interbedded pelite and sandstone (siltstone); Ta or Ta-Tb Bouma divisions missing; moderately high to very low sandstone (siltstone) to pelite ratios.
Facies E	**Pelitic-Arenaceous Facies II**
Description	Lenticular beds of sandstone characterized by flat, sharp bases and wavy tops interbedded with pelite.
Comments:	Facies E in the Carrabassett Formation are composed of medium fine-grained sandstone. Sandstone (siltstone) to pelite ratio is variable. Ripple tops may be graded and contain pelite laminae which thicken toward the troughs. Interpreted as overbank deposits.

Table 1. Sandstone and siltstone-rich turbidite and related lithofacies. (Modified from Mutti and Ricci Lucchi 1972.)

Pelitic Lithofacies. Non-disrupted pelitic strata are divided into only two facies, based on the recognition of fine-grained sand or silt laminae (table 2). Most pelitic strata in the Carrabassett Formation contain silt laminae spaced a few millimeters to as much as 30 cm apart. In overbank and interchannel deposits the thickness and density of laminae reflect the distance from channel margins. There also appears to be a continuum between these facies and the more sandstone-rich facies D and E. Many thick, apparently massive pelitic units have been found to be muddy debris-flow deposits and are often difficult to distinguish from non-disrupted massive pelite. Contourites have not been recognized in the Carrabassett Formation; the observed sedimentary structures and lack of extensive bioturbation suggest that most pelitic beds were deposited from turbidity currents.

Disrupted Lithofacies. Disrupted facies (table 3) are composed of either chaotically mixed lithologies, broken strata, or folded beds that were deformed or transported by syndepositional or premetamorphic-tectonic processes. facies F1, which is absent from these formations, contains clasts or blocks that are extraformational (not originating from within the basin). Intraformational chaotic facies (F2) are composed of deformed strata derived from deposits within the basin. All chaotic units within the Carrabassett Formation were derived from the mass-wasting or deformation of local strata. Subdivision of intraformational facies is based on the intensity of disruption. facies F2-1,-2 and -4 are common in the Carrabassett Formation and are the result of mass-wasting. Facies F2-3 is more problematic and may be related to premetamorphic faulting that accompanied early closure of the basin. (See Introduction.) Other processes, such as diapirism may have from chaotic units but would be difficult to identify.

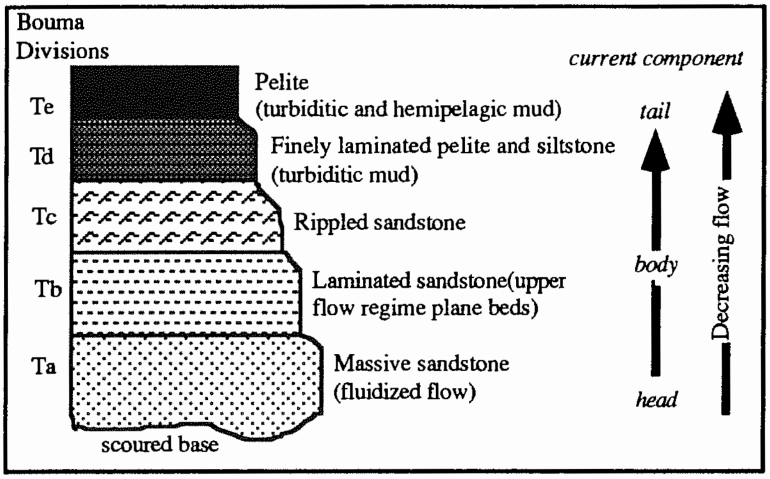

Figure 15. Complete Bouma sequence with description of Bouma divisions (Bouma, 1962)

Table 2. Pelitic lithofacies of the Carrabassett Formation. These facies are related to the mud-turbidite sequence described by Stow and Shanmugam (column 1980).

PELITIC FACIES (Hanson 1988)		SEDIMENTARY STRUCTURES (Stow and Shanmugam 1980)	
M	*Massive pelitic facies*	P	Bioturbated pelagic or hemipelagic pelite
		T7	Ungraded mud
		T6	Graded mud with or without silt lenses
L	*Laminated pelitic facies*	T5	Pelite with wispy, convolute silt laminae
		T4	Pelite with indistinct and discontinous silt laminae
		T3	Pelite with parallel silt laminae
		T2	Irregular to lenticular rippled silt layer in pelite
		T1	Convolute laminae in relatively thick pelite
		T0	Basal lenticular siltstone or fine-grained sandstone with climbing ripples

Table 3. Classification of disrupted lithofacies.

F1	***Chaotic deposits with exotic clasts***
F2	***Chaotic deposits with intraformational clasts***
F2-1	***Extensional chaotic facies.*** Strata are cut by minor normal faults.
F2-2	***Moderately-disrupted chaotic facies.*** Strata are faulted and folded, but topping direction and original lithofacies is still recognizable.
F2-3	***Highly disrupted, foliated-chaotic facies.*** Similar to F2-4 but with the appearance of a fragment foliation or phacoidal cleavage.
F2-4	***Highly disrupted,Non-foliated chaotic facies.*** original bedding is unrecognizable.

REFERENCES

Boone, G. M., and Boudette, E. L., 1989, Accretion of the Boundary Mountains Terrane within the northern Appalachian orthotectonic zone, *in* Horton, J.W., Jr., and Rast, N., eds., Melanges and olistostromes of the U.S. Appalachians: Geological Society of America, Special Paper 228, p. 17-42.

Boone, G. M., Doty D. T., and Heizler, M.T., 1989, Hurricane Mountain Formation Melange: Description and tectonic significance of a Penobscottian accretionary complex, *in* Marvinney, R.G., and Tucker, R.D., eds., Structure and stratigraphy: Studies in Maine geology, v. 1: Augusta, Maine, Maine Geological Survey, p. 333-84.

Boucot, A.J., 1961, Stratigraphy of the Moose River Synclinorium, Maine: U.S. Geological Survey Bulletin 1111E, p. 153-187.

Bradley, D.C., 1983, Tectonics of the Acadian orogeny in New England and adjacent Canada: Journal of Geology, v. 91, p. 381-400.

Bradley, D. C., 1987, Tectonic controls of stratigraphy in the Acadian foreland basin, Northern Appalachians: Geological Society of America, Abstracts with Programs, v. 19, p. 6.

Bradley, D.C., Hanson, L.S., 1989, Melanges and turbidite facies of the Madrid Formation, Central Maine, *in* Berry, A.W., Jr., ed., Guidebook for field trips in southern and west-central Maine: Farmington, Maine, University of Maine, New England Intercollegiate Geological Conference, 81st Annual Meeting, p. 183-199.

Breen, N.A., Silver, E.A., and Hussong, D.M., 1986, Structural styles of an accretionary wedge south of the island of Sumba, Indonesia, revealed by SeaMARC II side scan sonar: Geological Society of America Bulletin, v. 97, p. 1250-1261.

Caldwell, D.W., 1972, The geology of Baxter State Park and Mt. Katahdin: Maine Geological Survey Bulletin no. 12, 57 p.

Denning, S. A., and Lux, D. R., 1990, $^{40}Ar/^{30}Ar$ isotopic dating of the Horserace quartz diorite and its bearing on age relationships in the Katahdin batholith - Traveler Rhyolite system, *in* Marvinney, R.G., and Tucker, R.D., eds., Igneous and metamorphic geology: Studies in Maine geology, v. 1: Augusta, Maine, Maine Geological Survey, p. 115-124.

Donley, D.T., 1993, Acadian polyphase deformation in the Sherman-Island Falls area, Maine: Chestnut Hill, Massachusetts, Boston University, Unpublished Master's thesis, 102 p.

Fitzgerald, J.P., 1991, Geochemistry of the Spider Lake and West Branch Penobscot volcanic suites, northern Maine: tectonic implications from a complex petrogenesis: Chestnut Hill, Massachusetts, Boston University, Unpublished Master's thesis, 254 p.

Goldthwait, 1914, Remnants of an old graded upland of the Presidential Range of the White Mountains: American Journal of Science, 4th Series, v. 37, p. 451-463.

Griscom, Andrew, 1976, Bedrock geology of the Harrington Lake area, Maine: Harvard University, Ph.D. dissertation, 373 p.

Hall, B.A., Pollock, S.G., and Dolan, K., 1976, Lower Devonian Seboomook Formation and Matagamon Sandstone, northern Maine: a flysch basin-margin delta complex: Geological Society of America Memoir 148, p. 57-63.

Hanson, L.S., 1988, Stratigraphy of the Jo-Mary Mountain area with emphasis on the sedimentary facies and tectonic interpretation of the Carrabassett Formation: Boston, Massachusetts, Boston University, Unpublished Ph.D. dissertation, 308 p.

Hanson, L.S., 1989, A depositional model for the Carrabassett Formation, central Maine [abs.]: Geological Society of America, Abstracts with Programs, v. 21, n. 2. p. 20.

Hanson, L.S., and Bradley, D.C., 1989, Sedimentary facies and tectonic interpretation of the Carrabassett Formation, north-central Maine, *in* Marvinney, R.G., and Tucker, R.D., eds., Structure and stratigraphy: Studies in Maine geology, v. 1: Augusta, Maine, Maine Geological Survey, p. 101-126.

Hatch, N.L., Moench, R.H., and Lyons, J.B., 1983, Silurian-Lower Devonian stratigraphy of eastern and south-central New Hampshire: extensions from western Maine: American Journal of Science, v. 283, p. 739-761.

Hon, R., 1980, Geology and petrology of igneous bodies within the Katahdin pluton, *in* Roy, D.C., and Naylor, R.S., eds., The geology of northeastern Maine and neighboring New Brunswick: Boston, Mass., Boston College, New England Intercollegiate Geological Conference, 72nd Annual Meeting, Annual, p. 65-79.

Loiselle, M., Hon, R., and Naylor, R.S., 1983, Age of the Katahdin batholith, Maine [abs.]: Geological Society of America, Abstracts with Programs, v. 15, p. 146.

Lyons, J.B., Boudette, E.L., and Aleinikoff, J.N., 1982, The Avalonian and Gander zones in central eastern New England, *in* St. Julien, P., and Beland, J., eds., Major structural zones and faults in the northern Appalachians: Geological Association of Canada, Special Paper 24, p. 43.

Moench, R.H., and Pankiwskyj, K.A., 1988, Geologic map of western interior Maine: U.S. Geological Survey, Miscelaneous Investigations Map I-1692, 21 p., scale 1:250,000.

Mutti, E., and Ricci Lucchi, F., 1972, Le Torbiditi dell'Appennine settentroinale: introduzione all'analisi di facies: Memorie della Societa Geologica Italiana, v. 11, p. 161-199. (Translated into English by T. H. Nilsen, 1978, International Geology Review, v. 20, no. 2, p. 125-166)

Osberg. P. H., Hussey, A.H., and Boone, G.M., 1985, Bedrock geologic map of Maine: Augusta, Maine, Maine Geological Survey, scale 1:500,000.

Osberg, P.H., Tull, J.F., Robinson, P., Hon, R., and Butler, J.R., 1989, The Acadian Orogen, *in* Hatcher, R.D., Jr., Thomas, W.A., and Viele, G.W., eds., The Appalachian-Ouachita orogen in the United States: Boulder, Colorado, Geological Society of America, The Geology of North America, v. F-2, p. 179-232.

Philbrick, S.S., 1936, The contact metamorphism of the Onawa pluton, Piscataquis County, Maine: American Journal of Science, v. 31, p. 1-40.

Pollock, S.G., 1987, The Lower Devonian slate problem of western and northern Maine revisited: Northeastern Geology, v. 9, no. 1, p. 27-50.

Rankin, D., 1968, Volcanism related to tectonism in the Piscataquis volcanic belt, an island arc of Early Devonian age in north-central Maine, *in* Zen, E-an, White, W.S., Hadley, J. B., and Thompson, J., Jr., eds., Studies of Appalachian geology; Northern and maritime: New York, Interscience Publishers, p. 255-369.

Shreve, R.L., 1985, Late Wisconsin ice-surface profile calculated from esker paths and types, Katahdin esker system, Maine: Quaternary Research, v. 23, p. 27-37.

Stow, D.A.V., and Shanmugam, G., 1980, Sequence of structures in fine-grained turbidites: comparison of recent deep-sea and ancient flysch sediments: Sedimentary Geology, v. 25, p. 23-42.

Thoreau, H.D., 1864, The Maine Woods: Boston, Tichnor and Fields.

Woodcock, N.H., 1979, The use of slump structures as paleoslope orientation estimators: Sedimentology, v. 26, p. 83-99.

Chapter DD

Highlights of Metamorphic Stratigraphy and Tectonics in Western Maine to Northeastern Vermont

By Robert H. Moench

Field Trip Guidebook for the Northeastern United States:
1993 Boston GSA

Volume 2
Contribution No. 67, Department of Geology and Geography, University of Massachusetts, Amherst, Massachusetts

HIGHLIGHTS OF METAMORPHIC STRATIGRAPHY AND TECTONICS IN WESTERN MAINE TO NORTHEASTERN VERMONT

By
Robert H. Moench, U.S. Geological Survey, 905 Federal Center, Denver, CO 80225

INTRODUCTION

This 3-day trip covers the basis for currently evoloving interpretations of northern New England geology, resulting from six decades of geologic mapping, remapping, and related studies by many geologists. Since the publication of Marland Billings' classic work in New Hampshire (Billings, 1935, 1937, 1956) the broad outlines of northern New England geology that he established have been greatly "fleshed out." And, naturally, some of the stratigraphic and tectonic concepts that he developed were modified, in places radically, as new information became available. Figure 1, showing the locations of larger scale maps (figs. 3-5), is simplified from a geologic map of the Lewiston and part of the Sherbrooke 1^{o} x 2^{o} quadrangles (scale 1:250,000) edited by Moench, ed. (in press), with area compilations by W.A. Bothner, G.M. Boone, E.L. Boudette, N.L. Hatch, Jr., A.M. Hussey, II, R.G. Marvinney, and R.H. Moench; this map and the accompanying pamphlet also contains isotopic age control edited by J.N. Aleinikoff, who furnished new data, and the locations and brief descriptions of all fossil localities from many sources. The part of figure 1 that extends south and west of the Lewiston quadrangle is derived from a geologic map (1:48,000) that I prepared, with U-Pb zircon data furnished J.N. Aleinikoff; an intermediate version of this map has been displayed at a recent GSA poster session (Moench and Aleinikoff, 1991b). Figures 4 and 5, maps of the southern part of that area, show the numbered stops for day 3. Stratigraphic nomenclature of this field guide is updated from previous sources to the usage of the map of Moench, ed. (in press). Figures 1 and 5 show selected metamorphic isograds. Because primary features are typically well preserved, sedimentary nomenclature is emphasized in the following descriptions.

Recent mapping and related studies for the 1:250,000 and 1:48,000 maps described above was initiated in 1978 under the Conterminous United States Minerals Assessment Program (CUSMAP) of the U.S. Geological Survey, and was considered to be complete, at least in reconnaissance form, by the end of the 1984 field season. Early in 1985, however, I was asked to investigate the bedrock geology of the Mount Cube 15-minute quadrangle, just southwest of the Lewiston sheet, as part of the Glens Falls CUSMAP project. The intention was to extend our findings in the Lewiston sheet to the southwest. I quickly learned, however, that new information was to flow the other way, requiring much additional fieldwork and ultimately resulting in the delineation of what I now call the Piermont-Frontenac allochthon, inferred to contain all Silurian rocks exposed west of the Monroe-Foster Hill-Thrasher Peaks line (figs. 1 and 2, M-F-T). The existence of the allochthon has been debated (Billings, 1992; Moench, 1992).

Until recently, I have interpreted the (Piermont) allochthon as a fault-bounded Acadian thrust sheet rooted to the east, in an inferred Silurian sub-basin marginal to the Central Maine trough (fig. 1, CMT); I proposed that the sub-basin existed just west of the Silurian tectonic hinge (STH) and was destroyed by Acadian compression (Moench, 1990, fig. 5; Moench and Aleinikoff, 1991a). On the basis of newer mapping, I now recognize that this scenario is not viable. Instead, the allochthon is bounded only on its east side by a major fault system (fig. 1; M-F-T), and is rooted to the west in the Connecticut Valley trough (fig. 1, CVT), as shown by evidence of a lateral gradation between the sequence of Silurian rocks previously included in the allochthon (the Piermont sequence of fig. 1) and the Silurian Frontenac Formation, a major component of the CVT. These relationships present the enigma of an eastern source, based on stratigraphic sequential similarity, but a western root. On the assumption that these relationships are correct, rocks of the Piermont sequence and the Frontenac Formation (and possibly other Silurian rocks of the CVT) now appear to be equally allochthonous relative to the tectonic belts to the southeast. This is why I have changed the name of the allochthon from Piermont allochthon to Piermont-Frontenac allochthon. Possible resolution of this enigma and other problems concerning the allochthon are developed later.

Although a major focus of the trip is on the Piermont-Frontenac allochthon, the trip can also be considered a transect across parts of three major tectonic belts (fig. 1). So, even though some participants might disagree with my allochthonous views, they are sure to see many fine rocks.

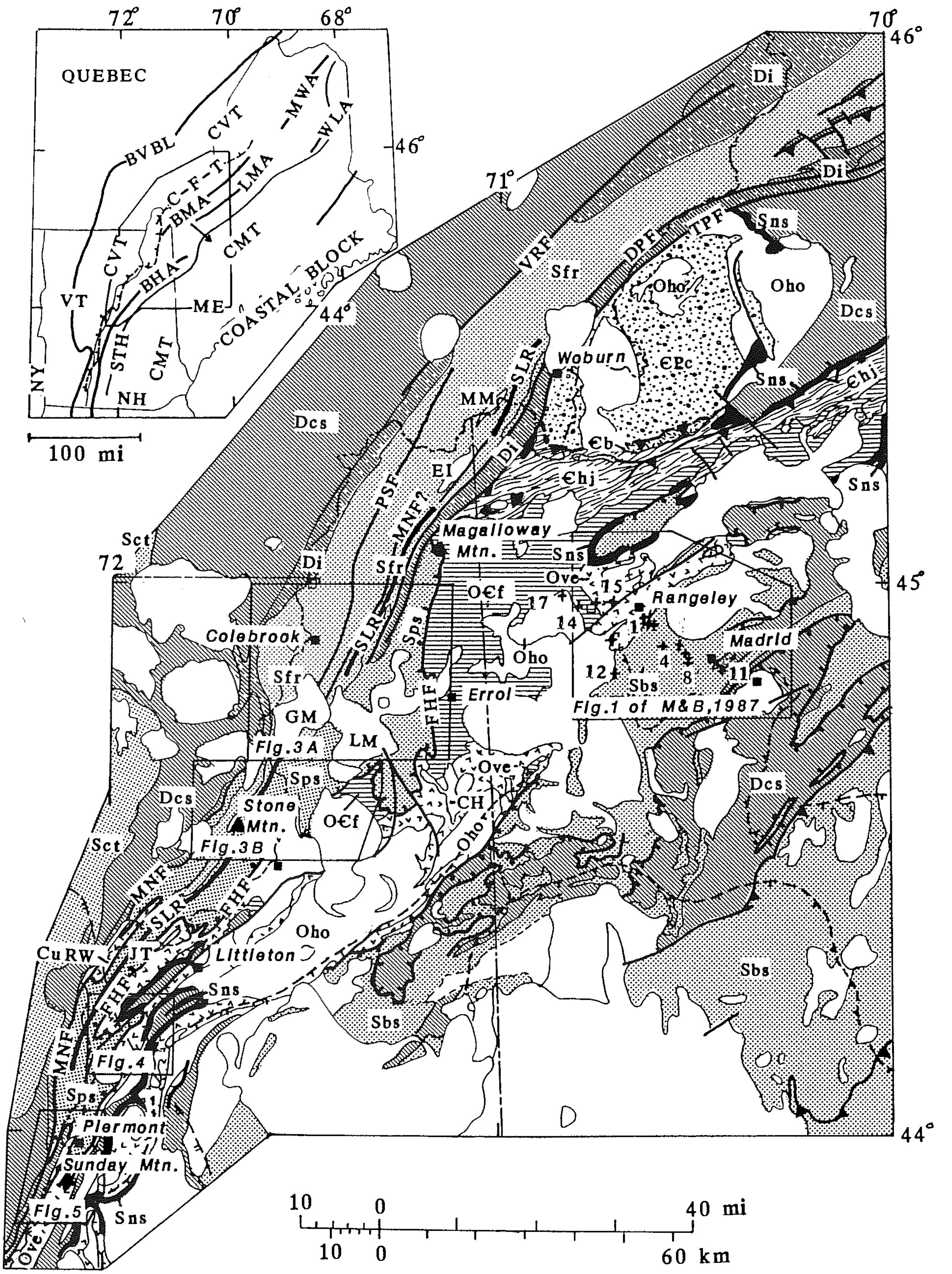
72°
70°
68°
46°
44°
QUEBEC
BVBL
CVT
MWA
WLA
C-F-T
LMA
BMA
CMT
BHA
COASTAL BLOCK
VT
ME
STH
NY
NH
100 mi
70°
46°
71°
Di
Sns
Oho
Dcs
DPF
TPF
VRF
Sfr
Woburn
ЄPc
SLR
MM
Єhj
Єb
EI
PSF
MNF?
Magalloway
Mtn.
Sct
72
Di
Sfr
Ove
15
Rangeley
45°
OЄf
17
14
Colebrook
Sps
Madrid
Oho
12
4
8
11
Sbs
Errol
Fig.1 of M&B,1987
GM
Fig.3 A
LM
FHF
Ove
Dcs
CH
Stone
Mtn.
Fig.3B
Sct
MNF
SLR
Littleton
CuRW
JT
Sns
Sbs
Fig.4
Sps
Piermont
Sunday Mtn.
Fig.5
Ove
44°
10
0
40 mi
10
0
60 km

Figure 1. Simplfied geologic map of western Maine, northern New Hampshire, and northeastern Vermont. Modified from Moench, ed. (in press), St. Julien and Slivitsky (1987), and unpublished map of Littleton-Piermont area Moench and Aleinikoff (1991b).

Oho **Plutonic rocks (Mesozoic to Ordovician):** Oho, Oliverian and Highlandcroft Plutonic Suites (Ordovician). Other units not shown. Cited plutons: **JT**, Joslin Turn; **CH**, Chickwolnepy; **IE**, East Inlet; **MM**. Marble Mountain sheeted dikes; **LM**, Long Mountain; **GM**, Gore Mountain

Dcs **Cover sequence of all tectonic belts (Lower Devonian):** Seboomook Group (except Di), Littleton and Compton Formations, and possibly Gile Mountain Formation

Di **Parallochthonous deposits above P-F allochthon (Lower Devonian, Gedinnian?):** Ironbound Mountain Formation, possibly Meetinghouse Slate Member of Gile Mountain Formation

Sns **Near-shore formations coeval with deposits of CMT and P-F allochthon (Silurian, Pridolian to upper Llandovierian:** Fitch Formation, Clough Quarzite and related units

Sbs **Basin sequence of CMT (Silurian, Pridolian through Llandoverian):** Greenvale Cove, Rangeley, Perry Mountain, Smalls Falls and Madrid Formations; Waterville and Sangerville Formations

Sps **Piermont sequence of P-F allochthon (Silurian, Pridolian through Llandoverian):**

Sfr **Frontenac Formation of P-F allochthon (Silurian, Pridolian? through Llandoverian?)**

Sct **Calcareous turbidites of CVT (Silurian):** Waits River and Ayers Cliff Formations

Ove **Volcanic and euxinic sedimentary rocks of Bronson Hill arc (Ordovician, Cincinnatian to late Whiterockian):** Ammonoosuc Volcanics and Partridge and Quimby Formations

O€f **Pelitic to arenaceous flysch (Ordovician, Whiterockian, to Upper Cambrian?):** Aziscohos and Dead River Formations

€hj **Euxinic melange of Hurricane Mountain Formation and volcanic and clastic rocks of Jim Pond Formation (Cambrian?).**

€b **Ophiolitic Boil Mountain Complex (Cambrian?).** Ultramafic rocks, gabbro, epidiorite, trondhjemite

€Pc **Diamictite and related rocks of Chain Lakes massif (Cambrian or Proterozoic)**

Acadian and younger faults; teeth on side of upper plate of thrust fault: **MNF**, Monroe, **PSF**, Perry Stream, **DPF**, Deer Pond, **TPF**, Thrasher Peaks

FHF **Foster Hill and other preAcadian faults and slides;** ticks point to upper plate or downthrown side: Includes soles of major slumps in CMT

CuRW **Coppermine Road window**

Penobscottian(?) surface of tectonic ramping: Lower boundary of Boil Mountain Complex

GAA AB **Selected metamorphic boundaries;** ticks point to higher grade. **GAA**, greenschist through lower amphibolite facies. **AB**, middle amphibolite facies (first sillimanite). **AC**, upper amphibolite facies (sillimanite + K-feldspar).

Aluminum silicate triple point isobar; double ticks point to area of higher pressure (Thompson and Norton, 1968)

Tectonic lines and belts: BVBL, Baie Verte-Brompton line. **M-F-T**, Monroe-Foster Hill-Thrasher Peaks line. **CVT**, Connecticut valley trough. **CMT**, Central Maine trough. **BHA**, Bronson Hill, **BMA**, Boundary Mountains, **LMA**, Lobster Mountain, **MWA**, Munsungen-Winterville, anticlinoria; **BHBMA**, BHA+BMA. **STH**, Silurian tectonic hinge. **SLR**, magmatic axis of Second Lake rift

+1 Field trip stop for day 1: Numbered where sufficient space

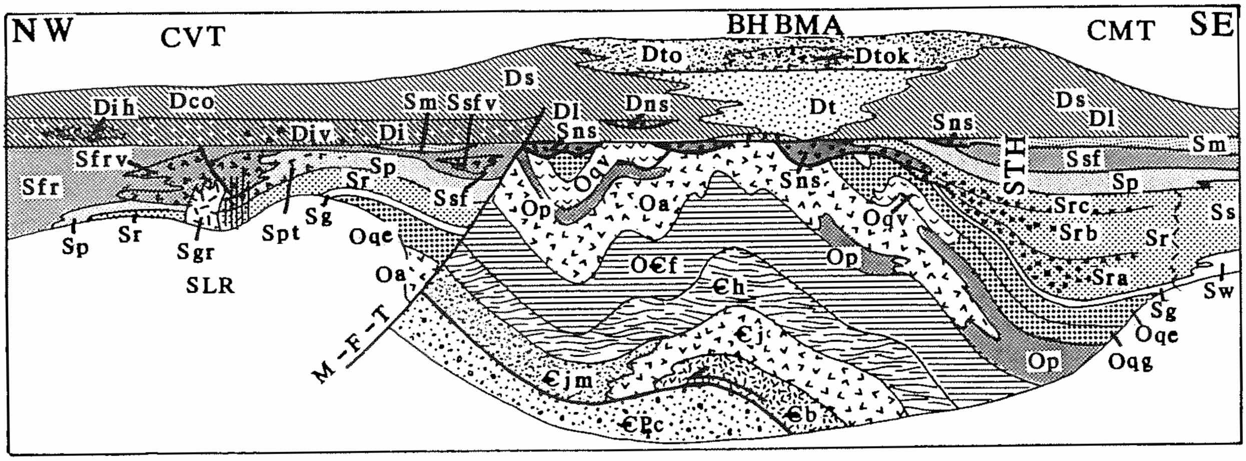

Figure 2. Schematic stratigraphic diagram for area of figure 1. Not to scale. Thick line at lower contact of a unit indicates a disconformity or an unconformity. Lower Devonian(?) Gile Mountain Formation and Silurian Waits River and Ayers Cliff Formations of CVT are not shown, because of uncertain correlations.

Tectonic lines and belts: **CVT**, Connecticut Valley trough (includes Ordovician and Silurian units of Piermont-Frontenac allochthon, and Lower Devonian parallochthonous and autochthonous cover sequence. **BHBMA**, Bronson Hill-Boundary Mountains anticlinorium. **CMT**, Central Maine trough. **SLR**, magmatic axis of Second Lake rift. **M-F-T**, Monroe-Foster Hill-Thrasher Peaks line (southeast side of Piermont-Frontenac allochthon). **STH**, Silurian tectonic hinge

Lower Devonian units: **Dns**, near-shore formations. **Di**, Ironbound Mountain Formation of Seboomook Group; **Dih**, grit lenses at Halls Stream; **Div**, volcanic member. **Ds**, Seboomook Group, undivided. **Dl**, Littleton Formation. **Dco**, Compton Formation. **Dt**, Tarratine Formation. **Dto**, Tomhegan Formation; **Dtok**, Kineo Volcanic Member

Silurian and Silurian(?) units: **Sns**, near-shore formations. **Sfr**, Frontenac Formation; **Sfrv**, bimodal volcanic members. **Sg**, Greenvale Cove Formation. **Sr**, Rangeley Formation; **Sra**, member A; **Srb**, member B; **Src**, member C. **Sp**, Perry Mountain Formation; **Spt**, variably tuffaceous and local volcanic facies. **Ssf**, Smalls Falls Formation; **Ssfv**, bimodal volcanic facies. **Sm**, Madrid Formation. **Sw**, Waterville Formation. **Ss**, Sangerville Formation. **Sgr**, granite of East Inlet pluton

Ordovician (Cincinnatian to upper Whiterockian) units of Bronson Hill arc: **Op**, Partridge Formation. **Oa**, Ammonoosuc Volcanics. **Oqe**, shale and graywacke member, **Oqg**, graywacke member, **Oqv**, volcanic member of Quimby Formation

Ordovician (Whiterockian) to Upper Cambrian(?) flysch: **OЄf**, Aziscohos and Dead River Formations.

Cambrian(?) ophiolitic melage: **Єb**, Boil Mountain Complex. **Єjv**, bimodal volcanic member, **Єjm**, Magalloway arenite member of Jim Pond Formation. **Єh**, Hurricane Mountain Formation.

Cambrian or Proterozoic rocks: **ЄPc**, diamictite and related rocks of Chain Lakes massif

STRATIGRAPHIC AND TECTONIC FRAMEWEORK

As shown on figure 1, the tectonic framework of the area consists of the Bronson Hill-Boundary Mountains anticlinorium (BHBMA), and the flanking Connecticut Valley and Central Maine troughs (CVT, CMT). The stratigraphy of all three belts is illustrated schematically in figure 2, which depicts the Lower Devonian formationsas a cover sequence, subhorizontal before Acadian deformation. I consider the basal unit of the Lower Devonian sequence west of the BHBMA to be parallochthonous above the Piermont-Frontenac allochthon; i.e., to have accumulated on the allochthon while in transit.

Parallochthonous to autochthonous rocks of Lower Devonian cover sequence

Covering all of the tectonic belts is a sedimentary and locally volcanic blanket, at least 2 km thick, of Early Devonian age characterized by spectacularly graded mud-silt-sand turbidites (fig. 1, Dcs). The principal units are the Littleton Formation (Dl), several formations of the Seboomook Group (Ds), the Compton Formation (Dco), and possibly the Gile Mountain Formation. Fossils from these units (except the Gile Mountain) indicate an Early Devonian (Emsian to late Gedinnian) age, but the lowest beds are generally unfossiliferous. Where these deposits cover near-shore and on-shore Silurian deposits and Ordovician and older sequences of the Bronson Hill-Boundary Mountains anticlinorium, described later, they locally contain lenses of weakly metamorphosed fossiliferous limestone, siltstone, arkose, or conglomerate, or mixtures of all these lithologies (fig. 2, Dns); lower contacts of these units are local unconformities. In the Moose River syncline, which lies between the Boundary Mountains and Lobster Mountain anticlinoria (fig. 1; BMA, LMA), the turbidites of the Seboomook Group grade laterally and upward to very thick-bedded quartzose sandstone mapped as the Tarratine Formation (Dt). Disconformably above the Tarratine Formation is the Tomhegan Formation (Dto), composed of shallow marine tuffaceous sandstone, siltstone and slate, and the Kineo Volcanic Member of the Tomhegan (Dtok), composed of mainly subaerial rhyolitic ash-flow tuff, flows, domes, and volcaniclastic deposits, and garnet-bearing intrusive rhyolite. These volcanic rocks represent the south end of the Piscatiquis volcanic belt of Rankin (1968). The Tomhegan Formation and the uppermost rocks of the Seboomook Group and Compton and Littleton Formations are Emsian in age and were deposited just prior to Acadian folding.

The Ironbound Mountain Formation (Di), defined as the lowermost formation of the Lower Devonian Seboomook Group, covers the Silurian rocks of the Piermont-Frontenac allochthon (fig. 2). This formation is composed mainly of highly pelitic gray slate with graded siltstone laminations, but, as shown on figs. 2 and 3A, it also contains volcaniclastic grit (Dih) and metavolcanic rocks (Div). The Ironbound Mountain Formation is conformably underlain by the Silurian Frontenac Formation of the allochthon, but where the Ironbound Mountain is underlain by formations of the Piermont sequence of the allochthon the contact is sharp and conformable to possibly unconformable. Small remnants of the formation are cut by the Foster Hill fault (FHF), at the east margin of the allochthon. According to the two models discussed later, Ironbound Mountain Formation was deposited over the Piermont-Frontenac allochthon while the allochthon was still in transit.

Autochthonous rocks of Bronson Hill-Boundary Mountains anticlinorium

The anticlinorium is cored at its north end by the Chain Lakes massif, a large, structurally resistant body composed mainly of poorly dated, Proterozoic or Cambrian diamictite and related rocks (€Pc) of controversial age and origin (see Boone and Boudette, 1989; Trzcienski, et al, 1992). Structurally above the south side of the massif is a Cambrian(?) ophiolitic melange sequence composed, as shown in figure 2, of the mafic-ultramafic-trondhjemitic Boil Mountain Complex (€b), bimodal volcanic rocks and the volcaniclastic Magalloway Member of the Jim Pond Formation (€jv, €jm), and euxinic trench melange of the Hurricane Mountain Formation (€h). Available U-Pb zircon data indicate an age of about 520 Ma for Boil Mountain trondhjemite and Jim Pond dacite (Eisenberg, 1981, 1982; J.N. Aleinikoff in Moench, ed., in press); primitive sponges found in the Hurricane Mountain Formation (Harwood, 1973, p. 23) suggest a Cambrian age for the formation, although an Ordovician age is not ruled out (R.M. Finks, oral commun., 1983). According to Boone and Boudette (1989), the lower boundary of the ophiolitic melange is an early Paleozoic (Penobscottian) suture between a buried (Gander?) terrane of uncertain character to the southeast and their Boundary Mountains terrane to the northwest, represented by rocks of the Chain Lakes massif. Boone and Boudette infer that their Boundary Mountains terrane extends northwest to the Baie Verte-Brompton line (fig. 1, index), which is widely considered the principal middle Ordovician (Taconian) suture. [North American divisions of Ordovician time (Ross, et al, 1982) are used herein, and the terms early, middle, and late (lower, middle, upper) Ordovician are used informally].

The ophiolitic melange sequence is overlain to the south by an Upper Cambrian(?) to middle Ordovician (Whiterockian) flysch sequence (figs. 1 and 2, O€f) composed of arenaceous to pelitic turbidites mapped as the Dead River and Aziscohos Formations. Abruptly but probably conformably above the flysch is a sequence possibly as much as 4 km thick of subaqeous basaltic to soda-rhyolitic volcanic and euxinic sedimentary rocks of middle and late Ordovician (late Whiterockian through Cincinnatian) age mapped as the Ammonoosuc Volcanics (Oa), and the Partridge and Quinby Formations. The Partridge Formation (Op) is composed mainly of interbedded black slate and metagraywacke, and locally abundant metachert. The Ammonoosuc and Partridge intertongue with one another and both are conformably to unconformably overlain by the Quimby Formation. In its type area near Rangeley, the Quimby Formation contains basal, laterally intergradational graywacke and felsic volcanic members (Oqg, Oqv), and an upper euxinic sedimentary member (Oqe), much like parts of the Partridge Formation. In the Littleton area, the volcanic member is much more prominant and contains both felsic and mafic rocks.

The Ammonoosuc Volcanics and the Partridge and Quimby Formations represent the stratified component of the Bronson Hill magmatic arc in the area of figure 1 (Ove). Plutonic components are represented by granitic rocks of the Highlandcroft and Oliverian plutonic Suites (Oho), the Chickwolnepy intrusions (fig. 1, CH, 10 mi south of Errol), composed of gabbro, sheeted diabase, and tonalite, and the Joslin Turn pluton (fig. 1, OJ, 5 mi northwest of Littleton), composed of granophyric tonalite and strongly altered and locally mineralized granitic rock of undetermined composition. The arc, which extends at least from Connecticut to the north end of the Munsungen-Winterville anticlinorium (MWA) in northern Maine, is widely considered to have to have been active during subduction that preceded and accompanied the Taconian collision (for example Stanley and Ratcliffe, 1985). However, whereas the Taconian collision and metamorphism apparently culminated at about 465 Ma (Sutter, et al, 1985), U-Pb zircon ages obtained recently from metavolcanic rocks and associated intrusive plagioclase-rich gneisses of the arc in Massachussetts indicate magmatic activity in the range of 454-445 Ma (Tucker and Robinson (1990). In contrast, data from the area of this map indicate that the earliest arc eruptions accompanied emplacement of the Joslin Turn pluton, dated at 469+-1.3 Ma, and the Chickwolnepy intrusions, dated at 467+-3 Ma (Aleinikoff and Moench, 1992), during or not long before the collision. J.N. Aleinikoff (in Moench, ed. in press) has dated Ammonoosuc metarhyolite exposed about 20 km south of Littleton, NH, at 461+-8 Ma, and an age of about 460 Ma is appropriate (R.J. Ross, Jr., written commun., 1992) for Climacograptus bicornis zone graptolites (Harwood and Berry, 1967) recovered from the approximate middle of the Partridge Formation; the locality is about 8 km north of stop 15 (fig. 1). Basal felsic metatuff from the volcanic member of the Quimby Formation has yielded a U-Pb zircon age of 444+-4 Ma (Aleinikoff and Moench, 1992; locality is on fig.4), and available data indicate that magmas of the Highlandcroft and Oliverian plutonic suites were emplaced in the range of 458-440 Ma (Zartman and Leo, 1985; Foland and Loiselle, 1981; Lyons, et al,1986; J.N. Aleinikoff, in Moench,ed. in press). Interestingly, these data and the descriptions and data of Tucker and Robinson (1990) indicate that the duration of magmatism in the southern part of the Bronson Hill was much shorter than it was in the area of this guide. Additionally, the thick sequence of flysch and ophiolitic melange found in the area of figure 1 is absent to the south.

Mapping indicates that all of the Ordovician and older stratified rocks exposed along the axial zone of the anticlinorium were strongly folded and cleaved, uplifted, and eroded before deposition of the Silurian near-shore and on-shore deposits (Sns) represented by the Clough Quartzite (mainly of quartz conglomerate and quartzite), the Fitch Formation (metamorphosed limestone and fine-grained calcareous siliciclastic deposits), and other named and unnamed Silurian near-shore formations. The Clough and Fitch are distinguished on figures 4 and 5 (Sc, Sf). As shown in figure 2, the near-shore and on-shore formations are facies of much thicker basin deposits exposed in the Central Maine trough (Sbs), southeast of the Silurian tectonic hinge (STH) and in the Piermont-Frontenac allochthon.

The uplifted anticlinorium is the only specifically identified source area for the thick Silurian deposits of the Central Maine trough to the east, but it is surely too small to have been the sole source of these deposits, even if it was, say, twice as wide before Acadian folding. This problem is compounded further by the fact that much of the deformation within the anticlinorium occurred before that area became a Silurian source area. Almost certainly, the exposed part of the anticlinorium is only a small fragment of the original Silurian source area. Contributing to this view is the fact that the anticlinorium is truncated on the west by the Foster Hill and Thrasher Peaks faults (figs. 1, 2), which also mark the western limit of the known Silurian near-shore deposits.

Autochthonous deposits of Central Maine trough

In marked contrast with the profound unconformity that exists below the near-shore Silurian deposits exposed along the Bronson Hill-Boundary Mountains anticlinorium, no unconformity is recognized on the southeast limb (fig. 2). Here, strongly euxinic rocks of the Quimby Formation (Oqe) are conformably overlain by noneuxinic deposits of the Greenvale Cove Formation (Sg), at the base of the Silurian sequence in the Central Maine trough. The Greenvale Cove Formation is about 200 m thick, and is composed of mildly calcareous, interlaminated feldspathic metasandstone and metasiltstone. I interpret the Greenvale Cove Formation as a deltaic deposit that marks the initial emergence of the western source area. This formation is considered to be approximately coeval with the Waterville Formation (Sw) of the southeastern part of the Central Maine trough.

Abruptly gradationally above the Greenvale Cove Formation is the Rangeley Formation (Sr), as much as 3 km thick, and divided into members A, B, and C (ascending order), which are further subdivided. Member A is about 1,200 m thick; it is divided into facies of metamorphosed polymictic conglomerate, massive arkose, and interbedded gray shale and sandstone. The conglomerate and arkose facies define a subaqueous fanglomerate body that coarsens upward, fines southeastward, and was shed from a growing mountain range to the northwest. Member B (Srb), also about 1,200 m thick, is composed mainly of metamorphosed interbedded dark-gray, sulfidic shale and poorly graded feldspathic quartzite, but with extensive lenses of polymictic conglomerate and conglomeratic mudflow deposits.

The B-member conglomerates have a higher quartz content than those of member A, but also become finer grained and less abundant southeastward. Member C (Src), about 600 m thick, is divided into a lower submember (maximum thickness about 200 m) composed of metamorphosed interbedded quartz conglomerate, feldspathic quarztite, and dark-gray, sulfidic metashale, and local laminated impure metalimestone, and an upper submember (about 450 m thick) composed of interbedded dark-gray sulfidic metashale and metasandstone.

The quartz conglomeratic rocks of member C are a marine basin facies of the near-shore Clough Quartzite (fig. 2, Sc), exposed above Ordovician and older rocks of the anticlinorium to the west. Similar late Llandoverian shelly faunas have been recovered from quartz conglomeratic beds of the unit and an associated lens of laminated metalimestone north of Rangeley (Moench and Boudette, 1987; Boudette,1991) and from the Clough Quartzite in southwestern New Hampshire (Boucot and Thompson, 1963). The Rangeley Formation as a whole becomes increasingly distal in character to the southeast, and is inferred to grade to the generally finer-grained Sangerville Formation (fig. 2, Ss) of the southeastern part of the Central Maine trough. In addition to siliciclastic turbidtites, the Sangerville Formation contains externsive layers of thinly bedded metalimestone, probably calcareous turbidties.

Gradationally above the moderately euxinic Rangeley Formation is the noneuxinic Perry Mountain Formation (Sp), which is about 600 m thick in the Rangeley area. The Perry Mountain Formation is characterized by sharply interbedded potassic, muscovite-rich pelitic schist, and planar-bedded white, slightly feldspathic quartzite that commonly displays features of bouma turbidites and evidence of reworking by bottom currents. Sparse trachyte is exposed in the formation north of Rangeley (Boudette, 1991), and volcaniclastic rocks have been mapped in the Perry Mountain Formation just east of the area of figure 1 (Moench and Pankiwskyj, 1988a; pamphlet p. 4). Lithofacies indicate a northwestern source for the Perry Mountain Formation. By Perry Mountain time the mountain range that shed the coarsely clastic deposits of the Rangeley Formation was reduced to low hills that shed the more mature Perry Mountain clastics.

Sharply but conformably above the Perry Mountain Formation is the strongly euxinic Smalls Falls Formation (Ssf), having a maximum thickness of more than 700 m. The contact is marked by an abrupt change from the nonsulfidic, light-colored rocks of the Perry Mountain to rust-encrusted, richly pyrrhotitic gray to black metashale and quartzite of the Smalls Falls. Otherwise the two formations have similar sedimentary styles. A calcareous member is recognized in the upper part of the Smalls Falls Formation along the western side of the Central Maine trough. The formation represents a time of strongly euxinic, closed basin conditions probably produced by nonuniform basin subsidence. Again, lithofacies indicate northwestern provenance.

Conformably above the Smalls Falls Formationis are noneuxinic, variably calcareous rocks mapped as the Madrid Formation (Sm), which is the uppermost unit of the Silurian sequence. This unit is about 300 m thick at Madrid village, the type locality, but is much thicker farther southeast. At Madrid, the formation divides into a lower member of thinly bedded metasiltstone and weakly to strongly calcareous metasandstone (now calcsilicate rock), and an upper member of thickly bedded mildly calcareous feldspathic metasandstone of uniform composition, with partings and interbeds of gray pelitic schist similar to that of the overlying Carrabassett Formation of the Lower Devonian cover sequence. Although unfossiliferous, the Madrid Formation is almost certainly coeval with the well dated upper Ludlovian and Pridolian Fitch Formation of the Bronson Hill anticlinorium. In contrast with the underlying Silurian units, the Madrid sands probably came from the northeast.

Connecticut Valley trough and Piermont-Frontenac allochthon

According to my interpretations, the Piermont-Frontenac allochthon contains all of the Silurian and older rocks of the Connecticut Valley trough exposed west of the Monroe-Foster Hill-Thrasher Peaks line (fig. 1, index). In the area of figure 1, these rocks include six formations that make up the Piermont sequence, the Frontenac Formation, and, tentatively, the Ayers Cliff and Waits River Formations. Although the Lower Devonian rocks are considered to represent a mainly autochthonous cover sequence deposited after the allochthon docked, the highly pelitic Ironbound Mountain Formation, at the bottom of the cover sequence, is interpreted to be parallochthonous; i.e., deposited while the allochthon was still in transit.

Monroe-Foster Hill-Thrasher Peaks line (fig. 1, M-F-T)--The Foster Hill fault (fig. 1, FHF), originally considered the folded sole and eastern margin of the Piermont allochthon (Moench, et al, 1987), has been mapped in variable detail from Sunday Mountain about 150 km northeast to Magalloway Mountain (fig. 1). The FHF has the map pattern of a strongly folded, east-directed thrust fault, complete with one large window (Coppermine Road window, CuRW, 5 mi west of Littleton) and two others that are too small to show on figure 1.

Where seen in outcrops, however, the fault typically is a tight, sharp, pre-cleavage surface showing no confirmed evidence of cataclasis. So far I have not recognized meaningful tectonic indicators, but more work is needed. However, the internal stratigraphy of the allochthon, described later, indicates that the FHF must be a surface of major displacement.

Possibly the most important relationship shown by the FHF, and by the Monroe fault (MNF) south of Sunday Mountain and the Thrasher Peaks fault (TPF) northeast of Magalloway Mountain, is the fact that all three form a line that marks the western limit of known Silurian near-shore deposits that unconformably truncate significantly older rocks (M-F-T on fig. 1, index). Whereas a transition between these deposits and the thick turbiditic Silurian sequence of the Central Maine trough to the east is well defined, no such transition is recognized to the west.

In its formative years, the allochthon was considered to be truncated on the west by the Monroe fault (fig. 1, MNF), which I incorrectly thought to join the Victoria River fault (VRF) in Quebec and extend as a single major feature at least as far as the Caucomgomoc Lake area in northern Maine (Moench, 1990, and references therein). I did not address the question of the whereabouts of the allochthon to the west of this presumed through-going fault, an area underlain by the Silurian and Lower Devonian rocks of the Connecticut Valley trough (CVT). On the basis of more recent mapping and observations by Tremblay, et al, (1993), and W.A. Bothner (unpub. mapping, 1990-92), it now appears that the Monroe and Victoria River faults are not colinear, and that neither fault is a major feature in Quebec and northernmost New Hampshire. Instead, new mapping now indicates that the Silurian rocks that previously defined the Piermont allochthon, shown as the Piermont sequence on figure 1, grade laterally to those of the Silurian Frontenac Formation, a major stratgraphic component of the CVT. The Foster Hill fault, however, remains fundamental; I propose that it is a complexly folded but originally "flat connector" between fundamental segments of the Monroe fault (MNF) south of Sunday Mountain and Thrasher Peaks fault (TPF) northeast of Magalloway Mountain.

About 3.5 mi northwest of Sunday Mountain the Foster Hill fault converges with the Monroe fault (fig. 5); it reappears 5 mi farther south, where it markd the east side of a thin slice of Rangeley Formation. Farther south the MNF is a long-recognized major structure that separates very different rocks of the "Vermont" and "New Hampshire" sequences, respectively the Waits River-Gile Mountain sequence of the Connecticut Valley trough and the Ammonoosuc-Partridge-Clough-Fitch-Littleton sequence of the Bronson Hill anticlinorium. Between the approximate latitude of Sunday Mountain and the Gore Mountain plutons (fig.1, GM), the Monroe fault is an easily recognized feature that sharply separates the Waits River-Gile Mountain sequence from the Silurian formations of the Piermont sequence and the southernmost mapped exposures of the Frontenac Formation. According to my reconstruction (fig. 6) the Monroe fault dips west in the Piermont area. North of the Gore Mountain plutons, however, the Monroe fault might correlate with either of two faults, shown as the Perry Stream (PSF) and Monroe? (MNF?) faults, both of which die out to the northeast within rocks now mapped as the Frontenac Formation; neither fault has geophysical expression (Spencer, et al, 1989; Stewart, et al, 1991).

A short distance northwest of Magalloway Mountain the Foster Hill fault is truncated by the Thrasher Peaks fault (TPF). Although the TPF and the actual point of truncation were not seen in outcrop, rocks of the Dead River Formation (fig. 1, OCf) exposed immediately southeast of the mapped trace of the TPF are strongly deformed by northeast-trending cataclastic foliation that dips 50°-70°NW, and is decorated by stretching lineations that plunge downdip to the northwest. The foliation is conspicuous through an exposed width of about 200 m. About 50 mi northeast of Magalloway Mountain (fig. 1), where the Lower Devonian Ironbound Mountain Formation (Di) is faulted by the TPF against Ordovician granite, the granite is deformed by another zone of mainly NW-dipping cataclastic foliation as much as 1,200 m wide; the foliation is most strongly developed in granite outcrops that are closest to the fault (Albee and Boudette, 1972, p. 27, 28, 72). Albee and Boudette did not map the fault, which Westerman (1983) later mapped in detail in this area.

Seismic relflection and refraction profile data indicate that the Thrasher Peaks fault is a major, moderately NW-dipping structure where it cuts the northwest side of the Chain Lakes massif (Spencer,et al, 1989; Stewart, et al, 1991). The TPF is visible in the profile to a depth of about 10 km. The Deer Pond fault (DPF) to the north (fig. 1) also is visible; it dips more steeply NW than the TPF, which it joins at a depth of about 5 km. The belt of Lower Devonian Ironbound Mountain Formation that lies between the DPF and TPF is wedge-like in cross section, possibly a graben that was later compressed and overturned against the massif to the south. These movements were probably minor relative to the total pre-Devonian history that I infer for the TPF.

Southwest of the truncation of the FHF near Magalloway Mountain I traced the TPF a maximum distance of about 13 mi. Features of brittle deformation occur locally along this segment of the TPF, but only minor displacement is inferred, because rocks on both sides of the fault are in almost their normal statigraphic order.

In summary, I interpret the Foster Hill fault, the Monroe fault south of Sunday Mountain, and the Thrasher Peaks fault northeast of Magalloway Mountain to be a major crustal feature, probably a transcurrent fault. The complexly folded FHF probably originated as a "flat" segment of the rupture. Because of its gentle dip in comparison to the MNF and TPF, the Foster Hill fault was strongly folded by subhorizontal Acadian compression, whereas the other faults were relative unaffected. According to the strike-slip model discussed later, this feature was active mainly in Silurian time. The evidence for Devonian activity is more conspicuous, but actual Devonian displacement was comparatively minor. I interpret the present alignments of the MNF and TPF across their intersections with the Foster Hill fault to be the result of Devonian and possibly younger reactivations.

Piermont sequence--This sequence is composed of variants of the Quimby, Greenvale Cove, Rangeley, Perry Mountain, Smalls Falls, and Madrid Formations, whose type localities are near Rangeley, Maine. The sequence also contains small remnants of the Lower Devonian Ironbound Mountain Formation, which is more conveniantly treated as a parallochthonous part of the cover sequence, already described. These units supplant the Albee Formation of Billings (1935, 1937, 1956), and parts of the Dixville Formation of Green (1964, 1968), both originally considered major Ordovician components of the anticlinorium. Other parts of Green's Dixville Formation are now mapped as the Hurricane Mountain Formation (fig. 2, Ꞓh), and the Magalloway Member of the Jim Pond Formation (Ꞓjm).

The occurrence of the Quimby to Madrid sequence that originally defined the Piermont allochthon is most convincing in the Piermont area of the Mount Cube 15-minute quadrangle (fig. 5), which I consider to be the type area of the allochthon. This quadrangle was originally mapped by Hadley (1942, 1950), and later partly modified by Rumble (1969). The north-adjacent Woodsville 15-minute quadrangle was mapped by White and Billings (1951), and partly revised by Hafner-Douglass (1986). My revisions in parts of these quadrangles are described and illustrated by Moench (1990, p. J2-J10). Figures 5 and 6 are slightly modified from figures 2 and 3 of Moench (1990). The Ammonoosuc fault (AF), a Triassic normal fault that has an average dip of about 40°W, divides rocks of the area into a greenschist-facies block on the west, and an epidote-amphibolite and amphibolite-facies block on the east. As shown on the restored structure section (fig. 6) the western block has dropped about 5 km relative to the eastern block in the Piermont area, assuming that the AF orginally dipped 40°W above ground; displacement decreases northward to about 3 km near Littleton, NH.

The area of figure 5 contains the only known exposures of the Quimby (Oqe) and Greenvale Cove (Sg) Formations in the allochthon. Only the uppermost 100 m of the Quimby is exposed. The rocks are interbedded rusty-weathering black schist and metagraywacke, similar to the euxinic shale and graywacke member exposed in the type area of the formation near Rangeley, Maine. However, the rocks also are similar to much of the Partridge Formation (Op) of the autochthonous sequence and are distinguished from the Partridge only by the higher stratigraphic position of the Quimby. The Quimby Formation is overlain by the Greenvale Cove Formation, about 200 m thick,and composed of interlaminated, light-purplish gray garnetiferous two-mica schist and calcsilicate rock, interpreted as calcareous feldspathic siltstone and sandstone. Cobble metaconglomerate is exposed locally; it is characterized by deformed cobbles of metasandstone, probably cannibalized from underlying Greenvale Cove sediments, in a matrix of finer grained similar material. The conglomerate suggests that the Greenvale Cove Formation of this area is a proximal facies relative to the type Greenvale Cove Formation.

Conformably above the Greenvale Cove Formation are rusty-weathering, dark-gray, thinly to thickly interbedded pelitic schist and poorly graded to well graded feldspathic quartzites assigned to the Rangeley Formation, which is about 500 m thick in the area of figure 5. The contact is marked by an abrupt change in sedimentary style, and by lenses, rarely more than a few meters thick, of polymictic metaconglomerate (Srp) containing deformed pebbles and cobbles of quartz and various sedimentary, volcanic, and plutonic rocks. These basal conglomerate lenses are thought to be equivalent to the polymictic conglomerates of members A or B in the type area of the Rangeley Formation. This type of conglomerate is unknown farther north in the allochthon. At a higher stratigraphic level are lenses composed of interstratified quartz pebble conglomerate, gray schist, and feldspathic quartzite (Srq) much like the quartz conglomeratic submember of member C of the type Rangeley. The quartz conglomerates of the Rangeley are interpreted to be a marine basin facies of the Clough Quartzite (Sc) of the autochthonous sequence. The Rangeley Formation of the area of figure 5 is far thinner than the type Rangeley south of Rangeley, Maine (0.5 km vs. 3 km), but it is comparable in thickness and relatively proximal facies to the Rangeley Formation exposed about 20 km north of Rangeley village.

The Perry Mountain Formation is about 500 m thick in the Piermont area, and varies from about 200 m to possibly more than 1 km thick elsewhere in the allochthon. Much of the formation is composed of sharply interbedded slightly feldspathic quartzite and muscovite-rich pelitic schist similar to that of the type Perry Mountain Formation of western Maine. These rocks grade laterally and vertically, however, to facies composed of variably feldspathic rocks, interpreted to be tuffaceous, with scattered centers of felsic and sparse mafic volcanic rocks, and locally abundant hypabyssal intrusive rocks; this is the variably tuffaceous and local volcanic facies shown on figures 2-5 (Spt). U-Pb-zircon ages of 412+-2 and 414+-4 Ma were obtained from metarhyolite at two localities about 20 km southwest of Littleton (Moench and Aleinikoff, 1991a, b, 1992; Moench, 1992). Although I now recognize that both dated bodies are probably sills, it is unlikely that they are not related to the stratified volcanic assemblage within the Perry Mountain Formation. In addition to extensive planar-bedded turbidite sequences that are comparable to the type Perry Mountain, in the allochthon this formation has lenticular-bedded sequences suggestive of a shallower, more proximal environment of deposition also occur. Also suggestive of a relatively proximal environment is the local occurrence of thick basal quartzite beds with ripups of dark-gray phyllite derived from the underlying Rangeley Formation. The Perry Mountain Formation is conformably overlian by the Smalls Falls Formation. The contact is sharp and marked by an abrupt change from noneuxinic to strongly euxinic compositions, but only minor changes in bedding style.

In the Piermont area (fig. 5), the Smalls Falls Formation is about 100 m thick . Throughout the allochthon it appears to thin westward from a maximum thickness of about 800 m west of Errol, NH. Thin layers of super-black, sulfidic phyllite several centimeters to several meters thick that occur within rock sequences mapped as the Frontenac Formation, described later, are interpreted to represent the western feather edge of the Smalls Falls Formation. Much of the formation in the allocthon is composed of interbedded rust-encrusted quartzite, and coaly-black, pyrrhotite-rich pelitic phyllite, but parts are somewhat less graphitic and sulfidic. West of Errol is a thick sequence of basalt-dominated bimodal metavolcanic rocks that is underlain and overlain by strongly euxinic sedimentary rocks assigned to the Smalls Falls Formation (fig. 3A). The volcanic sequence was originally mapped as the Clear Stream Member of the Ordovician Dixville Formation (Green, 1964). The rocks are massive and pillowed metabasalt (now amphibolite), greatly subordinate felsic metatuff, sparse intrusive felsite, and volumetrically minor but spectaular exposures of laminated exhalative metachert, manganiferous metachert (now garnet coticule), and magnetite iron-formation. Petrochemically, the metabasalts are tholeiites having rather low titanium contents. I assigned these rocks to the Smalls Falls Formation on the basis of their mapped stratigraphic position within the well-defined stratigraphic sequence of the area, and on an approximate Silurian U-Pb zircon age obtained from felsic metatuff (Aleinikoff and Moench, 1985; lower intercept at about 434 Ma, which is possibly 20 m.y. too old). These felsic metavolcanic rocks are part of a volcanic belt in the Smalls Falls Formation mapped from Magalloway Mountain to Stone Mountain (figs. 1 and 3). Where the overlying Madrid Formation is recognized, the Smalls Falls-Madrid contact is sharp, conformable, and marked by an abrupt change to less ruxty to nonrusty, somewhat calcareous rocks of the Madrid Formation.

Only locally do I confidently recognize the Madrid Formation, at the top of the Piermont sequence. Rocks assigned to the formation have a maximum thickness of about 200 m east of Piermont (fig. 5), but they are much thinner or absent elsewhere. At low metamorphic grade the rocks are laminated, brownish-gray or purplish-gray, weakly calcareous slaty siltstone and metasandstone, massively bedded, purplish-brown, fine-grained, feldspathic metasandstone, local feldspathic metatuff, and sparse basaltic greenstone. Where seen at higher metamorphic grade, the formation locally contains calc-silicate rocks and light-purplish-gray metasandstone (now granofels) similar to much of the type Madrid. At several localities, rocks assigned to the formation are conformably succeeded by dark-gray pelitic slate or schist of the Ironbound Mountain Formation, in the same way that the type Madrid is overlain by similar metapelite of the Carrabassett Formation (the basal unit of the Seboomook Group in the CMT).

Frontenac Formation, Second Lake rift, and Waits River Formation--The Frontenac Formation (fig. 1, Sfr) was defined (McGerrigle, 1935; Marleau, 1968) as a sequence of interbedded green to gray slates and arenites with extensive layers of weakly metamorphosed mafic and felsic volcanic rocks that are widely exposed in Frontenac County Quebec. The name, extended by Green (1968) into northernmost New Hampshire, is now applied to a belt of rocks exposed west of Stone Mountain (figs. 1, 3B; Moench, ed., in press), and in an inlier too small to show on the map within the Coppermine Road window (fig. 1, CuRW). Long considered Devonian age, the Frontenac Formation is now considered Silurian on the basis of U-Pb dating cited later, and on the basis of the stratigraphic position of the formation below the Lower Devonian (Gedinnian?) Ironbound Mountain Formation (Marvinney, 1986). On the basis of a concordant U-Pb zircon age of about 500 Ma (Aleinikoff and Moench, 1985), now considered to represent detritus, Moench, ed. (1984) previously correlated the main volcanic belt of the Frontenac Formation with the Cambrian(?) (or early Ordovician) Jim Pond Formation. That was just before I began to recognize the Piermont allochthon. Harwood (1969) suggested an Ordovician age for this same volcanic belt, in the core of his Second Lake anticline; he suggested that these rocks are unconformably flanked by Lower Devonian sedimentary sequences. On the basis of mapping information and the isotopic age data, it is now recognized that the volcanic and sedimentary sequences mapped as the Frontenac Formation belong to the same Silurian lithotectonic package.

According to Marvinney, et al (1992), rocks of the Frontenac Formation were deposited in a Silurian rift basin shown as the Frontenac rift on the profiles of Stewart, et al (1991). Moench, et al (1992) further suggested that the main volcanic belt of the formation is the axial belt of a magmatic spreading ridge that separated two rift basins: the basin of Frontenac deposition on the west, and the basin of Piermont sequence deposition on the east. The belt is anticlinal in form, as Harwood (1969) recognized, but it is "creased" longitudinally by a faulted syncline interpreted to have originated as an axial half-graben. Along the line of the faulted syncline are the volcanogenic massive sulfide deposits of the Clinton River district in Quebec, and at the Ledge Ridge prospect in northernmost New Hampshire. Modifying Harwood's nomenclature, Moench, et al (1992) called this anticlinal belt the axis of the Second Lake rift (fig. 1, SLR).

The volcanic center of the Second Lake rift is a belt of weakly metamorphosed pillowed and massive basalt flows and pyroclastic rocks, rhyolitic tuff and local fragmental rhyolite, and local exhalative deposits and associated volcanogenic massive sulfide deposits extending about 35 mi southwest from near Woburn, Quebec (fig. 1). The metabasalts and related greenstone dikes of the Frontenac Formation have iron- and titanium-rich compositions that are characteristic of basalts erupted in regions undergoing tectonic extension (references in Moench, 1990, p. J13). Felsic rocks exposed at three localities have yielded U-Pb zircon ages of 432+-10 Ma, 418+-4, and <430 Ma; volcanic rocks of the belt are intruded by high-level biotite granite of the East Inlet pluton (fig. 1, EI), dated at 430+-4 Ma, and by the undated, but presumably Silurian, gabbro, diabase, and felsite of the Marble Mountain sheeted dikes (MM). These ages were determined by Eisenberg, 1982; Lyons, et al, 1986, by Aleinikoff (in Moench, ed. in press). The volcanic and intrusive rocks of the belt are assumed to be comagmatic. Though assigned to the Frontenac Formation, volcanic rocks of this belt are conformably overlain by black sulfidic slate mapped as Smalls Falls Formation (exposed in the faulted synclinal "crease"), by slate and arenite of the Frontenac Formation (west of the belt), and by slate and quartzite assigned to the Perry Mountain Formation (east of the belt). If the Perry Mountain Formation of this area is correctly identified, the most active (proximal) part of the Second Lake rift is reasonably inferred to have been a prominant subaqueous ridge that separated the Frontenac and Piermont sequence basins, as proposed by Moench, et al (1992).

Farther south, between the Monroe(?) and Deer Pond faults (figs. 1 and 3A; MNF?, DPF) and north of the Jurassic Gore Mountain and Carboniferous Long Mountain plutons (fig. 1, GM, LM), volcanic rocks of the belt are more distal in character and are interstratified with siliciclastic metasedimentary rocks; the outcrop of a probably small volcanogenic(?) polymetallic sulfide deposit was found by L.J. Cox and M.J. Carnese during mapping for the CUSMAP project. Rocks of the belt in this area are intruded by a bimodal dike swarm, one felsic dike of which has been dated at 418+-4 Ma (Lyons, et al, 1986). This part of the belt appears to be in a transition zone between rocks of the Frontenac Formation and the Piermont sequence. Near the center of the belt is a narrow synclinal(?) lens of black sulfidic phyllite mapped as Smalls Falls Formation, which is inferred to lie above volcanic and sedimentary rocks of the Frontenac Formation. Between the mapped southern terminus of the Deer Pond fault and the Carboniferous pluton rocks of the Frontenac Formation are apparently conformably underlain by thin belts of rocks assigned to the Perry Mountain and Rangeley Formations.

South of the Gore Mountain plutons (GM), the Second Lake rift axis is less well defined. It is expressed by sporadic occurrences of volcanic-bearing sequences mainly in the Perry Mountain Formation, but also in the Smalls Falls Formation, between Stone Mountain and the Gore Mountain plutons. This part of the rift axis was probably sufficiently low to permit much sedimentary communication between the Frontenac and Piermont sequence basins. For example, in the area of Stone Mountain (fig. 3B), the transition occurs west of the inferred rift axis. Here, metasedimentary rocks characteristic of the Perry Mountain Formation grade laterally to metasedimentary rocks characteristic of the Frontenac Formation. The transition from Perry Mountain Formation to Frontenac Formation, best seen along ridges west of Stone Mountain, is broadly gradational and is expressed mainly by the loss of typically poorly cleaved, resistant, matrix-poor quartzite or feldspathic quartzite beds characteristic of the Perry Mountain, and the gain of pervasively cleaved, less resistant, probably matrix-rich arenite beds characteristic of the Frontenac. The Frontenac Formation, thought to be a lateral facies of the Madrid, Smalls Falls, and Perry Mountain Formations, has not been adequetely subdivided but it does contain weakly calcareous, brownish-weathering metasandstone and slaty metasiltstone similar to much of the Madrid Formation of the Piermont sequence, and sparse thin layers of black sulfidic phyllite thought to represent the western feather edge of the Smalls Falls Formation. A strongly calcareous member of the Frontenac Formation that is possibly equivalent to the Waits River Formation, discussed below, is exposed north of the Gore Mountain plutons.

The Waits River Formation (fig. 1, Sct), composed mainly of well stratified calcareous wacke and metasiltstone, graphitic phyllite, and impure marble, is exposed along the west side of the area of figure 1. These rocks are conformably overlain by arenaceous and pelitic rocks of the Gile Mountain Formation exposed west of the Monroe fault. The Gile Mountain Formation is undated; although widely considered to be Early Devonian in age, it might be partly equivalent to the Silurian Frontenac Formation. This is suggested by the facts that metasedimentary rocks of the two formations are not radically different, and that the highly pelitic Meetinghouse Slate Member, possibly at the top of the Gile Mountain (Hatch, 1988), is remarkably similar to the Lower Devonian Ironbound Mountain Formation above the Frontenac. The Ayers Cliff Formation of Quebec (fig. 1, Sct) is correlated with the Waits River Formation.

Locally along and near the Waits River-Gile Mountain contact are basaltic metavolcanic rocks, some pillowed, and sparse felsic metavolcanic rocks, in the same apparent position as the Silurian Standing Pond Volcanics (Aleinikoff and Karabinos, 1990) of southeastern Vermont. Like the metabasalts of the Frontenac Formation, those of the Standing Pond Volcanics have chemical characteristics of basalt erupted in regions undergoing tectonic extension (Hepburn, 1991). Hepburn recognized high and low titanium basaltic sequences that seem comparable to the high-Ti Frontenac basalts and the low-Ti Smalls Falls basalts. The Standing Pond Volcanics and the underlying Waits River Formation probably represent an extensional volcano-sedimentary environment much like that of the Frontenac Formation. Because no major structural break is recognized to exist between the areas underlain by the Frontenac and Waits River Formations, it is worthwhile to consider that the Waits River Formation and the Standing Pond Volcanics are part of the Piermont-Frontenac allochthon.

MODELS FOR ORIGIN OF PIERMONT-FRONTENAC ALLOCHTHON

I propose two radically different models for the origin of the allochthon that are consistent with all that I know so far. The main question is whether the Silurian deposits of the Central Maine and Connecticut Valley troughs accummulated in two separate Silurian basins, or in different parts of one basin that have been faulted together. The critical relationships are: 1) The presence along the eastern side of the Connecticut Valley trough (CVT) of the Piermont sequence, composed of the Quimby, Greenvale Cove, Rangeley, Perry Mountain, Smalls Falls, and Madrid Formations, which from Maine to Connecticut define the stratigraphy of the western part of the Central Maine trough (CMT). The Piermont sequence, deposited without break through Silurian time, occurs west of the western Silurian shore of the CMT, in an area that should now represent the source area for the Silurian deposits of the CMT. Although the CMT and CVT are widely considered to represent two separate sedimentary basins, it is unlikely that sediments forming the same stratigraphic sequence would have accummulated on opposit sides of a landmass. 2) The landmass, represented by the Bronson Hill-Boundary Mountains anticlinorium (BHBMA), is almost certainly too small to have supplied all of the Silurian deposits of the CMT; it is truncated on the northwest by the Monroe, Foster Hill, and Thrasher Peaks faults. Evidently a major part of the source area has been faulted away. 3) The Perry Mountain, Smalls Falls, and Madrid Formations of the Piermont sequence grade laterally northwestward into the Frontenac Formation, which is one of the fundamental units of the CVT. Therefore, if the Piermont sequence is allochthonous, the Frontenac Formation and probably the other Silurian deposits of the CVT would be equally allochthonous according to the strike-slip model, described later, but less allochthonous to possibly autochthonous according to the gravity slide model. 4) The Fairlee pluton, considered a granitic body of the Bethlehem Granodiorite Gneiss, intrudes the allochthonous Perry Mountain Formation and the autochthonous Littleton Formation in the Piermont area (fig. 5). This body, dated at 410+-5 Ma (Moench and Aleinikoff, 1991a, b), is interpreted as a downdropped slice of the Indian Pond pluton (fig. 6), dated at 407+-5 Ma (Kohn, et al, 1992). These age determinations are within error of one another, and both closely agree with the age of 408.5 Ma that Harland, et al (1989) favor for the Silurian-Devonian time boundary. If these three numbers are accurate within several million years, the allochthon must have docked before deposition of most of the Lower Devonian cover sequence. If these relationships are valid, they imply, furthermore, that the Fairlee pluton and all other bodies of Bethlehem Granodiorite Gneiss are subvolcanic and perhaps comagmatic with the extensive metavolcanic rocks in the lower part of the Lower Devonian Littleton Formation (see discussion for stop 46).

My original model (Moench, 1990, and references therein) that the allochthon is an east-derived Acadian thrust sheet rooted along the western margin of the Central Maine trough (CMT) is not valid for two reasons: 1) The Piermont sequence is bounded on the east but not the west by the trace of a through-going sole fault, and intstead grades westward into the Frontenac Formation. Accordingly, under the thrust model the Frontenac Formation and (and probably the other Silurian deposits of the CVT), as well as the Piermont sequence, would have to have been thrust over the anticlinorium. The size of the thrust sheet would be too great. Moreover, possible counterparts of the Frontenac Formations and other Silurian units of the CVT are unknown in the CMT. 2) On the assumption that the previously cited ages for the Fairlee and Indian Pond plutons and the Silurian-Devonian time boundary are approximately correct, this thrusting would have occurred while the entire region was being blanketed by the Early Devonian cover sequence, and long before the onset of compressional Acadian deformation.

Strike-slip model: This model accounts for the apparent inadequate size of the Bronson Hill-Boundary Mountains anticlinorium as the main source area for the Silurian deposits of the CMT. The model also utilizes the Monroe-Foster Hill-Thrasher Peaks line interpreted as a major transcurrent fault that truncates the northwestern side of the anticlinorium. The Foster Hill segment is considered a "flat connector" between the Monroe and Thrasher Peaks segements; it was complexly folded during Acadian compression because of its gentle original dip, whereas the steeper Monroe and Thrasher Peaks faults were relatively unaffected. Possibly the major part of the anticlinorium was excised by strike-slip along this surface and the rocks of the Piermont-Frontenac allochthon were emplaced in its stead. Transport occurred mainly in Silurian time and was subaqueous. In Early Devonian time the allochthon was buried by parallochthonous to autochthonous deposits of the cover sequence. But where did the allochthonous rocks come from? On stratigraphic grounds, at least the Piermont sequence must have accumulated in some part of the Central Maine trough, probably, according to the model, several hundreds of kilometers northeast or southwest of the recognized ends of the CMT. The site, according to the model, was an area where the basins of deposition of the Piermont-CMT sequence and the Frontenac Formation were separated by a low to prominant subaqeous magmatic spreading ridge (Second Lake rift axis). Was movement left-slip or right-slip? Pollock and Marvinney (1993), and Marvinney (1988) propose dextral and reverse senses of motion for the Thrasher Peaks and Deer Pond faults where they cut Lower Devonian rocks of the Seboomook Group in northern Maine. I propose, however, that by far the greatest motion along the Thrasher Peaks fault occurred in Silurian time. So far, I have found no tectonic indicators that can be conclusively tied to the movement in question. Possible sites of origin have not been identified, and probably all of the central and northern parts of the Appalachian orogen would have to be searched. Is it possible, for example, that the remarkably similar diamictites and related rocks of the Chain Lakes massif and the Sykesville Formation of the Washington-Baltimore area, now 900 km apart, originated as a single body? The Monroe-Foster Hill-Thrasher Peaks line is in an appropriate place to have been part of the linking structure.

Two problems in this model are the lack of a specific source area, and the lack of recognized major cataclasis along the Foster Hill fault.

Gravity slide model: According to this model, the Piermont-Frontenac allochthon is far less allochthonous, and the Frontenac Formation is less allochthonous than the Piermont sequence, which slid westward and piled against the Frontenac Formation. This model takes advantage of two facts: 1) The absence of known near-shore Silurian deposits (Sns) along the trend of the Bronson Hill-Boundary Mountains anticlinorium from Littleton, NH, to about 6 mi northeast of Magalloway Mountain (fig. 1), a distance of more than 60 mi. 2) The near absence of conglomerate in the Rangeley Formation of the allochthon for almost the same distance northeast of Piermont, NH. According to this model, the 60 mi length of the anticliorium that lacks the near-shore deposits was awash through Silurian time, perhaps as a strait or sound connecting the large CMT and CVT basins. En echelon to the northeast and southwest were major island ranges represented by the separate Bronson Hill and Boundary Mountains parts of the anticlinorium that contain the near-shore deposits. To judge from conspicuous left-rotational "twists" seen in the map patterns (figs. 1 and 4), the islands might have been much farther apart than their remnants are today. The sound, lying west of the Silurian tectonic hinge, might have been the site of deposition of the Piermont sequence, and possibly also the locus of the magmatic axis of the Second Lake spreading ridge. The basin of deposition of the Frontenac Formation and other Silurian units of the CVT was west of the ridge and, as proposed by Marvinney, et al (1992), anterior to (west of) the Bronson Hill-Boundary Mountains anticlinorium.

According to the model, the Silurian sediments and volcanics that accumulated in the sound were uplifted and "dumped" westward in latest Silurian and earliest Devonian time. Uplift was sufficient to initiate subaqueous sliding, but probably not sufficient to cause subaerial erosion. Probably at about the same time, major southeastward slumping occurred along the northwestern side of the Central Maine trough (see Moench and Pankiwskyj, 1988a, b, and references therein). Whereas the strike-slip model might be supported by evidence of major shearing along the Foster Hill fault, little evidence of shearing is seen in the actual outcrops. In fact, features seen along Foster Hill fault and the major premetamorphic slides of the Central Maine trough (fig. 1) described by Moench (1970) are remarkably similar; all are sharp premetamorphic surfaces that rarely show evidence of cataclasis and only minor disruption of bedding in the opposing walls. I have interpreted the slides as the soles of giant slumps. According to the model, uplift and westward "dumping" was accompanied by a sinistral translation of the two island ranges; this movement forced the southern part of the Piermont sequence to a position that is now west of the Clough Quartzite and Fitch Formation of the Bronson Hill anticlinorium for a distance of about 45 mi southwest of Littleton, NH. A similar juxtaposition of rocks assigned to the Piermont sequence west of Magalloway Mountain might have been produced by a southwestward "wedging" motion of the south end of the Chain Lakes massif and overlying autochthonous units.

Possibly damaging to this model is the occurrence of polymictic and quartz conglomerates in the Rangeley Formation as far as 45 mi SW of Rangeley village, along the western side of the CMT. I have long considered these conglomerates to have been shed from the part of the anticlinorium that I now suggest was awash in Rangeley time. Furthermore, the gravity slide model, as written, requires the division of the western source area, already too small, into smaller land masses; and it does not address the question of the truncation of the northwestern side of the Bronson Hill-Boundary Mountains anticlinorium.

ACKNOWLEDGEMENTS

I am greatly indebted to John N. Aleinikoff for the high quality U-Pb zircon ages that he has determined on a large number of plutonic and metavolcanic rocks in northern New England; some supported my original interprtetations, but others caused me to return and agonizingly reappraise my erroneous ideas. Discussions with Wallace A. Bothner and John B. Lyons have contributed to my understanding of the allochthon, and I much appreciate the efforts of Bothner, Robert G. Marvinney, and Stephen G. Pollock to educate me concerning the subtle characteristics of the Ironbound Mountain and Frontenac Formations. Critical aspects of my interpretation hinge on Bothner's understanding of Ironbound Mountain-Frontenac relationships in northernmost New Hampshire.

ROAD LOG AND DESCRIPTION OF STOPS

Althought the Piermont-Frontenac allochthon is mainly a feature of western New Hampshire and northeastern Vermont, there is little chance that I would have recognized its existence if it weren't for my previous experience in the Rangeley area of western Maine, which contains the type areas of the five Silurian formations and one Ordovician formation that make up the Piermont sequence of the allochthon. Day one of this trip, from Oquossoc to Madrid, ME, is therefore both a survey of the enormously thick sequence of Ordovician, Silurian, and Lower Devonian rocks that make up a major part of the Central Maine trough (fig. 1, CMT), and a preview of the same sequence, with variations, in the allochthon. Most stops for day 1 are taken from Moench and Boudette (1987). Other field guides that have been prepared for this area include Moench and Boudette (1970), and Moench (1989a). Stops for day 2 have not been described previously; all but one are on figure 3. Stops for day 3 are on figures 4 and 5; several are listed in Moench,et al (1987) and Moench (1989b), but readers are cautioned about mapping changes made since those field guides were prepared.

Most unit symbols in the stop descriptions are on figure 2; exceptions are on other figures, as cited. States and compass directions, and tectonic lines and belts (fig. 1), are abbreviated. The term allochthon refers to the Piermont-Frontenac allochthon.

Mileage for day 1. Refer to figure 1 of Moench and Boudette (1987), cited as follows: **Stop 1** (5 of M&B). The five 15-minute quadrangles shown in Moench and Boudette (1987, fig. 1) were mapped by Harwood (197), Cupsuptic qd, Boudette (1991), Kennebago Lake qd, Guidotti (197), Oquossoc qd, and Moench (1971), Rangeley and Phillips qds. Credit by 15-minute quadrangle.

0.0 Farmhouse Inn, on E side of ME 4 about 1.4 mi. S of Rangeley village. From the inn parking lot descend to the long streamwashed outcrops along Nile Brook. just upstream from ME 4.

Stop 1 (5 of M&B). Euxinic shale and Graywacke member of Quimby Formation (Oqe). Part of the type area of the Quimby Formation (Ordovician, Cincinnatian), named for Quimby Pond and Quimby Brook about 4 mi. WNW of Rangeley village. The rocks are interbedded black sulfidic slate and metagraywacke near the top of the formation. Graded beds top NW; the SE-topping upper contact is exposed on the lake shore, about 0.5 mi. to the S. The unit is exposed in a small area near the S end of the allochthon (fig. 5, Oqe).

0.8 Park on right shoulder, at N end of nearly continuous outcrops along the E side of ME 4.

Stop 2 (2 and 3 of M&B). Greenvale Cove Formation (Sg), and subaqeous fanglomerate of Rangeley Formation (member A, Sra). The northernmost outcrops represent the type locality of the Greenvale Cove Formation (Silurian? Llandoverian?), named for the southeast arm, Greenvale Cove, of Rangeley Lake. The rocks, in the biotite zone, are laminated slate, metasiltstone, and mildly calcareaous, feldspathic metasandstone. The formation is about 200 m thick; its abruptly gradational, conformable upper contact is exposed on the hillside about 0.3 mi to the NE. Rocks assigned to the Greenvale Cove Formation are extensively exposed near the S end of the allochthon (fig. 5, Sg). At stop 2, rocks of member A of the overlying Rangeley Formation to the SE are massively bedded metaarkose (Sras) and gradationally overlying polymictic pebble to boulder metaconglomerate (Srac), having a combined thickness of about 1,200 m. In the allochthon, metaconglomerates of member A (or possibly B, seen at stop 3) are represented by thin lenses of polymictic metaconglomerate at the lower contact of the Rangeley Formation (fig. 5, Srp).

1.9 Park near the intersection of ME 4 and the road that follows the south shore of Rangeley Lake.

Stop 3 (8 of M&B). Slump-folded and conglomeratic rocks of Rangeley Formation (member B, Srb). Riprap quarry and long outcrop along Cascade Stream, a short distance upstream from the old Greenvale Cove schoolhouse, which is due east of the intersection. Private property; permission to enter denied in 1993. This is the type locality of the Rangeley Formation. Rocks exposed here represent member B. They are well stratified mildy euxinic interbedded dark-gray, pseudomorphous staurolite schist and feldspathic quartzite, quartz-rich polymictic metaconglomerate, and matrix-supported conglomeratic mudflow deposits (Srac); structures include an intraformational unconformity that truncates the limb of a slump fold. Member B is about 1,200 m thick; its conformable upper contact is placed just below the lowest beds of quartz metaconglomerate of member C, but where conglomerates are absent rocks of members B and C are indistinguishable.

5.3 Park on right shoulder, near Long roadside outcrop on the S side of ME 4.

Stop 4 (just E of Long Pond, on M&B). Pelitic rocks of Rangeley Formation (member B, Srb). The rocks are unusually pelitic rocks of member B. This lithology is seen locally in the allochthon, where rusty-weathering quartzite beds are typically more abundant.

7.7 Roadcut on the SW side of ME 4; park on SW shoulder an old shed. Watch out for traffic!

Stop 5 (10 of M&B). Quartz conglomerate-bearing rocks of Rangeley Formation (member C, Src). Walk S on the E side past the outcrops, then N on the W side. Staurolite zone. Quartz metaconglomerate is exposed on the nose of a steeply NE-plunging fold, and is flanked by interbedded dark-gray pelitic schist and quartzite, all of member C. The conglomerate, better exposed at stop 12, is dated by an upper Llandoverian shelly fauna found by R.J. Willard, more extensively collected by E.L. Boudette, and dated by A.J. Boucot, about 10 mi. (16 km) north of Rangeley village (see Moench and Boudette, 1987, fig. 1, p. 276). The quartz conglomerates of member C are interpreted as the basin facies of near-shore or on-shore deposits of the Clough Quartzite (Sc), of the same age (Boucot and Thompson, 1963). In the allochthon, quartz conglomerate is sparse but found in the areas of figures 3A, B, and 5 (Srq).

8.9 Long roadcut on the W side of ME 4; park in logging staging area just N of the bridge over the Sandy River, and walk N about 0.1 mi. to the outcrops.

Stop 6 (10 and 11 of M&B). Perry Mountain Formation (Sp). This is in the type area of the formation; the top of Perry Mountain is about 1 mi. to the E. The rocks are sharply interbedded muscovite-rich staurolite schist and quartzite, in part somewhat rusty-weathering.

9.8 Near N end of a long roadcuts, which extend around the sharp curve farther S. Watch out for traffic! Park on W shoulder and walk on E side of ME 4 to the N end of the outcrops.

Stop 7 (11 of M&B). Perry Mountain (Sp) and Smalls Falls (Ssf) Formations. The rocks, extending around the curve, are cyclically interbedded planar quartzite turbidites and muscovite-rich, pseudomorphous staurolite schist of the upper part of the Perry Mountain Formation. The formation is about 600 m thick; its upper contact, exposed elsewhere at many places, is sharp to abruptly gradational. In the allochthon, nearly identical rocks are mapped separately from a variably tuffaceous and volcanic facies (figs 2-5, Spt). Strongly euxinic, black, pyrrhotitic schist and quartzite of the Smalls Falls Formation is seen in the southernmost outcrop.

10.6 Turn right (W) into the Smalls Falls picnic area.

Stop 8 (12 of M&B). Smalls Falls Formation (Ssf). Type locality of the Smalls Falls Formation (Silurian, Ludlovian). Dated by graptolites found by Alan Ludman in central Maine (see Moench and Pankiwskyj, 1988a). Extensive exposures of black, pyrrhotitic schist and quartzite occur in falls and cascades along the Sandy River, and particularly along Chandler Mill Stream, a major tributary from the W. Staurolite zone, but staurolite absent owing to high sulfide content; andalusite (chiastolite) is conspicuous. A calcaeous upper member of the formation is mapped farther S. The maximum thickness of the formation in western ME is about 750 m; the upper contact is sharp but conformable. The Smalls Falls Formation is widely exposed in the allochthon, where it is generally much thinner, and where a bimodal volcanic facies also is mapped (Ssfv).

13.5 Madrid village. Park at the small church about 0.1 mi. E of the bridge across the Sandy River, and descend at the bridge to the outcrops along the river and in Saddleback Stream, a major tributary from the N.

Stop 9 (14 of M&B). Madrid Formation (Sm). Type locality of the Madrid Formation (Silurian?, Pridoian?). Rocks of the lower member are thin-bedded calcsilicate rocks of the lower member, best exposed in Saddleback Stream. Rocks of the upper member, exposed along the Sandy River, are thick-bedded, mildly calcareous, feldspathic, fine-grained metasandstone of the upper member, which also contains about 20 percent of gray pelitic schist with staurolite pseudomorphs. Graded bedding and crossbedding consistently top southeast. The formation is about 300 m thick here; its upper contact is abruptly gradational. The Madrid Formation is correlated with the well dated Fitch Formation (Sf) of the BHA. In the allochthon the Madrid Formation has a maximum thickness of about 200 m, but the formation is typically much thinner and locally absent; and, furthermore, locally contains metavolcanic rocks.

14.4 Outcrops along Sandy River, below and downstream from a ME 4 bridge. Visit only in dry weather and at low water. Park on the S shoulder and descend S of the bridge.

Stop 10 (15 of M&B). Carrabassett Formation of Seboomook Group (Ds). The rocks near the bridge are dark-gray staurolite schist displaying cyclic mud-silt turbidites and scattered thin lenses of sulfidic, garnetiferous ironstone, some copper-bearing; these rocks are part of the massively bedded member of the Carrabassett Formation, named by Boone (1973). The formation is the basal unit of the Seboomook Group (Ds) in the CMT, where it is also recognized, locally, in the lower parts of rocks mapped as the Littleton Formation. Beds of metasandstone similar to the upper member of the Madrid Formation, but mapped in the Carrabassett, are exposed farther downstream. The Carrabassett Formation is correlated with the lithologically similar Ironbound Mountain Formation (Di), above rocks of the allochthon.

15.5 Bold outcrops on the NE side of ME 4; reverse direction and park on N shoulder.

Stop 11 (1.1 mi SE of 15 of M&B). Madrid (Sm) and Carrabassett (Ds) Formations. The rocks are calcareous metasandstone of the Madrid Formation, overlain to the SE by dark-gray pelitic rocks of the Carrabassett Formation (Lower Devonian). The contact is not exposed here, but graded beds in both units indicate the Carrabassett is younger. Return N along ME 4 to the intersection at stop 3.

29.1 Intersection at stop 3. Take road to the W along the south side of Rangeley Lake.
36.6 Turn left (S) onto ME 17.
38.1 Rangeley Lake overlook on the left (E), and rocks of stop 13 on the right, to be seen later.
43.7 Small parking area at Mooselookmeguntic Lake overlook, known locally as the "height of land."

Stop 12 (On ME 17, S 65 W of Four Ponds Mtn., on fig. 1 of M&B). Quartz conglomerate-bearing rocks of Rangeley Formation (member C, Src). About 900 ft of nearly continuously exposed member C, in the first sillimanite zone above the gently E-dipping upper contact of the Mooselookmeguntic batholith. Interstratified, rusty-weathering pelitic schist, feldspathic quartzite, and quartz granule to pebble metaconglomerate. Early folds plunge NE and are redeformed by minor late reclined folds having late AP schistosity that is subparallel to the upper contact of the batholith. The batholith, composed in this area of 2-mica granite, is interpreted as a subhorizontal sheet emplaced in the ductile-brittle transition zone near the boundary of the middle and upper crust (Moench and Zartman, 1976; Moench, et al, 1982).

44.3 Reverse direction at parking lot at Four Ponds Brook. This is the approximate location of a core hole that confirmed the mapped gentle E dip of the top of the batholith. Drive N.
50.5 Park in overlook on right (E).

Stop 13 (On ME 17, about 5 mi NW of Four Ponds Mtn, on fig. 1 of M&B). Graywacke member of Quimby Formation (Oqg). Extensive roadcuts on W side of ME 17 expose rusty-weathering metagraywacke. Also exposed is a probable sill, about 20 m thick, of dense felsite, probably a feeder to the volcanic member (Oqv), exposed farther N.

56.1 Oqoussoc village, where ME 17 terminates at its intersection with ME4. Turn left (W).
57.1 Park near small green house with white trim, and walk about 0.4 mi. N along driveway to causeway to Spots Island.

Stop 14 (1 of M&B). Pelitic rocks of Dead River Formation (O€d). Rocks exposed on the island near the causeway are strongly crenulated greenish-gray pelitic phyllite containing abundant stringers and pods of quartz. Similar to parts of the pelitic Aziscohos Formation of Green (1964). Return to vehicle and drive E through Oquossoc village, continuing towards Rangeley.

58.3 Junction ME 16 from NW with ME 4; continue E on ME 4/16.
59.0 Park on S side of ME 4/16; outcrops along N side.

Stop 15 (2 of M&B). Ammonoosuc Volcanics (Oa) and Partridge Formation (Op). Basaltic greenstone of the Ammonoosuc Volcanics is succeeded to the E by black slate of the Partridge Formation. The contact is a NW-trending brittle fault, marked by quartz veins. Early Mohawkian graptolites of the climacograptus bicornis zone were recovered from the black slate about 5 mi. (8 km) to the N (Harwood and Berry, 1967).

61.3 Park on S shoulder at large roadcut near Dodge Pond.

Stop 16 (3 of M&B). Graywacke member of Quimby Formation (Oqg). Interbedded metagaywacke and subordinate dark-gray slate of the member, near its contact with the overlying euxinic shale and graywacke member, seen at stop 1. Continue E on ME 4/16 to Rangeley, then S on ME 4.

65.7 Farmhouse Inn.

Mileage for day 2. Stop 1 is on figure 1; stops 18-32 are on figure 3A; stops 33-36 are on figure 3B.

7.4 Drive from the Farmhouse Inn N to Rangeley village and W almost to Oquossoc village, where ME 16 departs to the N from ME 4/16. Drive N on ME 16 towards Errol, NH.
12.3 Cupsuptic Camp Ground. Outcrop of Dead River Formation on right.
15.2 Park on shoulder at bold outcrop on the N side.

Stop 17. Granite of Highlandcroft Plutonic Suite (Oh). Foliated, metamorphosed, feldspar-porphyritic granite or granodiorite of Adamstown pluton; dated at 452+-4 Ma (Lyons,et al, 1986). Intrudes Dead River and Aziscohos Formations (O€f). Considered a plutonic member of the Bronson Hill magmatic arc.

23.9 Large outcrops on S side of Devonian 2-mica granite (fig. 1, Dn), at northwest end of Mooselookmeguntic batholith..At 26.1 is outlet of Aziscohos Lake, and diversion pipeline.

41.8 Entrance to dam and power station on the Androscoggin River; park on the W side of NH 16 and walk driveway to the S to outcrops near the dam, on the W side of the river.

Stop 18. Dead River Formation (O€d). Complexly deformed, spectacularly "pinstriped" quartzite and phyllite. The "pinstripes," which are emphasized by dark minerals, are interpreted as pressure-solution features developed along early slaty cleavage.
41.5 Junction of NH 16 (N) with NH 26. Turn W through Errol village. At 41.8 turn S on NH 16 towards Berlin, NH.
49.3 Large parking area at Seven Islands bridge, which crosses the Androscoggin River.

Stop 19. Dead River Formation (O€d) faulted against Rangeley Formation (Sr) at E edge of the allochthon. Walk E across the bridge, and follow the logging road 1,100 ft. from the E end of the bridge; turn due S into the woods about 775 ft., along a flagged line to the principal outcrops of this stop, marked with severaltapes. From the logging road to this point are several outcrops of thickly bedded

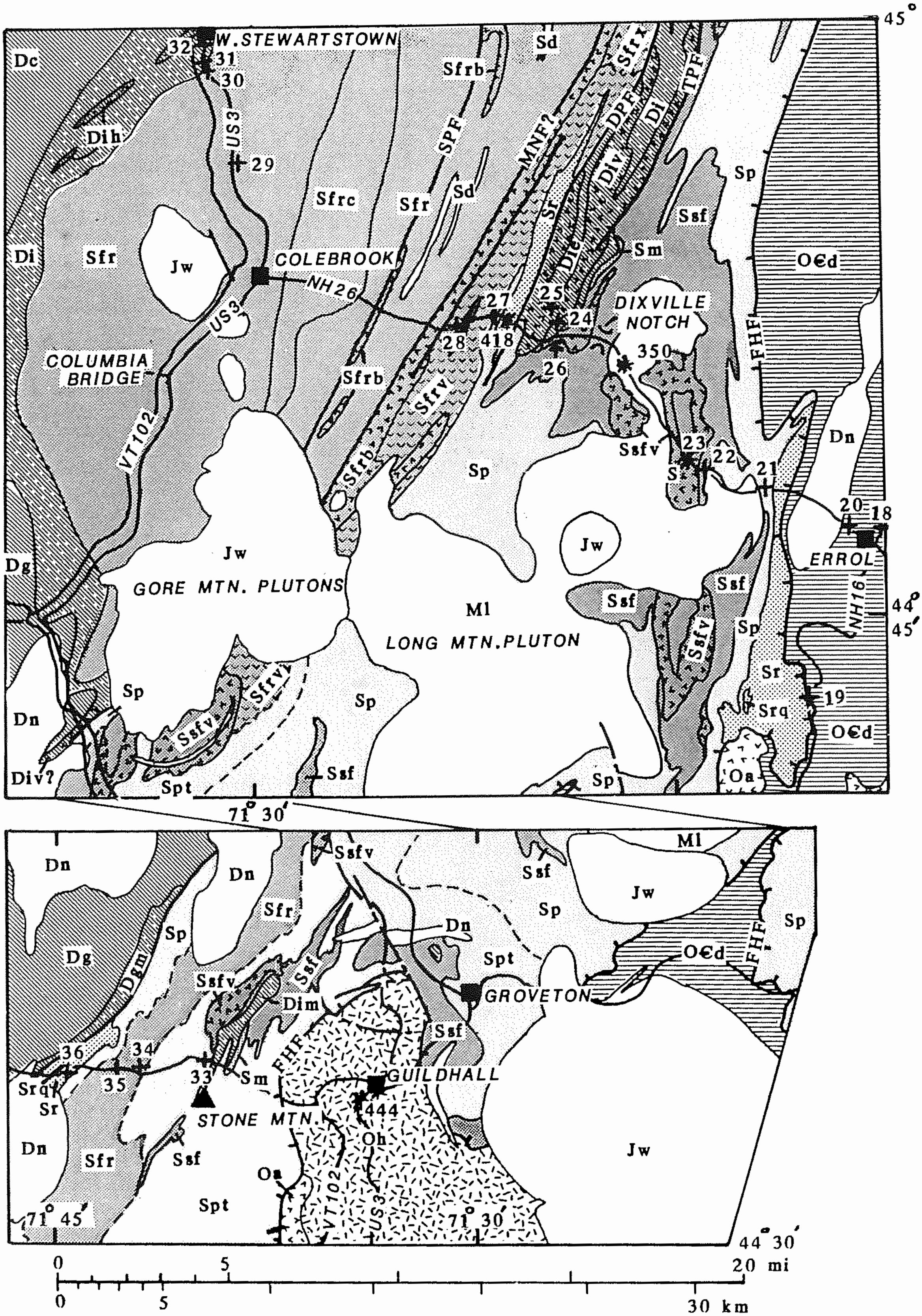
W. STEWARTSTOWN
COLEBROOK
COLUMBIA BRIDGE
DIXVILLE NOTCH
ERROL
GORE MTN. PLUTONS
LONG MTN. PLUTON
GROVETON
GUILDHALL
STONE MTN.
US3
NH26
VT102
NH16
SPF
MNF?
DPF
TPF
FHF
Dc
Dih
Di
Dg
Dn
Div?
Dgm
Dim
Sfr
Sfrc
Sfrb
Sfrv
Sfrx
Sd
Sr
Srq
Sm
Ssf
Ssfv
Sp
Spt
Jw
Ml
OЄd
Oa
Oh
Dic
Div
45°
44° 45′
71° 30′
71° 45′
44° 30′
0 5 20 mi
0 5 30 km

Figure 3. Geologic maps of the Errol-Colebrook area (3A), and the Stone Mountain area (3B), NH-VT. Area A modified by R.H. Moench and W.A. Bothner from Green (1964), Errol qd, Hatch (1963), Dixville qd, and Swift (1966) and Myers (1964), Averill qd. Area B modified by R.H. Moench, L.J. Cox, A.R. Pyke, and J.L. Schneider from Chapman (1935), Percy qd, Johansson (1963), Guildhall qd, and Woodland (1965), Burke qd.

Intrusive rocks: Oh, Highlandcroft Plutonic Suite (Ordovician). **Sd**, Metadiabase (Silurian?). **Dn**, New Hampshire Plutonic Suite. **Ml**, granite of Long Mountain pluton (Mississippian). **Jw**, White Mountain Plutonic-Volcanic Suite

Autochthonous to parallochthonous cover sequence (Lower Devonian and Lower Devonian?): Di, Ironbound Mountain Formation; **Dim**, magnetite-bearing member; **Div**, volcanic member; **Dih**, grit lenses at Halls Stream; **Die**, euxinic shale and tuff member. **Dc**, Compton Formation. **Dg**, Gile Mountain Formation; **Dgm**, Meetinghouse Slate Member

Sequences of Piermont-Frontenac allochthon (Silurian and Silurian?): Sfr, siliciclastic facies, **Sfrc**, calcareous facies, **Sfrv**, mixed sedimentary and volcanic facies, **Sfrx**, proximal bimodal volcanic facies, **Sfrb**, basalt lenses of Frontenac Formation. **Sr**, Rangeley Formation; **Srq**, quartz granule and pebble conglomerate lenses. **Sp**, quartzite and schist facies of Perry Mountain Formation; **Spt**, variably tuffaceous and local volcanic facies. **Ssf**, Smalls Falls Formation; **Ssfv**, bimodal volcanic-bearing member. **Sm**, Madrid Formation

Autochthonous sequence (Ordovician to Upper Cambrian?): OЄd, Dead River Formation. **Oa**, Ammonosuc Volcanics

*** S Site of U-Pb zircon age determination**: S, indefinite Silurian age from felsic volcanic rocks of Smalls Falls Formation. **418**, age of 418+-4 Ma from rhyolite dike (Lyons, et al, 1986). **350**, age of about 350 Ma from granite of Long Mountain pluton (Harrison, et al, 1987). **442**, age of 442+-4 Ma from granodiorite of Lost Nation pluton (J.N. Aleinikoff, in Moench, ed., in press)

+ 18 Numbered field trip stop

Brittle fault. **Brittle to ductile fault**; **SPF**, Perry Stream, **MNF**, Monroe, **DPF**, Deer Pond, **TPF**, Thrasher Peaks. **FHF** **Foster Hill fault**; ticks on side of upper plate

"pinstriped" quartzite and phyllite of the Dead River Formation. The Foster Hill fault, marking the E boundary of the allochthon, is not exposed here but is placed within about 2 m. Exposed immediately to the S, is rusty-weathering, dark-gray to black phyllite and quartzite of the Rangeley Formation. Additional outcrops of the Rangeley Formation are seen along a flagged route that cricles back to this point. Where seen in outcrop about 11 mi. to the S, the fault is marked by a 3-cm thick layer of disturbed black pelitic to silty slate that shows no evidence of cataclasis, except for an oblique set of irregular quartz veins. The features are similar to those of several major prematamorphic faults in western ME (Moench, 1970; Moench and Pankiwskyj, 1988a, b). Return to Errol.

56.8 Intersection of NH 16(S) and NH 26 at Errol; turn W toward Colebrook, NH.
57.3 Park on N shoulder, at outcrops on both sides of NH 26.

Stop 20. Dead River Formation (OЄd). Medium-gray pelitic hornfels with thin to thick beds of quartzite, representing a somewhat more pelitic facies of the formation. The rocks are contact metamorphosed by 2-mica granite of the Greenough Pond pluton, immediately to the W.

60.2 Park on N side, just W of large roadcuts.

Stop 21. Perry Mountain Formation (Sp). The rocks are interbedded muscovite-rich garnetiferous staurolite schist and quartzite, originally mapped as the Ordovician Albee Formation (Green, 1964; Moench, ed. 1984), before the allochthon was recognized. The rocks are deformed by a tight upright syncline that plunges gently N. The Perry Mountain Formation of this belt is underlain to the E by the Rangeley Formation and overlain to the W by the Smalls Falls Formation, on the E limb of a major N-trending sycline originally mapped by Green (1964).

62.2 Park on N side and walk E along the road to the W edge of a field, then cross road and walk W along outcrops in the woods and along the road.

Stop 22. Volcanic member of Smalls Falls Formation (Ssfv). From E to W granite of the Greenough Pond pluton is followed by a thin zone of schist and quartzite of the Perry Mountain Formation, then by about 100 ft of rusty-weathering schist and quartzite of the Smalls Falls Formation, and then by about 65 ft of laminated felsite, granite, variably rusty schist, quartzite and metachert?, in sharp contact on the W with basaltic amphibolite. On the N side of the road the amphibolite is sharply interlayered with pink, garnetiferous metachert. The metavolcanic rocks and metachert are assigned to the volcanic member of the Smalls Falls Formation, which regionally lies above and below strongly euxinic rocks more characteristic of the formation.

62.7 Park at long roadcuts on both sides of road.

Stop 23. Volcanic member of Smalls Falls Formation (Ssfv). The rocks are mafic, felsic, and possibly some intermediate metavolcanic rocks and metachert of the volcanic member. A large sample of cherty fragmental felsic rock obtained about 4 ft from the east end of the guard rail on the N side yielded an approximate Silurian U-Pb zircon lower intercept age, and an apparently inherited upper intercept age of about 1,500 Ma (Aleinikoff and Moench, 1985).

67.6 Dixville Notch.
67.8 Turnoff to the N to The Balsams, a resort hotel. Follow the road through the hotel parking area; at 68.7 take right (N) fork and continue to the N end of a small pond at 69.2.
69.2 Park on E shoulder just N of pond.

Stop 24. Magnetite-bearing facies of Ironbound Mountain Formation (Dim). Directly N of the pond are bold outcrops of poorly bedded, medium-gray, pelitic to semipelitic schist, most of which contain scattered magnetite crystals. These rocks grade northward to more characteristic dark-gray pelitic slate of the formation. About 3 mi NE of this stop, the slate is conformably underlain by metasandstone and calcsilicate rock mapped as the Madrid Formation (Sm), which in turn is underlain by rocks of the Smalls Falls Formation (Ssf). Continue N and W along road.

70.4 Road forks; park. The S fork leads to a golf course and the N fork leads of Upper Kidderville village.

Stop 25. Volcanic facies of Ironbound Mountain Formation (Div). On the steep hillside just N of the fork are abundant outcrops of metavolcanic rocks mapped as the volcanic facies. For a distance of about 300 ft from E to W the rocks are amphibolite and amphibole schist, fine-grained gray metasedimentary rocks like those at stop 24, passing to more felsic amphibole-bearing metatuff(?), and a thick sequence of massively bedded, coarse-grained quartz-feldspar crystal metatuff. These rocks are part of an assemblage of weakly metamorphosed mafic to felsic volcanic rocks and volcaniclastic grit mapped in the Ironbound Mountain Formation for a distance of 35 mi N of this stop; they intertongue with dark-gray pelitic slate of the formation. Reverse direction and return to the intersection of the road to The Balsams and NH 26 near Dixville Notch.

72.0 Turn right (W) onto NH 26. At 72.6 is a large outcrop of amphibolite on N side.
73.3 Park on N shoulder at large roadcut on S side.

Stop 26. Smalls Falls Formation (Ssf). Rusty-weathering, sulfidic black schist and quartzite of the formation, strongly folded along steeply plunging axes; as shown by graded bedding, the folds face N toward rocks of the Ironbound Moutain Formation seen at stops 24 and 25.

74.9 Sharp curve to right (N) and steep driveway down to house on the bank of the Mohawk River. Park where safe on shoulder of NH 26, watch out for traffic, and walk down the driveway to the house. The Owner has kindly granted access permission for the trip participants, provided they don't hammer on the rocks. Please leave hammers in the vehicle!

Stop 27. Bimodal dike swarm of Second Lake rift. Outcrops along the river display a N-trending bimodal dike swarm that obliquely intrudes interbedded schist and quartzite of the Perry Mountain Formation. Graded beds top W and rocks of the formation are underlain, upstream to the E, by rusty-weathering schist and quartzite of the Rangeley Formation. The Perry Mountain Formation is no thicker than about 100 m in this area; it is overlain to the W by mixed metasedimentary and metavolcanic rocks assigned to the Frontenac Formation (Sfrv). One of the felsite dikes, collected from a nearby outcrop on NH 26, and rhyolite metatuff of the Frontenac Formation sampled 20 mi (32 km) onstrike to the NE have yielded identical U-Pb zircon ages of 418+-4 Ma (Lyons, et al, 1986).

75.8 Intersection of NH 26 with road to the N, Kidderville and Coleman State Park.76.3. Outcrops on the N side, along the bank of the Mohawk River just west of a resaurant and motel with large parking area.

Stop 28. Basalt-dominated volcanic rocks of Frontenac Formation (Sfrv) of Second Lake rift. Stratified basaltic amphibolite and interlayered felsite and felsic schist representing the magmatic axis of the Second Lake rift. These rocks are distal relative to the near-vent facies (Sfrx), mapped from the N border of the area of figure 3A to Woburn, Quebec (fig. 1). One of several zircon size fractions obtained from the felsic schist yielded a concordant age of about 500 Ma (Aleinikoff and Moench, 1985), now considered a detrital age.

82.5 Intersection of NH 26 and US 3 at Colebrook, NH. Turn right (N) onto US 3. Roadcuts at 83.4, opposite Colebrook cemetary, and 85.4 to 85.9 expose the Frontenac Formation.
86.4 Park on E shoulder, near outcrop on the E side, at Colebrook-Stewartstown line

Stop 29. Metagraywacke and phyllite of Frontenac Formation (Sfr). Thick and thin beds of gray metagraywacke interbedded with subordinate darker-gray, biotite-bearing pelitic phyllite, representing a nonvolcanic facies of the formation. Warped slaty cleavage that dips 30- 50 E is AP to reclined folds; the most uniform attitude of bedding is about N 75 W, 20N.

89.3 Park on E shoulder of US 3 at S end of long roadcut.

Stop 30. Frontenac Formation (Sfr). The S face of the outcrop displays upright, pervasively cleaved graded beds of metagraywacke about 20 cm thick alternating with thinner beds of gray, biotite-bearing pelitic phyllite (bedding attitude N 40 E, 30 N; cleavage N 5 W, 65 E).

89.6 N end of same long roadcut on E side of US 3.

Stop 31. N-dipping contact between Frontenac Formation (Sfr) and Ironbound Mountain Formation (Di). Walk S through brush to long pavement at the top of the roadcut. The contact between interbedded metagraywacke and pelitic phyllite of the Frontenac Formation to the south and overlying faintly bedded to massive dark-gray phyllite (metamudstone) of the Imonbound Mountain Formation is in the approximate middle of the outcrop. The contact is confonnable and may be placed just above the appearance of the first graded metagrawacke beds of the Frontenac Formation. Bedding attitudes throughout the outcrop are consistent with the measurements at stops 29 and 30; folds in the uppermost rocks of the Frontenac plunge gently N and are upright, as shown by graded bedding.

90.1 S end of long roadcut on downhill grade to West Stewartstown; park on E shoulder.

Stop 32. Ironbound Mountain Formation (Di). Poorly bedded to massive, dark-gray pelitic phyllite, or metamudstone, characteristic of the formation. Near West Stewartstown, the formation contains lenses of feldspathic grit characteristic of the Grenier Ponds Grit Member of the formation in northern ME, and found also in rocks mapped as the volcanic facies north of stops 24 and 25, and in rocks assigned to the formation near Littleton, NH. Unpublished mapping by Wallace A. Bothner (in Moench, ed., in press) indicates that the Ironbound Mountain Formation is conformably overlain to the NW of this stop by the Compton Formation (Dco), which contains Lower Devonian (Emsian) plant fossils (Hueber, et al, 1990). These relationships establish the tie between the Frontenac Formation of the allochthon and overlying rocks of the CVT. Reverse direction and follow US 3 to S.

97.7 Intersection of NH 26 and US 3 in Colebrook. Continue S on US 3. At 101.7, at turnoff to Columbia Bridge, is a large outcrop of Frontenac Formation (Srf). Cross to VT 102, just S of Lemington, VT; drive S on VT 102. At 110.7 is Bloomfield, VT.
125.9 Guildhall, VT; bridge to Northumberland, NH to E. Continue W on VT 102.
128.1 Intersection of VT 102 with road W to Granby, VT. Turn W onto Granby Road.
131.7 Junction of logging road on left (S); park on the logging road.

Stop 33. Variably tuffaceous and local volcanic facies of Perry Mountain Formation (Spt). Outcrops along the logging road and on the sides of the Granby Road expose feldspathic stratified rocks of the variably tuffaceous and local volcanic facies; biotite zone. These rocks are intruded by dikes of weakly metamorphosed fine-grained rhyolite quartz porphyry of the type that yielded a late Silurian U-Pb zircon age SW of Littleton. Walk 500 ft W along Granby Road to a logging road that leads N; follow the logging road N about 960 ft to a large block, one face of which displays interbedded chalky-weathering feldspathic quartzite and pale-green phyllite characteristic of the facies. Retrace about 40 ft and follow flagged line about 250 ft, S 50 W, diagonally up the steep side of a knoll, to a 12 x 25 ft rock face exposing similar rocks; these rocks are deformed by downward-facing late

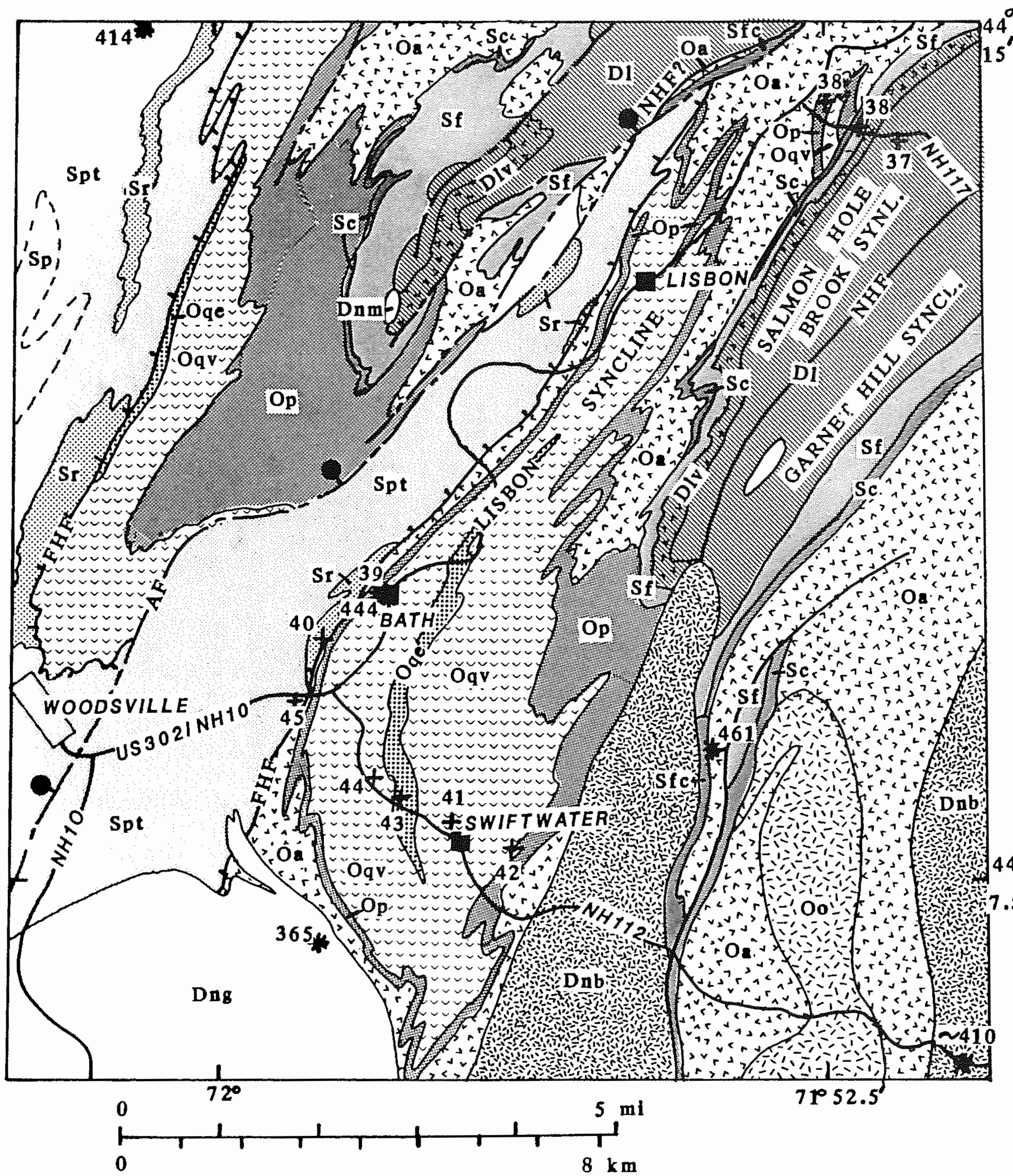

folds with AP spaced cleavage, a common structural feature seen in the P-F allochthon. Continue S an additional 50 ft to outcrops on the knoll crest exposing sharp and abruptly graded quartzite beds, 1 to 50 cm thick, separated by greatly subordinate beds of green, biotite-bearing phyllite. This is a characteristic bedding style of the Perry Mountain Formation. Return to vehicle.

133.7 Park on logging road, which branches to the S; cross to N side of Granby Road and follow flagged line N 25 W to partly cleared outcrops at about 100 and 200 ft from the road.

Stop 34. Frontenac Formation (Sfr) with Perry Mountain "hybrid." The rocks are a hybrid of interbedded phyllite and feldspathic quartzite that resembles the Perry Mountain Formation, and less contrasty,

Figure 4. Geologic map of the Lisbon area, New Hampshire. Modified by R.H. Moench from Billings (1935), Moosilauke qd; White and Billings (1951), Woodsville qd; and Hafner-Douglass, 1986, part of Woodsville qd. Credit by 15-minute quadrangle.

Intrusive rocks: Oo, granite of Oliverian Plutonic suite (Ordovician). **Dnb**, Bethlehem Granodiorite Gneiss, **Dnm**, Moulton Diorite, and **Dng**, granite of New Hampshire Plutonic Suite (Devonian)

Autochthonous sequence: Oa, Ammonoosuc Volcanics, **Op**, Partridge Formation (both Ordovician, Mohawkian and upper Whiterockian). **Oqv**, volcanic member, **Oqe**, euxinic shale and graywacke member of Quimby Formation (Ordovician, Cincinnatian). **Sc**, Clough Quartzite Silurian (Silurian, upper Llandoverian). **Sf**, Fitch Formation (Silurian, Pridolian and upper Ludlovian). **Sfc**, Clough Quartzite and Fitch Formation, undivided. **Dl**, Littleton Formation (Lower Devonian, Emsian, Siegenian, and Gedinnian?); **Dlv**, volcanic member

Piermont sequence of Piermont-Frontenac allochthon: Sr, Rangeley Formation (Silurian, Llandoverian). **Sp**, quartzite and schist facies of Perry Mountain Formation (Silurian, Ludlovian? and Wenlockian?); **Spt**, variably tuffaceous and local volcanic facies

* **365 Site of U-Pb zircon age determination: 365**, age of 365+-3 Ma for granite of French Pond Pluton (Aleinikoff and Moench, 1987). **414,** age of 414+-4 Ma (Moench and Aleinikoff (1991a, b) for fine-grained quartz porphyry in Perry Mountain Formation, previously reported as a bed (flow) (Moench, 1992), but possibly a sill. **~410**, data from Bethlehem Granodiorite Gneiss consistent with age of 410+-5 Ma obtained from Fairlee pluton (fig. 5) (Moench and Aleinikoff, 1991a, b). **461**, age of 461+-8 Ma obtained from felsic metatuff of Ammonoosuc Volcanics (Aleinikoff in Moench, ed., in press). **444**, age of 444+-4 Ma for basal felsic metatuff of Quimby Formation (Aleinikoff and Moench, 1992)

\+ **37 Numbered field trip stop**

AF Ammonosuc fault; ball on downthrown side. **NHF Northey Hill fault.**

FHF Foster Hill fault; ticks on side of upper plate

pervasively cleaved arenite and phyllite characteristic of the Frontenac Formation. Most of the talus blocks from higher parts of Harris Mountain to the NW show more typical Frontenac lithologies that lack resistant quartzite, and hav darker gray metagraywacke and phyllite. Probably because of more abundant labile rock fragments and micaceous matrix, metagraywackes of the Frontenac Formation tend to be more pervasively cleaved than the feldspathic quartzites of the Perry Mountain Formation.

134.5 Just E of a major power line, park at intersection of road that follows the line and walk about 200 ft W to pavements near the closest power pole, and as far as 180 ft S 30 E from the pole.

Stop 35. Frontenac Formation (Sfr). The rocks are pervasively cleaved, gray to brownish-gray, interbedded phyllite and arenite characteristic of the formation. Spectacular outcrops of the Frontenac Formation, and some hybrid Frontenac-Perry Mountain types, can be seen where the power line and its access road cross the W ridge of Cow Mountain about 1.5 mi to the S. Continue W on Granby Road.

136.0 Park on N side of Granby Road, opposite the ruins of an octagonal wooden silo. Walk directly up to the crest of the ridge to the NW (ascent of 160 ft), and 175 ft, or so, over the crest.

Stop 36. Rangeley-Perry Mountain sequence, lying below Frontenac Formation. The rocks on the ridge are thick to thin beds of variably rusty-weathering quartzite with minor interbeds of gray to black, garnet-bearing schist, considered a quartzite-rich facies of the Rangeley Formation. Several of the quartzite beds have a coarse sandy texture, charactertistic of member C (Src) of the type Rangeley. A large outcrop of quartzite and schist near the W end of the ridge contains a bed, several centimeters thick, of poorly sorted quartz granule conglomerate. The conglomerate, first recognized by D.W. Rankin in my company, is the coarsest material recognized so far in the Rangeley Formation of the allochthon between the quartz pebble conglomerate beds found near Piermont, NH, (fig. 5) and about 6 mi SW of Errol, NH (fig. 3A).

Return to Granby Road and walk about 700 ft farther SE across a field to the edge of the woods. Most outcrops in the field are rusty-weathering metadiabase dikes that intrude rocks of the Rangeley Formation. About 40 ft into the woods, on the N side of a small knoll, is a large outcrop of rusty-weathering quartzite and schist near the top of the Rangeley Formation, with SE-topping graded quartzite beds. Following the topographic contour through spruce thickets around the E end of the knoll it can be seen that rocks of the Rangeley Formation are overlain by nonrusty interbedded schist and quartzite characteristic of the Perry Mountain Formation. Farther SE rocks of Perry

Mountain and Rangeley character are not easily separated, because of the thickets and tight folding. The Perry Mountain Formation is well exposed in large outcrops 500 and 700 ft SSE of the knoll.

Relationships exposed at stops 33 to 36, from Stone Mountain to the Monroe fault, indicate: 1) that the bulk of the Perry Mountain Formation grades laterally westward into the Frontenac Formation; 2) that a thin basal layer of Perry Mountain and the underlying Rangeley Formation extend farther west, at least to the Monroe fault, below the Frontenac Formation. Return to vehicle; continue W.

136.9 Granby village. At 138.2, Gallup Mills, take sharp turn to S. The road goes through Victory Bog, in part a boreal forest wildlife sanctuary. At 148.0, North Concord, VT, turn W onto US 2, and drive W through Concord and East St. Johnsbury, VT. At 156.0 turn S onto VT 18. At 56.5, take I-93 to Franconia, NH.

176.5 Exit 37 at Franconia. Drive N through Franconia village on NH 18, and at 177.0 turn W onto NH 117 toward Sugar Hill. At 179.0 is the Homestead Inn, on left (S).

Mileage for day 3. Stops 37 to 45 are on figure 4, and stops 46 to 49 are on figure 5.

0.0 Homestead Inn. Continue W on NH 117 through Sugar Hill village.

4.8 Park on right shoulder W of bridge over Salmon Hole Brook.

Stop 37. Littleton Formation (Dl), on W limb of Salmon Hole Brook syncline. Descend to the brook on the S side, and walk 200 ft upstream to the waterfall at an old bridge abutment. The rocks are massive to faintly bedded gray garnetiferous pelitic schist characteristic of the lower part of the Littleton Formation. Bedding dips gently E, on the W limb of the syncline, and is crossed by steeply W-dipping schistosity.

5.2 Stop on N shoulder for dropoff at E end of the stop. Vehicle to continue to W for pickup at E end of of the stop; at mileage 5.8, just E of the junction of NH 117 and US 302, turn N on the dirt the road that follows the E side of the Ammonoosuc River, cross railroad tracks and park of the W side of the road about 0.25 mi N of NH 117. The W end is stop 2M of Moench, et al (1987).

Stop 38. Clough Quartzite (Sc), volcanic member of Quimby Formation (Oqv), Partridge Formation (Op), and Ammonoosuc Volcanics (Oa), with a potential "ore horizon." From the dropoff point, descend the steep bank to Salmon Hole Brook and walk downstream. The first outcrop is the Clough Quartzite, the bottom of which marks the basal unconformity of the Clough-Fitch-Littleton sequence. Exposed a short distance farther downstream is black schist and metagraywacke assigned to the Partridge Formation; these rocks are interpreted to form the E limb of a Taconian syncline that is truncated by the basal Silurian unconformity. After a covered interval of a few hundred ft are massively bedded, coase-grained felsic metatuff characteristic of the volcanic member of the Quimby Formation of this area, exposed over a width of about 500 ft. Along a short sequence of cascades farther downstream are interbedded black schist and white, sugary metachert of the Partridge formation, complexly folded along subvertical axes. Here the Partridge Formation is no thicker than about 100 ft, probably tectonically thinned. The Ammonoosuc Volcanics are exposed for a distance of about 350 ft, from the western contact of the Partridge Formation to the junction of Salmon Hole Brook with the Ammonoosuc River. From E to W the rocks are amphibolite, massive to thinly layered felsic gneiss interpreted as felsic metatuff, and strikingly laminated gneiss of volcanic and altered volcanic compositions, somewith anthophyllitesunbursts, interpreted as metamorphosed resedimented volcanics and chemical sediments.

The laminated gneiss is best exposed in two peninsulas about 50 ft apart the protrude into the Ammonoosuc River. The downstream peninsula exposes a potential volcanogenic "ore horizon," composed, from E to W, of: 1) siliceous, pyritic felsic gneiss (hydrothermally altered probable rhyolite); 2) about 15 cm of garnet-chlorite-actinolite-anthophyllite gneiss with gossan pockets (silicate iron-formation and sulfides of the "ore horizon"); 3) nonsulfidic garnetiferous felsic gneiss (unaltered post-mineralization volcanic cover). This sequence is interpreted to top W toward an inferred (unexposed) folded digitation of the Ammonoosuc-Partridge contact.

5.9 Junction; turn left onto US 302/NH 10. At 8.1 is center of town of Lisbon.

13.7 Bath village. If transport is by tour bus, participants must walk from stop 39 to stop 40 and return (total distance 1.5 mi).

Stop 39. Partridge Formation (Op) overlain by dated felsic volcanic rock of Quimby Formation (Oqv). Cross to W side of bridge. This is stop 2F of Moench, et al (1987); felsic metatuff then assigned to the upper member of the Ammonoosuc Volcanics is now mapped in the volcanic member of the Quimby Formation. Amphibolite of the Ammonoosuc Volcanics (Oa) is exposed just SW of the W end of the bridge, on the side of the road that leads S to Woodsville (Woodsville Rd.). Walk N and down the driveway that leads to railroad tracks, then S along the tracks, under the bridge; a path that leads to the shore of the Ammonoosuc River leaves the tracks about 180 ft S of the bridge. Walk N to the cascades, but stay away from the small wooden dam at the top.

Most of the cascades expose rusty-weathering black schist of the Partridge Formation; about midway is a thin graded bed of felsic metatuff that is overturned to the SE. The lower part of the cascades exposes massively bedded felsic metatuff of the stratigraphically overlying Quimby Formation. The Partridge-Quimby contact is sharp, overturned to the SE, and is intruded at a low angle by an amphibolite dike (about 3 m thick); the contact climbs diagonally across the cascades to about midway on the E side. The basal metatuff bed of the Quimby, several meters thick, is coarse-grained quartz-feldspar gneiss containing matrix-supported slivers and slices of dark-gray to black slate, metachert, and other rocks derived from the underlaing Partridge Formation. The metatuff, sampled here, has yielded a U-Pb zircon age of 444+-4 Ma (Aleinikoff and Moench, 1992). Where the same contact is exposed 10.5 mi (17 km) to the NNE, the basal Quimby metatuff bed contains large angular blocks of slate derived from thePartridge Formation, which farther N appears to have been eroded away. Regionally, I interpret the Quimby-Partridge contact to change from an abruptly gradational conformity at stop 41, to a sharp conformity or disconformity here, to an unconformity farther N.

14.5 Small parking areas on Woodsville Road are on the W side of the bridge over Childs Brook (mileage is from E end of covered bridge at Bath).

Stop 40. Outcrop of Foster Hill fault (FHF) between Ammonoosuc Volcanics (Oa) and Rangeley Formation (Sr). This is stop 1C of Moench, et al (1987), and stop 23 of Moench (1989b), both prepared before I recognized the nonexistence of the Dead River Formation along Childs Brook; the shear zone described on p. 253 of Moench, et al (1987) is minor. At low water, descend W bank to the brook (E bank at high water) to the lip of a waterfall about 100 ft S of the bridge. The face of the waterfall exposes black sulfidic schist of the Partridge Formation. The fall's lip is held up by about 5 m of strongly foliated actinolitic greenstone and schist of the Ammonoosuc Volcanics, which I interpret to be all that remains of possibly more than 2 km of Ammonoosuc that has been excised by the Foster Hill fault. Exposed farther upstream is interbedded quartzite and rusty-weathering dark-gray schist of the Rangeley Formation, succeeded about 1,000 ft to the west by nonrusty schist and quartzite of the Perry Mountain Formation.

The FHF, exposed on a low rock face just upstream from the lip of the waterfall, is a knife-sharp surface at the base of a quartzite layer about 50 cm thick. The fault surface has an attitude of N 43 E, 55 NW; ribbing at the base of the quartzite and mineral lineations in the underlying amphibole schist plunge 45, N 78 W, but these features might be unrelated to the faulting. Return to Bath.

15.3 Bath village. Continue S on US 302/NH 10. At 16.6 turn left (S) onto NH 112 for stops 41 to 45 across the Lisbon syncline, interpreted as a major unconformably truncated Taconian fold The four stops (41-44) are stops 2J to 2M of Moench, et al (1978), and stops 19 to 22 of Moench (1989b). At 18.7 is Swiftwater village; turn left (N) toward covered bridge (load limit 3 tons) over the Wild Ammonoosuc River.

18.8 Park bus near S end of the bridge; smaller vehicles in parking area on the N side. Bus-transported trip will not visit stop 42.

Stop 41. Felsic metatuff sequence in Quimby Formation (Oqv). Outcrops upstream from the bridge, under the bridge, and in the cascade downstream expose stratified felsic metavolcanic rocks of the Quimby Formation, interpreted, from E to W, as a graded subaqueous agglomeratic ash-flow deposit, and massive felsic tuff, and well stratified ash tuff. The bedding attitude is N 30 E, 50 NW; grading and minor channeling indicate tops to NW, on the SE limb of the Lisbon syncline. Continue NNE along dirt road.

19.8 Intersection at Nutter; turn right (E). At 19.9, intersection; turn right (SE) onto South Landaff Rd.. At 21.0, ; turn right (SSW) onto graded road extending downhill.

21.5 Turn right (W) at the fork and park where convenient (4 WD vehicles may continue).

Stop 42. Partridge Formation (Op) conformably overlain by felsic metatuff of Quimby Formation (Oqv). Continue W to a second fork at about 50 ft, and then right (W) on road, at first down a steep, rough grade, to large pavement outcrops along N bank of the Wild Ammonoosuc River, about 3,000 ft from the parking place. The rocks are black schist of the Partridge Formation, conformably overlain by felsic metatuff of the Quimby Formation. The metavolcanic rocks are on the limbs of an anticlinal digitation on the

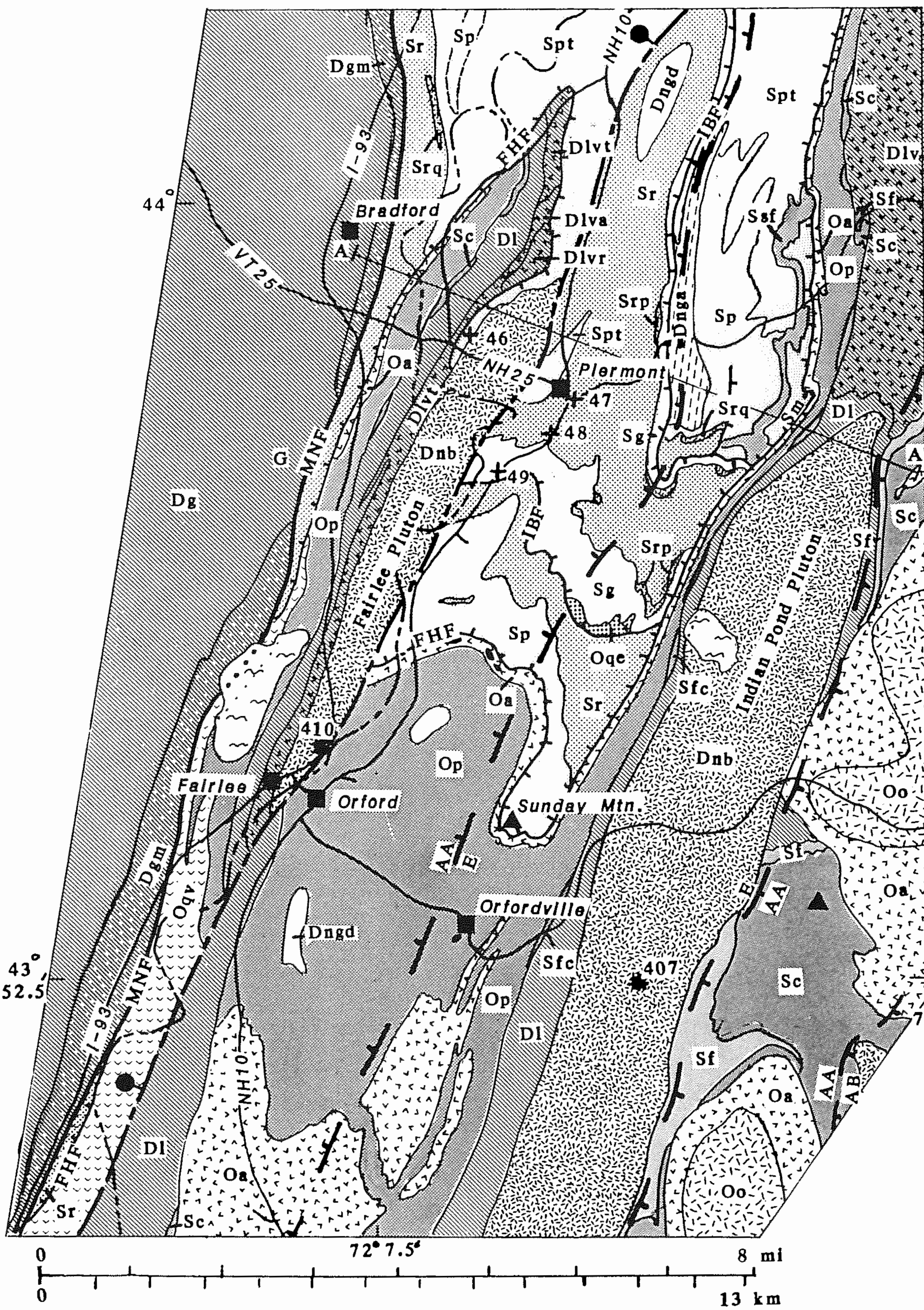

Bradford
Piermont
Fairlee
Orford
Orfordville
Sunday Mtn.
Fairlee Pluton
Indian Pond Pluton
I-93
VT25
NH25
NH10
MNF
FHF
IBF
44°
43° 52.5
72°
72° 7.5'
A
A'
0
8 mi
0
13 km

Figure 5. Geologic map of Piermont area, New Hampshire and Vermont. Modified from Hadley (1942, 1950), Rumble (1969), Mt. Cube qd, and White and Billings (1951), Woodsville qd. Credit by 15-minute quadrangle.

New Hampshire Plutonic Suite (Devonian): Dnga, sheeted metagabbro and metadiabase; possibly Silurian and allochthonous. **Dnb**, granite to granodiorite of Bethlehem Granodiorite Gneiss. **Dngd**, unfoliated granodiorite

Oliverian Plutonic Suite Ordovician): Oo, mainly granite

Autochthonous stratified rocks: Oa, Ammonoosuc Volcanics, **Op**, Partridge Formation (both Ordovician, Mohawkian to upper Whiterockian). **Oqv**, volcanic member of Quimby Formation (Ordovician, Cincinnatian). **Sc**, Clough Quartzite (Silurian, upper Llandoverian). **Sf**, Fitch Formation (Silurian, Pridolian and upper Ludlovian). **Sfc**, Clough Quazrtzite and Fitch Formation, undivided. **Dl**, Littleton Formation (Lower Devonian); **Dlv**, undivided volcanic member; **Dlvt**, felsic tuff; **Dlva,** agglomerate; **Dlvr**, flow-banded rhyolite. **Dg**, Gile Mountain Formation (Lower Devonian?); **Dgm**, Meetinghouse Slate Member

Piermont sequence of Piermont-Frontenac allochthon: Oqe, euxinic shale and graywacke member of Quimby Formation (Ordovician, Cincinnatian). **Sg**, Greenvale Cove Formation (Silurian?, Llandoverian?). **Sr**, main body, **Srq**, quartz conglomerate lenses, **Srp**, polymictic conglomerate, of Rangeley Formation (Silurian, Llandoverian). **Sp**, quartzite and schist member, **Spt** variably tuffaceous and local volcanic facies, of Perry Mountain Formation (Silurian). **Ssf**, Smalls Falls Formation (Silurian, Ludlovian). **Sm**, Madrid Formation (Silurian?, Pridolian?); locally includes Ironbound Mountain Formation (Lower Devonian)

***410 Site of U-Pb zircon age determination: 410**, age of 410+-5 Ma for Fairlee pluton (Moench and Aleinikoff, 1991a, b). **407**, age of 407+-5 Ma for Indian Pond pluton (Kohn, et al, 1992; 407+-5 Ma)

+46 Numbered field trip stop

AF Ammonoosuc fault; ball on downthrown side. **MNF Monroe fault.**

FHF IBF Foster Hill and Indian Brook Faults of Piermont-Frontenac allochthon; ticks on side of upper plate or downthrown side.

G E AA Metamorphic facies boundary; ticks point to higher grade: **G**, greenschist. **E**, epidote-amphibolite. **AA**, lower Amphibolite (staurolite). **AB**, middle amphibolite (first sillimanite).

SE limb of the Lisbon syncline. The stratigraphic sequence is demonstrated by graded bedding, best exposed on the NW limb of the digitation. Return to Swiftwater.

24.3 Intersection with NH 112 S of covered bridge; turn right (NW) onto NH 112.
24.9 Park on right (NE) shoulder.

Stop 43. Euxinic shale and graywacke member of Quimby Formation (Oqe). Descend steep bank to large outcrops along the river exposing black schist and metagraywacke, along the axial trace of the Lisbon syncline. Graded beds top NW and SE on opposite limbs.

25.3 Park on right (NE) shoulder.

Stop 44. Mafic tuff and pyroclastic rocks of Quimby Formation (Oqv). Descend to outcrops along the river exposing mafic volcanic rocks of the member. The outcrops display a set spectacularly graded beds, locally with load casts, of basaltic or andesitic metatuff with abundant blocky feldspar phenocruysts supported by a matrix of black amphibolite. The beds are overturned to the E. Farther downstream are probable agglomeratic pyroclastic flow deposits.

26.4 Intersection; turn left (W) onto US 302/NH 10.
26.7 Park on right (NW), at E end of long roadcut.

Figure 6. Section A-A' across Piermont area. Line of section shown on figure 5. Restoration based on assumed uniform dip of 40° W for Ammonoosuc fault. Note that Monroe fault (MNF) must dip west.

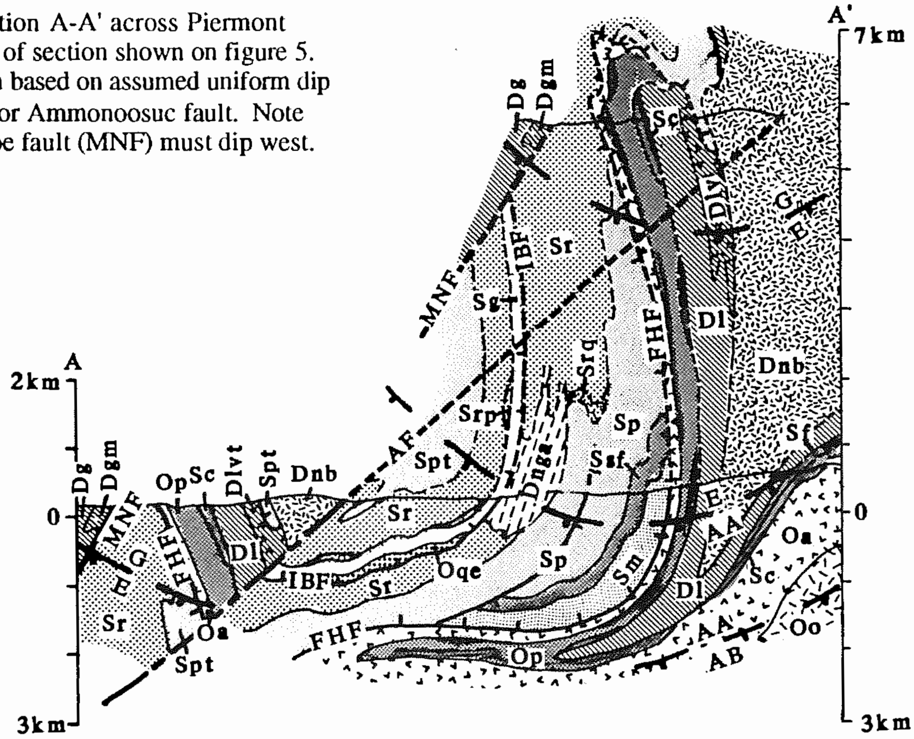

Stop 45. Perry Mountain Formation, of variably tuffaceous facies (Spt). The rocks, within the allochthon just W of the mapped trace of the Foster Hill fault, are interbedded quartzite and garnetiferous 2-mica schist of the Perry Mountain Formation, intruded by many amphibolite dikes. Continue SW on US 302/NH 10.

29.0 NH 10 branches S from US 302, which leads through the town of Woodsville, NH. Continue S on NH 10. At 31.0 is a large roadcut of granite of French Pond pluton. At 33.1, North Haverhill at Benton Road. At 37.0 NH 25 branches to the SE; continue S on NH 10. At 37.7, center of Haverhill village.

38.6 Turn right (SW) onto River Road; mapped trace of the Ammonoosuc fault is about 1/2 mi to the E.

42.0 Glen Farm (G.F. Ritchie) on the right (W)

42.2 Sharp knoll on the right (W) held up by quartz conglomeratic Clough Quartzite (Sc), beautifully exposed as a rock garden at the residence of N.R. Provost. This outcrop is part of a sequence, bounded on the W by the FHF, that includes (ascending order) units: Oa, OP, unconformity, Sc, and Dl, all in the downthrown block of the Ammonoosuc fault. The Littleton Formation (Dl) contains felsic metatuff (Dlvt), agglomerate (Dlva), and flow-banded rhyolite (Dlvr), a short distance north of the chilled intrusive contact of the Fairlee pluton, seen at stop 46.

42.4 Park on the left (E), near two unpainted sheds, and walk the farm trail S 70 E at the S end of the Glen Farm cornfield. At 1,000 ft the trail crosses a brooklet and climbs NE through woods and into a pasture.

Stop 46. Chilled contact of Fairlee pluton (Dnb) against Perry Mountain Formation (Spt) of P-F allochthon, and nearby rhyolite of Littleton Formation (Dlvr). After about 250 ft from the brooklet, still in the woods, walk SE along the SW side of a small knoll. Exposed here is a sequence at least 300 ft wide of interbedded quartzite and greenish-gray slate characteristic of the Perry Mountain Formation. Continue around the SE end of the knoll and E into the pasture, where outcrops of foliated granite of the Fairlee pluton are seen about 200 ft E, at the far side of the pasture.

Lines of outcrops of the granite and Perry Mountain Formation converge uphill to the E; they join at an elevation of about 670 ft, or about 180 ft above the pasture. Follow the flagged line to the intrusive contact, at about el. 690 ft. Here, fine-grained chilled granite is in solid contact with slaty hornfels of the Perry Mountain Formation. The chill zone is about 150 ft wide, and grades from strongly-foliated, medium-coarse (0.5 to 1 cm) granite at the outer margin of the chill zone, through unfoliated, fine-grained porphyry about midway, and almost dense porphyry at the contact.

Continue about 700 ft N and NE along the contour to a farm trail, then another 600 ft steeply uphill to the E along the trail. At this point the grade of the trail flattens, and outcrops of Perry Mountain Formation on the SE and the dense rhyolite of the Littleton Formation on the NW come into view on opposite sides of a broad gully. Is the Fairlee pluton, a short distance uphill to the SE, subvolcanic to the Littleton rhyolite? Return to vehicle.

42.7 Junction; turn left onto NH 25, toward Piermont village.

43.7 Approximate mapped trace of the Ammonosuc fault; garnet zone rocks to the E represent an approximately 5 km deeper structural level. At 44.0 pass through Piermont village.

44.1 Junction of NH 25 and NH 10; continue E through the intersection and park on the wide shoulder on the right (S).

Stop 47. Rangeley Formation (Sr), with quartz granule conglomerate. Descend to Eastman Brook about 200 ft upstream from the NH 10 bridge and walk downstream to the W side of the bridge. Exposed here are rusty-weathering dark-gray schist and impure quartzite of the Rangeley Formation, with several beds of quartz granule conglomerate about 8 cm thick. Well stratified quartz pebble conglomerate, representing approximately the same horizon in the Rangeley Formation, is exposed at two other locations in the Piermont area (fig. 5). These beds are correlated with the quartz conglomerates of the lower part of member C of the type Rangeley, and are considered a basin turbidite facies of the Clough Quartzite, exposed 1.75 mi NW of this stop. Reverse direction and drive S on NH 10.

44.7 Prominant outcrop on the right (W).

Stop 48. Rangeley Formation (Sr). Characteristic rusty-weathering quartzite and schist of the Rangeley Formation.

45.8 Park in the Connecticut River overlook on the right (W), and walk N to the roadcut.

Stop 49. Greenvale Cove Formation (Sg). The roadcut exposes faintly to conspicuously laminated, purplish-gray, garnetiferous, feldspathic 2-mica schist and granofels, and small amounts of calcsilicate rock. The compositions and bedding styles strongly resemble those of the upper member of the Greenvale Cove Formation at its type locality S of Rangeley, ME. In the Piermont area these rocks are in sequence with the overlying Rangeley Formation and the underlying euxinic shale and graywacke member of the Quimby Formation, which is exposed only in a small area (fig. 5). Continue S 4.4 mi to Orford village; turn right (NW) across Connecticut River to Fairlee, VT and access to I-93.

REFERENCES CITED

Albee, A.L., and Boudette, E.L., 1972, Geology of the Attean quadrangle, Somerset County, Maine: U.S. Geological Survey Bulletin 1297, 110 p.

Aleinikoff, J.N., and Karabinos, Paul, 1990, U-Pb zircon data for the Moretown and Barnard Volcanic Members of the Missisquoi Formation and a dike cutting the Standing Pond Volcanics, southeastern Vermont: U.S. Geological Survey Bulletin 1887, p. D1-D10.

Aleinikoff, J.N., and Moench, R.H., 1985, Metavolcanic stratigraphy in northern New England--U-Pb zircon geochronology: Geological Society of America Abstracts with Programs, v. 17, no. 1, p. 1.

______1987, U-Pb geochronology and Pb isotopic systematics of plutonic rocks in northern New England--Ensimatic vs. ensialic sources: Geological Society of America Abstracts with Programs, v. 24, no. 2, p. 2.

______1992, U-Pb zircon ages of the Ordovician Ammonoosuc Volcanics and related plutons, near Littleton and Milan, New Hampshire: Geological Society of America Abstracts with Programs, v. 24, no.2, p. 2.

Billings, 1935, Geology of the Littleton and Moosilauke quadrangles, New Hampshire: Concord, New Hampshire Planning and Development Commission, 51 p.

______1937, Regional metamorphism of the Littleton-Moosilauke area, New Hampshire: Geological Society of America Bulletin, v. 48, p. 463-566.

______1956, The geology of New Hampshire, Part II, Bedrock geology: Concord, N.H., New Hampshire State Planning and Development Commission, 203 p., map scale 1:250,000.

______1992, The "Piermont allochthon" in the Littleton-Moosilauke area of west central New Hampshire: Alternative interpretation: Geological Society of America Bulletin, v. 103, p. 1539-1541.

Boone, G.M., 1973, Metamorphic stratigraphy, petrology, and structural geology of the Little Bigelow Mountain map area, western Maine: Maine Geological Survey Bulletin 24, 136 p.

Boone, G.M., and Boudette, E.L., 1989, Accretion of the Boundary Mountains terrane within the northern Appalachian orthotectonic zone, *in* Horton, J.W., Jr., and Rast, N.M., eds., Melanges and olistostromes of the U.S. Appalachians: Geological Society of America Special Paper 288, p. 17-42.

Boucot, A.J., and Thompson, J.B., Jr., 1963, Metamorphosed Silurian brachiopods from New Hampshire: Geological Society of America Bulletin, v. 74, p. 1313-1334.

Boudette, E.L. 1991, Geologic map of the Kennebago Lake quadrangle, Franklin County, Maine: U.S. Geological Survey Miscellaneous Investigations Series Map I-2058, scale 1:62,500; pamphlet, 12 p.

Chapman, R.W., 1939, Petrology and structure of the Percy quadrangle, New Hampshire: Geological Society of America Bulletin,v. 59, p. 1059-1100.

Eisenberg, R.A., 1981, Chronostratigraphy of metavolcanic and associated intrusive rocks of the Boundary Mountains anticlinorium: Geological Society of America Abstracts with Programs, v. 13, no. 3, p. 131.

______1982, Chronostratigraphy and lithogeochemistry of lower Paleozoic rocks from the Boundary Mountains, west-central Maine: Berkeley, University of California, Ph. D. dissertation, 180 p.

Foland, K.A., and Faul, Henry, 1977, Ages of the White Mountain intrusives--New Hampshire, Vermont, and Maine, U.S.A.: American Journal of Science, v. 277, p. 888-904.

Foland, K.A., and Loiselle, M.C., 1981, Oliverian syenites of the Pliny region, northern New Hampshire: Geological Society of America Bulletin, v. 92, Part 1, p. 179-188.

Green, J.C., 1964, Stratigraphy and structure of the Boundary Mountain anticlinorium in the Errol quadrangle, New Hampshire: Geological Society of America Special Paper 77, 78 p.

______1968, Geology of the Connecticut Lakes-Parmachenee area, New Hampshire and Maine: Geological Society of America Bulletin, v. 79, p. 1601-1638.

Guidotti, C.V., 1977, Geology of the Oquossuc 15' quadrangle, west-central Maine: Maine Geological Survey Open-File Report 77-2, 26 p.

Hadley, J.B., 1942, Stratigraphy, structure, and petrology of the Mt. Cube area, New Hampshire: Geological Society of America Bulletin, v. 53, p. 113-176.

______1950, Geology of the Bradford-Thetford area, Orange County, Vermont: Vermont Geological Survey Bulletin 1, 36 p.

Hafner-Douglas, Katrin, 1986, Stratigraphic, structural, and geochemical analysis of bedrock geology, Woodsville quadrangle, New Hampshire-Vermont: Hanover, N.H., Dartmouth College, M.S. thesis, 117 p.

Harland, W.B., Armstrong, R.L., Cox, A.V., Craig, L.E., Smith, A.G., and Smith, D.G, 1989, A geologic time scale: Cambridge, Cambridge University Press, 263 p.

Harrison, T.M., Aleinikoff, J.N., and Compton, W., 1987, Observations and controls on the occurrence of inherited zircon in Concord-type granitoids, New Hampshire: Geochimical et Cosmochimica Acta, v. 51. p. 2549-2555.

Harwood, D.S., 1969, The Second Lake anticline--A major structure on the northwest limb of the Boundary Mountain anticlinorium, northern New Hampshire, west-central Maine, and adjacent Quebec: U.S. Geological Survey Professional Paper 650-D, p. D106-D115.

______1973, Bedrock geology of the Cupsuptic and Arnold Pond quadrangles, west-central Maine: U.S. Geological Survey Bulletin 1346, 90 p.

Harwood, D.S., and Berry, W.B.N., 1967, Fossiliferous lower Paleozoic rocks in the Cupsuptic quadrangle, west-central Maine: U.S. Geological Survey Professional Paper 575-D, p. D16-D23.

Hatch, N.L., Jr., 1963, Geology of the Dixville quadrangle, New Hampshire: Concord, N.H., New Hampshire Department of Economic Resources and Development Bulletin 1, 81 p.; includes map, scale 1:62,500.

______1988, Some revisions to the stratigraphy and structure of the Connecticut Valley trough, eastern Vermont: American Journal of Science, v. 288, p. 1041-1059.

Hepburn, J.C., 1991, Geochemical evidence for post-Taconic rift origin of the Connecticut Valley-Gaspe synclinorium, VT-NH: Geological Society of America Abstracts with Programs, v. 23, No. 5, p. A133.

Hueber, F.M., Bothner, W.A., Hatch, N.L., Jr., Finney, S.C., and Aleinikoff, J.N., 1990, Devonian plants from southern Quebec and northern New Hampshire and the age of the Connecticut Valley trough: American Journal of Science, v. 290, no. 4, p. 360-395.

Johansson, W.I., 1963, Geology of the Lunenburg-Brunswick-Guildhall area, Vermont: Vermont Geological Survey Bulletin 22, 86 p.

Kohn, M.J., Orange, D.L., Spear, F.S., Rumble, D., III, and Harrison, M T., 1992, Pressure, temperature, and structural evolution of west-central New Hampshire: Hot thrusts over cold basement: Journal of Petrology, v. 33, p. 521-556.

Lyons, J.B., Aleinikoff, J.N., and Zartman, R.E., 1986, Uranium-thorium-lead ages of the Highlandcroft Plutonic Suite, northern New England: American Journal of Science, v. 286, no. 6, p. 489-509.

Marleau, D.A., 1968, Woburn-East Megantic-Armstrong area, Frontenac and Beauce Counties: Quebec Department of Natural Resources Geologic Report 131, 55 p.

Marvinney, R.G., 1986, Tectonic implications of stratigraphy, structure, and metamorphism in the Penobscot Lake region, northwestern Maine: Syracuse, N.Y., Syracuse University, Ph. D. dissertation, 261 p.

______1989, Thrust and strike-slip faults near Jackman, Maine, *in* Tucker, R.D., and Marvinney, R.G., Studies in Maine geology, vol. 2: Augusta, Maine Geological Survey, p. 173-185.

Marvinney, R.G., Bothner, W.A., and Pollock, S.G., 1992, The Frontenac Formation: A record of Silurian marginal basin development in Maine, Quebec, New Hampshire, and northeastern Vermont: Geological Society of America Abstracts with Programs, v. 24, no. 3, p. 61.

McGerrigle, H.W., 1935, Mount Megantic area, southeastern Quebec, and its placer gold deposits: Quebec Bureau of Mines Annual Report 1934, pt. D, p. 63-104.

Moench, R.H., 1970, Premetamorphic down-to-basin faulting, folding, and tectonic dewatering, Rangeley area, western Maine: Geological Society of America Bulletin, v. 81, p. 1463-1496.

______1971, Geologic map of the Rangeley and Phillips quadrangles, Franklin and Oxford Counties, Maine: U.S. Geological Survey Miscellaneous Geologic Investigations Map I-605, scale 1:62,500.

______1989a, Metamorphic stratigraphy of the northwestern part of the Kearsarge-Central Maine synclinorium, western Maine, *in* Moench, R.H. and St. Julien, Pierre, leaders, IGC Field Trip T358, Northern Appalachian Transect: Southeastern Quebec, Canada, through western Maine, U.S.A., 28th International Geological Congress: Washington, D.C., American Geophysical Union, Field Trip Guidebook T358, p. 38-47.

______1989b, Metamorphic stratigraphy of the Connecticut Valley area, Littleton to Piermont, New Hampshire, *in* Lyons, J.B. and Bothner, W.B. leaders, IGC Field Trip T162, A transect through the New England Appalachians, 28th International Geological Congress: Washington, D.C., American Geophysical Union, Field Trip Guidebook T162, p. 45-53.

______1990, The Piermont allochthon, northern Connecticut valley area, New England--Preliminary description and resource implications, *in* Slack, J.S., ed., Summary results of the Glens Falls CUSMAP project, New York, Vermont, and New Hampshire: U.S. Geological Survey Bulletin, p. 1887-J, p. J-1 to J-23.

______1992, The "Piermont allochthon" in the Littleton-Moosilauke area of west central New Hampshire--Reply: Geological Society of America Bulletin, v.103, p. 1541-1545.

Moench, R.H., ed., 1984, Geologic map of the Sherbrooke-Lewiston area, Maine, New Hampshire, and Vermont: U.S. Geological Survey Open-File Report 84-0650, scale 1:250,000, one sheet (superseded by Moench, ed., in press).

______in press, Geologic map of the Sherbrooke-Lewiston area, Maine, New Hampshire, Vermont, United States, and Quebec, Canada: U.S. Geological Survey Miscellaneous Investigations Map I-1898-D; scale 1:250,000; includes p. pamphlet.

Moench, R.H., and Aleinikoff, J.N., 1991a, The Piermont allochthon of northern New England: A displaced remnant of a post-Taconian extensional sub-basin marginal to the central Maine trough: Geological Society of America Abstracts with Programs, v. 23, no. 1, p. 106.

______1991b, Geologic map of the Littleton-Moosilauke-Piermont area, NH-VT: Type area of the Piermont allochthon: Geological Society of America Abstracts with Programs, v. 23, no. 1, p. 106.

Moench, R.H., Bothner, W.A.,and Carnese, M.J., 1982, Nature of the Devonian transition from upper to middle crust in New England: Geological Society of America Abstracts with Programs, v. 14, no. 7, p. 567.

Moench, R.H., and Boudette, E.L., 1970, Stratigraphy of the northwest limb of the Merrimack synclinorium in the Kennebago Lake, Rangeley, and Phillips quadrangles, western Maine, *in* Boone, G.M., ed., Guidebook for field trips in the Rangeley Lakes-Dead River basin region: New England Intercollegiate Geological Conference, 62nd Annual Meeting, Rangeley, Maine, October 2-4, 1970, trip A-1, p. 1-25.

______1987, Stratigraphy of the Rangeley area, western Maine: Geological Society of America Centennial Field Guide, Northeastern Section, p. 273-278.

Moench, R.H., Bothner, W.A., Marvinney, R.G., and Pollock, S.G., 1992, The Second Lake rift, northern New England: Possible resolution of the Piermont allocthon-Frontenac Formation problem: Geological Society of America Abstracts with Programs, v. 24, no. 2, p. 63-64.

Moench, R.H., Hafner-Douglass, Katrin, Jahrling, C.E., II, and Pyke, A.R., 1987, Metamorphic stratigraphy of the classic Littleton area, New Hampshire: Geological Society of America Centennial Field Guide, Northeastern Section, p. 247-256.

Moench, R.H., and Pankiwskyj, K.A., 1988a, Geologic map of western interior Maine, *with contributions by* G.M. Boone, E.L. Boudette, Allan Ludman, W.R. Newell, and T.I. Vehrs: U.S. Geological Survey Miscellaneous Investigations Series Map I-1692, scale 1:250,000 (includes pamphlet, 21 p.).

______1988b, Definition, problems, and reinterpretation of early premetamorphic faults in western Maine and northeastern New Hampshire, *in* Tucker, R.D., and Marvinney, R.G., Studies in Maine geology, Volume I: Augusta, Maine Geological Survey, p. 35-50.

Moench, R.H., and Zartman, R.E., 1976, Chronology and styles of multiple deformation, plutonism, and polymetamorphism in the Merrimack synclinorium of western Maine, *in* Lyons, P.C., and Brownlow, A.H., Studies in New England geology: Geological Society of America Memoir 146, p. 203-238.

Myers, P.B., 1964, Geology of the Vermont portion of the Averill quadrangle, Vermont: Vermont Geological Survey Bulletin 27, 69 p.

Rankin, D.W., 1968, Volcanism related to tectonism in the Piscataquis volcanic belt, an island arc of Early Devonian age in north-central Maine, *in* Zen, E-an, and others, eds., Studies of Appalachian geology--Northern and maritime: New York, Interscience Publishers, p. 355-369.

Pollock, S.G., and Marvinney, R.G., 1993, Acadian dextral transpression in western Maine: Geological Society of America Abstracts with Programs, v. 25, no. 2, p. 70.

Ross, R.J., and others, 1982, The Ordovician System in the United States: International Union of Geological Science Publication No. 12, 73 p.

Rumble, Douglass, III, 1969, Stratigraphic, structural, and petrologic studies in the Mt. Cube area, New Hampshire: Cambridge, Massachussetts, Harvard University, Ph.D. dissertation, 120 p.

Spencer, C., Green, A., Morel-a-Huissier, P., Milkereit, B., Luetgert, J., Stewart, D., Unger, J., and Phillips, J., 1989, The extension of Grenville basement beneath the northern Appalachians: Results from the Quebec-Maine seismic reflection and refractions surveys: Tectonics, v. 8, no. 4, p. 677-696.

Stanley, R.S., and Ratcliffe, N.M., 1985, Tectonic synthesis of the Taconian orogeny in western New England: Geological Society of America Bulletin, v. 96, p. 1227-1250.

Stewart, D.S., Wright, B.E., Unger, J.D., Phillips, J.D., Hutchinson, D.R., Luetgert, J.H., Bothner, W.A., Klitgord, K.D., Liberty, L.M., and Spencer, C., 1991, Global geoscience transect, southeastern Canada, northeastern U.S.A.: U.S. Geological Survey Open-Files Series OF 91-0353; map scale 1:1,000,000 (includes pamphlet, 34 p.).

St. Julien, Pierre, and Slivitsky, Anne, 1987, Compilation geologique de la region de l'Estrie-Beauce: Ministere de l'Energie et des Ressources, Quebec, Carte no. 2030 du rapport MM-85-04, scale 1:250,000 (includes pamphlet, 40 p., by Anne Slivitsky and Pierre St. Julien).

Sutter, J.F., Ratcliffe, N.M., and Musaka, S.B., 1985, 40Ar/39Ar, and K-Ar data bearing on the metamorphic and tectonic history of western New England: Geoogical Society of America Bulletin, v. 96, p. 123-136.

Swift, C.M.,Jr., 1966, Geology of the southeast portion of the Averill quadrangle, New Hampshire: Concord, New Hampshire Department of Resources and Economic Development, 19. p.

Thompson, J.B., Jr., and Norton, S.A., 1968, Paleozoic regional metamorphism in New England and adjacent areas, *in* Zen, E-an and others, eds., Studies of Appalachian geology--Northern and maritime: New York, Interscience Publishers, p. 319-327.

Tremblay, Alain, Lebel, Daniel, and Van Grootl, Geert, 1993, Stratigraphy and structure of the Connecticut Valley-Gaspe trough in southern Quebec: Geological Society of America Abstracts with Programs, v.25, no. 2, p. 85.

Trzcienski, W.E., Jr., Rodgers, John, and Guidotti, C.V., 1992, Alternative hypotheses for the Chain Lakes "massif," Maine and Quebec: American Journal of Science, v.292, p. 508-532.

Tucker, R.D., Krogh, T.E., Ross, R.J., Jr., and Williams, S.H., 1990, Time-scale calibration by high-precision U-Pb zircon dating of interstratified volcanic ashes in the Ordovician and Lower Silurian stratotypes of Britian: Earth and Planetary Science Letters, v. 100, p. 51-58.

Tucker, R.D., and Robinson, Peter, 1990, Age and setting of the Bronson Hill magmatic arc: A re-evaluation based on U-Pb zircon ages in southern New England: Geological Society of America Bulletin, v. 102. p. 14-4-1419.

Westerman, D.S., 1983, The nrothwest boundary fault of the Boundary Mountain anitclinorium, in D.W. Caldwell and L.S. Hanson, eds, New England Intercollegiate Conference Guidebook, 75th Annual Meeting, October 7, 8, and 9, 1983, Maine, p. 87-101.

White, W.S., and Billings, MP., 1951, Geology of the Woodsville quadrangle, Vermont-New Hampshire: Geological Society of America Bulletin, v. 62, p. 647-696.

Zartman, R.E., and Leo, G.W., 1985, New radiometric ages on gneisses of Oliverian domes in New Hampshire and Massachusetts: American Journal of Science, v. 285, no. 3, p. 267-280.

Chapter EE

Multiple Glaciations and Deglaciation Along a Transect from Boston, Massachusetts, to the White Mountains, New Hampshire

By P. Thompson Davis, Woodrow B. Thompson, Byron D. Stone, Robert M. Newton, and Brian K. Fowler

Field Trip Guidebook for the Northeastern United States: 1993 Boston GSA

Volume 2
Contribution No. 67, Department of Geology and Geography, University of Massachusetts, Amherst, Massachusetts

MULTIPLE GLACIATIONS AND DEGLACIATION ALONG A TRANSECT FROM BOSTON, MASSACHUSETTS, TO THE WHITE MOUNTAINS, NEW HAMPSHIRE

by
P. Thompson Davis, Department of Natural Sciences, Bentley College, Waltham, MA 02154-4705,
Woodrow B. Thompson, Maine Geological Survey, Augusta, ME 04333,
Byron D. Stone, U.S. Geological Survey, Reston, VA 22092,
Robert M. Newton, Department of Geology, Smith College, Northampton, MA 01063,
and
Brian K. Fowler, Mt. Washington Observatory, North Conway, NH 03260

INTRODUCTION

The purpose of this field trip is to visit and evaluate critical sites for understanding late Quaternary glaciations, the last deglaciation, and climate of a transect between northeastern Massachusetts and the White Mountains in northern New Hampshire. This two-day trip will examine drumlin exposures in northeastern Massachusetts that exhibit two tills separated by a weathering profile; glacial outwash features and eskers in central New Hampshire; and preglacial weathering profiles ("rottenstone"), glacial depositional features (till, erratics, moraines, alluvial fans, lake sediments), and erosional landforms (grooves, striations, potholes, roches moutonnees, cirques, U-shaped valleys, the "Old Man of the Mountains") in northern New Hampshire. Of particular interest are: 1) the "two-till problem;" 2) the mode and chronology of continental deglaciation, and 3) the relative sequence of continental and cirque glaciation in the White Mountains. Bogs and lakes in the area not only provide meaningful paleoecological records of postglacial climate, but also provide our only significant dating control for deglacial events.

This field trip is in memory of the late Dr. Richard P. Goldthwait, professor emeritus at Ohio State University, and founder and first director of the University's Institute of Polar Studies (now the Byrd Polar Research Center). His name is synonymous with Quaternary geology in New Hampshire; without his decades of research on and around the White Mountains, this field trip would have little meaning. Dick Goldthwait led field trips to the Mt. Washington area beginning in the 1940s; in this present effort we have made extensive use of materials from guidebooks for three of his more recent trips: the International Symposium on Antarctic Glaciological Exploration, 1968; the Friends of the Pleistocene, 1970; and the American Quaternary Association, 1988. More recent geological efforts by numerous workers in the area have merely expanded on his cornerstone work. In 1986, the Quaternary Geology and Geomorphology Division of the Geological Society of America bestowed upon Dick Goldthwait their first Distinguished Service Award, an award destined to become the most coveted in the profession.

Other recent field trips to the area covered by the present effort include the 40th reunion of the Friends of the Pleistocene to the lowlands just southeast of the White Mountains (Newton, 1977); Trip C-1 of the 78th annual meeting of the New England Intercollegiate Geological Conference to the foothills east of the Presidential Range (Thompson, 1986); and part of Trip A-2 of the 81st annual meeting of the New England Intercollegiate Geological Conference to northeastern Massachusetts (Weddle et al., 1989).

Brief directions are provided as a guide to the locations of the stops, which are numbered sequentially from 1 to 18 for the two days (Fig. 1). The primary leaders are noted (within parentheses) for each stop. We will spend the intervening evening at the Appalachian Mountain Club's Pinkham Notch Camp, at the foot of the east slope of Mt. Washington, which has been carved up by numerous deep and broad cirque glaciers.

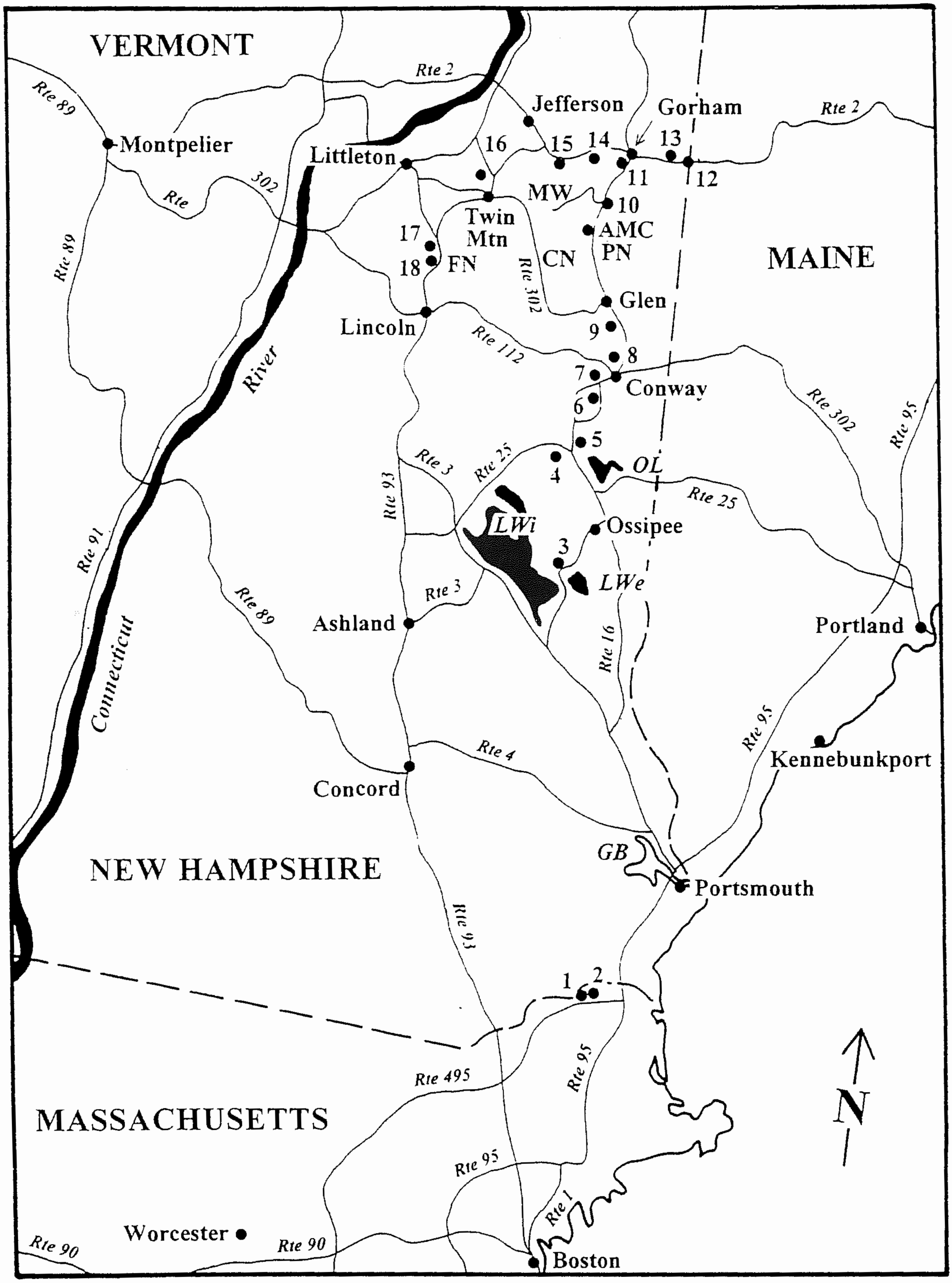

Figure 1. Location map for stops, numbered 1 through 18. MW = Mt. Washington; AMC = Appalachian Mountain Club's Pinkham Notch Camp; PN = Pinkham Notch; CN = Crawford Notch; FN = Franconia Notch; LWi = Lake Winnipesaukee; LWe = Lake Wentworth; OL = Ossipee Lake; GB = Great Bay estuary.

THE TWO-TILL STRATIGRAPHY OF NEW ENGLAND

Byron D. Stone

Two till units are correlated with two late Pleistocene glaciations of southern New England. At present, the tills are designated by informal stratigraphic names or by proposed formal names for local varieties of till (Fig. 2). No regional study of varietal members of the upper, surface till of late Wisconsinan age or the lower, pre-late Wisconsinan till supports an inclusive formal nomenclature for the two tills. In the field, physical criteria differentiate local varieties of the tills, always on a basis of comparative characteristics in areas of similar bedrock type. Because of the close relation of till composition and texture to very local bedrock lithologies, differences within one till unit may be greater in some areas than differences between varieties of both units.

The general terms **upper till** and **lower till** (Schafer and Hartshorn, 1965) seem confusing to some workers because the terms emphasize an expected superposition of the units. In most exposures, this superposed stratigraphy consists of a very thin (<1 m) sandy upper till with cobbles overlying a mixed-till zone that contains discrete angular fragments of the lower till within a rusty-oxidized sandy matrix. Thick, compact gray upper till is present above such a mixed zone or above oxidized lower till in few exposures (Pessl and Schafer, 1968). The upper till forms a discontinuous till blanket of highly variable composition over the upland bedrock landscape and is present as a thin unit beneath most stratified glacial deposits (Fig. 3). The upper till's composition likewise reflects the local source material in drumlins. The lower till is preserved chiefly in drumlins and related thick bodies of till with glacially smoothed and streamlined morphology. The terms **new till** and **old till** also have been used (Schafer and Hartshorn, 1965), in reference to the correlated ages of the units.

In this report, the **upper till** is referred to as the **surface till**. The surface till is the material referent of the late Wisconsinan glacial episode in southern New England, which occurred from about 24 ka to deglaciation about 15 ka - 14 ka. The surface till is dated by radiocarbon from preglacial subtill materials incorporated in the drift and from postglacial materials that overlie the drift (Stone and Borns, 1986). The surface till is highly variable in composition, dependent on the composition of local bedrock and older surficial materials. The surface till includes a compact basal unit of lodgement and meltout origin; a discontinuous, thin overlying unit of loose sandy till, of meltout origin; and the mixed-till zone that overlies the weathered till in drumlins.

SINGLE GLACIATION 1880-1958	Southern New England, New Hampshire	Maine
WISCONSIN	till, drumlin till	till

MULTIPLE GLACIATIONS 1900-1959	Southern New England, Long Island	Maine
WISCONSIN	thin till, surface till, upper till	till
ILLINOIAN	drumlin till, lower till, Montauk till	drumlin till lower till

MULTIPLE WISCONSINAN GLACIATIONS 1949-1986		Southern New England, Long Island	Maine
WISCONSINAN	Late	upper till, surface till, new till, proposed local formal units	upper till
	Mid-		middle till at New Sharon
	Early	lower till, drumlin till, Montauk Till, proposed local formal units	lowest till at New Sharon, lower till, Austin Stream till, Nash Stream till
ILLINOIAN		lower till at Sankaty Head	

THIS REPORT WISCONSINAN AND ILLINOIAN GLACIATIONS		Southern New England, Long Island	Maine	Quebec
WISCONSINAN	Late	surface till	upper till, surface till, Sandy River till at New Sharon	Lennoxville Till
ILLINOIAN		drumlin till, Montauk Till, lower till at Sankaty Head	drumlin till, lower till	Johnville Till

Figure 2. Correlation diagrams showing the development of the multiple glacial stratigraphic framework of southern New England, Long Island, New Hampshire, and Maine. Compiled by B.D. Stone; see Weddle et al., 1989, Fig. 2, p. 29, for specific references.

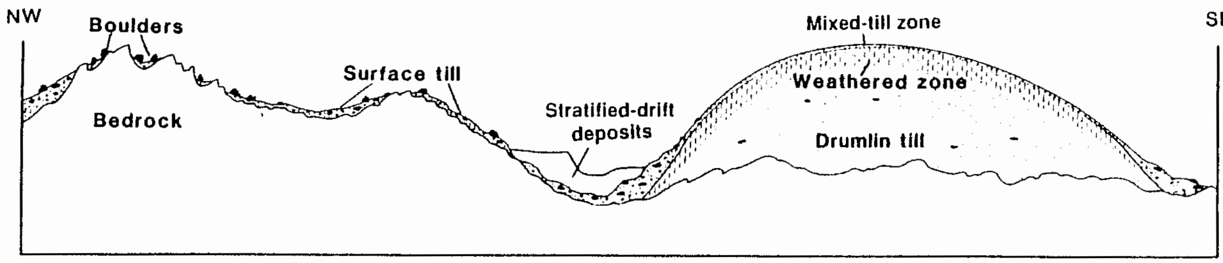

Figure 3. Generalized geologic section showing distribution of surface and drumlin tills and weathered and mixed-till zones. Vertical exaggeration x 6. From Melvin et al., 1992, Fig. 3, p. 9.

The **lower till** is referred to in this report as the **drumlin till**. The drumlin till is preserved chiefly in glacially smoothed landforms that were resistant to late Wisconsinan glacial erosion. The drumlin till is the material referent of the Illinoian glacial episode; which is older than 133 ka. The drumlin till is dated by consideration of the depth and degree of the weathering in its upper part, and by correlation with the Sankaty lower till, which lies beneath dated marine beds of Sangamonian age on Nantucket Island (Oldale et al., 1982). The weathering zone in the upper part of the drumlin till is related to a relatively long or intense period of weathering that postdated drumlin formation in the region. Only a compact basal drumlin till unit is known; its texture and composition vary with bedrock composition.

Physical characteristics that differentiate the two tills of southern New England are summarized in Table 1. These characteristics are related to source materials of the tills, glacial erosional and depositional processes, and weathering effects.

MODE AND CHRONOLOGY OF CONTINENTAL DEGLACIATION OF NORTHERN NEW HAMPSHIRE

W. B. Thompson

The deglaciation history of northern New Hampshire, and the White Mountains in particular, has been the subject of much study and spirited debate since the late 1800s. Early controversies centered on whether the White Mountains had been glaciated by a local icecap, a continental icesheet, or both (Thompson and Fowler, 1989). Packard (1867) and Vose (1868) supported the icecap theory. Vose noted the presence of NE-SW trending striations in the Peabody River valley between Pinkham Notch and Gorham. He interpreted the striation data as supporting the northeastward (downvalley) flow of a glacier originating in the local mountains. Hitchcock (1878) disproved this theory by finding examples of stoss-and-lee bedrock topography indicating that the actual direction of ice flow was southwestward (up the valley). Some of the outcrops examined by these workers can still be observed along Rte 16, near the entrance to the Mount Washington Auto Road, and will be visited on this trip.

Agassiz (1870) and Hitchcock (1878) thought that a local icecap persisted in the White Mountains following the recession of the last continental icesheet. They claimed that a local glacier flowed northward down out of the Franconia Range and deposited the Bethlehem Moraine in the Ammonoosuc River valley. Upham (1904) carried this concept even farther when he proposed that a belt of moraines could be traced around the full circumference of the White Mountains. Goldthwait (1916) disagreed with the icecap model and pointed out numerous flaws in the arguments that had been advanced in support of it.

Once it was realized that the late Wisconsinan icesheet was the dominant factor in the last glaciation of northern New Hampshire, a major controversy arose in the early 1900s regarding the mode of deglaciation. Was there a distinct northward-retreating ice margin, which maintained some degree of active flow, or did the icesheet experience widespread rapid stagnation due to thinning over the mountainous terrain? Earlier workers in the area, including Packard (1867) and Hitchcock (1878), had assumed the presence of active ice, and listed many

Table 1. Selected characteristics of surface and drumlin tills that are derived from crystalline bedrock. Modified from Melvin et al., 1992, Table 1, p. 10.

	SURFACE TILL (late Wisconsinan)	**DRUMLIN TILL** (Illinoian)
Color (naturally moist material, Munsell color symbols)	Gray to light gray (2.5-5Y 6-7/1-2), to olive gray to light olive gray (5Y-4-6/2)	Olive to olive gray (5Y 4-5/2-3) to olive-brown (2.5Y 4-5/3-5) in weathered zone, dark gray (5Y 3.5-5/1) in unweathered till
Texture of matrix (< 2mm [-1 phi] range)	62-80% sand, 20-38% silt & clay, and < 1-7% clay	35-60% sand, 40-65% silt & clay, and 11-38% clay
Stone content	19-54% > 2 mm 5-30% > 76 mm (3 in.)	19-42% > 2 mm 1-11% > 76 mm (3 in.)
Layering	Textural laying common, generally subhorizontal; consists of thin, lighter sandy layers interbedded	Textural layering not common; thin, oxidized sand layers and vertical sand dikes locally with darker, silty layers; layering is laterally discontinuous
Jointing	None; subhorizontal parting is related to layering and fabric of matrix	Well-developed, closely-spaced subhorizontal joints and less numerous subvertical joints impart a blocky or thin platey structure to till
Distribution and thickness	Lies directly on bedrock; less than 3 m thick in areas of rock outcrop; commonly 3-6 m thick on lower valley slopes	Forms cores of drumlins and related bodies of thick till; generally > 10 m thick, commonly 20-30 m thick; maximum known thickness 70 m
Soils and weathering (representative USDA S.C.S. soil series)	Canton series, Charlton series (Typic Dystrochrepts)	Paxton series (Typic Dystrochrepts); soil developed in mixed-till zone that overlies weathered zone in drumlin till; weathered zone <9 m thick; zone is oxidized, leached in some areas, and contains altered clay minerals and iron-bearing minerals

end moraines that they believed to exist in the White Mountains. Goldthwait (1925) likewise described the deglaciation of New Hampshire in terms of a receding ice margin that remained active and deposited moraines in some areas. However, he later changed his opinion and concluded that deglaciation of the White Mountains was characterized by down-wastage and stagnation of the icesheet (Goldthwait, 1938). He dismissed the hummocky deposits of the Bethlehem Moraine as nothing more than kettled outwash, while Crosby (1934) and Lougee (1940) attributed these deposits to the readvance of active ice. Lougee (1939) was a leading proponent of active-ice retreat, claiming that the receding glacier margin dammed a succession of glacial lakes in north-draining valleys of the Connecticut River basin.

Later work by the Goldthwait family continued to stress the role of regional stagnation in dissipation of the late Wisconsinan icesheet (Goldthwait et al., 1951). However, recent detailed field investigations have demonstrated the presence of late-glacial active ice in parts of northern New Hampshire, especially where valleys were favorably oriented relative to the flow of the thinning icesheet (Gerath et al., 1985; Thompson and Fowler, 1989). The Androscoggin Moraine (Stop 12), which is located on the Maine-New Hampshire border in the Androscoggin River valley, provides evidence of vigorous ice flow during an advanced stage of deglaciation in the northern White Mountains. There are also meltwater channels, heads-of-outwash, and glaciolacustrine deposits (e.g. Stops 15 and 16) that consistently indicate a distinct ice margin that was receding to the northwest, as described by Lougee (1939, 1940). However, some of these same features have been used to support the regional stagnation model (Goldthwait and Mickelson, 1982). Intensive field work in the forested terrain of northern New Hampshire will be required to clarify the mode of ice retreat.

The chronology of deglaciation in northern New Hampshire is poorly known because of the lack of datable materials in ice-marginal deposits. Thompson and Fowler (1989) discussed the problems inherent in correlating with the chronology of glaciomarine deposits in coastal Maine. Active ice may have lingered in the latter area when parts of the White Mountains were deglaciated. Continental ice probably disintegrated very rapidly in the White Mountains, as radiocarbon ages from basal sediments in bogs and ponds suggest that both alpine zones and valley bottom were ice-free by as early as about 13.6 ka (Davis et al., 1980; Spear, 1989). Formation of the Androscoggin Moraine as early as 14 ka would be consistent with regional reconstructions such as those of Davis and Jacobson (1985) and Dyke and Prest (1987). The deglacial features in northern New Hampshire are believed to be the product of the receding Connecticut Valley lobe of the Laurentide Icesheet, rather than the later Appalachian ice mass that developed over northern Maine and adjacent Quebec in response to marine drawdown in the St. Lawrence Lowland.

SEQUENCE OF CONTINENTAL AND CIRQUE GLACIATION

P. Thompson Davis

A long-standing controversy in Quaternary geology concerns whether mountainous areas in northeastern United States and adjacent parts of Canada supported isolated icecaps or cirque glaciers after continental ice recession in late Wisconsin time. For nearly a century arguments for post-icesheet local glaciers at various high-mountain areas in New England and adjacent areas (Tarr, 1900; Rich, 1906, 1935; Johnson, 1917, 1933; Antevs, 1932; Flint, Desmorest, and Washburn, 1942; Flint, 1951; Thompson, 1960, 1961; Caldwell, 1966, 1972, 1980; Wagner, 1970; Craft, 1979; Bradley, 1981) have been countered by various arguments against post-icesheet local glaciers (Fairchild, 1913; J.W. Goldthwait, 1913, 1916; R.P. Goldthwait, 1939, 1940, 1970a; Davis, 1976, 1978, 1983, 1989; Borns and Calkin, 1977; Davis and Davis, 1980; Gerath and Fowler, 1982; Fowler, 1984; Gerath et al., 1985; Davis and Waitt, 1986; Davis et al., 1988; Waitt and Davis, 1988). At the Presidential Range in New Hampshire, Thompson (1960, 1961) and Bradley (1981) argue for a rebirth of local ice, but Goldthwait (1970a), Fowler (1984), Davis and Waitt (1986), Davis et al. (1988), and Waitt and Davis (1988) against them.

Proponents for post-icesheet local ice at the Presidential Range argue that the steep cirques and sharp arêtes are evidence for local ice erosion following recession of continental ice. Opponents contend that this evidence is irrelevant because continental ice could have eroded out the basins or icesheet modification of older alpine forms was minor. Proponents interpret till-like drift downvalley from cirques rich in lithologies derived from upslope as evidence for rebirth of local ice. Opponents counter that this evidence is also irrelevant because the till-like drift was more probably deposited by postglacial mass wastage processes.

Opponents for post-icesheet local ice at the Presidential Range support their views with the following evidence, which all suggest continental ice was last: 1) upcirque-pointing roches moutonnées on cirque floors, 2) striae on cirque headwalls, 3) icesheet erratics in cirque-floor drift, and 4) apparent absence of moraines in and downvalley of cirques. Proponents for post-icesheet local ice counter that cirque glaciers did not completely remove icesheet drift and that moraines in cirques are obscure because they are small, subdued by postglacial mass wasting processes, or thickly forested. However, at Mount Katahdin a lateral moraine system that flanks two sides of the mountain is thickly forested, yet is a prominent topographic feature.

An important theoretical argument against post-icesheet local ice in alpine areas in northeastern United States is that equilibrium-line altitudes rose rapidly to elevations well above cirque floors at the end of the late Wisconsinan. For example, average summer temperatures must be lowered at least 17° F (9.3° C) to permit contemporary snowline to intersect cirque floors on Mt. Washington. Thus, temperatures warmed too rapidly to support renewed cirque glacier activity during the waning phases of the late Wisconsinan on Mt. Washington.

ACKNOWLEDGMENTS

The research related to this field trip benefitted from the help, inspiration, and suggestions of many persons. All of the authors were inspired by the pioneering work on the glacial history of the White Mountains by the late Richard P. Goldthwait. The authors also have benefitted from recent discussions in the field with Richard B. Waitt, Robert Gerath, George Haselton, and Carl Koteff. Robert Johnston (Maine Geological Survey) helped with figure preparation, Maureen Malloy (Bentley College) assisted with word processing, and Nancy M. Eyster-Smith (Bentley College) provided editorial assistance. Landowners, without whose permission we could not access the properties at many of the stops, include the Mairofrides Brothers (Stop 2), Alvin J. Coleman & Son (Stop 6), the White Mountain Hotel (Stop 9), Ken W. Corrigan, Inc. (Stop 15), and Twin Mountain Sand and Gravel (Stop 16).

ROAD LOG - DAY ONE

From Boston, proceed about 30 mi N on Rte 93 and take Exit 44A to Rte 495 N. Proceed about 9 mi N on Rte 495 to Exit 48 (Ward Hill, Rte 125), follow road about 0.5 mi to light at Riverview St. for U-turn, then proceed about 0.6 mi N to facility.

STOP 1 - HAVERHILL RESOURCE RECOVERY FACILITY, THE NECK, HAVERHILL, MA (Stone)

The large excavation is in a lowland area of thick till, surrounded by numerous drumlins with crests above 75 m altitude. The excavated hill is elongate but is irregular in shape and morphology; it is not a drumlin. The Canton fine sandy loam soil series was mapped on the original landform (Fuller and Hotz, 1981).

The pit exposes 3-6 m of gray sandy till in bench cuts at the west end. The base of the lowest cut is about 12 to 15 m below the top of the original landform. The till is light brownish gray to light gray (2.5Y 6/7-2), compact, thinly layered silty sand matrix with 15% gravel and boulders by volume. It is composed of gray to light brownish gray (2.5Y 6/0-2) massive, compact, nonplastic diamict material in irregular patches and lenses, <2 m long, which are associated with zones of gravel clasts (15-20%) pebbles and cobbles. The bulk of the till comprises laterally extensive zones of alternating thin (<3 cm) layers of gray, massive, compact, silty-sand diamict material and thin layers of light gray to pale yellow (2.5Y 2/2-4) less compact sandy material. The massive material contains minute, and irregularly shaped, angular pebble-to-cobble-sized clasts of compact gray clayey silt. These clasts are composed of indistinctly laminated and microlaminated gray clayey silt and white medium-to-coarse silt. Microlaminae are bounded by sharp contacts; laminae are folded in truncated open or isoclinal folds. Many of these silt clasts and gravel clasts are oriented with long axes dipping northerly at $\leq 20^\circ$. Layering also dips northerly; individual layers cannot be traced much more than 20 cm. Sandy layers pinch out at or are truncated by the silty-sand layers. The till weathers and fractures along the layering. Sets of layers that dip as much as 50-60° are truncated by other sets that dip 15-20°. Some steeply dipping resistant gray silty-sand diamict layers can be matched across the gently dipping planes of truncation, indicating thrust displacement of a few centimeters. Gravel clasts and boulders as much as 2.5 m long are subangular with subrounded ends or faces, and with angular, hackly terminations on some faces. Some faces of large boulders retain glacial polish and grooves. Till stones composed of fine-grained metasedimentary rock show some evidence of glacial shaping and many are striated.

The till is interpreted as a basal lodgement facies of the surface till, based on the degree of compaction, strongly preferred orientation of till stones, and preferred orientation of layering. The till-stone fabric records a southerly flow during deposition of the lower part of the exposed till. The till contains clasts of laminated silt that preserve primary laminae, indicating a source component of older stratified materials in the valley or materials deposited subglacially and re-entrained during till sedimentation. Layers also contain minute clasts of the laminated silt. The layering of the till is very well developed here, and it is a regional characteristic. It is of probable subglaciogenesis, perhaps related to some primary segregation of material, which was enhanced by shear or thrust displacement along with sandy layers. Rotation of sets of layers took place during till sedimentation. The youngest planar sets of thrust show movement toward the southeast, parallel to the axes of surrounding drumlins.

On leaving facility, return about 0.6 mi to lights for U-turn, and proceed about 0.5 mi to Rte 495 N. Proceed about 5.3 mi N on Rte 495 to Exit 52 (Haverhill, Rte 110), turn left (S) on Rte 110, proceed about 1.0 mi past Northern Essex Community College and turn left on Kenosha St. (unmarked), follow for 0.9 mi to left fork on Center St. (Walnut Cemetery on right), proceed 0.1 mi to T-junction and turn left, proceed 0.1 mi and turn right on Millvale Rd. (unmarked), proceed 0.7 mi and bear right on East Broadway, and proceed 0.5 mi to pit entrance on right.

STOP 2 - MAIROFRIDES BROTHERS SAND AND GRAVEL PIT, EAST BROADWAY STREET, HAVERHILL, MA (Stone)

This pit exposes till in the sides and top of an irregularly shaped, double crested drumlin. Paxton extremely stony, or very stony, fine sandy loam soils were mapped in areas coincident with the mixed-till zone. The pit also exposes a thick section of glaciomarine deltaic beds, normal to paleocurrent flow, and younger glaciomarine silt and sand to the north. The fine sediments are overlain unconformably by cross-bedded medium-coarse pebbly sand of fluvial origin.

The west-facing cut exposes an upper set of units that contain about 10% pebbles, cobbles and few boulders. These units overlie an oxidized stone-poor till that grades downward into gray till. Bedrock crops out beneath the gray till on the floor of the pit. A generalized section is described, from top to bottom:

Unit	Thickness	Description
1	1-2 m	Pale yellow (2.5Y 7/4) and strong brown to reddish yellow to yellowish brown to brownish yellow (7.5-10YR 5-6/8) silty sand diamict material, noncompact to moderately compact, massive, containing pebbles, angular blocks and subrounded cobbles and boulders (10-25%); loose and easily excavated at north end of exposure; irregular base with 1 m relief
2	2 m	Pale yellow (2.5Y 7/4) silty-sand till, compact, massive; unit is gradationally more stony from bottom to top (to about 10-15% but is less stony than overlying unit; pale yellow till matrix contains angular clasts of compact silty till; faces of these clasts are stained strong brown (7.5YR 5/8) with Fe-Mn coating; subangular gravel clasts include weathered brown metapelites; clasts are not coated with Fe-Mn stain; vesicles are common in parts of the matrix; base of unit is irregular, distinguished by color and stone content
3	2-3 m	Olive (5Y 4-5/4) silty fine-sand till consisting of discontinuous layers of olive silty-sandy till, less than 2 cm thick, that contain subangular-to-blocky compact clasts of clayey-silty till; till clasts are less than 3 cm long and are coated with strong brown (7.5YR 4/6) Fe-Mn stain; pebbles and cobbles are 2-5%; base of unit is locally sharp
4	2-4 m	Olive (5Y 5/4) clayey-silty till; compact, massive, subhorizontal and subvertical joints well developed at top and more widely spaced downward through unit; joint faces stained with Fe-Mn coating; unit mottled at base where it grades by color and loss of joint structure into underlying unit
5	1-3 m	Gray till, compact, massive, tough, moderate to high plasticity, pebbles and small cobbles are 2-5%; gravel clasts composed of fine-grained rock types are subrounded and striated, but not well faceted

Gravel Clast Compositions at STOP 2:

Dark gray to black, fine-grained metapelite (local bedrock)	28%
Granite, granitic gneiss, pink, gray, and white	26%
Gray, fine-grained biotite schist	15%
Gray amphibolite, garnet schist, and gneiss	12%
Gray, fine-to-medium grained gneiss, hornblende(?), muscovite, biotite	11%
Gray, very fine-grained aplite (volcanic?), weathered to silt	4%
Quartz	3%
Brown, weathered biotite schist or metapelite	1%

Unit 1 is interpreted to be chiefly of supraglacial meltout origin, based on its loose, cobbly character, and degree of soil development. However, an early postglacial colluvial origin cannot be ruled out. Units 2 and 3 contain oxidized and fresh clasts of the underlying units within a sandy matrix that is similar in texture to the overlying unit and to the surface till at Stop 1. These units are stony varieties of the mixed-till zone; genetically they are local varieties of the surface till, with the materials locally eroded and deposited on the drumlin skin by the late Wisconsinan icesheet. Unit 4 is the pervasively oxidized and jointed weathering zone developed in the top of unit 5, the drumlin till of Illinoian age.

Leave pit, turn left onto East Broadway and retrace route 0.8 mi to left onto Millvale Rd., proceed 0.8 mi and bear right at Middle Rd., proceed under Rte 495 about 1.5 mi to T-junction and turn left onto Rte 101, proceed 1.0 mi to junction with Rte 495 N (2nd entrance), turn left and proceed about 10 mi N on Rte 495, merge with Rte 95, proceed about 15 mi N on Rte 95 through Hampton tollbooths and bear left at Exit 4 (Rte 16/4, NH Lakes, White Mtns.), proceed W about 4.5 mi over Great Bay estuary on General Sullivan Bridge, continue about 14 mi N on Rte 16 through Dover and Rochester tollbooths, continue another 20 mi N on Rte 16 noting eskers on right, continue another 16 mi N on Rte 16 and turn S on Rte 28, proceed 8.5 mi S on Rte 28 through Ossipee to sand and gravel pit on right.

STOP 3 - ALLEN A. PIT, RTE 28, WOLFEBORO, NH (Newton, Davis)

Most of the larger lakes in central New Hampshire lie in bedrock basins 15 to 60 m deep scoured out by repeated glacial erosion of weaker and deeply rotted rock types (granitic ?). They are surrounded by discontinuous hills and low mountains (schists, quartzites, and volcanics) that reach elevations up to 450 m higher than the lakes.

As the last Wisconsinan icesheet disappeared from this area 13,000 to 14,000 years ago, it left abundant evidence of meltwater flow in the form of channels, kame terraces, and high deltas. The ice did not disappear simultaneously from all lake basins; nor did it retreat with one uniform steep edge across basin to basin. Rather it thinned first in one basin and then in another as shown by meltwater flow. These basin sequences are illustrated by details in the Ossipee-Wolfeboro-Winnipesaukee area. The order of opening of the basins from thick ice lenses to open lakes was generally south to north and east to west.

Where broad and deep north-south valleys, like the Merrimack and Connecticut River valleys, penetrate the hills and mountains, the residual but thinning ice sources in northern New Hampshire and Vermont kept broad streams of ice flowing into these valleys long after surrounding basins were deglaciated (12 ka?). This is shown by the steep ice-contact features (Merrimack River valley, sequential outwashes) and ice-contact deltas (Connecticut River valley, glacial Lake Hitchcock). These areas open up from south to north as demonstrated by the work of Newton (1974).

The final stage of ice retreat from central New Hampshire was melting of ice from valley bottoms (Goldthwait and Mickelson, 1982). The deepest parts of valleys held the thickest ice, hence were the last to become deglaciated. Ice-marginal lakes developed locally where ice blocked the surface drainage. Drainage also occurred around and over separated ice masses, leaving terraces with ice-content faces. When the Lake Wentworth basin first became ice-free, water could not drain to the southwest (Goldthwait, 1968). A large sand delta with a lobate front, foreset beds, and a flat top near the overflow threshold, 21 m above the present lake, is evidence for a former glacial lake (Fig. 4). Therefore, the northern part of the Lake Winnipesaukee basin was under ice when the Wentworth basin opened up (Goldthwait and Mickelson, 1982).

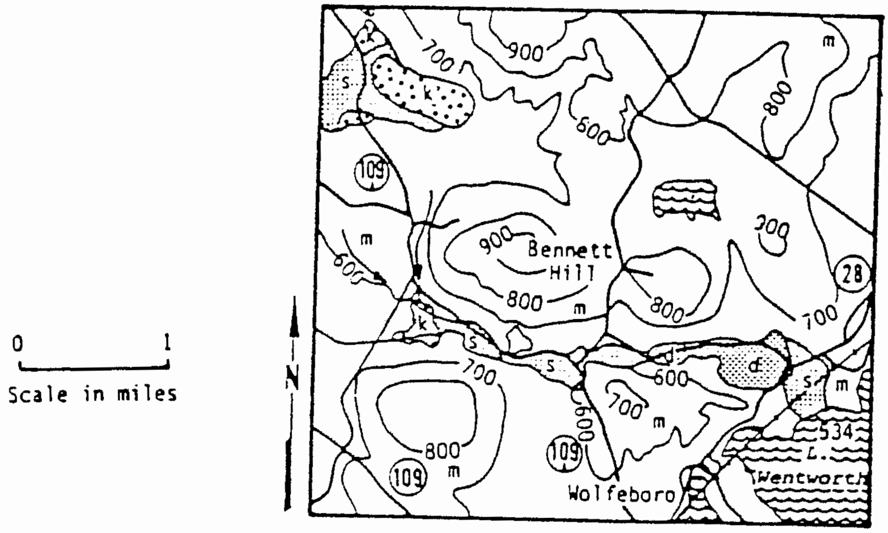

Figure 4. Channels crossing shoulder of hill near Wolfeboro, and chain of ice-contact deposits formed by meltwater flowing eastward into glacial Lake Wentworth. k = kame, d = delta, s = sand plain, m = till and bedrock hills. From Goldthwait and Mickelson (1982). Kay still resides at the Goldthwait summer home on Lake Wentworth, where Richard passed away while collecting water samples in July, 1992.

Retrace about 8.5 mi N on Rte 28 to left turn on Rte 16, proceed about 10.5 mi N on Rte 16 to left turn at Rte 25, proceed about 1.0 mi W on Rte 25 to till pit.

STOP 4 - DRUMLIN TILL, RTE 25, TAMWORTH, NH (Newton)

The Tamworth area (Fig. 5) is covered by a loose, sandy till with numerous cobbles and boulders. Some of the boulders lying on the surface are quite large; the largest is the "Madison Boulder," measuring 25 m x 11 m x 7 m. This till correlates with the **surface till** found throughout most of New England (Koteff and Pessl, 1985). A second, older till outcrops sporadically throughout the area, with the most numerous exposures within the Ossipee Mountains. The till seen at this stop correlates with the **drumlin till** found in southern New England and here averages 57 percent sand, 21 percent silt, and 22 percent clay. Exposures in the Ossipee Mountains reveal both a brown, weathered "oxidized" zone and an olive-gray unweathered zone. There are both vertical and horizontal sets of clastic dikes cutting through many of the exposures.

Retrace about 1 mi E on Rte 25 to left turn on Rte 16, follow Rte 16 less than 0.2 mi N to right turn on Rte 41, proceed about 1 mi E on Rte 41 to pits in outwash plain.

STOP 5 - OUTWASH PLAIN, NEAR SILVER LAKE, MADISON, NH (Newton)

A large outwash plain lies in the area between Ossipee and Silver Lakes and covers an area of approximately 15 km^2 (Fig. 5). The outwash grades from coarse gravel on the north to medium sand to the south. Much of the southern part of the fan is deltaic. There are a series of kame deltas south of the outwash fan that indicate an early high-level stage of the glacial lake into which the outwash built.

Retrace about 1 mi W on Rte 41 to right turn on Rte 16, proceed about 12 mi N on Rte 16 to right turn onto Rte 113 to sand and gravel pit.

STOP 6 - KAME TERRACE-ESKER COMPLEX, ALVIN J. COMAN & SON SAND & GRAVEL PIT, RTE. 113, MADISON, NH (Newton)

There are extensive deposits of stratified drift throughout the lowland areas. The through valleys are filled with ice-contact deposits that feed into extensive areas of outwash farther south. In some cases the ice-contact deposits may be directly correlated to meltwater erosion features at higher elevations. The ice-contact deposits include kames, kame terraces, and eskers. The eskers occur primarily along the bottoms of the through valleys. In at least one case the meltwater stream that formed the esker can be shown to be hydrostatically controlled so that the flow direction was opposite to the topographic gradient.

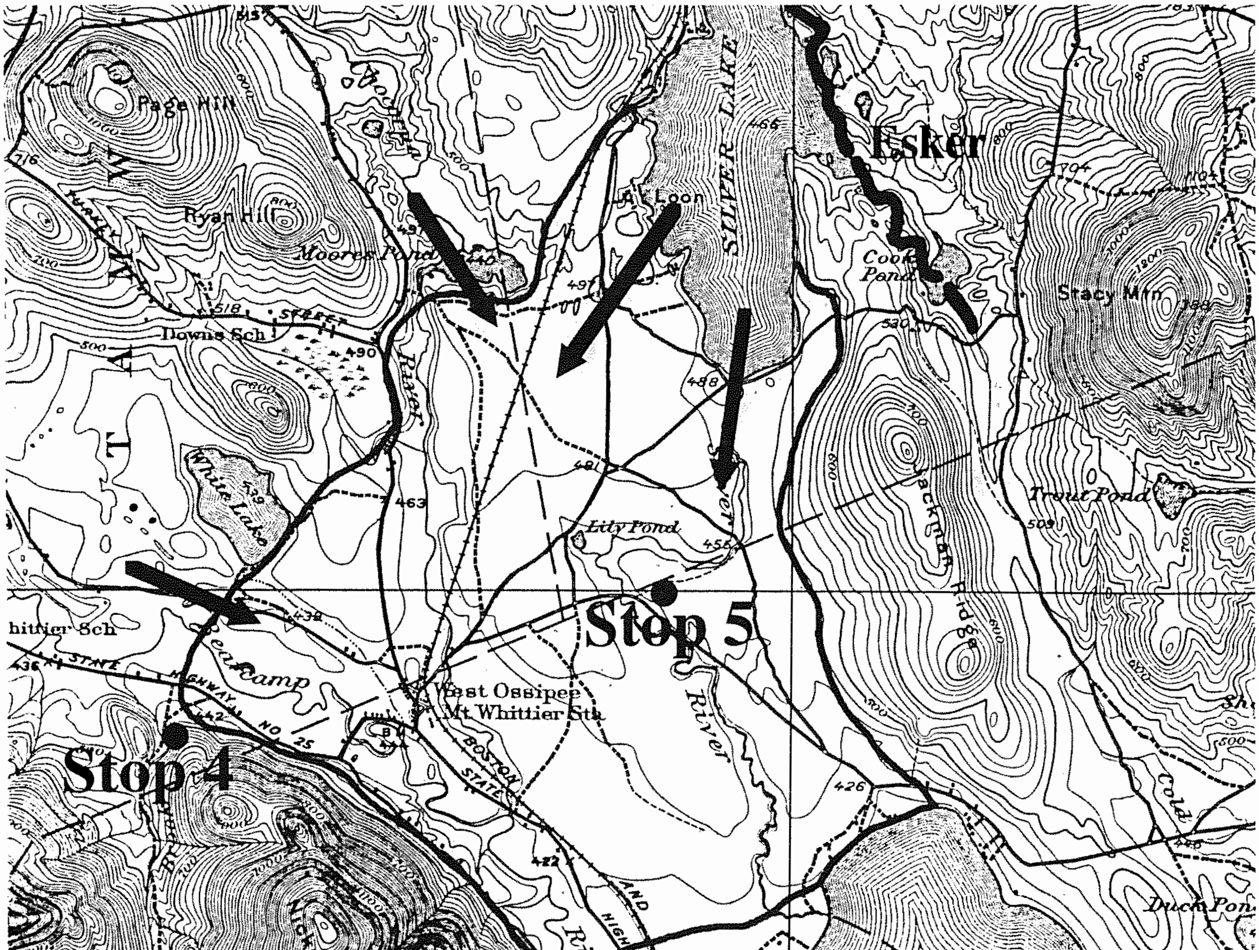

Figure 5. Map of the maximum extent of the Silver Lake outwash fan. Arrows indicate the flow directions of source streams onto the outwash fan. From Newton (1974).

Return to Rte 16, proceed 0.8 mi N on Rte 16 to left turn onto Bald Hill Rd., follow Bald Hill Rd. about 2 mi W to meltwater channels.

STOP 7 - BALD HILL MELTWATER CHANNEL, ALBANY, NH (Newton)

Meltwater channels occur on steeper, higher elevation slopes than the meltwater deposits. Some of the channels may be related to the progressive melting of stagnant ice, while others appear to have formed between stagnant and active ice. A set of eight parallel lateral channels on the side of Mt. Chocorua range in elevation from 200 to 400 m. These channels appear to have been formed because of the progressive thinning of stagnant ice occupying the adjacent valley. Another set of channels is found in the area of Bald Hill, just west of the village of Conway. Here two channels were cut through adjacent gaps in an east-west ridge and can be traced 3 km downslope to kame terraces in the Silver Lake through valley (Fig. 6). For meltwater to have flowed through this system the ice at the north end of the channel must have stood at an elevation of at least 300 m, while at the downstream end the ice appears to have been at an elevation of only 180 m. This suggests a rather steep gradient for the ice front (22 m/km).

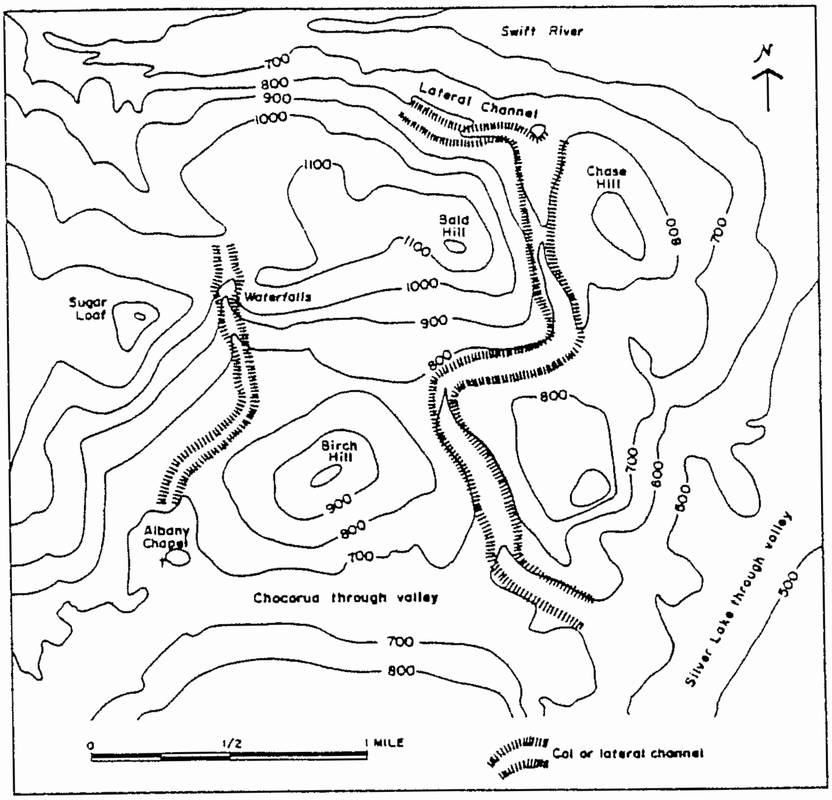

Figure 6. Map showing locations of col channels west of Conway. The Sugarloaf channel formed first, followed by the Chase Hill channel. From Newton (1974).

Return to Rte 16, turn left and proceed about 1 mi N on Rte 16 into Conway and turn left onto West Side Rd., proceed about 1 mi N to left turn onto Passaconway Rd., proceed 1.2 mi W to right fork onto unmarked dirt road, proceed about 1.5 mi to "rottenstone" pits.

STOP 8 - "ROTTENSTONE," GOVERNMENT PIT, ALBANY, NH (Newton, Davis)

At Conway the Saco River valley makes a right-angle turn to the east. However, much of the glacial ice continued streaming southward, eroding a series of "through valleys" across the divide between the Saco River and Ossipee River watersheds. These through valleys range up to 13 km in length and 100 m in depth. The surrounding hills also show strong evidence of glacial erosion as many have well-developed stoss-and-lee forms comparable to roches moutonnees.

Not all the bedrock in the region was glacially scoured down to fresh solid rock. There are some exposures of deeply weathered granite on the lee sides of hills, which appear to have been protected from glacial erosion. The weathered granite is mined as it makes excellent road metal. The resulting exposures frequently reveal sets of vertical and horizontal clastic dikes that have been injected into weathered granite, presumably during glaciation. Similar features can also be found in some exposures of pre-late Wisconsinan till.

The Government Pit shows excellent exposures of disintegrated Conway Granite ("rottenstone"). The granite is weathered to a depth of at least 6 m at this locality. Weathering is concentrated along joint planes, and in places has resulted in rottenstone surrounding cores of relatively fresh bedrock. Till overlies the rottenstone in part of the pit area (Newton, 1977).

The Government Pit is also one of the best known mineral localities in the state. Collectors have honeycombed the weathered rock in search of miarolitic cavities containing crystals of smoky quartz, feldspar, topaz, and rare beryllium minerals.

Return to West Side Rd., proceed about 3.5 mi N to left turn onto access road to White Mountain Hotel - Resort, proceed about 1.5 mi W to parking lot.

STOP 9 - CATHEDRAL AND WHITE HORSE LEDGES, WEST SIDE ROAD, BARTLETT AND HALES LOCATION, NH (Davis)

The lowland extending from the town of Conway in the Saco River valley to Ossipee in the Ossipee River valley contains numerous erosional and depositional features associated with Pleistocene glaciation (Newton, 1974). The area lies at the edge of the Lakes Region, bounded on the north by the White Mountains. This topographic setting greatly influenced the flow of ice through the area and resulted in a number of deeply scoured valleys. Perhaps the best example of this is the portion of the Saco River valley extending northward from Conway to the village of Intervale. The valley here appears to have been overdeepened by coalescing ice streams flowing out of Crawford and Pinkham Notches. These ice streams trimmed the valley walls to form Cathedral and White Horse Ledges near the village of North Conway.

Meltwater channels and meltwater deposits suggest that deglaciation in this region was controlled by the underlying topography. The ridges acted as barriers separating areas of active ice to the north from stagnant ice to the south. The through valleys were occupied by tongues of ice that received tremendous amounts of meltwater and sediment from the melting ice to the north. Most of this sediment was transported through the valleys and out onto the outwash plains seen at the previous stops to the south.

Although the steep east faces of Cathedral and White Horse Ledges appear to be parallel to the regional ice flow in the Saco River valley in the North Conway area, Ellis (1972) considered the cliffs to be lee sides of classic roches moutonnées. The ledges are composed of Conway Granite, which was intruded as coalescing stocks at the eastern edge of the White Mountain batholith. The Conway Granite is part of the White Mountain plutonic-volcanic series, dating about 185 mya. Although the granite crystallized at depth, volcanism is evidenced by flows, tuffs and breccias of the Moat Volcanics on Moat Mountain, a few kilometers southwest of the ledges.

The Conway Granite is a coarse, pink biotite granite that generally weathers to a dull gray. The granite is not foliated, but in a few places schlieren with oriented quartz, biotite, and feldspar grains may be found. Miarolitic cavities lined with smoky quartz and feldspar crystals are locally abundant.

The Conway Granite is generally massive with joints commonly tens of meters apart. Ellis (1972) summarized a detailed study that he made of the two types of joints. Primary jointing formed during deep burial soon after the magma crystallized. Based on the presence or absence of quartz, aplite, or basalt dikes, Ellis (1972) distinguished two ages of near-vertical primary joints with variable orientations. Sheeting, as is well displayed by exfoliation slabs on White Horse Ledge, formed by unloading of the rock by erosion. Sheets of rock on the tops and sides of the ledges are common and less than a meter thick; however, sheets are less common and much thicker with depth at the bases of the ledges. The sheeting is younger than the primary jointing because exfoliation joints cut across the primary joints, dikes, and schlieren. Also, the sheeting is preglacial in origin because exfoliation joints have been partially removed by glacial erosion.

On the stoss (northwest) sides of the ledges, sheeting is generally intact, as glacial ice only abraded the bedrock surfaces. Grooves, crescentic gouges, polish, and perched boulders are common. However, on lee (southeast) sides of the ledges, sheeting is truncated by the cliff faces (east side of Cathedral Ledge and south side of White Horse Ledge), as evidenced by some sheets overhanging space created by removal of bedrock by glacial plucking. Much of this erosion may have occurred when continental ice thinned. The topography controlled a generally southward ice flow, which polished bedrock surfaces, such as the slabs of White Horse Ledge. Very little evidence exists for development of sheeting caused by glacial unloading, except perhaps in a few places on the slabs of White Horse Ledge. Thus Ellis (1972) suggested that a longer period of time than the postglacial was required to develop the extensive sheeting observed on Cathedral and White Horse Ledges and in other quarries in New England.

Note: Because of the generally unweathered character of the Conway Granite, along with the variety of cracks that follow the vertical primary jointing and the moderate-angled exfoliation slabs that follow the sheeting, Cathedral and White Horse Ledges are one of the most popular rock-climbing areas in North America. In recent years, hang gliding from the tops of the ledges also has become common.

Return to West Side Rd., proceed about 1 mi N to T-junction, turn right and proceed about 1 mi E to Rte 16, turn left and proceed about 16 mi N to Pinkham Notch Camp.

ROAD LOG - DAY TWO

Proceed about 3 mi N on Rte 16 to the Glen House site.

STOP 10 - PANORAMA OF CIRQUES, GLEN HOUSE SITE, RTE 16, GREENS GRANT, NH (Davis, Fowler)

Late Wisconsinan continental ice probably covered the highest peaks of the Presidential Range, including Mt. Washington, with a summit elevation of 1917 m above sea level. The cols between peaks have striae and roches moutonnées oriented 140° (Goldthwait, 1940, 1970a,b). In the area around the Glen House site, striae are oriented 180-200°, which leads to the question of whether or not these erosional features are contemporaneous (Goldthwait, 1970b).

If the weather cooperates, a fine panoramic view of the great cirques cut into the east slope of the Presidential Range should be visible. As discussed in the Introduction section, a long-standing controversy concerns whether or not cirque glaciers existed following deglaciation of the continental icesheet.

Proceed 6.4 mi N on Rte 16 to a parking area at the Peabody River section.

STOP 11 - STRATIGRAPHY OF THE LOWER PEABODY RIVER VALLEY, RTE 16, GORHAM, NH (Fowler)

The exposures at this stop, with lacustrine sediments overlain by two diamict units and an intermediate lacustrine unit, have been the source of much study and controversy during the past fifty years. Crosby (1934) cited these exposures, along with a number of others scattered across northern New Hampshire, as evidence of till overlying lacustrine deposits, and suggested they were part of the so-called Bethlehem Moraine. He postulated the moraine to be the result of a late Wisconsinan readvance or stillstand of the Laurentide Icesheet.

Goldthwait (1938) soundly refuted Crosby's proposition on geomorphological grounds, but later Lougee (1940) and Flint (1953) mentioned the deposits again in support of a proposed late Wisconsinan readvance (perhaps of Valders age). Since that time sporadic studies have focused on better stratigraphic description of the section and the search for organic materials for dating.

In 1971, Fowler (unpublished data) examined the rhythmite sequence at the bottom of the westerly exposures and demonstrated that approximately 275 irregular but distinguishable couplets are present in the lower lacustrine unit. Later, Gosselin (1971) published the first detailed description of this section and its multiple exposures, and Goldthwait (1972) performed detailed fabric analyses and stone counts on the two diamict units, demonstrating a strong fabric parallel to the valley's axis, and a definite north to northeast provenance for both of the units. This evidence refuted earlier suggestions of northward ice flow from a highland icecap to the south (Flint, 1951), but requires that the deposits were related exclusively to ice moving from the north.

Gerath (1978) suggested that the sediments in the lower Peabody River valley were a morainal "plug" inserted between the steep valley walls. Although he considered the origin of these sediments to be uncertain, he suggested the possibility of concomitant Wisconsinan ice to the north in the Androscoggin valley. Bradley (1981) also investigated this section and resurrected Crosby's suggestion for widespread moraine segments in this region. On the basis of geomorphic observations, he concluded that the Peabody valley deposits were formed by ice flowing southward, possibly as a late-glacial ice tongue pushing up the valley and damming a proglacial lake. Gerath and Fowler (1982) refuted Bradley's contention that this and other moraine segments are of regional significance, but did not dispute the importance of the Peabody River section to the regional deglaciation history.

Haselton and Fowler (1991) completed a detailed stratigraphic description and analysis of the exposures seen at this stop. Their research has become more significant because of work on the nearby Androscoggin Moraine in Shelburne, New Hampshire (Thompson and Fowler, 1986, 1989). The possible existence of an active ice tongue in the Androscoggin valley and its relationship to these two localities has renewed the need for an accurate interpretation of this complex section.

Stratigraphic description

The 150-ft thick (46 m) section consists of several distinct units (Figure 7a). The basal unit is composed of 70-80 ft (21-24 m) of lacustrine rhythmites and varves. Couplets vary widely in thickness and gradation and suggest a complex, rapidly changing lacustrine environment located close to glacial ice. This unit contains blocks of compact, stony diamict with clasts of northeasterly provenance. Dropstones with conformal bedding surrounding them and scattered thick lenses of fine to coarse sand with graded bedding are also present. It has been reported that this unit lies directly on bedrock at this locality (Goldthwait, personal communication), although bedrock is not presently exposed in the riverbed.

The basal unit is overlain by 20-25 ft (6-8 m) of compact, silty, clayey, locally cobbly to bouldery diamict. The contact between these units is sharp; no rip-up clasts or deformation of the contact or the underlying lacustrine unit has been observed. The fabric of the clasts in the diamict is predominately N 40°E (Figure 7b), and stone counts clearly indicate the clasts came from an area lying about 6 miles (10 km) to the north-northeast (Table 2). The lower diamict unit is overlain by 8-10 ft (3 m) of bouldery/cobbly gravel, which displays little internal bedding or other sedimentary structure except for a locally discontinuous bed of coarse to fine sand near its base. This gravel overlies the diamict along a sharp contact. Above the lower diamict is a very distinctive 18-20 ft (6 m) sequence of severely deformed, sandy-silty rhythmites and more massive lacustrine beds. Shearing and thickening/thinning of beds has been observed along micro-faults and sheared structures suggest the deformation was caused by compression from the north. The contact with the underlying gravel is sharp and undeformed, and no rip-up clasts have been observed. Finally, the deformed lacustrine unit is overlain sharply by 6-10 ft (3 m) of loose silty, sandy stony diamict. The fabric of the clasts has a predominate orientation of N 45°E (Figure 7c); clast provenance is identical to that of the lower diamict unit. The top of this unit has an abrupt gradational contact with winnowed, bouldery ground moraine, typical of the surficial deposits in this area.

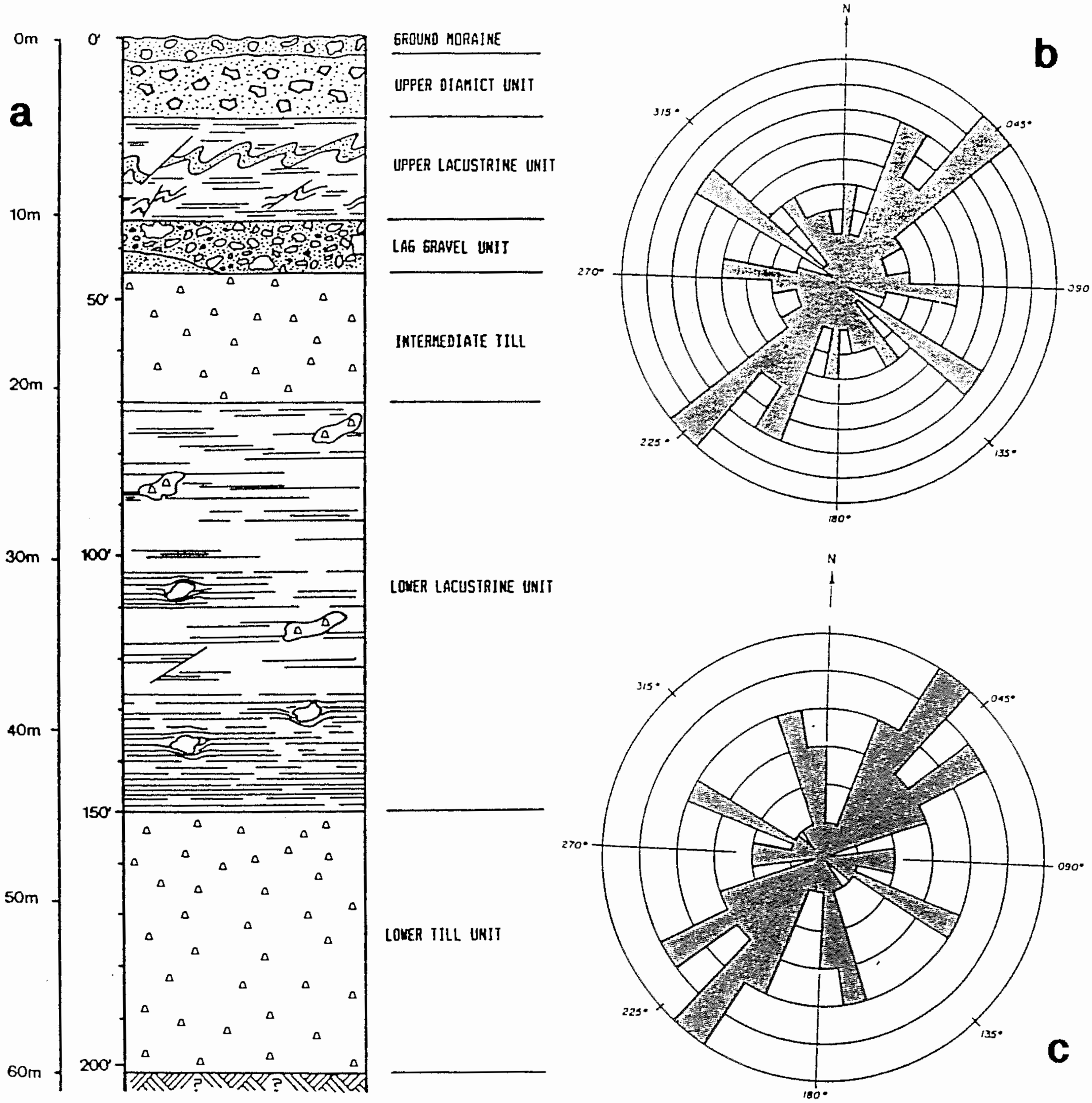

Figure 7a. Composite stratigraphic diagram of lower Peabody River valley, Gorham, New Hampshire; 7b. composite rose diagram, clast orientation, intermediate till unit (diagram based on 150 clast measurements from 3 counts); 7c. composite rose diagram, clast orientation, upper diamict unit (diagram based on 92 clast measurements from 2 counts). From Haselton and Fowler (1991).

Status of Interpretation

The latest studies of the lower Peabody River valley section (Haselton and Fowler, 1991) suggest that the section represents various types of deposition in an ice-contact proglacial lake formed between ice in the northernmost river valley and the reverse slope to the south. Ashley (1985) has characterized the sedimentary environment in such a lake as complex and rapidly changing because of the types of deposition possible from interactions between glacially-derived detritus, solid and melting ice, and water. As Davis et al. (1980) have shown, the local climate in this area alternated between periods of warmth with heavy runoff and cold periods with hard freezes of long duration. In such a climate, the alternating sedimentary units could have been deposited rapidly during the warm periods of meltwater discharge, and then could have been consolidated and perhaps frozen during the following periods of cold quiescence. These units have sharp contacts and lack of grading and incorporation between them. This suggests their emplacement during independent episodes, over the possibly frozen surface of the previously deposited unit. The repetitive character of the section (lacustrine-diamict-lacustrine-diamict) appears more likely caused by dynamic fluctuation in this sedimentary environment, than to widespread late Wisconsinan climatic events. The foregoing interpretation suggests that these deposits are not the result of a widespread regional readvance of late Wisconsinan ice of the sort contemplated by Crosby and Bradley, but does suggest a local readvance of ice in the Androscoggin River valley, pushing southward to this site and damming at least one proglacial lake.

Table 2. Summary of stone count percentages, lower Peabody River valley, Gorham, New Hampshire

	Lower Diamict Samples				Upper Diamict Samples					
Lithologies #	1*	2*	3+	4+	1*	2*	3*	4*	5+	6+
Amphibolite	14	12	16	10	12	22	6	6	15	13
Biotite Granitics	38	40	36	43	34	32	33	22	28	30
Quartzite	1	4	2	0	6	6	4	0	0	0
Quartz Diorite	10	9	15	20	16	17	14	16	18	21
Quartz Monzonite	1	0	2	5	3	0	0	0	0	0
Biotite Granite	29	29	21	18	29	19	21	17	15	18
Binary Granite	4	1	6	4	0	1	14	35	24	18
Biotite Schist	0	0	0	0	0	2	1	0	0	0
Undifferentiated	3	5	2	0	0	1	7	4	0	0
Totals	100	100	100	100	100	100	100	100	100	100

Assemblages are derived from area north-northeast of Peabody River section, dominated by widespread outcrops of biotite granites and granitic gneisses of the Oliverian Plutonic Series, which have been extensively intruded by biotite granite and quartz diorite with some secondary quartz monzonite of the White Mountain Plutonic Series. Rock types to the south consist primarily of sillimanite-grade, aluminous metasedimentary rocks (primarily mica schist and para-gneiss, with minor amounts of quartzite).

* Count percentages summarized from Goldthwait, 1972.

\+ Unpublished count percentages of Fowler.

Proceed 1.7 mi N on Rte 16 to Gorham, turn right and proceed 12.2 mi E on Rte 2 into Maine, turn left onto North Rd. and proceed about 0.5 mi across RR tracks and over bridge on Androscoggin River, turn left and proceed about 2.5 mi to foot of a ridge of the Androscoggin Moraine system.

STOP 12 - ANDROSCOGGIN MORAINE, NORTH ROAD, SHELBURNE, NH, AND GILEAD, ME (Thompson)

The Androscoggin Moraine system, which is a large cluster of en-echelon moraine ridges, is located in the Androscoggin River valley (Fig. 8). Stone (1880) discovered part of the moraine system, and illustrated the segment seen here in his book titled "The Glacial Gravels of Maine" (Stone, 1899). Thompson investigated the area in detail and found numerous additional moraine segments that had not been previously reported (Thompson, 1983; Thompson and Fowler, 1989). The moraine ridge at this stop is located adjacent to North

Road, and is crossed by the Portland-Montreal pipeline. Unfortunately, no stratigraphic records were kept when the pipeline trenches were excavated through here.

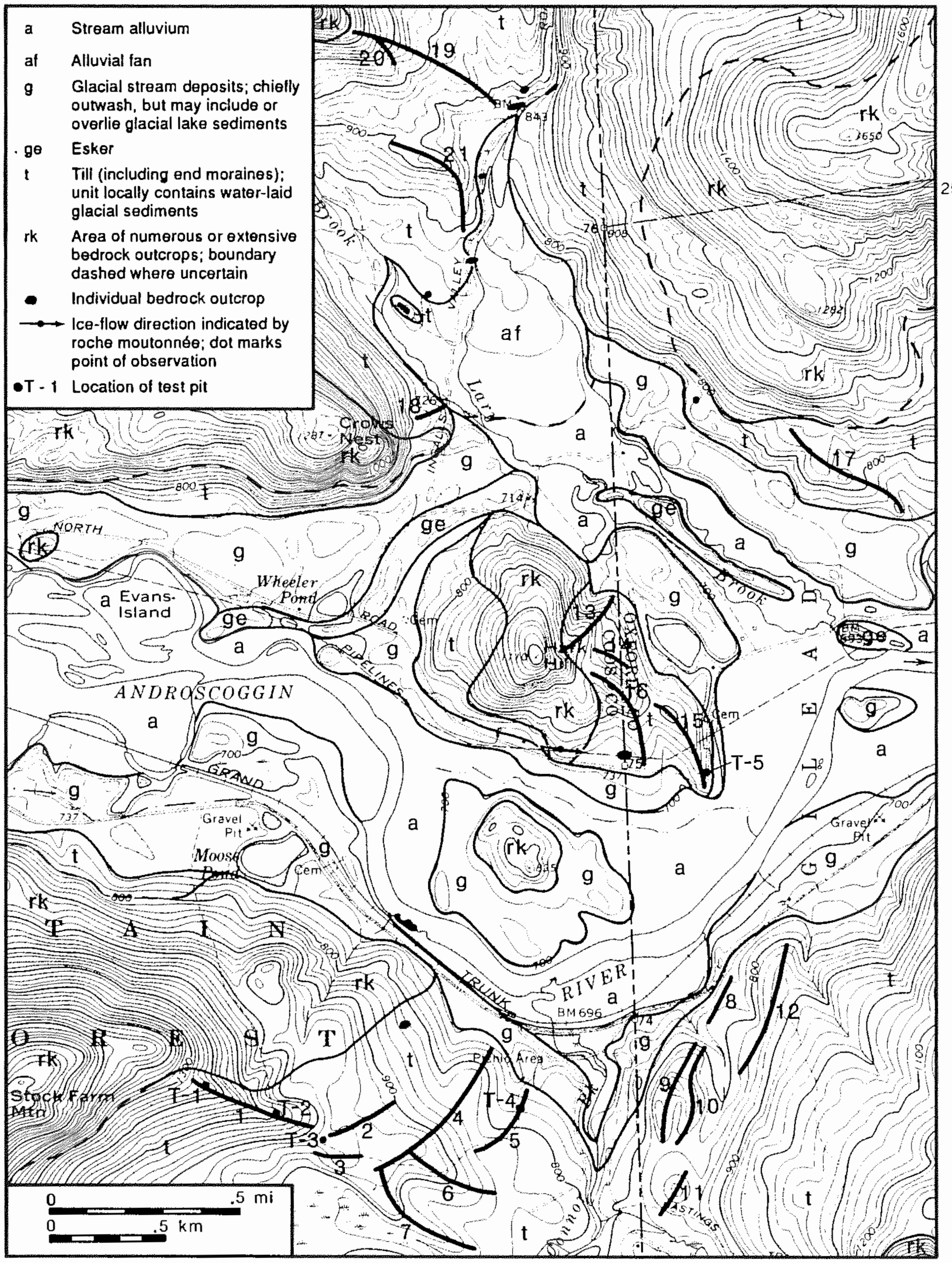

Figure 8. Surficial geologic map of southeastern part of the Shelburne 1:24,000 quadrangle (from Thompson and Fowler, 1989). Numbered lines indicate crests of moraine ridges in Androscoggin Moraine system. Stop 12 is where pipeline crosses ridge no. 15. Stop 13 is roche moutonnee indicated by arrow near center. T = test pits..

The ridges comprising the Androscoggin Moraine are mostly sharp-crested, up to 100 ft (30 m) high, and are littered with boulders derived from bedrock a short distance up the valley; the largest of these boulders found to date is 25 ft (8 m) in diameter. The moraine crests range in elevation from 720 ft (219 m) next to the river to about 900 ft (274 m) on the north and south walls of the valley. Test pits dug at five locations (Fig. 8) have shown that the moraines consist of sandy diamictons (mostly flowtills) with variable percentages of interbedded water-lain silt, sand, and gravel (Thompson and Fowler, 1989).

The Androscoggin Moraine was deposited by a tongue of glacial ice flowing eastward down the valley from the Gorham area. Striation evidence, together with meltwater channels and deposits between Gorham and Jefferson, suggest that the source of the ice was the Connecticut River valley lobe of the Laurentide Icesheet. This lobe spilled across the divide between the Connecticut and Androscoggin River basins, following the prominent valley seen along Rte 2 west of Gorham (Gerath, 1978; Thompson and Fowler, 1978; see also Stop 15). The steep profile of the moraine system suggests an advancing ice margin, but it is not known what triggered this event. The trigger may have been a climate change, or perhaps simply an adjustment of icesheet equilibrium resulting from deglaciation of the Carter and Mahoosuc Ranges on either side of the Androscoggin River valley. As these mountains emerged from the glacier, active ice flowing through the Gorham area would have been funneled into the narrow valley where the moraines were deposited.

Proceed 0.6 mi W on North Rd. to roche moutonnee.

STOP 13 - ROCHE MOUTONNÉE, NORTH ROAD, SHELBURNE, NH (Thompson)

The east end of the bedrock outcrop has been disturbed by blasting for the pipeline where it crosses the base of Hark Hill (Fig. 8), but the overall form clearly indicates the direction of glacial flow. The ledge has been sculpted by ice flowing eastward down the Androscoggin River valley. The axis of the roche moutonnee trends 100°, parallel to glacial striations found nearby in this part of the valley. This orientation suggests that the outcrop was shaped at the same time that the late-glacial ice tongue deposited the Androscoggin Moraine. However, it is possible that the icesheet was topographically deflected parallel to the valley during the late Wisconsinan maximum as well, and that the outcrop was sculpted over a longer period of time.

Proceed 2.4 mi W on North Rd., then 1.0 mi S on Meadow Rd., and retrace Rte 2 W to Gorham, continue 1.4 mi W on Rte 2 to junction with Rte 16 N, continue 5.6 mi W on Rte 2 over Randolph Hill to Appalachia parking lot on S side of Rte 2.

STOP 14 - DEPOSITS NEAR DURAND LAKE, RTE 2, RANDOLPH, NH (Davis, Fowler)

Gravelly deposits at the mouths of several narrow valleys draining on the northern Presidential Range contain stones derived from higher parts of the valleys to the south. Because of the large boulders of schist and the high percentages of schist in stone counts (Fig. 9; Table 3), Bradley (1981) interpreted these deposits as till emplaced by alpine glaciers issuing from cirques in the Presidential Range during late-glacial time. Fowler (1984) subsequently presented evidence that the deposits near Durand Lake resulted from colluvial processes, rather than glacial transport from the King Ravine cirque. The latter view is shared by Davis and Waitt (1986), who also have mapped this area. Waitt and Davis (1988) summarized the arguments and data pertaining to the sequence of cirque glaciers and continental ice in the Presidential Range, as well as on Mt. Katahdin in Maine and the Green Mountains in Vermont.

Proceed about 4 mi W on Rte 2, then proceed about 0.5 mi S on Valley Rd.; sand and gravel pits are on the W side of Valley Rd.

STOP 15 - CORRIGAN SAND & GRAVEL PIT, NEAR RTE 2, RANDOLPH, NH (Thompson)

The Corrigan Pit is located in the upper part of the Israel River valley. The Israel River drains northwest and joins the Connecticut River at Lancaster. A short distance east of the Corrigan Pit, in the Bowman section of Randolph, Rte 2 crosses the divide into the Androscoggin River basin. The elevation of this drainage divide is 1500 ft (457 m). As the late Wisconsinan glacier margin receded down the Israel River valley, a glacial lake was impounded in this area and spilled eastward across the Bowman divide. Glaciolacustrine fan and deltaic deposits that accumulated in the lake are exposed in several pits in Randolph and Jefferson. An ice-contact delta graded to this 1500-ft lake level forms a narrow terrace along Rte 2 northeast of the Corrigan Pit.

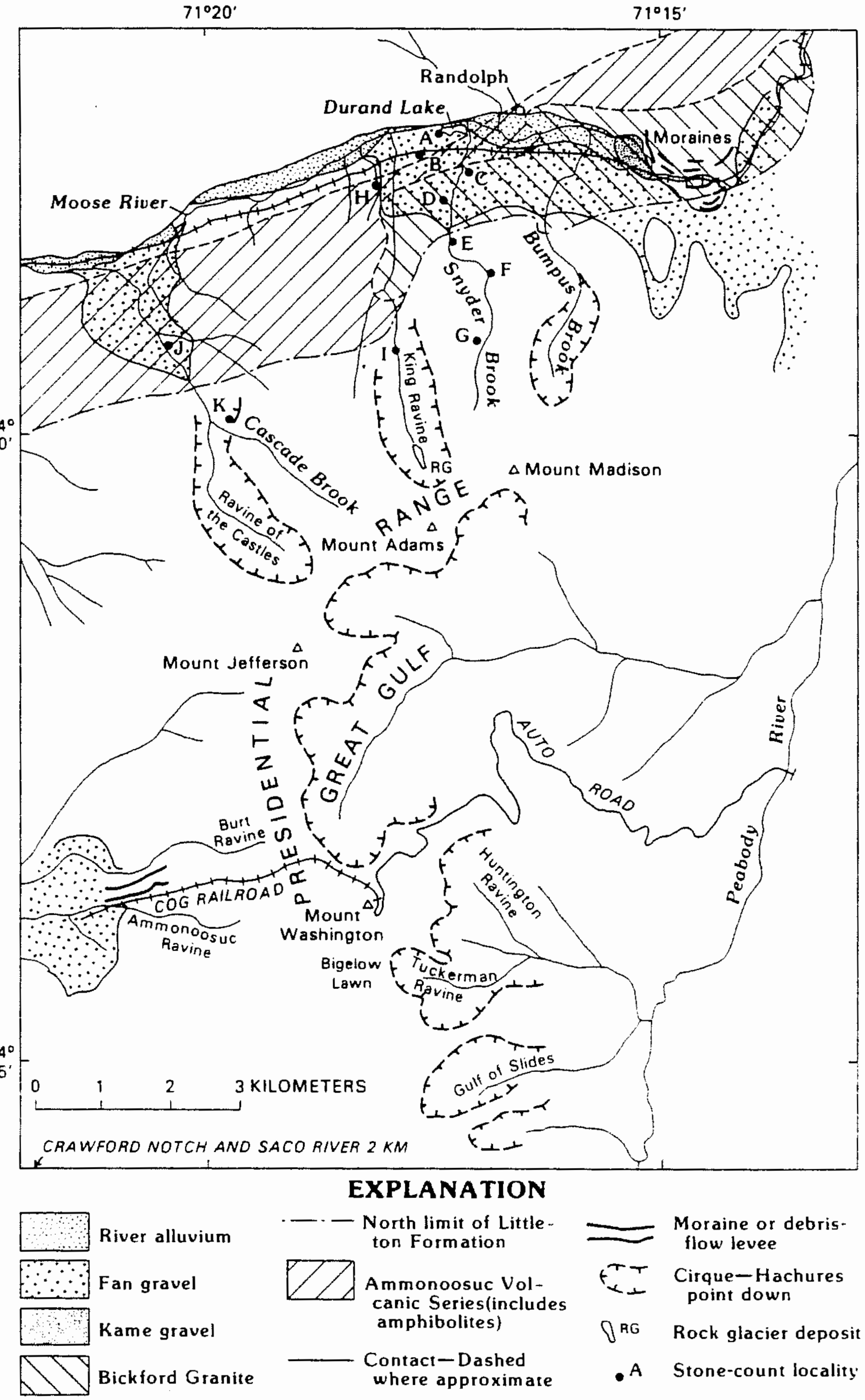

Figure 9. Map of northern Presidential Range and adjacent Randolph valley, New Hampshire, showing generalized geology and distribution of cirques, debris fans, and other features. From Waitt and Davis, 1988, Fig. 10, p. 522.

Table 3. Lithology of pebble fraction of till and fan material, northern Presidential Range. From Waitt and Davis, 1988, Table 4, p. 523.

	Localities**										
Rock Types	A	B	C	D	E	F	G	H	I	J	K
Muscovite-biotite schist***	19	17	12	8	8	4	4	24	8	24	—
Micaceous gneiss†	35	38	36	48	24	60	48	40	20	28	12
Pegmatites, quartzite, vein quartz, undiff. mafics††	37	31	28	32	44	28	28	32	40	48	40
Binary granite (Bickford)†††	—	—	—	—	—	—	—	—	—	—	—
Biotite-quartz monzonite and coarse pink granite (White Mountain Magma Series)[7]	4	3	—	4	4	—	4	4	8	—	12
Amphibolite and volcanics (Ammonoosuc Volcanic Series)[8]	3	9	20	4	16	8	12	—	20	—	32
Diorite (Lost Nation)[9]	1	1	4	4	—	—	—	—	—	—	4
Hornblende gneiss[9]	—	1	—	—	4	—	—	—	—	—	—
Quartzite[9]	1	—	—	—	—	—	4	—	4	—	—

*Expressed as percent of 25 pebbles counted (100 for localities A and B) with long axes 2 to 5 cm.

**Localities specified in figure 10: A, Durand Lake, south shore; B, railroad cut about 200 m south of Durand Lake; C,D,E,F,G, in ascending order, stream cuts in Snyder Brook valley; H, stream cut in fan below King Ravine; I, stream cut in lower part of King Ravine floor; J, stream cut in fan below Ravine of the Castles; K, stream cut in lower sidewall of Ravine of the Castles.

***Upper unit of Littleton Formation (Billings and others, 1979), possibly upvalley source for pebbles at all localities.

†Lower unit of Littleton Formation (Billings and others, 1979), possibly upvalley source for pebbles at all localities.

††Unknown source, but possibly derived from Littleton Formation.

†††Probable upvalley source for pebbles at localities A,B,C,D,H.

[7] Probable upvalley source for pebbles at all localities.

[8] Probable source for pebbles at localtiies E,F,G,I,K.

[9] Probable downvalley source at all localities.

In 1992 the main working face in the Corrigan Pit exposed four units, which are described below. This section was located in the southern part of the pit area, close to the river. The pit face trended NNE-SSW and was excavated in a low NE-SW ridge that reaches an elevation of 1440 ft (439 m). The general stratigraphy seen here consists of a glaciolacustrine sand and gravel deposit which coarsens upward and is overlain by a stony glacial diamict. There is much deformation evident throughout the section. Starting with the lowest unit, the following materials were observed in late 1992:

UNIT 1: This unit consists of at least 7 ft (2 m) of glaciolacustrine sand and silty sand (base not exposed). The sand shows thin planar foreset beds that dip between northeast and east. Current ripples are present locally in the foresets. There is much faulting in the central to upper parts of this unit. The deformation may have been caused by ice shove, but measurements taken on several fault planes were inconclusive in this respect.

UNIT 2: The sand is abruptly overlain by 4.6 ft (1.4 m) of massive to weakly stratified pebble-cobble gravel. This gravel is poorly sorted, angular, and variably sandy. The contact between Unit 2 and Unit 1 was unconformable and channeled in the small part of the section where it could be seen.

UNIT 3: In the SSW end of the pit face, Unit 2 is overlain by 7 ft (2 m) of coarse gravel, which consists of a chaotic mixture of pebble-cobble-boulder gravel with sand lenses. The contact with Unit 2 is sharp.

UNIT 4: The uppermost unit consists of 20 ft (6 m) of bouldery, silty-sandy glacial diamict containing abundant lenses of washed sediment. This unit appears identical with the regional late Wisconsinan surface till. It is olive-gray (5Y-5/2), rather loose-textured, and non-fissile. The stones show a wide variety of bedrock lithologies. They are mostly subangular to angular, and few are striated. Sand lenses seen in the diamict unit during an earlier visit were greatly deformed and suggestive of ice shove.

A shallow opening in the northern part of the pit complex (next to Valley Road) revealed a thin veneer of pebbly sand and pebble gravel overlying glaciolacustrine silt. The silt is unusually compact, and the sediments in this exposure are complexly deformed. Bedding in the silt is locally contorted, with fragmented sand pods and dropstones. Overall, the deposits in the Corrigan Pit are believed to record the advance of a glacier margin into a lake ponded in the Israel River valley. Unit 1 is probably a subaqueous fan deposit that was blanketed by coarser fan gravel, gravelly diamict flows, and finally by flowtill as ice approached the site. It is not certain whether this was a minor readvance in late-glacial time or the earlier onset of late Wisconsinan glaciation. However, the ridge-shaped or hummocky topography suggests that these deposits resulted from a readvance during the recession of the last icesheet.

Return to Rte 2 and proceed about 3 mi W to Rte 115. Proceed about 9 mi SW on Rte 115 to a jct with Rte 3; a sand and gravel pit is located on the W side of the jct.

STOP 16 - TWIN MOUNTAIN SAND & GRAVEL PIT, RTE 3 AND 115, CARROLL, NH (Thompson)

This large pit is located in an ice-contact delta that was built southward into glacial Lake Ammonoosuc (Fig. 10). The lake was named by Goldthwait (1916), who recognized that it was dammed by a receding continental ice margin in the Ammonoosuc River valley. He described the delta seen at this stop as a "pitted outwash plain," and proposed that the Bethlehem Moraine (a series of hummocky deposits in the Bethlehem - Littleton area) was deposited into the same lake at a slightly later time. Goldthwait noted the terraces extending southward from the delta along both sides of Alder Brook, and described them as kame terraces built against remnant ice in the Alder Brook valley. These terraces connect in turn with a "deeply pitted kame plain" to the south, near Twin Mountain village (Goldthwait, 1916).

Lougee (1940) examined this area in detail and agreed that a glacial lake had existed here. However, he demonstrated that the Alder Brook terraces are not kame terraces, but simply resulted from incision of the distal portion of the Carroll delta. This downcutting resulted from lowering of the lake level while the ice margin was still located at the head of the delta and continued to discharge meltwater. A deep channel cut into the west side of the delta at this time is clearly evident at this stop (Fig. 10). Lougee also described the meltwater channels on the hillside northeast of the delta. He thought that these channels formed by the sudden drainage of a glacial lake that was situated east of Cherry Mountain. Water escaping along the ice margin, around the north and west sides of the mountain, supposedly carved these channels and deposited the eroded sediment on the delta. Lougee observed that channels on the delta surface originate at the northeast corner of the delta where the hillside drainage would be expected to have entered the delta plain. A major problem with this scenario is that the channels can only be traced a short distance, and are absent from the remainder of the long proposed drainage route around Cherry Mountain. But, more likely drainage from within the ice contributed most of the water and sediment to the Carroll delta. This drainage probably occurred via tunnels in the glacier.

There were no large fresh exposures in the pit at this stop when this guidebook was prepared. However, the coarse gravels forming the delta topset beds can be seen along the east wall of the pit and sandy foreset beds are exposed in a few places. According to Goldthwait (1916) the delta plain (which has since been removed in the pit area) was "strongly pitted" in the proximal part, but smooth and uncollapsed in the central and distal portions. He also noted that the topset gravels were less bouldery toward the front of the delta. The elevation of the delta plain indicates that the upper level of glacial Lake Ammonoosuc was approximately 1475 ft (450 m). The probable spillway for this lake stage is located along Rte 3, southwest of Twin Mountain village. The lower lake level is indicated by the surface at about 1378 ft (420 m) in the Twin Mountain area, south of here (Fig. 10). Lake Ammonoosuc dropped to this level when ice retreat opened a lower spillway west of Twin Mountain. Both lake stages drained into the Gale River, which flows through Franconia.

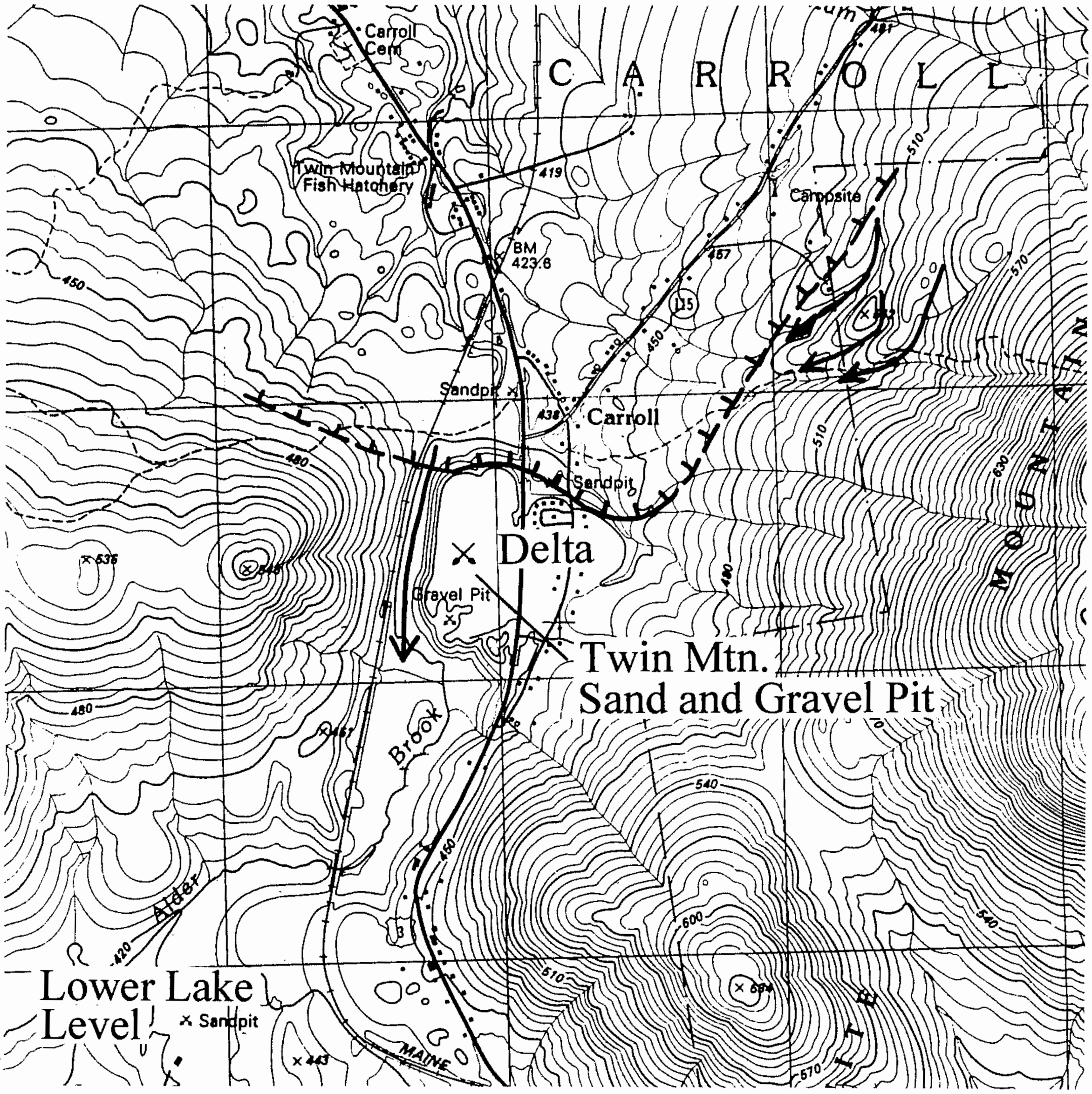

Figure 10. Map showing location of the Twin Mountain Sand and Gravel pit (Stop 16) in glacial Lake Ammonoosuc delta. Arrows indicate meltwater channels. Hachured line shows position of glacier margin when delta was deposited. Topography from Bethlehem 7.5 x 15-minute quadrangle.

Proceed about 2 mi S on Rte 3 to Twin Mountain village, and about 10 mi SW on Rte 3 to Franconia Notch and the parking lot at Profile Lake.

STOP 17 - OLD MAN OF THE MOUNTAINS, RTE 93, FRANCONIA NOTCH, FRANCONIA, NH (Fowler, Davis)

The "Old Man of the Mountains," perhaps New Hampshire's most important landmark, consists of seven large blocks of Conway Granite bedrock that are juxtaposed in such a way to provide the profile seen from Profile Lake on the floor of Franconia Notch. These seven blocks are positioned on the profile as follows: 1) forehead plate with detached crest block, 2) eyebrow, 3) nose, 4) upper lip and base of nose, 5) chin and lower lip, 6) continuation of block five at rear of central cavern, and 7) Adam's Apple, just below block 5. Five discrete structural elements with seven separate joint sets are involved in the rock mass comprising the profile

(Fowler, 1982). Fowler (1982) concluded that: 1) the dead weight load of the blocks comprising the profile and the location of the center of gravity of the rock mass are primarily responsible for the stability of the profile, 2) the rock mass from the nose up is more stable than the chin and upper lip blocks below, which pose the most critical stability problems on the profile, and 3) active reinforcement of the rock mass comprising the profile might be possible. At the moment, the profile is protected by water diversion ditches, grouting in cracks, and turnbuckles joining various blocks.

Proceed about 5 mi S on Rte 93 to a parking lot on the W side of the highway.

STOP 18 - THE BASIN POTHOLES, RTE 93, FRANCONIA NOTCH, LINCOLN, NH (Davis)

The Basin Potholes are classical erosional features presumably formed from high meltwater discharge during the waning stages of the most recent continental glaciation in Franconia Notch. Although larger and more spectacular potholes occur elsewhere in the White Mountains, such as those on the Ammonoosuc River just west of Mt. Washington, the Basin Potholes are the most accessible for this field trip. This stop also provides a fine view of Franconia Notch to the north, a classical U-shaped glacial valley, with Cannon Mountain to the west and Mts. Lafayette, Lincoln, and Little Haystack to the east.

Proceed about 135 mi S on Rte 93 directly to Boston.

REFERENCES

Agassiz, Louis, 1870, On the former existence of local glaciers in the White Mountains: American Naturalist, v. 4, p. 550-558.

Antevs, E. 1932, Alpine zone of Mt. Washington Range: Auburn, Maine, Merrill and Webber, 118 p.

Ashley, G.M. 1985, Introduction in Ashley, G.M. Shaw, J., and Smith, N. D., eds., Glacial sedimentary environments: Society of Economic Paleontologists and Mineralogists, Short Course No. 16, p. 1-6.

Billings, M.P., Fowler-Billings, K., Chapman, C.A. Chapman, R.W., and Goldthwait, R.P., 1946 (reprinted 1979), The geology of the Mt. Washington Quadrangle: Concord, New Hampshire Department of Resources and Economic Development, 56 p.

Borns, H.W., Jr., and Calkin, P.E., 1977, Quaternary glaciation, west-central Maine, Geological Society of America Bulletin, v. 88, p. 1773-1784.

Bradley, D.C., 1981, Late Wisconsinan mountain glaciation in the northern Presidential Range, New Hampshire: Arctic and Alpine Research, v. 13, no. 3, p. 319-327.

Caldwell, D.W., 1966, Pleistocene geology of Mt. Katahdin, in Mount Katahdin region, Maine, Guidebook for 58th annual New England Intercollegiate Geological Conference, p. 51-61.

Caldwell, D.W., 1972, The geology of Baxter State Park and Mt. Katahdin, Maine Geological Survey Bulletin 12, 57 p.

Caldwell, D.W., 1980, Alpine glaciation of Mount Katahdin, Guidebook for 72 annual meeting of New England Intercollegiate Geological Conference, p. 80-85.

Craft, J.L., 1979, Evidence for local glaciation, Adirondack Mountains, New York, Guidebook for 42nd annual reunion of the Friends of the Pleistocene, Eastern Cell, 75 p.

Crosby, I.B. 1934, Extension of the Bethlehem, New Hampshire, moraine: Journal of Geology, v. 42, p. 411-421.

Davis, M.B., Spear, R.W., and Shane, L.C.K., 1980, Holocene climate of New England: Quaternary Research, v. 14, p. 240-250.

Davis, P.T., 1976, Quaternary glacial history of Mt. Katahdin, Maine: Orono, Maine, University of Maine, M.S. thesis, 155 p.

Davis, P.T., 1978, Late Quaternary paleoenvironmental history of Mt. Katahdin, Maine: Implications for vertical extent of late Wisconsinan Laurentide ice: Geological Society of America and Geological Association of Canada, Abstracts with Programs, v. 10, no 7, p.386.

Davis, P.T., 1983, Glacial sequence, Mount Katahdin, north-central Maine, Geological Society of America, Abstracts with Programs, v. 18, p. 11.

Davis, P.T., 1989, Quaternary glacial history of Mt. Katahdin and the nunatak hypothesis, in Tucker, R.D., and Marvinney, R.G., eds., Studies in Maine Geology, v. 6, Quaternary Geology, p. 119-134: Augusta, Maine, Maine Geological Survey.

Davis, P.T., Thompson, W.B., et al., 1988, Late Quaternary glacial and vegetational history of the White Mountains, New Hampshire, Guidebook for Trip A.1, 10th biennial meeting of the American Quaternary Association, University of Massachusetts, Amherst, 68 p.

Davis, P.T., and Davis, R.B., 1980, Interpretations of minimum-limiting radiocarbon ages for deglaciation of Mt. Katahdin area, Maine: Geology, v. 8, p. 396-400.

Davis, P.T., and Waitt, R.B., 1986, Cirques in the Presidential Range revisited: No evidence for post-Laurentide mountain glaciation: Geological Society of America, Abstracts with Programs, v. 18, no. 5, p. 11.

Davis, R.B., and Jacobson, G.L., Jr., 1985, Late-glacial and early Holocene landscapes in northern New England and adjacent areas of Canada: Quaternary Research, v. 23, p. 341-368.

Dyke, A.S., and Prest, V.K., 1987, Late Wisconsinan and Holocene history of the Laurentide Ice Sheet: Geographie physique et Quaternaire, v. 41, no. 2, p. 237-263.

Ellis, E.G., 1972, The geology of Whitehorse and Cathedral Ledges, in Cote, J., A climber's guide to Mt. Washington Valley: Topsfield, Massachusetts, Fox Run Press, p. 22-31.

Fairchild, H.L., 1913, Pleistocene geology of New York state, Geological Society of America Bulletin, v. 24, p. 133-162.

Flint, R.F., 1951, Highland centers of former glacial outflow in northeastern North America: Geological Society of America Bulletin, v. 62, p. 21-37.

Flint, R.F., 1953, Probable Wisconsinan substages and late-Wisconsin events in northeastern North America: Geological Society of America Bulletin, v. 64., p. 879-920.

Flint, R.F., Desmorest, M., and Washburn, A.L., 1942, Glaciation of the Shickshock Mountains, Gaspe Peninsula: Geological Society of America Bulletin, v. 53, p. 1211-1230.

Fowler, B.K., 1982. Preliminary stability reconnaissance, Old Man of the Mountains, New Hampshire, in: Farquhar, O.C. (ed.), Geotechnology in Massachusetts; Proceedings of a Conference in March, 1980: Amherst, University of Massachusetts, p. 141-149.

Fowler, B.K., 1984, Evidence of a late-Wisconsinan cirque glacier in King Ravine, northern Presidential Range, New Hampshire, U.S.A.: Alternative interpretations: Arctic and Alpine Research, v. 16, no. 4, p. 431-437.

Fuller, D.C., and Hotz, C.F., 1981, Soil survey of Essex County, Massachusetts, northern part: U.S. Department of Agriculture, Soil Conservation Service, 194 p.

Gerath, R.F., 1978, Glacial features of the Milan, Berlin, and Shelburne map areas of northern New Hampshire: Montreal, McGill University, M.S. thesis, 129 p.

Gerath, R.F., and Fowler, B.K., 1982, Discussion of "Late Wisconsinan mountain glaciation in the northern Presidential Range, New Hampshire," by Dwight C. Bradley: Arctic and Alpine Research, v. 14, no. 4, p. 369-370.

Gerath, R.F., Fowler, B.K., and Haselton, G.M., 1985, The deglaciation of the northern White Mountains of New Hampshire, in Borns, H.W., Jr., LaSalle, P., and Thompson, W.B., eds., Late Pleistocene history of northeastern New England and adjacent Quebec: Geological Society of America, Special Paper 197, p. 21-28.

Goldthwait, J.W., 1913, Glacial cirques near Mount Washington: American Journal of Science, v. 235, p. 21-28.

Goldthwait, J.W., 1916, Glaciation in the White Mountains of New Hampshire: Geological Society of America Bulletin, v. 27, p. 263-294.

Goldthwait, J.W., 1925, The geology of New Hampshire: New Hampshire Academy of Science, Handbook No. 1, Rumford Press, Concord, New Hampshire, 86 p.

Goldthwait, J.W., Goldthwait, Lawrence, and Goldthwait, R.P., 1951, The geology of New Hampshire, Part I, Surficial geology: Concord, New Hampshire State Planning and Development Commission, 83 p.

Goldthwait, R.P., 1938, The uncovering of New Hampshire by the last ice sheet: American Journal of Science, fifth series, v. 36, p. 345-372.

Goldthwait, R.P., 1939, Mount Washington in the great ice age, New England Naturalist, no. 5 (Dec.), p. 12-19.

Goldthwait, R.P., 1940, Geology of the Presidential Range: New Hampshire Academy of Science, Bulletin, No. 1, 43 p.

Goldthwait, R.P., 1968, Surficial geology of the Wolfeboro-Winnipesaukee area, New Hampshire: Concord, New Hampshire Department of Resources and Economic Development, 60 p.

Goldthwait, R.P., 1970a, Mountain glaciers of the Presidential Range in New Hampshire: Arctic and Alpine Research, v. 2, no. 2, p. 85-102.

Goldthwait, R.P., 1970b, Scientific aspects of Mount Washington in New Hampshire: Guidebook for 33rd reunion of the Friends of the Pleistocene, Mt. Washington, New Hampshire.

Goldthwait, R.P., and Mickelson, D.M. 1982, Glacier Bay: A model for the deglaciation of the White Mountains in New Hampshire, in Larson, G.J., and Stone, B.D., eds., Late Wisconsinan glaciation of New England: Dubuque, Iowa, Kendall/Hunt, p. 167-181.

Goldthwait, T., 1972, Two-till exposure along the Peabody River, Gorham, New Hampshire: Hanover, New Hampshire, Dartmouth College, unpublished senior paper, 14 p.

Gosselin, G.W., 1971, A Pleistocene legacy: Mount Washington Observatory Bulletin, v. 12, no. 1, p. 3-13.

Haselton, G.M. and Fowler, B.K., 1991, Stratigraphy in the lower Peabody valley, Gorham, New Hampshire, USA: Northeastern Geology, v. 13, no. 1, p. 11-20.

Hitchcock, C.H., 1878, The geology of New Hampshire - Volume III, Part III: Surface geology: Concord, New Hampshire, E.A. Jenks, 386 p.

Ives, J.D., 1974, Biological refugia and the nunatak hypothesis, in Ives, J. D., and Barry, R.G., eds., Arctic and alpine environments: London, Methuen, p. 605-636.

Johnson, D.W., 1917, Date of local glaciation in the White, Adirondack, and Catskill Mountains: Geological Society of America Bulletin, v. 28, p. 543-552.

Johnson, D.W., 1933, Date of local glaciation in the White Mountains: American Journal of Science, v. 225, p. 339-405.

Koteff, C. 1974, The morphologic sequence concept and deglaciation of southern New England in Coates, D.R., ed., Glacial Geomorphology: Binghamton, State University of New York, p. 121-144.

Koteff, C. and Pessl, F., Jr., 1985, Till stratigraphy in New Hampshire: Correlations with adjacent New England and Quebec, in Borns, H.W., Jr.,. LaSalle, P., and Thompson, W.B., eds., Late Pleistocene history of America: Geological Society of America, Special Paper 197, p. 1-12.

Lawson, D.E., 1979, Sedimentological analysis of the western terminus region of the Matanuska Glacier, Alaska: Gold Regions Research and Engineering Laboratory, Report 79-9, 112 p.

Lawson, D.E., 1982, Mobilization, movement and deposition of active subaerial sediment flows, Matanuska Glacier, Alaska: Journal of Geology, v. 90, p. 279-300.

Leavitt, H.W. and Perkins, E.H., 1935, A survey of road materials and glacial geology of Maine, v. II, Glacial Geology of Maine: Orono, Maine Technology Experiment Station, Bulletin 30, 232 p.

Lougee, R.J., 1939, Geology of the Connecticut watershed, in Warfel, H.E., ed., Biological Survey of the Connecticut watershed: Concord, New Hampshire, New Hampshire Fish and Game Department, Survey Report No. 4, p. 131-149.

Lougee, R.J., 1940, Deglaciation of New England: Journal of Geomorphology, v. 3, p. 189-217.

Melvin, R.L., deLima, Virginia, and Stone, B.D., 1992, The stratigraphy and hydraulic properties of tills in southern New England: U.S. Geological Survey Open File Report 91-481, 53 p.

Newton, R.M., 1974, Surficial geology of the Ossipee Lake Quadrangle, New Hampshire: Concord, New Hampshire, Department of Resources and Economic Development, 52 p.

Newton, R.M., 1977, Glacial features in east-central New Hampshire: Guidebook for 40th reunion of Friends of the Pleistocene, North Conway, New Hampshire.

Oldale, R.N., Cronin, T.M., Valentine, P.C., Spiker, E.C., Blackwelder, B., Belknap, D.F., Wehmiller, J.F., and Szabo, B.J., 1982, The stratigraphy, absolute age, and palynology of the upper Pleistocene deposits at Sankaty Head, Nantucket Island, Massachusetts: Geology, v. 10, p. 246-252.

Packard, A.S., 1867, Ice-marks and ancient glaciers in the White Mountains: American Naturalist, v. 1, p. 260-269.

Persson, C., 1983, Glacial deposits and the central Swedish end moraine zone in eastern Sweden, in Ehlers, J., ed., Glacial deposits in North-west Europe: Rotterdam, A.A. Balkema, p. 131-139.

Pessl, F., Jr. and Schafer, J.P., 1968, Two-till problem in Naugatuck-Torrington area, western Connecticut, in Orville, P.M. (ed.), Guidebook for Field Trips in Connecticut, for 62nd annual meeting of New England Intercollegiate Geological Conference, State Geological and Natural History Survey, Hartford, Connecticut, Guidebook No. 2, 25 p (each article paged separately).

Rich, J.L., 1906. Local glaciation in the Catskill Mountains: Journal of Geology, v. 14, p. 113-121.

Rich, J.L., 1935, Glacial geology of the Catskills: New York Museum Bulletin 229, 180 p.

Schafer, J.P. and Hartshorn, J.H., 1965, The Quaternary of New England, in Wright, H.E., Jr, and Frey, D.G., eds., The Quaternary of the United States: Princeton, New Jersey, Princeton University Press, p. 113-128.

Shaw, J., 1985, Subglacial and ice marginal environments, in Ashley, G.M., Shaw, J., and Smith, N.D., eds., Glacial sedimentary environments: Society of Economic Paleontologists and Mineralogists, Short Course No. 16, p. 47-52.

Smith, G.W., 1985, Chronology of late Wisconsinan deglaciation of coastal Maine, in Borns, H.W., Jr., LaSalle, P., and Thompson, W.B., eds., Late Pleistocene history of northeastern New England and adjacent Quebec: Geological Society of America, Special paper 197, p. 29-44.

Spear, R.W., 1989, Late-Quaternary history of high-elevation vegetation in the White Mountains of New Hampshire: Ecological Monographs, v. 59, no. 2, p. 125-151.

Stone, G.H., 1880, Note on the Androscoggin glacier: American Naturalist, v. 14, p. 299-302.

Stone, G.H., 1899, The glacial gravels of Maine: U.S. Geological Survey, Monograph 34, 499 p.

Stone, B.D. and Borns, H.W., Jr., 1986, Pleistocene glacial and interglacial stratigraphy of New England, Long Island, and adjacent Georges Bank and the Gulf of Maine, in Sibrava, V., Bowen, D.Q., and Richmond, G.M., eds., Quaternary glaciations in the Northern Hemisphere, IGCP Project 24, Pergamon Press, Oxford, England, p. 39-53.

Tarr, R.S., 1900, Glaciation of Mount Ktaadn [sic], Maine: Geological Society of America Bulletin, v. 11, p. 433-448.

Thompson, W.B., 1983, The Androscoggin Moraine: The Maine Geologist (newsletter of the Geological Society of Maine), v. 9, no. 3, p. 5.

Thompson, W.B., 1986, Glacial geology of the White Mountain foothills, southwestern Maine, Field Trip C-1, in Newberg, D.W., ed., Guidebook for Field Trips in Southwestern Maine, 78th annual meeting of the New England Intercollegiate Geological Conference, Bates College, Lewiston, Maine, p. 275-288.

Thompson, W.B. and Fowler, B.K., 1986, The Androscoggin Moraine: Evidence of late-glacial ice flow in the White Mountains: Geological Society of America, Abstracts with Programs, v. 18, no. 1, p. 71.

Thompson, W.B. and Fowler, B.K., 1989, Deglaciation of the upper Androscoggin River valley and northeastern White Mountains, Maine and New Hampshire, in Tucker, R.D. and Marvinney, R.G., eds., Studies in Maine Geology, v. 6, Quaternary Geology: Augusta, Maine, Maine Geological Survey, p. 71-88.

Thompson, W.W., 1960, The shape of New England Mountains, Part I: Appalachia, v. 26, p. 145-159.

Thompson, W.W., 1961, The shape of New England Mountains, Parts II and III: Appalachia, v. 27, p. 316-335 and 457-478.

Upham, Warren, 1904, Moraines and eskers of the last glaciation in the White Mountains: American Geologist, v. 33, p. 7-14.

Vose, G.L., 1868, Traces of ancient glaciers in the White Mountains of New Hampshire: American Naturalist, v. 2, p. 281-291.

Wagner, P.W., 1970, Pleistocene mountain glaciation, northern Vermont, Geological Society of America Bulletin, v. 81, p. 2465-2470.

Waitt, R.B. and Davis, P.T., 1988, No evidence for post-icesheet cirque glaciation in New England: American Journal of Science, v. 288, p. 495-533.

Weddle, T.K., Stone, B.D., Thompson, W.B., Retelle, M.J., Caldwell, D.W., and Clinch, J.M., 1989. Illinoian and late Wisconsin tills in eastern New England: A transect from northeastern Massachusetts to west-central Maine, Field Trip A-2, in Berry, A.W., Jr., ed., Guidebook for Field Trips in Southern and West-Central Maine, 81st annual meeting of the New England Intercollegiate Geological Conference, University of Maine at Farmington, Farmington, Maine, p. 25-85.